Université de Montréal

The Synthesis and Characterization of Rh_2(II,II) Templated Photoactive Assemblies

Par

Michael Cooke

Département de chimie

Faculté des arts et des sciences

Thèse présentée à la Faculté des études supérieures en vue de l'obtention du grade de Philosophiae Doctor (Ph.D.) en chimie

July 2007

Université de Montréal
Faculté des études supérieures

Cette thèse intitulée

The Synthesis and Characterization of Rh_2(II,II) Templated Photoactive Assemblies

présenté par:
Michael Cooke

à été évalué par un jury compose des personnes suivantes:

Prof. Davit Zargarian
président
Prof. Garry Hanan
directeur de recherche
Prof. André Beauchamp
membre du jury
Prof. Frederick MacDonnell
examinateur externe
Prof. Christian Reber
représentant du doyen de la FES

Abstract

The dirhodium(II,II) tetracarboxylate motif has been shown to serve as a structural template for the self-assembly of carboxylate-appended photoactive units of the form [(tpy)(4'-(4-carboxyphenyl)tpy)Ru]$(PF_6)_2$ (tpy = 2,2':6'2'' terpyridine). Efficient quenching of the emissive ^{3}MLCT state of these photoactive complexes upon formation of these higher-order assemblies suggested irreversible energy transfer to the non-emissive excited state of the Rh_2(II,II) center, which was verified through the preparation of analogous assemblies based upon the triazine-based photoactive units [(2-phenyl-4,6-di(2-pyridyl)triazine)(4'-(4-carboxyphenyl)tpy)Ru]$(PF_6)_2$ and [(2-(4-carboxyphenyl)-4,6-di(2-pyridyl)triazine)(tpy)Ru]$(PF_6)_2$.

To expand on the synthetic utility of the dirhodium(II,II) tetracarboxylate motif, a series of homoleptic Ru(II) complexes based on the ligands 4'-(carboxy)tpy, 4'-(4-carboxyphenyl)tpy, and (2-(4-carboxyphenyl)-4,6-di(2-pyridyl)triazine) were prepared. Incorporation of the Rh_2(II,II) motif to these dicarboxylates could be performed in the absence of deleterious polymerization to give both bis-Rh_2 and mono-Rh_2-adducts, which have been unambiguously characterized. To ameliorate the general insolubility of such dicarboxylate complexes, the ligand 4'-(4-carboxyphenyl)-4,4''-di-(*tert*-butyl)tpy was prepared, along with its subsequent homoleptic Ru(II) complex which was shown to be abundantly soluble in a range of organic solvents and to possess an unusual, porous solid-state structure.

To improve the integrity of the highly-charged Ru(II) assemblies constructed about the Rh_2(II,II) motif, amidinate analogues [(4'-(*N,N'*-dipropylbenzamidine)-tpy)(tpy)Ru]$(PF_6)_2$ and [(4'-(*N,N'*-diphenylbenzamidine)-tpy)(tpy)Ru]$(PF_6)_2$ were prepared, along with the polytopic amidine ligand *N,N'*-di-(4'-phenyl-tpy) formamidine. However, coordination of these amidinate-Ru(II) complexes to a Rh_2(II,II) center was not possible using conventional methods. Moreover, the elusiveness of the ligand *N,N'*-di-(4'-phenyl-tpy) formamidine was shown to be due to an unusual and unanticipated susceptibility of this compound to undergo hydrolysis, presumably due to the presence of tpy fragments bound to the amidine nitrogen atoms.

A divergent strategy was therefore developed by creating a family of reactive building blocks based upon the Rh_2(*N,N'*-diphenylbenzamiinate)$_4$ motif. This family stemmed from the initial creation of Rh_2(*N,N'*-diphenyl-4-bromobenzamidinate)$_4$, from which reactive functionality was installed to the central phenyl ring of the amidinate ligand. Such functionality was shown to include $-NH_2$ and –CCH groups, the periodicity and proportion of which could be controlled based upon the efficient isolation of mixed diphenylketimine/bromine Rh_2-complexes from the C-N coupling reaction of benzophenone imine with Rh_2(*N,N'*-diphenyl-4-bromobenzamidinate)$_4$. As proof of principle, both di- and penta-nuclear Rh_2(II,II) complexes were prepared. Where formylation was desired but inaccessible through a 'chemistry-on-the- complex' approach, suitable ligand preparation (i.e. *N,N'*-diphenyl-4-formyl-benzamidine) gave access to Rh_2 (*N,N'*-diphenyl-4-formyl-benzamidine)$_4$, from which the carboxylate analogue Rh_2 (*N,N'*-diphenyl-4-carboxybenzamidine)$_4$ could be prepared. All complexes were unambiguously characterized by ^{1}H NMR, ESI-MS, UV-vis, cyclic voltammetry and, in some cases, single-crystal X-ray crystallography.

Key Words: ruthenium(II), dirhodium(II,II), tpy, triazine, carboxylate, amidinate, self-assembly, templation, photoactive, excited–state, energy transfer.

Résumé

Le complexe tétracarboxylate de dirhodium(II,II) peut servir comme motif de base pour l'auto-assemblage de systèmes polynucléaires basés sur des complexes photo-actifs fonctionnalisés avec le groupement carboxylate. Plus particulièrement, la coordination du complexe [(tpy)(4'-(4-carboxyphenyl)tpy)Ru]$(PF_6)_2$ (tpy = 2,2':6'2'' terpyridine) sur le Rh_2(II,II) empêche l'émission de l'état excité ^{3}MLCT, ce qui suggère un transfert irréversible vers l'état excité non-emissif du centre Rh_2(II,II). Afin de confirmer ce phénomène, une série d'analogues basée sur les complexes [(2-phenyl-4,6-di(2-pyridyl)triazine)(4'-(4-carboxyphenyl)tpy)Ru]$(PF_6)_2$ et [(2-(4-carboxyphenyl)-4,6-di(2-pyridyl)triazine)(tpy)Ru]$(PF_6)_2$ ont été préparés et étudiés.

Pour augmenter l'utilité synthétique du complexe tétracarboxylate de dirhodium(II,II) dans ce domaine, une série de complexes homoleptiques de Ru(II) basés sur les ligands 4'-(carboxy)tpy, 4'-(4-carboxyphenyl)tpy et (2-(4-carboxyphenyl)-4,6-di(2-pyridyl)triazine) ont été preparés. La coordination de ces complexes au centre Rh_2(II,II) a pu se faire efficacement sans polymérisation pour donner des complexes mono- et bis-Rh_2(II,II). Afin d'améliorer la solubilité des complexes dicarboxylate, le ligand 4'-(4-carboxyphenyl)-4,4''-di-(*tert*-butyl)tpy a été préparé, avec le complexe subséquent de Ru(II), qui a manifesté une grande solubilité dans les solvents organiques. De plus, à l'état solide, ce complexe adopte une structure comportant de grandes cavités.

Afin d'améliorer la stabilité des assemblages hautement chargés de Ru(II), les complexes [(4'-(*N,N'*-dipropylbenzamidine)-tpy)(tpy)Ru]$(PF_6)_2$ et [(4'-(*N,N'*-diphenylbenzamidine)-tpy)(tpy)Ru]$(PF_6)_2$ ont été préparés et caractérisés ainsi que le ligand polytopique *N,N'*-di-(4'-phenyl-tpy)formamidine. Malheureusement, les complexes amidinates ne pouvaient pas se coordonner au centre Rh_2(II,II) en utilsant les voies bien connues dans la litérature. De plus, la difficulté avec la synthèse du ligand *N,N'*-di-(4'-phenyl-tpy)formamidine a été attribuée à sa sensibilité a une attaque de l'eau. Cette sensibilité n'était pas anticipée, mais maintenant qu'elle est connue, il est évident qu'elle résulte de l'effect d'un groupement tpy attaché directement à l'atome d'azote de l'amidinate.

Il a donc fallu créer une autre voie qui se concentre sur l'approche inverse. Dans ce concept, le complexe Rh_2(*N,N'*-diphenylbenzamiinate)$_4$ a été fonctionnalisé. Pour ce faire, le complexe Rh_2(*N,N'*-diphenyl-4-bromobenzamidinate)$_4$ a été préparé en vue de faire la chimie directement sur le complexe. Ceci a permis l'introduction des groupements réactifs, comme -NH_2 et –CCH, sur le phényle situé au centre du ligand amidinate. Le nombre et la disposition de ces groupements ont été contrôlés en fassant la séparation de complexes intermédiares diphenylketimine/brome lors du couplage C-N du benzophénone imine avec Rh_2(*N,N'*-diphenyl-4-bromobenzamidinate)$_4$. Pour démontrer l'utilité de ces complexes, des assemblages di- et penta-nucléaire de Rh_2(II,II) ont été préparés et caractérisés. Dans le cas de la formylation, la chimie sur le complexe n'était pas réussi et le ligand *N,N'*-diphenyl-4-formyl-benzamidine et le complexe Rh_2(*N,N'*-diphenyl-4-formyl-benzamidine)$_4$ ont été préparés. De cela, le complex Rh_2(*N,N'*-diphenyl-4-carboxybenzamidine)$_4$ a pu être fait selon l'approche 'chimie sur le complexe'. Tous les complexes ont été caractérisés par spectroscopie de résonance magnétique nucléaire en solution, spectrométrie de masse ESI, spectroscopie UV-visible, voltampérométrie cyclique et analyse cristallographique à l'état solide par diffraction des rayons X.

Mots clés: ruthénium(II), dirhodium(II,II), tpy, triazine, carboxylate, amidinate, auto-assemblage, transfert d'énergie.

Table of Contents

List of Figures

List of Schemes

List of Equations

List of Tables

List of Abbreviations

Å	Angstrom
δ	chemical shift
EA	elemental analysis
bpy	2,2'-bipyridine
br	broad
BINOL	1,1'-Bi-2-naphthol
Bu	butyl
cif	crystallographic information file
COSY	correlation spectroscopy
Cy	cyclohexyl
d	doublet
dba	dibenzylideneacetone
dpb	*N,N'*-diphenylbenzamidine
DCM	1,2-dichloromethane
DMF	N,N-dimethylformamide
DMSO	dimethylsulfoxide
eq	equivalent
EtOH	ethanol
Et_2O	diethyl ether
ESI	electrospray ionization
form	formamidine
hr	hour
HOMO	highest-occupied molecular orbital
ILCT	inter-ligand charge transfer
J	coupling constant
LUMO	lowest-unoccupied molecular orbital
m	multiplet
MC	metal-centered
MLCT	metal-to-ligand charge transfer

MS	mass spectrometry
min	minute
Me	methyl
MeCN	acetonitrile
MeOH	methanol
NMR	nuclear magnetic resonance
n-Bu	n-butyl
ns	nanosecond
OAc	acetate
ORTEP	Oak Ridge Thermal ellipsoid program
OSWV	Osteryoung square-wave voltammetry
p	para
Ph	phenyl
ppm	parts per million
py	pyridine
t	triplet
r.t.	room temperature
^{t}Bu	*tert*-butyl
THF	tetrahydrofuran
tpy	2,2':6',2''-terpyridine
TOF	time-of-flight
Φ_p	phosphorescence quantum yield

Acknowledgments

First off, I would like to thank my supervisor, Prof. Garry Hanan., for providing me the autonomy to pursue my ideas and the guidance and encouragement to see them to fruition. You have reinforced my belief that creativity and imagination is everything in this business, and to you I owe my transformation into a synthetic chemist.

From Waterloo to Montreal, I have had both the privilege and pleasure of working alongside talented and dedicated scientists as a member of Prof. Garry Hanan's group. From my time in Waterloo, I am grateful for the camaraderie of Dr. Matt Polson, Dr. Joanne Yu, and Dr. Craig Robertson. Beating one's head off the wall is only fun when you have company.

I would like to thank both past and present members of Prof. Hanan's group since my arrival at the Université de Montréal, in particular Dr. Elaine Medlycott, Joseph Wang, Elena Ioachim, Pierre Tremblay, Francois Laverdiere, Marie-Pierre Santoni, Daniel Chartrand, and Isabelle Theobald, whose friendship has made my time here all the more memorable.

The time required to tackle the synthetic challenges that comprise this body of work would not have been possible if not for the aid of those adept at resolving single-crystal X-ray diffraction data, of which I have generated my fair share. From my time in Waterloo, I would like to say thank you to the late Dr. Nick Taylor. From my time in Montreal, I would like to thank the X-ray staff of Francine Bélanger-Gariépy and Dr. Michel Simard, along with Marie-Pierre Santoni, Elaine Medlycott, and Daniel Chartrand.

I would also like to thank the technical services at the Université de Montréal, including Sylvie Bilodeau for assistance with variable-temperature NMR and, in particular, Alexandra Furtos and Karine Venne for mass spectrometry. Prof. Yasu Tanaka and Masashi Watanabe of Shizuoka University, Japan, are also thanked for performing mass spectrometry on some challenging compounds.

I am grateful to Prof. Sebastiano Campagna and Dr. Frédérique Loiseau of the Università di Messina, Italy, for their photophysical contribution which has added a valued dimension to this work.

I wish to thank my family, including my mother Michelle, father Milton, and brother David for their support over the years, and for instilling in me that which made this possible.

Finally, I wish to thank my wife Vanessa for her support and patience. You believed in me when I wasn't sure I did.

Chapter 1: Introduction

1.1 Introductory Remarks

The harnessing of light energy by photoactive units has led to the pursuit of artificial light harvesting systems (LHS) promising a myriad of potential applications ranging from catalysis,[1] sensitizers for photovoltaic and fuel cell devices,[2,3] electroluminescent devices,[4] molecular sensors,[1a, 5] and photodynamic therapeutics.[6] The LHS's which exist in nature represent the pinnacle of complexity and function, and the lessons learned in their elucidation continues to be instrumental en route to efficient devices. While several important issues need be addressed in the development of functional artificial devices, perhaps the most significant is the assembly of many photoactive units by means conducive to energy and / or electron transfer. The reason for this stems from two considerations. The first is that the targeted function, particularly in catalysis, can involve multiple electron transfer and so multiple photon absorption is required for every molecule produced. The second is that energy transfer is never completely efficient, succumbing often to heat dissipation, and so a high input of light energy is required.[7] Nature utilizes many weak interactions in a true supramolecular sense (H-bonding, dipole-dipole) to effect connectivity, recognition, and energetic/electronic relay. The reversibility of such supramolecular interactions is instrumental to the self-assembly process.

Although elegant, constructing artificial LHS in this manner may not be suitable to the photoactive unit employed and / or to the conditions of operation for the device. Recent examples have focused on utilizing elaborate ligand design and / or performing many iterative chemical transformations with compromised efficiency and demanding purification.[8] Although limitations of this nature have been recognized,[9] synthesis remains tedious and structures of high nuclearity often possess a large degree of freedom which can preclude structural characterization and frustrate energy transfer processes. The covalent bond gives more durable, inert systems but low yields and exceedingly labourious synthesis often precludes practical application. In between lies the strongest supramolecular interaction, dative bonding, whose inherent reversibility allows for pre-

organization / self-assembly while offering bond strengths suitable to afford robust systems.

The vectorial and "self-seeking" nature of metal-ligand bonding, along with various possible coordination geometries, is conducive to rapid synthesis of multinuclear photoactive arrays with pre-determined architectures. Apart from facilitating construction, incorporation of metals can also serve to greatly affect energy and/or electron transfer processes. Considering the large number of metals to choose from, it is easy to see how photophysical properties can be readily fine-tuned for any given coordination motif. In addition, control of the overall 3-D organization and morphology of the photoactive array have been found to dramatically affect energy migration, [10] something that can be controlled to a great extent when incorporating metal units. Such a wide range of modification has served to provide ideal systems for study of electron and energy transfer processes and permitted access to a wide range of potential applications. Herein is presented a cross-section of current literature regarding metallo-directed assembly of photoactive systems, classified according to the coordination motif employed in their assembly.

1.2 Luminescent Assemblies from Four-Coordinate Metal Ions

1.2.1 Tetrahedral Metals

Carbon and silicon serve as non-metallic points of origin from which to grow a branched photoactive assembly adopting a central tetrahedral coordination geometry.[11] However, their utilization dictates a divergent synthetic approach which is inherently more labourious relative to convergent strategies employing metal centers as the central assembling unit. Of the metal centers adopting such a coordination motif, those with d^{10} configurations are most frequently encountered in the literature. Owing to their electron count, their coordination number and geometry can vary greatly, the outcome of which is usually dictated by the nature (i.e. hapticity, periodicity, bite angle, steric bulk) and flexibility of the ligand(s) involved. As a result, ideal tetrahedral motifs are seldom encountered, being distorted to some degree. With regard to photoactive assemblies, Ag(I), Au(I), and Cu(I) are most prevalent. Both Ag(I) and Au(I) are prone to metal-

metal bonding interactions. Combined with non-specific coordination numbers, it is not surprising, then, that these metals are often found in the context of luminescent cluster and polymeric compounds.[12, 13]

The outcome of the resulting supramolecular structure depends strongly on external factors in addition to the choice of the ligand(s) used. Their capacity for coordination extends beyond the ligand employed, and often the solvent used and the presence of weakly coordinating counter-anions can have a dramatic affect on the isolated product, invariably obtained upon crystallization.[14] This reflects a dynamic solution equilibrium rendered by such kinetically labile metal centers.

Ag(I) is regarded as a soft acid that favours coordination of soft bases, such as ligands that contain sulfur and phosphorous. Such donors have typically been in the context of simple chelating ligands.[15] Current literature reflects a dominance of nitrogen containing ligands, particularly with regard to N-heterocycles.[16] While polymeric structures and clusters still prevail, appropriate design of such ligands can lead to discrete, open structures normally exhibited by square planar and octahedral metal centers.[17] Here, bis-bidentate N-heterocycles derived from imine formation, like those depicted in Figure 1.1, are readily obtained by condensation of an appropriate diamine with 2-formyl pyridine.[17a]

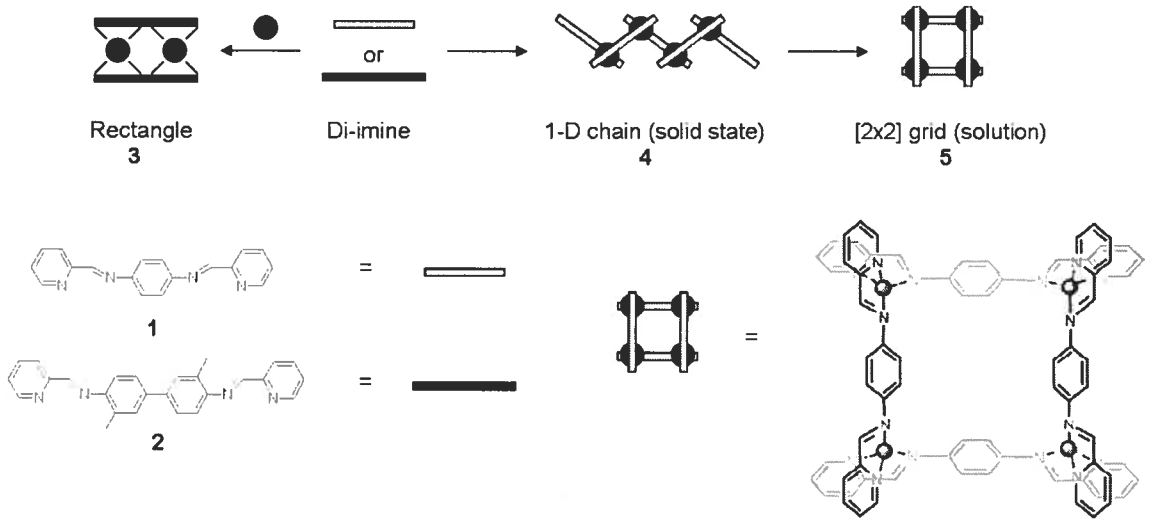

Figure 1.1. Characteristic solution equilibria of Ag(I) complexes containing dinucleating ligands.

Layering of an $AgClO_4$ / CH_3CN solution over a THF solution containing an equimolar amount of ligand **1** produced crystalline material comprising a zig-zag 1-D chain exhibiting intermolecular π-π stacking interactions. However, upon dissolution in polar media, this polymer was observed to rearrange into a [2x2] grid structure, as evidenced by a symmetric ^1H NMR spectrum and confirmed by FAB-MS, both in acetonitrile solution. However, when a methanol solution of $AgClO_4$ was layered over a solution of **2** in nitrobenzene / toluene, a rectangular structure was formed which showed no evidence of rearrangement in solution. Ag(I) containing complexes, like those presented here, do not possess significant MLCT bands in their absorption spectra, and so luminescence must derive from the ligand itself. Here, neither **1** nor **2** is luminescent in either the solid state or solution. However, upon complexation to form the polymer / grid or the rectangle, luminescence from ligand-centered π-π^* states is observed, even at room temperature in strongly coordinating deoxygenated acetonitrile (τ = 1.2-12.7 ns). This is due to a reduction in structural perturbation upon excitation of the ligands, afforded by an increase in ligand rigidity by complexation to the metal. This is a common theme with regard to d^{10} metals such as Ag(I) and Zn(II). However, the metal is not completely innocent in this regard, since decay profiles are clearly bi-exponential with both short-lived $^1\pi$-π^* and longer-lived $^3\pi$-π^* intraligand transitions, the latter stemming from heavy-atom relaxation of spin-forbidden processes. This case is unique considering that most Ag(I)-based systems display luminescence only in the solid state or at 77 K. Also, the inert nature and luminescence of the rectangle **3** indicates that this approach is certainly a step in the right direction toward viable applications.

In the pursuit of suitable photoactive units, much work has been devoted in the last twenty years to Cu(I) (bis)diimine complexes, where the diimine ligand is typically 1,10-phenanthroline (phen) or a derivative thereof.[18] Like Ru-polypyridyls, these complexes are characterized by relatively weak MLCT bands in the visible region. However, modification of the 1,10-phenanthroline ligand has much more dramatic affects on both the MLCT absorption profile and the excited-state lifetime and emission intensity. Considering that the parent complex $Cu(phen)_2^+$ is non-emissive in solution, homo and heteroleptic analogues have been prepared exhibiting strong luminescence.

This enhancement has mirrored much of the attenuation strategies that have been employed with ruthenium(II) polypyridyls,[19] such as increasing ligand delocalization and lowering thermal accessibility of upper-lying deactivating states. However, much of this attenuation stems from unique phenomena associated with the $Cu(phen)_2^+$ unit. Upon photo-excitation, a transient Cu(II) center is generated which distorts to a square-planar arrangement, making nucleophilic attack by coordinating solvent or anions possible.[20] From this 5-coordinate exciplex species, non-radiative deactivation of the emissive state is rapid and efficient. However, modification of the phen ligand so as to frustrate nucleophilic attack has led to large improvements in emission.[18, 21] In addition, the use of bulky phosphines, and especially diphosphine chelates, has yielded heteroleptic Cu(phen)(P-P) complexes with emission lifetimes of up to 16 μs in dichloromethane at room temperature.[22] Moreover, such complexes have proven to be emissive even in strongly coordinating solvent such as methanol and acetonitrile. The extent to which the emissive properties may be tuned bodes well for device applications, as does the fact that the excited state of such Cu(I) complexes leads to more powerful reductants than that of their $Ru(bpy)_3$ counterparts (-1.11 V for $Cu^*(phen)_2^+ \rightarrow Cu(phen)_2^{2+}$ vs -0.85 V for $Ru^*(bpy)_3^{2+} \rightarrow Ru(bpy)_3^{3+}$). This has naturally led to such potential applications as electroluminescence,[4a,23] sensitization of photovoltaic devices,[24] and DNA intercalation.[25]

The incorporation of Cu(I) phenanthrolines into multicomponent photoactive systems has, for the most part, been in the context of rotaxanes, catenanes, and dendritic systems.[18] With regard to these systems, fullerenes have been an attractive partner for Cu(I) phenanthrolines considering that it is fluorescent, exhibits diagnostic singlet and triplet transient absorption spectra, and is an excellent electron acceptor. Recently,[26] such incorporation has been in the context of helicate formation, as shown below for related helicates formed from bismethanofullerene (**A**) and methanofullerene (**B**). At the outset, it should be pointed out that the absorption spectra of each helicate was found to be the sum of the spectra of their individual components, thus suggesting no ground-state electronic interaction between the Cu(I)-phenanthroline and C_{60} moieties.

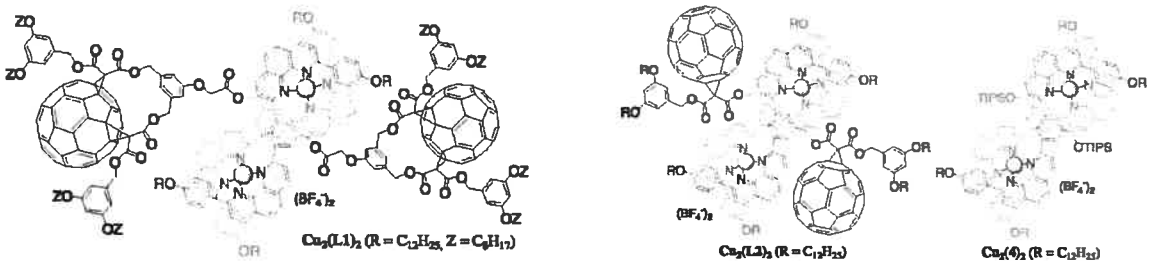

A B

Figure 1.2. Cu(I) helical fullerene structures: bismethanofullerene (**A**) and methanofullerene (**B**)

Fluorescence from the bismethanofullerene was unaffected relative to a related model compound consisting of nearly the same ligand but without the bis-phenanthroline portion. This is in accord with other supramolecular assemblies containing such photoactive units. Considering the energies for the ^{3}MLCT of Cu(I)(phen)$_2$, the singlet emissive state of the bismethanofullerene, and the charge separated state (Cu^+-C_{60}^-) produced upon electron transfer, it was determined that excitation of either photoactive unit could lead to exergonic electron transfer. Although this driving force was found to be larger upon excitation of bismethanofullerene, the maintenance of the fullerene emission upon helicate formation points to electron transfer from the ^{3}MLCT of the Cu(I) core. Although this process is less thermodynamically favoured, it is likely that the occurrence of a MLCT prior to electron transfer serves to reduce kinetic activation barriers to electron transfer by affecting favourably the external and internal reorganization energy contributions.

More recent is their incorporation into polynuclear racks,[27] grids,[28] boxes,[29] and baskets.[30] Shown below are representative examples of a 1D rack (**A**) and 2D grid (**B**) and a box-like cavity (**C**). These structures represent important synthetic achievements considering that a prerequisite for such architectures has typically been the use of more kinetically inert 2nd and 3rd row transition metals. Their synthesis relies on the incorporation of bulky substituents in the 2 and 9 positions of phenanthroline on one of the ligand components. Doing so limits the potential thermodynamic possibilities (homoleptic oligomers) that are otherwise quite accessible using Cu(I) and Ag(I). This

leads to efficient "one-pot" self-assembly of polynuclear structures possessing large voids and internal cavities (e.g. 5000 $Å^3$ for **C**) that, given the photoactive nature of their components, are ideally suited for applications in molecular sensing and catalysis. Unfortunately, to date, elucidation of their photophysical properties has not been undertaken. It is noteworthy that structure **C** was assembled using both Cu(I) and Ag(I), which is a testament to the utility of this approach considering that Ag(I) complexes are relatively less stable. This point was made quite nicely by Schmittel et al, when the structure **C** assembled by Ag(I) was cleanly exchanged with the isostructural compound composed of Cu(I) by addition of equimolar quantities of CuI at room temperature. That this occurs despite obvious steric barriers underscores the prevalence of Cu(I) as a tetrahedral assembling unit.

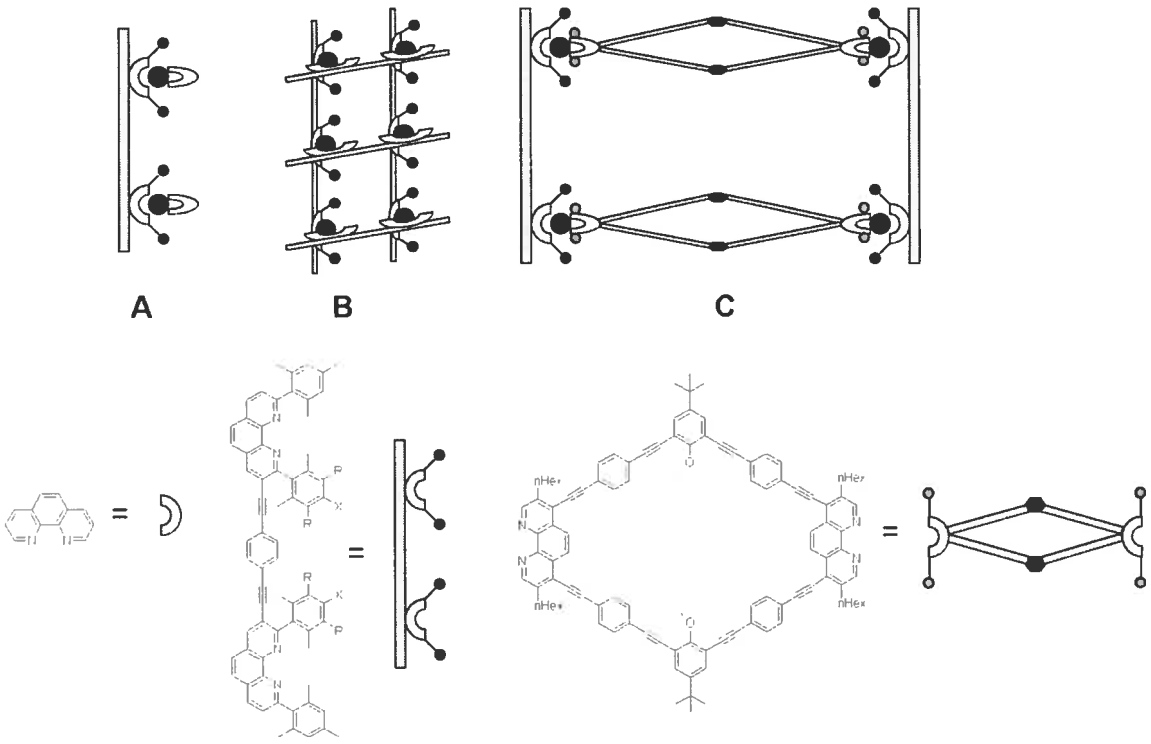

Figure 1.3. Rack (**A**), grid (**B**), and box-like (**C**) assemblies based upon (phen)Cu(I).

1.2.2 Square Planar Metals

As we have seen, tetrahedral metal centers can, with appropriate ligand design, lead to porous structures. However, most often they lead to closed structures such as helices and polymers. This, in addition to an intrinsic tendency to undergo fluxional processes where d^{10} metals are concerned, compromises their potential for applications to some extent, necessitating increasingly elaborate ligand design. Their four-coordinate relatives predisposed to square planar coordination are inherently advantageous with respect to both of these points. They are more prone to formation of open, discrete structures and relatively more kinetically inert, thus making them well suited for application purposes, particularly with regard to luminescent sensors and catalysis.[1a] It is not surprising, then, that this is one of the most heavily investigated motifs en route to metal-directed assemblies.

Of the transition metals predisposed to form square planar complexes, Pd^{2+} and Pt^{2+} are the most prevalent, with and without regard to forming luminescent assemblies. Their synthesis relies on a self-assembly strategy where appropriate precursor transition-metal units possessing labile coordination sites are combined with complementary bridging bidentate ligands to yield a target geometry according to thermodynamic control (see Figure 4). Thus, many metallo-supramolecular systems can contain several species in equilibrium where no clear thermodynamic preference is given, the distribution of which depends strongly on the steric demand and flexibility of the bridging ligand as well as on the presence of potential guest molecules.[31] To make matters more complicated, the reversible nature of dative bonds can give rise to persistent kinetically controlled species en route to the final thermodynamically favoured product. Therefore, the choice of metal ion used in the precursor units and its affect on dative bond strength (e.g. $Pt^{2+} > Pd^{2+}$) influences both the stability of the end product and the reaction conditions necessary to generate it efficiently.[32]

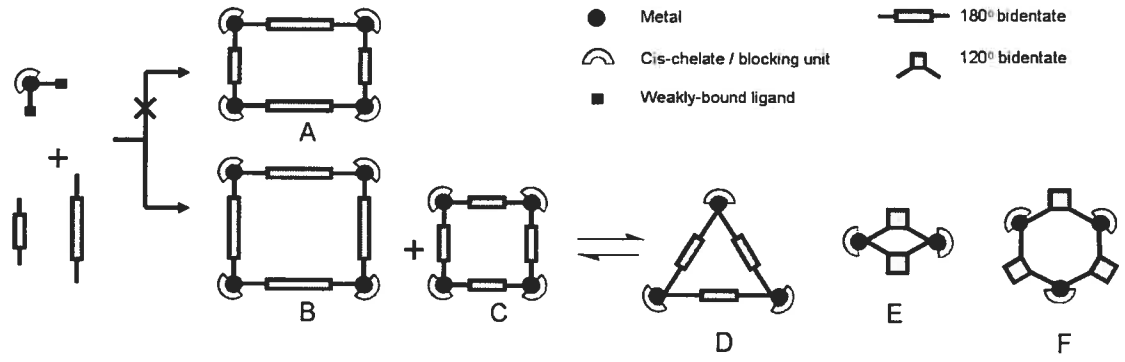

Figure 1.4. Metal-directed self-assembly leads to several possible discrete products (**A-F**).

The role of a square planar metal in producing photoactive assemblies may be solely structural, as with the majority of d^{10} metal ions. In this case, suitable photoactive units coordinated to the assembling metal can experience an increase in rigidity, which can in turn influence emission energy and intensity by enhancing ligand π-delocalization and minimizing excited state structural perturbations. However, there exists a plethora of mononuclear square planar complexes which exhibit MLCT and, depending on the ligand, ILCT states from which emission may occur. It is therefore reasonable to develop polynuclear systems wherein these metals comprise the photoactive unit. Of these, Pt^{2+} complexes have received a great deal of attention,[33] while Pd^{2+} has received relatively little.[34] This is due to the larger ligand field produced with Pt^{2+} compared to Pd^{2+} for any given ligand, making upper lying ^{3}MC states less thermally accessible from the emissive ^{3}MLCT or ^{3}ILCT states. In this way, efficient non-radiative decay from these highly distorted ^{3}MC states to the ground state is reduced, thereby preserving emissive–state population. The result is often room temperature solution luminescence for Pt^{2+} complexes while only solid state or 77 K emission is observed with Pd^{2+} complexes, although a few examples of room temperature emission are known.[34] Metal-directed, photoactive assemblies based on the square-planar coordination motif have been discussed in recent reviews,[1a, 5a] and the following discussions concern developments since that time.

With regard to forming square assemblies, the conventional self-assembly approach outlined in Figure 1.4 has inherent limitations, owing to the relative thermodynamic stabilities of all possible species in solution. This becomes evident in

pursuit of larger square assemblies where one relies on longer, linear bridging ligands whose increased flexibility diminishes the enthalpic advantage of square formation over that of a triangle, allowing the entropic advantage of triangle formation to become significant in determining product distribution. An additional disadvantage is the inability to form structures of particular topologies via a one-pot self- assembly approach. This has been well exemplified by Lin and co-workers in the pursuit of constructing chiral, enantiopure squares and triangles composed of Pt^{2+} corners and BINOL-derived, linear bis(4,4'-alkynyl) ligands (L_1 and L_2, Figure 5).[35] A related square employing the same bridging ligands, but using bulky phosphines in place of 4,4'-di-tert-butyl-2,2'-bipyridine (dtbPy), was reported earlier and shown to be enantiopure, exhibiting dual room temperature emission from intra-ligand $^1\pi$-π^* (425 nm, $\tau < 400$ ps) and $^3\pi$-π^* (582 nm, $\tau \sim 100$ μs), the latter being observed in argon de-gassed solution.[36] Considering that the ligand itself is strictly fluorescent, the effect of Pt^{2+} incorporation has led to efficient singlet-triplet intersystem crossing via spin-orbit coupling. The exclusive production of such squares was previously accomplished after multiple steps wherein two mono-nuclear $(Et_3P)_2Pt(L)_2^{2+}$ corner units were covalently coupled to two corner units of $(Et_3P)_2PtCl_2$ in 34-46 % yield. More recently, Lin et al have produced the species shown in Figure 5, utilizing once again covalent bond synthesis, but in the context of a one-pot assembly. The consequence of reduced synthetic steps has been compromised yield for square formation, but this was shown to be readily countered by attenuating the steric bulk of the linear bridging ligand such that the square **7b** could be formed exclusively. Interestingly, although **6a** and **7a** are isolated form the same reaction mix, dissolution of **6a** cleanly produces **7a** with a half-life of 4 days. The incorporation of the chelating ligand dtbPy was done in pursuit of electroluminescent device applications, since phosphorescence emanating from the ^{3}MLCT [Pt – π^*(diimine)] transition of simple (diimine)-Pt(acetylide)$_2$ complexes has been of interest for the fabrication of light-emitting devices.[4a] Here, square **7a** was shown to be strongly phosphorescent ($\Phi_p = 9.4$ %) and stable, giving electroluminescent performance exceeding that for simple (diimine)-Pt(acetylide)$_2$ complexes.[37]

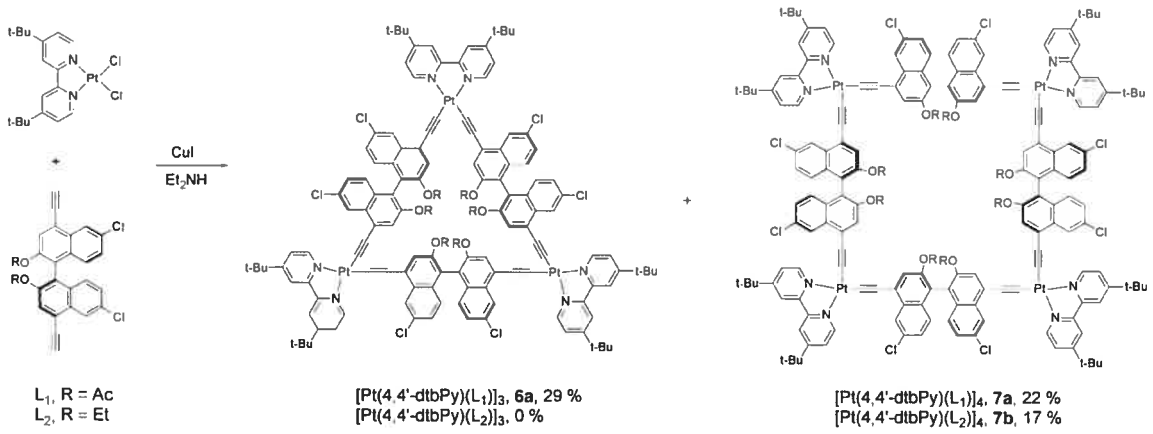

Figure 1.5. Topological discrimination: generation of enantio-pure geometries from chiral sub-units with potential electroluminescence application.

Coordination to a square planar assembling unit is also of interest with regard to the "complex as the ligand" approach where transition-metal containing photoactive groups are prepared with suitable secondary functionality to allow for subsequent coordination. This approach has been particularly popular amongst ruthenium polypyridyl and metallo-phorphyrin researchers, owing to their robust nature and the potential to perform chemical modifications directly on the complex. Most often, the secondary functionality is installed through preparation of homo- or hetero-ditopic ligands, as illustrated in Figures 6 and 7. Complex **9** and its precursor complex **8** (Figure 6) were synthesized for the purposes of fundamental investigations into electron and energy transfer between subunits of metal-based light harvesting antennas.[38] Such studies have, to date, dealt primarily with ruthenium and osmium complexes. Here, precursor complex **8** has a ^{1}MLCT excitation at 490 nm, with room temperature solution emission at 650 nm and a luminescence decay of 363 ns, while complex **9** has a red-shifted ^{1}MLCT excitation at 530 nm, with room temperature solution emission at 658 nm and a luminescence decay of 244 ns. Monitoring of the excited-state relaxation processes leading to the equilibrated ^{3}MLCT by time-resolved transient absorption revealed a very fast ($\geq$ 200 fs) time constant and a slower solvent-dependent time constant ($\approx$ 1.5 ps) upon fitting of the initial rise for both **8** and **9**, corresponding to intersystem crossing and solvent reorganization processes, respectively. An additional time constant (50 ps) was observed for **9** corresponding to a mono-exponential transient decay. This indicated

charge transfer to the $Pd(allyl)^{2+}$ unit. Upon monitoring the ground state recovery kinetics of the ruthenium complex, a fourth time constant (220 ps) was found in addition to those found on examination of the excited state kinetics. Since it did not occur in the excited-state absorption, back-electron transfer to the ruthenium complex was ruled out, and the process was assigned to excitation equilibration between $Pd(allyl)^{2+}$ units subsequent to charge transfer from the ruthenium chromophore. Since charge transfer is initiated on the periphery and terminates on the central Pd(allyl) units, which are rather open to substrate binding, this system serves as a functional model for the photosynthesis reaction center in plants.

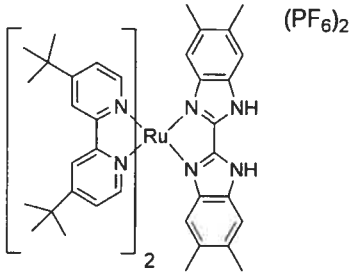

8

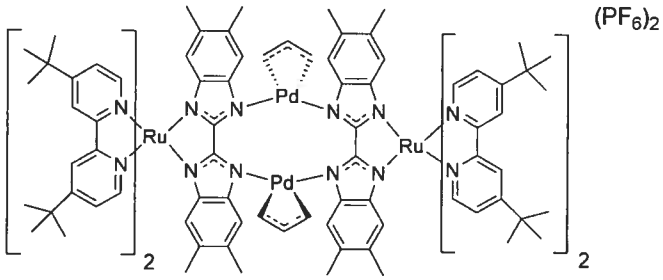

9

Figure 1.6. Model compound exhibiting photo-initiated electron collection at Pd(II) sub-units.

A recent potential host-guest assembly has been described by Wolf and co-workers using the typically strongly luminescent $[Ru(bpy)_3]^{2+}$ motif.[39] Here, the "complex as the ligand" approach is once again utilized where the datively unsaturated $[Ru(bpy)_2(qpy)]Cl$ (see Figure 7 below, where qpy is 2,2':4,4":4',4'''-quarterpyridyl) is heated with 0.5 equivalents of either the solvated adduct $[M(en)(solv)_2]^{2+}$ (where M = Pd^{2+}(**A**) or Pt^{2+}(**B**), en is 1,2-ethylenediamine) or $ClRe(CO)_5$ (**C**). Considering that every coordination compound is ultimately in an assembly/disassembly equilibrium to some degree in solution, the rapid build-up of charge can be a concern considering that large electrostatic repulsions arising from close proximity of cationic units can compromise coordination strength, leading to an equilibrium more easily affected by such variables as solvent polarity, temperature, and trace competing ligands. As expected, complex **B** is more kinetically robust than **A.** All complexes show strong, characteristic absorption and

solution luminescence in both organic and aqueous solvent. The absorption spectra show intense bands at high energy associated with intra-ligand $\pi \rightarrow \pi^*$ processes and lower energy, less intense bands ranging from 350-550 nm arising from Pd/Pt(d) $\rightarrow L(\pi^*)$ and Ru(d) $\rightarrow L(\pi^*)$ processes. Relatively intense emission occurs between 650-670 nm. This is slightly red shifted relative to $[Ru(bpy)_2(qpy)]^{2+}$, as expected since coordination serves to stabilize the ligand-centered π^* orbitals (i.e. MLCT state). Also, this emission is insensitive to the excitation wavelength which indicates efficient energy transfer from the other MLCT states to the Ru-^{3}MLCT state. To accommodate coordination to both octahedral metals, **C** has a bent shape when looking down the Re-Re axis. The maintenance of room temperature luminescence, particularly in water, and the limited number of counter-anions within the internal cavity for **C** encouraged further host-guest complexation / sensing study which showed that the "puckered" cavity of **C** can enhance binding of guest aromatic molecules.

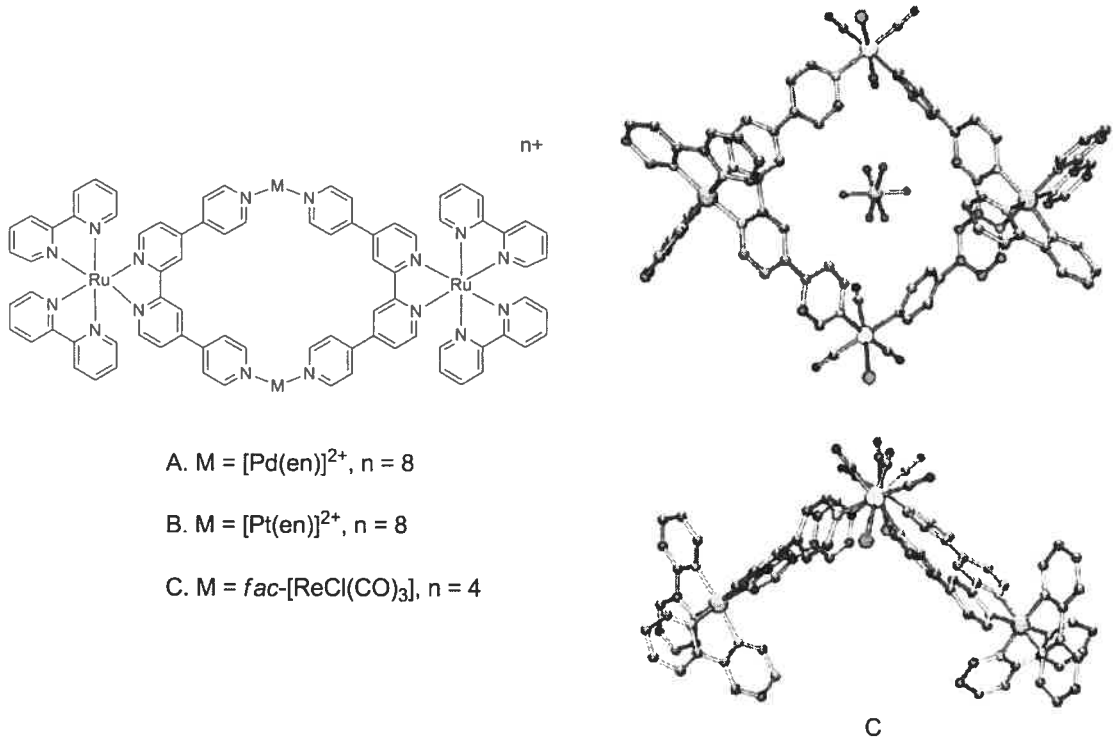

Figure 1.7. Kinetically-locked metallomacrocycles based upon $Ru(bpy)_3^{2+}$, assembled from Pd(II) (**A**), Pt(II) (**B**), and Re(I) (**C**) sub-units.

Much effort has been directed toward the synthesis of multinuclear porphyrinoid assemblies, owing to a wide range of potentially exploitable physical properties, including luminescence.[40] Of the existing strategies, metal-directed assembly is particularly attractive considering the influential electronic role played by the linking metal unit(s) and a wide variety of such subunits that can be prepared with secondary dative functionality, afforded by advancements in their synthesis. Shown below (Figure 8) is a recent, elegant example by Drain and co-workers which embodies typical synthetic considerations.[41]

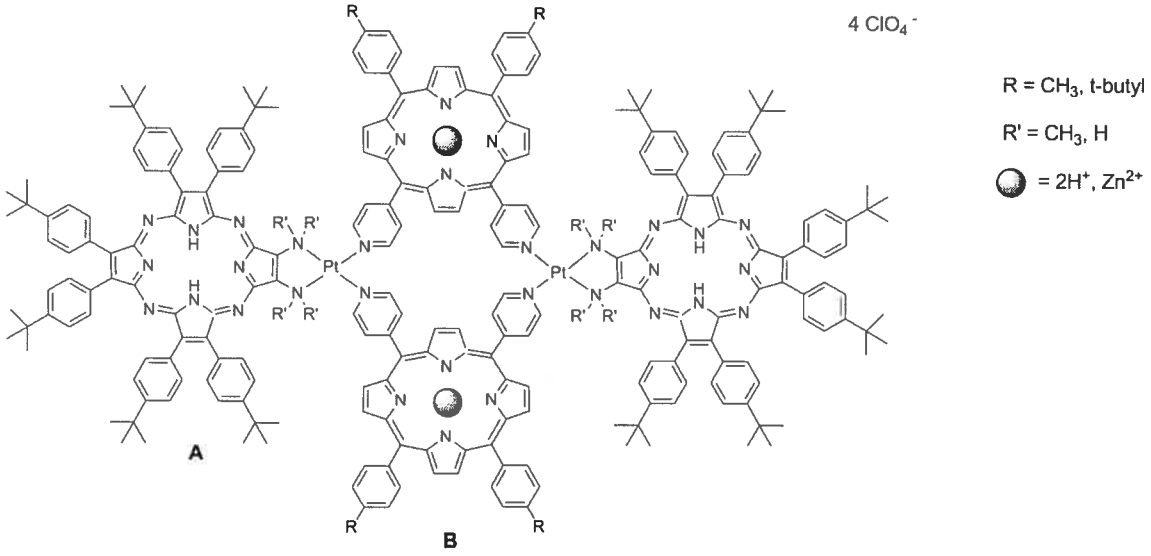

Figure 1.8. Dative assembly of porphyrin (**B**) and porphyrazine (**A**) chromophores exhibiting efficient energy transfer phenomena.

Here, dipyridyl-porphyrin subunits (**B**, Figure 8) and diamine-porphyrazine subunits (**A**) were incorporated into a tetra-porphyrinic assembly upon coordination of Pt^{2+}. A one-pot self assembly approach using stoichiometric equivalents of each component yields only small amounts of the desired structure, since the dative functionality instilled on the exterior of the subunits is not exclusively predisposed to closed structures. Such alternative outcomes are made particularly troublesome considering a distinct difference in binding kinetics between the pyridyls of **B** and the diamine unit of **A**, particularly when dimethylamine is employed. A stepwise synthesis is thus taken, whereby preparation of the precursor $(\mathbf{B})_2Pt_2Cl_4$, followed by dechlorination with $AgClO_4$ in the

presence of **A** leads to the desired target in 60 % yield. Large changes in the electronic absorption profile of this compound relative to those of the subunits **A** and **B** indicate significant electronic mixing between subunits, facilitated by coordination to the Pt^{2+} centers. This is reflected also in the emission spectra, whereby selective excitation of the Zn(II) complexes of **B** results in strong emission from **A**, and *vice versa*, indicating efficient energy transfer.

1.3 Octahedral Metals

1.3.1 Discrete Structures

The creation of porous photoactive structures is inherently facilitated by transition metals predisposed to mutually perpendicular dative bonds. To this end, octahedral metal centers have received much attention, with preference being given to second and third row transition metals owing to their more inert character.

Of these, Re(I) has been particularly emphasized as an assembling unit, as we have seen already in Figure 7. Its popularity stems from attractive photophysical properties of the *fac*-$[ClRe(CO)_3LL]$ complex (where LL is a diimine ligand) since they display intense luminescence in the visible region and are stable to photodecomposition.[5c, 42] Complexes composed of such units have, therefore, been of interest for solar energy conversion.[43] In addition, unlike its more prevalent counterparts based on Pt^{2+} and Pd^{2+}, these assemblies can be prepared with charge neutrality which means that the cavities are not occupied by counterions and are available for inclusion of guest molecules. Such events can have large effects on the luminescence of the parent complex, and so solution-phase molecular sensing has become intensely studied of late.[42] An added feature for such assemblies has been the formation of channels due to stacking of these molecular cavities in the solid state, making such applications as solid state chemical sensing and molecular sieving possible as well.[5b, 44]

A wide range of porous geometries, like those shown in Figure 4, have been prepared from the octahedral coordination motif $XRe(CO)_5$ (X = Cl or Br), where carbonyls are thermally liberated in non or weakly coordinating solvent for coordination

to a suitable bis-monodentate ligand. The resultant geometry is often dictated by the flexibility and steric bulk of the bridging ligand. Most often these ligands have been linear and applied to square formation via a "one-pot" self-assembly. Recently, focus in the literature has shifted from the self-assembly of squares to rectangles, in part because the lower symmetry of a rectangle should lead to greater selectivity and binding, especially for planar aromatic guests.[45] However, a "one-pot" self-assembly approach using bridging ligands of different lengths is precluded by the thermodynamically favoured production of square assemblies (Figure 4).

A promising aspect of coordination based assemblies is the range of properties that can be introduced and/or perturbed simply by changing the transition metal used for a given coordination motif or upon their incorporation into a given assembly. The later has been well illustrated by Hupp and co-workers, where both square and rectangular charge-neutral assemblies have been prepared using moderately fluorescent ($^1\pi \rightarrow {}^1\pi^*$) Zn(salen) complexes (Figure 9) and the anionic benzimidazolate bridging ligand.[46] Considering that Zn(II) possesses a closed shell d^{10} configuration, its incorporation into the salen framework serves more of a structural role as it rigidifies this bridging ligand, making it more suitable for charge delocalization. This effect is evidenced through decreased emission energy and an increase in its intensity relative to the free ligand. However, upon coordination of Re(I), a reduction in emission intensity is observed. This is likely due to facilitation of intersystem crossing from the excited singlet to the non-emissive triplet state ($^3\pi^*$) of the salen ligand. Also, no ^{3}MLCT emission is observed from these assemblies even though it lies 3000 cm^{-1} below the salen emissive state, suggesting that the promoted $^3\pi^*$ state lies even lower in energy.

The coordinative flexibility of Zn(II) afforded by its d^{10} configuration also allows for axial coordination and hence the potential to incorporate guest molecules in a dative fashion. Here, the bridging ligands are the two variations of the Zn(II)salen complex used to construct the square assemblies. The red shift in both absorption and emission for the phenyl (yellow) derivative relative to the aliphatic (blue), along with good spectral overlap, prompted the formation of the bridged-square assemblies depicted in Figure 9. These assemblies demonstrate that the aliphatic derivative behaves as a donor for energy transfer and the phenyl derivative as an acceptor, whereby the outer assembly of

Zn(II)salen-aliphatic complexes can behave collectively as antennae for efficient energy transfer to the encapsulated Zn(II)salen-phenyl complex for subsequent fluorescence emission.

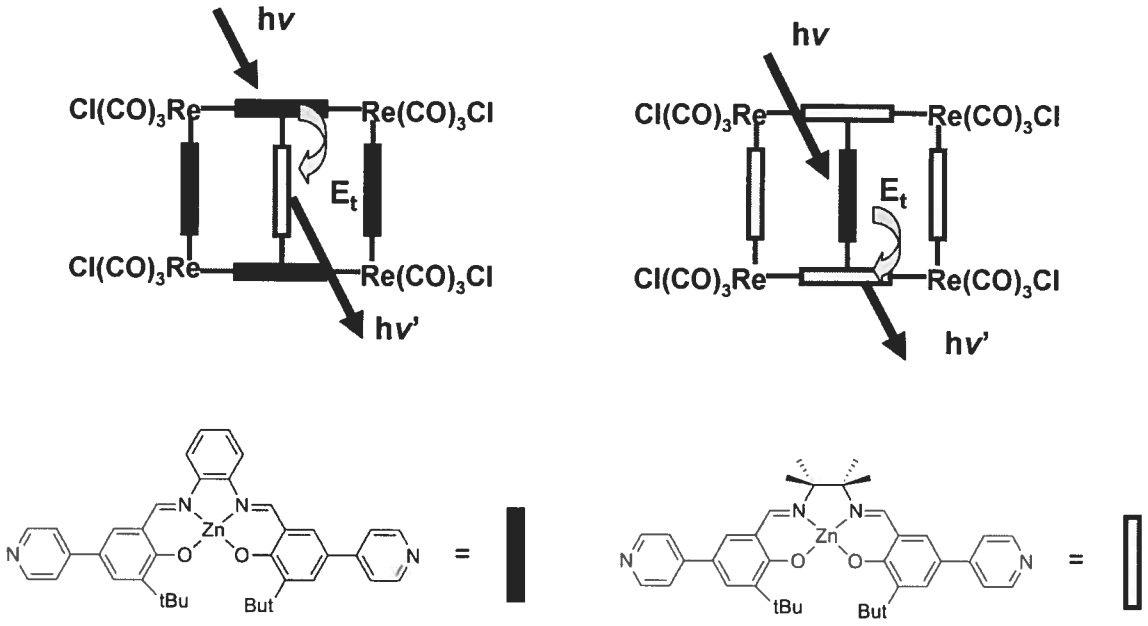

Figure 1.9. Mediation of energy transfer in Re(I)-based photoactive assemblies upon installation of Zn(II) (salen) complexes.

In addition to Re(I) carbonyls, Ru(II), and Os(II) polypyridyls have been heavily investigated owing to their relatively strong luminescence and the ease with which their photophysical properties may be altered through either synthetic manipulation of their ligands or changes in environmental conditions (i.e. temperature, pH, and solvent).[19, 47] Their incorporation into larger assemblies can be attained through covalent bond formation, design of polytopic ligands, or using the "complex as the ligand" approach whereby appropriately-functionalized polypyridyl complexes are used as pre-organized units in self-assembly. With regard to the latter approach, Lees and co-workers have prepared square assemblies in a step-wise synthesis using $(pytpy)_2M^{2+}$ (where pytpy = 4'(4-pyridyl)terpyridine, M = Fe(II), Ru(II), and Os(II)) along with corner units of either *fac*-$Re(CO)_4Br$ or *cis*-protected $[1,1'\text{-}(PPh_2)Fc]Pd^{2+}$ (Figure 10).[48] The squares **1-4** were synthesized in high yield by simply heating a 1:1 mix of corner unit / $(pytpy)_2M^{2+}$ in an appropriate solvent, where the highly charged product precipitates from solution. The

electronic effect of square formation is reflected in both their solution electrochemistry and their solution absorption and emission spectra. The absorption spectra for **1-3** indicates a red shift for the $(pytpy)_2M^{2+}$ based MLCT, the origin of which could be either an electronic effect of the Re(I) unit or an extended π-delocalization effect upon formation of the square. Cyclic voltammetry of **1-3** along with their component subunits shows a shift to higher potential for both the M^{2+}/M^{3+} oxidation and the first ligand-centered reduction processes, the latter of which is more pronounced and thus indicates a net lowering of the MLCT energy, in accordance with electronic absorption spectra. This suggests an electron-withdrawing effect upon coordination to the Re(I) unit. In terms of luminescence, **10**, **11**, and **13** have no detectable emission at room temperature, as with their mononuclear $(pytpy)_2Fe^{2+}$and $(pytpy)_2Ru^{2+}$ starting materials. Despite a net stabilization of the ^{3}MLCT state for $(pytpy)_2M^{2+}$, deactivation via non-radiative relaxation from upper-lying ^{3}MC states is significant and, in the case of **13**, there is an additional affect of upper-lying ^{3}MC states centered on the ferrocene units. It is for this reason and the potential reductive quenching of the ^{3}MLCT state by electron releasing *cis*-protecting ligands that have precluded the formation of luminescent assemblies based on such preorganized units. On the other hand, the Os(II) based structure **12** is luminescent. This is due to the stronger ligand field effected by Os(II) compared to both Fe(II) and Ru(II) which results in a higher energy ^{3}MC state that is not as readily thermally accessible. Newkome and co-workers have prepared related,[49] open structures composed of tri-, penta-, and hexa-nuclear bis(terpyridyl)M^{2+} units using appropriately angular ditopic bis(terpyridyl) ligands assembled from Fe(II), Ru(II), and Zn(II) coordination. Again, thermal population of deactivating ^{3}MC states led to efficient quenching in all cases, even when typically fluorescent ligands were employed, the exception being those structures incorporating Zn(II) owing to its closed-shell configuration. In the end, these complexes illustrate some of the factors that govern luminescence in larger assemblies and show that beginning with luminescent components does not guarantee luminescent products. In addition, even if they did show emission, the large number of counter-anions located within their cavities would likely preclude their application as luminescent sensors.

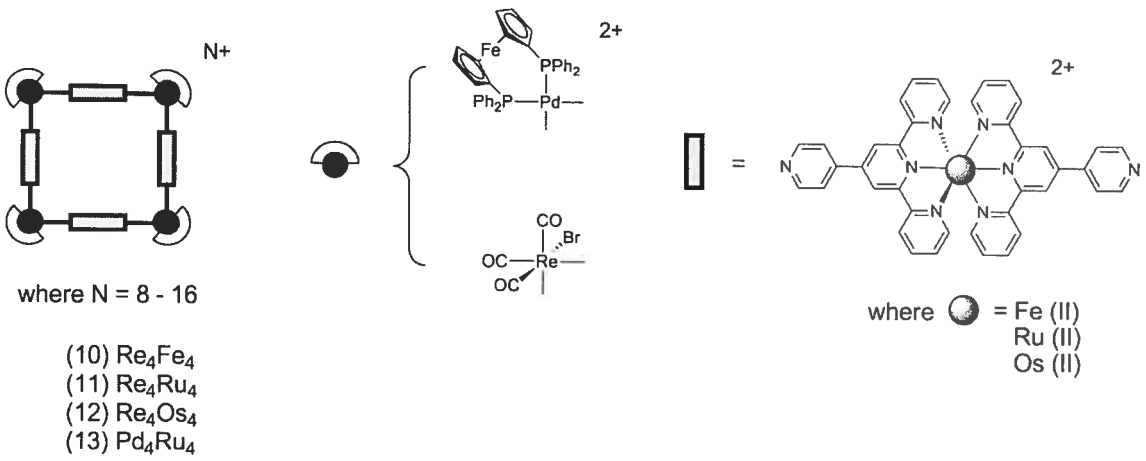

Figure 1.10. The "complex-as-ligand" approach: Re(I)-based assemblies using various homoleptic 4-pyridyl-tpy complexes.

1.3.2 Closed-Structures: Photoactive Grid Arrays

The formation of metal-ion arrays with regular grid-like patterns using appropriate multi-dentate ligands holds potential in information storage and processing where it can be demonstrated that external triggers reversibly produce distinct physicochemical states.[50] Their synthesis relies primarily on a self-assembly approach whereby the ligand binding motif is repeated regularly to give *N* binding sites. Metals are selected and added in the correct stoichiometry such that placement of a second ligand with *M* binding sites mutually perpendicular to the first satisfies the preferred coordination motif(s) of all metal(s) added. However, if one is using different metals with the same predisposition of coordination, differences in the relative kinetic stability of these metal-ions must be exploited to achieve spatial control of their placement. To this end, rigid aromatic N-heterocycles such as pyridines offer both kinetically labile intermediates and thermodynamically stable end products with most metals (M^{1+}, M^{2+}, and M^{3+}), and so many of the examples found are based upon chelating aromatics related to bipyridine and terpyridine. Since transition metal polypyridyls are characterized by a photo-generated MLCT state, such networks should be well suited for photonic device applications. Lehn and co-workers have elegantly demonstrated the synthetic strategies and potential applications of such grids in recent years,[50, 51] of which the following nicely illustrates some important synthetic and photophysical considerations.

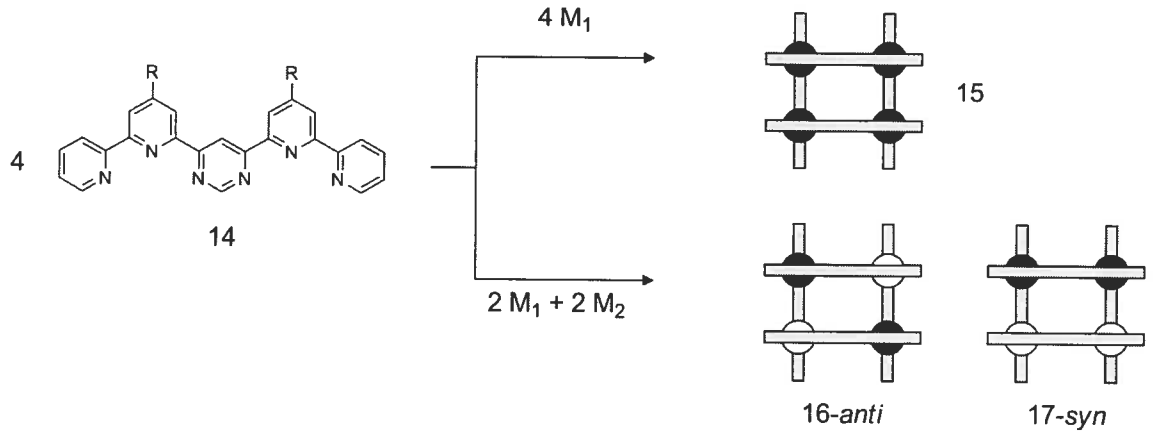

Figure 1.11. Potential outcomes to strict self-assembly approach to homo- and hetero-tetrametallic grids.

Here,[52] a ditopic hexadentate ligand (**14**, Figure 11) based on bis-terpyridine satisfies octahedral coordination mutually perpendicular to itself. Generation of homometallic grids (**15**) would simply entail a one-step reaction using an octahedral predisposed metal. However, if incorporation of two different octahedral metals is attempted in such a manner, both *anti* (**16**) and *syn* (**17**) topoisomers will result. This necessitates a sequential strategy based on the kinetically inert Ru(II) and Os(II), and the relatively kinetically labile Fe(II) where coordination of the inert metals first forms a corner precursor (**19**, Figure 12). Subsequent coordination of the second, more labile metal ion under mild conditions avoids ligand scrambling to yield the desired structure. The formation of **19** is straightforward in the case of Os(II) where **14** refluxed directly with 0.5 equivalents of NH_4OsCl_6 to give the corner precursor in 40% yield. However, such an approach with the more kinetically labile Ru(II) results in scrambling and the undesired $[Ru_4]^{8+}$ grid. It was therefore necessary to invoke a protection sequence using trimethyloxonium tetrafluoroborate, which prefers to methylate the outer pyridines due to lower steric encumbrance and a higher basicity of these nitrogens relative to those of the electron deficient pyrimidine. The resulting mono-protected ligand **18** can then be coordinated to give the desired corner unit **19**, which is then de-protected with 1,4-

diazabicyclo[2.2.2] octane (DABCO) and complexed under mild conditions with hexaaqua iron(II) to yield the *anti* isomer **20**.

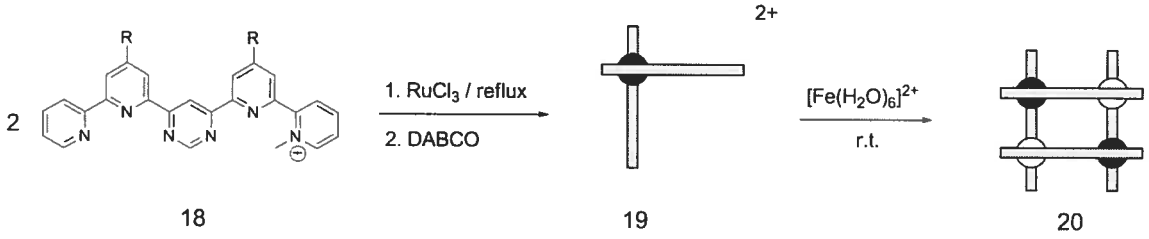

Figure 1.12. Controlled, step-wise assembly of heterometallic photoactive grids.

Since the energy of the MLCT state is sensitive to the nature of the metal, polymetallic grids offer broad absorption in the visible spectrum, a prerequisite for suitable light-harvesting arrays. Equally appealing is the variation of the emissive ^{3}MLCT state simply through selection of the metals employed. Thus, energy gradients can be created to effect vectorial energy transfer, another desired property of such arrays. In this example, however, the mixed-metal grids [Os_2Fe_2] and [Ru_2Fe_2] do not emit due to the presence of the Fe(II) unit which has a relatively weak ligand field strength and a ^{3}MC state located below its ^{3}MLCT state. This creates an efficient energy sink upon excitation of Os(II) and Ru(II), resulting in rapid energy transfer to the Fe(II) ^{3}MC state from which deactivation readily occurs. Such energy transfer has been found from pump-probe femtosecond spectroscopy to be less than 200 fs for dinuclear Os-L-Ru and Ru-L-Ru complexes, where L is electronically very similar to **1**.[53] This is a rate on par with ^{1}MLCT-^{3}MLCT conversion,[54] and such rapid transfer is likely present in the grid presented here. When considering large antennae networks for light harvesting devices, such rapid energy transfer is required to effectively compete with excited-state deactivation pathways which, over long distances involving many energy transfer steps, would otherwise render the device inefficient for practical purposes. Unfortunately, to date, such luminescent grids are very rare.[55] However, great advances have been made in recent years toward prolonging the emissive-state lifetime of mononuclear polypyridyl complexes. [19] Thus, it stands to reason that a combination of such advancements with intelligent methodology, such as that described here, holds tremendous potential for the creation of high nuclearity photoactive grids well suited for device applications.

1.3.3 Closed Structures: Branched Arrays

As discussed previously, it is necessary to absorb a large quantity of light energy for efficient device operation. As such, it is inherently more advantageous to develop spherically dense photoactive assemblies, and to this end dendritic arrays have been prepared utilizing photoactive sub-units. However, to make the device functional, it is required that the assembly possesses an available "docking" site where the substrate can receive the electrical equivalents to the initial photoexcitation. This requires the design of lower symmetry assemblies, relative to their potential dendritic counterparts. Where catalysis is concerned, photo-reduction of the substrate requires an electron acceptor site capable of collecting and relaying electrical equivalents while at the same time maintaining structural integrity. The incorporation of photoactive units displaying photo-initiated charge transfer is obviously required, and as such ruthenium(II) osmium(II) polypyridyl complexes have, amongst others, received particular attention.[9, 11a, 53] Suitable electron acceptor sites may also be served by various transition metal units based upon, for instance, iridium(III), rhodium(III), and platinum(IV). The advantage of their incorporation over purely organic acceptor sites is their capacity to transmit charge directly through dative bonding interactions, the consequence thereof should be enhanced efficiency over other scenarios involving hopping or tunneling processes. To do this requires that such a metal-containing motif be, or become, datively unsaturated for substrate binding subsequent to photo-excitation. In addition, to promote and facilitate ^{3}MLCT excitation and subsequent charge transfer, it is required that the ligand systems employed be rigid, aromatic, and amenable to minimizing donor-acceptor internuclear distance, considering the distant dependence of electron and energy transfer. Several of these systems have been reported,[56] recent examples of which have been given by Brewer and co-workers,[57] as outlined in Figure 13. Here, the ditopic ligand 2,3-di-2-pyridylpyrazine is used to coordinate simultaneously to ruthenium(II) centers in the reference complex **A** and to the rhodium(III) center in **B**. Cyclic voltammetry of **B** shows no significant electronic interaction between Ru(II) centers as evidenced by superimposed and reversible Ru(II/III) couples at 1.63 V (vs Ag/AgCl), while the Rh(III) center undergoes typical irreversible reduction to Rh(I) at -0.37 V, along with two

reversible $dpp^{0/-}$ reductions at -0.76 and -1.00 V. The irreversibility of the Rh(III) reduction illustrates the Rh($d\sigma^*$) nature of the LUMO of the acceptor unit. The lowest energy absorption band is at 520 nm, due to a Ru → dpp CT transition. Emission from this ^{3}MLCT state (760 nm) is slightly red-shifted with respect to that of **A** (744 nm), reflecting the stabilizing influence of the Rh(III) center on the dpp π^* orbital. Moreover, **B** exhibits 95 % quenching of the ^{3}MLCT emission and concurrent excited-state lifetime reduction relative to that of **A**, indicating efficient charge transfer to Rh(III), thereby populating the lower lying ^{3}MMCT state. Since the ^{3}MLCT states for **A** and **B** are similar in energy, it is reasonable to estimate that k_r and k_{nr} are equivalent for **B**, giving a rate constant for electron transfer of $k_{et} = 1.2 \times 10^8\ s^{-1}$. Upon forming a Rh(I) center, a square planar coordination motif is preferred and so two chloride ions are lost, making room for potential substrate binding. The capacity for such an assembly to serve as an efficient photo-catalyst for substrate reduction was tested in the context of water reduction to form hydrogen. This is a thermodynamically uphill process and requires multiple electron exchange. To ensure reasonable device efficiency, then, it is advantageous to construct an assembly bearing more photoactive units, such as for the related assembly **C** in Figure 13. This complex was prepared using a step-wise approach whereby the terminal ruthenium(II) units are assembled first containing available coordination sites via the bridging ligand dpp, and these complexes are then in turn used as "ligands" in subsequent complexation steps to render controlled design of the assembly. For the catalyst to function, it is necessary to complete the redox cycle, and so a sacrificial electron donor, N,N-dimethylaniline (DMA) is added, which serves to regenerate the catalyst by reducing Ru^*(III) back to Ru(II). In the presence of DMA in a H_2O / CH_3CN mix, irradiation of complex **C** was found to produce significant amounts of hydrogen gas, detected by gas chromatography, upon irradiation at the MLCT excitation wavelength or any wavelength overlapping with the absorption spectrum of **C**.

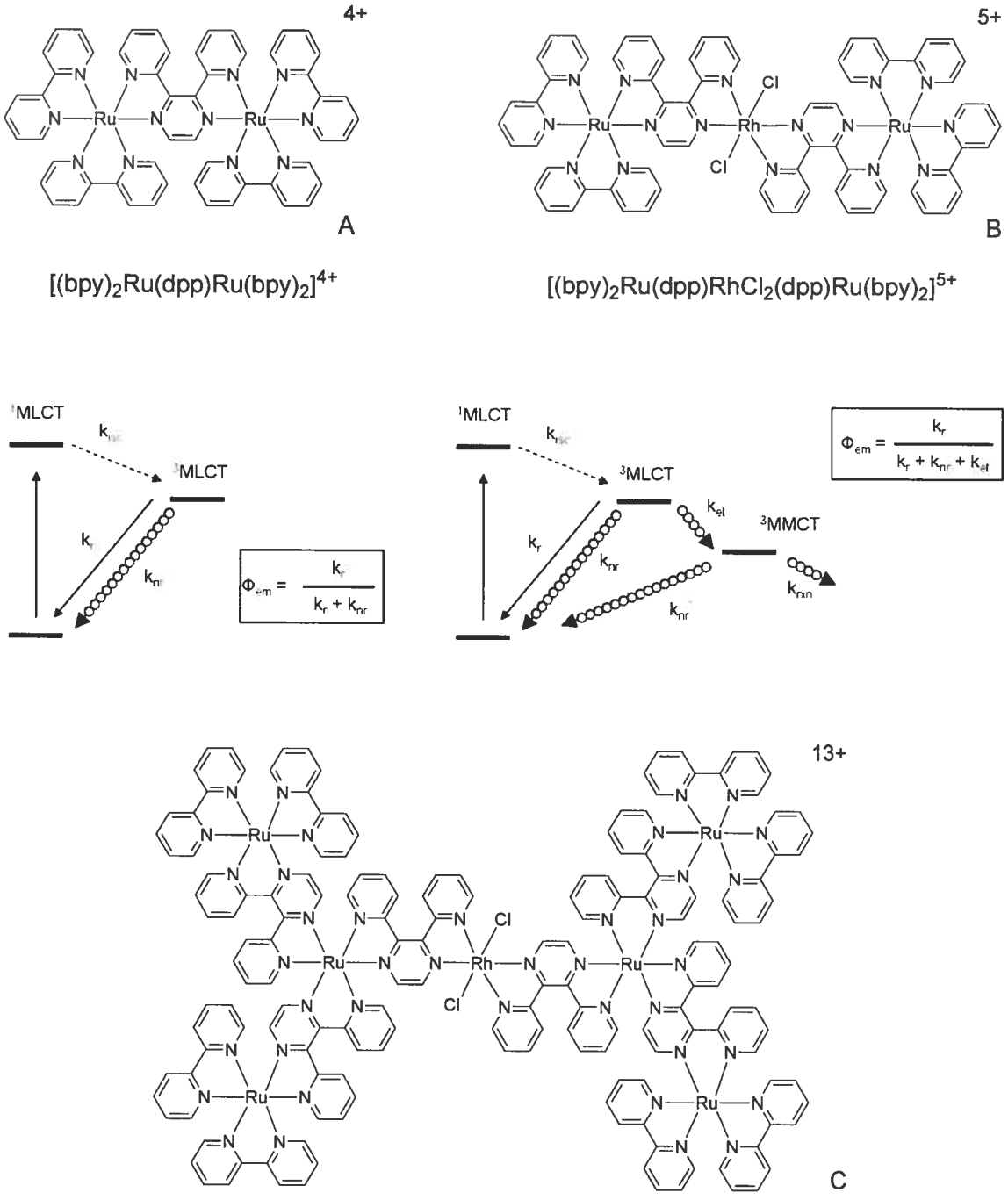

Figure 1.13. Branched photo-active assemblies assembled about a Rh(III) center, illustrating the governing processes subsequent to photo-excitation.

The potential utility of such photo-initiated donor-acceptor assemblies toward catalysis depends in large part on the number of electrons involved in the process. For instance, both hydrogen production and dioxygen reduction require concerted multi-

electron transfer. The incorporation of high-valent transition metals such as Rh(III) and Ir(III) are conducive to significant electronic mixing with the ligand acceptor component to the photo-produced ^{3}MLCT state and possess stable low-valent forms, which permits the occurrence of multi-electron transfer. It is attractive, then, to establish acceptor components capable of undergoing even greater reduction, which could in turn permit access to catalytic processes requiring proportionately greater multi-electron transfer. To this end, MacDonnell and co-workers have established the capacity for bridging ligands based upon tetraazatetrapyridopentacene to undergo multi-electron photoreduction.[58] This ligand, depicted in Figure 14 below, serves to bridge metal centers, in this case two photo-active $(phen)_2Ru^{2+}$ fragments, and is capable of accepting up to four electrons from two one-electron processes and a single double electron reduction process. Moreover, in its doubly reduced state, this ligand binds two protons in aqueous media,[58a] and cleaves DNA in low-oxygen environments.[58c] Such behaviour holds promise with regard to hydrogen production and therapeutics, respectively.

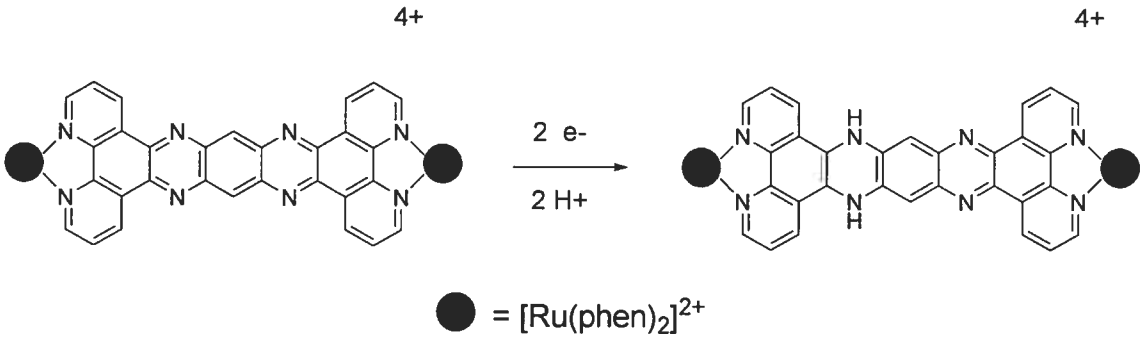

Figure 1.14. Dinuclear $(phen)_2Ru^{2+}$ complex assembled about a tetraazatetrapyridopentacene bridge, capable of undergoing multiple electron photo-reduction and subsequent protonation.

1.3.4 Pseudo-Octahedral

Numerous transition metals exhibit dimeric structures based on a characteristic "paddlewheel" arrangement of four mutually perpendicular bidentate chelates. Depending on the metal and the nature of the chelate, a wide range of physical properties

can be exhibited, including long-lived photo-excited states.[59] Considering their use as building blocks in a number of supramolecular architectures,[60] investigations into their potential structural and functional roles toward photoactive assemblies seems to be a natural progression.

Both axial and equatorial coordination sites of metal dimers may be used to assemble larger structures using appropriate bridging ligands. With regard to photoactive assemblies, porphyrins are attractive since a wide range of functionality can be introduced in the course of their synthesis. Dirhodium(II,II) units are attractive as assembling units owing to their rigidity, diamagnetic nature, and an inherent kinetic advantage over other metal dimers regarding ligand displacement.[61] Toward creating directing units for square geometries, the complex *cis*-$Rh_2(form)_2(O_2CCF_3)_2$ (where form = N,N'-di-p-tolylformamidinate) is ideal since it incorporates kinetically inert amidinates as protecting / blocking units and kinetically labile trifluoroacetates. Self-assembly of **A** (Figure 15) proceeds upon metathesis of *cis*-$Rh_2(form)_2(O_2CCF_3)_2$ with the disodium salt of 15,20-di-(4-carboxyphenyl)-5,10-diphenylporphyrin.[62] The larger assembly **B** was prepared upon displacement of weakly, axially bound solvent molecules with the stronger bis-monodentate ligand *cis*-5,10-diphenyl-15,20-dipyridylporphyrin.[63] These square assemblies are neutral, which is desired for potential guest uptake analogous to previous discussion pertaining to luminescence detection of host-guest interaction. However, the installation of amidinates leads to electrochemically rich dirhodium(II,II) units, exhibiting facilitated one-electron oxidations relative to their tetracarboxylate counterparts. As such, given the $Rh_2^{4+/5+}$ potential and the excited-state reduction potential for the porphyrin for both **A** and **B**, reductive electron-transfer quenching was found to be energetically favorable in both cases (ΔG = -0.4 eV and ΔG = -0.2 eV, respectively). The difference in driving force can be attributed to the relatively greater electron richness of the dirhodium(II,II) unit used in **A**. Porphyrin-based emission from **B** is quenched completely, but **A** is very slightly emissive with $\tau < 500$ ps and $\Phi = 7 \times 10^{-5}$ compared to τ = 10 ns and Φ = 0.017 for the parent porphyrin. This trend seems contradictory to the energetic difference for reductive electron transfer. However, given the irreversible nature of the Rh_2 based oxidations for **A**, it is likely that such electron transfer is not as efficient as for that in **B**.

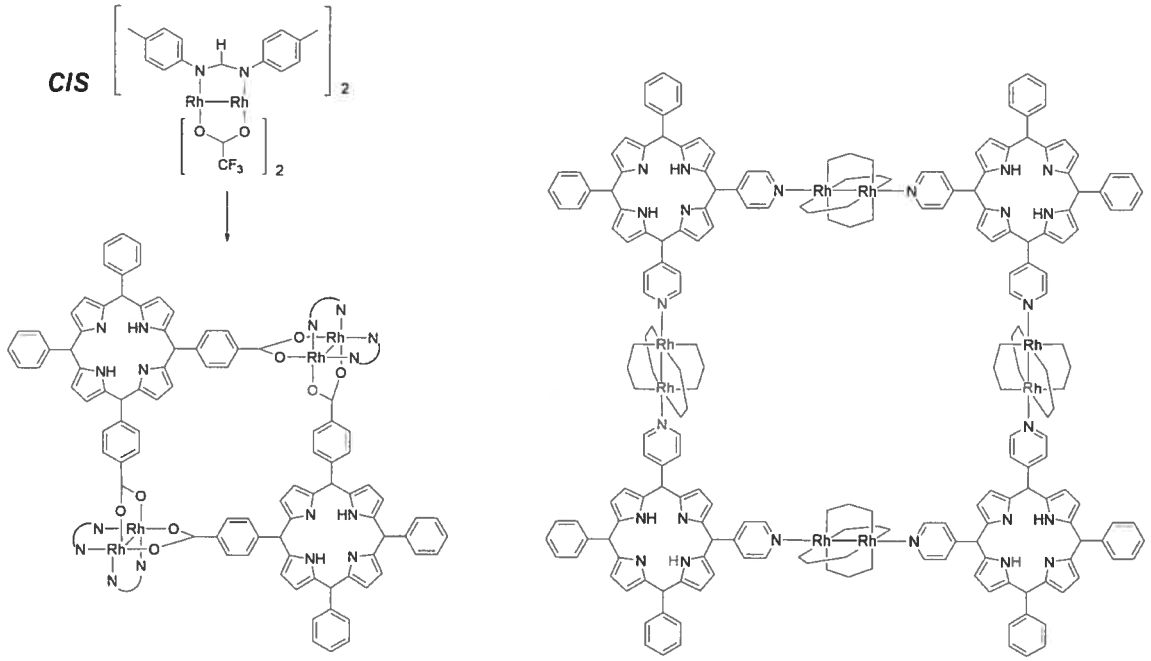

Figure 1.15. Dirhodium(II,II)-based porphyrinic assemblies utilizing equatorial (**A**) and axial (**B**) coordination modes of the dimeric unit.

Kamar and co-workers have utilized the di-anionic 2,2'-biimidazolate ligand (biim), which is capable of supporting both μ-bidentate and (bis)monodentate modes of coordination in a back-to-back manner (see Figure 16). Installation of the $(bpy)_2Ru^{2+}$ fragment to the μ-bidentate portion yields the datively unsaturated photoactive unit $[Ru(bpy)_2(H_2biim)](ClO_4)_2$ which, upon de-protonation to form the free-base $[Ru(bpy)_2(biim)]$, can then be assembled around a templating metal amenable a (bis)monodentate mode of coordination. The nuclearity and overall structure of the assembly depends on the dative predisposition of the metal selected. To this end, a dinuclear linear assembly based around a dimeric Ag_2^{2+} unit has been described,[64a] along with a more recent report of a tetranuclear assembly supported by a dimeric Cu_2^{4+} unit (Figure 16).[64b] The synthesis of this latter assembly is straight-forward and entails refluxing the free-base precursor Ru(II) complex with $Cu(ClO_4)_2$ in methanol. The resulting tetrameric structure is twisted about the Cu_2^{4+} center, with the $biim^{2-}$ and Cu_2^{4+} units deviating from co-planarity by ~ 40°. This twist is repeated in a staggered manner

about the Cu_2^{4+} center and induces chirality, both enantiomers of which are found in equal proportions in the crystal structure. This stands in contrast to the eclipsed conformation of the related $Cu_2(O_2C_2H_3)_4$. [61] Cu^{2+} is a d^9 metal with S = ½ in octahedral-pseudooctahedral coordination motifs, and so it is often incorporated for magnetic investigations. Fitting of variable temperature magnetic susceptibility data here established antiferromagnetic coupling between S = ½ Cu^{2+} centers through the $biim^{2-}$ ligand, although no intra-dimer coupling parameters are mentioned to address direct metal-metal bonding. The electronic absorption spectrum of this tetramer was conducted and showed a red-shift of the Ru(d)→L(π^*) MLCT and a four-fold increase in its intensity relative to [Ru(bpy)$_2$(biim)], due to the presence of four photoactive units. Unfortunately, no emission studies were conducted to investigate energy transfer phenomena, and so the potential of these units toward the development of photoactive arrays cannot be assessed. However, the prospects of altering electron and / or energy transfer processes for the creation of tailor-made arrays (or subunits thereof) simply through the choice of metallic assembling unit are very promising. This is particularly true considering that photoactive polypyridyl complexes, especially those based on $(tpy)Ru^{2+}$, are robust and can tolerate synthetic modification to a great degree.

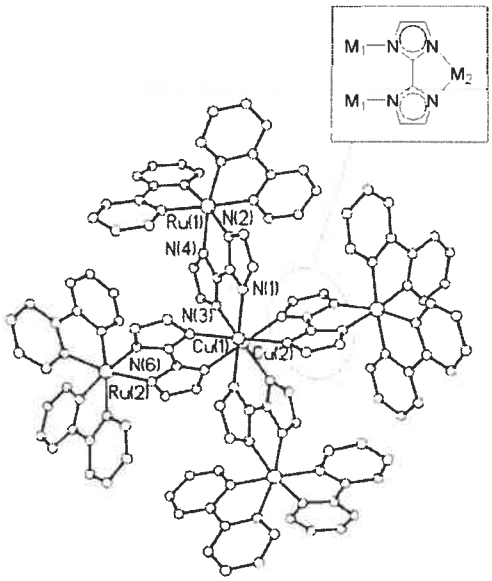

Figure 1.16. Convergent, directed-assembly of photo-active [Ru(bpy)$_2$(biim)] units about a Cu_2(II,II) core.

1.4 Research Objectives and Outline

In light of the motivations outlined in Section 1.1, and as an extension of the systems discussed in Sections 1.2-1.3, it is the intent of this thesis to investigate the structural and functional utility of dirhodium paddlewheel complexes toward the assembly of multi-nuclear photoactive assemblies. The photoactive sub-unit chosen to be incorporated is based upon the $(tpy)_2Ru^{2+}$ motif, due to its achiral nature and suitability to a wide range of synthetic modification. Initial forays to this end will focus on dirhodium(II,II) tetra-carboxylate motifs as assembling units, owing to inherent properties that make them both synthetically amenable and photophysically intriguing to constructing such assemblies. These multi-nuclear complexes will serve to elaborate energy transfer processes and guide the evolution toward more robust and varied assemblies.

Chapter 1. This introduction addresses the motivation toward constructing multi-nuclear photoactive assemblies, using naturally occurring systems as a point of reference and inspiration. The amelioration of their synthesis and attenuation of their properties through metal-based assembly will be discussed in the context of a recent literature cross-section of this area.

Chapter 2. This chapter introduces the convergent, self-assembly of multi-nuclear complexes based upon carboxy-derived $(tpy)_2Ru^{2+}$ sub-units grafted to a dirhodium(II,II) tetra-carboxylate core. Their assembly exemplifies unusual reaction control, the source of which is linked to observations regarding both solid-state and solution behaviour. Moreover, these systems indicate irreversible energy transfer to the non-emissive excited state of the dirhodium(II,II) motif, the nature of which is elaborated upon through incorporation of triazine analogues to $(tpy)_2Ru^{2+}$.

Chapter 3. The unusual reaction control demonstrated in chapter 2 is used to advantage toward assembling linear hetero-metallic assemblies. Here, the dirhodium(II,II) tetra-carboxylate motif is shown to be appended in a controlled manner to various

dicarboxylate-derived $(tpy)_2Ru^{2+}$, forgoing polymer formation normally encountered with charge-neutral components using such an approach. This has given symmetric 'dimer-bridge-dimer' complexes and asymmetric, mono-substituted products with an available carboxy group for incorporation of additional dimetal units. Complexes based on the former, symmetric model can serve to evaluate the capacity of the $(tpy)_2Ru^{2+}$ complex to electronically couple such dimetal units, while the latter asymmetric models give unprecedented access to a wide array of hetero-metallic systems. In addition, to compensate for the high-insolubility of these dicarboxy-$(tpy)_2Ru^{2+}$ complexes, an expedient protocol for the preparation of a highly soluble dicarboxy-$(tpy)_2Ru^{2+}$ complex is described based upon the synthesis of the novel ligand, 4'-(4-carboxyphenyl)-4,4''-di-(*tert*-butyl) tpy. The solid-state structure of this soluble dicarboxy-$(tpy)_2Ru^{2+}$ complex displays serendipitous porosity.

Chapter 4. In an effort to address decomposition concerns encountered with the systems prepared in Chapter 2, both *N,N'*-dipropyl and *N,N'*-diphenyl amidinate $(tpy)_2Ru^{2+}$ analogues were prepared and characterized. The extent of this characterization includes determination of their respective pKa values. In anticipation of a convergent approach using these amidinate analogues in the same manner as that described in Chapter 2, the polytopic ligand *N,N'*-di-(4'-phenyl-tpy)-formamidine was also prepared, but was found to be quite susceptible to decomposition by hydrolysis. This reactivity is quite unexpected and serves as a valuable lesson toward the creation of such polynuclear assemblies incorporating amidinates. The incapability of both the *N,N'*-dipropyl and *N,N'*-diphenyl amidinate $(tpy)_2Ru^{2+}$ to be grafted to the dirhodium(II,II) core via numerous, well-known procedures forces the development of another approach.

Chapter 5. This chapter describes a viable, divergent strategy based upon the Rh_2(*N,N'*-diphenylbenzamidinate)$_4$ motif, wherein synthetic modifications may be performed both on the exterior of the complex and through the preparation of suitably modified analogues to *N,N'*-diphenylbenzamidinate. A range of complementary functionality is introduced, and the resulting dimetal complexes are fully characterized. To demonstrate the synthetic utility of such complexes, a covalently-assembled tetra-nuclear $(tpy)_2Ru^{2+}$

complex is prepared and its preliminary characterization is described. To further demonstrate the versatility of such building-blocks, covalently assembled dinuclear-Rh_2(II,II) and pentanuclear-Rh_2(II,II) templates were assembled and characterized, both of which have the potential for the creation of photoactive systems of very-high nuclearity.

Chapter 6. This chapter will describe some of the possible future directions based upon the work described in Chapters 2-5.

1.5 References

1. a) Amijs, C. H. M.; van Klink, G. P. M.; van Koten, G. *Dalton. Trans.* **2006**, 308. b) Funyu, S.; Isobe, T.; Takagi, S.; Tryk, D. A.; Inoue, H. *J. Am. Chem. Soc.* **2003**, 125, 5734. c) Otruba, J. P.; Neyhart, G. A.; Dressick, W. J.; Marshall, J.L.; Sullivan, B. P.; Watkins, P. A.; Meyer, T. J. *J. Photochem.* **1986**, 35, 133.
2. Grätzel, M. *Inorg. Chem.* **2005**, 44, 6841 and references therein.
3. Dempsey, J. L.; Esswein, A. J.; Manke, D. R.; Rosenthal, J.; Soper, J. D.; Nocera, D. G. *Inorg. Chem.* **2005**, 44, 6879 and references therein.
4. a) Armaroli, N.; Accorsi, G.; Holler, M.; Moudam, O.; Nierengarten, J.-F.; Zhou, Z.; Wegh, R. T.; Welter, R. *Adv. Mat.* **2006**, 18, 1313, and references therein. b) Stagni, S.; Palazzi, A.; Zacchini, S.; Ballarin, B.; Bruno, C.; Marcaccio, M.; Paolucci, F.; Monari, M.; Carano, M.; Bard, A. J. *Inorg. Chem.* **2006**, 45, 695.
5. a) Wurthner, F.; You, C.-C.; Saha-Moller, C. R. *Chem. Soc. Rev.* **2004**, 33, 133. b) Mines, G. A.; Tzeng, B. C.; Stevenson, K. J.; Li, J.; Hupp, J. T. *Angew. Chem. Intl. Ed.* **2002**, 41, 154. c) Sun, S.-S.; Lees, A. J. *Coord. Chem. Rev.* **2002**, 230, 171 and references therein.
6. a) Milanesio, M. E.; Alvarez, M. G.; Rivarola, V.; Silber, J. J.; Durantini, E. N. *Photochem. and Photobiol.*, **2005**, 81, 891. b) Stochel, G.; Wanat, A.; Kulis, E.; Stasicka, Z. *Coord. Chem. Rev.* **1998**, 171, 203.
7. a) Huynh, M. H. V.; Dattelbaum, D. M.; Meyer, T. J. *Coord. Chem. Rev.* **2005**, 249, 457. b) Alstum-Acevedo, J. H.; Brennaman, M. K.; Meyer, T. J. *Inorg. Chem.* **2005**, 44, 6802.
8. see, for example a) Ruben, M.; Rojo, J.; Romero-Salguero, F. J.; Uppadine, L. H.; Lehn, J.-M. *Angew. Chem. Int. Ed.* **2004**, 43, 3644 and references therein. b) Fang Y.-Q.; Polson, M. I. J.; Hanan, G. S. *Inorg. Chem.* **2003**, 42, 5. c) Denti, G.; Campagna, S.; Sabatino, L.; Serroni, S.; Ciano, M.; Balzani, V. *Inorg. Chem.* **1990**, 29, 4750. d) Denti, G.; Campagna, S.; Sabatino, L.; Serroni, S.; Ciano, M.; Balzani, V. *J. Am. Chem. Soc.* **1992**, 114, 2944.
9. Constable, E. C. *Chem. Commun.* **1997**, 1073 and references therein.

10. a) Jiang, D. L.; Aida, T. *J. Am. Chem. Soc.* **1998**, 120, 10895. b) Wakabayashi, Y.; Tokeshi, M.; Hibara, A.; Jiang, D. L.; Aida, T.; Kitamori, T. *J. Phys. Chem. B* **2001**, 105, 4441.

11. a) Jiang, H.; Lee, S. J.; Lin, W. *Org. Lett.* **2002**, 4, 2149. b) Constable, E. C.; Eich, O.; Fenske, D.; Housecroft, C. E.; Johnston, L. A. *Chem. Eur. J.* **2000**, 6, 4364.

12. see, for example a) Wang, Q. M.; Lee, Y. A.; Crespo, O.; Deaton, J.; Tang, C.; Gysling, H. J.; Gimeno, M. C.; Larraz, C., M.; Villacampa, D.; Laguna, A.; Eisenberg R. *J. Am. Chem. Soc.* **2004**, 126, 9488. b) Yam, V. W.-W.; Lo, W.-Y.; Zhu, N. *Chem. Commun.* **2003**, 2446. c) Catalano, V. J.; Kar, H. M.; Garnas, J. *Angew. Chem. Intl. Ed.* **1999**, 38, 1979.

13. see, for example a) Dong, Y.-B.; Geng, Y.; Ma, J.-P.; Huang, R.-Q. *Organomet.* **2006**, 25, 447. b) Catalano, V. J.; Moore, A. L. *Inorg. Chem.* **2005**, 44, 6558. c) Sun, D.; Cao, R.; Weng, J.; Hong, M.; Liang, Y. *J. Chem. Soc. Dalton Trans.* **2002**, 291.

14. see, for example Lin, R.; Yip, J. H. K. *Inorg. Chem.* **2006**, 45, 4423 and references therein.

15. see, for example a) Yin, G.-Q.; Wei, Q.-H.; Zhang, L.-Y.; Chen, Z.-N. *Organomet.* **2006**, 25, 580. b) Feazell, R. P.; Carson, C. E.; Klausmeyer, K. K. *Eur. J. Inorg. Chem.* **2005**, 3287. c) Fournier, E.; Decken, A.; Harvey, P. D. *Eur. J. Inorg. Chem.* **2004**, 4420.

16. a) Valencia, L.; Bastida, R.; Macias, A.; Vicente, M.; Perez-Lourido, P. *New J. Chem.* **2005**, 29, 424. b) Wang, C.-C.; Yang, C.-H.; Tseng, S.-M.; Lin, S.-Y.; Wu, T.-Y.; Fuh, M.-R.; Lee, G.-H.; Wong, K.-T.; Chen, R.-T.; Cheng, Y.-M.; Chou, P.-T. *Inorg. Chem.* **2004**, 43, 4781. c) Fei, B.-L.; Sun, W.-Y.; Okamura, T.-A.; Tang, W.-X.; Ueyama, N. *New J. Chem.* **2001**, 25, 210.

17. a) Wu, H.-C.; Thanasekaran, P.; Tsai, C.-H.; Wu, J.-Y.; Huang, S.-M.; Wen, Y.-S.; Lu, K.-L. *Inorg. Chem,* **2006**, 45, 295. b) Zhang, G.; Yang, G.; Ma, J. S. *Inorg. Chem. Commun,* **2004**, 7, 994.

18. Armaroli, N. *Chem. Soc. Rev.* **2001**, 30, 113 and references therein.

19. Medlycott, E. A.; Hanan, G. S. *Coord. Chem. Rev.* **2006**, 250, 1763.

20. a) Chen, L. X.; Shaw, G. B.; Novozhilova, I.; Liu, T.; Jennings, G.; Attenkofer, K.; Meyer, G. J.; Coppens, P. *J. Am. Chem. Soc.* **2003**, 125, 7022. b) Gunaratne, T.;

Rodgers, M. A. J.; Felder, D.; Nierengarten, J.-F.; Accorsi, G.; Armaroli, N. *Chem. Commun.* **2003**, 3010.

21. Kalsani, V.; Schmittel, M.; Listorti, A.; Accorsi, G.; Armaroli, N. *Inorg. Chem.* **2006**, 45, 2061.
22. a) Cuttell, D. G.; Kuang, S.-M.; Fanwick, P. E.; McMillan, D. R.; Walton, R. A. *J. Am. Chem. Soc.* **2002**, 124, 6. b) Kuang, S.-M.; Cuttell, D. G.; McMillan, D. R.; Fanwick, P. E.; Walton, R. A. *Inorg. Chem.* **2002**, 41, 3313.
23. Jia, W. L.; M^{c}Cormick, T.; Tao, Y.; Lu, J.-P.; Wang, S. *Inorg. Chem.* **2005**, 44, 5706.
24. Ruthkosky, M.; Kelly, C. A.; Castellano, F. N.; Meyer, G. J. *Coord. Chem. Rev.* **1998**, 171, 309.
25. McMillan, D. R.; McNett, K. M. *Chem Rev.* **1998**, 98, 1201.
26. Holler, M.; Cardinali, F.; Mamlouk, H.; Nierengarten, J.-F.; Gisselbrecht, J.-P.; Gross, M.; Rio, Y.; Barigelleti, F.; Armaroli, N. *Tetrahedron* **2006**, 62, 2060.
27. Kalsani, V.; Bodenstedt, H.; Fenske, D.; Schmittel, M. *Eur. J. Inorg. Chem.* **2005**, 1841.
28. Schmittel, M.; Kalsani, V.; Fenske, D.; Wiegrefe, A. *Chem. Commun.* **2004**, 490.
29. Schmittel, M.; Ammon, H.; Kalsani, V.; Wiegrefe, A.; Michel, C. *Chem. Commun.* **2002**, 2566.
30. Kalsani, V.; Ammon, H.; Jackel, F.; Rabe, J. P.; Schmittel, M. *Chem. Eur. J.* **2004**, 10, 5481.
31. a) Fujita, M.; Sasaki, O.; Mitsuhashi, T.; Fujita, T.; Yazaki, J.; Yamaguchi, K.; Ogura, K. *Chem. Commun.* **1996**, 1535. b) Lee, S. B.; Hwang, S.; Chung, D. S.; Yun, H.; Hong, J. I. *Tetrahedron Lett.* **1998**, 39, 873.
32. Fujita, M.; Yazaki, J.; Ogura, K. *Chem. Lett.* **1991**, 1031.
33. see, for example a) Adams, C. J.; Fey, N.; Weinstein, J. A. *Inorg. Chem.* **2006**, 45, 6105. b) Laskar, I. R.; Hsu, S.-F.; Chen, T.-M. *Polyhedron* **2005**, 24, 881. c) Wadas, T. J.; Chakraborty, S.; Lachicotte, R. J.; Wang, Q.-M.; Eisenberg, R. *Inorg. Chem.* **2005**, 44, 2628. d) Tao, C.-H.; Zhu, N.; Yam, V. W.-W. *Chem. Eur.* **2005**, 11, 1647.
34. La Deda, M.; Ghedini, M.; Aiello, I.; Pugliese, T.; Barigelletti, F.; Accorsi, G. *J. Organomet. Chem.* **2005**, 690, 857 and references therein.
35. Zhang, L.; Niu, Y.-H.; Jen, A.K.-Y.; Lin, W. *Chem. Commun.* **2005**, 1002.

36. Lee, S. J.; Luman, C. R.; Castellano, F. N.; Lin, W. *Chem. Commun.* **2003**, 2124.

37. Chan, S.-C.; Chan, M. C. W.; Wang, Y.; Che, C.-M.; Cheung, K.-K.; Zhu, N. *Chem. Eur. J.* **2001**, 7, 4180.

38. Dietzek, B.; Kiefer, W.; Blumhoff, J.; Bottcher, L.; Rau, S.; Walther, D.; Uhlemann, U.; Schmitt, M.; Popp, J. *Chem. Eur. J.* **2006**, 12, 5105.

39. de Wolf, P.; Waywell, P.; Hanson, M.; Heath, S.L.; Meijer, A. J. H. M.; Teat, S. J.; Thomas, J. A. *Chem. Eur. J.* **2006**, **12**, 2188.

40. see, for example, a) Milic, T. N.; Chi, N.; Yablon, D. G.; Flynn, G. W.; Batteas, J. D. Drain, C. M. *Angew. Chem. Intl. Ed.* **2002**, 41, 2117. b) Drain, C. M.; Goldberg, I.; Sylvain, I; Falber, A. *Top. Curr. Chem.* **2005**, 245, 55 and references therein.

41. Cheng, K. F.; Thai, N. A.; Grohmann, K.; Teague, L. C.; Drain, C. M. *Inorg. Chem.* **2006**, 45, 6928.

42. Slone, R. V.; Benkstein, K. D.; Belanger, S.; Hupp, J. T.; Guzei, I. A.; Rheingold, A. L. *Coord. Chem. Rev.* **1998**, 171, 221.

43. Wong, H. L.; Lam, L. S. M.; Cheng, K. W.; Man, K. Y. K.; Chan, W. K.; Kwong, C. Y.; Djurisic, A. B. *Appl. Phys. Lett.* **2004**, 84, 2557.

44. Belanger, S.; Hupp, J. T.; Stern, C. L.; Slone, R. V.; Watson, D. F.; Carrell, T. M. *J. Am. Chem. Soc.* **1999**, 121, 557.

45. Thanasekaran, P.; Liao, R. T.; Liu, Y. H.; Rajendran, T.; Rajagopal, S.; Lu, K. L. *Coord. Chem. Rev.* **2005**, 249, 1085.

46. Splan, K. E.; Massari, A. M.; Morris, G. A.; Sun, S.-S.; Reina, E.; Nguyen, S. T.; Hupp, J. T. *Eur. J. Inorg. Chem.* **2003**, 2348.

47. a) Balzani, V.; Juris, A.; Venturi, M.; Campagna, S.; Serroni, S. *Chem. Rev.* **1996**, 96, 759. b) Sauvage, J.-P.; Collin, J.-P.; Chambron, J.-C.; Guillerez, S.; Coudret, C. *Chem. Rev.* **1994**, 94, 993. c) Chen, P.; Meyer, T. J. *Chem Rev.* **1998**, 98, 1439.

48. Sun, S.-S.; Lees, A. *Inorg. Chem.* **2001**, 40, 3154.

49. a) Hwang, S.-H.; Moorefield, C. N.; Fronczek, F. R.; Lukoyanova, O.; Echegoyen. L.; Newkome, G. R. *Chem. Commun.* **2005**, 713. b) Hwang, S.-H.; Wang, P.; Moorefield, C. N.; Godinez, L. A.; Manriquez, J.; Bustos, E.; Newkome, G. R. *Chem. Commun.* **2005**, 4672. c) Hwang, S.-H.; Moorefield, C. N.; Wang, P.; Fronczek, F. R.; Courtrey, B. H.; Newkome, G. R. *Dalton Trans.* **2006**, 3518.

50. Ruben, M.; Rojo, J.; Romero-Salguero, F. J.; Uppadine, L. H.; Lehn, J.-M. *Angew. Chem. Intl. Ed.* **2004**, 43, 3644 and references therein.

51. Stadler, A. M.; Puntoriero, F.; Campagna, S.; Kyritsakas, N.; Welter, R.; Lehn, J.-M. *Chem. Eur. J.* **2005**, 11, 3997.

52. Bassani, D.; Lehn, J.-M.; Serroni, S.; Puntoriero, F; Campagna, S. *Chem. Eur. J.* **2003**, 9, 5936.

53. Baudin, H. B.; Davidson, J.; Serroni, S.; Juris, A.; Balzani, V.; Campagna, S.; Hammarstrom, L. *J. Phys. Chem. A* **2002**, 106, 4312.

54. Damrauer, N. H.; Cerullo, G.; Yeh, A.; Boussie, T. R.; Shank, C. V.; McCusker, J. K. *Science*, **1997**, 275, 54.

55. a) Zhang, J.; Xiong, R.-G.; Chen, X.-T.; Xue, Z.; Peng, S.-M.; You, X.-Z. *Organomet.* **2002**, 21, 235. b) Rojo, J.; Romero-Salguero, F. J.; Lehn, J.-M.; Baum, G.; Fenske, D. *Eur. J. Inorg. Chem.* **1999**, 1421.

56. a) Molnar, S. M.; Nallas, G. N. A.; Bridgewater, J. S.; Brewer, K. J. *J. Am. Chem. Soc.* **1994**, 116, 5206. b) Konduri, R.; Ye, H.; MacDonnell, F. M.; Serroni, S.; Campagna, S.; Rajeshwar, K. *Angew. Chem.* **2002**, 41, 3185. c) Watson, D. F.; Wilson, J. L.; Bocarsly, A. B. *Inorg. Chem.* **2002**, 41, 2408.

57. a) Elvington, M.; Brewer, K. J. *Inorg. Chem.* **2006**, 45, 5242. b) Elvington, M.; Brewer, K. J. *PCT Intl. Appl.* **2006**, IPN WO 2006/060039.

58. a) Konduri, R.; de Tacconi, N. R.; Rajeshwar, K.; MacDonnell, F. M. *J. Am. Chem. Soc.* **2004**, 126, 11621. b) Chiorboli, C.; Fracasso, S.; Ravaglia, M.; Scandola, F.; Campagna, S.; Wouters, K. L.; Konduri, R.; MacDonnell, F. M. *Inorg. Chem.* **2005**, 44, 8368. c) Janaratne, T. K.; Yadav, A.; Ongeri, F.; MacDonnell, F. M. *Inorg. Chem.* **2007**, 46, 3420.

59. a) Byrnes, M. J.; Chisholm, M. H.; Gallucci, J. A.; Liu, Y.; Ramnauth, R.; Turro, C. *J. Am. Chem. Soc.* **2005**, 127, 17343. b) Bradley, P. M.; Bursten, B. E.; Turro, C. *Inorg. Chem.* **2001**, 40, 1376.

60. a) Bickley, J.; Bonar-Law, R.; McGrath, T.; Singh, N.; Steiner, A. *New J. Chem.* **2004**, 28, 425. b) Schiavo, S. L.; Serroni, S.; Puntoriero, F.; Tresoldi, G.; Piraino, P. *Eur. J. Inorg. Chem* **2002**, 79. c) Cotton, F. A.; Murillo, C. A. *Acc. Chem. Res.* **2001**, 34, 759. d) Eddaoudi, M.; Kim, J.; Wachter, J. B.; Chae, H. K.; O'Keeffe, M.; Yaghi,

O. M. *J. Am. Chem. Soc.* **2001**, 123, 4368. e) Bonar-Law, R.; McGrath. T.; Singh, N.; Bickley, J. F.; Femoni, C.; Steiner, A. *J. Chem. Soc. Dalton Trans.* **2000**, 4343.

61. Cotton, F. A.; Walton, R. A. *Multiple Bonds Between Metal Atoms*, 3rd ed., Wiley, New York, **1994**.
62. Schiavo, S. L.; Pocsfalvi, G.; Serroni, S.; Cardiano, P.; Piraino, P. *Eur. J. Inorg. Chem.* **2000**, 1371.
63. Schiavo, S. L.; Serroni, S.; Puntoriero, F.; Tresoldi, G.; Piraino, P. *Eur. J. Inorg. Chem.* **2002**, 79.
64. a) Majumdar, P.; Kamar, K. K.; Castineiras, A.; Goswami, S. *Chem. Comm.* **2001**, 1292. b) Kamar, K. K.; Falvello, L. R.; Fanwick, P. E.; Kim, J.; Goswami, S. *Dalton Trans.* **2004**, 1827.

Chapter 2: Polynuclear Ru(II) Complexes Self-Assembled About a Rh-Rh Core

2.1 Introduction

Natural light harvesting systems (LHS) and the myriad of complex functions they perform serve as inspiration for the development of artificial LHS capable of performing tailored functions ranging from catalysis to the development of efficient fuel and solar cells.[1] Such functional systems present numerous challenges, the largest of which is arguably the efficient connection of multiple photoactive units by means conducive to energy and electron transfer. This need stems from two considerations. The first is that the targeted function, particularly in catalysis, can involve multiple electron transfer and so multiple photon absorption is required for every molecule produced. The second is that energy transfer is never completely efficient, succumbing often to heat dissipation, and so a high input of light energy is required.[2] Nature utilizes many weak interactions in a true supramolecular sense (H-bonding, dipole-dipole) to effect connectivity, recognition, and energetic / electronic relay. The reversibility of such supramolecular interactions is instrumental to the self-assembly process. Although elegant, constructing artificial LHS in this manner may not be suitable to the photoactive unit employed and / or to the conditions of operation for the device. Recent examples have focused on utilizing elaborate ligand design and / or performing many iterative chemical transformations with compromised efficiency and demanding purification.[3] Although limitations of this nature have been recognized,[4] synthesis remains tedious and structures of high nuclearity often possess a large degree of freedom which can preclude structural elucidation and frustrate energy transfer processes. The covalent bond gives more durable, inert systems but low yields and exceedingly labourious synthesis often precludes practical application. In between lies the strongest supramolecular interaction, dative bonding, whose inherent reversibility allows for pre-organization / self-assembly while offering bond strengths suitable to afford robust systems. This approach can lead to simplified synthesis with

readily accessible modification or installation of new physical properties simply with the selection of metallic connecting unit employed.

Dirhodium (II,II) tetra-carboxylates have found extensive application in catalysis, including cyclopropanation,[5] alkyne cyclopropenation,[6] C-H insertion,[7] and carbeonid initiated C-C bond formation.[8] The complex $Rh_2(OCCH_3)_4(L)_2$ has been shown to bind duplex DNA and inhibit DNA replication where L is a labile axially coordinated ligand (e.g. water), [9] while the use of nitrogen chelates such as 1,10-phenanthroline and 2,2'-bipyridine as the axially coordinated ligand yields adducts capable of acting as antibacterial agents and exhibit cytostatic activity against human oral carcinoma.[10, 11] Complementary to these applications was the report of a long-lived, non-emissive lowest excited state, determined by energy transfer experiments to lie between 1.34 and 1.77 eV with a lifetime of up to 5 μs depending on the solvent used.[12] Subsequently, photoexcitation of $Rh_2(O_2CCH_3)_4(L)_2$, in the presence of electron acceptors, has been shown to catalyze the conversion of isopropanol to acetone and to cleave DNA,[13] while the related solvato complex *cis*-$[Rh_2(O_2CCH_3)_2(CH_3CN)_6]^{2+}$ has been shown to serve as a photoactivated *cis*-platin analogue.[14]

Dimetal paddlewheel complexes, including dirhodium (II,II) tetra-carboxylates, have received much attention of late as building blocks for the creation of electrochemically rich supramolecular architectures.[15] More recently, we have identified this motif as a suitable template for growth of polynuclear systems based upon carboxylate-functionalized photoactive units (Figure 2.2) with potential excited-state interaction as suggested by near-complete emission quenching of the appended chromophore.[16] Herein, we elaborate on the nature of this interaction through the preparation and characterization of a complete family of related, electron-deficient triazine analogues (Figure 2.3) as well as elaborate on factors affecting the overall stability of such multi-metallic systems.

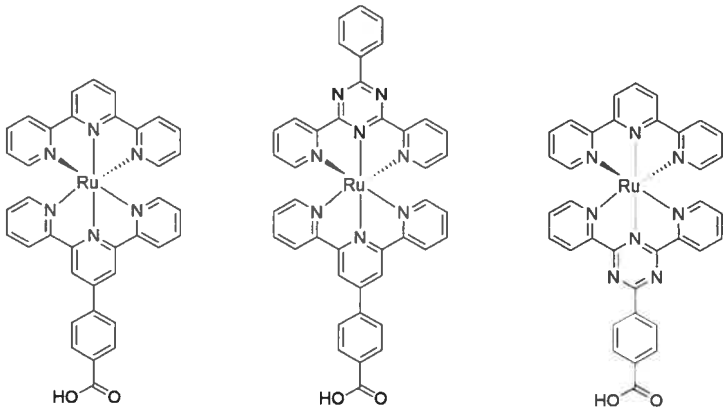

Figure 2.1 The series of carboxy-appended ruthenium (II) complexes.

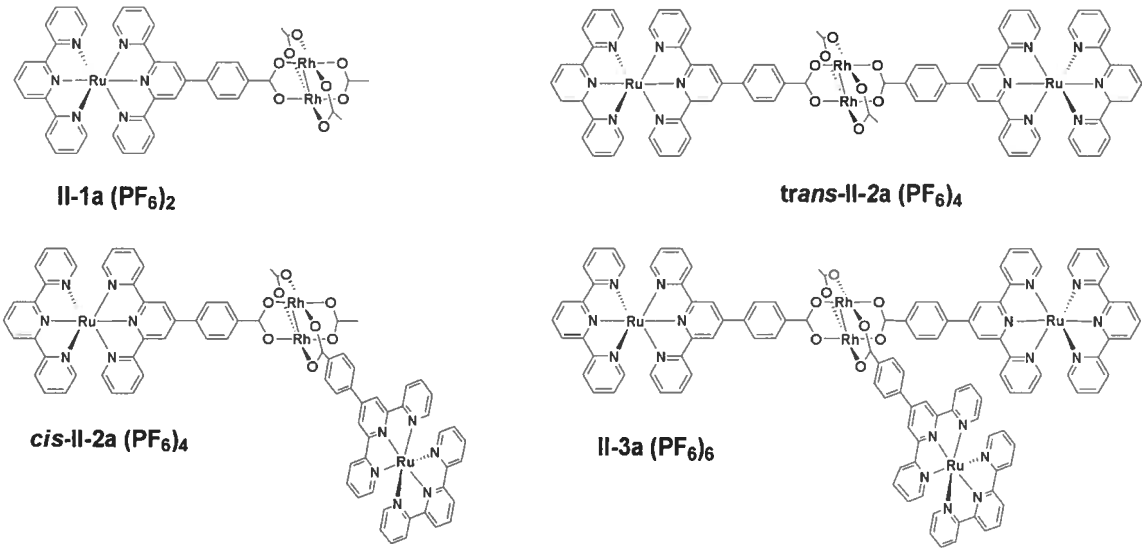

Figure 2.2 Family of oligonuclear complexes based on **II-5a $(PF_6)_2$**.

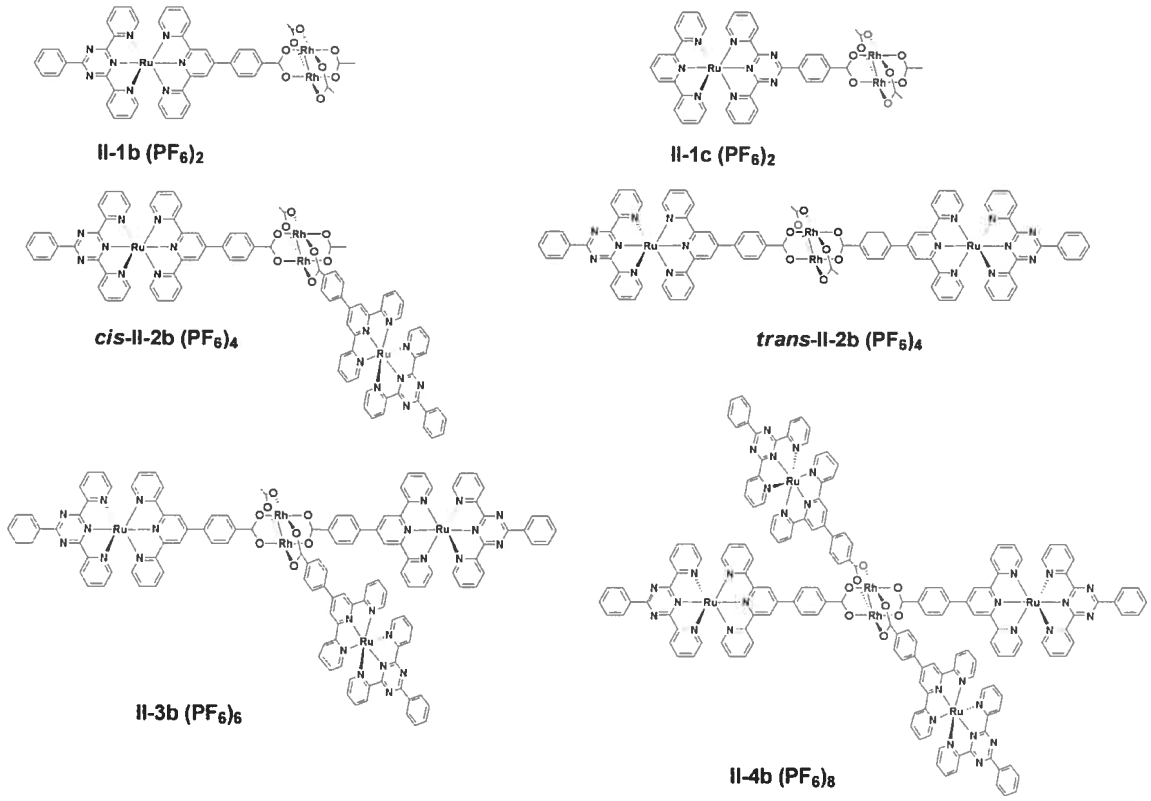

Figure 2.3 Family of oligonuclear complexes based on **II-5b $(PF_6)_2$ / II-5c $(PF_6)_2$**.

2.2 Synthesis

The mixed-metal polynuclear complexes are assembled following a classical ligand exchange process according to Scheme 2.1, in which acetic acid is removed by distillation from the reaction mixture. Considerable influence can be exerted on both the rate and extent to which substitution proceeds simply by varying temperature, concentration, stoichiometry, and rate of acetic acid distillation. Since these products are strongly coloured and stable to chromatographic separation, the reaction process may be monitored by TLC and the products of different nuclearity are easily separated by column chromatography. The precursor complex **II-5b $(PF_6)_2$** can be synthesized as was **II-5a**,[16] by heating to reflux 4'-(*p*-carboxyphenyl)-2,2':6',2"-terpyridine (**La**) and Ru(**Lb**)Cl_3 (Lb = 6-phenyl-2,4-di(2-pyridyl)-s-triazine) in EtOH / H_2O in the presence of the dechlorinating agent $AgNO_3$, which affords **II-5b $(PF_6)_2$** in 41 % yield after column

purification. In a typical preparation of the oligonuclear complexes of the **b** series, **II-1b-II-4b** $(PF_6)_2$ can be prepared in 69 % overall yield after column chromatography, based on recovered **II-5b** $(PF_6)_2$, which is very similar to that obtained for the series **II-1a-II-3a** $(PF_6)_2$.[16] Solvents other than acetonitrile were tried (e.g. DMF, benzonitrile); however, in all cases acetonitrile was found to be optimal with regard to controlling the reaction and minimizing the number of unidentified decomposition side-products. Unfortunately, ***trans*-II-2b** $(PF_6)_4$ and ***cis*-II-2b** $(PF_6)_4$ proved to be inseparable using the same technique as that used to separate ***trans*-II-2a** $(PF_6)_4$ and ***cis*-II-2a** $(PF_6)_4$. As such, the spectroscopic, luminescence, and redox properties of the **II-2b** $(PF_6)_4$ complexes were not studied.

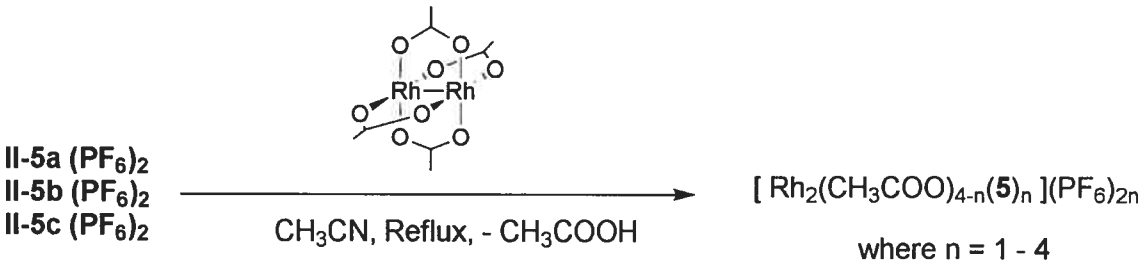

Scheme 2.1 Synthesis of oligonuclear complexes in acetonitrile.

To complete the family, it was desired to move the ligand component responsible for the emissive ^{3}MLCT state closer to the dirhodium(II,II) core, which was afforded by synthesizing the novel ligand 6-(4-carboxyphenyl)-2,4-di(2-pyridyl)triazine (**Lc**) (see Section 2.10). Preparation of the precursor complex **II-5c** $(PF_6)_2$ proceeded as with complexes **II-5a**,[16] involving simple reflux of **Lc** with $Ru(tpy)Cl_3$ in the presence of the dechlorinating agent $AgNO_3$ in a EtOH / H_2O mix, giving **II-5c** $(PF_6)_2$ in 36 % yield after column purification. The application of **II-1c**$(PF_6)_2$ in the same manner as depicted in Scheme 2.1 does lead to a product distribution analogous to that for the series **II-1a-II-3a** $(PF_6)_2$, **II-1b-II-4b** $(PF_6)_2$. Instead, insignificant quantities of higher substitution products were found, as determined by high-resolution mass spectrometry. The mono-substitution product **II-1c** $(PF_6)_2$ could be produced in 57 % yield, although this required longer reaction times (~ 7 days) than that needed to produce **II-1a** $(PF_6)_2$ and **II-1b**

$(PF_6)_2$ (~ 1 day) using the same proportion of $Rh_2(OAc)_4$. These observations were not unexpected, since placement of the triazine moiety nearer to the carboxylate group would be expected to reduce its dative bonding capacity to some degree. Nevertheless, **II-1c $(PF_6)_2$** was stable to chromatographic separation and could be isolated cleanly for further electrochemical and photophysical analysis.

2.3 Spectrophotometric and Spectrofluorometric Determination of Ground State pKa Values for Complexes II-5a $(PF_6)_2$ and II-5c $(PF_6)_2$

The pKa values of complexes **II-5a $(PF_6)_2$** and **II-5c $(PF_6)_2$** were determined by means common to analogous Ru(II) polypyridyl complexes bearing secondary and protic dative functionality.[17] The experimental details are outlined in Section 2.10. In short, this entailed monitoring the ^{1}MLCT and ligand-centered transitions, observed in their respective electronic absorption spectra, as well as the ^{3}MLCT emission intensity as a function of changing pH. These subsequent changes in intensity were plotted to give clear inflection points that correspond to the pKa of the carboxylate fragment for the respective complex.

In the case of complex **II-5a $(PF_6)_2$**, modest but clear diminution of the intensity of the bands centered at 485 nm and 271 nm with decreasing pH gave, in both cases, pKa values of 5.18 from first derivative plots of the titration data (Figures 2.4 and 2.5). Conversely, the emission intensity, centered at 650 nm, was augmented as a function of decreasing pH (Figure 2.6). However, no clear inflection point could be obtained from the subsequent emission data (Figure 2.7), and so we take the pKa determined from the absorption data for consideration.

In the case of complex **II-5c $(PF_6)_2$**, the absorption profiles are relatively insensitive to changing pH (Figure 2.8). However, like complex **II-5a $(PF_6)_2$**, the emission intensity centered at 730 nm changed substantially, although this was found to decrease with lower pH. As such, we take into consideration the pKa determined from a first-derivative plot of the emission data in Figure 2.10, which corresponds to pKa = 3.75.

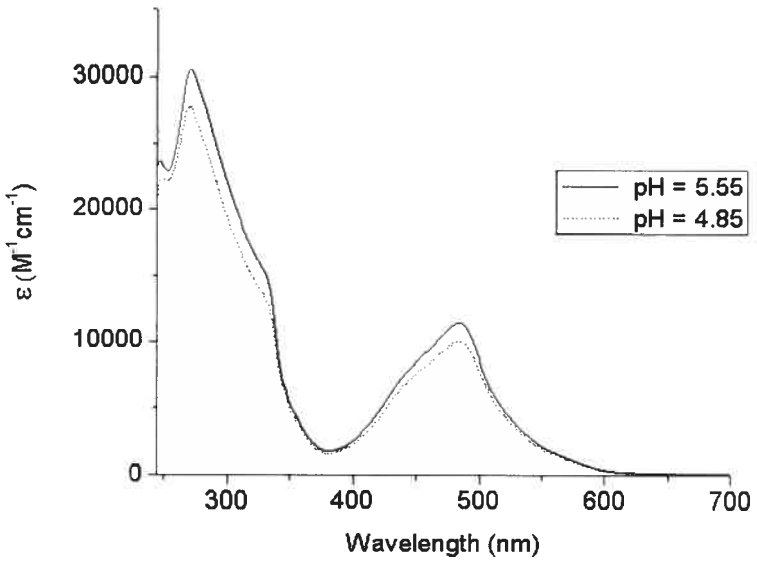

Figure 2.4 Absorption profiles for complex **II-5a $(PF_6)_2$** at pH values bracketing pKa.

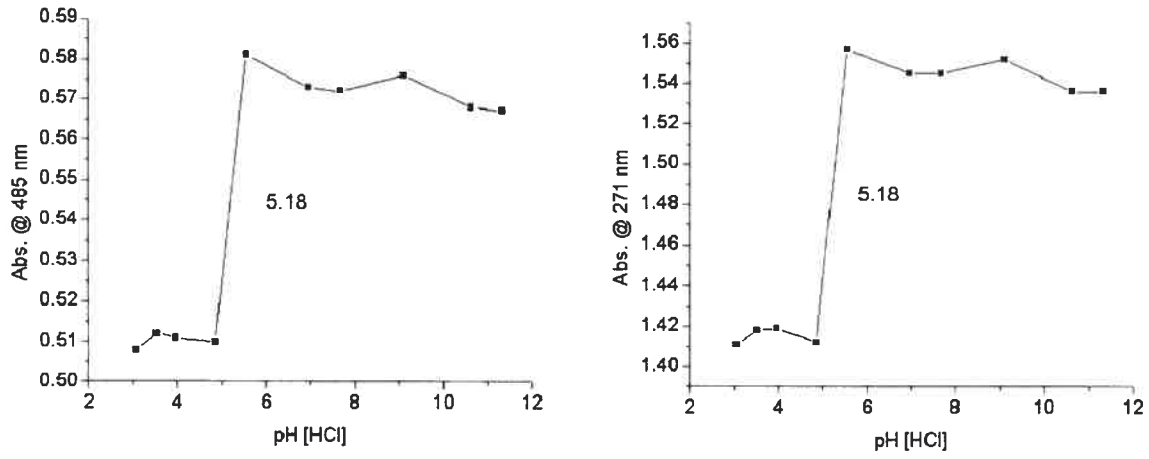

Figure 2.5 Titration data for complex **II-5a $(PF_6)_2$** from absorption at 485 nm (left) and 271 nm(right).

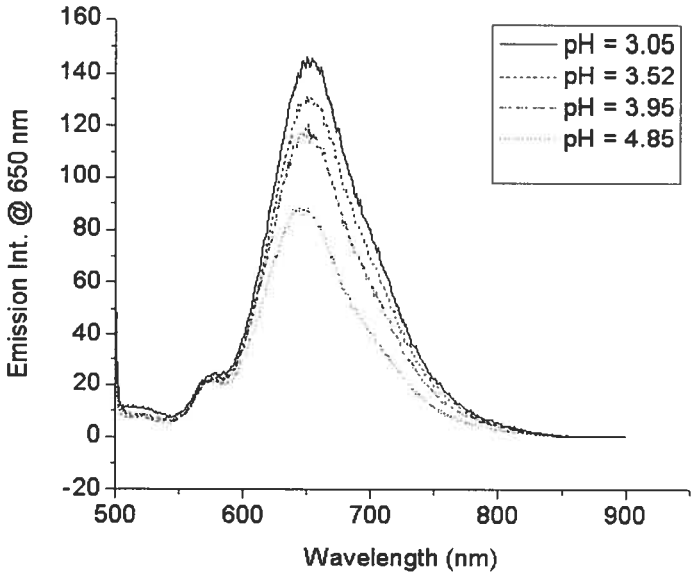

Figure 2.6 Emission profiles for complex **II-5a** $(PF_6)_2$ at pH values bracketing pKa.

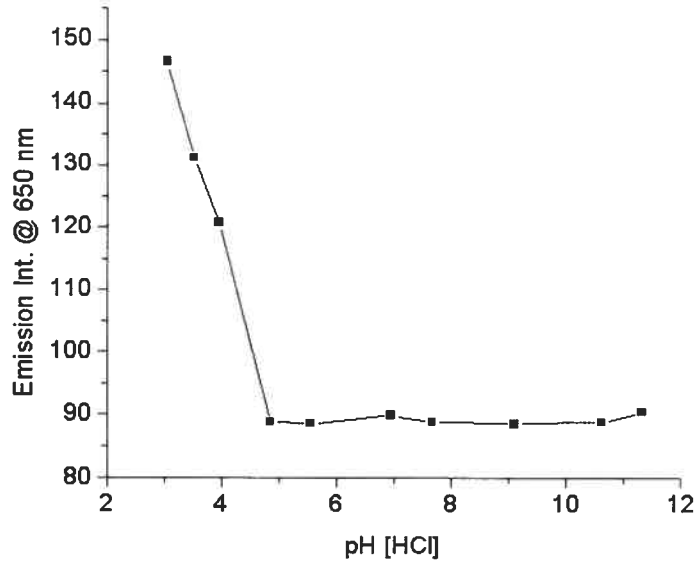

Figure 2.7 Titration data for complex **II-5a** $(PF_6)_2$ from emission at 650 nm.

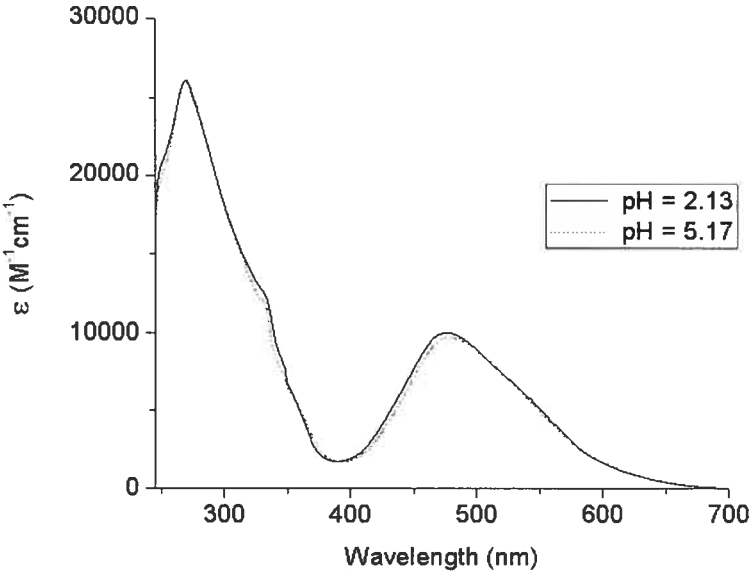

Figure 2.8 Absorption profiles for complex **II-5c** $(PF_6)_2$ at pH values bracketing pKa.

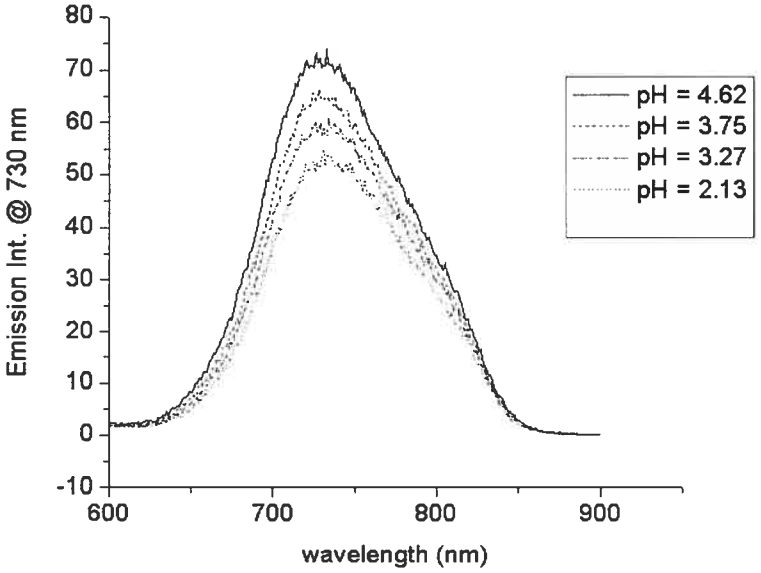

Figure 2.9 Emission profiles for complex **II-5c** $(PF_6)_2$ at pH values bracketing pKa.

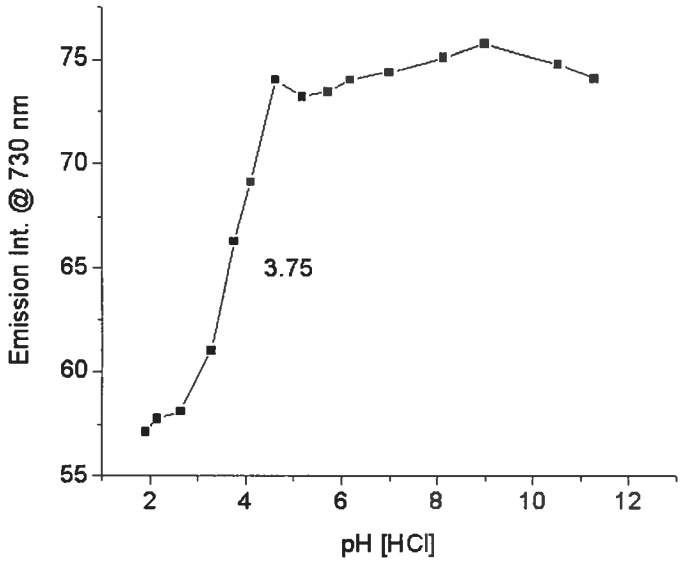

Figure 2.10 Titration data for complex **II-5c** $(PF_6)_2$ from emission at 730 nm.

2.4 NMR and Solution Behaviour

In general, the ^{1}H NMR of the parent complexes **II-5a** $(PF_6)_2$, **II-5b** $(PF_6)_2$, and **II-5c** $(PF_6)_2$ are very similar to those of their dirhodium(II,II) adducts. However, some notable differences are exhibited which lead to unambiguous identification of these higher-order complexes.

Located between 1.7-2.0 ppm are resonances stemming from the acetates bound to the dimetal unit. The number and proportion of these resonances is quite diagnostic as to the degree of substitution. As more Ru(II) complexes are grafted to the dirhodium core, the position of these resonances shifts slightly downfield. Interestingly, spectra of the resolved isomers ***trans*-II-2a** $(PF_6)_4$ and ***cis*-II-2a** $(PF_6)_4$ show distinct methyl singlets at 1.85 and 1.88 ppm, respectively. These singlets were located at almost the exact same position for the unresolved isomeric mix ***cis/trans*-II-2b** $(PF_6)_2$, and their relative integration gives a 3.3:1 *cis/trans* distribution. This is significantly greater than the statistical 2:1 *cis/trans* ratio expected in the absence of a difference in donor capacities between acetate and the ligand **II-5b** $(PF_6)_2$. The labilizing *trans* effect, well documented in mononuclear square planar and octahedral complexes, applies also to dimetal paddlewheel complexes.[18] Here, one would expect a greater proportion of the

trans isomer if ligand **II-5b $(PF_6)_2$** is significantly more basic than acetate. That this is not the case suggests the opposite scenario. The origin of this occurrence may lie in consideration of electrostatic factors, which will be elaborated on later in this section and the section to come.

A dramatic change in the phenyl doublets of the parent ligands is observed upon complexation to the dirhodium core, indicating a strong electronic influence. The well defined doublets of the parent carboxylate complexes merge into a singlet upon formation of the mononuclear adducts (Figures 2.11, 2.15, 2.19), but gradually separate and resolve with successive incorporation of the ruthenium complex. The conclusion of this effect is illustrated by the tetranuclear adduct **II-4b $(PF_6)_8$** (Figure 2.18), which displays phenyl resonances very similar to that for its parent complex **II-5b $(PF_6)_2$**.

Lastly, the 3', 5' resonance of complexes **II-5a $(PF_6)_2$** and **II-5b $(PF_6)_2$** appears as a singlet and is displaced very slightly (~0.05 ppm) upfield upon complexation to the dirhodium unit, providing another diagnostic marker for adduct formation. However, the contribution of this resonance has been most pronounced in the assignment of the tris-adducts **II-3a $(PF_6)_6$** and **II-3b $(PF_6)_6$**, where the presence of two distinct 3', 5' singlets in 2:1 proportion firmly supports the presence of symmetrically non-equivalent photoactive units.

Although the dirhodium adducts outlined in Figures 2.2 and 2.3 are stable in acetonitrile solution and to chromatographic separation, higher substitution adducts based on **II-5c $(PF_6)_2$** were found to decompose significantly under the purification conditions used, giving a mix of the desired product and the starting complex **II-5c $(PF_6)_2$**. The dissociation of these higher substitution adducts is no doubt linked to the more forcing conditions required to form even the mono-substituted adduct **II-1c $(PF_6)_2$** compared to the conditions used to form the analogues **II-1a $(PF_6)_2$** and **II-1b $(PF_6)_2$**. These observations are rationalized by the relatively lower dative capacity of **II-1c $(PF_6)_2$**, owing to the proximity of the electron deficient triazine moiety (see Section 2.3). However, that this is also a function of the overall nuclear charge of the adduct points to an electrostatic origin for this instability, which is made more problematic upon compromising the basicity of the complex / ligand employed. To further support this argument, the preparation of complexes **II-1-3a** was attempted using dirhodium(II,II)

tetra-*fluoro*acetate as the dative substrate. Tetra-fluoroacetate dimetal complexes typically undergo ligand exchange reactions with relatively more electron-rich chelates much more quickly compared to those using a tetra-acetate dimetal complex, owing to the reduced basicity of the tetrafluoroacetates.[19] Such exchange reactions have, until now, exclusively involved neutral or anionic chelates. In this case, however, no substitution whatsoever was observed under the same reaction conditions using $Rh_2(O_2C_2F_3)_4$. It is unlikely that the dative capacity of **II-5a $(PF_6)_2$** is lower than that of tetrafluoroacetate and, if it was, its use in large excess should otherwise ensure some substitution product. That this is not the case implies that installation of cationic complexes onto the already electron deficient dirhodium core of $Rh_2(O_2C_2F_3)_4$ is highly unfavourable due to Coulombic repulsion. This sort of decomposition is not unprecedented for highly-charged polynuclear coordination systems,[20] but it is with regard to dirhodium (II,II) solution behaviour.

To elaborate more on this point, dissolution of complex **II-1a $(PF_6)_2$** in d_5-pyridine and periodic monitoring of the 3', 5' proton resonance reveals gradual decomposition to give a dominant and minor intermediate at 9.36 ppm and 9.30 ppm, respectively, along with the unbound complex **II-5a $(PF_6)_2$** at 9.33 ppm (Figure 2.20). This solution equilibrated after 11 days to give complete decomposition of **II-1a $(PF_6)_2$**. Such behaviour denotes active competition between d_5-pyridine and **II-1a $(PF_6)_2$** for coordination to the dirhodium core. This has been demonstrated previously for $Mo_2(O_2CCF_3)_4$,[21] but it is the first such example for dirhodium carboxylates which are otherwise known to be much more inert to ligand scrambling processes.[19a, 22] The nature of these intermediates can only be speculated upon, but it is likely that they are mono-dentate adducts en route to full dissociation of ligand **II-5a $(PF_6)_2$**, in accord with previous observations of $Mo_2(O_2CCF_3)_4$ in pyridine.[21c] The fact that there are two such intermediates may be rationalized considering that a mono-dentate mode of coordination of **II-5a $(PF_6)_2$** leaves an oxygen atom available for simultaneous coordination to the axial site of the dirhodium complex, albeit in competition with d_5-pyridine. This is supported by the generally accepted mechanism for ligand scrambling wherein the incoming chelate coordinates axially first, followed by dissociative ring opening of the leaving chelate which frees an equatorial site for coordination of the incoming chelate.[23]

Notably, only relatively small amounts of the unbound complex **II-5a $(PF_6)_2$** are observed after equilibration of the solution, suggesting large activation barriers to its complete dissociation from the dimer.

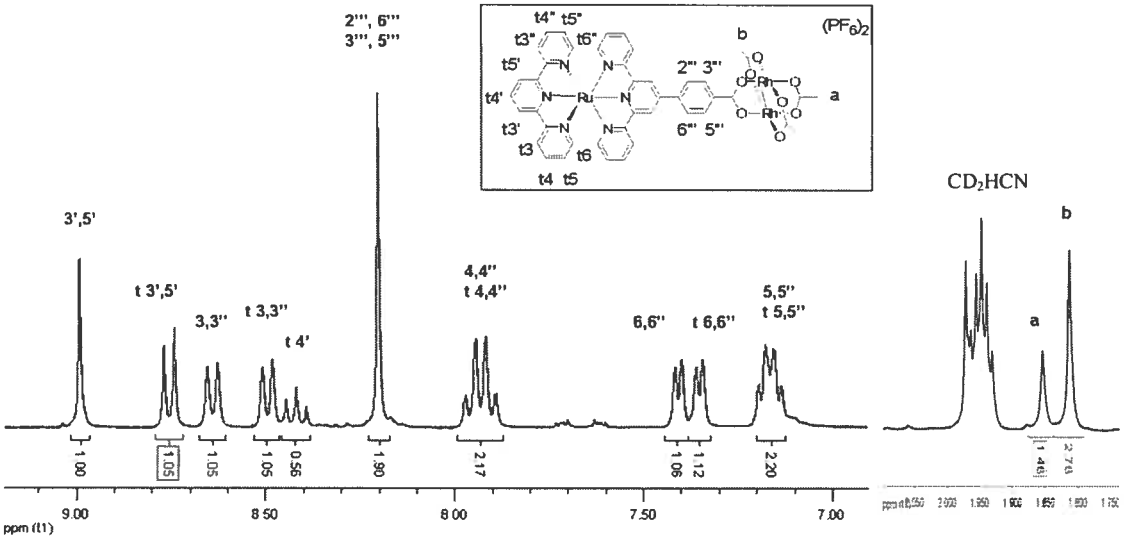

Figure 2.11 ^{1}H NMR spectrum of complex **II-1a $(PF_6)_2$** displaying aromatic (left) and acetate (right) resonances recorded in CD_3CN.

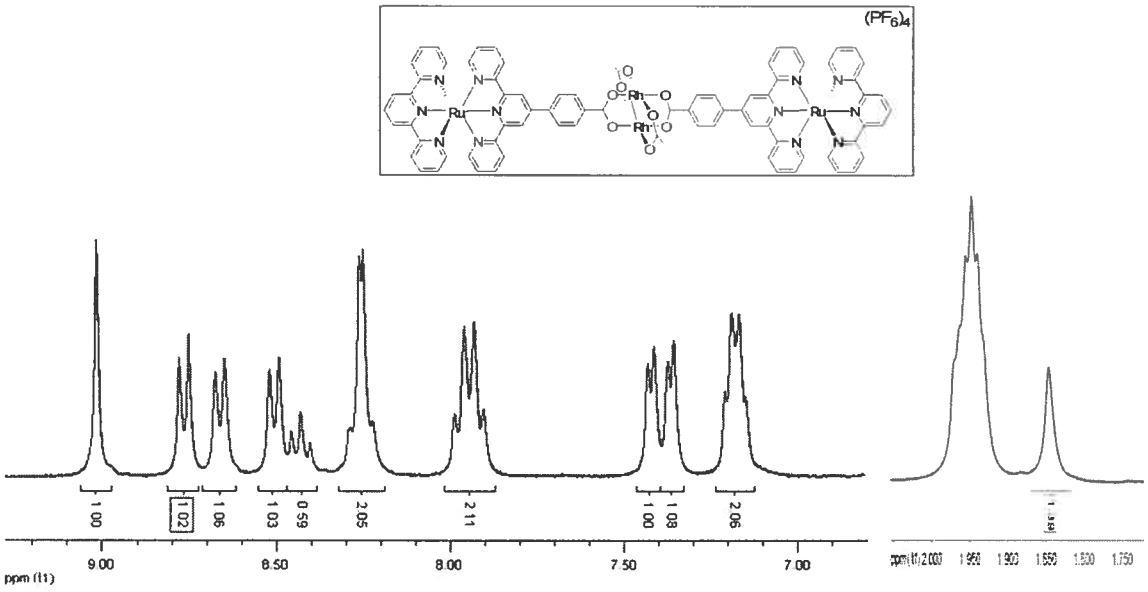

Figure 2.12 ^{1}H NMR spectrum of complex ***trans*-II-2a $(PF_6)_4$** displaying aromatic (left) and acetate (right) resonances recorded in CD_3CN.

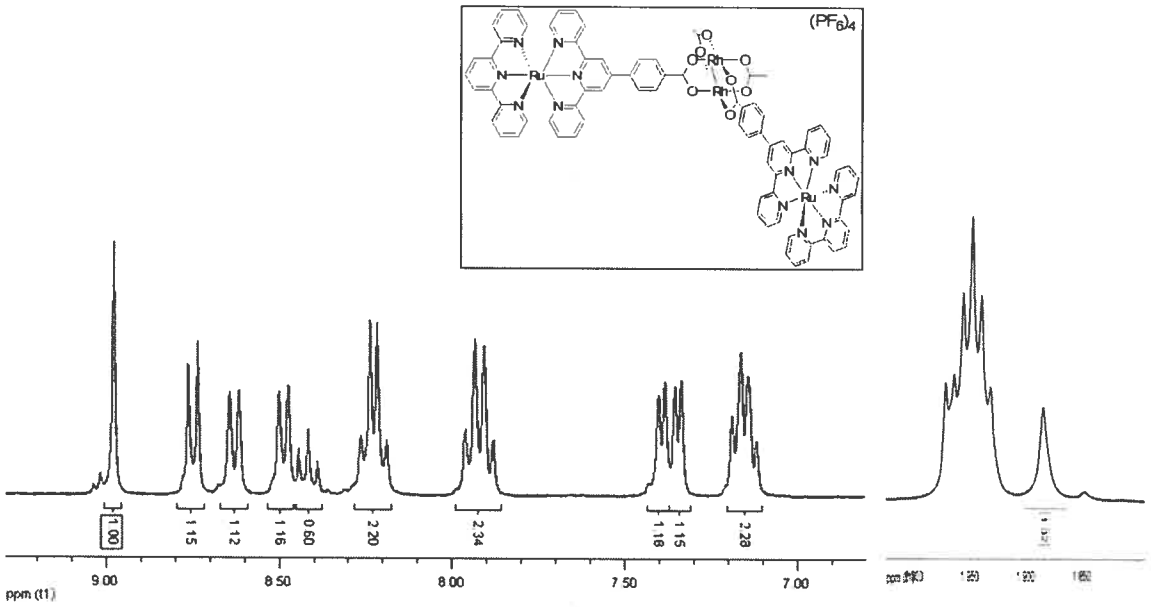

Figure 2.13 ^{1}H NMR spectrum of complex ***cis*-II-2a $(PF_6)_4$** displaying aromatic (left) and acetate (right) resonances recorded in CD_3CN.

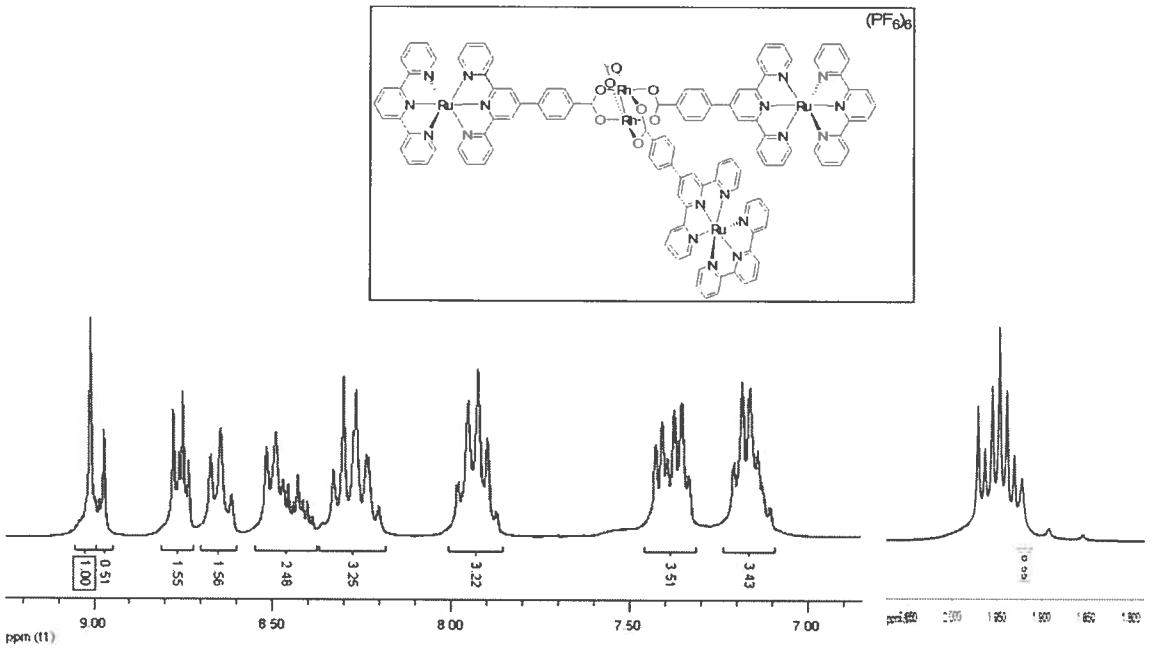

Figure 2.14 ^{1}H NMR spectrum of complex **II-3a $(PF_6)_6$** displaying aromatic (left) and acetate (right) resonances recorded in CD_3CN.

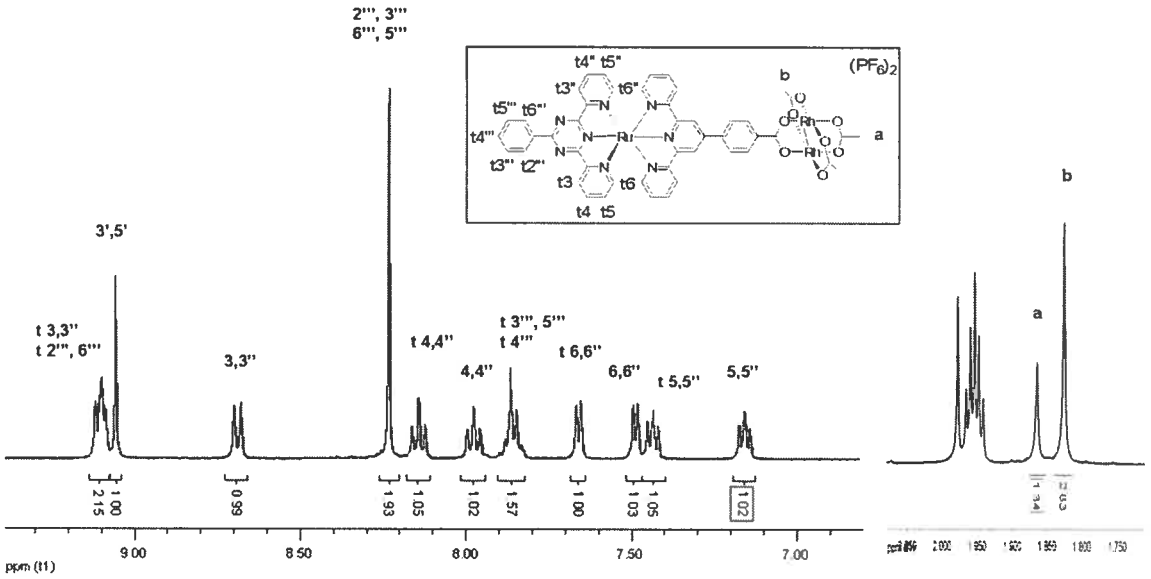

Figure 2.15 ^{1}H NMR spectrum of complex **II-1b $(PF_6)_2$** displaying aromatic (left) and acetate (right) resonances recorded in CD_3CN.

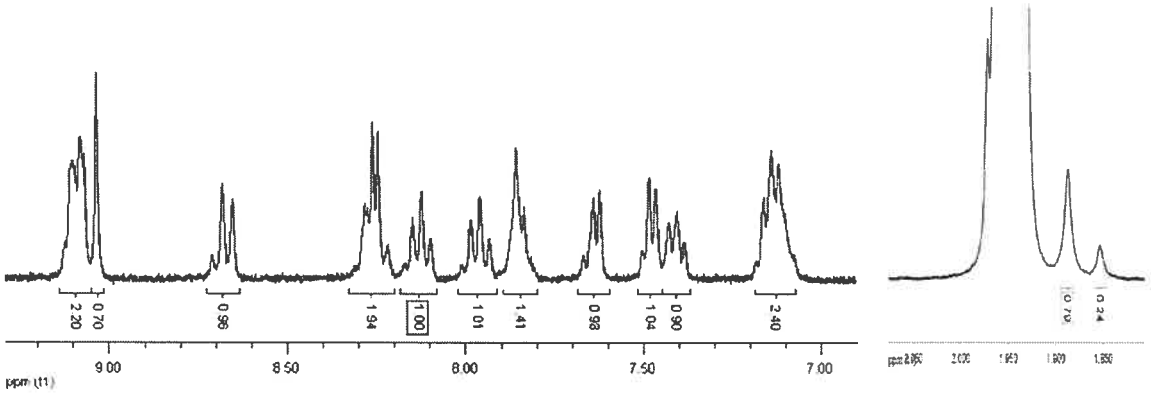

Figure 2.16 ^{1}H NMR spectrum of unresolved isomeric mix of complexes ***cis / trans*-II-2b $(PF_6)_4$** displaying aromatic (left) and acetate (right) resonances recorded in CD_3CN.

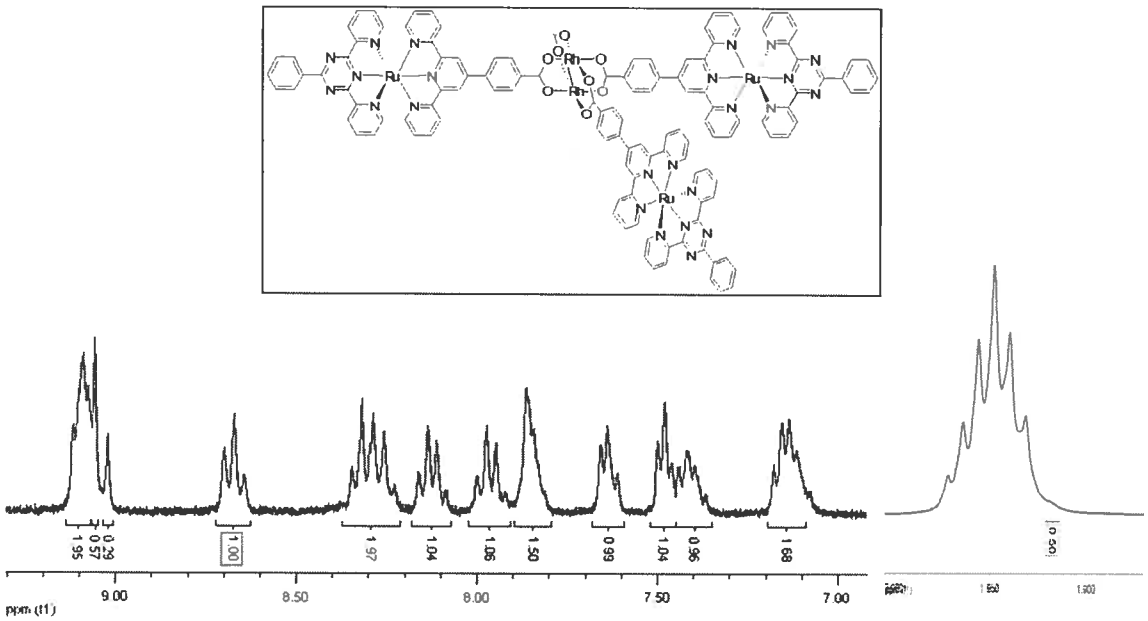

Figure 2.17 ^{1}H NMR spectrum of complex **II-3b** $(PF_6)_6$ displaying aromatic (left) and acetate (right) resonances recorded in CD_3CN.

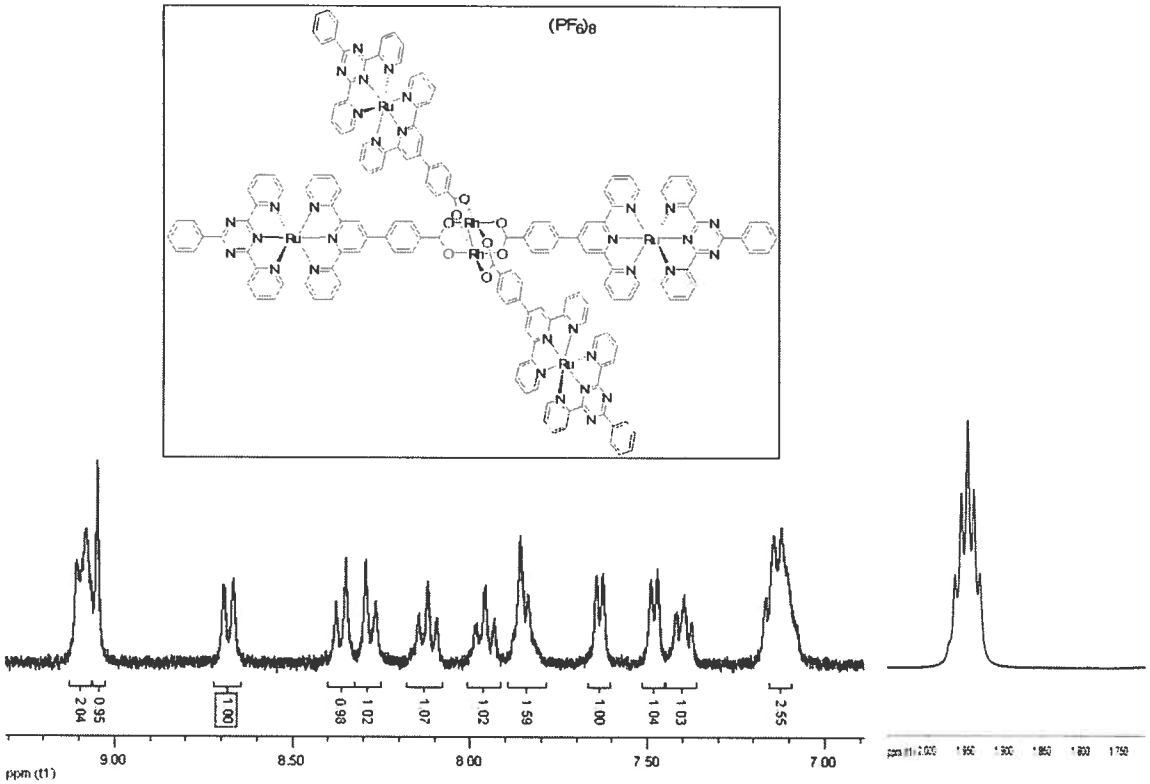

Figure 2.18 ^{1}H NMR spectrum of complex **II-4b** $(PF_6)_8$ displaying aromatic (left) and absence of acetate resonances (right) recorded in CD_3CN.

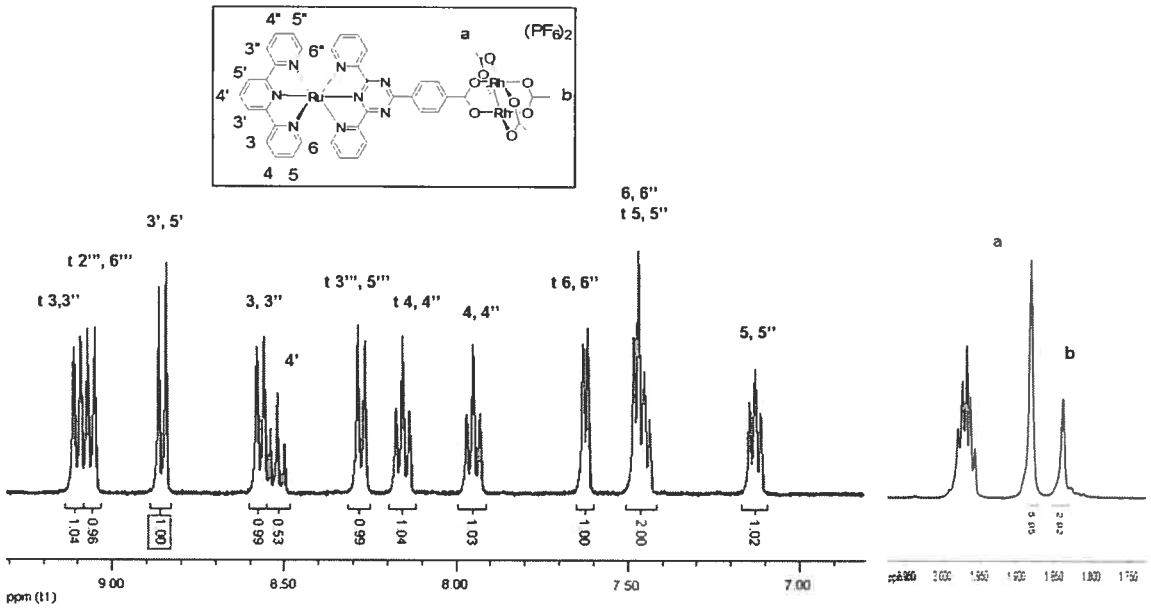

Figure 2.19 ^{1}H NMR spectrum of complex **II-1c** $(PF_6)_2$ displaying aromatic (left) and acetate (right) resonances recorded in CD_3CN.

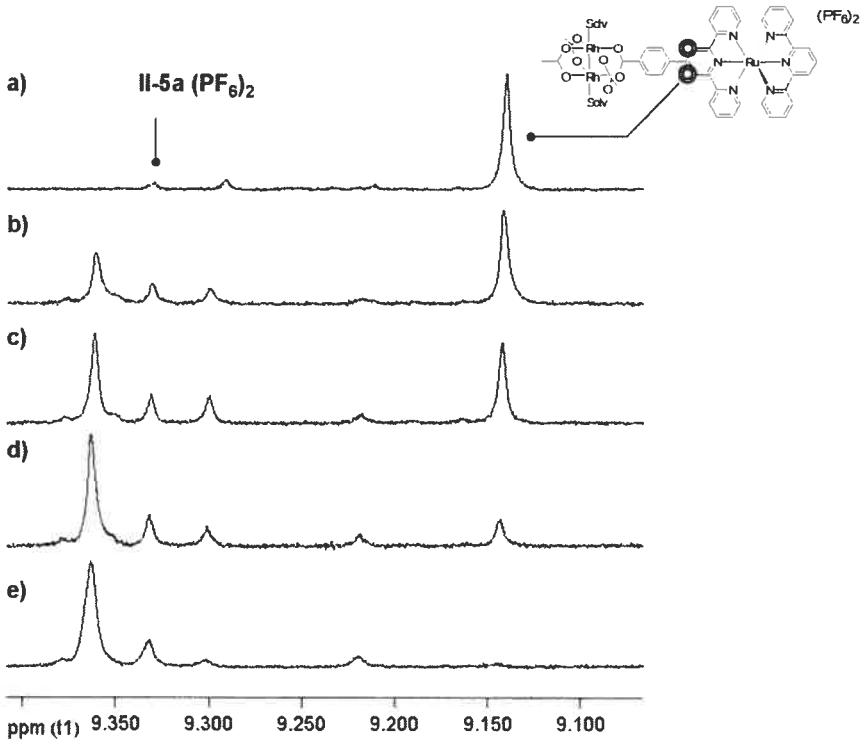

Figure 2.20 ^{1}H NMR spectrum of complex **II-1a** $(PF_6)_2$ in d_5-pyridine at r.t., exhibiting decomposition and formation of dative intermediates after (a) 0 hr (b) 24 hr (c) 48 hr (d) 72 hr (e) 11 days.

2.5 Crystal Structure Determination of II-5a $(BPh_4)_2$, II-5b $(BPh_4)(PF_6)$, and *trans*-II-2a $(CH_3CN)_2(BPh_4)_2(BF_4)_2$ (refer to pages II, VI, and XII of Appendix 2, respectively, for X-ray data and parameters)

For all crystal structures reported herein, single crystals of suitable quality for diffraction studies were grown from acetonitrile solutions containing the complex (as either the PF_6^- or BF_4^- salt) saturated with NH_4BPh_4. Although complex **II-5a** has been reported previously,[24] no X-ray structural data has been given until now. The structure is depicted below in Figure 2.21. Like that of $Ru(tpy)_2^{2+}$, **II-5a** contains mutually orthogonal ligands with a pseudo-octahedral geometry about the ruthenium atom.[25] The phenyl ring bearing the carboxylic acid group is twisted with respect to the central pyridyl ring by 44°. Each oxygen atom of the carboxylic acid group, and hence the acidic proton as well, can be found in two unique dispositions throughout the crystal lattice as indicated by site occupancy factors of 0.5 for each. As expected, the C-O bond lengths of this carboxylic acid group are 1.405(4) and 1.280(4) Å, corresponding to C-O single and double bonds, respectively. No hydrogen bonding is observed in the extended lattice structure.

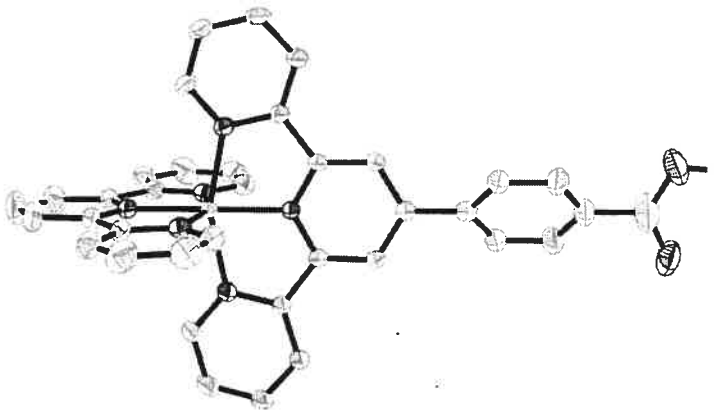

Figure 2.21 X-ray crystal structure of complex **II-5a $(BPh_4)_2$** with thermal ellipsoids at 30% probability. Solvent and counter-anions have been omitted for clarity.

The structure of **II-5b** (Figure 2.22) possesses a characteristic distorted octahedral geometry about the ruthenium atom with no relevant discrepancy in Ru-N bond lengths associated with the two electronically distinct ligands (e.g. Ru-N = 1.975(3) Å (central

triazine ring) and Ru-N = 1.980(2) Å (central tpy ring). However, the phenyl ring of the tpy ligand is twisted out of the plane of the central pyridyl ring by only 17°. Hydrogen bonding of the phenyl protons to the triazine nitrogen lone-pair electrons has been found to yield a near co-planar orientation in some instances,[26] but here the phenyl ring is twisted by 20° with respect to the central triazine ring. Also, unlike **II-5a**, complex **II-5b** exhibits hydrogen bonding between molecular units with an oxygen donor-acceptor distance of 2.630 (3) Å, a hydrogen-acceptor distance of 1.82 Å, and an O-H---O angle of 166.7°

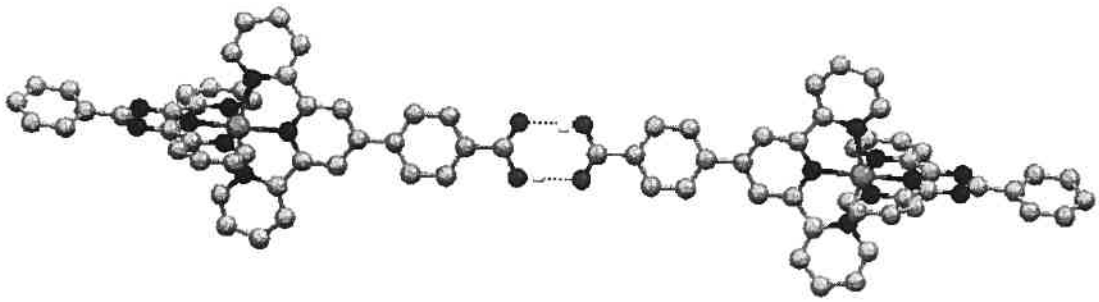

Figure 2.22 Ball-and-stick representation of the hydrogen bonding interaction in complex **II-5b** $(BPh_4)(PF_6)$. Solvent and counter-anions have been omitted for clarity.

For adduct ***trans*-II-2a** (Figure 2.23), the two appended ruthenium complexes possess structural features similar to that for **II-5a** with the exception that the phenyl ring is twisted out of the plane of the tpy ligand to a lesser extent (26°). With respect to dirhodium(II,II) tetra-carboxylates in general, the metal-metal bond has been found to vary inversely with the basicity of the axially coordinated ligand and, to a lesser degree, the electronic influence of the carboxylate bridging ligand.[19, 27] It should also be noted that packing forces have been implicated in minor changes of 0.01 Å.[19] The Rh-$O_{(caboxylate)}$ bond lengths are largely invariant among dirhodium carboxylates, with an average length of 2.04 Å. Here, the Rh-Rh and Rh-$N_{(CH3CN)}$ bond lengths are 2.367(2) Å and 2.200(15) Å, respectively, while the unique Rh-O bond lengths associated with the ruthenium complex have been found to be 2.051(2) and 2.052(5) Å. These distances are quite consistent with those found in other tetracarboxylate complexes of (bis)acetonitrile adducts.[28] However, the Rh-O bond length associated with the acetates is considerably

shorter with bond lengths of 1.86(1) and 1.936(11) Å. The discrepancy between these two values is due to problems resolving one of these oxygen atoms, as evidenced by larger anisotropic displacement parameters. Regardless, the Rh-O bond of 1.936(11) Å is about 0.1 Å shorter than expected, well outside justifiable implication of packing effects. This suggests that the acetates are bound more strongly than the ruthenium complexes, which is consistent with the solution behaviour discussed previously in Section 2.4. Any strong electron donating/withdrawing affect exerted by the equatorially coordinated carboxylate should have ramifications on the strength of coordination by the axial ligand which in turn will affect the metal-metal bond length.[27a, 29] However, these bond lengths are in good agreement with related dirhodium carboxylates. For this reason, and in consideration of the observations made in Section 2.4, we are convincingly led to believe that the effect is not inductive but rather *electrostatic* in nature. In essence, we have appended multiply charged cations to a cationic Rh_2^{4+} core. To offset unfavourable electrostatic repulsions, the anionic acetates have been subsequently drawn closer to the dirhodium(II,II) unit.

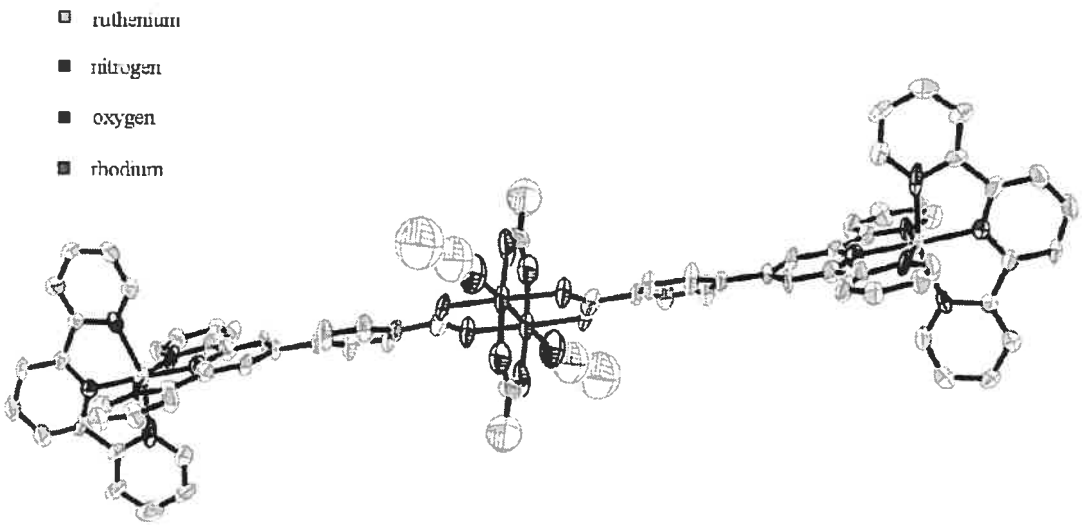

Figure 2.23 X-ray crystal structure of complex ***trans*-II-2a** $(CH_3CN)_2(BPh_4)_2(BF_4)_2$ with thermal ellipsoids at 30 % probability. Solvent and counter-anions have been omitted for clarity.

2.6 Electrochemistry

Cyclic voltammetry of complexes **II-1a-II-3a** revealed little difference compared to that of the parent complex **II-5a** $(PF_6)_2$ (Table 2.1). The absence of the characteristically reversible $Rh_2^{5+/4+}$ process, normally observed at ~1.02 V vs SCE,[30] was originally attributed to it being shifted outside the potential range of the solvent. However, the cyclic voltammetry of complexes **II-1b** $(PF_6)_2$ and **II-1c** $(PF_6)_2$ reveal two distinct and reversible redox couples corresponding to one electron oxidations which, on the basis of the oxidation behaviour of the model compounds $Rh_2(OAc)_4$, **II-5b** $(PF_6)_2$, and **II-5c** $(PF_6)_2$ (Table 2.1), are assigned to the Rh_2^{4+} and the Ru^{2+} centers (see Figure 2.24 and Table 2.1). In **II-1b** $(PF_6)_2$ and **II-1c** $(PF_6)_2$, the $Rh_2^{5+/4+}$ couple is shifted to higher potential by ~0.2 V relative to that of the parent $Rh_2(OAc)_4$, as expected based on the fact that the species is no longer neutral. It is therefore more likely that the $Rh_2^{5+/4+}$ couple is simply superimposed with the $Ru^{3+/2+}$ couple in **II-1a** $(PF_6)_2$, but becomes resolved in **II-1b** $(PF_6)_2$ and **II-1c** $(PF_6)_2$ because of the higher potential for their $Ru^{3+/2+}$ couples, owing to their more electron deficient triazine-based ligands.

However, for the higher substitution products, only one oxidation process is observed, and it is assigned as the $Ru^{3+/2+}$ couple based upon similarity to that for the respective Ru(II) parent complex. Interestingly, this couple exhibits chemical irreversibility in these higher adducts, the extent of which depends on the degree of substitution (Table 2.1), such that the return cathodic wave is diminished in intensity relative to the corresponding anodic wave. The absence of the $Rh_2^{5+/4+}$ couple for these higher nuclearity systems can be rationalized considering the observed 0.2 V anodic shift of the $Rh_2^{5+/4+}$ couple upon incorporation of a single Ru(II) moiety to form both **II-1b** $(PF_6)_2$ and **II-1c** $(PF_6)_2$. As more Ru(II) units are connected to the dirhodium unit, it is expected that this shift will increase. Notably, this shift need not occur in a linear fashion, considering in particular a point where the ruthenium(II) oxidation no longer lies at higher potential relative to the $Rh_2^{5+/4+}$ couple, since this entails the generation of even greater charge en route to oxidizing the dirhodium unit.

At negatively applied potentials lie ligand based reductions for all species.[26] It is noteworthy that the triazine analogues possess one more reduction process than those

based solely on tpy, the first of which is assigned to a triazine-based reduction whose position and reversibility depends upon the degree of substitution. For adducts **II-3b** $(PF_6)_6$ and **II-4b** $(PF_6)_8$, this reduction becomes chemically irreversible in their respective cyclic voltammograms, while their square-wave voltammograms show an anodic shift of 0.07 V (**II-3b** $(PF_6)_6$) and 0.15 V (**II-4b** $(PF_6)_8$) relative to the parent complex **II-5b** $(PF_6)_2$. Such a shift can be rationalized by the high positive charge of these complexes, which should facilitate reduction. The second reduction process is tpy-based and is reversible for the complexes **II-5b** $(PF_6)_2$ and **II-5c** $(PF_6)_2$ but becomes irreversible upon adduct formation (Table 2.1), being shifted to slightly higher potential with increasing substitution / charge. This shift is most pronounced for **II-4b** $(PF_6)_8$ relative to **II-5b** $(PF_6)_2$ (ΔE_c = 0.08 V). The final reduction process is triazine-based and is either not observed or chemically irreversible by cyclic voltammetry (Table 2.1), with the exception of **II-5c** $(PF_6)_2$ which shows a reversible process but with diminished current response relative to the two preceding one-electron reductions. Enhanced resolution inherent to the square wave experiment shows clearly this third reduction process in all cases and, again, a pronounced anodic shift (0.16 V) is observed for the highly charged adduct **II-4b** $(PF_6)_8$ relative to the parent complex **II-5b** $(PF_6)_2$.

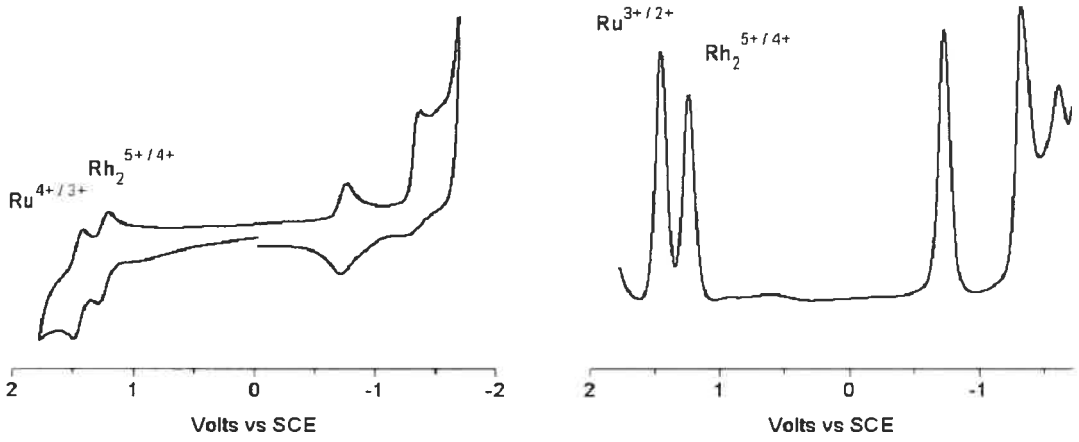

Figure 2.24 Cyclic voltammogram (left) and square-wave voltammogram (right) of complex **II-1c** $(PF_6)_2$ at 100 mVs^{-1}.

Table 2.1 Electrochemical Data for All Complexes.[a, b]

Cmpd	Potential [V] vs SCE. ΔE_p (mV).[a]						I_c / I_a[c] (Ru)	I_c / I_a[c] (Rh_2)
	$Ru^{3+/2+}$	$Rh_2^{5+/4+}$	Red.					
II-1a	1.27 (100)	-	-1.21 (irr)	-1.55 (irr)	-	-	0.70	-
II-1b	1.43 (80)	1.23 (70)	-0.76 (60)	-1.33 (irr)	-	-	0.72	0.95
II-1c	1.46 (70)	1.25 (80)	-0.74 (60)	-1.37 (irr)	-	-	0.95	1.14
***cis*-II-2a**	1.29 (80)	-	-1.18 (irr)	-1.53 (irr)	-	-	0.95	-
***trans*-II-2a**	1.29 (80)	-	-1.20 (irr)	-1.48 (irr)	-	-	1.06	-
II-3a	1.29 (80)	-	-1.18 (irr)	-1.53 (irr)	-	-	0.94	-
II-3b	1.44 (100)	-	-0.78 (irr)	-1.31 (irr)	-1.38 (irr)	-1.70 (irr)	0.25	-
II-4b	1.46 (90)	-	-0.73 (irr)	-1.35 (irr)	-1.66 (irr)	-	0.19	-
II-5a	1.28 (70)	-	-1.24 (irr)	-1.49 (irr)	-	-	0.73	-
II-5b	1.43 (80)	-	-0.78 (60)	-1.43 (120)	-	-	0.67	-
II-5c	1.46 (70)	-	-0.74 (60)	-1.41 (110)	-1.64 (80)	-	0.88	-
$Rh_2(OAc)_4$[d]	-	1.02	-1.08 (irr)	-	-	-	-	-
$(tpy)Ru^{2+}$[e]	1.30	-	-1.24	-1.49	-	-	-	-

a) Scan rate 100 mV s^{-1}. $E_{1/2}$ = ½ (E_{pa} + E_{pc}), where E_{pa} and E_{pc} are the anodic and cathodic peak potential respectively. $\Delta E_p = E_{pa} - E_{pc}$. Reported values for irreversible processes, labeled ir, are peak potentials. Potentials are corrected by internal reference, ferrocene (395 mV); b) the *cis* and *trans* isomers of **2b** could not be separated and complex **4a** was not obtained; c) I_c = cathodic peak current, I_a = anodic peak current; d) ref. (30); e) ref (31).

2.7 Electronic Absorption

The absorption characteristics and profiles of these adducts are dominated by the appended ruthenium complex, resembling strongly the absorption spectra of other ruthenium(II) polypyridyl complexes (Figure 2.25).[26, 32] In the visible region at ~ 480 nm is found the spin-allowed metal-to-ligand charge transfer (MLCT) band, which is assigned as a Ru(II)-to-tpy transition. The UV region is dominated by $\pi \rightarrow \pi^*$ and $n \rightarrow \pi^*$ processes with additional bands being resolved in some cases at 300 nm and 330 nm, owing to lower energy $\pi \rightarrow \pi^*$ transitions of the triazine ligand. The $Rh_2(O_2CCH_3)_4$ species is characterized by two bands in the visible region. The lower energy band (552 nm in CH_3CN), has been assigned to the π^* (Rh_2) $\rightarrow \sigma^*$ (Rh_2) transition and is shifted strongly to higher energy as a function of the solvent basicity owing to increased destabilization of the (Rh_2) σ^* orbital.[33a] The second, higher energy band (440 nm) assignment is still debatable but has been attributed to a π (Rh-O) $\rightarrow \sigma^*$ (Rh-O) transition.[33b] Of these transitions, only the lower energy band is solvent dependent, owing to the predominantly metal-based σ^* (Rh_2) component. Both of these bands are quite weak ($\varepsilon = 235\ M^{-1}cm^{-1}$ and $112\ M^{-1}cm^{-1}$ for π^* (Rh_2) $\rightarrow \sigma^*$ (Rh_2) and π (Rh-O) $\rightarrow \sigma^*$ (Rh-O), respectively) owing to poor orbital overlap, with the exception of a third observed band in the UV region which has been assigned as a σ (Rh_2) $\rightarrow$ (Rh_2) σ^* transition (221 nm, $\varepsilon = 18400\ M^{-1}cm^{-1}$).[33b, c] As such, the ^{1} MLCT absorption intensity for these Rh_2-adducts occurs as near integral multiples in accord with the degree of substitution of the appended Ru(II) complex onto the Rh_2 core, with the exception of adducts **II-1a-II-3a** for which the intensity is disproportionately high (see Table 2.2).

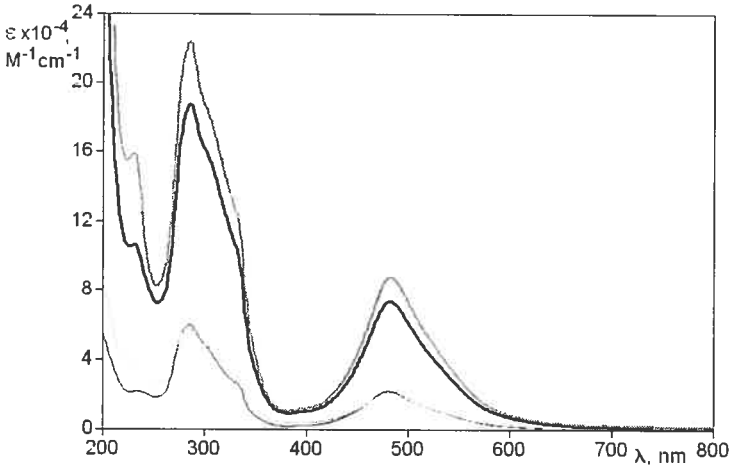

Figure 2.25 Absorption spectra of compounds **II-1b** $(PF_6)_2$ (gray line), **II-3b** $(PF_6)_6$ (bold black line), **II-4b** $(PF_6)_8$ (bold gray line) and **II-5b** $(PF_6)_2$ (black line), in acetonitrile solution.

Table 2.2 Electronic Absorption Data. [a] x = a, b, c.

Cpd	^{1}MLCT λ_{max} (nm) ε (M^{-1} cm^{-1}) [ε / ε $_{II\text{-}5x}$] [a]	LC transitions λ_{max} (nm), ε ($M^{-1}cm^{-1}$)				
II-1a	484 (19200), [1.8]	330 (34700)	307 (63800)	281 (45400)	273 (46800)	230 (49400)
II-1b	481 (23100), [1.0]	307 (49600)	285 (61900)	-	-	-
II-1c	480 (17800), [0.8]	330 (24400)	299 (38400)	283 (40300)	-	-
***trans*-II-2a**	485 (43100), [4.0]	330 (83600)	308 (139400)	281 (93900)	274 (96200)	230 (88900)
***cis*-II-2a**	485 (39400), [3.6]	330 (76100)	307 (136500)	281 (101400)	274 (103500)	230 (98400)
II-3a	485 (57200), [5.3]	330 (102800)	307 (175000)	281 (134800)	274 (137600)	230 (126700)
II-3b	482 (73600), [3.3]	286 (190100)	232 (107200)	-	-	-
II-4b	482 (87100), [3.9]	285 (225100)	231 (165800)	-	-	-
II-5a	484 (10800)	331 (15000)	272 (34500)	230 (39200)	-	-
II-5b	481 (22200)	286 (60000)	232 (24500)	-	-	-
II-5c	478 (22100)	299 (57600)	283 (59100)	-	-	-

2.8 Luminescence

All of the complexes emit at 77 K in butyronitrile matrix, whereas only the complexes containing the triazine-based ligand (i.e., the **b** and **c** series) show room temperature emission in fluid solution. Luminescence energies, lifetimes, and quantum yields, along with comparison with suitable model compounds, identify the emitting level as a ^{3}MLCT state in all cases.[26, 34] More specifically, this state involves the phenyl-tpy ligand for the **a** series, and the (bis)pyridyl triazine ligand for the **b** and **c** series.[35] The luminescence data is collected in Table 2.4, and the luminescence spectra of some representative species is displayed in Figures 2.26 and 2.27.

Considering first the **a** series of complexes, the emissive state of **II-5a $(PF_6)_2$** is essentially quenched upon attachment to the Rh_2 core. From the 77 K emission energy for **II-5a $(PF_6)_2$**, we can determine a 0.18 eV lower-limit and a 0.61 eV upper-limit driving force for energy transfer to the non-emissive state of the Rh_2 moiety, based on the upper limit of 1.77 eV and the lower limit of 1.34 eV, respectively, for its non-emissive state.[12] However, this does not in itself preclude quenching by electron transfer, for which two scenarios may be considered.

1. <u>Reductive Quenching</u> **2. <u>Oxidative Quenching</u>**

$$[Rh_2]^{0/+} \xrightarrow{e^-} [Ru]^{*/-} \qquad [Ru]^{*/+} \xrightarrow{e^-} [Rh_2]^{0/-}$$

Scheme 2.2 Electron-transfer quenching scenarios for the adducts **II-1a-II-3a**.

Unfortunately, because the $Rh_2^{5+/4+}$ redox couple is not observed in the series **II-1a-II-3a**, we cannot determine the thermodynamic driving force for reductive quenching. Any approximation to this end using the oxidation couple for $Rh_2(OAc)_4$ (Table 2.1) would be severely flawed considering the likelihood that the $Rh_2^{5+/4+}$ couple for **II-2a-II-3a** lies outside the potential cut-off for the solvent (refer to Section 2.6). Fortunately, the $Rh_2^{5+/4+}$ process was observed in the adducts **II-1b (PF_6)** and **II-1c $(PF_6)_2$**, for which reductive thermodynamic parameters may be calculated.[35] For all adducts, approximating the reductive thermodynamic parameters was done based on the irreversible $Rh_2^{4+/3+}$

couple observed in the model compound $Rh_2(OAc)_4$ (Table 2.1). That this process cannot be identified with any confidence in these Rh_2-adducts places a cautionary note on such approximation. However, the $Rh_2^{4+/3+}$ couple for $Rh_2(OAc)_4$ is probably a *low limit* for the reduction of the dirhodium core in these adducts, so that the calculated ΔG is also a low limit. These values are summarized below in Table 2.3. In all cases, both reductive and oxidative quenching are energetically disfavoured, which makes energy transfer to the non-emissive Rh_2 motif more plausible for the **a** series of adducts. Moreover, the fact that a part of the emission is recovered for these **a** series adducts at 77 K points to a significant nuclear barrier to energy transfer and a Dexter- type, electron exchange mechanism.[36]

Table 2.3 Approximate thermodynamic parameters for electron-transfer quenching.

Complex	ΔG (eV)	
	Red.	Ox.[a]
II-1a	-	0.41
II-1b	0.23	0.71
II-1c	0.00	0.77
***trans*-II-2a**	-	0.41
cis-II-2a	-	0.42
II-3a	-	0.42
II-3b	-	0.73
II-4b	-	0.73

[a] Calculated based on the $Rh_2^{4+/3+}$ couple (-1.08 V vs SCE) for $Rh_2(OAc)_4$.

The triazine analogues **II-5b** $(PF_6)_2$ and **II-5c** $(PF_6)_2$ possess emissive ^{3}MLCT states (1.80 and 1.78 eV, respectively, from 77 K emission maxima) considerably lower in energy relative to that for **II-5a** $(PF_6)_2$ (1.95 eV, from 77 K emission). This is attributable to the electron-deficient triazine moiety which lowers the emissive ^{3}MLCT

state, thus reducing thermal population and deactivation from upper lying ^{3}MC states.[37] In fact, their incorporation into the Rh_2 motif entails a reduction in the driving force for energy transfer to the non-emissive state of Rh_2, corresponding to lower-limits of only 0.03 eV and 0.01 eV for the **b** and **c** series, respectively. The fact that the emissive state for the **c** series is slightly lower in energy relative to that for the **b** series accounts for this difference and may be due to direct incorporation of the electron-withdrawing carboxy group onto the (bis)pyridyl triazine ligand in the **c** series.[37] Regardless, such a large reduction in driving force for energy transfer in both cases accounts for the solution emission observed at both room temperature and 77 K for the **b** and **c** series, and reinforces the invocation of energy transfer in the **a** series of Rh_2-adducts. Moreover, by taking into account the non-negligible nuclear barrier for the energy transfer process, as inferred by the 77 K emission properties of the **a** series, it is reasonable that energy transfer from the Ru-based ^{3}MLCT states to the dirhodium excited states does not occur appreciably at room temperature in the **b** and **c** series. More specifically, inspection of the emissive state lifetimes for the **b** series of adducts relative to that for the parent complex **II-5b** $(PF_6)_2$ at 77 K indicates that energy transfer to the Rh_2 core is partially effective. However, there is essentially no real difference in the emissive state lifetimes at 77 K between **II-1c** $(PF)_6$ and the parent complex **II-5c** $(PF_6)_2$, which indicates the complete absence of energy transfer to the Rh_2 core. This dismisses spin-orbit coupling by the dirhodium unit as a basis to explain the partial decay of the ^{3}MLCT in adducts of series **a** and **b** relative to their respective parent complexes. Since the acceptor ligand for the MLCT state extends to the carboxylate moiety for adducts of both series **a** and **c**, it is possible that they will have larger inner reorganization contributions to their respective nuclear barriers to energy transfer. Considering that complexes of series **c** possess a slightly lower energy emissive state than their **b** series counterparts, the absence of energy transfer to the Rh_2 unit in series **c** can be attributed to both lowered driving force and a relatively higher nuclear barrier to energy transfer.

That emission is still observed for the **b** and **c** series suggests that the non-emissive state of the dirhodium unit lies at or near the upper limit of 1.77 eV, since proximity to the lower limit of 1.34 eV would entail driving forces of 0.46 eV and 0.44 eV for energy transfer, respectively, and so likely render emission quenching analogous

to the **a** series at room temperature. It is highly unlikely that the nuclear barrier to energy transfer would be large enough in both cases to preclude energy transfer if in fact the excited-state of the Rh_2 core lied at or near 1.34 eV, considering that inner sphere reorganization energy (the principle component of the nuclear barrier for energy transfer) has been determined to be small for Ru(II) polypyridine complexes.[36] In addition, even for systems where electronic coupling is weak (coupling cannot be negligible in this case, otherwise energy transfer in the **a** complexes would be impossible) barriers on the order of 0.25 eV are readily bypassed at room temperature when a considerable exothermic driving force is present.[36]

Energy transfer rate constants can be calculated from the equation $k_{en} = 1/\tau_i - 1/\tau_0$, where τ_1 and τ_0 are the 77 K emission lifetimes of the compound in question and of the model compound, respectively. From the data in Table 2.5, the rate constants of the compounds of the **a** series are close one another, as expected because of the roughly identical donor / acceptor pair involved. Small differences in rate are still appreciable, and they can be tentatively attributed to small modifications in the energy of the Rh_2-based excited state (with subsequent modification to the driving force for energy transfer) or to small changes in the reorganization energy within the acceptor unit as a function of the different arrangements of the appended Ru(II) chromophore.

Interestingly, the rate constants for energy transfer at 77 K for the **b** series adducts is similar to those of the **a** series. This is somewhat odd, considering the aforementioned large difference in driving-force for energy transfer to the Rh_2 excited-state. Electronic coupling cannot be held responsible for this effect. The MLCT state in the **a** series of adducts is directed toward the Rh_2 unit, while in the **b** series it is directed toward the periphery. As such, electronic coupling should be higher for the **a** series, since the donor / acceptor distance is smaller. This should lead to the reverse effect. So the decisive effect has to be linked to nuclear factors. It should be considered that the acceptor ligand of the MLCT state of the **a** series also extends to the carboxylate moieties. Reorganization energy within the Ru(II) partner of the energy transfer process would therefore be larger for **a** compounds than for **b** compounds. Larger reorganization energy can compensate for larger driving forces in Dexter-type energy transfer processes, and could explain the similarity in energy transfer rate constants between **a** and **b** complexes at 77 K.

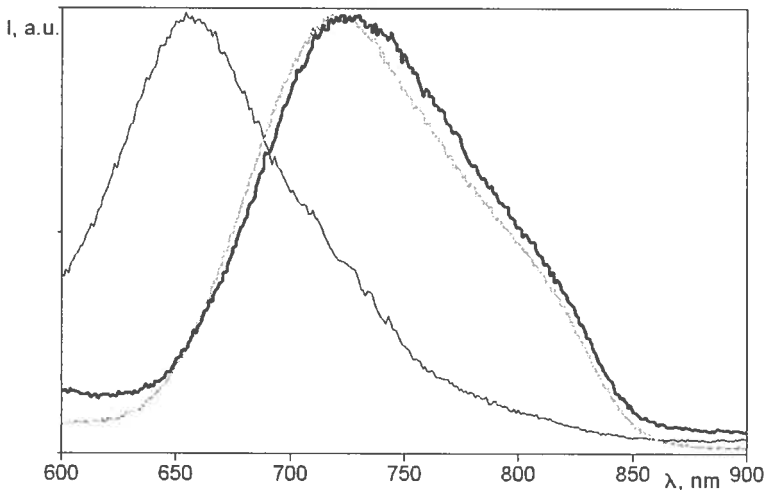

Figure 2.26 Uncorrected emission spectra of compounds **II-1a** $(PF_6)_2$ (black line), **II-1b** $(PF_6)_2$ (gray line), **II-1c** $(PF_6)_2$ (bold black line) in acetonitrile fluid solution at room temperature. For corrected values see Table 2.4.

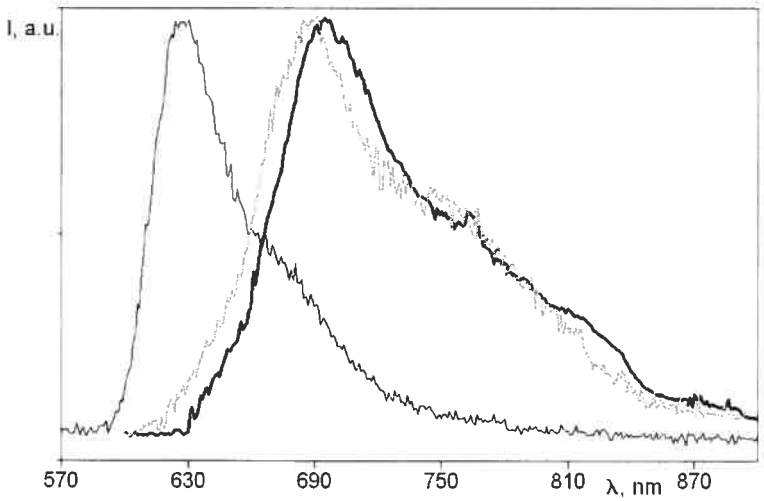

Figure 2.27 Uncorrected emission spectra of compounds **II-1c** $(PF_6)_2$ (bold black line), **II-3a** $(PF_6)_6$ (black line), **II-4b** $(PF_6)_8$ (gray line) in butyronitrile rigid matrix at 77 K. For corrected values see Table 2.4.

Table 2.4 Spectroscopic and photophysical data in de-aerated CH_3CN solutions at 298 K, unless otherwise stated.[a]

	Luminescence, 298 K			Luminescence, 77 K [b]	
cpd	λ_{max} (nm)	τ, (ns)	Φ ($x10^{-4}$)	λ_{max} (nm)	τ, (μs)
II-1a	-	-	-	639	2.50
II-1b	731	4.3	1.2	690	0.75
II-1c	750	14.3	0.7	703	1.30
***cis*-II-2a**	-	-	-	636	0.80
***trans*-II-2a**	-	-	-	634	1.2
II-3a	-	-	-	635	0.80
II-3b	731	5.8	1.1	692	0.86
II-4b	733	5.3	1.3	692	0.77
II-5a	666	9.5	0.8	635	13.2
II-5b	735	5.3	1.2	689	1.37
II-5c	745	14.4	1.9	698	1.38
$Ru(tpy)_2^{2+}$ [c]	629	0.25	$\leq$0.05	-	-
$Ru(Ph\text{-}tpy)_2^{2+}$ [c]	715	1.0	0.4	-	-

a) the *cis* and *trans* isomers of **II-2b** could not be separated and complex **II-4a** was not obtained; b) in butyronitrile rigid matrix; c) ref (38).

Table 2.5 Calculated rate constants of the Ru-to-Rh_2 energy transfer processes at 77 K.[a]

cpd	**1a**	***cis*-2a**	***trans*-2a**	**3a**	**1b**	**3b**	**4b**
k_{en} (10^5 s^{-1})	3.2	12.0	7.5	12.0	6.0	4.3	5.8

(a) Calculated values are based on the 77 K lifetimes given in Table 2.4. Reference species are **II-5a** $(PF_6)_2$ for the **a** series and **II-5b** $(PF_6)_2$ for the **b** series.

2.9 Conclusion

The capacity of the dirhodium(II,II) tetra-carboxylate motif to serve as a template for convergent and controlled synthesis of polynuclear photoactive compounds has been demonstrated, based upon suitable carboxy-functionalized $Ru(tpy)_2^{2+}$ photoactive units. To this end, inherent advantages of the dirhodium(II,II) tetra-carboylate unit regarding its relative inertness to ligand scrambling and its diamagnetic nature make it amenable to such a synthetic approach. In addition to this, it appears that there exists some difficulty to append such cationic complexes onto the Rh_2^{4+} core, the origins of which are likely electrostatic in nature, as evidenced by the crystal structure of ***trans*-II-2a** and non-reactivity to ligand displacement when employing the relatively electron-deficient $Rh_2(O_2CCF_3)_4$. The net result is control over the extent of substitution en route to polynuclear species. Contributions of electron transfer to the efficient quenching observed in the series **II-1a-II-3a** are precluded on thermodynamic grounds and through the preparation of relatively electron-deficient triazine analogues **II-1b-II-4b** and **II-1c**, which have enabled direct observation of the $Rh_2^{4+/5+}$ couple (**II-1b** and **II-1c**) previously unobserved for **II-1a**. Moreover, the triazine analogues emit almost unperturbed relative to their respective parent complexes **II-5b** and **II-5c** subsequent to initial photo-excitation, which places the non-emissive state of the dirhodium(II,II) tetra-acetate near the previously reported upper limit of 1.77 eV. Considering the recent elucidation of other long-lived dimetal photo-excited states,[39] more evolved examples of these systems should prove to be ideal models for study of energy and electron transfer processes.

2.10 Experimental

2.10.1 Materials and Methods Solvents used in the preparation and purification of complexes **II-1a-5a**, **II-1b-5b**, and **II-1c** and **II-2c** were reagent grade. The preparation of **II-5a**,[24] 2, 2': 6', 2''-terpyridine,[40] 2-*para*-tolyl-4,6-di(2-pyridyl)triazine,[26] (2-phenyl-4,6-di(2-pyidyl)triazine)$RuCl_3$,[26] and 4'-(4-carboxyphenyl)tpy [41] have been described previously. Silica used for chromatographic isolation of all complexes was 400-450 Å mesh. The starting materials $Rh_2(O_2CCH_3)_4(MeOH)_2$,[42] $Rh_2(O_2CCF_3)_4(MeOH)_2$,[43] and (tpy)$RuCl_3$ [44] were prepared and purified according to established procedures.

2.10.2 Physical Measurements All ^1H NMR spectra were recorded using a Bruker 400RG at 400 MHz. Electrochemical data was recorded using a BAS Epsilon potentiostat using argon-degassed, spectroscopic grade acetonitrile solutions of 0.1 M tetrabutylammonium hexafluorophosphate ($TBAPF_6$) as supporting electrolyte. A three electrode set-up was employed using a working Pt button electrode, a Pt wire auxiliary electrode, and a Ag wire pseudo-reference electrode with addition of ferrocene as an internal reference. All data is corrected to the Fc/Fc^+ couple vs SCE. Single crystal X-ray diffraction data for **II-5a**, ***trans*-II-2b**, and **II-5b** were collected on a Bruker Apex at 100 K using Cu-Kα radiation (λ= 1.54178 Å) and refined by Francine Bélanger-Gariépy. Mass spectrometry was performed by direct injection using an LC-MSD TOF (Agilent) spectrometer with electrospray ionization.

The ground-state pKa values for complexes **II-5a $(PF_6)_2$ and II-5c $(PF_6)_2$** were determined by UV-Vis (Cary 500i spectrophotometer, 1 cm path length quartz cell) and emission measurements (Cary Eclipse spectrophotometer) over the range of pH = 2-13 for air-equilibrated solutions. Stock solutions (**II-5a $(PF_6)_2$**, 5.1 x 10^{-5} M; **II-5c $(PF_6)_2$**, 6.1 x 10^{-5} M) were prepared in 100 mL of H_2O containing 20% DMSO and 0.1 M KCl. The addition of DMSO ensured complete dissolution of the complexes over the measured pH range. The pH of the solution was initially adjusted by addition of 0.2 M NaOH(aq) and subsequently lowered by careful addition of HCl(aq) solution. The acid solution was added such that the total volume change was negligible, and the solutions were allowed to equilibrate for 5 min. prior to recording the UV-vis spectrum.

2.10.3 Synthesis and Purification

Note: Single crystals of compound **II-5a**, suitable for structure determination by X-ray diffraction, were grown upon vapour diffusion of isopropyl ether into an acetonitrile / toluene solution of **II-5a** $(PF_6)_2$, wherein the title compound crystallized as **II-5a** $(BPh_4)_2$.

2-(4-Carboxyphenyl)-4,6-di(2-pyridyl)triazine (Lc) In a typical preparation, $KMnO_4$ (6.3 g, 40 mmol) is dissolved in H_2O (250 ml) made basic to pH = 14 with addition of KOH. 2-(p-Tolyl)-4,6-di(2-pyridyl)triazine (1.0 g, 3.1 mmol) is then added and the mixture heated to reflux for 16 h, after which a 10% solution of $Na_2S_2O_3$ is added until coloration ceases to ensure removal of excess $KMnO_4$. Filtration over celite of the still hot solution, followed by adjustment to pH = 5 with dropwise addition of HCl, forms a colourless precipitate on standing overnight that is collected by filtration and dried *in vacuo*. Yield: 75 %. ^{1}H NMR (400 MHz, d_6-DMSO) δ ppm 7.73 (m, 2H), 8.15 (m, 2H), 8.23 (d, J = 8.6 Hz, 2H), 8.79 (d, J = 7.9 Hz, 2H), 8.83 (d, J = 8.6 Hz, 2H), 8.93 (d, J = 4.6 Hz, 2H). ^{13}C (300 MHz, d_6-DMSO) δ ppm 126.23, 128.24, 130.24, 131.21, 135.99, 138.84, 140.26, 151.54, 154.02, 168.15, 172.48, 172.62. ESI-MS: $[M + H]^+$ cald. for $C_{20}H_{14}N_5O_2$, 356.11475; found, 356.11437.

[(2-Phenyl-4,6-di(2-pyridyl)triazine)(4'-(4-carboxyphenyl)tpy)Ru]$(PF_6)_2$ (II-5b) In a typical preparation, (2-phenyl-4,6-di(2-pyidyl)triazine)$RuCl_3$ (0.20 g, 0.39 mmol), 4'-(4-carboxyphenyl)tpy (0.136 g, 0.39 mmol), and $AgNO_3$ (0.197 g, 1.16 mmol) are triturated briefly in ethanol (60 mL), then refluxed under ambient conditions for 12 h. The crude mix is filtered hot over celite to remove AgCl(s) and the solvent is removed by distillation. The residue is dissolved in a 2:1 mix of CH_3CN / H_2O and eluted on silica using 7:2 CH_3CN / KNO_3 (sat, aq) as eluent. The collected fractions are combined in a separatory funnel with addition of CH_3CN, H_2O and NH_4PF_6, followed by enough CH_2Cl_2 to effect phase separation. After removal of the aqueous phase, the process is repeated again until no colouration of the aqueous phase persists, at which point the organic layer is washed with two 100 mL portions of H_2O The organic layer is then

removed and dried, then dissolved in a minimal amount of CH_3CN and precipitated in H_2O to remove excess NH_4PF_6. The precipitate is removed by filtration and dried *in vacuo*. Yield: 41 %. R_f = 0.37 (SiO_2 substrate, 7:2 CH_3CN / KNO_3 (sat, aq) as eluent). Single crystals suitable for structure determination by X-ray diffraction were prepared by vapour diffusion of isopropyl ether into an acetonitrile solution of **II-5b $(PF_6)_2$** saturated with ammonium tetraphenylborate, wherein the title compound crystallized as **II-5b $(PF_6)(BPh_4)$**. ^{1}H NMR (400 MHz, CD_3CN) δ ppm 7.17 (m, 2H), 7.45 (m, 2H), 7.50 (d, J = 5.5 Hz, 2H), 7.67 (d, J = 5.4 Hz, 2H), 7.87 (m, 3H), 7.98 (m, 2H), 8.15 (m, 2H), 8.33 (d, J = 8.4 Hz, 2H), 8.40 (d, J = 8.4 Hz, 2H), 8.70 (d, J = 8.0 Hz, 2H), 9.10 (m, 6H). ESI-MS: $[M]^{2+}$ cald. for $C_{41}H_{28}N_8O_2Ru$, 383.06894; found, 383.06886.

[(2-(4-Carboxyphenyl)-4,6-di(2-pyridyl)triazine)(tpy)Ru]$(PF_6)_2$ (II-5c) Prepared and purified as for **II-5b $(PF_6)_2$**, using 2-(4-carboxyphenyl)-4,6-di(2-pyridyl)triazine (0.20 g, 0.56 mmol), $(tpy)RuCl_3$ (0.25 g, 0.56 mmol), and $AgNO_3$ (0.29 g, 1.68 mmol) in a 1:1 ethanol / H_2O mix (60 mL). Yield: 36% (R_f = 0.35). ^{1}H NMR (400 MHz, CD_3CN) δ ppm 7.15 (m, 2H), 7.45 (m, 2H), 7.47 (d, J = 5.6 Hz, 2H), 7.62 (d, J = 5.6 Hz, 2H), 7.96 (m, 2H), 8.17 (m, 2H), 8.44 (d, J = 8.5 Hz, 2H), 8.52 (t, J = 8.1 Hz, 1H), 8.54 (d, J = 7.2 Hz, 2H), 8.83 (d, J = 8.2 Hz, 2H), 9.13 (d, J = 8.0 Hz, 2H), 9.18 (d, J = 8.5 Hz, 2H). ESI-MS: $[M]^{2+}$ cald. for $C_{35}H_{24}N_8O_2Ru$, 345.05328; found, 345.05267.

General Procedure for II-1a-II-3a and II-1b-II-4b The product distribution and extent of reaction depends on the quantity of the carboxy complexes **II-5a / 5b $(PF_6)_2$** relative to $Rh_2(OAc)_4$, in addition to reaction temperature and duration, and the removal of acetic acid. In a typical preparation, **II-5a $(PF_6)_2$** (0.175 g, 0.18 mmol)) and $Rh_2(OAc)_4(CH_3OH)_2$ (0.022 g, 0.043 mmol) are refluxed in acetonitrile (40 mL) for 5 days. During the course of the reaction, the solvent was removed periodically (after ~ 24 h) and acetic acid was removed by sublimation. After this time, the intensities of the bands corresponding to the substitution products **II-1a-3a** were deemed to be sufficiently intense, and the reaction mix was concentrated and applied to a short plug of silica for elution under pressure to separate excess **II-5a**. Adducts **II-1a-II-3a** were collected as one band and then converted to their PF_6^- salts as outlined above for **II-5b $(PF_6)_2$**. After filtration and

washing with water on the frit, the material was re-dissolved in CH_3CN and applied to a silica column using 7:1 CH_3CN / KNO_3(sat, aq) as eluent. The collected fractions are converted to their respective PF_6^- salts as outlined above. The organic layer is then dried and the residue taken up in a minimal amount of CH_3CN and added to a minimal amount of H_2O giving a precipitate which is then filtered and dried *in vacuo*, affording **II-1a $(PF_6)_2$** (24 mg, $R_f = 0.56$), ***trans*-II-2a $(PF_6)_4$** (28 mg, $R_f = 0.45$), ***cis*-II-2a $(PF_6)_4$** (35 mg, $R_f = 0.43$), **II-3a $(PF_6)_6$** (39 mg, $R_f = 0.34$), 11 mg of unreacted **II-5a $(PF_6)_2$**. Overall yield = 63 %.

As above, but using **II-5b $(PF_6)_2$** (0.20 g, 0.19 mmol) and $Rh_2(OAc)_4(CH_3OH)_2$ (0.016 g, 0.032 mmol), which afforded: **II-1b $(PF_6)_2$** (30 mg, $R_f = 0.51$), ***cis/trans*-II-2b $(PF_6)_4$** (15 mg, $R_f = 0.38$), **II-3b $(PF_6)_6$** (21 mg, $R_f = 0.30$) and **II-4b $(PF_6)_8$** (19 mg, $R_f = 0.20$) along with 95 mg of **II-5b $(PF_6)_2$**. Overall yield = 69 %. **Note:** the *cis / trans* isomers of **II-2b** could not be resolved despite numerous efforts with various eluents and solid supports.

[(tpy)Ru(tpy-ph-CO_2)$Rh_2(O_2CCH_3)_3$](PF$_6$)$_2$ (II-1a): ^{1}H NMR (400 MHz, CD_3CN) δ ppm 7.17 (m, 4H), 7.36 (d, J = 5.1 Hz, 2H), 7.41 (d, J = 5.2 Hz, 2H), 7.95 (m, 4H), 8.21 (s, 4H), 8.43 (t, J = 8.2 Hz, 1H), 8.50 (d, J = 8.0 Hz, 2H), 8.65 (d, J = 8.0 Hz, 2H), 8.76 (d, J = 8.2 Hz, 2H), 9.00 (s, 2H), 1.82 (s, 3H), 1.86 (s, 6H). % Cald. for $C_{43}H_{38}N_6O_8RuRh_2P_2F_{12}$·2 H_2O: C (36.90), H (3.02), N (6.00). % Found: C (36.36), H (3.20), N (5.92). ESI-MS: $[M(BF_4)]^+$ cald. for $C_{43}H_{34}N_6O_8BF_4RuRh_2$, 1156.96; found, 1155.00. $[M]^{2+}$ cald. for $C_{43}H_{34}N_6O_8RuRh_2$, 534.98; found, 534.22.

[(tpy)Ru(tpy-ph-CO_2)$_2$$Rh_2(O_2CCH_3)_2$](PF$_6$)$_4$ (*trans*-II-2a): ^{1}H NMR (400 MHz, CD_3CN) δ ppm 7.18 (m, 8H), 7.37 (d, J = 5.2 Hz, 4H), 7.42 (d, J = 5.1 Hz, 4H), 7.95 (m, 8H), 8.26 (m, 8H), 8.43 (t, J = 8.2 Hz, 2H), 8.51 (d, J = 8.0 Hz, 4H), 8.66 (d, J = 8.0 Hz, 4H), 8.77 (d, J = 8.2 Hz, 4H), 9.02 (s, 4H), 1.85 (s, 6H). % Cald. for $C_{78}H_{60}N_{12}O_8Ru_2Rh_2P_4F_{24}$·3 H_2O: C(40.12), H (2.85), N (7.20). % Found: C (40.09), H (2.97), N (7.17). ESI-MS: $[M(BF_4)_3]^+$ cald. for $C_{78}H_{56}N_{12}O_8B_3F_{12}Ru_2Rh_2$, 1959.06; found, 1956.81. $[M(BF_4)_2]^{2+}$ cald. for $C_{78}H_{56}N_{12}O_8B_2F_8Ru_2Rh_2$, 936.03; found, 934.08. Single crystals suitable for structure determination by X-ray diffraction were grown upon diffusion of isopropyl ether into an acetonitrile solution of ***trans*-II-2a $(BF_4)_4$** saturated

with ammonium tetraphenylborate, wherein the title compound crystallized as the (bis) acetonitrile adduct ***trans*-II-2a $(CH_3CN)_2(BPh_4)_2(BF_4)_2$**.

[(tpy)Ru(tpy-ph-CO_2)$_2$$Rh_2$($O_2CCH_3$)$_2$](PF$_6$)$_4$ (*cis*-II-2a): ^{1}H NMR (400 MHz, CD_3CN) δ ppm 7.15 (m, 8H), 7.35 (d, J = 5.3 Hz, 4H), 7.39 (d, J = 5.5 Hz, 4H), 7.92 (m, 8H), 8.23 (m, 8H), 8.42 (t, J = 8.2 Hz, 2H), 8.49 (d, J = 8.0 Hz, 4H), 8.63 (d, J = 8.2 Hz, 4H), 8.75 (d, J = 8.2 Hz, 4H), 8.98 (s, 4H), 1.88 (s, 6H). % Cald. for $C_{78}H_{60}N_{12}O_8Ru_2Rh_2P_4F_{24}$·2 H_2O: C (40.43), H (2.78), N (7.25). % Found: C (40.51), H (2.80), N (7.22). ESI-MS: $[M(BF_4)_3]^+$ cald. for $C_{78}H_{56}N_{12}O_8B_3F_{12}Ru_2Rh_2$, 1959.06; found, 1955.13. $[M(BF_4)_2]^{2+}$ cald. for $C_{78}H_{56}N_{12}O_8B_2F_8Ru_2Rh_2$, 936.03; found, 934.28.

[(tpy)Ru(tpy-ph-CO_2)$_3$$Rh_2$($O_2CCH_3$)](PF$_6$)$_6$ (II-3a): ^{1}H NMR (400 MHz, CD_3CN) δ ppm 7.17 (m, 12H), 7.35 (m, 6H), 7.41 (m, 6H), 7.93 (m, 12H), 8.27 (m, 12H), 8.43 (m, 3H), 8.49 (m, 6H), 8.65 (m, 6H), 8.75 (m, 6H), 8.97 (s, 2H), 9.01 (s, 4H), 1.92 (s, 3H). % Cald. for $C_{113}H_{82}N_{18}O_8Ru_3Rh_2P_6F_{36}$·3 H_2O: C (41.72), H (2.73), N (7.75). % Found: C (41.77), H (2.81), N (7.70). ESI-MS: $[M(BF_4)_3]^{3+}$ cald. for $C_{113}H_{78}N_{18}O_8B_3F_{12}Ru_3Rh_2$, 862.39; found, 861.74. $[M(BF_4)_2]^{4+}$ cald. for $C_{113}H_{78}N_{18}O_8B_2F_8Ru_3Rh_2$, 625.04; found, 624.26.

[(2-phenyl-4,6-di(2-pyidyl)triazine)Ru(tpy-ph-CO_2)Rh_2(O_2CCH_3)$_3$](PF$_6$)$_2$ (II-1b): ^{1}H NMR (400 MHz), CD_3CN) δ ppm 7.16 (m, 2H), 7.44 (m, 2H), 7.49 (d, J = 5.4 Hz, 2H), 7.66 (d, J = 5.3 Hz, 2H), 7.86 (m, 3H), 7.98 (m, 2H), 8.14 (m, 2H), 8.23 (s, 4H), 8.69 (d, J = 8.1 Hz, 2H), 9.06 (s, 2H), 9.10 (m, 4H), 1.83 (s, 6H), 1.86 (s, 3H). ESI-MS: $[M(PF_6)]^+$ cald. for $C_{47}H_{36}N_8O_8PF_6RuRh_2$, 1292.94; found, 1292.49. $[M]^{2+}$ cald. for $C_{47}H_{36}N_8O_8RuRh_2$, 573.99; found, 574.17.

[(2-phenyl-4,6-di(2-pyidyl)triazine)Ru(tpy-ph-CO_2)$_2$$Rh_2$($O_2CCH_3$)$_2$](PF$_6$)$_4$ (*cis/trans*-II-2b): ^{1}H NMR (400 MHz, CD_3CN) δ ppm 7.14 (m, 4H), 7.41 (m, 4H), 7.48 (m, 4H), 7.64 (m, 4H), 7.86 (m, 6H), 7.96 (m, 4H), 8.13 (m, 4H), 8.26 (m, 8H), 8.68 (m, 4H), 9.04 (s, 4H), 9.10 (m, 4H), 1.85 (s, *trans*-CH_3COO), 1.89 (s, *cis*-CH_3COO). ESI-MS:

$[M(PF_6)_3]^+$ cald. for $C_{86}H_{60}N_{16}O_8P_3F_{18}Ru_2Rh_2$, 2288.99; found, 2288.61. $[M(PF_6)_2]^{2+}$ cald. for $C_{86}H_{60}N_{16}O_8P_2F_{12}RuRh_2$, 1072.01; found, 1071.71.

[(2-phenyl-4,6-di(2-pyidyl)triazine)Ru(tpy-ph-CO_2)$_3$$Rh_2$($O_2CCH_3$)]($PF_6$)$_6$ (II-3b): ^{1}H NMR (400 MHz), CD_3CN) δ ppm 7.14 (m, 6H), 7.42 (m, 6H), 7.48 (m, 6H), 7.64 (m, 6H), 7.85 (m, 9H), 7.96 (m, 6H), 8.12 (m, 6H), 8.29 (m, 12H), 8.67 (m, 6H), 9.02 (s, 2H), 9.06 (s, 4H), 9.09 (m, 12H), 1.92 (s, 3H). ESI-MS: $[M(PF_6)_4]^{2+}$ cald. for $C_{125}H_{84}N_{24}O_8P_4F_{24}Ru_3Rh_2$, 1570.04; found, 1569.26. $[M(PF_6)_3]^{3+}$ cald. for $C_{125}H_{84}N_{24}O_8P_3F_{18}Ru_3Rh_2$, 998.37; found, 997.83.

[(2-phenyl-4,6-di(2-pyidyl)triazine)Ru(tpy-ph-CO_2)$_4$$Rh_2$]($PF_6$)$_8$ (II-4b): ^{1}H NMR (400 MHz, CD_3CN) δ ppm 7.13 (m, 8H), 7.40 (m, 8H), 7.48 (d, J = 5.5 Hz, 8H), 7.64 (d, J = 5.4 Hz, 8H), 7.85 (m, 12H), 7.96 (m, 8H), 8.12 (m, 8H), 8.28 (d, J = 8.5 Hz, 8H), 8.36 (d, J = 8.5 Hz, 8H), 8.68 (d, J = 8.3 Hz, 8H), 9.05 (s, 8H), 9.08 (m, 16H). ESI-MS: $[M(PF_6)_6]^{2+}$ cald. for $C_{164}H_{108}N_{32}O_8P_6F_{36}Ru_4Rh_2$, 2068.06; found, 2068.66. $[M(PF_6)_5]^{3+}$ cald. for $C_{164}H_{108}N_{32}O_8P_5F_{30}Ru_4Rh_2$, 1330.39; found, 1330.36.

[(tpy)Ru(2-(4-carboxyphenyl)4,6-di(2-pyridyl)triazine)Rh_2(O_2CCH_3)$_3$](PF_6)$_2$ (II-1c): Preparation and purification followed as described previously for **II-1a-3a** and **II-1b-4b**, but with some notable exceptions. In a typical preparation, **II-1c (PF_6)$_2$** (0.115 g, 0.12 mmol) and $Rh_2(OAc)_4(CH_3OH)_2$ (0.015 g, 0.03 mmol) are refluxed in CH_3CN (25 mL) for 7 days with periodic removal of solvent and acetic acid, giving a range of products analogous to the series **II-1a-3a** but heavily favouring the mononuclear adduct.. Yield: 0.040 g with 0.050 g of **II-5c (PF_6)$_2$** recovered. Overall yield = 57 %. R_f = 0.30. ^{1}H NMR (400 MHz, CD_3CN) δ ppm 7.13 (m, 2H), 7.44 (m, 2H), 7.47 (d, J = 5.3 Hz, 2H), 7.62 (d, J = 5.3 Hz, 2H), 7.95 (m, 2H), 8.16 (m, 2H), 8.28 (d, J = 8.4, 2H), 8.52 (t, J = 8.2 Hz, 1H), 8.57 (d, J = 8.1 Hz, 2H), 8.86 (d, J = 8.2 Hz, 2H), 9.06 (d, J = 8.4 Hz, 2H), 9.10 (d, J = 8.0 Hz, 2H), 1.84 (s, 6H), 1.88 (s, 3H). ESI-MS: $[M(PF_6)]^+$ cald. for $C_{41}H_{32}N_8O_8PF_6RuRh_2$, 1216.91; found, 1217.11. $[M]^{2+}$ cald. for $C_{41}H_{32}N_8O_8RuRh_2$, 535.98; found, 536.19.

2.11 References

1. a) Funyu, S.; Isobe, T.; Takagi, S.; Tryk, D.A.; Inoue, H. *J. Am. Chem. Soc.* **2003**, 125, 19, 5734. b) Otruba, J.P.; Neyhart, G.A.; Dressick, W.J.; Marshall, J.L.; Sullivan, B.P.; Watkins, P. A.; Meyer, T.J. *J. Photochem.* **1986**, 35, 133. b) Gratzel, M.; *Inorg. Chem.* **2005**, 44, 6841 and references therein. c) Dempsey, J.L.; Esswein, A.J. ; Manke, D.R. ; Rosenthal, J. ; Soper, J.D.; Nocera, D.G. *Inorg. Chem.* **2005**, 44, 6879 and references therein.
2. a) Baudin, H.B.; Davidsson, J.; Serroni, S.; Juris, A.; Balzani, V.; Campagna, S.; Hammarstrom, L. *J. Phys. Chem.* A **2002**, 106, 4312. b) Chen, P.; Meyer, T.J. *Chem. Rev.* **1998**, 98, 1439. c) Balzani, V.; Juris, A.; Venturi, M.; Campagna, S.; Serroni, S. *Chem. Rev.* **1996**, 96, 759 and references therein.
3. see, for example a) Ruben, M.; Rojo, J.; Romero-Salguero, F.J.; Uppadine, L.H.; Lehn, J.M. *Angew. Chem. Int. Ed.* **2004**, 43, 3644, and references therein. b) Fang, Y.-Q.; Polson, M. I. J.; Hanan, G. S. *Inorg. Chem.* **2003**, 42, 5. c) Denti, G.; Campagna, S.; Sabatino, L.; Serroni, S.; Ciano, M.; Balzani, V. *Inorg. Chem.* **1990**, 29, 4750. d) Denti, G.; Campagna, S.; Sabatino, L.; Serroni, S.; Ciano, M.; Balzani, V. *J. Am. Chem. Soc.* **1992**, 114, 2944.
4. Constable, E.C. *Chem. Commun.* **1997**, 1073 and references therein.
5. a) Manitto, P.; Monti, D.; Zanzola, S.; Speranza, G. *Chem. Comm.* **1999**, 543. b) Doyle, M.P.; Pieters, R.J.; Martin, S.F.; Austin, R.E.; Oalmann, C.J.; Muller, P. *J. Am. Chem. Soc.* **1991**, 113, 1423.
6. a) Doyle, M. P.; Protopopova, M.; Muller, P.; Ene, D.; Shapiro, E.A. *J. Am. Chem. Soc.* **1994**, 116, 8492. b) Doyle, M.P.; van Oeverne, A.; Westrum, L.J.; Protopopova, M.N.; Clayton, T.W. *J. Am. Chem. Soc.* **1991**, 113, 8982.
7. a) Srikrishna, A.; Gharpure, S. J. *Chem. Commun.* **1998**, 1589. b) Taber, D.F.; You, K. K.; Rheingold, A. L. *J. Am. Chem. Soc.* **1996**, 118, 547.
8. Wood, J. L; Moniz, G. A.; Pflum, D. A.; Stoltz, B. M.; Holubec, A. A.; Dietrich, H. J. *J. Am. Chem. Soc.* **1999**, 121, 1748.

9. a) Bear, J. L.; Gray, H. B.; Rainen, L.; Chang, I. M.; Howard, R. A.; Serio, G.; Kimball, A. P. *Cancer Chemother. Rep.* **1975**, 59, 611. b) Howard, R. A.; Kimball, A. P.; Bear, J. L. *Cancer Res.* **1979**, 39, 2568.
10. Bien, M.; Pruchnik, F. P.; Seniuk, A. ; Lachowicz, T. M. ; Jakimowicz, P. *J. Inorg. Biochem.* **1999**, 73, 49.
11. Chifotides, H. T. ; Dunbar, K. M. *Acc. Chem. Res.* **2005**, 38, 146 and references therein.
12. Bradley, P. M.; Bursten, B. E.; Turro, C. *Inorg. Chem.* **2001**, 40, 1376.
13. Bradley, P. M.; Fu, P. K.-L.; Turro, C. *Comments Inorg. Chem.* **2001**, 22(6), 393.
14. Lutterman, D. A.; Fu, P. K-L.; Turro, C. *J. Am. Chem. Soc.* **2006**, 128, 739.
15. a) Bickley, J.; Bonar-Law, R.; McGrath, T.; Singh, N.; Steiner, A. *New J. Chem.* **2004**, 28, 425. b) Schiavo, S.L.; Serroni, S.; Puntoriero, F.; Tresoldi, G.; Piraino, P. *Eur. J. Inorg. Chem.* **2002**, 79. c) Cotton, F.A.; Murillo, C.A. *Acc. Chem. Res.* **2001**, 34, 759. d) Eddaoudi, M.; Kim, J.; Wachter, J. B.; Chae, H. K.; O'Keeffe, M.; Yaghi, O. M. *J. Am. Chem. Soc.* **2001**, 123, 4368. e) Bonar-Law, R.; McGrath, T., Singh, N.; Bickley, J.F.; Femoni, C.; Steiner, A. *J. Chem. Soc., Dalt. Trans.* **2000**, 4343.
16. Cooke, M. W.; Hanan, G. S.; Loiseau, F.; Campagna, S.; Watanabe, M. ; Tanaka, Y. *Angew. Chem. Intl. Ed.* **2005**, 44, 4881.
17. See, for example a) Montalti, M.; Wadhwa, S.; Kim, W. Y.; Kipp, R. A.; Schmehl, R. H. *Inorg. Chem.* **2000**, 39, 76. b) Nazeeruddin, M. K.; Zakeeruddin, S. M.; Humphry-Baker, R.; Kaden, T. A.; Grätzel, M. *Inorg. Chem.* **2000**, 39, 4542. c) Nazeeruddin, M. K.; Zakeeruddin, S. M.; Humphry-Baker, R.; Jirousek, M.; Liska, P.; Vlachopoulos, N.; Shklover, V.; Fischer, C.-H.; Grätzel, M. *Inorg. Chem.* **1999**, 38, 6298. d) Lay, P.A.; Sasse, W. H. F. *Inorg. Chem.* **1984**, 23, 4123.
18. a) Drago, R. S.; Long, J. R.; Cosmano, R. *Inorg. Chem.* **1982**, 21, 2196. b) Norman, J. G.; Kolari, H. J. *J. Am. Chem. Soc.* **1978**, 100, 791.
19. a) Cotton, F.A.; Walton, R. A. *Multiple Bonds Between Metal Atoms*, 3rd, ed., Wiley, New York, **1994**. b) Telser, J.; Drago, R. *Inorg. Chem.* **1984**, 23, 2599.
20. You, C.-C.; Wurther, F. *J. Am. Chem. Soc.* **2003**, 125, 9716.

21. a) Girolami, G. S.; Mainz, V. V.; Andersen, R. A. *Inorg. Chem.* **1980**, 19, 805. b) Cotton, F. A.; Lay, D. G. *Inorg. Chem.* **1981**, 20, 935. c) Webb, T. R.; Dong, T.-Y. *Inorg. Chem.* **1982**, 21, 114.

22. Casas, J. M.; Cayton, R. H.; Chisholm, M. H. *Inorg. Chem.* **1991**, 30, 359.

23. Webb, T. R.; Dong, T.-Y. *Inorg. Chem.* **1982**, 21, 114.

24. Figgemeier, E.; Aranyos, V.; Constable, E. C. ; Handel, R. W. ; Housecroft, C. E.; Risinger, C.; Hagfeldt, A.; Mukhtar, E. *Inorg. Chem. Commun.* **2004**, 7, 117.

25. Pyo, S.; Perez-Cordero, E.; Bott, S. G.; Echegoyen, L. *Inorg. Chem.* **1999**, 38, 3337.

26. Polson, M. I. J.; Medlycott, E. A.; Hanan, G. S.; Mikelsons, L.; Taylor, N. J.; Watanabe, M.; Tanaka, Y.; Loiseau, F.; Passalacqua, R.; Campagna, S. *Chem. Eur. J.* **2004**, 10, 3640.

27. a) Cotton, F. A.; Hillard, E. A.; Liu, C. Y.; Murillo, C. A.; Wang, W.; Wang, X. *Inorg. Chim. Acta* **2002**, 337, 233. b) Lichtenberger, D.; Pollard, J. R.; Lynn, M. A.; Cotton, F. A.; Feng, X. *J. Am. Chem. Soc.* **2000**, 122, 3182. c) Pirrung, M. C.; Morehead, Jr., A. *J. Am. Chem. Soc.* **1994**, 116, 8991.

28. a) Barron, A. R.; Wilkinson, G.; Motevalli, M.; Hursthouse, M. B. *Polyhedron*, **1985**, 4(6), 1131. b) Cotton, F. A.; Thompson, J. L.; *Acta Cryst. (B): Structural Crystallography and Crystal Chemistry* **1981**, B37 (12), 2235.

29. Cotton, F. A.; Felthouse, T. R. *Inorg. Chem.* **1980**, 19, 323.

30. Tikkanen, W. R.; Binamira-Soriaga, E.; Kaska, W. C.; Ford, P. C. *Inorg. Chem.* **1984**, 23, 141.

31. Beley, M.; Collin, J.-P.; Sauvage, J.-P.; Sugihara, H.; Heisel, F.; Miehé, A. *J. Chem. Soc. Dalton Trans.* **1991**, 3157.

32. see, for example a) Sun, L.; Hammarstrom, L.; Akermark, B.; Styring, S. *Chem. Soc. Rev.* **2001**, 30, 36. b) Barigelletti, F.; Flamigni, L. *Chem. Soc. Rev.* **2000**, 29, 1. c) Hagfeldt, A.; Graetzel, M. *Acc. Chem. Res.* **2000**, 33, 269. d) Sauvage, J.-P.; Collin, J.-P.; Chambron, J.-C.; Guillerez, S.; Coudret, C. ; Balzani, V. ; Barigelletti, F. ; De Cola, L. ; Flamigni, L. *Chem. Rev.* **1994**, 94, 993.

33. a) Trexler, J. W.; Schreiner, A. F.; Cotton, F. A. *Inorg. Chem.* **1988**, 27, 3265. b) Miskowski, V. M.; Schaefer, W. P.; Sadeghi, B.; Santarsiero, B. D.; Gray, H. B.

Inorg. Chem. **1984**, 23, 1154. c) Norman, J. G. Jr.; Renzoni, G. E.; Case, D. A. *J. Am. Chem. Soc.* **1979**, 101, 5256.

34. a) Polson, M. I. J.; Taylor, N. J.; Hanan, G. S. *Chem. Comm.* **2002**, 1356. b) Medlycott, E. A.; Hanan, G. S.; Loiseau, F.; Campagna, S. *Chem. Eur. J.* **2007**, in press.
35. The driving force for electron-transfer was approximated using the expression $\Delta G = e(E_{ox.} - E_{red.})$, neglecting work terms and entropy contributions. Excited–state potentials (E^*) were determined using $E([Ru]^*/[Ru]^-) = E([Ru]/[Ru]^-) + E_{00}$ in the case of reductive-electron quenching, and $E([Ru]^+/[Ru]^*) = E([Ru]^+/[Ru]) - E_{00}$ in the case of oxidative electron-transfer, where E_{00} corresponds to the emission maxima at 77 K.
36. Balzani, V.; Scandola, F. *Supramolecular Photochemistry*, Horwood, Chichester, UK, **1991**.
37. Medlycott, E. A.; Hanan, G. S. *Chem. Soc. Rev.* **2005**, 34, 133.
38. Maestri, M.; Armaroli, N.; Balzani, V.; Constable, E. C.; Thompson, A. M. W. C. *Inorg. Chem.* **1995**, 34, 2759.
39. Byrnes, M. J.; Chisholm, M. H.; Gallucci, J. A.; Liu, Y.; Ramnauth, R.; Turro, C. *J. Am. Chem. Soc.*, **2005**, 127, 17343.
40. Cooke, M. W.; Wang, J.; Theobald, I.; Hanan, G. S. *Synthetic Commun.* **2006**, 36, 1721.
41. Storrier, G. D.; Colbran, S. B. *Inorg. Chim. Acta* **1999**, 284, 76.
42. Rempel, G. A.; Legzdins, P.; Smith, H.; Wilkinson, G. *Inorg. Synth.* **1972**, 13, 90.
43. Johnson, S. A.; Hunt, H. R.; Neumann, H. M. *Inorg. Chem.* **1963**, 960.
44. Sullivan, B. P.; Calvert, J. M.; Meyer, T. J. *Inorg. Chem.* **1980**, 19, 1404.

Chapter 3: A Novel Series of Linear Dicarboxylate "Ligands" Based on the $Ru(tpy)_2^{2+}$ Motif: Asymmetric and Symmetric $Rh_2(II,II)$-Capped Complexes and an Unexpected Porous Structure

3.1 Introduction

Polytopic carboxylic acids, and their anionic counterparts, are heavily valued in the domain of supramolecular chemistry owing to their amenability toward formation of both discrete and extended coordination-based structures with promising applications.[1, 2] Within this realm, supramolecular architectures based upon the classical paddlewheel motif exhibited by metal-dimer complexes pioneered by Cotton and co-workers have emerged as a valued building-block from which to design such frameworks.[3] From an architectural perspective, this is evident since the motif is highly symmetric and rigid. However, such an approach is also well-suited for the design of *functional* supramolecular materials since most transition metals have been found to adopt such a dimeric motif, and thus a wide range of electronic and magnetic properties are accessible for exploitation.[4]

With respect to these points, we have demonstrated the utility of the dimetal paddlewheel motif of dirhodium(II,II) tetraacetate toward generation of polynuclear ruthenium(II) bis-terpyridyl systems wherein the ruthenium(II) complexes have been equipped with peripheral carboxylic acid functionality to allow for conventional ligand displacement on the dirhodium core.[5] These systems are structurally well-defined and sufficiently robust, attributable to the inherent kinetic inertness of dirhodium(II,II) carboxylates. Moreover, we have demonstrated efficient energy transfer to the non-emissive state of the dirhodium(II,II) unit that may be attenuated by modification of the emissive state of the appended ruthenium(II) complex.[6] In this respect, the dimeric unit may act as an energy reservoir and thus serve dual structural and functional roles, the latter of which is underscored by the recent elucidation of the emissive and non-emissive states of related dimeric units.[7]

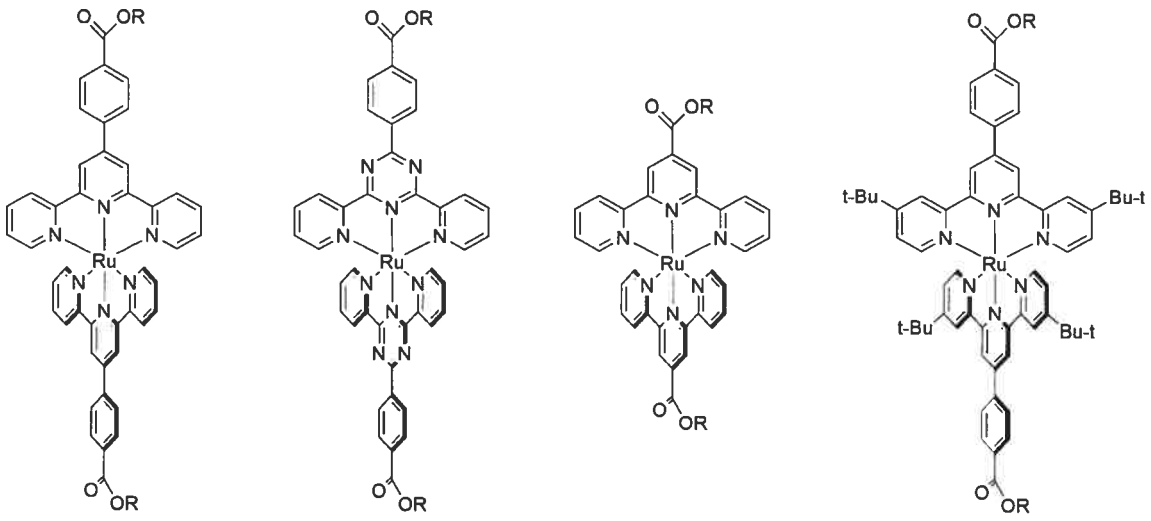

Figure 3.1. Series of dicarboxylate Ru(II) complexes and their methyl ester precursors.

As an extension of this work, we have prepared a series of homoleptic, dicarboxylic acid functionalized $(tpy)_2Ru^{2+}$ complexes (Figure 3.1) suitable for binding dimetal units in a linear fashion. Such "dimer of dimer" complexes have been heavily investigated by Chisholm and Cotton, particularly in the context of the relatively kinetically labile dimolybdenum(II,II) tetracarboxylate and ditungsten(II,II) tetracarboxylate motifs, owing to their ideal nature for studying electronic coupling and mixed-valency.[8] To our knowledge, no examples of such complexes have been reported utilizing a cationic bridging ligand, nor have non-symmetric complexes bearing just one dimetal unit connected the bridge. Herein we show how utilizing the former can yield surprising reaction control to give both symmetric and non-symmetric dimetal-bridging systems by means typically unsuited to the formation of discrete structures using dicarboxylates. Moreover, to counter the high degree of insolubility of such dicarboxylic acid complexes, an expedient synthetic protocol for installation of solubilizing t-butyl groups at the 4,4''-pyridyls of the terpyridine ligand is described.

The synthesis of bridged dimeric complexes of the form M_2-bridge-M_2 (where M = Mo or W) is most commonly accomplished by stirring the $M_2(O_2CR)_4$ precursor (where R is commonly ^{t}Bu) with the HO_2C-R'-CO_2H bridge in a non-coordinating solvent in the absence of oxygen, during which time the desired M_2-bridge-M_2 species precipitates from solution (Eqn. 3.1). Considering that this reaction is in equilibrium, one can either

remove acetic acid or precipitate the product to arrive at acceptable yields. Given the sensitivity of the dimeric materials, one must rely on precipitating the M_2-bridge-M_2 species, and so solvent selection (and also bridge selection) is critical. In addition, Mo_2 and W_2 dimeric units readily undergo ligand displacement / scrambling of their carboxylates and,[9] considering the possibility for *cis / trans* substitution, uncontrolled polymer/oligomer formation may proceed.[10] Thus, the reaction is typically performed at room temperature and requires a considerable amount of time (~ 1 week). Moreover, once isolated, the M_2-bridge-M_2 species must be handled with care, considering its oxygen sensitivity and its susceptibility to ligand scrambling and disproportionation.

$$2\ M_2(O_2CR)_4 + HO_2C\text{-}R'\text{-}CO_2H \underset{\text{r.t.}}{\overset{\text{toluene}}{\rightleftharpoons}} (O_2CR)_3M_2(O_2C\text{-}R'\text{-}CO_2)M_2(O_2CR)_3 + 2\ HO_2CR$$

Equation 3.1. 'One-pot' dimer-bridge-dimer formation from a dicarboxylic acid.

Considering that amidinates are relatively more basic than carboxylates and are not subject to ligand scrambling, Cotton and co-workers have prepared mixed dimeric units of the forms $[M_2(am)_{4-n}(CH_3CN)_{2n}]^{n+}$,[11] $[M_2(am)_{4-n}(X_{2n})]$,[12] and $M_2(am)_{4-n}(O_2CR)_n$ (am = amidinate, X = monodentate anion).[13] Such building blocks have enabled the controlled synthesis of various robust supramolecular architectures,[3, 14] including M_2-bridge-M_2 species,[15] without the deleterious production of oligomeric species. Here, monodentate solvent or anionic equatorial ligands are selectively displaced during metathesis reactions with suitable dicarboxylate salts (Eqn. 3.2), or labile carboxylates are displaced in a manner akin to Eqn. 3.1, but at elevated temperature and with reduced reaction times.

$$2\ [M_2(am)_3(CH_3CN)_2](BF_4) + [{}^tBu_4N]_2[O_2C\text{-}R\text{-}CO_2] \longrightarrow (am)_3M_2(O_2C\text{-}R\text{-}CO_2)M_2(am)_3 + 2\ [{}^tBu_4N](BF_4) + 4\ CH_3CN$$

Equation 3.2. Dimer-bridge-dimer formation by metathesis with a dicarboxylate salt.

However, the cationic dicarboxylic acid ligands **III-2b** and **III-3b, III-4** are not amenable to the metathesis procedures mentioned above for two main reasons. The first is the inability to cleanly prepare suitable dicarboxylate salts owing to the presence of

requisite counter-anions associated with the ruthenium(II) complex. The second reason stems from electrostatic considerations in that cationic precursors of the form $[M_2(am)_{4-n}(CH_3CN)_{2n}]^{n+}$ have proven to be essentially non-reactive to carboxy-functionalized cationic ruthenium(II) complexes. Such non-reactivity is consistent with observations made previously regarding appendage of related complexes to $Rh_2(O_2CCF_3)_4$.[6] In this regard, precursors of the form $M_2(am)_{4-n}(O_2CR)_n$ are likely more suited as building-blocks for polynuclear arrays based upon ruthenium(II) polypyridyls since the presence of amidinates may serve to buffer such electrostatic effects.

3.2 Synthesis and Characterization of Diacid Precursor Complexes (refer to page XVIII of Appendix 3 for X-ray data and parameters for complex **III-1b (PF_6)**)

Though the dimethyl ester precursors **III-1a-II-3a $(PF_6)_2$** could be prepared in modest to high yield upon reflux of the appropriate methylcarboxy-tpy ligand with 0.5 eq. of $RuCl_3$ and 3 eq. of $AgNO_3$, the high degree of insolubility of the related dicarboxylic acids **III-1b-III-3b $(PF_6)_2$** precludes their direct formation by complexation of the carboxy-tpy ligands. However, solubility of **III-1b $(PF_6)_2$** was sufficient to grow single crystals suitable for structure determination by X-ray diffraction. The ratio of counter-anions to ruthenium(II) complex is 1:1 and denotes a formal de-protonation. The molecular structure is depicted below in Figure 3.2, along with selected bond lengths and angles. Partial packing diagrams are shown below in Figures 3.3 and 3.4, wherein an inversion center relates oppositely propagating polymeric chains based upon a hydrogen bonding interaction. Reasonably close association of the pendant pyridyl rings with the phenyl spacer of adjacent molecules suggests potential "face-to-face" (3.5-3.7 Å) and "edge-to-face" (3.0 Å) π-π interactions that may play a role in the intimate packing (Figure 3.2, b) reminiscent of the "tpy embrace" noted for other $M(tpy)_2^{2+}$ type complexes.[16]

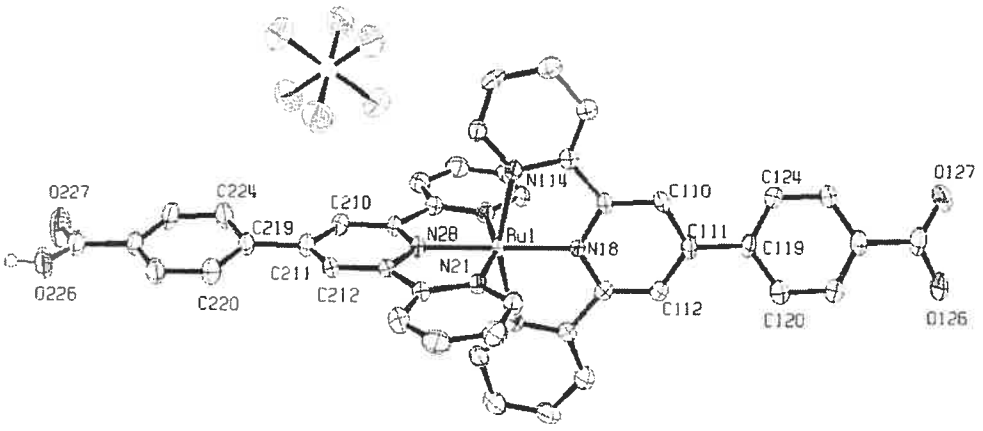

Selected Bond Angles (°)		**Selected Bond Distances (Å)**	
C_{110}-C_{111}-C_{119}-C_{124}	-35.5(8)	O_{127}-C	1.229(6), O_{126}-C 1.277(6)
C_{210}-C_{211}-C_{219}-C_{220}	-9.1(7)	O_{227}-C	1.222(6), O_{226}-C 1.299(6)
N_{18}-Ru-N_{21}	102.11(14)	N_{18}-Ru	1.978(3)
N_{18}-Ru-N_{114}	79.11(13)	N_{21}-Ru	2.077(3)

Hydrogen Bonding

D-H···A	**D-H (Å)**	**H···A (Å)**	**D···A (Å)**	**D-H···A (°)**
O_{126}-H_{126}···O_{226i}	0.83	1.68	2.491(4)	166.6
O_{226}-H_{226}···O_{126ii}	0.83	1.69	2.491(4)	161.7

Figure 3.2 ORTEP of **III-1b (PF_6)** (asymmetric unit). Carboxyl proton is disordered over O226 and O126. Thermal ellipsoids at 50 % probability. Aromatic hydrogen atoms are omitted for clarity. Oppositely propagating chain (related through inversion) defined by i, ii.

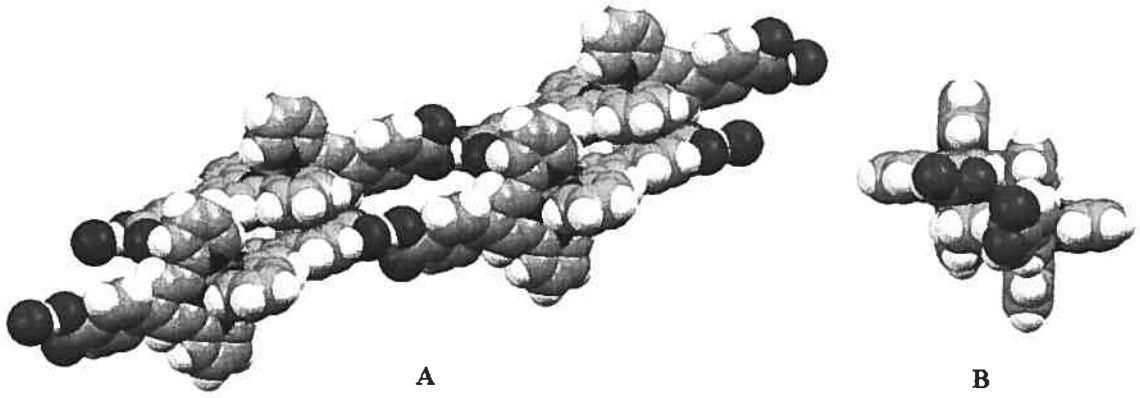

Figure 3.3. **A:** Partial packing diagram for complex **III-1b (PF_6)**. **B:** End-on view exhibiting "tpy embrace". Counter-anions have been omitted for clarity.

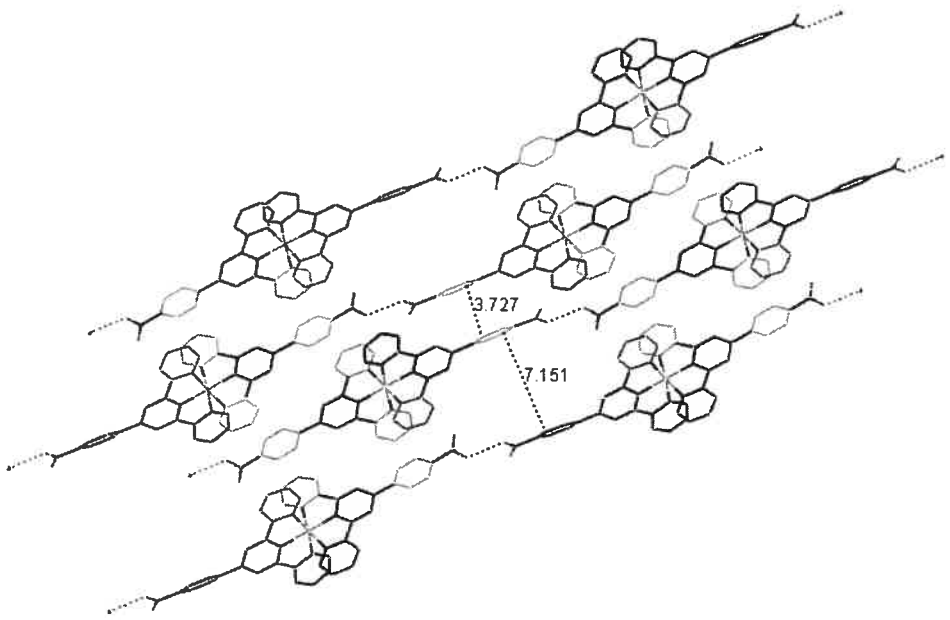

Figure 3.4 Simplified representation of hydrogen-bonding network in **III-1b (PF_6)** depicting intra (~ 7.1 Å) and inter-unit cell (~ 3.7 Å) relationships. Green aromatic rings denote possible "face-to-face" π interactions while red aromatic rings denote possible "edge-to-face" interactions with a perpendicular "green" neighbor. Protons and counter-ions are omitted for clarity.

With the exception of complex **III-3b (PF_6)$_2$**, insolubility of the diacid complexes outlined in Figure 3.1 precluded their characterization by ^{1}H NMR. However, their corresponding dimethyl ester analogues are abundantly soluble and hence amenable to such characterization. Two of these spectra are depicted below in Figures 3.5 and 3.6.

3.3 Synthesis and Characterization of Mono- and Bis-Rh_2(II,II) Appended Complexes (refer to page XXV of Appendix 3 for X-ray data and parameters for complex **III-5b (CH_3CN)$_4$(PF_6)$_2$)**

Using a mix of either DMF / H_2O or CH_3CN / H_2O provided sufficient solubility of these dicarboxylic acids to permit appendage of dirhodium(II,II) units at elevated temperatures and with reasonable reaction durations (Scheme 3.3) to give the symmetric and asymmetric dimer-capped complexes shown in Figure 3.7, all of which are sufficiently stable for column purification on silica gel.

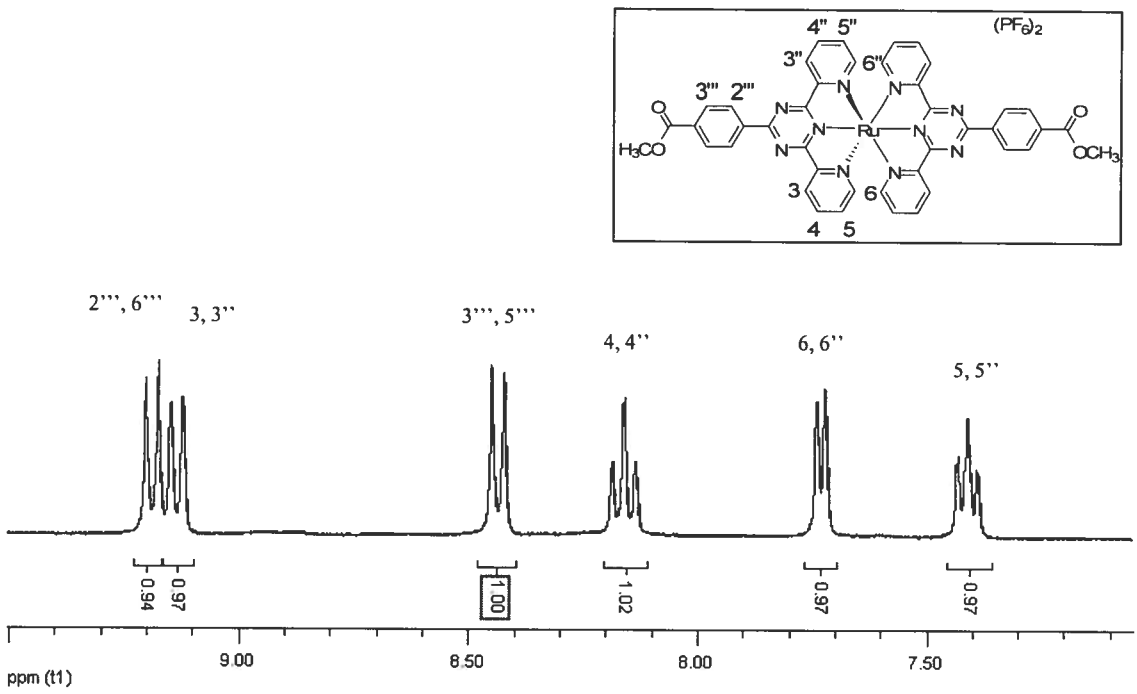

Figure 3.5 ^{1}H NMR spectrum of complex **III-2a $(PF_6)_2$** in CD_3CN (aromatic region). Methyl resonance at 4.02 ppm (not shown).

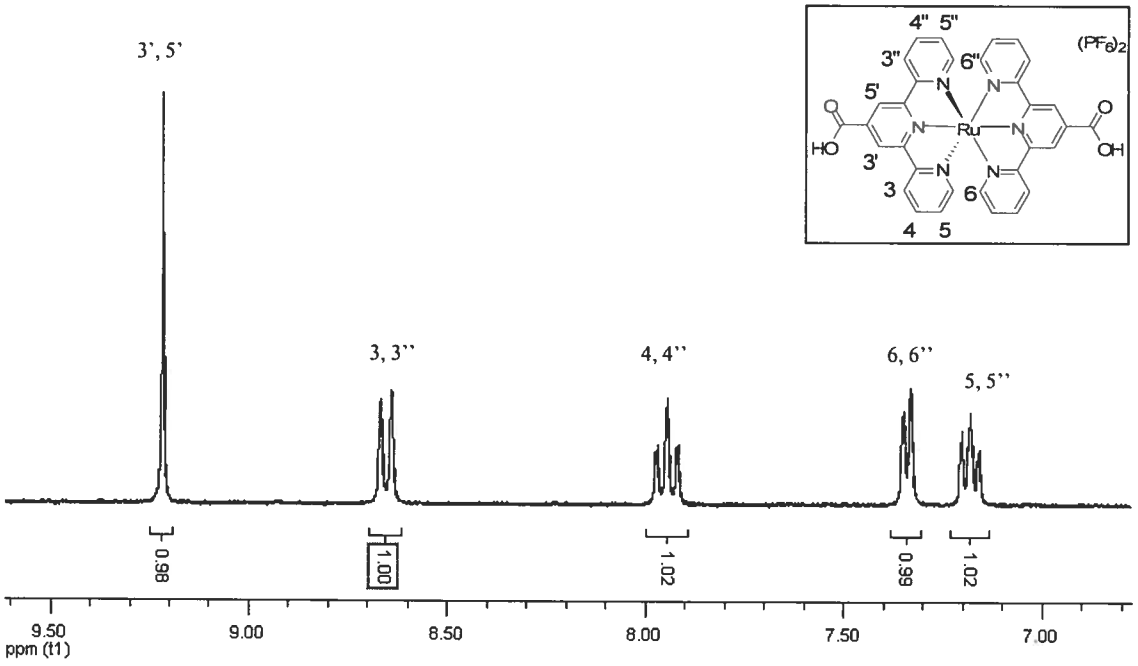

Figure 3.6 ^{1}H NMR spectrum of complex **III-3b $(PF_6)_2$** in CD_3CN (aromatic region).

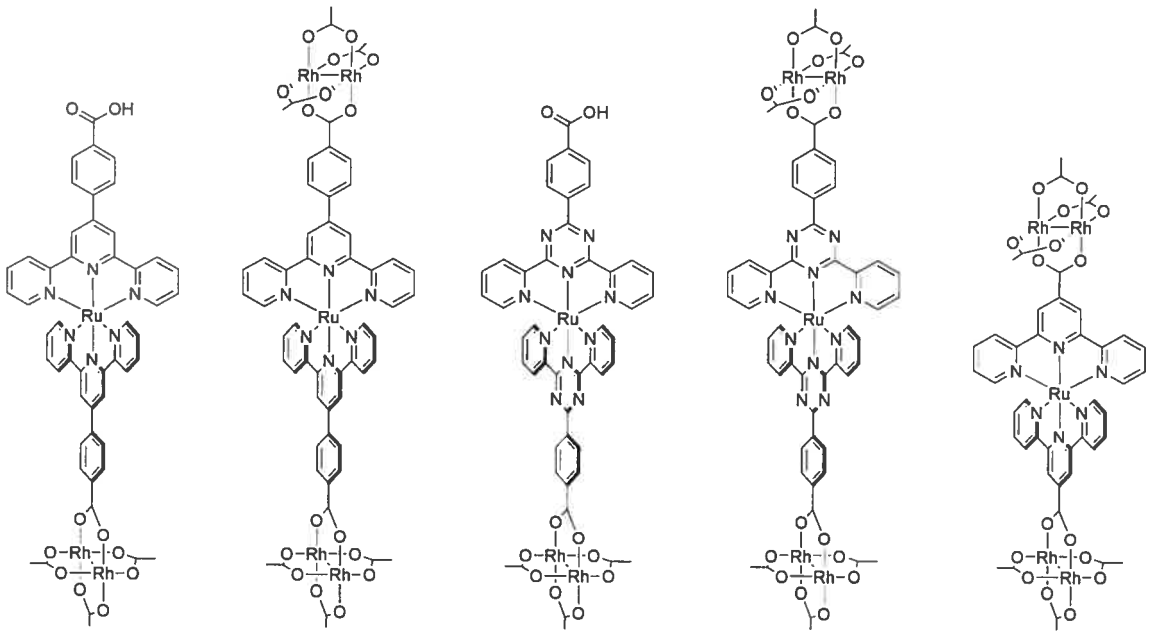

Figure 3.7. Series of Rh_2-appended dicarboxylate complexes.

^{1}H NMR of these symmetrically and asymmetrically Rh_2-appended complexes are shown in Figures 3.8-3.13. These spectra provide unambiguous assignment of their identity and degree of substitution, which is aided in particular by relative integration of the acetate resonances located between 1-2 ppm.

$$\begin{matrix} \text{III-1b } (PF_6)_2 \\ \text{III-2b } (PF_6)_2 \\ \text{III-3b } (PF_6)_2 \end{matrix} + 2\ Rh_2(O_2CCH_3)_4(CH_3OH)_2 \underset{CH_3CN\ ^b}{\overset{6:1\ DMF/H_2O\ ^a}{\rightleftharpoons}} \begin{matrix} \text{III-5a } (PF_6)_2 \text{ (44\%)} \\ \text{III-5b } (PF_6)_2 \text{ (28\%)} \\ \text{III-6a } (PF_6)_2 \text{ (39\%)} \\ \text{III-6b } (PF_6)_2 \text{ (26\%)} \\ \text{III-7 } (PF_6)_2 \text{ (56\%)}^c \end{matrix}$$

Equation 3.3 Synthesis of Rh_2-appended dicarboxylate complexes. (a) 100°C for 24 h, used for complexes **III-5a $(PF_6)_2$**, **III-5b $(PF_6)_2$** and **III-6a $(PF_6)_2$**, **III-6b $(PF_6)_2$**. (b) At reflux temperature for 40 h, used for complex **III-7 $(PF_6)_2$**. (c) For which 8 equivalents $Rh_2(O_2CCH_3)_4(CH_3OH)_2$ were used. Yields are based on recovered diacid complexes.

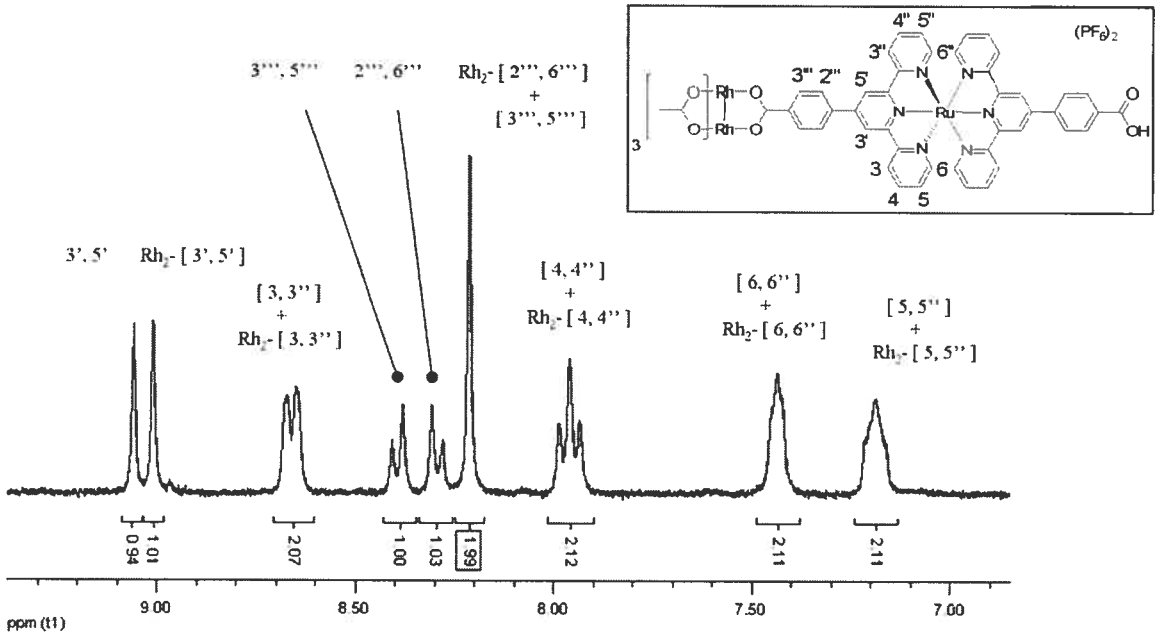

Figure 3.8 ^{1}H NMR spectrum of **III-5a $(PF_6)_2$** in CD_3CN (aromatic region).

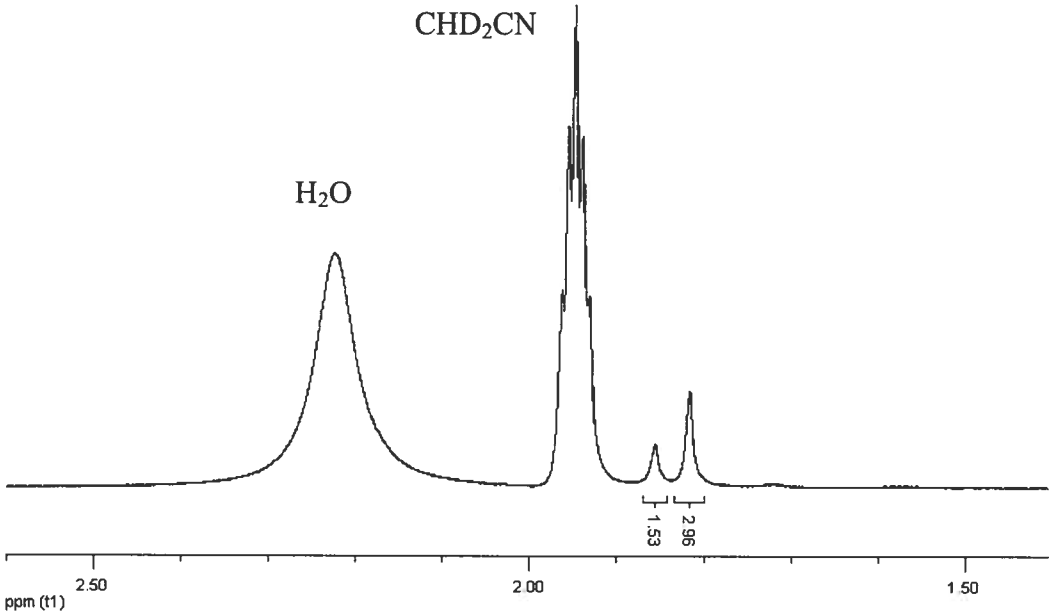

Figure 3.9 ^{1}H NMR spectrum of **III-5a $(PF_6)_2$** in CD_3CN (acetate resonances).

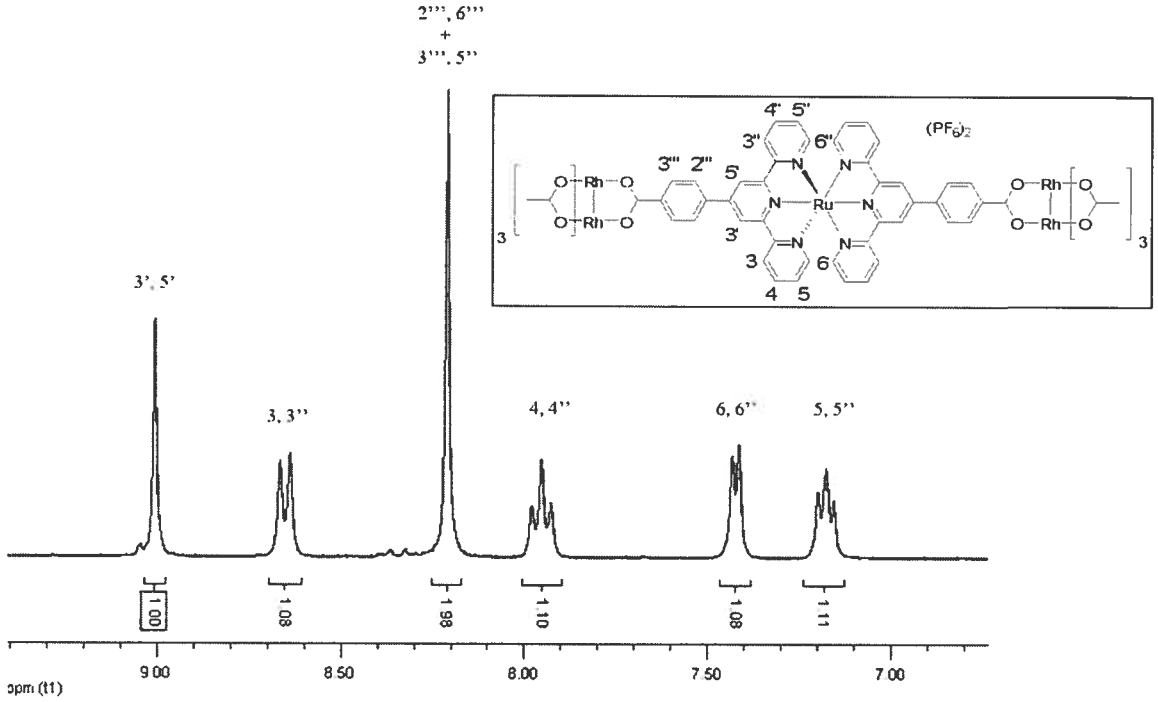

Figure 3.10 ^{1}H NMR spectrum of **III-5b $(PF_6)_2$** in CD_3CN (aromatic region). Methyl resonances at 1.86 ppm (6 H) and 1.82 ppm (12 H) not shown.

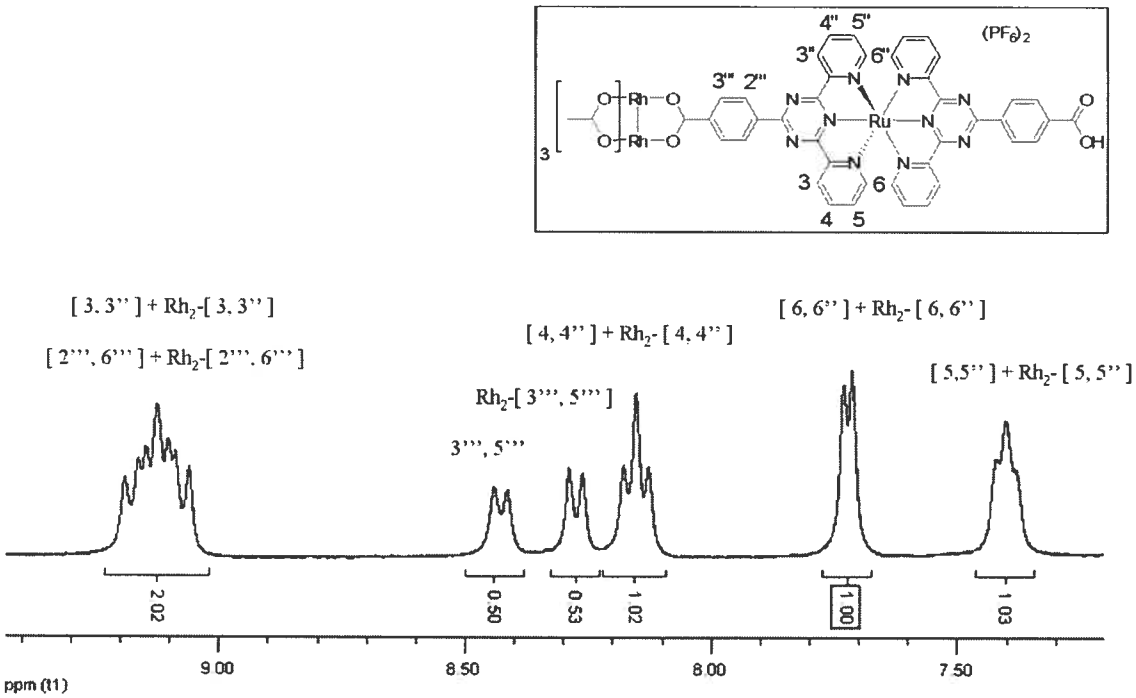

Figure 3.11 ^{1}H NMR spectrum of **III-6a $(PF_6)_2$** in CD_3CN (aromatic region). Methyl resonances at 1.86 ppm (3 H) and 1.82 ppm (6 H) not shown.

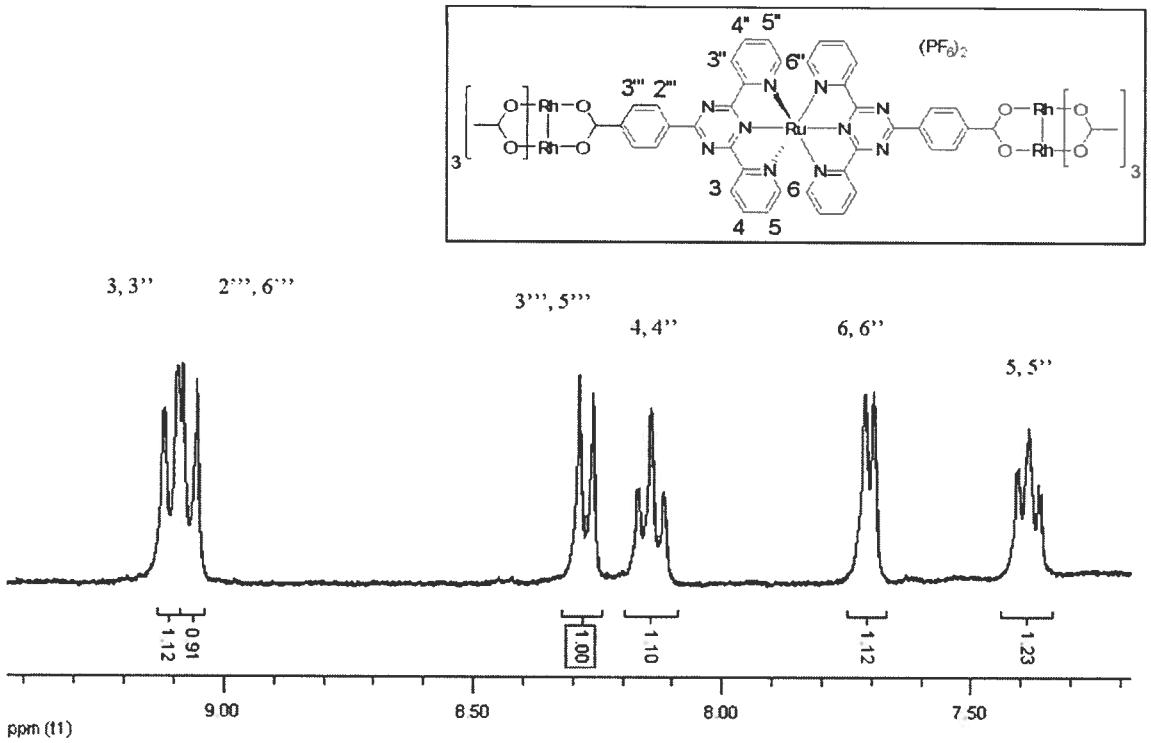

Figure 3.12 ^{1}H NMR spectrum of **III-6b $(PF_6)_2$** in CD_3CN (aromatic region). Methyl resonances at 1.86 ppm (6 H) and 1.82 ppm (12 H) not shown.

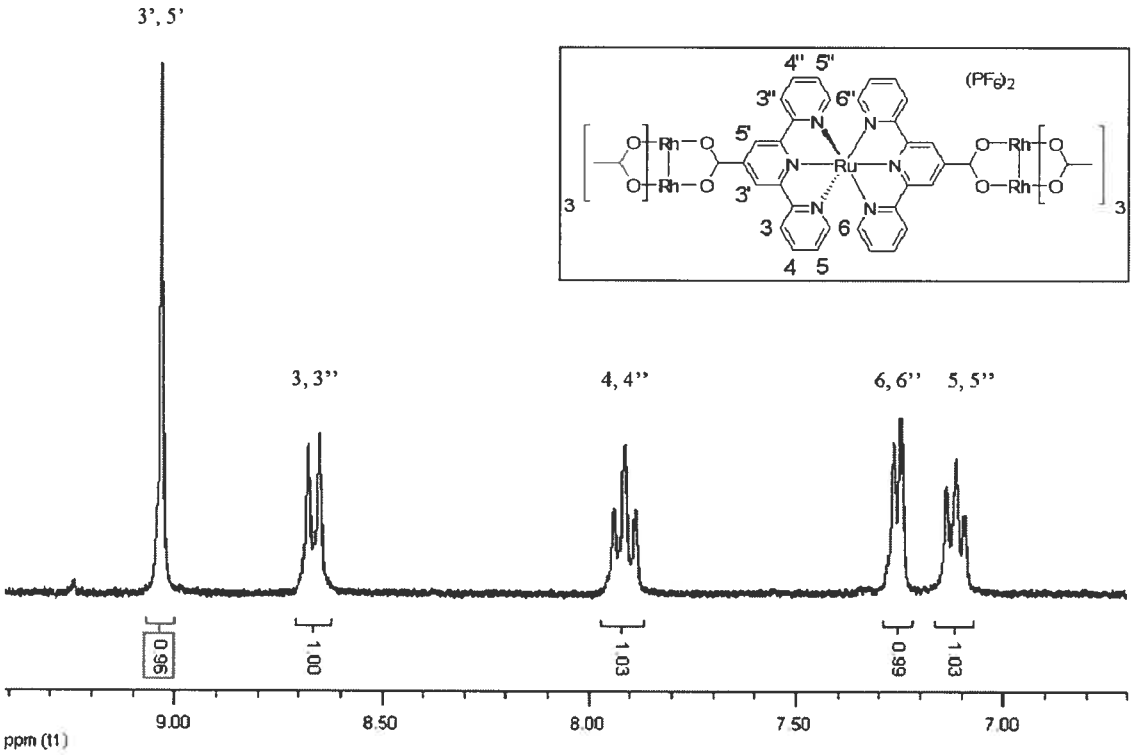

Figure 3.13 ^{1}H NMR spectrum of **III-7 $(PF_6)_2$** in CD_3CN (aromatic region). Methyl resonances at 1.88 ppm (6 H) and 1.86 ppm (12 H) not shown.

Coordination of the dimer leads to pronounced electronic effects, as evidenced by the asymmetry of the spectra for the partially substituted species **III-5a $(PF_6)_2$**. Here, the resonances of the 3', 5' protons of the central pyridyl ring and those of the phenyl group (between 9.10-8.90 ppm and 8.50-8.10 ppm, respectively) are split, with components stemming from proximity to the dirhodium(II,II) unit being located downfield by ~ 0.1 ppm relative to those of the non-coordinated carboxy group, indicating an electron-releasing effect by the dimer. Moreover, the phenyl doublets occur as a characteristic 'doublet of doublets' at 8.35 ppm for an uncoordinated moiety but are merged into a single peak at 8.20 ppm upon complexation to the dimer. As expected, the spectra of the symmetric species **III-5b $(PF_6)_2$** is relatively simplified.

Complexes **III-5b** and **III-6a** could be crystallized as their PF_6^- salts from acetonitrile / toluene solutions upon vapour diffusion of isopropylether. However, single crystals of suitable quality could only be obtained for complex **III-5b $(PF_6)_2$**, the structure of which is depicted below as the acetonitrile adduct (Figure 3.14) wherein the molecular unit lies on a mirror plane.

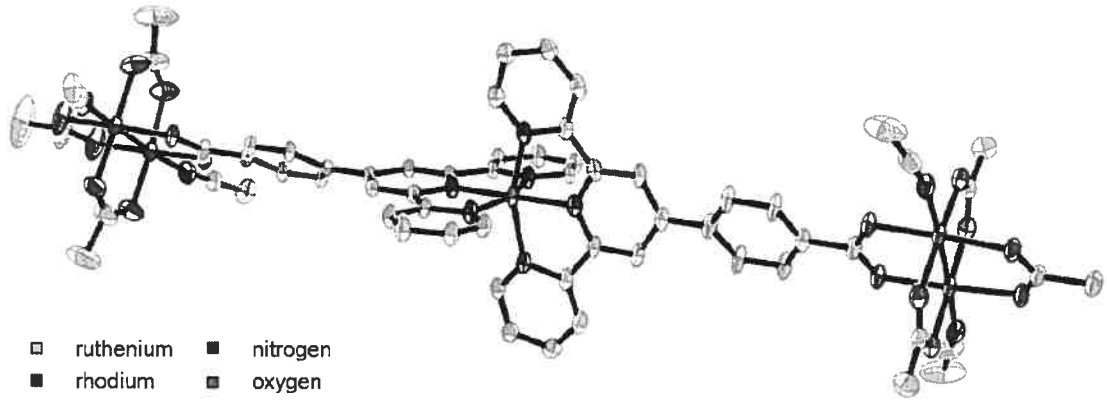

Figure 3.14 X-ray crystal structure of complex **III-5b $(CH_3CN)_4(PF_6)_2$** with thermal ellipsoids at 50 % probability. Solvent and counter-ions have been omitted for clarity.

Bond lengths and angles related to the $(tpy)_2Ru^{2+}$ fragment are, as expected, essentially unchanged relative to that for the precursor diacid complex discussed in Section 3.2. The absence of an inversion center gives two unique Rh_2 units, each of which displays a paddlewheel motif typical of other $Rh_2(O_2CR)_4$ complexes.[4] In addition, two unique tpy-phenyl torsion angles exist, corresponding to 28.3 (4) ° and 33.5 (3) °.

The Rh-Rh bond lengths are 2.3933 (9) Å and 2.3913 (9) Å, while the Rh-$N_{(axial)}$ bond distances to ligated CH_3CN are, respectively, 2.231 (6) Å and 2.233 (7) Å.

It was noted in Chapter 2 that there existed a significant difference in the Rh-O bond lengths associated with the acetates and the carboxy-appended Ru(II) complex, such that the former was significantly shortened (~ 0.1 Å) relative to values typically reported for similar complexes. The origin of this was ascribed to electrostatic effects, wherein the acetates are drawn closer to the dimetal core to help buffer electrostatic repulsion between the cationic Rh_2^{4+} core and the $(tpy)_2Ru^{2+}$ moiety. In this case, the Rh-O bond lengths are relatively uniform considering that variations on the order of ~ 0.01 Å have been attributed to packing effects. The Rh-O bond distances to the bridging Ru(II) complex are, for each unique dimetal unit, 2.036 (3) Å and 2.023 (3) Å. The Rh-$O_{acetate}$ bond distances range from 2.034 (4) - 2.042 (3) Å in the former case, and from 2.009 (4)-2.027 (5) Å in the latter. This should not discount the aforementioned explanation, considering that the formal overall charge here in complex **III-5b $(PF_6)_2$** is only half that of complex **II-3a(*trans*) $(PF_6)_4$**. As such, any real variation may be lost in the consequence of such packing effects.

3.4 Electrochemistry

It has been ascertained that the principal bonding interactions responsible for electronic coupling in such dimer-bridge-dimer complexes involve the M_2 δ and bridge π^* molecular orbitals.[17] Since the M_2 δ-orbital is also the HOMO for quadruply-bonded metal-dimer species, it is involved in electrochemical oxidation and reduction processes. As such, inter-dimer electronic coupling in symmetric systems based upon dimolybdenum(II,II) and ditungsten(II,II) are ideally suited to electrochemical assessment. With regard to dirhodium(II,II) systems, the M_2–based HOMO is of doubly degenerate π^* symmetry which, along with their kinetic resilience to ligand scrambling and affinity for axial ligation, highlights their primarily structural role with regard to polynuclear dimer-based systems.[3e,f, 14a,b,d] Here, electrochemical investigation using cyclic and square-wave voltammetry provides additional confirmation as to the composition of these complexes since the appended Ru(II) bis-terpyridyl complex undergoes a characteristic reversible / quasi-reversible $Ru^{3+/2+}$ process in the vicinity of the $Rh_2^{5+/4+}$ couple (see Figures 3.15-3.19). All electrochemical data for both the

precursor and dimer-appended complexes is summarized in Table 3.1. While the $Ru^{3+/2+}$ and $Rh_2^{5+/4+}$ couples were not resolved for the mixed-metal complexes **III-5a $(PF_6)_2$** and **III-5b $(PF_6)_2$**, they were for the analogous triazine complexes **III-6a $(PF_6)_2$** and **III-6b $(PF_6)_2$**, as well as for complex **III-7 $(PF_6)_2$**. The parentage of the metal-centered processes in these mixed-metal complexes is made based on similarity to those for the parent homometallic complexes and based on their relative integration for reversible one-electron processes (Table 3.1). In some cases, additional irreversible reduction processes in the range of -0.5 to -1.0 V appear (see Figures 3.15, 3.16, 3.19). These may be due to trace impurities adsorbed onto the electrode surface, but are more likely due to the presence of water and / or the emergence of the characteristically irreversible $Rh_2^{4+/3+}$ couple.

The ruthenium(II) complexes incorporating a triazine moiety are electron deficient relative to their purely tpy-based analogues, resulting in a somewhat reduced ligand field and an anodically displaced $Ru^{3+/2+}$ couple.[18] This is valuable in helping to resolve the metal-centered processes (Figures 3.17 and 3.18). In addition, the first one-electron triazine-based reduction at ~ -0.7 V (vs SCE) is well resolved into two processes in the homoleptic complex **III-2b $(PF_6)_2$** (ΔE_c = 170 mV), indicating significant stabilization of a reductive intermediate, the electronic-coupling contribution of which is very likely supported by co-planarity induced through hydrogen-bonding between the nitrogen lone-pairs of the triazine moiety and the 2,6 protons of the phenyl ring.[18] Such splitting is also evident for complex **III-6b $(PF_6)_2$** ((ΔE_c = 190 mV), and suggests that such a bridging unit may provide for efficient electronic coupling between termini despite a tip-to-tip distance of ~ 22 Å.[19] This is additionally significant considering the scarcity of such long-range coupling found in the literature.[20] Lastly, the chemical reversibility of the metal-centered processes for the mixed-metal complexes is indicative of their integrity in general. However, it should be noted that complex **III-5b $(PF_6)_2$** did exhibit a degree of chemical irreversibility upon repeated cycling of the metal-centered processes such that a shoulder became increasingly apparent on the return anodic sweep (Figure 3.16). The origin is uncertain but may be due to decomposition at oxidation potentials at or exceeding that for the $Ru^{3+/2+}$ couple, considering that variation of the magnitude of the cathodic switching potential had no effect. Complexes **III-6b $(PF_6)_2$** and **III-7 $(PF_6)_2$**, however, did not exhibit such behaviour.

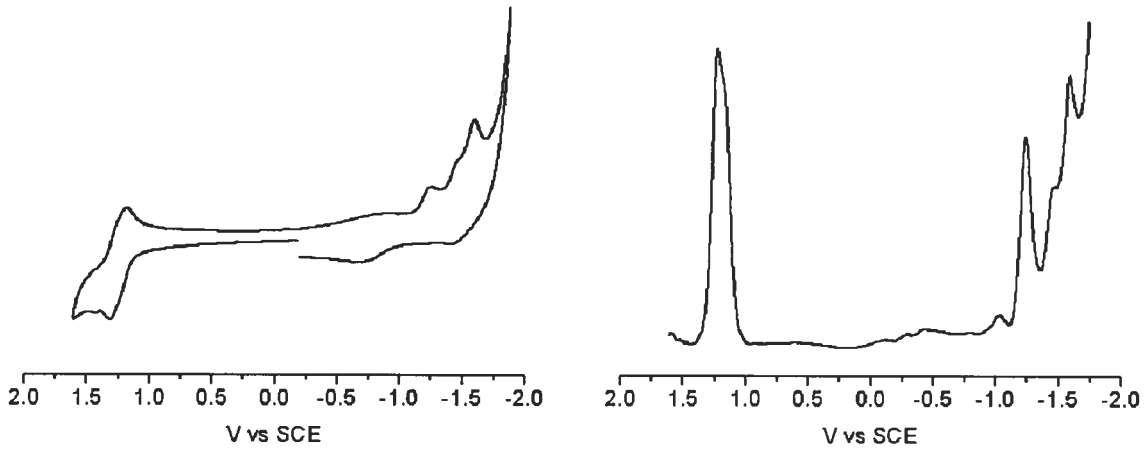

Figure 3.15 Cyclic voltammogram (left) and Square-wave voltammogram (right) of complex **III-5a $(PF_6)_2$** at 100 mVs^{-1}.

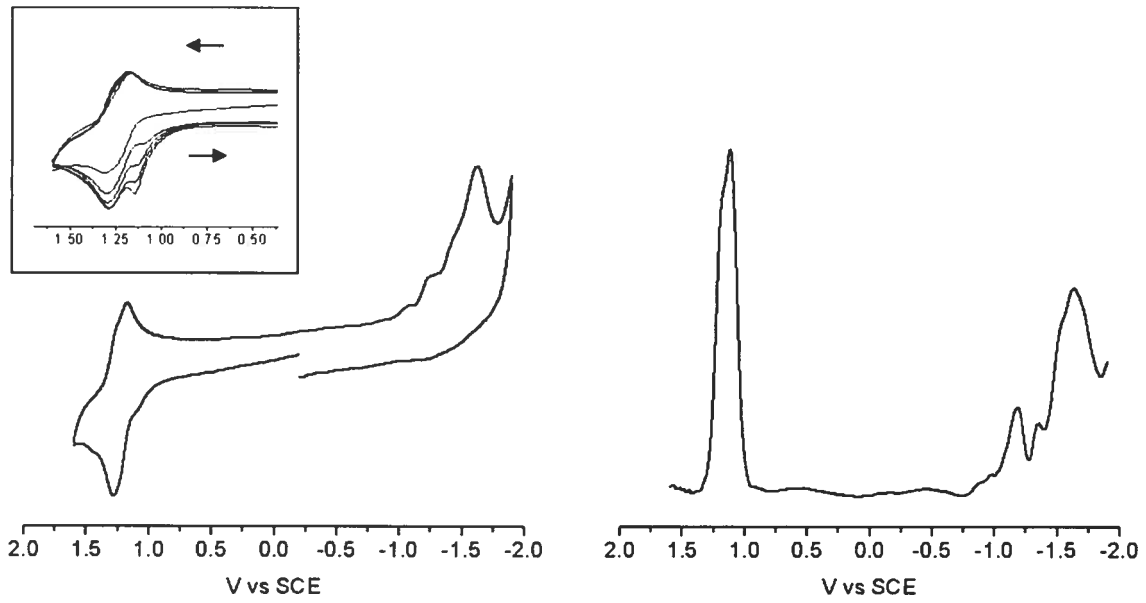

Figure 3.16 Cyclic voltammogram (left) and square wave voltammogram (right) of complex **III-5b $(PF_6)_2$** at 100 mVs^{-1} with cycled decomposition shown as inset.

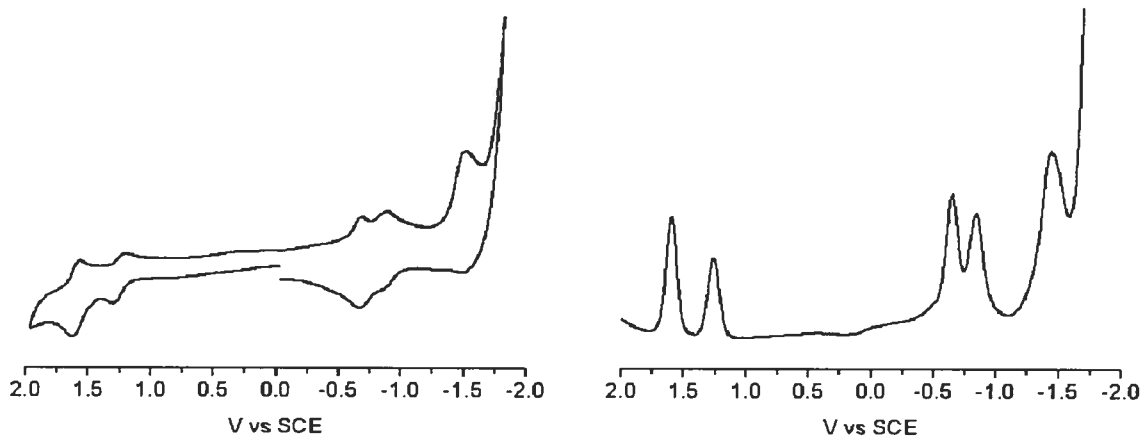

Figure 3.17 Cyclic voltammogram (left) and square wave voltammogram (right) of complex **III-6a $(PF_6)_2$** at 100 mVs^{-1}.

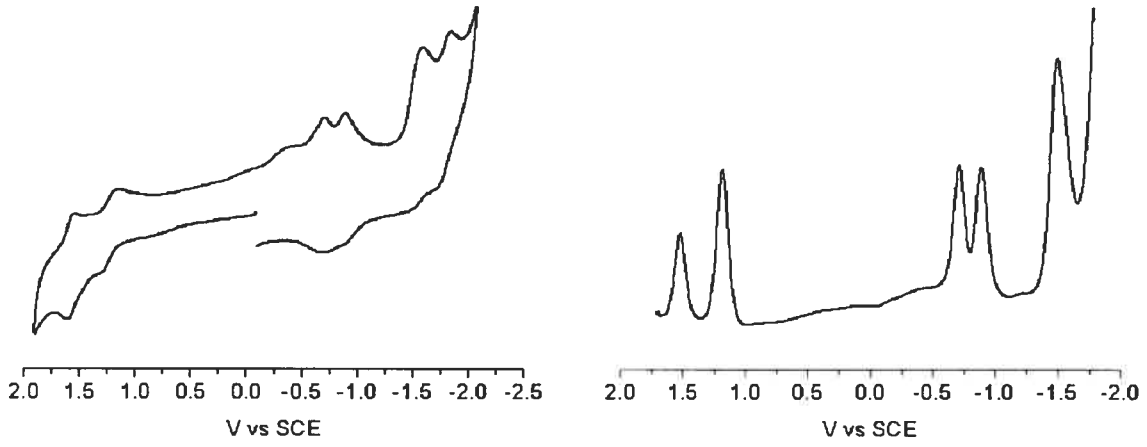

Figure 3.18 Cyclic voltammogram (left) and square wave voltammogram (right) of complex **III-6b $(PF_6)_2$** at 100 mVs^{-1}.

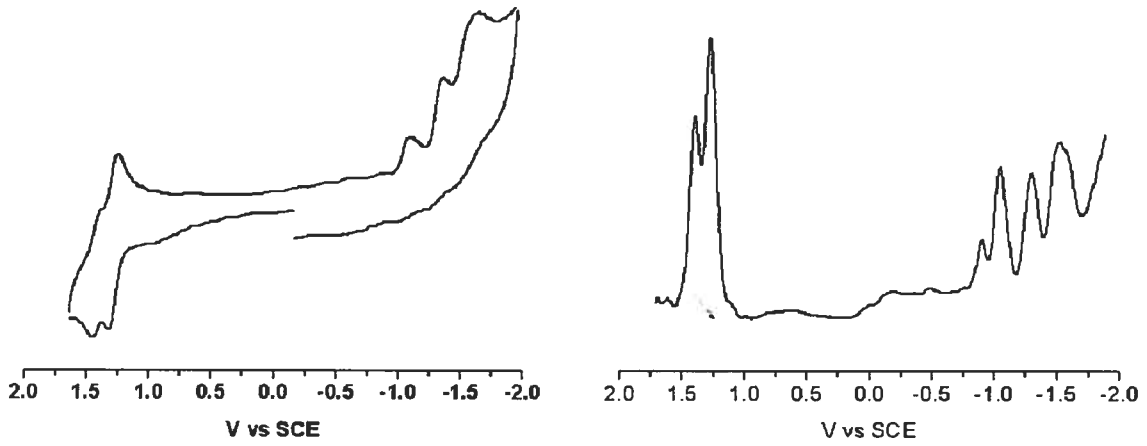

Figure 3.19 Cyclic voltammogram (left) and square wave voltammogram (right) of complex **III-7 $(PF_6)_2$** at 100 mVs^{-1}.

Table 3.1 Electrochemical Data.

Cpd	Potential [V] vs SCE. ΔE_p (mV)[a]						
	$Ru^{3+/2+}$	$Rh_2^{5+/4+}$	i_{Ru}/i_{Rh2} [c]	Ligand Red.			
III-1a	1.22 (90)	-		-1.27 (70)	-1.51 (90)	-1.70 (80)	-
III-2a	1.56 (80)	-		-0.68 (60)	-0.85 (60)	-1.47 (80)	-1.70 (80)
III-3a	1.42 (70)	-		-0.99 (60)	-1.25 (60)	-	-
III-3b	1.40 (80)	-		-1.37 (60)	-1.61 (80)	-	-
III-4	1.22 (70)	-		-1.25 (60)	-1.45 (irr)	-1.52 (70)	-
III-5a	1.26 (130)	-		-1.24 (irr)	-1.46 (irr)	-1.60 (irr)	-
III-5b	1.22 (110)[b]	-		-1.18 (irr)	-1.35 (irr)	-1.63 (irr)	-
III-6a	1.60 (60)	1.26 (90)	1.8	-0.69 (irr)	-0.89 (irr)	-1.52 (irr)	-
III-6b	1.58 (70)	1.23 (120)	0.5	-0.70 (irr)	-0.89 (irr)	-1.59 (irr)	-1.84 (irr)
III-7	1.42 (70)	1.28 (70)	0.5	-1.09 (irr)	-1.36 (irr)	-1.63 (irr)	-

a) Cyclic voltammogram scan rate is 100 mV s^{-1}. $E_{1/2}$ = ½ (E_{pa} + E_{pc}), where E_{pa} and E_{pc} are the anodic and cathodic peak potential, respectively. $\Delta E_p = E_{pa} - E_{pc}$. Reported values for irreversible processes, labeled irr, are peak potentials taken from the corresponding square-wave voltammograms. Potentials are corrected by internal reference to ferrocene (395 mV vs SCE). Data was recorded in 0.1 M $TBAPF_6$ / CH_3CN solution.

b) Irreversible shoulder observed in cathodic scan direction at 1.25 V for single scan.

c) $Ru^{3+/2+}$ / $Rh_2^{5+/4+}$ current ratios determined by relative integration of current responses observed in their respective square-wave voltammograms.

3.5 Electronic Absorption

The electronic absorption data is summarized in Table 3.2 below. The distinguishing absorption features normally associated with $Rh_2(OAc)_4$ [21] are two bands in the visible at 552 nm and 437 nm in CH_3CN, both of which are quite weak ($\varepsilon = 235$ and 112 $M^{-1}cm^{-1}$, respectively) and have been assigned to $\pi^*(Rh_2) \rightarrow \sigma^*(Rh_2)$ and π (Rh-O) $\rightarrow \sigma^*$(Rh-O) transitions, respectively. Relatively more intense bands can be found at 250 nm ($\varepsilon \approx 6000$ $M^{-1}cm^{-1}$) and 220 nm ($\varepsilon \approx 18000$ $M^{-1}cm^{-1}$), the former of which has not been assigned while the latter has been attributed to a $\sigma(Rh_2) \rightarrow \sigma^*(Rh_2)$ transition. As such, the absorption characteristics and profiles of these adducts are dominated by the appended ruthenium complex, resembling strongly the absorption spectra of other ruthenium(II) polypyridyl complexes.[22] A spin-allowed metal-to-ligand charge transfer (MLCT) band, assigned as a Ru(II)-to-tpy transition, is found in the visible region at ~490 nm for those complexes derived from tpy and at ~ 500 nm for those derived from the triazine analogue. The UV region is dominated by ligand centered (LC) transitions of $\pi \rightarrow \pi^*$ and $n \rightarrow \pi^*$ parentage, stemming from the tridentate ligand coordinated to Ru(II).

The ruthenium(II) complexes incorporating dirhodium(II) acetate units show no significant shifts in band maxima relative to the methylcarboxy ruthenium(II) complexes from which they derive. However, a marked change in the intensity of these transitions is noted upon incorporation of the dimetal units which is well beyond that arrived at from summation of contributions from the individual components. This is attributable, in part, to changes in the spectral envelope for certain transitions upon complexation to the dimer. This is apparent when comparing the MLCT bands of complexes **III-1a $(PF_6)_2$** and **III-5b $(PF_6)_2$**, for which incorporation of the dimer has significantly sharpened the MLCT profile (Figure 3.20). However, the spectral profiles of complexes **III-5a $(PF_6)_2$** and **III-5b $(PF_6)_2$** are quite similar, as are those of **III-6a $(PF_6)_2$** and **III-6b $(PF_6)_2$** relative to the related complex **III-2a $(PF_6)_2$**. As such, marked changes in intensity are interpreted as reflecting, to some degree, electronic mixing between the dimeric units and the bridging complex ligand. This is particularly noted upon comparing complexes **III-5a $(PF_6)_2$** and **III-5b $(PF_6)_2$**, where incorporation of a second dimetal unit leads to an increase in absorption for both MLCT and ligand-centered transitions by ~ 7000 and 15000 $M^{-1}cm^{-1}$, respectively (Table 3.2).

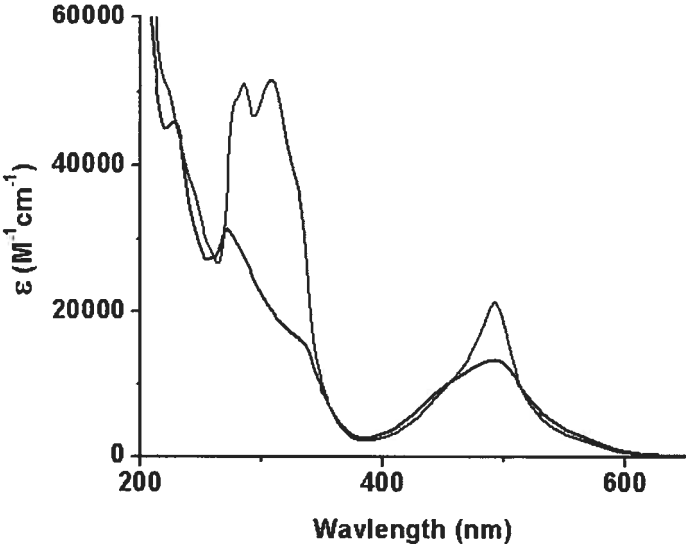

Figure 3.20 Absorption spectra of complexes **III-1a** $(PF_6)_2$ (black trace) and **III-5b** $(PF_6)_2$ (red trace).

Table 3.2 Electronic Absorption [a]

Complex	^{1}MLCT λ_{max} (nm) ε ($M^{-1}cm^{-1}$)	LC transitions λ_{max} (nm), ε ($M^{-1}cm^{-1}$)			
III-1a	492 (13300)	336_{sh} (15600)	-	272 (31300)	-
III-2a	500 (14600)	-	-	270 (37600)	-
III-3a	489 (12400)	336_{sh} (16100)	306 (20900)	272 (31700)	-
III-4	494 (14400)	332_{sh} (21300)	309 (27400)	280 (39200)	-
III-5a	492 (14300)	331_{sh} (23600)	307 (34600)	285 (35200)	278_{sh} (33000)
III-5b	492 (21200)	330_{sh} (36800)	308 (51300)	285 (51000)	278_{sh} (48600)
III-6a	504 (12900)	325_{sh} (17500)	-	280 (41600)	-
III-6b	504 (15200)	325_{sh} (24400)	-	280 (44600)	-
III-7	492 (14000)	333_{sh} (19500)	317 (28300)	280_{sh} (26600)	274 (30100)

[a] All spectra recorded in air-equilibrated acetonitrile solutions.

3.6 Synthesis and Characterization of 4'-(4-carboxyphenyl)-4,4''-di-(*tert*-butyl) tpy and the Corresponding Homoleptic Complex III-4 $(PF_6)_2$ (refer to page XXXV of Appendix 3 for X-ray data and parameters for complex **III-4 $(PF_6)_{1.5}$**)

The general insolubility of the precursor diacid complexes prompted us to investigate the installation of solubilizing functionality in the 4,4'' positions of the peripheral pyridyl rings. Symmetrically substituted 4,4',4''-trialkyl terpyridines have been valued for their noted electron donating effect upon formation of their complexes and for their accessibility to other functionalities.[23, 24] Such ligands have typically been prepared upon reflux of the appropriate 4-alkyl pyridine over activated Pd(0) with non-trivial purification owing to formation of higher-order polypyridines.[25] The synthesis of symmetrically and asymmetrically 4,4''-disubstituted terpyridines is inherently more complicated.[26] Recent reports to this end have relied on modified Krohnke synthesis to selectively produce such ligands.[27, 28] However, these syntheses are multi-step and time consuming relative to the "one-pot" protocols normally followed to produce 4'-aryl-tpy ligands using two equivalents of 2-acetyl pyridine and one equivalent of the aromatic aldehyde in basic alcoholic media. Thus, we opted to synthesize 2-acetyl-4-*tert*-butylpyridine in an expedient fashion. This has previously been accomplished via a tedious three-step synthesis starting from 4-*tert*-butylpyridine,[29] requiring the preparation of 2-cyano-4-*tert*-butylpyridine from the *N*-oxide precursor.[30] Instead, the *in situ* generation of alkyl radicals by silver(I) catalyzed de-carboxylation of the corresponding carboxylic acid provides a rapid "one-pot" route to 2-and 4-alkylated pyridines.[31] While this method has been used with success for acetylation of 4-substituted pyridine,[28a, c] the presence of a deactivating *tert*-butyl group in the 4 position led us to take the inverse approach wherein 2-acetylpyridine was alkylated using pivalic acid (Scheme 3.1).

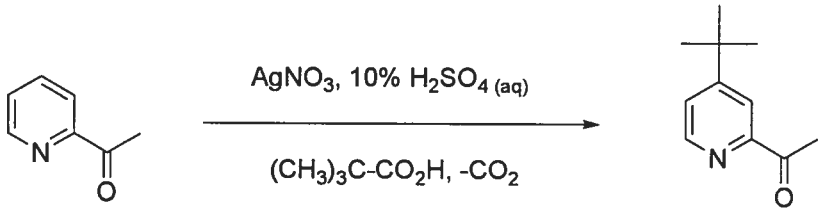

27 %

Scheme 3.1 Synthesis of 4-*tert*-butyl-2-acetylpyridine. Yield obtained after chromatographic purification.

The relatively low yield of the reaction is comparable to that obtained for the related synthesis of 4-isopropyl-2-acetylpyridine and is compensated by its simplicity and amenability to scale-up.[32] With 4-*tert*-butyl-2-acetylpyridine in hand, the "one-pot" protocol outlined in Scheme 3.2 could be undertaken to produce 4'-(4-carboxyphenyl)-4, 4''-di-(*tert*-butyl)tpy. However, owing to the increased solubility afforded by the *tert*-butyl groups, extended reaction times along with chromatographic purification were necessary since the product does not precipitate in appreciable quantity during the course of the reaction.

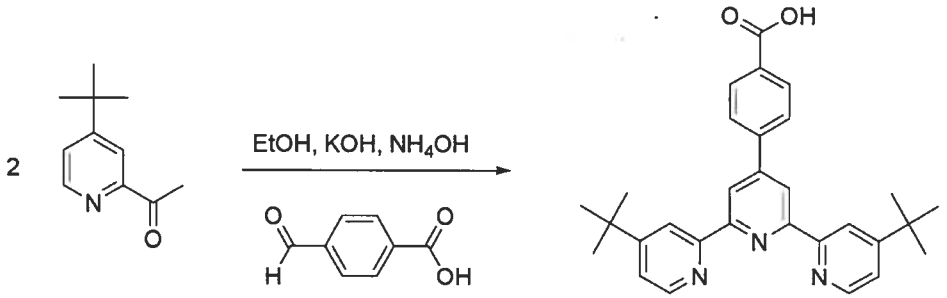

Scheme 3.2 Synthesis of 4'-(4-carboxyphenyl)-4,4''-di-(*tert*-butyl)tpy. Yield obtained after chromatographic purification.

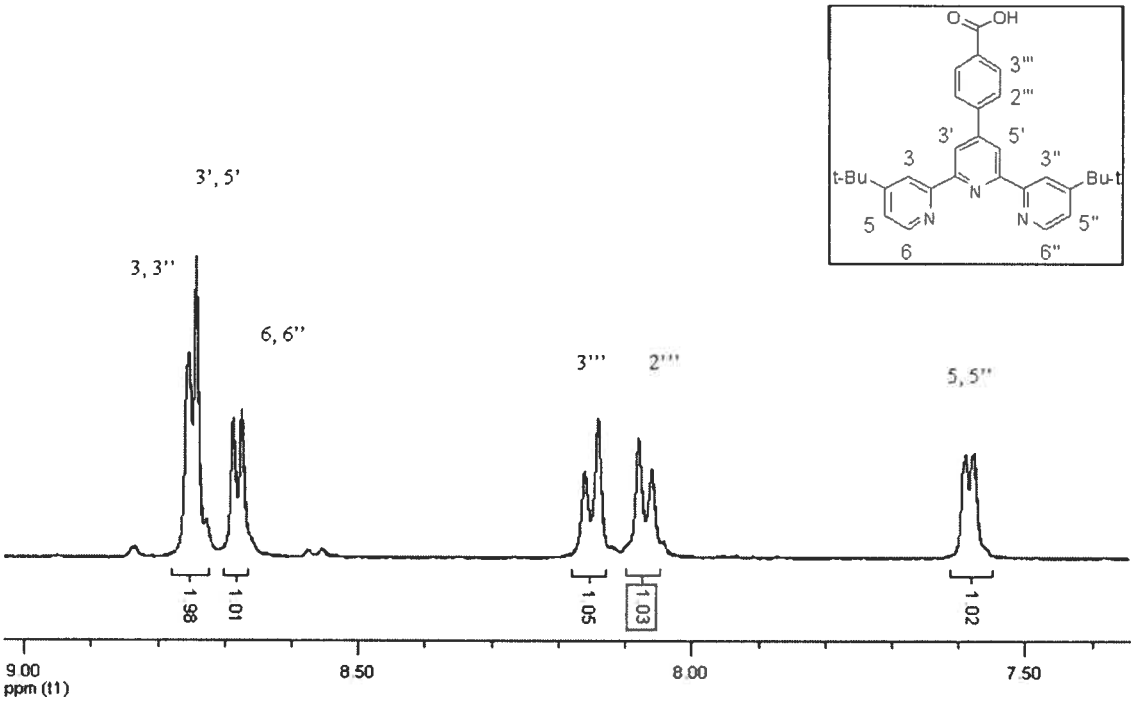

Figure 3.21 ^{1}H NMR spectrum of 4'-(4-carboxyphenyl)-4,4''-di-(*tert*-butyl)tpy in d_6-DMSO. Methyl resonance at 1.42 ppm (s, 18H) not shown.

Complexation of the target ligand with 0.5 eq $RuCl_3$ and 3 eq $AgNO_3$ in refluxing ethanol gave the homoleptic diacid complex **III-4 $(PF_6)_2$** in 52 % yield after column chromatography and anion exchange. Since the diacid complex is quite soluble in a wide range of both polar and non-polar solvents (e.g. DCM, $CHCl_3$), prior conversion of the ligand to the methyl ester was unnecessary. While there is a great enhancement of solubility relative to the structural analogue **III-1b $(PF_6)_2$**, there is no difference in their respective $Ru^{3+/2+}$ couples, which suggests no significant dative enhancement by the presence of the *tert*-butyl groups. This is in turn supported by crystallographic data which indicates no significant discrepancy in the Ru-N bond length involving the pendant pyridyl ring for complexes **III-1a $(PF_6)_2$** and **III-4 $(PF_6)_2$** (Figures 3.2 and 3.23). Moreover, the invariance of the MLCT band (Table 3.2) of **III-4 $(PF_6)_2$** (494 nm) compared to that for the related complex **III-1a $(PF_6)_2$** (492 nm) further reinforces this assessment considering that incorporation of electron releasing groups generally leads to some degree of red-shifting of the MLCT band, for which destabilization of Ru-based d-orbitals has been invoked.[33, 23b]

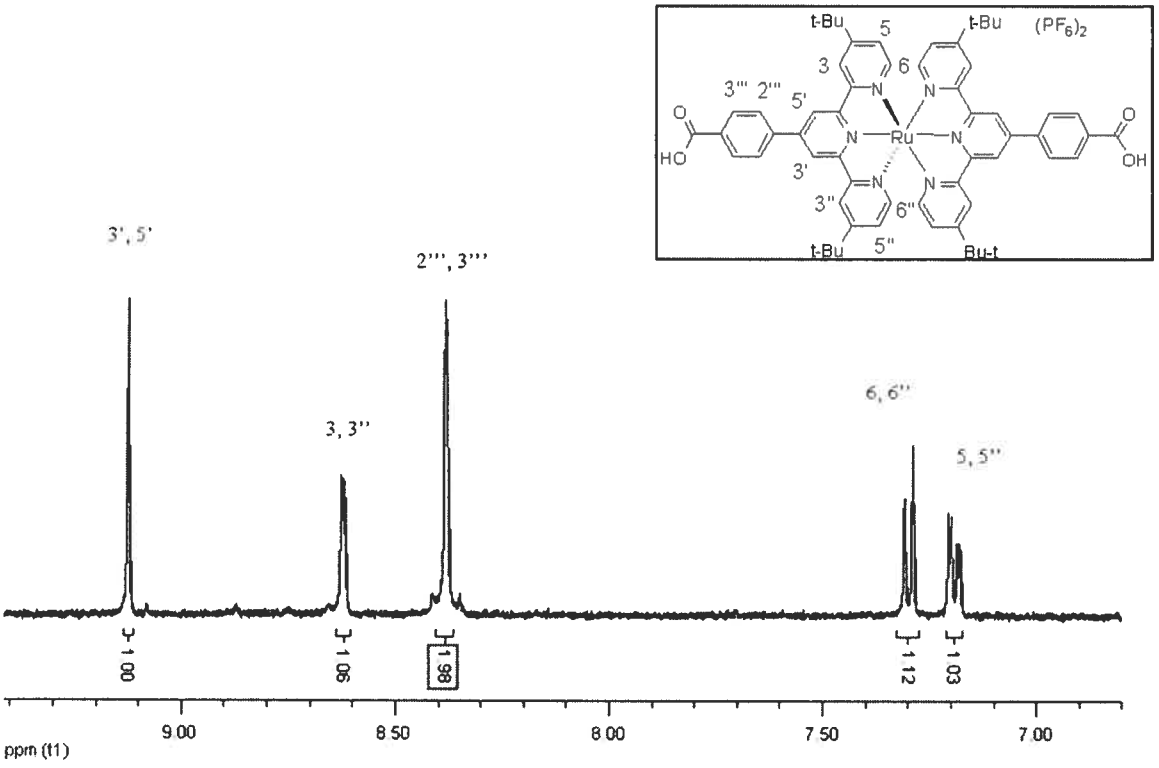

Figure 3.22 ^{1}H NMR spectrum of complex **III-4 $(PF_6)_2$** in CD_3CN (aromatic region). Methyl resonance at 1.33 ppm (s, 36H) not shown.

Single crystals suitable for structure determination by X-ray diffraction could be grown from an acetonitrile solution of the complex by vapour diffusion with isopropyl ether. The structure (Figure 3.23, below) confirms the spectroscopic assignment (Figure 3.22) of the *tert*-butyl group position and, like complex **III-1b** $(PF_6)_2$, exhibits a polymeric framework based upon hydrogen-bonding interactions.

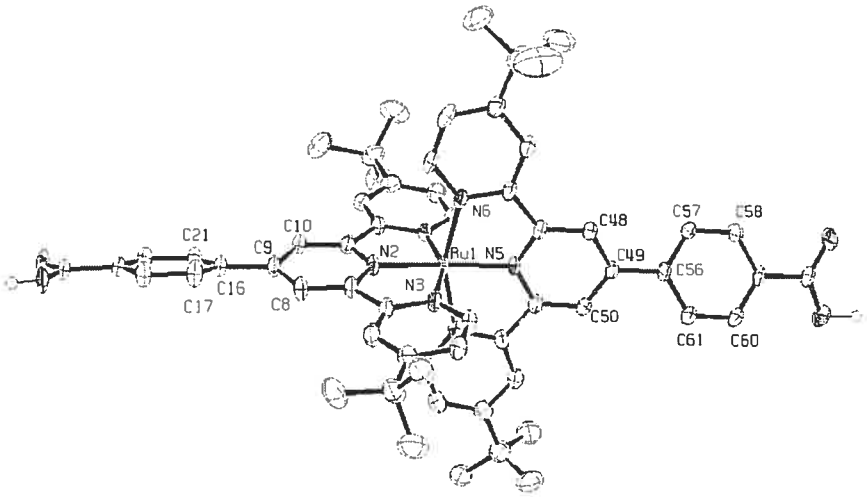

Figure 3.23 ORTEP of **III-4** $(PF_6)_{1.5}$ with thermal ellipsoids at 50% probability. Counter-anions are omitted for clarity.

Selected Bond Distances (Å)	**Selected Bond Angles (°)**	**Hydrogen Bonding**
O_{23}-C_{22} 1.215 (7)	C_{50}-C_{49}-C_{56}-C_{61} -35.5 (6)	O_{24}-H_{24} 0.82 Å
O_{24}-C_{22} 1.327 (6)	C_{10}-C_9-C_{16}-C_{21} 21.0 (7)	O_{64}-H_{24} 1.74 Å
O_{63}-C_{62} 1.267 (5)	N_5-Ru-N_3 98.78 (13)	O_{24}-O_{64} 2.552(4) Å
Ru-N_5 1.982 (3)	N_5-Ru-N_6 78.52 (13)	O_{24}-H_{24}-O_{64} 167.8 °
Ru-N_3 2.069 (4)		

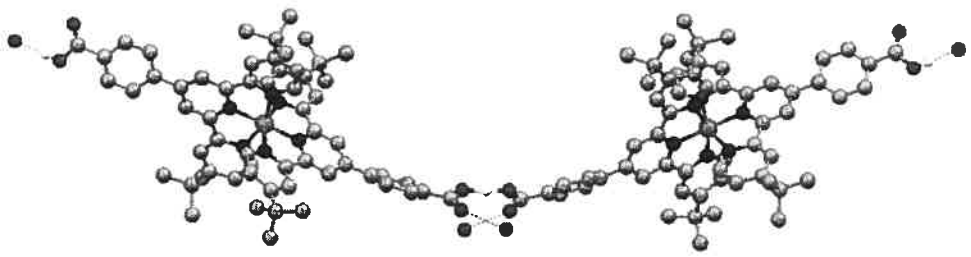

Figure 3.24 X-ray crystal structure of complex **III-4** $(PF_6)_{1.5}$ showing propagation of two polymeric chains 180° relative to one another based upon hydrogen bonding interactions. Solvent and counter-ions have been omitted for clarity.

The empirical formula for this structure gives a counter-anion:ruthenium(II) complex ratio of 1.5:1, indicating proton removal which may be understood considering the representation in Figure 3.24. Here, the asymmetric unit (complex **III-4**) generates its equivalent about a two-fold axis, wherein connectivity stems from sharing of a single proton between equivalent carboxy groups. This is supported by the length and similarity of the C-O bonds associated with these carboxy groups (1.267 (5) Å and 1.233 (5) Å for O_{63}-C_{62} and O_{64}-C_{64}, respectively) which indicates a strong anionic character. From this intersection extends polymeric chains based upon a hydrogen-bonding interaction like that seen with complex **III-1b** $(PF_6)_2$, but whose 180° relationship produces a 2-D grid, depicted in Figure 3.25 below.

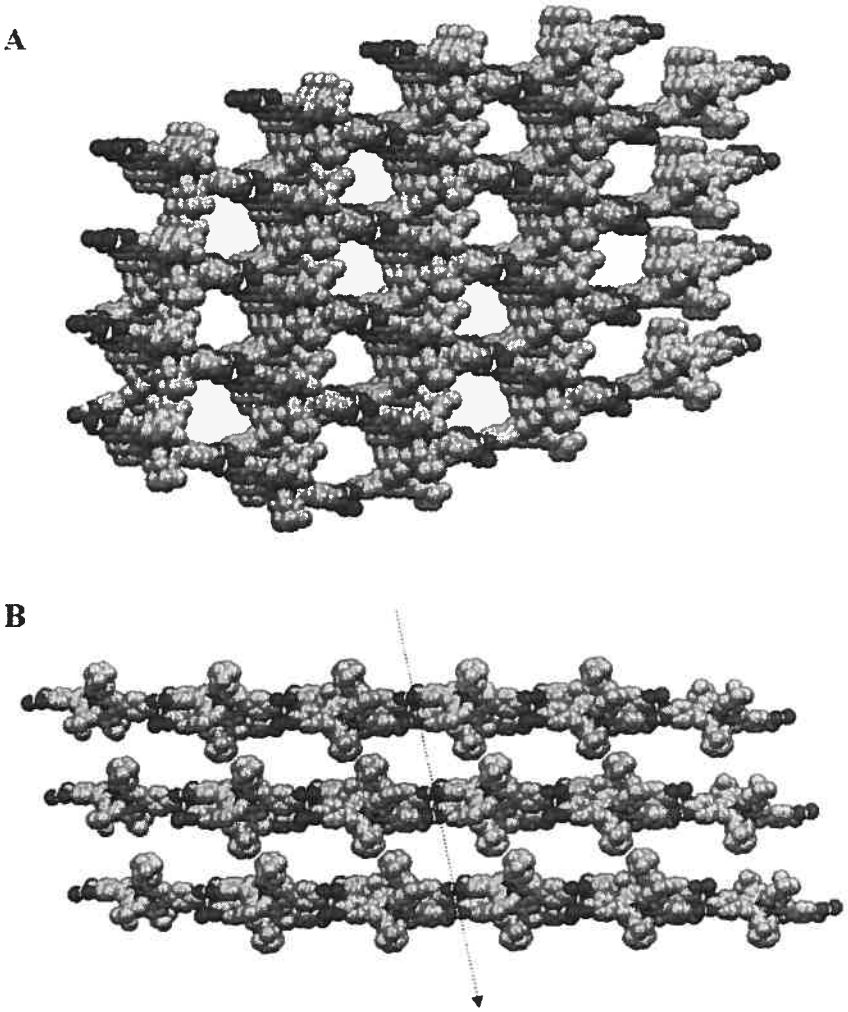

Figure 3.25 X-ray crystal structure of complex **III-4** $(PF_6)_{1.5}$ depicting three layers of the grid in a top-down (**A**) and side-on (**B**) view leading to channel formation, the propagation of which is indicated by the dashed arrow. Protons and counter-anions are omitted for clarity.

The cavities arising from this 2-D grid are approximately 15 Å x 14 Å, edge to edge. Successive layers are slightly offset, leading to channel formation in spite of the bulky *tert*-butyl groups (Figure 3.25, B). These channels are occupied by acetonitrile and isopropyl ether solvent molecules. Such occupation typically does not preclude incorporation of complementary guest molecules. Counter-anions may lead to such interference, but the PF_6^- anions in this case are located within close proximity to the intersection formed by the Ru(II) complexes and so do not overly obstruct these cavities. Although polypyridyl complexes of the form $(tpy)_2M^{2+}$ have been used as components to form discrete cavities,[34] this is, to the best of our knowledge, the first porous structure obtained exclusively from such units.

3.7 Concluding Remarks

A series of linear dicarboxylate complexes based upon the $Ru(tpy)_2^{2+}$ motif have been prepared and used to bridge Rh_2(II,II) acetate units in a controlled manner to yield both asymmetric, singly-substituted Rh_2(II,II)-appended complexes as well as the symmetric Rh_2(II,II)-bridge-Rh_2(II,II) systems. This is the first known report of a cationic bridging ligand used to span metal dimers, the use of which likely reinforces the relative inert nature of Rh_2(II,II) acetate units to permit straight-forward synthesis by direct complexation without need for elaborate, pre-organized starting materials. The asymmetric complexes are interesting in that they readily permit access to more diverse heterometallic complexes by direct complexation with dimeric units more substitutionally labile relative to Rh_2(II,II), such as Mo_2(II,II) and W_2(II,II). Moreover, symmetric dimer-bridge-dimer systems based upon Mo_2(II,II) and / or W_2(II,II) are of interest to help ascertain the potential of these $Ru(tpy)_2^{2+}$ complexes in mediating electronic coupling between such dimeric units. These systems are currently under investigation in our laboratory. Lastly, to address solubility problems generally encountered with the dicarboxylate complexes used, a dicarboxylate complex was prepared possessing solubilizing *tert*-butyl groups in the 4-pyridyl position of the peripheral rings of tpy. The structure of this diacid analogue reveals a porous network sustained by hydrogen-bonding, with cavities devoid of counter-anions and spanning ~15 Å.

3.8 Experimental

3.8.1 Materials and Methods. Solvents used in the preparation and purification of ligands and complexes were reagent grade and used without further purification. The preparation and characterization of 2-furyl terpyridine,[35] 4'-(4-methylcarboxyphenyl) tpy,[36] and 4'-(4-carboxyphenyl)tpy [37] have been described previously. Silica used for chromatographic isolation of all complexes was 400-450 Å mesh. $Rh_2(OAc)_4(MeOH)_2$ was prepared and purified according to an established procedure.[38]

3.8.2 Physical Measurements All ^{1}H NMR spectra were recorded using a Bruker 400 RG at 400 MHz.

Electrochemical data was recorded using a BAS Epsilon potentiostat using argon-degassed, spectroscopic grade acetonitrile solutions of 0.1 M tetrabutylammonium hexafluorophosphate ($TBAPF_6$) as supporting electrolyte. A three electrode set-up was employed using a working Pt button electrode, a Pt wire auxiliary electrode, and a Ag wire pseudo-reference electrode with addition of ferrocene as an internal reference. All data is corrected to the Fc/Fc^+ couple vs SCE. Single crystal X-ray diffraction data for **III-1b (PF_6)** and **III-4 ($(PF_6)_2$** were collected on a Bruker Apex at 100 K using Cu-Kα radiation (λ= 1.54178 Å) and refined by Francine Bélanger-Gariépy. Single crystal X-ray diffraction data for **III-5b ($(PF_6)_2$** was collected on a Microstar Apex 2 at 100 K using Cu-Kα radiation (λ= 1.54178 Å) and refined by Marie-Pierre Santoni. Mass spectrometry was performed by direct injection using an LC-MSD TOF (Agilent) spectrometer with electrospray ionization.

3.8.3 Synthesis and Purification:

4'-carboxy-tpy In a typical preparation, 2-furyl terpyridine (2.0 g, 6.7 mmol) and $KMnO_4$ (4.2 g, 26.7 mmol) are combined in H_2O (100 mL) made basic (pH = 10) with addition KOH and heated to reflux for 2 hr. The reaction mix is cooled to room temperature and filtered to remove MnO_2. The pH of the filtrate is adjusted to pH = 5 with addition of HCl (aq, conc.), forming an initial precipitate. Further precipitation was encouraged by reducing the volume of the filtrate under reduced pressure. The precipitate was then removed by filtration and washed with copious amounts of diethyl ether to obtain a pure white solid. Yield: 1.3 g (68%). ^{1}H NMR (400 MHz, d_6-DMSO) δ ppm 8.88

(s, 2H), 8.77 (d, J = 4.8 Hz, 2H), 8.67 (d, J = 7.9 Hz, 2H), 8.05 (m, 2H), 7.55 (m, 2H). ^{13}C NMR (300 MHz, d_6-DMSO): 167.35, 157.21, 155.49, 150.71, 141.86, 138.77, 126.03, 122.10, 120.87. ESI-MS: $[M + H]^+$ cald. for $C_{16}H_{12}N_3O_2$, 278.09295; found, 278.09376.

4-*tert*-butyl-2-acetylpyridine In a typical preparation, a 10% H_2SO_4 (aq) solution (140 mL) is charged with $AgNO_3$ (2.00 g, 11.8 mmol), pivalic acid (18.4 g, 180.4 mmol), and 2-acetylpyridine (7.2 g, 59.4 mmol). The solution is heated to 70 °C, at which point $(NH_4)_2S_2O_8$ (26.0 g, 114 mmol) in H_2O (60 mL) is added at once. The reaction mix is stirred at 70 °C until the evolution of CO_2 (g) ceases (~ 15 min). The temperature is then raised to 90 °C and the solution stirred for an additional 10 min. After cooling, the reaction mix is made basic (pH ≈ 10) with addition of Na_2CO_3 (aq, sat). Repeated extraction of the aqueous mix with DCM (3 x 100 mL), followed by washing of the combined organic extracts with brine and drying over $MgSO_4$, gave a dark oil upon removal of the DCM under reduced pressure. This oil is dissolved in a minimal amount of eluent (7:3 mix of hexanes / diethyl ether) and applied to a large silica column (l = 30 cm, w = 8 cm). The product is obtained as a lightly coloured yellow oil (R_f = 0.38). Yield: 2.84 g (27%). ^1H NMR (400 MHz, $CDCl_3$) δ ppm 8.61 (d, J = 5.2 Hz, 1 H), 8.08 (d, J = 2.0 Hz, 1 H), 7.48 (dd, ^3J = 5.2 Hz, ^4J = 2.0 Hz), 2.75 (s, 3H), 1.36 (s, 9H). ESI-MS: $[M+Na]^+$ cald. for $C_{11}H_{15}NONa$, 200.10513; found, 200.10453.

4'-(4-carboxyphenyl)-4,4''-di-(*tert*-butyl)tpy In a typical preparation, 4-*tert*-butyl-2-acetylpyridine (1.75 g, 9.87 mmol) is added to a stirred solution of 4-carboxy benzaldehyde (0.74 g, 4.93 mmol), KOH (0.8 g, 14 mmol), and NH_4OH (20 mL) in 150 mL ethanol. The reaction mixture is stirred at room temperature while open to air for 48 hr, after which the solution is made slightly acidic (pH = 5) with addition of HCl (aq, conc.). To the reaction mix is added 300 mL DCM, and the resultant solution is washed twice with 100 ml portions of H_2O. The organic phase is dried under reduced pressure, then dissolved in a minimal amount of eluent (4:1 ethyl acetate / methanol with 5% triethylamine) and applied to a silica column (l = 10 cm, w = 7.5 cm) to obtain a nearly pure off-white solid (R_f = 0.23) which can be crystallized from hot DMSO. Yield: 0.78 g (34%) ^1H NMR (400 MHz, d_6-DMSO) δ ppm 8.76 (d, J = 1.5 Hz, 2H), 8.74 (s, 2H), 8.68 (d, J = 5.1 Hz, 2H), 8.15 (d, J = 8.2 Hz, 2H), 8.07 (d, J = 8.2 Hz, 2H), 7.59 (dd, ^3J = 5.1 Hz, ^4J = 1.5 Hz, 2H), 1.42 (s, 18H). ^{13}C (300 MHz, d_6-DMSO): 161.91, 157.04,

156.01, 150.69, 131.66, 128.50, 123.20, 119.16, 118.56, 36.03, 31.40. ESI-MS: $[M + H]^+$ cald. for $C_{30}H_{32}N_3O_2$, 466.24945; found, 466.25001.

[(4'-(4-methylcarboxyphenyl)-tpy)$_2$Ru](PF$_6$)$_2$ (III-1a (PF$_6$)$_2$): Typically, 4'-(4-methylcarboxy phenyl)-terpyridine (0.20 g, 0.54 mmol), $RuCl_3$ (0.056 g, 0.27 mmol), and $AgNO_3$ (0.14 g, 0.81 mmol) were refluxed in *N,N'*-DMF for 2 hr. The reaction mix was filtered over celite to remove AgCl(s), and the filtrate then decanted into an equal volume of NH_4PF_6 (aq). The resulting precipitate was filtered and washed with water, then dissolved in acetonitrile and applied to a silica column for elution with a mix of 7:2 CH_3CN / KNO_3 (sat, aq). The column fractions are combined and to this added NH_4PF_6, H_2O, and enough DCM to effect a phase separation. The aqueous layer is removed and the process is repeated, followed by a final washing with water alone. The organic layer is dried and the residue dissolved in a minimal amount of acetonitrile, which is decanted into water to form a heavy precipitate. Filtration and drying of the solid in vacuo gives 0.221 g (72%) of **III-1a (PF$_6$)$_2$**. ^{1}H NMR (400 MHz, d_6-DMSO) δ ppm 9.23 (s, 4H), 8.65 (d, J = 8.0 Hz, 4H), 7.96 (m, 4H), 7.35 (d, J = 5.3 Hz, 4H), 7.19 (m, 4H), 4.20 (s, 6H). ESI-MS: $[M]^{2+}$ cald. for $C_{46}H_{34}N_6O_4Ru$, 418.08425; found, 418.08401.

[(4'-(4-carboxyphenyl)-tpy)$_2$Ru](PF$_6$)$_2$ (III-1b (PF$_6$)$_2$) This compound was prepared upon saponification of **III-1a (PF$_6$)$_2$**. Typically, **III-1a (PF$_6$)$_2$** (0.20 g, 0.18 mmol) is dissolved in a 2:1 mix of CH_3CN / H_2O (30 mL) to which is added NaOH(s) (0.29 g, 7.2 mmol). After stirring for 1 hr at room temperature, the solution is decanted into 100 mL H_2O and made acidic (pH = 2) with HPF_6 (aq) to give a heavy precipitate. The solid is filtered and washed with water, followed by copious amounts of diethyl ether, then dried in vacuo. This material is pure by TLC (7:2 CH_3CN / KNO_3 (sat, aq), silica, R_f = 0.19). Yield: 0.183 g (94%). Limited solubility in most solvents precludes characterization by NMR, and the material is used "as is" for subsequent complexation. Single crystals suitable for structure determination by X-ray diffraction could be grown by slow evaporation of a CH_3CN / H_2O solution of **III-1b (PF$_6$)$_2$**, wherein the title compound crystallized as **III-1b (PF$_6$)**. ESI-MS: $[M]^{2+}$ cald. for $C_{44}H_{30}N_6O_4Ru$, 404.06860; found, 404.06827.

[(2-(4-methylcarboxyphenyl)-4,6-di(2-pyridyl)triazine)$_2$Ru](PF$_6$)$_2$ (III-2a (PF$_6$)$_2$) Typically, 2-(4-carboxyphenyl)-4,6-di(2-pyridyl)triazine (1.0 g, 2.81 mmol) is heated to reflux in thionyl chloride (30 mL) for 0.5 hr, after which no solid suspension remains. The excess thionyl chloride is removed by distillation and the residue is dried under vacuum. The flask containing the residue is then purged with argon and dry methanol (60 mL) is charged via cannulae. The reaction mix is then equipped to a dry condenser with drying tube and heated to reflux until no solid suspension remains (~ 2 h). The solution is cooled to room temperature and tipped into H_2O (300 mL) forming a voluminous precipitate of the methyl ester ligand which is filtered off and dried in vacuo without further purification. Typically, the ligand (0.25 g, 0.68 mmol) is heated to reflux in DMF with $RuCl_3$ (0.07 g, 0.34 mmol) and $AgNO_3$ (0.173 g, 1.02 mmol) after which the solution is filtered to remove AgCl(s). The filtrate is then decanted into a solution of NH_4PF_6 (aq) (300 mL), and the resultant heavy precipitate is filtered off and washed with water, then dissolved in a minimal amount of acetonitrile for chromatographic purification using silica and a 7:2 (CH_3CN / KNO_3 (aq, sat) mix as eluent. The collected fractions are combined, and to this added NH_4PF_6 and enough DCM to effect a phase separation. After washing the organic phase, the aqueous phase is discarded and the process repeated, with a final washing with water alone. The organic phase is dried and the residue taken up in a minimal amount of acetonitrile, then poured into H_2O (300 mL) to give a heavy precipitate which is filtered and dried in vacuo. Yield: 0.263 g (69%), R_f = 0.55 (silica, 7:2 CH_3CN / KNO_3 (sat, aq) as eluent). ^{1}H NMR (400 MHz, CD_3CN) δ ppm 9.19 (d, J = 8.4 Hz, 4H), 9.14 (d, J = 7.7 Hz, 4H), 8.44 (d, J = 8.4 Hz, 4H), 8.16 (m, 4H), 7.73 (d, J = 5.3 Hz, 4H), 7.41 (m, 4H), 4.02 (s, 3H). ESI-MS: $[M]^{2+}$ cald. for $C_{42}H_{30}N_{10}O_4Ru$, 420.07475; found, 420.07499.

[(2-(4-carboxyphenyl)-4,6-di(2-pyridyl)triazine)$_2$Ru](PF$_6$)$_2$ (III-2b PF$_6$)$_2$) Typically, **III-2a (PF$_6$)$_2$** (0.20 g, 0.177 mmol) is dissolved in a 2:1 mix of CH_3CN / H_2O (40 mL) to which is added NaOH(s) (0.20 g, 5.0 mmol). After stirring at room temperature for 2 hr, the mix is decanted into H_2O made acidic with HPF_6 (aq) (pH = 2). The resultant precipitate is filtered and washed with H_2O followed by a small amount of CH_3CN, then dried in vacuo. Yield: 0.183 g, (94%) R_f = 0.17 (silica, 7:2 CH_3CN / KNO_3 (sat, aq) as eluent). This compound is pure by TLC but, like **III-1b (PF$_6$)$_2$**, is sparingly soluble in a wide range of solvents, precluding NMR analysis. This compound is used "as is" for

subsequent complexation. ESI-MS: $[M]^{2+}$ cald. for $C_{40}H_{26}N_{10}O_4Ru$, 406.05910; found, 406.05867.

[(4'-methylcarboxy-tpy)$_2$Ru](PF$_6$)$_2$ (III-3a (PF$_6$)$_2$) Typically, 4'-carboxy-tpy (1.0 g, 3.60 mmol) is converted to the methyl ester analogue using the procedure already outlined. This material is used without further purification for subsequent reaction. Complexation and purification followed identical procedures to that discussed previously for **III-2a (PF$_6$)$_2$**, using the methyl ester ligand (0.20 g, 0.72 mmol), $RuCl_3$ (0.075 g, 0.36 mmol), and $AgNO_3$ (0.184 g, 1.08 mmol), giving the dimethyl-ester complex **III-3a (PF$_6$)$_2$** (R_f = 0.56, silica, 7:2 CH_3CN / KNO_3 (sat, aq) as eluent). Yield: 0.238 g (68%). ^{1}H NMR (400 MHz, CD_3CN) δ ppm 9.23 (s, 4H), 8.65 (d, J = 8.0 Hz, 4H), 7.96 (m, 4H), 7.35 (d, J = 5.1 Hz, 4H), 7.19 (m, 4H), 4.20 (s, 6H). ESI-MS: $[M]^{2+}$ cald. for $C_{34}H_{26}N_6O_4Ru$, 342.05295; found, 342.05255.

[(4'-carboxy-tpy)$_2$Ru](PF$_6$)$_2$ (III-3b (PF$_6$)$_2$) Here, the dicarboxy complex is generated analogously to complex **III-2b (PF$_6$)$_2$**, using **III-3a (PF$_6$)$_2$** (0.20 g, 0.21 mmol) and NaOH (s) (0.42 g, 10.5 mmol), while stirring at room temperature for 1hr in a 2:1 mix of CH_3CN / H_2O. R_f = 0.04 (silica, 7:2 CH_3CN / KNO_3 (sat, aq) as eluent). Yield: 0.20 g (98%). ^{1}H NMR (400 MHz, CD_3CN) δ ppm 9.22 (s, 4H), 8.65 (d, J = 8.2 Hz, 4H), 7.95 (m, 4H), 7.34 (d, J = 5.3 Hz, 4H), 7.19 (m, 4H). ESI-MS: $[M]^{2+}$ cald. for $C_{32}H_{22}N_6O_4Ru$, 328.03730; found, 328.03721.

[(4'-(4-carboxyphenyl)-4,4''-di-(*tert*-butyl) tpy)$_2$Ru](PF$_6$)$_2$ (III-4 (PF$_6$)$_2$) The ligand 4'-(4-carboxyphenyl)-4,4''-di-(*tert*-butyl) tpy (0.10 g, 0.22 mmol) is combined with $RuCl_3$ (0.023 g, 0.11 mmol) and $AgNO_3$ (0.056 g, 0.33 mmol) is heated to reflux in ethanol (40 mL) for 24 hr, after which the solution is filtered over celite to remove AgCl(s). The filtrate is dried and the residue taken up in a minimal amount of acetonitrile, then applied to a silica column for elution with a 7:2 CH_3CN / KNO_3 (sat, aq) mix. The anion exchange is performed on the collected fractions analogously to that for **III-2a (PF$_6$)$_2$** with a final precipitation in water from an acetonitrile solution of the complex followed by drying in vacuo. Yield: 0.076 g (52%). R_f = 0.46 (silica, 7:2 CH_3CN / KNO_3 (sat, aq)). Single crystals suitable for structure determination by X-ray diffraction were grown upon vapour diffusion of isopropyl ether into an acetonitrile

solution of the complex, wherein the title compound crystallized as **III-4b $(PF_6)_{1.5}$**. ^{1}H NMR (400 MHz, CD_3CN) δ ppm 9.12 (s, 4H), 8.62 (d, J = 2.0 Hz, 4H), 8.38 (m, 8H), 7.30 (d, J = 6.0 Hz, 4H), 7.19 (dd, ^{3}J = 6.0 Hz, ^{4}J = 2.0 Hz, 4H), 1.33 (s, 36H). ESI-MS: $[M]^{2+}$ cald. for $C_{60}H_{62}N_6O_4Ru$, 516.19380; found, 516.19312.

$[(CH_3CO_2)Rh_2(O_2C\text{-}ph\text{-}tpy)Ru(tpy\text{-}ph\text{-}CO_2H](PF_6)_2$ (III-5a $(PF_6)_2$)

$[(CH_3CO_2)_3Rh_2(O_2C\text{-}ph\text{-}tpy)Ru(tpy\text{-}ph\text{-}CO_2)Rh_2(O_2CCH_3)_3](PF_6)_2$ (III-5b $(PF_6)_2$)

In a typical reaction, the diacid complex **III-1b $(PF_6)_2$** (0.10 g, 0.091 mmol) is dissolved in a 6:1 DMF / H_2O mix (20 mL) to which is added $Rh_2(OAc)_4(CH_3OH)_2$ (0.091 g, 0.18 mmol). The mixture is heated to 100°C for 24 hr, after which the solution is dried under vacuum and the residue dissolved in a minimal amount of acetonitrile. The solution is then applied to a silica column (l = 15 cm, w = 4 cm) and eluted using a mix of 14:3 CH_3CN / KNO_3 (sat, aq). Both III-**5a $(PF_6)_2$** (R_f = 0.35) and **III-5b $(PF_6)_2$** (R_f = 0.59), along with some starting material **III-1b $(PF_6)_2$**, are recovered and anion exchange to their PF_6 salts is done as described previously for complex **III-2a $(PF_6)_2$**. Owing to their partial water solubility, particularly for complex **III-5b $(PF_6)_2$**, the residue of each compound is triturated in a small amount of water and filtered to remove excess NH_4PF_6. Yield (**III-5a $(PF_6)_2$**): 0.050 g (44%). Yield (**III-5b $(PF_6)_2$**): 0.042 g (28%). ^{1}H NMR (**III-5a $(PF_6)_2$**) (400 MHz, CD_3CN) δ ppm 9.06 (s, 2H), 9.01 (s, 2H), 8.65 (m, 4H), 8.40 (d, J = 8.2 Hz, 2H), 8.30 (d, J = 8.2 Hz, 2H), 8.21 (s, 4H), 7.96 (m, 4H), 7.44 (m, 4H), 7.19 (m, 4H), 1.86 (s, 3H), 1.82 (s, 6H). ESI-MS: $[M]^{2+}$ cald. for $C_{50}H_{38}N_6O_{10}RuRh_2$, 594.98959; found, 594.98916. ^{1}H NMR (**III-5b $(PF_6)_2$**) (400 MHz, CD_3CN) δ ppm 9.00 (s, 4H), 8.65 (d, J = 8.0 Hz, 4H), 8.21 (s, 8H), 7.95 (m, 4H), 7.42 (d, J = 5.2 Hz, 4H), 7.18 (m, 4H), 1.86 (s, 6H), 1.82 (s, 12H). ESI-MS: $[M]^{2+}$ cald. for $C_{56}H_{46}N_6O_{16}RuRh_4$, 785.91114; found, 785.91355. Single crystals suitable for structure determination by X-ray diffraction were obtained upon vapour diffusion of isopropyl ether into an acetonitrile / toluene solution of **III-5b $(PF_6)_2$**, wherein the title compound crystallized as **III-5b $(PF_6)_2$**.

$[(CH_3CO_2)Rh_2(O_2C\text{-}ph\text{-}diazotpy)Ru(diazotpy\text{-}ph\text{-}CO_2H](PF_6)_2$ (III-6a $(PF_6)_2$)

$[(CH_3CO_2)Rh_2(O_2C\text{-}ph\text{-}diazotpy)Ru(diazotpy\text{-}ph\text{-}CO_2)Rh_2(O_2CCH_3)_3](PF_6)_2$ (III-6b $(PF_6)_2$) Identical protocols to those employed for the preparation and purification of **III-5a $(PF_6)_2$** and **III-5b $(PF_6)_2$** were undertaken here for the preparation of the triazine

analogues **III-6a $(PF_6)_2$** and **III-6b $(PF_6)_2$**, with the exception of using a 7:2 CH_3CN / KNO_3 (sat, aq) mix as eluent. Quantities used are as follows: **III-2b $(PF_6)_2$** (0.10 g, 0.090 mmol) and $Rh_2(OAc)_4.(CH_3OH)_2$ (0.0911 g, 0.18 mmol) in 6:1 N,N-DMF / H_2O (20 mL). Yield (**III-6a $(PF_6)_2$**): 0.041 g (39%), R_f = 0.41. Yield (**III-6b $(PF_6)_2$**): 0.035 g (26%), R_f = 0.62. ^1H NMR (**6a**) (400 MHz, CD_3CN) δ ppm 9.13 (m, 8H), 8.42 (d, J = 8.0 Hz, 2H), 8.28 (d, J = 8.2 Hz, 2H), 8.15 (m, 4H), 7.72 (d, J = 5.1 Hz, 4H), 7.40 (m, 4H), 1.86 (s, 3H), 1.82 (s, 6H). ESI-MS: $[M]^{2+}$ cald. for $C_{46}H_{34}N_{10}O_{10}RuRh_2$, 596.98009; found, 596.98031. ^1H NMR (**III-6b $(PF_6)_2$**) (400 MHz, CD_3CN) δ ppm 9.11 (d, J = 8.1 Hz, 4H), 9.07 (d, J = 8.6 Hz, 4H), 8.28 (d, J = 8.5 Hz, 4H), 8.15 (m, 4H), 7.71 (d, J = 5.1 Hz, 4H), 7.39 (m, 4H), 1.86 (s, 6H), 1.82 (s, 12H). ESI-MS: $[M]^{2+}$ cald. for $C_{52}H_{42}N_{10}O_{16}RuRh_4$, 787.90164; found, 787.90224.

$[(CH_3CO_2)_3Rh_2(O_2C\text{-}tpy)Ru(tpy\text{-}CO_2)Rh_2(O_2CCH_3)_3](PF_6)_2$ (III-7 $(PF_6)_2$) In a typical reaction, **III-3b $(PF_6)_2$** (0.095 g, 0.100 mmol) and $Rh_2(OAc)_4.(CH_3OH)_2$ (0.405 g, 0.8 mmol) are heated to reflux in CH_3CN (25 mL) for 40 hr. The reaction mix is dried and the residue purified by column chromatography using silica (l = 15 cm, w = 4 cm) and an eluent mix of 7:2 CH_3CN / KNO_3(sat, aq). Procedures for subsequent anion exchange and treatment of the collected fractions containing **7** have been described previously for **III-5a $(PF_6)_2$ / III-5b $(PF_6)_2$** and **III-6a $(PF_6)_2$ / III-6b $(PF_6)_2$**. Yield: 0.092 g (56%) R_f = 0.58. ^1H NMR (400 MHz, CD_3CN) δ ppm 9.03 (s, 4H), 8.67 (d, J = 8.1 Hz, 4H), 7.92 (m, 4H), 7.26 (d, J = 5.0 Hz, 4H), 7.2 (m, 4H), 1.88 (s, 6H), 1.86 (s, 12H). ESI-MS: $[M]^{2+}$ cald. for $C_{44}H_{38}N_6O_{16}RuRh_4$, 709.87984; found, 709.88001.

3.9 References:

1. see, for example: a) Mukherjee, P. S.; Das, N.; Kryschenko, Y. K.; Arif, A. M.; Stang, P. J. *J. Am. Chem. Soc.* **2004**, 126, 2464. b) Cui, Y.; Ngo, H. L.; Lin, W. *Inorg. Chem.* **2002**, 41, 1033.
2. see, for example: a) Kitagawa, S.; Uemura, K. *Chem. Soc. Rev.* **2005**, 34, 109. b) Hao, N.; Shen, E.; Li, Y.-G.; Wang, E.-B.; Hu, C.-W.; Xu, L. *Eur. J. Inorg. Chem.* **2004**, 4102. c) Lu, J.; Mondal, A.; Moulton, B.; Zaworotko, M. J. *Angew Chem. Intl. Ed.* **2001**, 40, 2113. d) Eddaoudi, M.; Li, H.; Yaghi, O. M. *J. Am. Chem. Soc.* **2000**, 122, 1391.
3. a) Petitjean, A.; Puntoriero, F.; Campagna, S.; Juris, A.; Lehn, J.-M. *Eur. J. Inorg. Chem.* **2006**, 3878. b) Cotton, F. A.; Murillo, C. A.; Stiriba, S.-E.; Wang, X.; Yu, R. *Inorg. Chem.* **2005**, 44, 8223. c) Cotton, F. A.; Murillo, C. A.; Yu, R. *Inorg. Chem.* **2005**, 44, 8211. d) Bursten, B. E.; Chisholm, M. H.; D'Acchioli, J. S. *Inorg. Chem.* **2005**, 44, 5571. e) Bickley, J.; Bonar-Law, R.; McGrath, T.; Singh, N.; Steiner, A. *New J. Chem.* **2004**, 28, 425. f) Schiavo, S.L.; Serroni, S.; Puntoriero, F.; Tresoldi, G.; Piraino, P. *Eur. J. Inorg. Chem.* **2002**, 79. g) Cotton, F. A.; Dikarev, E. V.; Petrukhina, M. A.; Schmitz, M.; Stang, P. J. *Inorg. Chem.* **2002**, 41, 2903. h) Eddaoudi, M.; Kim, J.; Wachter, J.B.; Chae, H.K.; O'Keefe, M.; Yaghi, O.M. *J. Am. Chem. Soc.* **2001**, 123, 4368. i) Cotton, F.A.; Murillo, C.A. *Acc. Chem. Res.* **2001**, 34, 759, and references therein.
4. Cotton, F.A.; Walton, R. A. *Multiple Bonds Between Metal Atoms*, 3rd, ed., Wiley, New York, **1994**.
5. Cooke, M. W.; Hanan, G. S.; Loiseau, F.; Campagna, S.; Watanabe, M.; Tanaka, Y. *Angew. Chem. Intl. Ed.* **2005**, 44, 4881.
6. Cooke, M. W.; Hanan, G. S.; Loiseau, F.; Campagna, S.; Watanabe, M.; Tanaka, Y. *J. Am. Chem. Soc.* **2007**, in press.
7. a) Burdzinski, G. T.; Ramnauth, R.; Chisholm, M. H.; Gustafson, T. L. *J. Am. Chem. Soc.* **2006**, 128, 6776. b) Byrnes, M. J.; Chisholm, M. H.; Gallucci, J. A.; Liu, Y.; Ramnauth, R.; Turro, C. *J. Am. Chem. Soc.*, **2005**, 127, 17343.
8. Chisholm, M. H.; Patmore, N. J. *Acc. Chem. Res.* **2007**, 40, 19. and references therein.

9. a) Chen, H.; Cotton, F. A. *Polyhedron* **1995**, 14, 2221. b) Chisholm, M. H.; MacIntosh, A. M. *Dalton Trans.* **1999**, 1205.

10. Cayton, R. H.; Chisholm, M. H.; Huffman, J. C.; Lobkovsky, E. B. *J. Am. Chem. Soc.* **1991**, 113, 8709.

11. Chisholm, M. H.; Cotton, F. A.; Daniels, L. M.; Folting, K.; Huffman, J. C.; Iyer, S. S.; Lin, C.; MacIntosh, A. M.; Murillo, C. A. *J. Chem. Soc., Dalton Trans.* **1999**, 1387.

12. a) Cotton, F. A.; Lin, C.; Murillo, C. A. *J. Chem. Soc., Dalton Trans.* **1998**, 3151.

13. b) Cotton, F. A.; Jordan IV, G. T.; Murillo, C. A.; Su, J. *Polyhedron* **1997**, 16, 1831.

14. a) Cotton, F. A.; Liu, C. Y.; Murillo, C. A. *Inorg. Chem.* **2004**, 43, 2267. b) Angaridis, P.; Cotton, F. A.; Murillo, C. A.; Villagran, D.; Wang, X. *Inorg. Chem.* **2004**, 43, 8290.

15. a) Cotton, F. A.; Murillo, C. A.; Yu, R. *Dalton Trans.* **2005**, 3161. b) Cotton, F. A.; Murillo, C. A.; Wang, X.; Yu, R. *Inorg. Chem.* **2004**, 43, 8394. c) Cotton, F. A.; Lei, P.; Murillo, C. A.; Wang, X.; Yu, S.-Y.; Zhang, Z.-X. *J. Am. Chem. Soc.* **2004**, 126, 1518. d) Cotton, F. A.; Daniels, L. M.; Lin, C.; Murillo, C. A.; Yu, S.-Y. *Dalton Trans.* **2001**, 502. e) Cotton, F. A.; Lin, C.; Murillo, C. A. *Inorg. Chem.* **2001**, 40, 6413. f) Cotton, F. A.; Daniels, L. M.; Lin, C.; Murillo, C. A. *J. Am. Chem. Soc.* **1999**, 121, 4538.

16. a) Cotton, F. A.; Liu, C. Y.; Murillo, C. A.; Zhao, Q. *Inorg. Chem.* **2006**, 45, 9493. b) Cotton, F. A.; Li, Z.; Liu, C. Y.; Murillo, C. A. *Inorg. Chem.* **2006**, 45, 9765. c) Cotton, F. A.; Liu, C. Y.; Murillo, C. A. *Inorg. Chem.* **2003**, 42, 4619. d) Cotton, F. A.; Liu, C. Y.; Murillo, C. A.; Villagran, D.; Wang, X. *J. Am. Chem. Soc.* **2003**, 125, 13564. e) Cotton, F. A.; Daniels, L. M.; Donahue, J. P.; Liu, C. Y.; Murillo, C. A. *Inorg. Chem.* **2002**, 41, 1354.

17. a) Chow, H. S.; Constable, E. C.; Housecroft, C. E.; Neuburger, M.; Schaffner, S. *Dalton Trans.* **2006**, 2881. b) Scudder, M. L.; Goodwin, H. A.; Dance, I. G. *New J. Chem.* **1999**, 23, 695.

18. a) Chisholm, M. H. *Dalton Trans.* **2003**, 3821. b) Chisholm, M. H. *J. Organomet. Chem.* **2002**, 641, 15.

19. a) Polson, M. I. J.; Loiseau, F.; Campagna, S. ; Hanan, G. S. *Chem. Commun.* **2006**, 1301. b) Polson, M. I. J. ; Medlycott, E. A. ; Hanan, G. S.; Mikelsons, L.; Taylor, N.

J.; Watanabe, M.; Tanaka, Y.; Loiseau, F.; Passalacqua, R.; Campagna, S. *Chem. Eur. J.* **2004**, 10, 3640.

20. Distance approximated based on tip-to-tip distance for X-ray structure of **1a** $(PF_6)_2$.
21. a) Rigaut, S.; Costuas, K.; Touchard, D.; Saillard, J.-Y.; Golhen, S.; Dixneuf, P. H. *J. Am. Chem. Soc.* **2004**, 126, 4072. b) Xu, G.-L.; DeRosa, M. C.; Crutchley, R. J.; Ren, T. *J. Am. Chem. Soc.* **2004**, 126, 3728. c) Jones, S. C.; Coropceanu, V.; Barlow, S.; Kinnibrugh, T.; Timofeeva, T.; Bredas, J.-L.; Marder, S. *J. Am. Chem. Soc.* **2004**, 126, 11782.
22. a) Trexler, J. W.; Schreiner, A. F.; Cotton, F. A. *Inorg. Chem.* **1988**, 27, 3265. b) Miskowski, V. M.; Schaefer, W. P.; Sadeghi, B.; Santarsiero, B. D.; Gray, H. B. *Inorg. Chem.* **1984**, 23, 1154. c) Norman, J. G. Jr.; Renzoni, G. E.; Case, D. A. *J. Am. Chem. Soc.* **1979**, 101, 5256.
23. a) Polson, M. I. J.; Medlycott, E. A.; Hanan, G. S.; Mikelsons, L.; Taylor, N. J.; Watanabe, M.; Tanaka, Y.; Loiseau, F.; Passalacqua, R.; Campagna, S. *Chem Eur. J.* **2004**, 10, 3640. b) Sun, L.; Hammarstrom, L.; Akermark, B.; Styring, S. *Chem. Soc. Rev.* **2001**, 30, 36. c) Barigelletti, F.; Flamigni, L. *Chem. Soc. Rev.* **2000**, 29, 1. d) Hagfeldt, A.; Graetzel, M. *Acc. Chem. Res.* **2000**, 33, 269. e) Sauvage, J.-P.; Collin, J.-P.; Chambron, J.-C.; Guillerez, S.; Coudret, C.; Balzani, V.; Barigelletti, F. ; De Cola, L.; Flamigni, L. *Chem. Rev.* **1994**, 94, 993.
24. a) Jones, G. D.; Martin, J. L.; McFarland, C.; Allen, O. R.; Hall, R. E.; Haley, A. D.; Brandon, R. J.; Konovalova, T.; Desrochers, P. J. Pulay, P.; Vicic, D. A. *J. Am. Chem. Soc.* **2006**, 128, 13175. b) Martineau, D.; Beley, M.; Gros, P. C. *J. Org. Chem.* **2006**, 71, 566. Matyjaszewski, K.; Gobelt, B.; Paik, H.-J.; Horwitz, C. P. *Macromolecules* **2001**, 34, 430. d) Murner, H.-R.; Chassat, E.; Thummel, R. P.; Bunzli, J.-C. G. *Dalton Trans*. **2000**, 2809.
25. Nazeeruddin, M. K.; Pechy, P.; Renouard, T.; Zakeeruddin, S. M.; Humphry-Baker, R.; Comte, P.; Liska, P.; Cevey, L.; Costa, E.; Shklover, V.; Spiccia, L.; Deacon, G. B.; Bignozzi, C. A.; Gratzel, M. *J. Am. Chem. Soc.* **2001**, 123, 1613.
26. Hadda, T. B.; Bozec, H. L. *Inorg. Chim. Acta* **1993**, 204, 103.
27. for a summary of synthetic routes, see a) Heller, M.; Schubert, U. S. *Eur. J. Org. Chem.* **2003**, 947. b) Cargill Thompson, A. M. W. *Coord. Chem. Rev.* **1997**, 160, 1.
28. Krohnke, F. *Synthesis*, **1976**, 1.

29. a) Eryazici, I.; Moorefield, C. M.; Durmus, S.; Newkome, G. R. *J. Org. Chem.* **2006**, 71, 1009. b) Duprez, V.; Krebs, F. C. *Tet. Lett.* **2006**, 47, 3785. c) Mikel, C.; Potvin, P. G. *Polyhedron* **2002**, 21, 49.

30. Gelling, A.; Orrell, K. G.; Osborne, A. G.; Sik, V. *Dalton Trans.* **1998**, 937.

31. Fife, W. K. *J. Org. Chem.* **1983**, 48, 1375.

32. Minisci, F.; Bernardi, R.; Bertini, F.; Galli, R.; Perchinummo, M. *Tetrahedron*, **1971**, 27, 3575.

33. Ishihara, M.; Tsuneya, T.; Shiga, M.; Kawashima, S.; Yamagishi, K.; Yoshida, F.; Sato, H.; Uneyama, K. *J. Agric. Food Chem.* **1992**, 40, 1647.

34. Medlycott, E. A.; Hanan, G. S. *Chem. Soc. Rev.* **2005**, 34, 133.

35. a) S.-H. Hwang, C. N. Moorefield, P. Wang, F. R. Fronczek, B. H. Courtrey and G. R. Newkome, *Dalton Trans.*, **2006**, 3518 and references therein. b) S.-S. Sun and A. Lees, *Inorg. Chem.*, **2001**, **40**, 3154.

36. Husson, J.; Beley, M.; Kirsch, G. *Tetrahedron Lett.* **2003**, 44, 1767.

37. a) Duprez, V.; Krebs, F. C. *Tet. Lett.* **2006**, 47, 3785. b) Winter, A.; van den Berg, A. M. J.; Hoogenboom, R.; Kickelbick, G.; Schubert, U. S. *Synthesis* **2006**, 2873.

38. Storrier, G. D.; Colbran, S. B. *Inorg. Chim. Acta* **1999**, 284, 76.

39. Rempel, G. A.; Legzdins, P.; Smith, H.; Wilkinson, G. *Inorg. Synth.* **1972**, 13, 90.

Chapter 4: Synthesis and characterization of a series of polytopic 4'-(amidinato)-tpy ligands and their subsequent heteroleptic Ru(II) complexes

4.1 Introduction

The synthetic versatility of amidines makes them an appealing class of compounds for use as ligands in coordination chemistry.[1] Mononuclear complexes are known with metals of both high and low oxidation states, spanning much of the periodic table. The subsequent reaction chemistry of these complexes, and the degree to which it may be tuned through derivatization of the amidine ligand, has shown promise for a multitude of catalytic applications.[2] Polytopic amidines have received attention in this respect,[3] and in the preparation of extended structures based upon their hydrogen-bonding interactions with complementary anions such as carboxylates and phosphates.[4] The repeating dative unit in these cases is invariably the amidine chelate, the vast majority of which are bis-amidines. While polytopic amidines incorporating secondary and unique dative functionality are attractive from both a medicinal and coordination based perspective, such ligands have very rarely been reported.[5]

Amidinates are capable of exhibiting coordination motifs analogous to carboxylates, but are, in general, more basic and possess fewer lone-pair electrons which are thought to play a role in ligand displacement.[6] The kinetic and thermodynamic advantages of utilizing amidinates in place of carboxylates are well known with regard to ligand displacement in metal dimers.[6a] As we have seen previously in Chapter 2, decomposition of polynuclear assemblies based on carboxylate-derived $Ru(tpy)_2^{2+}$ occurs in the presence of competing ligands, the extent of which is directly related to the nuclearity and overall charge of the assembly. Thus, amidine-derivatized $Ru(tpy)_2^{2+}$ complexes offer a potential solution to this problem if they can be appended to the dirhodium(II,II) core.

Ruthenium(II) polypyridyl complexes have long been studied as dye sensitizers for solar cell applications, owing to their charge separated photo-excited state.[7] Such dye

molecules are grafted to the oxide surface by installing suitable secondary functionality on the exterior of the dye sensitizer capable of coordinating to the oxide surface, allowing for charge injection into the conduction band upon photo-excitation of the dye molecule.[7,8] Selection of such functionality is critical with regard to 1) efficient electronic communication and charge injection, and 2) physical robustness related to conditions of operation of the device. To this end, there is a plethora of carboxylate and phosphonate-derived Ru(II) polypyridyl complexes. However, such amidinate-derived dyes have not, to date, been explored in this regard. This is unfortunate considering that the basicity of the amidinate moiety can be readily tuned by selection and installation of various *N*-bound substituents.

Thus, for the purposes of creating more robust Rh_2-templated multinuclear $Ru(tpy)_2^{2+}$ assemblies and potentially interesting solar cell dyes, we endeavoured to prepare the targets depicted in Figure 4.1 below.

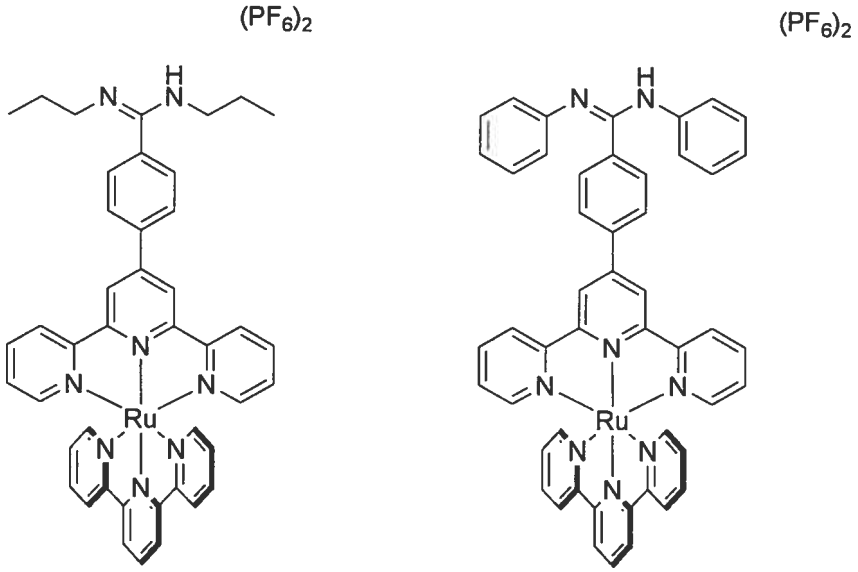

Figure 4.1 Targets: [{4'-(*N*,*N*'-dipropylbenzamidine)-tpy}(tpy)Ru]$(PF_6)_2$ **(IV-1)$(PF_6)_2$** and [{4'-(*N*,*N*'-diphenylbenzamidine)-tpy}(tpy)Ru]$(PF_6)_2$ **(IV-2)$(PF_6)_2$**.

In addition, it was also desired to prepare the polytopic ligand (Figure 4.2) as such a ligand holds much potential for the creation of polynuclear $Ru(tpy)_2^{2+}$ systems based on templation to metal centers.

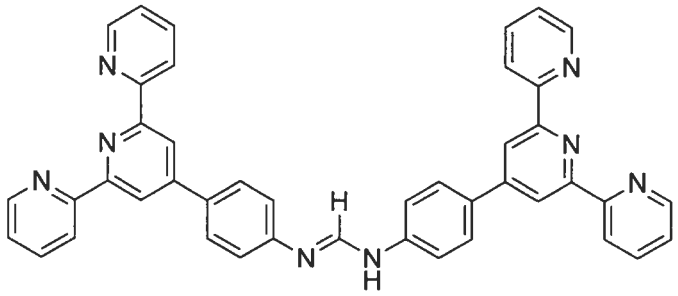

Figure 4.2 Target: *N,N'*-Di-(4'-phenyl-tpy) formamidine.

4.2 Synthesis and Characterization of Complexes IV-1 $(PF_6)_2$ and IV-2 $(PF_6)_2$ (refer to page XLIX of Appendix 4 for X-ray data and parameters for complex **IV-1 $(PF_6)(BPh_4)_2$**)

The novel tpy-amidine ligands 4'-(*N,N'*-dipropylbenzamidine)-tpy and 4'-(*N,N'*-diphenylbenzamidine)-tpy were prepared in modest to excellent yields using a conventional approach wherein chlorination of the corresponding 4'-(4-carboxyphenyl)-tpy and subsequent addition of the appropriate amine leads to the *N*-substituted amide ligand (Scheme 4.1).[9] The amide is isolated cleanly by precipitation in basic media and in turn chlorinated for reaction with a second equivalent of the amine to form the symmetric amidine.

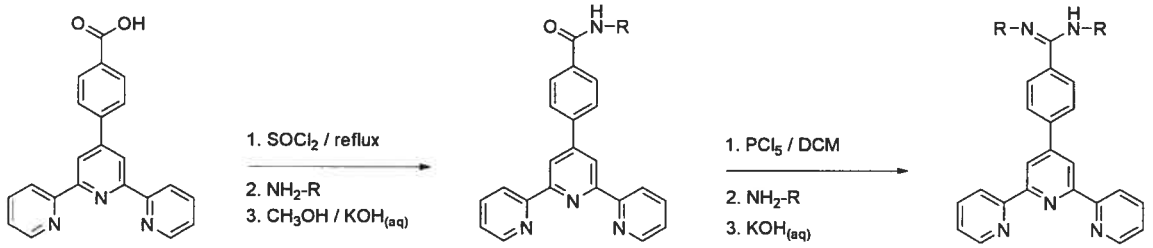

67 % R = n-propyl
93 % R = phenyl

79 % R = n-propyl [a]
84 % R = phenyl [b]

Scheme 4.1 Synthesis of 4'-(*N,N'*-dipropylbenzamidine)-tpy and 4'-(*N,N'*-diphenylbenzamidine)-tpy. (a) Yield obtained after chromatographic purification. (b) Yield obtained after crystallization.

Heteroleptic complex formation proceeds in modest yields in refluxing ethanolic solutions where the side products are mostly homoleptic amidine complexes, provided that the reaction time is kept to a minimum (Scheme 4.2). It is highly likely that the amidine moiety competes with tpy for coordination to Ru(II), as harsher reaction conditions gave rise to a large amount of dark material that does not move under various chromatographic conditions. Initially, this problem was approached by utilizing various *N*-protecting strategies,[10] but the problems encountered in each case did not justify the time invested, and so this approach was abandoned. Typically, a reaction time of 4 h in refluxing ethanol was found to be optimal.

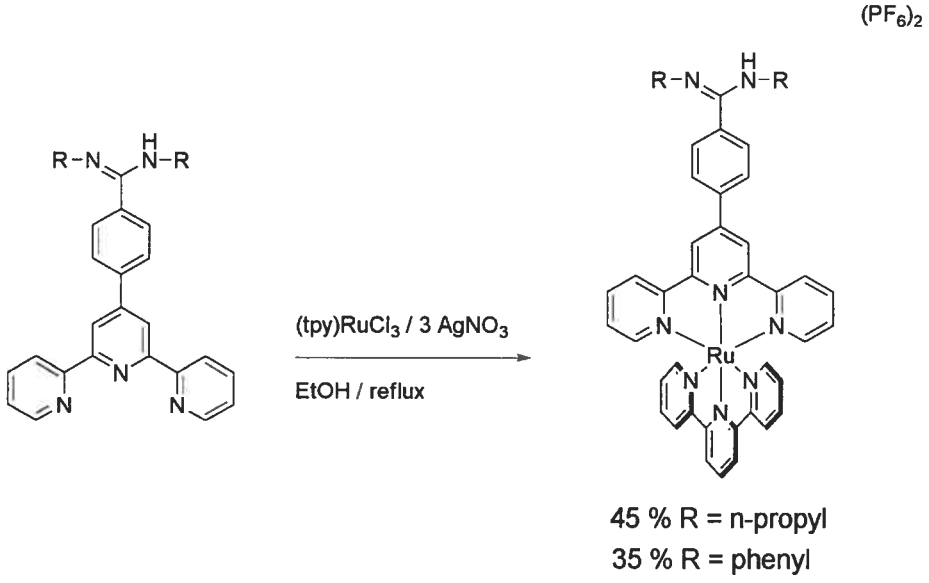

Scheme 4.2 Synthesis of complexes **IV-1** $(PF_6)_2$ and **IV-2** $(PF_6)_2$.

Single crystals suitable for X-ray structure determination were obtained for complex **IV-1** from acetonitrile in the presence of ammonium tetraphenylborate and reveal a protonated amidine moiety adopting a *trans* disposition of its *N*-propyl substituents. Two distinct molecules are found within the unit cell ($P2_1$), differentiated according to the twist of the phenyl spacer and the arrangement of their *N*-propyl groups, though both maintain the *transoid* arrangement of substituents. One of these is depicted below in Figure 4.3, along with selected bond lengths and angles.

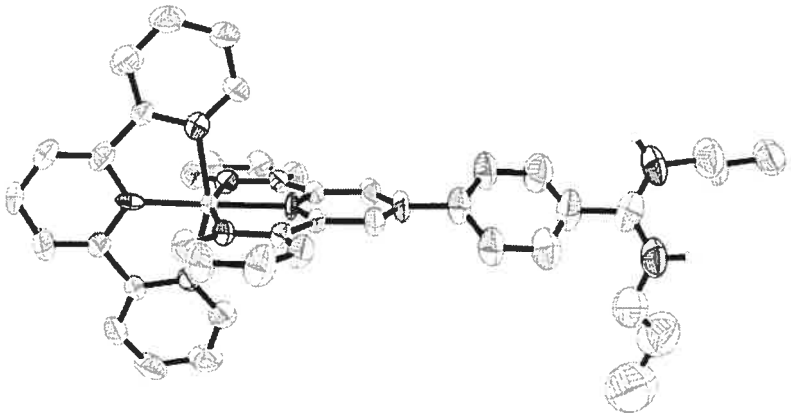

Selected Parameters

N_{11}-Ru-N_{21} = 96.1(2) °
N_{11}-Ru-N_{18} = 79.9(2) °
tpy-$ph_{(torsion)}$ = 44.0 $^{o}_{(av)}$

N_{18}-Ru = 2.038(5) Å
N_{11}-Ru = 2.083(6) Å
C_{125}-N_{130} = 1.318(8) Å
C_{125}-N_{126} = 1.313(8) Å

Figure 4.3 ORTEP of one of the two unique complexes of **IV-1 $(PF_6)(BPh_4)_2$** with thermal ellipsoids at 50 % probability. Solvent and counter-ions are omitted for clarity.

The ^{1}H NMR in CD_3CN of complex **IV-1 $(PF_6)_2$** (Figures 4.4, 4.5) is unambiguous, wherein all pyridyl and aliphatic signals are well resolved and give relative integration in agreement with the proposed structure. It is interesting to note that, at room temperature, the amidine-proton resonance occurs as two distinct signals, as does each multiplet of the *N*-propyl substituents. Moreover, each amidine-proton resonance corresponds to one proton from relative integration. However, at elevated temperature the amidine proton resonances coalesce to give a signal integrating to one proton, while the *N*-propyl multiplets remain unchanged (Figures 4.6, 4.7). In the case of *N,N'*-disubstituted benzamidines bearing an aryl group on the imino nitrogen, an *E* configuration about the C-N double bond has been found to be dominant.[1,11] Considering the invariance of the *N*-propyl amidines at elevated temperature, we postulate that rotational isomerism about the C-N single bond has differentiated the amidine proton resonance within the context of an *E* geometrical isomer, given the substantial steric encumbrance imposed about the amidine moiety.

At room temperature, the ^{1}H NMR spectrum of complex **IV-2 $(PF_6)_2$** in CD_3CN (Figure 4.8) is less clear, owing to severe broadening of the *N*-phenyl and amidine proton resonances along with an unobserved phenyl doublet. At elevated temperature (330 K), the broad amidine resonance at 9.68 ppm was lost completely while the missing phenyl doublet was shifted downfield and resolved from the multiplet arising from the 4, 4' protons of tpy at 8.0 ppm. The origin of this doublet is assigned to the phenyl protons

nearest the amidine on the basis of large shifts observed for this resonance upon protonation with HPF_6. The dynamic solution behaviour of the *N*-phenyl groups is evidenced by partial resolution, at elevated temperature, of the broad resonance that occurs at room temperature between 7.60-7.30 ppm. At 330 K, this broad resonance separates into two components, one of which is a broad doublet at 7.5 ppm and the other of which is coincident with the 6,6'' tpy resonances. The combined integration of these signals corresponds reasonably well to ten protons, as anticipated for the two *N*-phenyl groups.

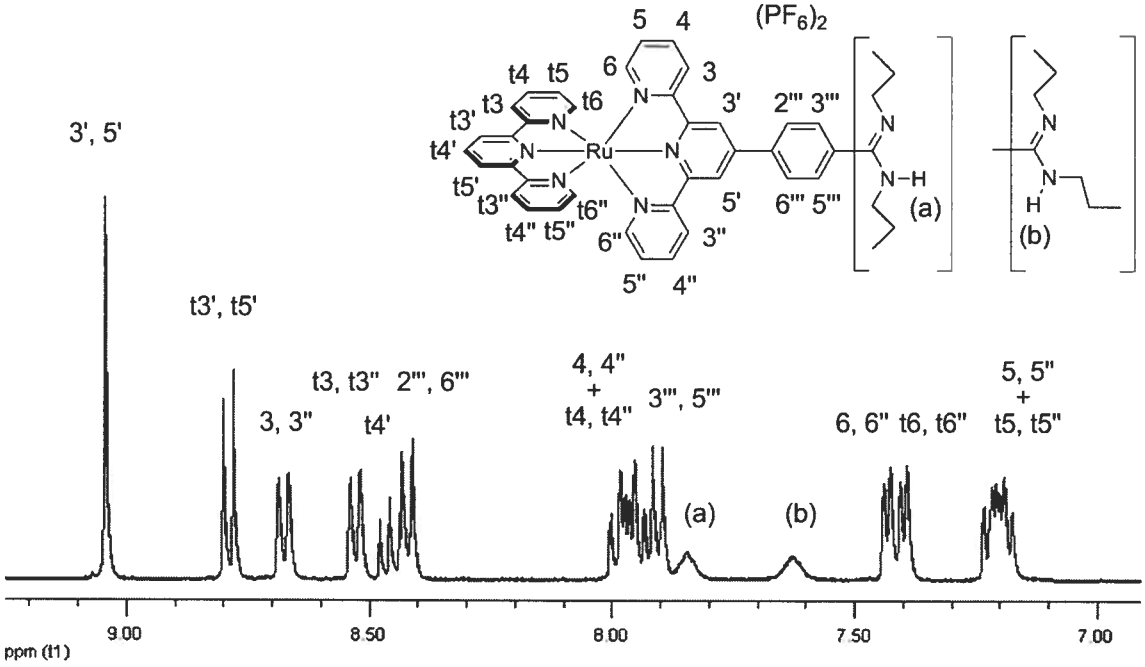

Figure 4.4. ^{1}H NMR spectrum of complex **IV-1 $(PF_6)_2$** in CD_3CN (aromatic region).

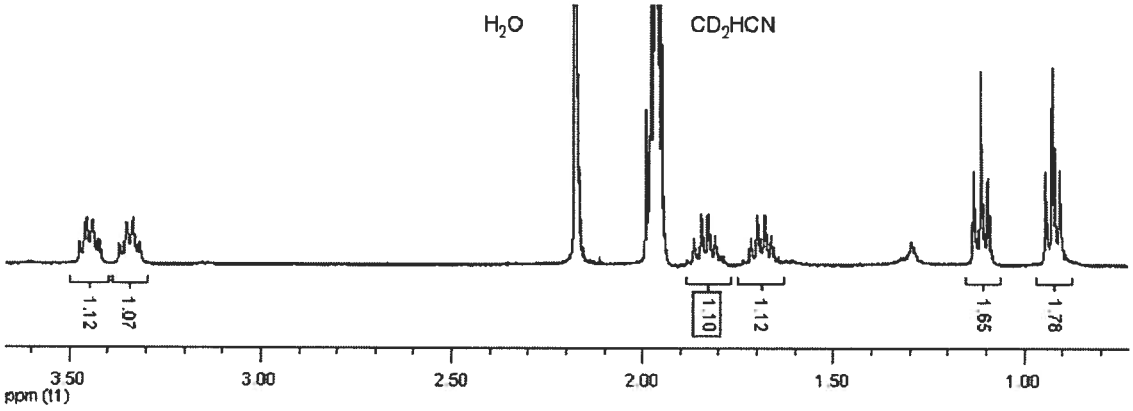

Figure 4.5 ^{1}H NMR spectrum of complex **IV-1 $(PF_6)_2$** in CD_3CN at r.t. (aliphatic region).

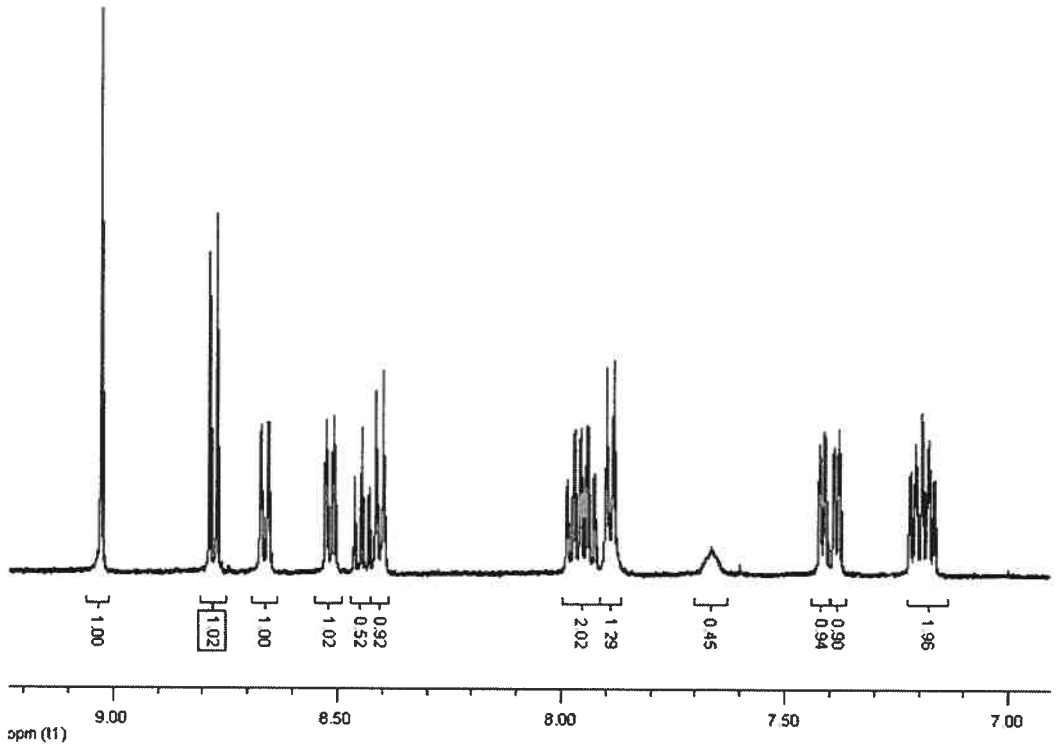

Figure 4.6 ^{1}H NMR spectrum of complex **IV-1 $(PF_6)_2$** in CD_3CN at 330 K (aromatic region).

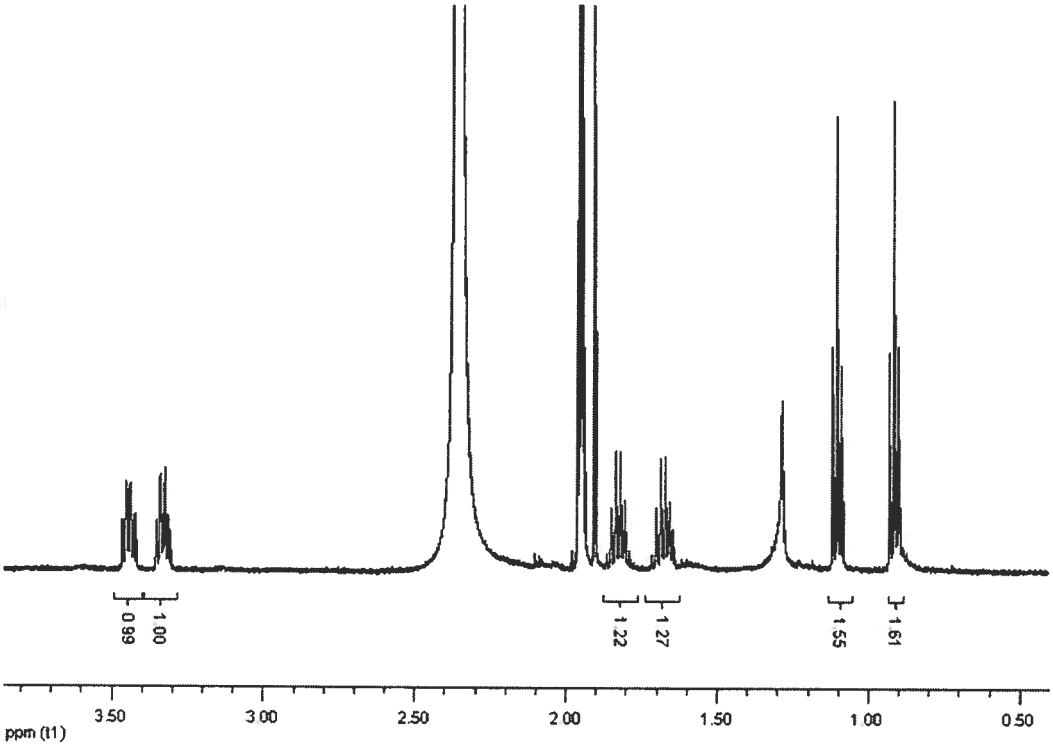

Figure 4.7 ^{1}H NMR spectrum of complex **IV-1 $(PF_6)_2$** in CD_3CN at 330 K (aliphatic region).

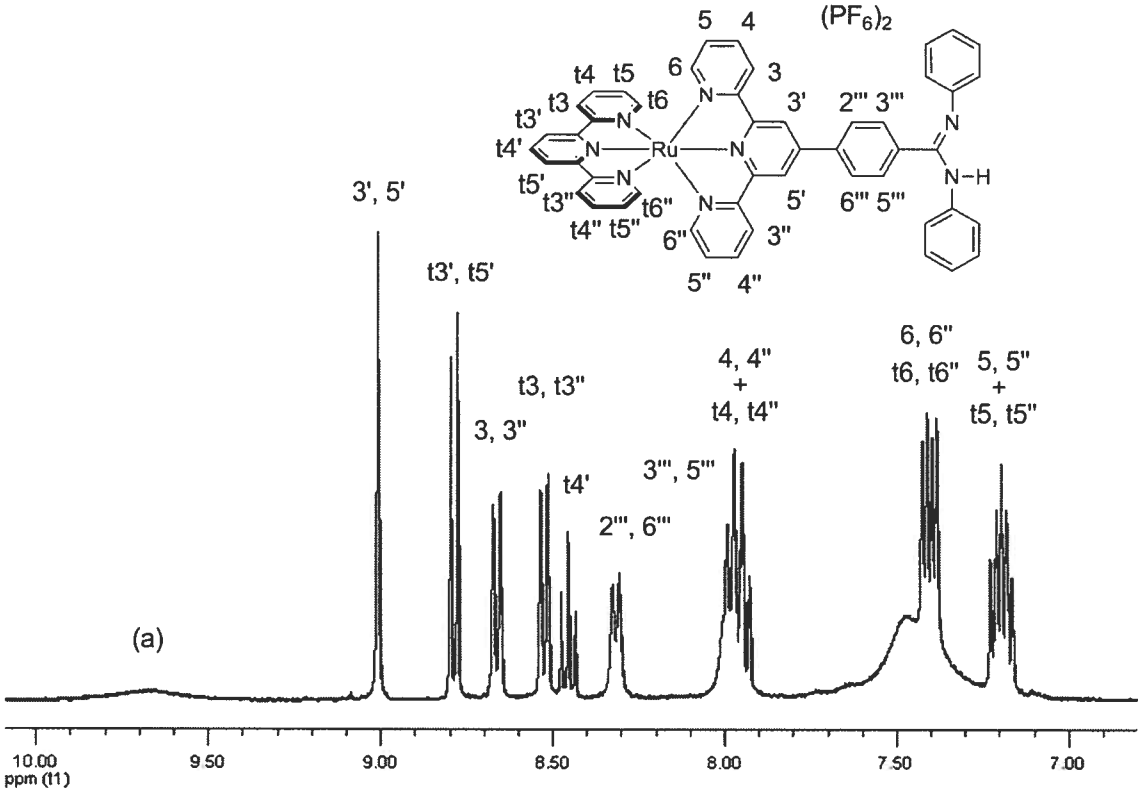

Figure 4.8 ^{1}H NMR spectrum of complex **IV-2 $(PF_6)_2$** in CD_3CN at r.t.

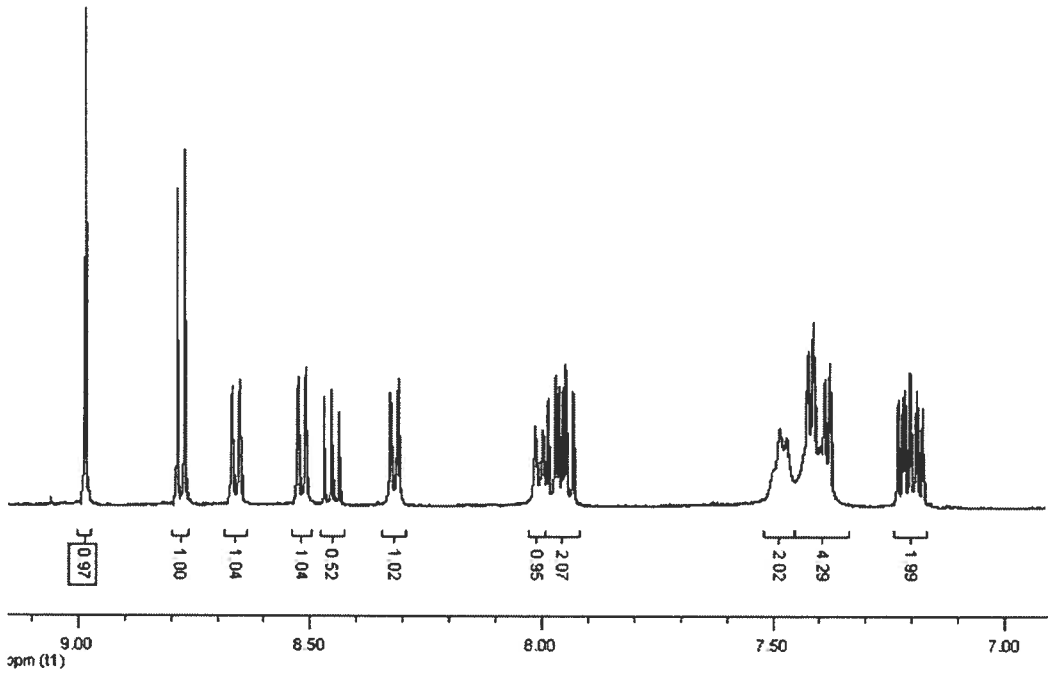

Figure 4.9 ^{1}H NMR spectrum of complex **IV-2 $(PF_6)_2$** in CD_3CN at 330 K.

4.3 Spectrophotometric and Spectrofluorimetric Determination of Ground-State pKa Values for Complexes IV-1 $(PF_6)_2$ and IV-2 $(PF_6)_2$.

Complexes **IV-1 $(PF_6)_2$** and **IV-2 $(PF_6)_2$** exhibit electronic absorption profiles characteristic of $(tpy)_2Ru^{2+}$ complexes.[12] A metal-ligand charge transfer (MLCT) band occurs in the visible at 486 nm for both complexes (Figures 4.10 and 4.15, respectively), while the UV region is dominated by ligand-based transitions of $\pi \rightarrow \pi^*$ and $n \rightarrow \pi^*$ origin at 271 and 331 nm, respectively, for complex **IV-2 $(PF_6)_2$**. For complex **IV-1 $(PF_6)_2$**, these bands appear to be split into components at 275 and 281 nm, and at 305 and 330 nm.

As with carboxylate and phosphonate-appended Ru(II) dye sensitizers, monitoring the intensity of the MLCT and / or ligand centered transitions of complexes **IV-2 $(PF_6)_2$** and **IV-1 $(PF_6)_2$** as a function of pH (pH = 2-13) produced clear inflection points for both complexes (Figures 4.12, 4.13, and 4.17) corresponding to their respective pKa values.[13] In general, very little if any displacement of the absorption maxima was observed as a function of pH. Likewise, the emission intensity of these complexes also produced very clear inflection points as a function of pH (Figures 4.14 and 4.18) that showed only minor (4-8 nm) shifts in the emission maxima at pH values bracketing the pKa. First-derivative plots of these data sets gave ground-state pKa data, which is summarized in Table 4.1 along with absorption and emission data recorded at pH values where the appended amidine moiety of the complex exists as the free-base.

Here, the intensity of the absorption and emission bands increases with decreasing pH for these amidine complexes. However, while the absorption maxima do not deviate as a function of pH, a slight red-shift is observed in the emission maxima corresponding to $\Delta\lambda = 4$ nm for **IV-1 $(PF_6)_2$** and $\Delta\lambda = 8$ nm for **IV-2 $(PF_6)_2$**. These observations are in accord with a previous report by Barigelletti and co-workers, which showed that protonation of appended, uncomplexed tpy ligands enhances emission from $(tpy)_2Ru^{2+}$ units through stabilization of the ^{3}MLCT state, likely due to electrostatic influence.[14] However, in the absence of excited-state pKa values (pKa^*) for the amidine complexes here, it is difficult to assess the degree of electronic mixing of the amidine fragments with that of the MLCT state. As such, it is quite possible that these amidines behave simply as

spectators, the protonation of which may serve to reduce energetic barriers to charge-separation, and hence the slight red-shift observed here in the emission spectra. To this end, numerous detailed studies have been reported for various polypyridyl-based sensitizers bearing secondary, protonable functionality.[15] With regard to variation of emission intensity with pH, quite often protonation of such secondary groups entails diminished emission, for which proton-induced quenching has been invoked. Interestingly, the opposite effect is observed for these amidine complexes.

The large difference in the measured pKa values for complexes **IV-1 $(PF_6)_2$** and **IV-2 $(PF_6)_2$** underscore the effect that the *N*-substituents have on the basicity of the amidine chelate. Here, it is clear that the *N*-propyl groups have a relatively large electron-releasing effect relative to the *N*-phenyl groups.

Lastly, it is interesting to note that the measured pKa for complex **IV-2 $(PF_6)_2$** is comparable to that for *N,N'*-diphenylbenzamidine (pKa = 6.15 ± 0.04),[16] although the near unitary difference suggests an electron releasing effect by the appended $(tpy)_2Ru^{2+}$ moiety. However, discrepancies in the conditions and manner in which these parameters were determined must be taken into consideration, and so no definitive effect may yet be attributed in this regard. This will be addressed further in Section 4.4.

Table 4.1 Absorption, Emission, and pKa Data for Complexes IV-1 $(PF_6)_2$ and IV-2 $(PF_6)_2$

Complex	^{1}MLCT λ_{max} (nm) ε ($M^{-1}cm^{-1}$)	LC transitions λ_{max} (nm), ε ($M^{-1}cm^{-1}$)				Em.	pKa (avg)
IV-1$(PF_6)_2$ [a]	486 (8200)	330 (13200)	305 (21000)	281 (24400)	275 (25100)	659	11.90 ± 0.18
IV-2 $(PF_6)_2$ [b]	486 (10400)	330 (15000)	-	-	271 (30200)	652	7.12 ± 0.10

(a) Absorption and emission data taken at pH = 12.80 in 0.1 M $KCl_{(aq)}$ soln. (4:1 (v/v) H_2O / DMSO).

(b) Absorption and emission data taken at pH = 8.88 in 0.1 M $KCl_{(aq)}$ soln. (4:1 (v/v) H_2O / DMSO).

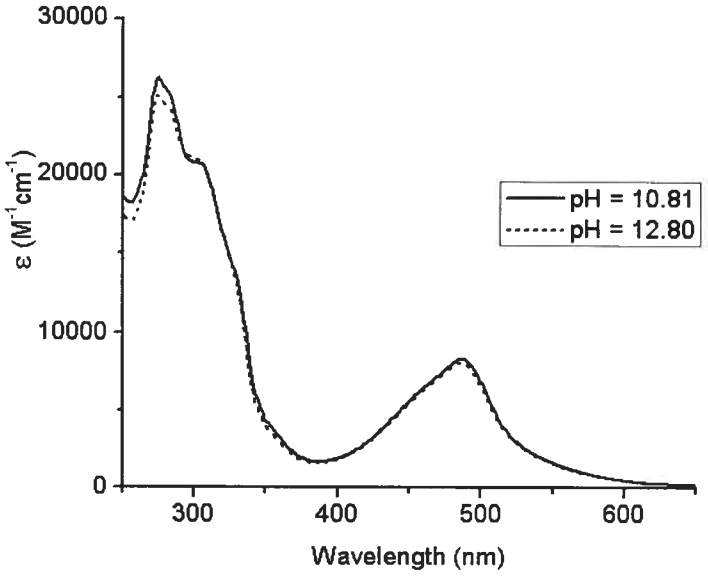

Figure 4.10 Absorption overlay of complex **IV-1** $(PF_6)_2$ at pH values bracketing the pKa.

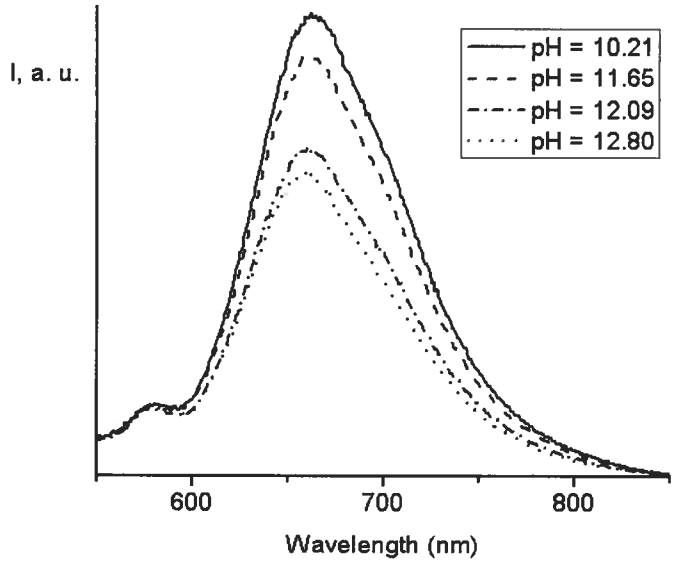

Figure 4.11 Emission overlay of complex **IV-1** $(PF_6)_2$ at pH values bracketing the pKa.

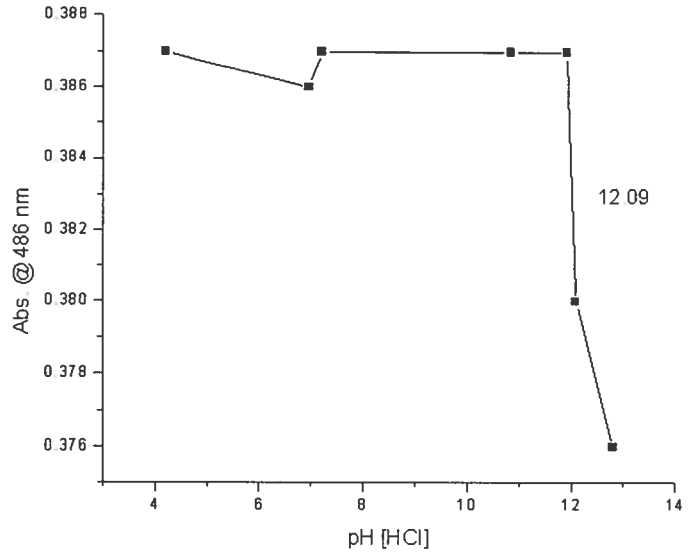

Figure 4.12 Spectrophotometric titration of complex **IV-1** $(PF_6)_2$ at 486 nm.

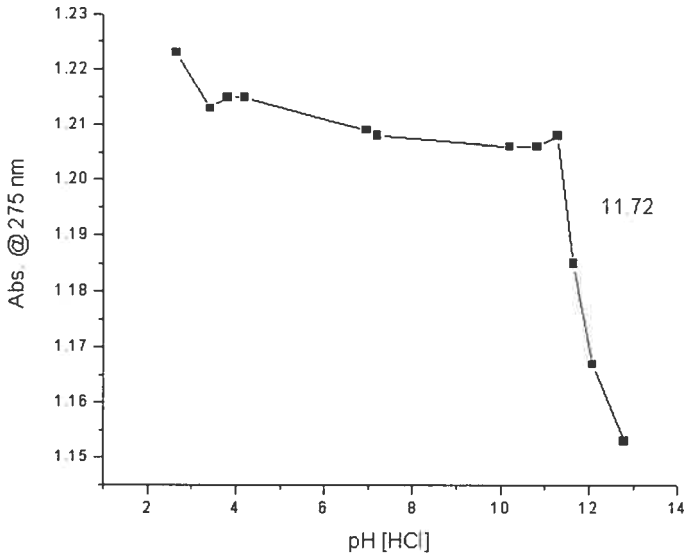

Figure 4.13 Spectrophotometric titration of complex **IV-1** $(PF_6)_2$ at 275 nm.

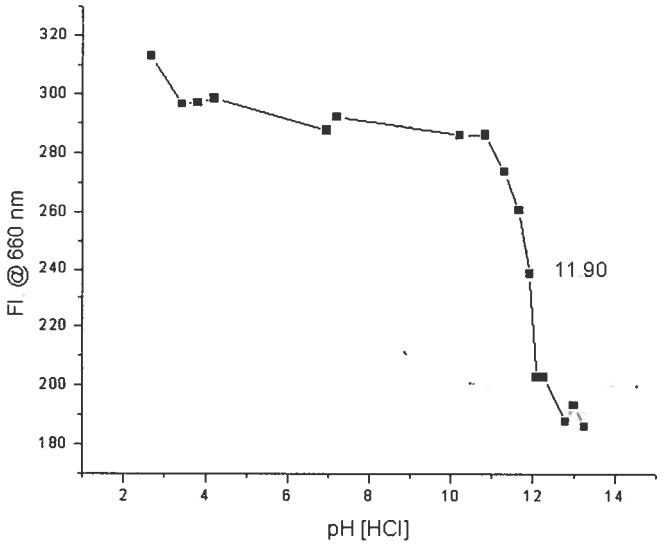

Figure 4.14 Spectrofluorimetric titration of complex **IV-1** $(PF_6)_2$ at 660 nm.

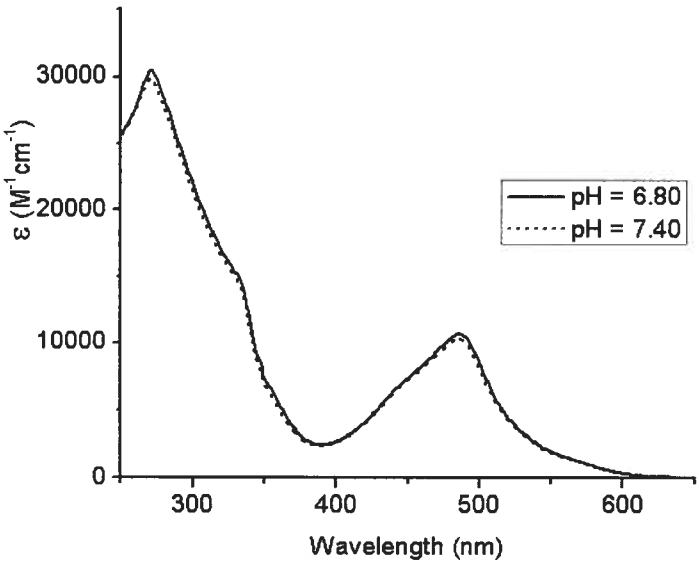

Figure 4.15 Absorption overlay for complex **IV-2** $(PF_6)_2$ at pH values bracketing the pKa.

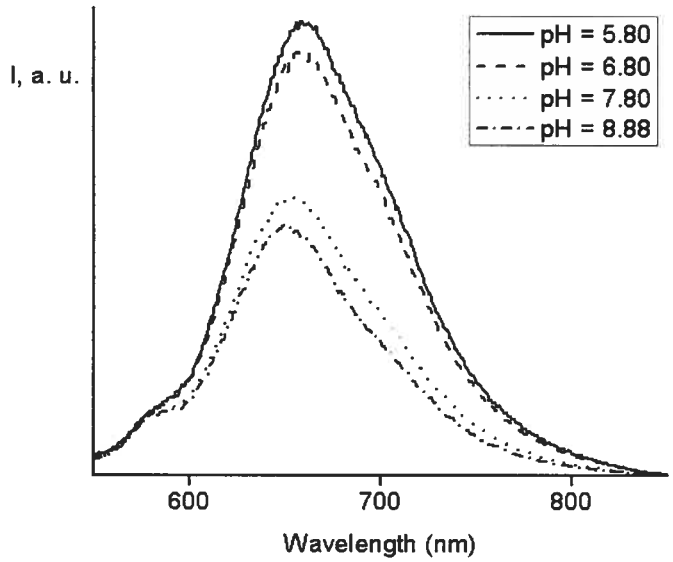

Figure 4.16 Emission overlay for complex **IV-2 $(PF_6)_2$** at pH values bracketing the pKa.

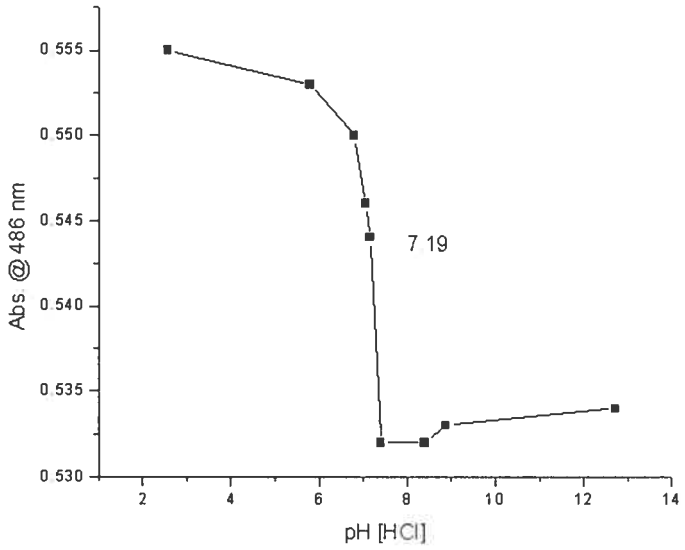

Figure 4.17 Spectrophotometric titration of complex **IV-2 $(PF_6)_2$** at 486 nm.

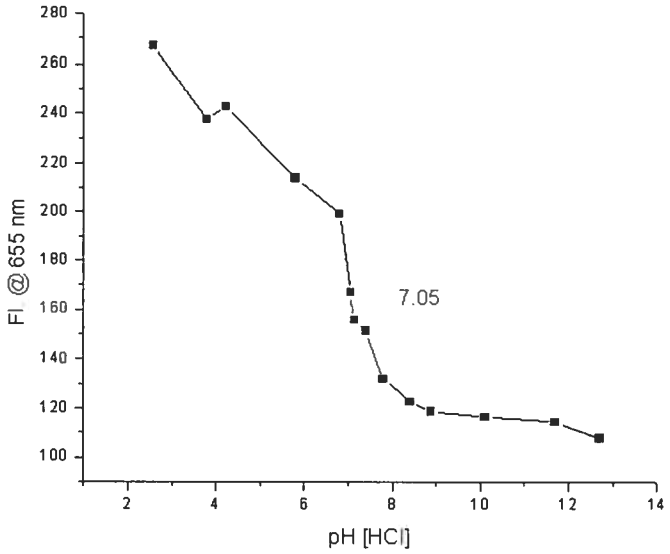

Figure 4.18 Spectrofluorimetric titration of complex **IV-2 $(PF_6)_2$** at 655 nm.

4.4 Electrochemistry of Complexes IV-1 $(PF_6)_2$ and IV-2 $(PF_6)_2$.

Summarized in Table 4.2 is the electrochemical data for complexes **IV-1 $(PF_6)_2$** and **IV-2 $(PF_6)_2$** obtained from their respective cyclic voltammograms (Figure 4.19). The profiles of these voltammograms are largely characteristic of $(tpy)_2Ru^{2+}$ complexes in general, in that one finds a reversible $Ru^{3+/2+}$ couple at oxidizing potential and two subsequent ligand-based reductions on the return cathodic scan.[12] All such redox processes here are both electrochemically and chemically reversible. Comparison of the half-wave potentials for both the metal-based and tpy-based redox processes indicate a strong electron releasing effect by the *N*-propyl substituents. This effect is most pronounced for the $Ru^{3+/2+}$ couple, for which the $E_{1/2}$ is cathodically displaced by 0.10 V relative to that for **IV-2 $(PF_6)_2$**, and is consistent with a significantly more basic *N,N'*-dipropyl benzamidine moiety as indicated by their respective pKa values (Table 4.1).

Amidines themselves are known to be electro-active, though very few reports exist in the literature concerning their electrochemistry.[17] The related compound *N,N'*-diphenylbenzamidine has been reported to possess two irreversible oxidations at 0.73 V and 1.93 V (vs SCE) and two irreversible reductions at -0.4 and -2.46 V (vs SCE), the former of which is very weak. With the exception of this higher-potential reduction, such processes are characteristic of most amidines. Complexes **IV-1 $(PF_6)_2$** and **IV-2 $(PF_6)_2$**

both possess similar irreversible and broad oxidations in their cyclic voltammograms at 0.85 and 0.94 V, respectively, the difference of which (0.09 V) is consistent with the electron releasing effect of the *N*-propyl substituents and analogous to that noted for the $Ru^{3+/2+}$ processes of the two complexes. However, only complex **IV-2 $(PF_6)_2$** was found to possess more than two reduction processes, of which a relatively weak and irreversible cathodic wave occurs at -0.90 V. These irreversible oxidations and reduction processes are tentatively assigned to the amidine fragment.

If we assume, then, that the irreversible oxidations observed at 0.85 and 0.94 V for complexes **IV-1 $(PF_6)_2$** and **IV-2 $(PF_6)_2$**, respectively, correspond to that at 0.73 V for *N,N'*-diphenylbenzamidine, it is interesting to note that there is an anodic shift of 0.21 V upon appendage of the $(tpy)_2Ru^{2+}$ moiety to *N,N'*-diphenylbenzamidine. This may be rationalized considering the charged nature of the complex and / or an electron withdrawing effect upon attachment of an extended aromatic system (tpy). This effect is contrary to that noted in Section 4.3 regarding comparison of the pKa values measured for complex **IV-2 $(PF_6)_2$** (pKa = 7.12) and that reported in the literature for *N,N'*-diphenylbenzamidine (pKa = 6.15). Considering that the difference in pKa values is modest and that discrepancies may arise from the manner in which they were determined, we place much more confidence in this electrochemical interpretation.

Table 4.2 Electrochemical Data for Complexes IV-1 $(PF_6)_2$ and IV-2 $(PF_6)_2$.

Complex	Potential [V] vs SCE. ΔE_p (mV) [a]				
	$Ru^{3+/2+}$	R-NCN-R		tpy	
IV-1 $(PF_6)_2$	1.25 (90)	0.85 (ir) [b]	-	-1.24 (70)	-1.48 (70)
IV-2 $(PF_6)_2$	1.35 (80)	0.94 (ir) [b]	-0.90 (ir) [c]	-1.18 (60)	-1.45 (60)

a) Scan rate 100 mV s^{-1}. $E_{1/2}$ = ½ (E_{pa} + E_{pc}), where E_{pa} and E_{pc} are the anodic and cathodic peak potential respectively. $\Delta E_p = E_{pa} - E_{pc}$. Reported values for irreversible processes, labeled ir, are peak potentials. Potentials are corrected by internal reference, ferrocene (395 mV). b) anodic wave peak potential. c) cathodic wave peak potential

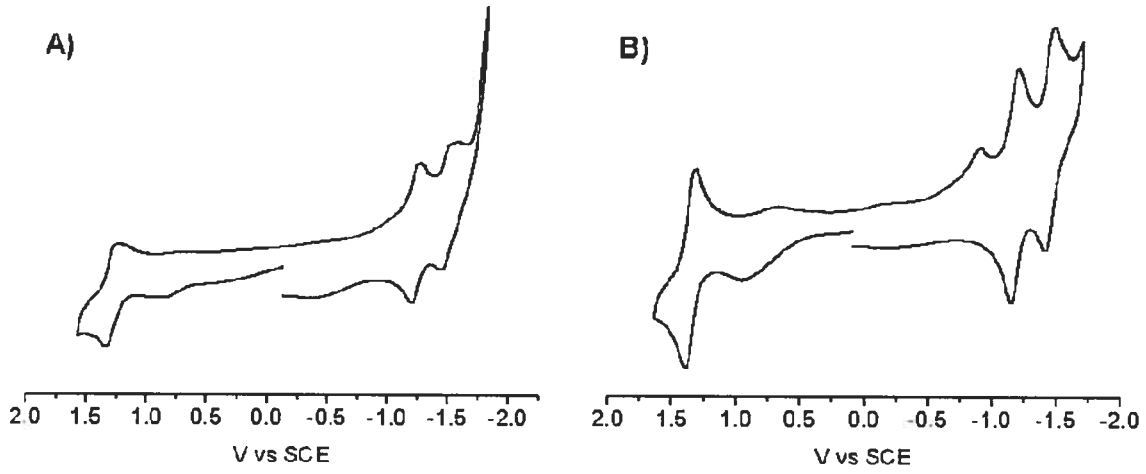

Figure 4.19 Cyclic voltammograms of **IV-1 $(PF_6)_2$ (A)** and **IV-2 $(PF_6)_2$ (B)** in 0.1 M $TBAPF_6$ CH_3CN solution at 100 mVs^{-1}.

4.5 Synthesis and Characterization of *N,N'*-Di-(4'-phenyl-tpy) formamidine (refer to page LXVIII of Appendix 4 for X-ray data and parameters of complex **IV-3 $(BPh_4)_2$**)

Synthesis of symmetric formamidines is typically accomplished by reaction of an aromatic or aliphatic amine with a trialkyl-orthoformate, such as triethyl-orthoformate, under distillation conditions to remove the alcohol by-product.[18] To this end, the precursor 4'-(4-aminopheny)-tpy was desired. Although this is a known compound, we have outlined a modified route based upon formation and reduction of the 4'-(4-nitrophenyl)-tpy precursor.[19] This nitro intermediate can be formed by reaction of 4-nitrobenzaldehyde with two equivalents of 2–acetylpyridine, either in the presence of $NH_4OH_{(aq)}$ in methanolic solution or using solvent-less conditions. The former route gives a black tar-like residue that is difficult to manipulate prior to reduction to the amino, while a solvent-less approach proceeds much more rapidly and with slightly improved yield. In both cases, while flash chromatography of the crude reaction mix affords pure 4'-(4-nitrophenyl)-tpy, reduction was typically performed directly on the crude reaction mix to save time considering that column purification of the desired 4'-(4-aminopheny)-tpy is required anyway.

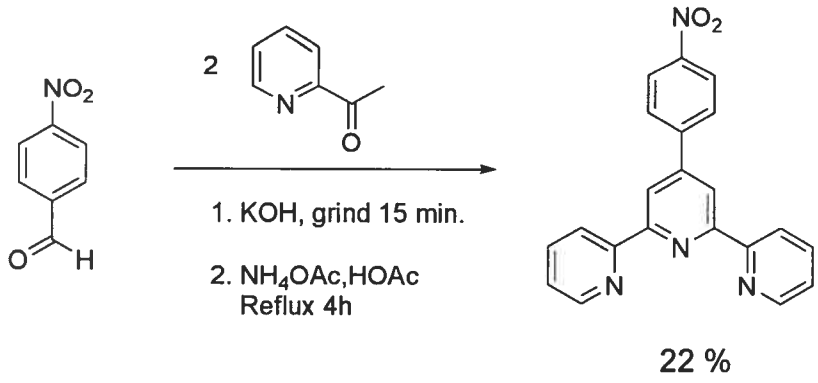

Scheme 4.3 Synthesis of 4'-(4-nitrophenyl)-tpy. Yield obtained after chromatography.

Pouring the reaction mix, obtained in the final step outlined in Scheme 4.3, into water gave a crude precipitate which was filtered off and reduced according to Scheme 4.4 below. Neutralization of the reaction mix, followed by extraction with DCM and purification by column chromatography, gave the desired amino starting material in sufficient yield (31%) considering the ease with which the reaction may be scaled-up.

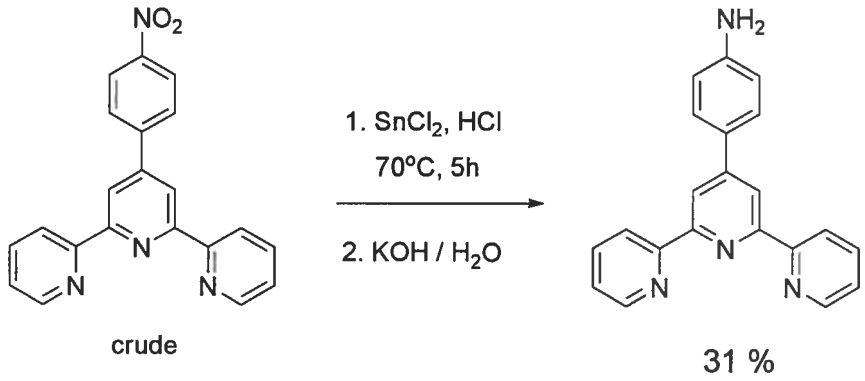

Scheme 4.4 Synthesis of 4'-(4-aminophenyl)-tpy. Yield is based on 4-nitro-benzaldehyde after column purification.

Reaction of 4'-(4-aminophenyl)-tpy with triethyl orthoformate (Scheme 4.5) at sufficiently elevated temperatures to distill ethanol by-product did not lead to the desired symmetric formamidine. Instead, thin-layer chromatography (TLC) revealed several species among which was a large amount of the amine starting material. This was invariant of whether the reaction was performed without solvent, by melting first the amine ligand (m.p. = 250 °C), or with solvent such as dry toluene.

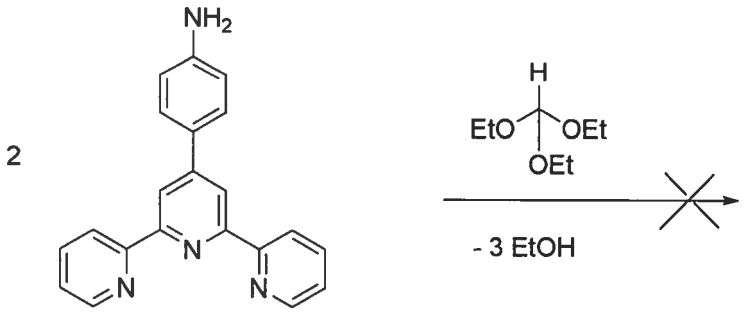

Scheme 4.5 First attempt to synthesize the symmetric formamidine upon distillation of ethanol by-product.

Another approach which may be taken to form symmetric formamidines involves reaction with *s*-triazine (Scheme 4.6 below).[20] Here, an excess of 4'-(4-aminophenyl)-tpy was heated to reflux in toluene with *s*-triazine. However, only starting materials were seen by TLC.

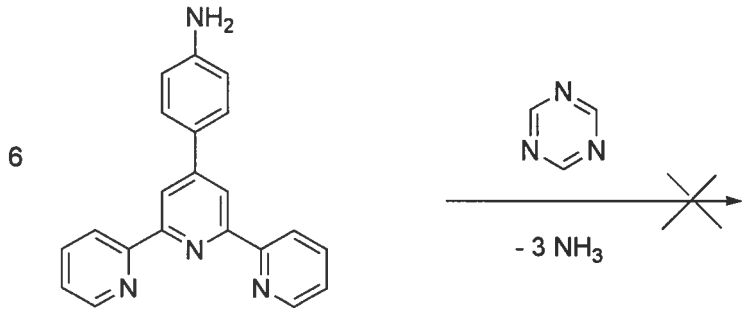

Scheme 4.6 Second attempt using s-triazine in refluxing toluene.

In light of the synthetic roadblocks outlined above, we were prompted to investigate ways in which one may install a formamidine moiety that would permit subsequent formation of the tpy ligands. The compound *N,N'*-di(4-formylphenyl) formamidine (Scheme 4.8) was therefore pursued.

Aldehyde functionality is accessible by mild oxidation of the corresponding benzyl alcohol,[21] and so the precursor *N,N'*-di(4-hydroxymethyl phenyl) formamidine was desired. However, the surprisingly high cost of 4-aminobenzyl alcohol motivated us

to synthesize it in an expedient manner from the much less costly 4-nitrobenzyl alcohol.

Reduction of 4-nitrobenzyl alcohol with sodium borohydride, followed by solvent extraction, gave pure 4-aminobenzyl alcohol in nearly quantitative yield (Scheme 4.7). With this material in hand, however, high temperature distillation protocols like those discussed previously proved to be too harsh for the benzyl functionality. Symmetric formamidines are also accessible from trialkyl orthoformates in the presence of a weak acid, which permits mild reaction conditions, although reaction times are considerably longer.[22] Such a protocol proved to be ideal for the 4-aminobenzyl alcohol substrate, wherein the use of DCM afforded the formamidine product as a pure precipitate from the reaction mix in decent yield (Scheme 4.7).

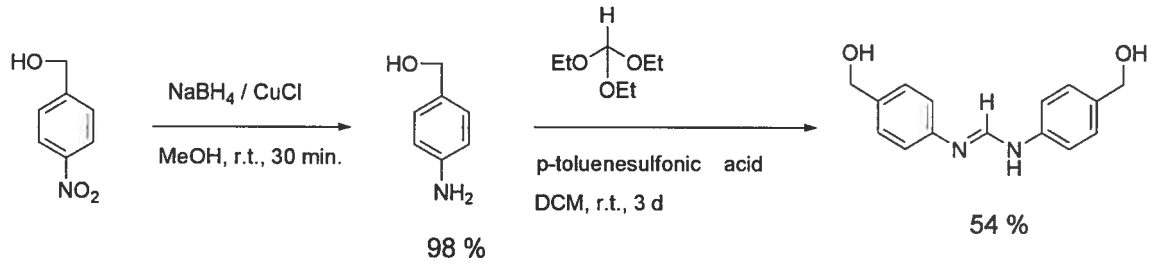

Scheme 4.7 Synthesis of *N,N'*-di(4-hydroxymethylphenyl) formamidine.

Mild oxidation of the dibenzyl formamidine proceeded smoothly using activated MnO_2 to give the desired dialdehyde formamidine precursor (Scheme 4.8).

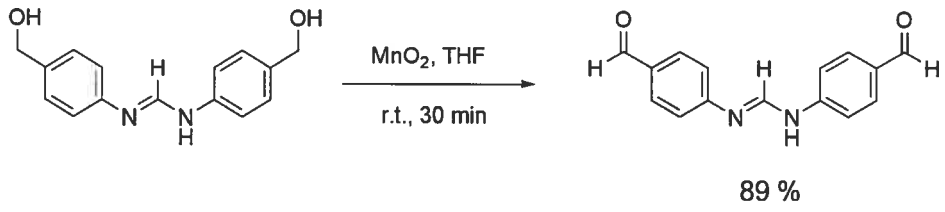

Scheme 4.8 Synthesis of *N,N'*-di(4-formylphenyl) formamidine.

Subsequent condensation of this dialdehyde with 2-acetylpyridine in a methanolic solution containing NH_4OH gave, after stirring at room temperature for 7 h, a heavy white precipitate which, when dissolved, looked to be mostly 4'-(aminophenyl)-tpy by

TLC. This was confirmed by mass spectrometry and ^{1}H NMR, both of which also suggested the presence of 4'-(*N*-phenylformamide)-tpy. The only explanation for the occurrence of these species is hydrolysis of the target amidine molecule once formed.

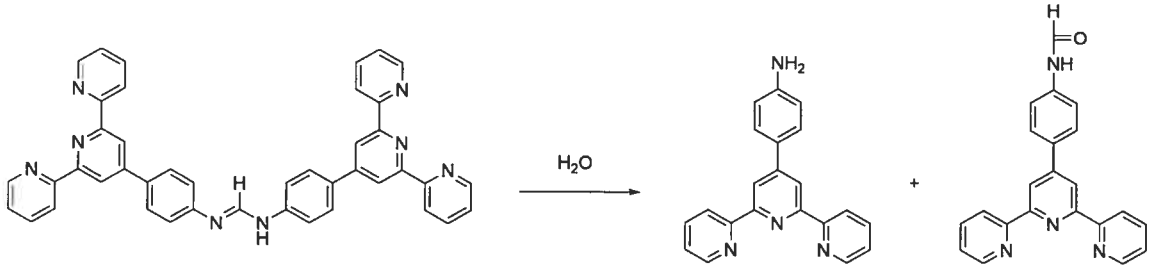

Scheme 4.9 Hydrolysis of *N,N'*-di-(4'-phenyl-tpy)-formamidine.

However, *N,N'*-diaryl amidines are generally regarded as being exceptionally stable to hydrolysis (Scheme 4.9).[18, 21] To be certain, 4'-(*N*-phenylformamide)-tpy was prepared independently according to the protocol outlined in Scheme 4.10. Inspection of this compound by ^{1}H NMR (Figure 4.20) reveals minor resonance components that were initially thought to arise from contamination by impurities. Relative integration, however, indicates that these are actually resonance contributions from another geometric arrangement in solution. It is known that the related compound *N*-phenylformamide exhibits a *cis / trans* distribution in solution at room temperature.[23] This is most evident by distinct carbonyl resonances in its ^{13}C NMR spectrum, which indicates a *cis / trans* ratio of 1.8:1. Here, preference for a *cisoid* structure is suggested by ^{13}C NMR (Figure 4.21), for which the carbonyl resonances agree almost exactly to that of the aforementioned reference compound, indicating a 2.7:1 *cis / trans* distribution.

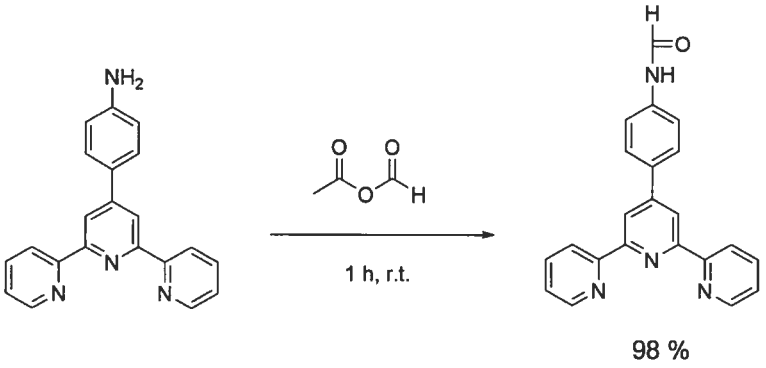

Scheme 4.10 Synthesis of 4'-(*N*-phenylformamide)-tpy.

Such decomposition is easier to ascertain if one is capable of obtaining the target molecule in a pure form. To this end, 4'-(aminophenyl)-tpy was revisited but using instead the acid-promoted conditions with triethyl orthoformate that were successful for the sensitive 4-aminobenzyl alcohol substrate. In this case, solvent selection was found to be critical. Using DCM as solvent in this manner (Scheme 4.11) afforded a heavy precipitate which was found to be pure 4'-(*N*-phenylformamide)-tpy, while the filtrate was found to contain large amounts of 4'-(aminophenyl)-tpy and smaller quantities of the formamide and the desired *N,N'*-di-(4'-phenyl-tpy)-formamidine. Changing the solvent to THF provided much enhanced solubility for both 4'-(aminophenyl)-tpy and 4'-(*N*-phenylformamide)-tpy, and so it was hoped that any precipitate that formed during the reaction would have a greater likelihood of being the target amidine. Over the course of several days, a precipitate indeed developed which was pure by TLC and found to be neither the amine nor the formamide.

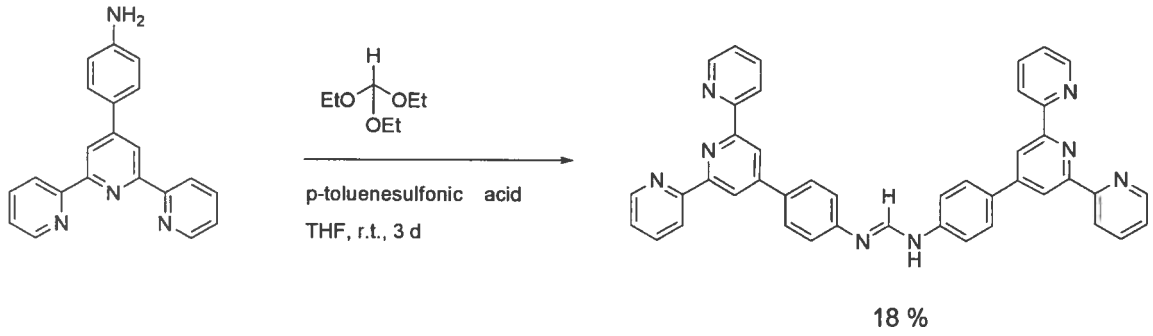

Scheme 4.11 Synthesis of *N,N'*-di-(4'-phenyl-tpy)-formamidine.

This material was found to be appreciably soluble in DMSO solutions only. Mass spectrometry of such a solution was dominated by the presence of the target amidine along with the formamide and amine materials. Initially, the ^{1}H NMR of this material (Figure 4.22) showed no presence of the formamide or the amine decomposition products, but on standing rapidly decomposed over several days to give one or more species resembling strongly 4'-(*N*-phenylformamide)-tpy (Figure 4.23). Interestingly, this decomposition material does not correspond exactly to 4'-(*N*-phenylformamide)-tpy that was prepared independently. This is consistent with the absence of 4'-(aminophenyl)-tpy

in solution, which is evident by the absence of the characteristic -NH_2 resonance normally observed at 5.64 ppm. At this point, however, chromatography of the ^{1}H NMR solution on silica substrate reveals exclusively 4'-(*N*-phenylformamide)-tpy and 4'-(aminophenyl)-tpy. Thus, it appears that this compound hydrolyses incompletely to give one or more species that readily decompose on silica to yield 4'-(aminophenyl)-tpy and 4'-(*N*-phenylformamide)-tpy. Regardless, the clean production of both components is in itself strong evidence for the synthesis of the target *N,N'*-di-(4'-phenyl-tpy)-formamidine.

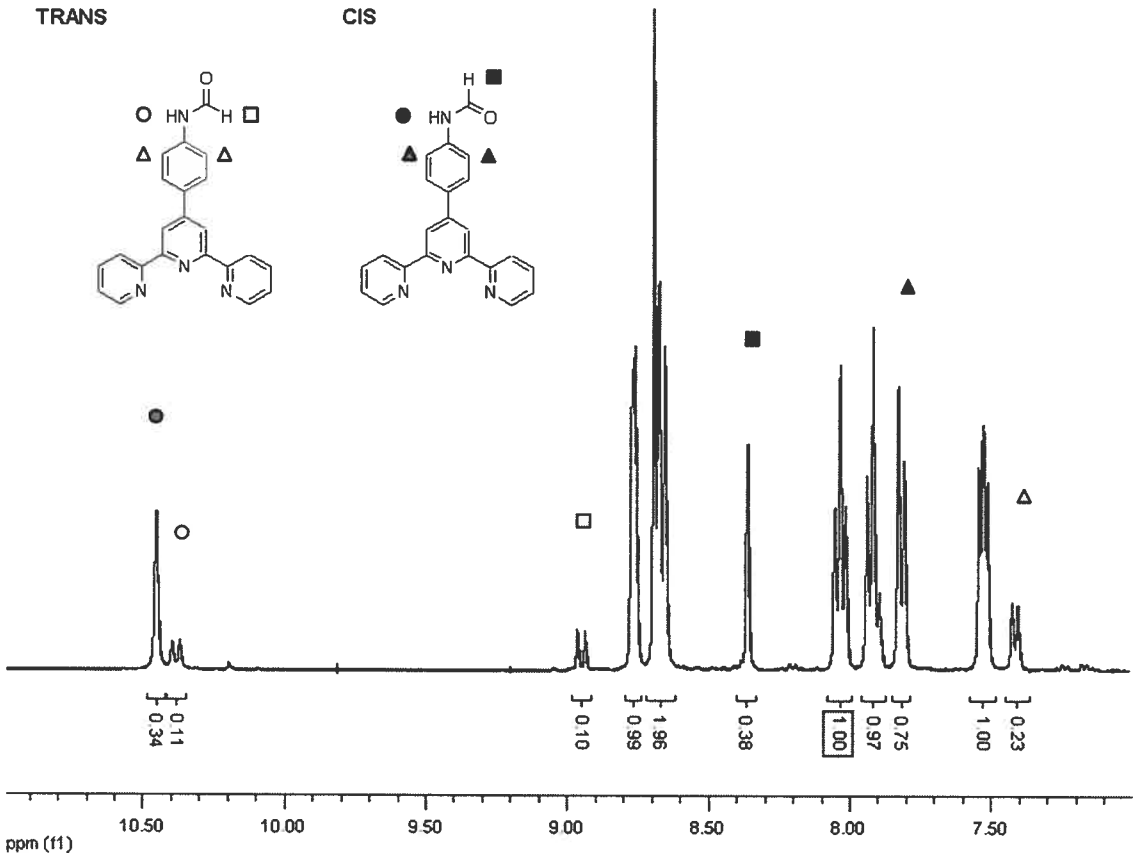

Figure 4.20 ^{1}H NMR of 4'-(*N*-phenylformamide)-tpy in d_6-DMSO at r.t.

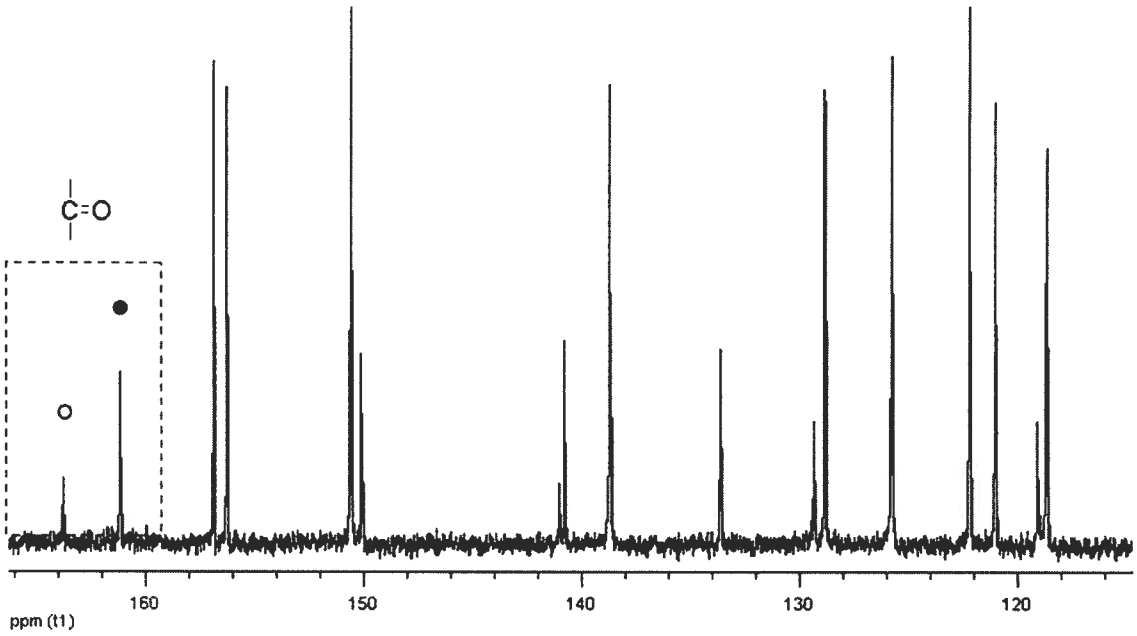

Figure 4.21 ^{13}C NMR of 4'-(*N*-phenylformamide)-tpy in d_6-DMSO at r.t.

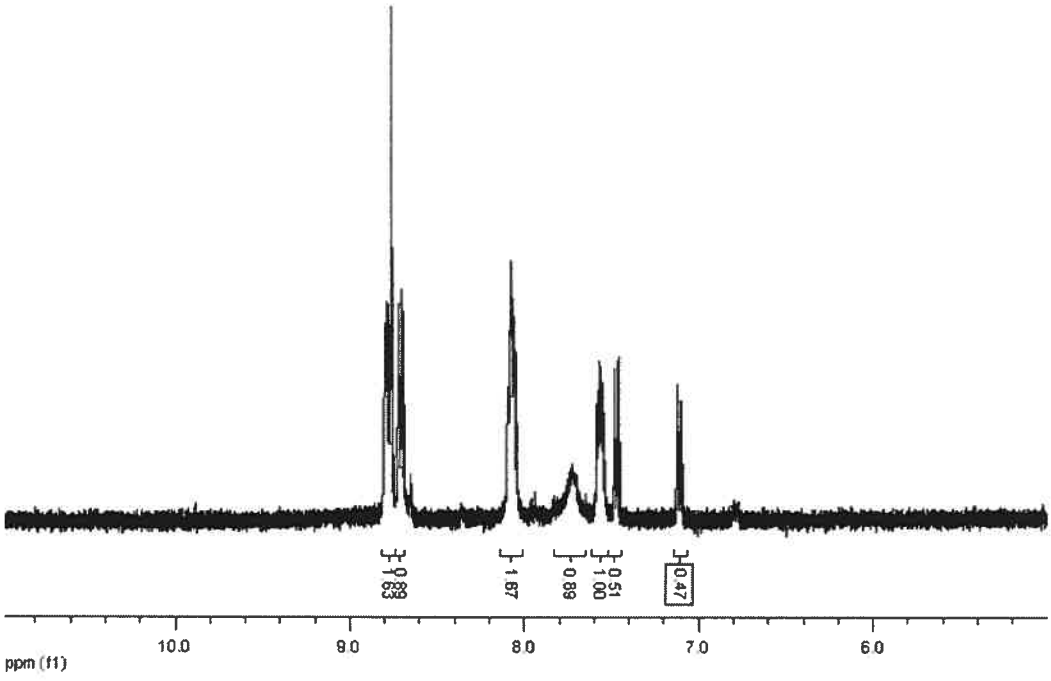

Figure 4.22 ^{1}H NMR of material from Scheme 4.11 in d_6-DMSO. Time = Ø

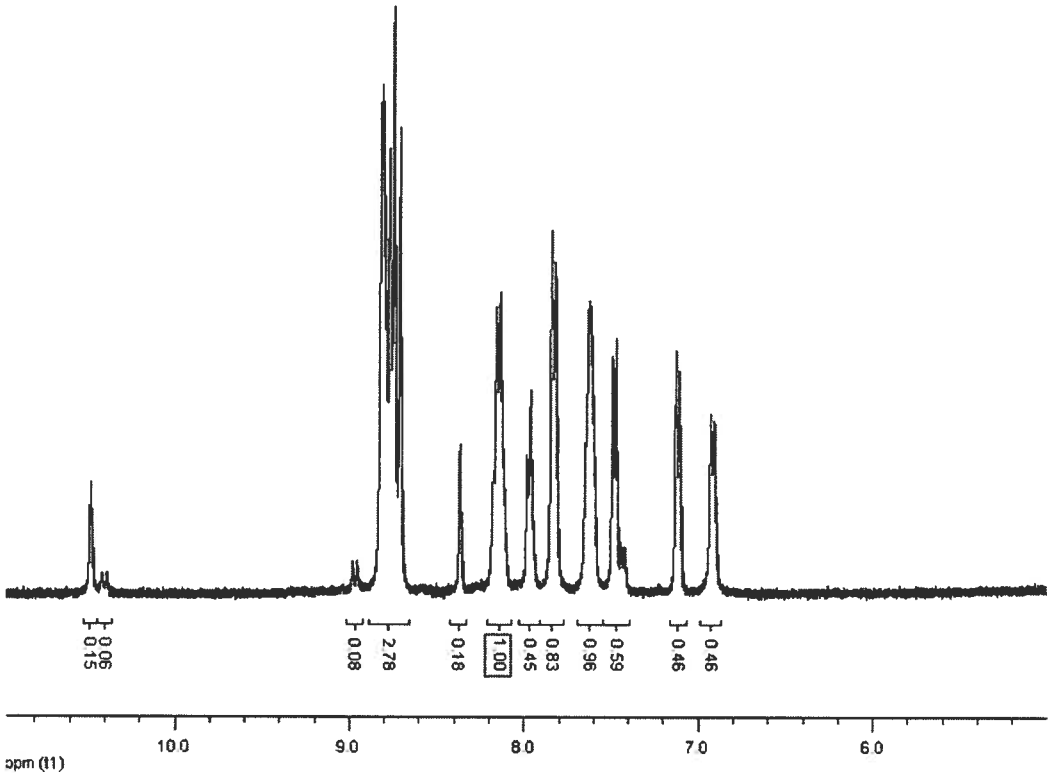

Figure 4.23 ^{1}H NMR of material from Scheme 4.11 in d_6-DMSO after standing for two weeks at r.t.

An obvious question is whether complexation of the tpy ligands could exert a stabilizing influence on the formamidine moiety. To this end, however, there are synthetic limitations imposed by the charged nature of a potential precursor complex such as [(4'-(4-aminophenyl)-tpy)Ru(tpy)]$(PF_6)_2$ if one adopts the synthetic protocols followed to this point. It was therefore opted to complex the material isolated from the reaction outlined in Scheme 4.11, believed to be *N,N'*-di-(4'-phenyl-tpy)-formamidine, directly with Ru(tpy)Cl_3 in the hopes that complexation would precede decomposition of the ligand if there were to be such a stabilizing influence. The reaction is outlined in Scheme 4.12 below.

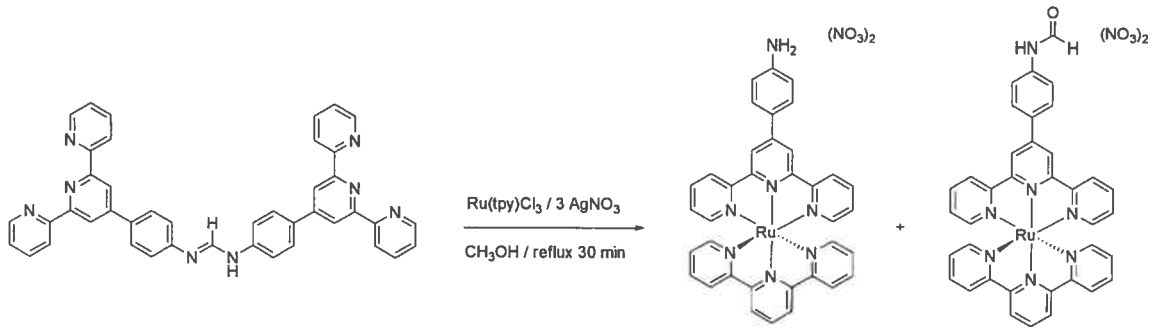

Scheme 4.12 Attempted complexation of *N,N'*-di-(4'-phenyl-tpy)-formamidine.

To help deter ligand decomposition, anhydrous conditions were used and reaction duration was minimized to 30 min at reflux temperature. Although TLC revealed two separable Ru(II) complexes and no starting ligand, their resolution by column chromatography using the same conditions (silica, 7:2 CH_3CN / KNO_3(sat, aq) as eluent) was unsuccessful. This isolated material was found, by ^1H NMR and ESI-MS, to be a mix of both [(4'-(*N*-phenylformamide)-tpy)Ru(tpy]$(PF_6)_2$ and [(4'-(4-aminophenyl)-tpy)Ru(tpy)]$(PF_6)_2$, the former of which gave suitable crystals for structure determination as a di-tetraphenylborate salt upon diffusion of isopropyl ether into an acetonitrile solution of the complex, saturated with NH_4BPh_4. The structure, depicted in Figure 4.24 below along with selected bond lengths and angles, was found to crystallize exclusively in a *cisoid* geometry with respect to the formamide group. The structural parameters are not particularly noteworthy, as they are typical for related complexes.[12] As the molecule lies on a two-fold axis, only one representation is shown in Figure 4.24. Both representations resulting from this two-fold symmetry are differentiated only by their respective 4'-*N*-phenylformamide substituents, as evidenced by partial occupancies of 0.5 for these atoms.

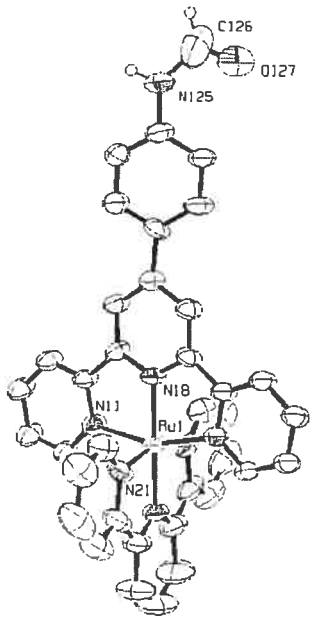

Selected Bond Lengths (Å) and Angles (°):

Ru-N18 = 1.995 (5)
Ru-N11 = 2.066 (4)
Ru-N21 = 2.078 (4)

N18-Ru-N21 = 100.92 (11)
N18-Ru-N11 = 78.81 (10)

C126-O127 = 1.179 (16)
C126-N125 = 1.457 (9)

Phenyl torsion (avg) = 40.9

Figure 4.24 ORTEP depiction of one (of two) unique **IV-3 $(BPh_4)_2$** units at 30% thermal ellipsoid probability. Solvent, counter-anions, and aromatic protons have been omitted for clarity.

Although such unusual susceptibility to hydrolysis precludes the use of this formamidine, it is quite conceivable that analogous compounds based upon *N,N*-di-(terpyridyl) *aryl*amidines (Figure 4.25, below) may show resiliency in this regard. This is particularly true considering the large extent to which such arylamidines may be electronically modified with appropriate functionalization, using the same or similar synthetic protocols outlined herein.

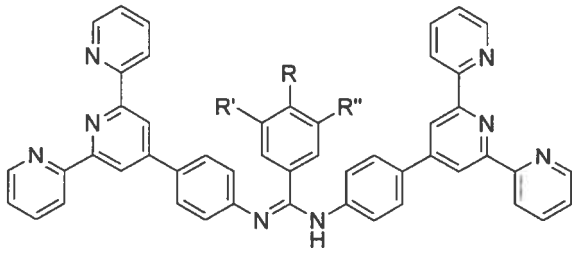

Figure 4.25 Proposed *N,N'*-Di-(4'-phenyl-tpy) arylamidine as potentially more robust alternatives.

4.6 Attempts to Append the Complexes IV-1 $(PF_6)_2$ and IV-2 $(PF_6)_2$ to the Dirhodium(II,II) Unit

The appendage of amidinates in a μ-bidentate fashion to a dimeric unit is, in general, accomplished by either 1.) ligand exchange / metathesis with a suitable dimeric precursor possessing readily displaced mono or μ-bidentate ligands, or 2.) *in-situ* reductive generation of the dimeric unit in the presence of an amidine.[24] Although variations exist within each general approach, one factor which has remained invariable to date is the use of purely organic amidine ligands. The following summarizes the synthetic strategies attempted using the amidine complexes **IV-1** $(PF_6)_2$ and **IV-2** $(PF_6)_2$ toward the convergent development of polynuclear complexes akin to those discussed in Chapter 2.

The simplest reactions performed in the context of the first category involve high temperature displacement with a pre-formed dimeric unit possessing relatively more labile carboxylates. The reaction is performed in a donor solvent with high-boiling point, such as DMF, in the presence of a strong base, typically triethyl amine. However, no reaction was observed after several days at reflux temperature for both the *N,N'*-dipropyl and *N,N'*-diphenyl amidine complexes (Scheme 4.13). This was somewhat surprising, particularly in the case of the *N,N'*-diphenyl amidine complex since this was found to have a modest pKa of 7.12.

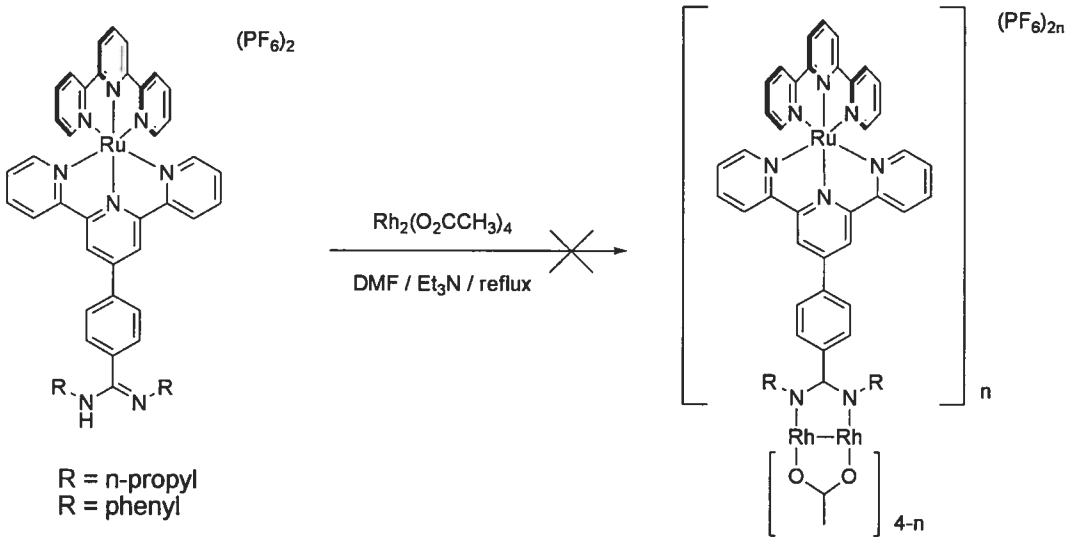

Scheme 4.13 Direct displacement approach at high-temperature.

A second approach in this first category, and by far the most utilized, involves metathesis between an appropriate amidinium salt and the pre-formed dimetal unit. Depending on the basicity of the amidine, either an alkoxide or lithiating reagent may be used, such as n-BuLi (Scheme 4.14), to prepare the amidinium salt *in situ*. Metathesis may be carried out either with a tetracarboxylate dimer or a solvato complex thereof, the latter of which typically shows much enhanced reaction rates. Solvent selection is critical, to ensure both solubility of starting materials and to ensure precipitation of the salt by-product, with THF being the mot commonly used. In this case, both *N,N'*-dipropyl and *N,N'*-diphenyl amidine complexes were sufficiently soluble in THF. Addition of equimolar amounts of either NaOMe or n-BuLi gave noticeable colour changes at -40°C. Upon warming of the solution to room temperature, addition of either $Rh_2(O_2CCH_3)_4$ or *cis*-$[Rh_2(O_2CCH_3)_2(CH_3CN)_{eq}](BF_4)_2$ resulted in solutions that revealed only the uncomplexed amidine over time. The presence of counter-anions in these amidine complexes likely complicates the clean formation of the required amidinium salts in solution, and so the same approach was taken using excesses of base. However, in all cases, only starting materials were observed.

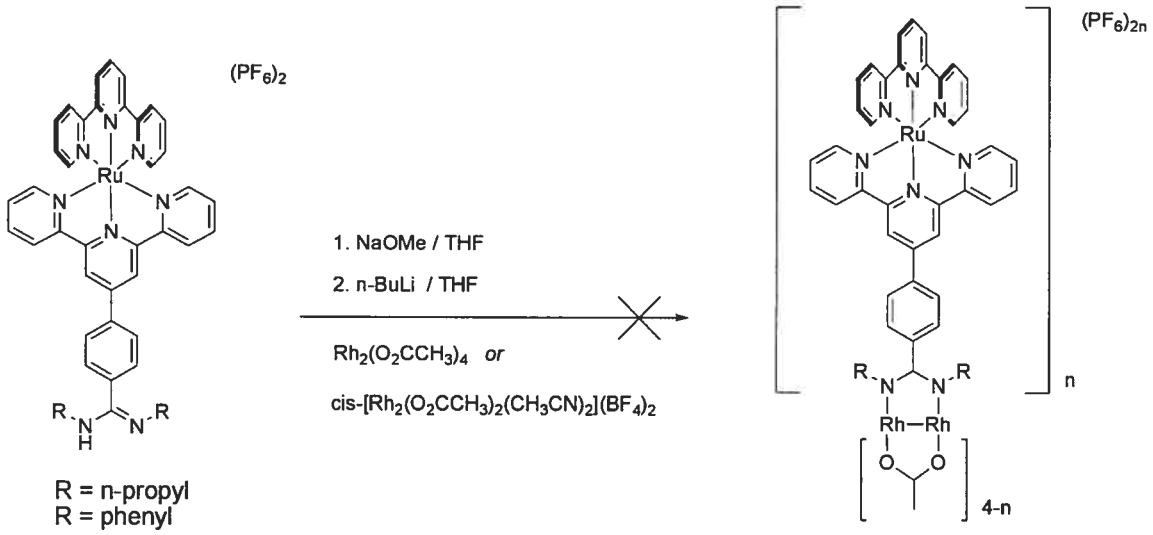

Scheme 4.14 Metathesis approach using both tetraacetate and *cis*-solvato Rh_2 precursors.

Finally, reductive generation of a dimetal "paddlewheel" complex may be formed in the presence of a suitable μ-bidentate starting from the mononuclear salt of the

transition metal. This reaction is outlined in Scheme 4.15 below, and was attempted using only the *N,N'*-dipropyl amidine complex. This reaction, if successful, permits only a tetrameric Ru(II) complex. After purging the combined reagents with three freeze-pump-thaw cycles, refluxing over an argon atmosphere for 24 h resulted in a solution which still contained a fairly large amount of starting amidine complex, along with two new species. The first of these to elute was found by ^{1}H NMR to be very clean but contained no resonances associated with n-propyl groups, while the second did contain the propyl resonances. ESI-MS indicated that both species were 2+ complexes, but formulations of their structures could not be proposed to account for their observed m/z peaks. Regardless, the recovery of starting material and the presence of 2+ species showed clearly that the desired reaction was not working.

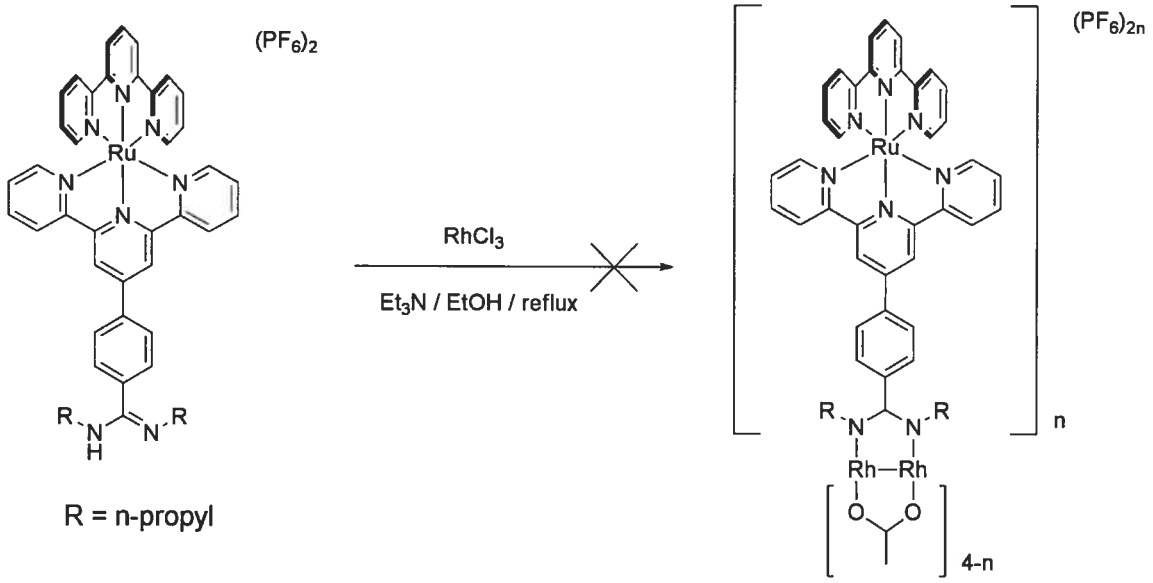

Scheme 4.15 Attempt to reductively form the dirhodium paddlewheel motif *in situ*.

4.7 Concluding Remarks

The incapability of the amidinato Ru(II) complexes **IV-1** and **IV-2** to self-assemble about the Rh_2(II,II) core by conventional, well-established means necessitates a more elaborate, divergent strategy. The success of such an approach should be more likely considering the lessons learned from the unanticipated decomposition of *N,N'*-di-(4'-phenyl-tpy) formamidine.

4.8 Experimental

Note: Although 4'-(4-nitro-phenyl)-tpy and 4'-(4-amino-phenyl)-tpy have been previously prepared and characterized,[19] their synthesis and purification in this work differs considerably, and so they are described herein.

4.8.1 Materials and Methods Solvents used for ligand synthesis were freshly distilled, while those used in the subsequent purification and complexation steps were reagent grade. The reagents *N*-propylamine and aniline were distilled over sodium sulfate and stored over activated 3Å molecular sieves. The preparation of 2,2':6',2''-terpyridine (tpy),[25] $Ru(tpy)Cl_3$,[26] $Rh_2(O_2CCH_3)(CH_3OH)_2$,[27] and 4'-(4-carboxyphenyl)-tpy [28] have been described previously. Silica used for chromatographic purification of all complexes was 400-450 Å mesh.

4.8.2 Physical Measurements Room-temperature ^1H NMR spectra were recorded using a Bruker 400RG at 400 MHz spectrometer, while those at 333 K were recorded using a Bruker 500RG at 500 MHz spectrometer.

Electrochemical data was recorded using a BAS Epsilon potentiostat using argon-degassed, spectroscopic grade acetonitrile solutions of 0.1 M tetrabutylammonium hexafluorophosphate ($TBAPF_6$) as supporting electrolyte. A three electrode set-up was employed using a working Pt button electrode, a Pt wire auxiliary electrode, and a Ag wire pseudo-reference electrode with addition of ferrocene as an internal reference. All data is corrected to the Fc / Fc^+ couple vs SCE.

UV-Vis and emission spectra were recorded in a 1 cm path length quartz cell using a Cary 500i and Cary Eclipse spectrophotometer, respectively, using air-equilibrated solutions. Emission spectra were recorded upon excitation of the sample according to its respective lowest energy MLCT band observed in the absorption spectrum. The ground-state pKa values for complexes **IV-1 $(PF_6)_2$ and IV-2 $(PF_6)_2$** were determined by UV-Vis and emission measurements over the range of pH = 2-13. Stock solutions (**IV-1 $(PF_6)_2$**, 4.6×10^{-5} M; **IV-2 $(PF_6)_2$**, 5.1×10^{-5} M) were prepared in 100 mL of H_2O containing 20% DMSO and 0.1 M KCl. The addition of DMSO ensured the

complete dissolution of the complexes over the measured pH range. The pH of the solution was initially adjusted by addition of 0.2 M NaOH(aq) and subsequently lowered by careful addition of HCl(aq) solution. The acid solution was added such that the total volume change was negligible, and the solutions were allowed to equilibrate for 5 min. prior to recording the UV-Vis spectrum.

Single crystal X-ray diffraction data for **IV-1 $(PF_6)_2$** was collected on a Bruker Apex at 100 K using Cu-Kα radiation (λ= 1.54178 Å) and refined by Francine Bélanger-Gariépy. Mass spectrometry was performed by direct injection using an LC-MSD TOF (Agilent) spectrometer with electrospray ionization.

4.8.3 Synthesis and Purification

4'-(4-*N*-propylbenzamide)-tpy In a typical preparation, 4'-(4-carboxyphenyl)-tpy (1.2 g, 3.4 mmol) is refluxed in neat thionyl chloride (30 mL) for 1.5 hr. Excess thionyl chloride is then removed by distillation and the residue is dried in vacuo. The residue is then charged with neat *N*-propylamine (25 mL) and the mix is stirred under an argon atmosphere at room temperature for 1 hr. The reaction mix is then poured into a 1:1 H_2O / CH_3OH mix (400 mL), made basic (pH = 12) with KOH, to give a heavy precipitate which is isolated by filtration. The product is then triturated in H_2O and re-filtered. Dissolution of the solid in DCM, followed by drying over $MgSO_4$ and filtration, gave 0.9 g of the product after drying in vacuo. Yield: 67 %. ^{1}H NMR (400 MHz, $CDCl_3$) δ ppm 8.76 (s, 4H), 8.70 (d, J = 8.0 Hz, 2H), 7.98 (d, J = 8.3, 2H), 7.92 (m, 4H), 7.39 (m, 2H), 6.30 (t, J = 5.2 Hz, 1H), 3.49 (m, 2H), 1.71 (m, 2H), 1.04 (t, J = 7.4 Hz, 3H). ^{13}C NMR (300 MHz, d_6-DMSO) δ ppm 166.82, 157.07, 156.12, 150.67, 149.97, 141.08, 138.83, 136.66, 129.52, 128.17, 125.93, 122.28, 119.35, 42.35, 23.694, 12.80. ESI-MS = $[M+H]^+$ cald. for $C_{25}H_{23}N_4O$, 395.18719 ; found, 395.18638

4'-(*N*-phenylbenzamide)-tpy In a typical preparation, 4'-(4-carboxyphenyl)-tpy (2.0 g, 5.7 mmol) is heated to reflux in thionyl chloride (35 mL) for 1.5 hr. Excess thionyl chloride is then removed by distillation and the residue is dried in vacuo. To the residue is charged, via cannulae, dry DCM (60 mL) followed by dry triethylamine (1.2 g, 12 mmol) under an argon atmosphere. The mix is cooled to -10 °C and charged with dry

aniline (5.16 g, 55.4 mmol) after which the solution is brought to room temperature and heated to reflux for 12 hr. The reaction mix is poured into a 2:1 CH_3OH / H_2O mix (400 mL) made basic with KOH (pH = 12) to give a heavy precipitate which is isolated by filtration. The product is then triturated in H_2O and re-filtered. Dissolution of the solid in DCM, followed by drying over $MgSO_4$ and filtration, gave 2.25 g of the product after drying in vacuo. Yield: 93 %. ^{1}H NMR (400 MHz, d_6-DMSO) δ ppm 10.40 (s, 1H), 8.77 (m, 4H), 8.68 (d, J = 7.8 Hz, 2H), 8.19 (d, J = 8.2 Hz, 2H), 8.09 (d, J = 8.2 Hz, 2H), 8.05 (m, 2H), 7.84 (d, J = 7.8 Hz, 2H), 7.54 (m, 2H), 7.39 (m, 2H), 7.14 (t, J = 7.3 Hz, 1H). ^{13}C NMR (300 MHz, d_6-DMSO) δ ppm 166.26, 157.03, 156.04, 150.61, 149.81, 141.60, 140.34, 138.85, 136.84, 130.04, 129.94, 128.27, 125.94, 125.12, 122.32, 121.80, 119.39. ESI-MS: $[M+H]^+$ cald. for $C_{28}H_{21}N_4O$, 429.17154; found, 429.16993.

4'-(*N*,*N*'-dipropylbenzamidine)-tpy In a typical preparation, PCl_5 (1.1 g, 5.1 mmol) is stirred in dry DCM (100 mL) under an argon atmosphere at -10 °C for 10 min. The solution is then charged with 4'-(4-*N*-propylbenzamide)-tpy (1.0 g, 2.5 mmol) and stirred for 15 min., then slowly brought to room temperature and stirred an additional 3 hr. The solution is again cooled to -10 °C and *N*-propylamine (1.44 g, 24.0 mmol) is then added slowly over the course of 5 min. The solution is slowly brought to room temperature and stirred an additional 6 hr. The solid suspension which has developed is removed by filtration and discarded. The filtrate is washed with an aqueous solution of KOH (100 mL, pH = 12) and then with H_2O alone (100 mL). Drying of the DCM layer over $MgSO_4$, followed by filtration and drying in vacuo gave an orange oil which is applied to a plug of alumina and eluted under pressure with ethyl acetate to remove any unreacted 4'-(4-*N*-propylbenzamide)-tpy. The desired product is then recovered by elution under pressure using a 4:1 mix of ethyl acetate / methanol. The residue is dried and then dissolved in DCM for subsequent filtration to ensure complete removal of any dissolved alumina particulates. The filtrate is dried in vacuo to give 0.87 g of the amidine. Yield: 79 %. ^{1}H NMR (400 MHz, $CDCl_3$) δ ppm 12.95 (s,br, 1H) 8.78 (s, 2H), 8.75 (d, J = 4.8 Hz, 2H), 8.72 (d, J = 8.0 Hz, 2H), 8.08 (d, J = 8.2 Hz, 2H), 7.93 (m, 2H), 7.45 (d, J = 8.2 Hz, 2H), 7.41 (m, 2H), 2.95 (m, 4H), 1.59 (m, 4H), 0.86 (t, J = 7.4 Hz, 6H). ^{13}C NMR (300 MHz, d_6-DMSO) δ ppm 175.85, 157.04, 156.04, 151.83, 150.60, 149.68, 140.91, 138.72,

130.10, 129.51, 128.53, 128.06, 125.87, 124.74, 122.21, 119.34, 24.77, 23.70, 12.56. ESI-MS: $[M+H]^+$ cald. for $C_{28}H_{30}N_5$, 436.25012; found, 436.24861.

4'-(*N,N'*-diphenylbenzamidine)-tpy In a typical preparation, PCl_5 (1.94 g, 9.3 mmol) is stirred in dry DCM (100 mL) under an argon atmosphere at -10 °C for 10 min. The solution is then charged with 4'-(*N*-phenylbenzamide)-tpy (2.0 g, 4.7 mmol), stirred cold for 20 min., then brought to room temperature and stirred for an additional 12 hr. The solution is cooled to -10 °C and dry aniline (5.16 g, 55.4 mmol) is then added slowly over the course of 5 min. The solution is brought to room temperature and stirred for an additional 8 hr, after which the mix is poured into a 2:1 CH_3OH / H_2O mix (400 mL) to form a heavy precipitate which is collected by filtration, triturated in H_2O, and re-filtered. The solid is re-dissolved in DCM, dried over $MgSO_4$, filtered, and dried in vacuo. Dissolution of the crude material in $CHCl_3$ (40 mL), followed by addition of 20 mL CH_3OH, led to crystallized product upon slow evaporation of the mix. Yield: 84 %. ^1H NMR (400 MHz, d_6-DMSO) δ ppm 9.35 (s, 1H), 8.75 (d, J = 4.6 Hz, 2H), 8.66 (m, 4H), 8.03 (m, 2H), 7.92 (d, J = 7.4 Hz, 2H), 7.87 (d, J = 8.2 Hz, 2H), 7.52 (m, 4H), 7.32 (m, 2H), 7.09 (m, 2H), 7.00 (t, J = 6.7 Hz, 1H), 6.79 (t, J = 7.0 Hz, 1H), 6.67 (J = 7.4 Hz, 2H). ^{13}C NMR (300 MHz, d_6-DMSO) δ ppm 157.05, 156.08, 155.47, 151.75, 150.66, 149.96, 142.54, 139.21, 138.81, 137.04, 131.31, 129.69, 127.88, 125.92, 123.57, 123.319, 122.44 122.24, 120.84, 119.22. ESI-MS: $[M+H]^+$ cald. for $C_{34}H_{26}N_5$, 504.21882; found, 504.21824.

[{4'-(*N,N'*-dipropylbenzamidine)-tpy}(tpy)Ru]$(PF_6)_2$ (IV-1 $(PF_6)_2$) In a typical preparation, $tpyRuCl_3$ (0.16 g, 0.36 mmol) and 4'-(*N,N'*-dipropylbenzamidine)-tpy (0.16 g, 0.36 mmol) are combined with $AgNO_3$ (0.185 g, 1.09 mmol) in ethanol (40 mL). The mix is triturated briefly and then heated to reflux for 4 hr under ambient conditions. The reaction solution is then filtered hot over a plug of celite, and the filtrate is dried. The residue is re-dissolved in acetonitrile and applied to a silica column using a 7:2 (CH_3CN / KNO_3 (sat., aq.) mix as eluent. The product (R_f = 0.48) is collected and extracted repeatedly with a CH_3CN / DCM / KPF_6 mixture. The organic layer is removed and dried, then dissolved in a minimal amount of CH_3CN and precipitated in H_2O to remove

excess KPF_6. The precipitate is removed by filtration and dried *in vacuo*. Yield: 0.173 g (45 %). Single crystals suitable for structure determination by X-ray diffraction were prepared by vapour diffusion of isopropyl ether into an acetonitrile solution of **IV-1 $(PF_6)_2$** saturated with ammonium tetraphenylborate, wherein the title compound crystallized as **IV-1 $(PF_6)(BPh_4)_2$**. **Note:** sample for elemental analysis prepared by precipitation from an aqueous solution made acidic with HPF_6 (aq, 60 wt %). ^{1}H NMR (400 MHz, CD_3CN, 298 K) δ ppm 9.05 (s, 2H), 8.79 (d, J = 8.2 Hz, 2H), 8.68 (d, J = 8.1 Hz, 2H), 8.53 (d, J = 8.2 Hz, 2H), 8.46 (t, J = 8.2 Hz, 1H), 8.42 (d, J = 8.6 Hz, 2H), 7.97 (m, 4H), 7.91 (d, J = 8.6 Hz, 2H), 7.85 (br, 1H) 7.63 (br, 1H), 7.43 (d, J = 5.6 Hz, 2H), 7.40 (d, J = 5.6 Hz, 2H), 7.20 (m, 4H), 3.45 (m, 2H), 3.34 (m, 2H), 1.84 (m, 2H), 1.69 (m, 2H), 1.12 (t, J = 7.3 Hz, 3H), 0.93 (t, J = 7.4 Hz, 3H). % Calcd. for $C_{43}H_{42}N_8F_{18}P_3Ru$: C (42.80), H (3.51), N (9.29). % Found: C (43.32), H (4.60), N (9.14). ESI-MS: $[M]^{2+}$ cald. for $C_{43}H_{40}N_8Ru$, 385.12097; found, 385.11986.

[{4'-(*N*,*N*'-diphenylbenzamidine)-tpy}(tpy)Ru]$(PF_6)_2$ (IV-2 $(PF_6)_2$) In a typical preparation, $tpyRuCl_3$ (0.22 g, 0.50 mmol) and 4'-(*N*,*N*'-diphenylbenzamidine)-tpy (0.25 g, 0.50 mmol) are combined with $AgNO_3$ (0.26 g, 1.50 mmol) in ethanol (50 mL). The mix is triturated briefly and then heated to reflux for 2.5 hr under ambient conditions. Purification and treatment followed that for **IV-1 $(PF_6)_2$**, giving the desired product (R_f = 0.56). Yield: 170 mg (35 %). ^{1}H NMR (400 MHz, CD_3CN, 298 K) δ ppm 9.68 (br, 1H), 9.01 (s, 2H), 8.79 (d, J = 8.2 Hz, 2H), 8.66 (d, J = 8.1 Hz, 2H), 8.53 (d, J = 8.1 Hz, 2H), 8.46 (t, J = 8.2 Hz, 1H), 8.32 (d, J = 8.2 Hz, 2H), 7.96 (m, br, 6H), 7.50 (br, 10 H), 7.42 (d, J = 5.4 Hz, 2H), 7.39 (d, J = 5.3 Hz, 2H), 7.20 (m, 4H). % Calcd. for $C_{49}H_{38}N_8F_{18}P_3Ru$: C (46.16), H (3.00), N (8.79). % Found: C (45.75), H (3.65), N (9.10). ESI-MS: $[M(PF_6)_2 + H]^+$ cald. for $C_{49}H_{37}F_{12}N_8P_2Ru$, 1129.14683; found 1129.14381; $[M(PF_6) + H]^{2+}$ cald for $C_{49}H_{37}F_6N_8PRu$, 492.09132; found, 492.09093. $[M]^{2+}$ cald. for $C_{49}H_{36}N_8Ru$, 419.10532; found, 419.10394.

4'-(4-Nitrophenyl)-tpy 4-nitrobenzaldehyde (4.0 g, 26.5 mmol) and 2-acetyl pyridine (6.4 g, 53.0 mmol) are combined in a large mortar and ground for 10 min, after which time the mix solidifies. The solid is ground for an additional 5 min, then transferred to a

flask containing acetic acid (40 mL) and NH_4OAc (16.0 g, 208 mmol). The mix is heated to reflux for 4 h, after which the solution is diluted to 250 mL with water, forming a heavy precipitate which is removed by filtration. The solid is triturated in hot methanol (500 mL) and filtered over celite. The methanol filtrate is discarded while the solid residue is removed from the celite plug upon washing with DCM (500 mL). Concentration of the DCM filtrate (60 mL) followed by application to a plug of neutral alumina and elution with ethyl acetate under pressure gave 2.1 g of pure product in 22 % yield.

4'-(4-aminophenyl)-tpy In the course of preparing 4'-(4-nitrophenyl)-tpy, the crude solid obtained prior to column purification is added to HCl (conc., 300 mL), followed by $SnCl_2$ dihydrate (15 .0 g, 66.5 mmol). The mix is stirred at 70°C for 5 h, then decanted into water (600 mL) and made basic (pH = 10) by slow addition of $KOH_{(s)}$, forming a heavy brown precipitate. The solution is decanted into a large separatory funnel and extracted five times with DCM (400 mL). The DCM washings are combined and filtered over a plug of celite, then washed with a saturated, aqueous solution of [EDTA]Na_2. The organic layer is separated and dried over Na_2SO_4. Flash chromatography over a plug of neutral alumina using ethyl acetate as eluent afforded 2.6 g of pure product in 31 % yield.

4'-(*N*-phenylformamide)-tpy The formic acetic anhydride solution was prepared by cooling a dry flask containing acetic anhydride (4.6 mL) to -15°C in an ice/methanol mixture and then adding of formic acid (5.5 mL) drop wise over the course of 1 h with stirring. The mix is stirred for 3 h under an argon atmosphere at -5°C, after which the solution is transferred via cannulae to a dry flask containing 4'-(4-aminophenyl)-tpy (0.52 g, 1.6 mmol). The solution is brought to room temperature and stirred for 1 h, after which it is decanted into water and extracted three times with DCM (100 mL). The DCM extracts are reduced to dryness to give an orange oil which is triturated with toluene (150 mL) to give 0.55 g of pure product as an off-white solid suspension. R_f = 0.27 (SiO_2 substrate, ethyl acetate as eluent). ^1H NMR (400 MHz, d_6-DMSO) δ ppm [10.46 (s) + 10.39 (d, J = 10.8 Hz), 1H], [8.95 (d, J = 10.8 Hz) + 8.36 (s), 1H], 8.77 (d, J = 4.4 Hz, 2H), 8.70 (s, 2H), 8.67 (d, J = 8.3 Hz, 2H), 8.04 (m, 2H), 7.93 (d, J = 8.6 Hz, 2H), [7.82

(d, J = 8.6 Hz) + 7.42 (d, J = 8.3 Hz), 2H], 7.53 (m, 2H). ^{13}C NMR (300 MHz, d_6-DMSO) δ ppm 163.79, 161.16, 156.89, 156.28, 150.60, 150.11, 141.01, 140.79, 138.71, 133.61, 129.34, 128.85, 125.78, 122.21, 121.03, 119.09, 118.69. ESI-MS: $[M + H]^+$ 353.3. Calcd.(%) for $C_{22}H_{16}N_4O$: C 74.98, H 4.58, N 15.90. Found (%): C 74.72, H 4.61, N 15.74.

4-aminobenzyl alcohol A flame-dried flask is charged with dry methanol (100 mL) followed by 4-nitrobenzyl alcohol (4.0 g, 26 mmol) and CuCl (anhydrous, 7.8 g, 79 mmol). The mix is stirred briefly, then $NaBH_4$ (7.0 g, 185 mmol) is added portion wise over the course of 20 min. The mix is stirred over an argon atmosphere at room temperature for an additional 25 min., after which water is slowly added to quench. All solvent is then removed by distillation, and the residue is triturated with a 1:1 mix of ethyl acetate/DCM (300 mL). The mix is filtered over celite, and the filtrate dried over Na_2SO_4. Filtration and removal of the solvent afforded 3.03 g of pure product in 98 % yield. ^{1}H NMR (400 MHz, d_6-DMSO) δ ppm 7.00 (d, J = 8.2 Hz, 2H), 6.52 (d, J = 8.2 Hz, 2H), 4.90 (s, 2H), 4.78 (t, J = 5.2 Hz, 1H), 4.25 (d, J = 5.2 Hz, 2H).

***N,N'*-Di-(hydroxymethyl phenyl) formamidine** A flame-dried flask is charged with dry DCM (40 mL) followed by 4-aminobenzyl alcohol (1.5 g, 12.2 mmol), which is stirred under an argon atmosphere until completely dissolved. Triethyl orthoformate (0.9 g, 6.1 mmol) is then added, followed by a catalytic amount of p-toluenesulfonic acid. After stirring at room temperature for 16 h, a precipitate develops, which is allowed to stir for an additional 56 h (3 d total). The solid is removed by filtration and washed with diethyl ether and dried under vacuum to give 0.84 g of pure product in 54 % yield. R_f = 0.10 (SiO_2 substrate, 2:1 DCM/acetone as eluent). ^{1}H NMR (400 MHz, d_6-DMSO) δ ppm 9.71 (s, br, 1H), 8.20 (s, br, 1H), 7.22 (m, 8H) 5.09 (t, J = 5.2 Hz, 2H), 4.41 (d, J = 5.2 Hz, 4H). ESI-MS: $[M + H]^+$ 257.2.

***N,N'*-Di-(4-formylphenyl) formamidine** To a flame-dried flask is charged, over an argon atmosphere, dry THF (40 mL) followed by *N,N'*-Di-(hydroxymethyl phenyl)-formamidine (0.5 g, 2.0 mmol). After dissolution of the substrate, MnO_2 (< 5 μ mesh, 3.4

g, 39.0 mmol) is added and the mix stirred for 2 h at room temperature. Removal of the MnO_2 by filtration and drying the filtrate gave 0.44 g of pure dialdehyde product in 89 % yield. R_f = 0.73 (SiO_2 substrate, 2:1 DCM/acetone as eluent). ^1H NMR (400 MHz, d_6-DMSO) δ ppm 10.64 (s, br, 1H), 9.89 (s, 2H), 8.55 (s, br, 1H), 7.85 (m, 5H), 7.47 (br, 3H). ESI-MS: $[M + H]^+$ 253.1.

***N,N'*-Di-(4'-phenyl-tpy) formamidine** To a flame-dried flask is charged dry THF (35 mL) followed by 4'-(4-aminophenyl)-tpy (0.44 g, 1.36 mmol) and triethyl orthoformate (0.10 g, 0.66 mmol). Upon dissolution of the substrate, a catalytic amount of ρ-toluenesulfonic acid is added and the reaction mix is stirred under an argon atmosphere at room temperature for 72 h, during which time a precipitate develops. This precipitate is removed by filtration, washed twice with 40 mL portions of THF, and dried under vacuum to give 0.08 g of material, pure by TLC, in 18 % yield. R_f = 0.16 (SiO_2 substrate, ethyl acetate as eluent). ^1H NMR (400 MHz, d_6-DMSO) δ ppm 8.80 (d, J = 4.5 Hz, 4H), 8.77 (s, 4H), 8.71 (d, J = 7.8 Hz, 4H), 8.08 (m, 5H), 7.73 (br, 4H), 7.57 (m, 4H), 7.48 (d, J = 8.0 Hz, 2H), 7.12 (d, J = 8.0 Hz, 2H). ESI-MS: $[M+H]^+$ calcd. for $C_{43}H_{31}N_8$, 659.26717; found, 659.26799.

4.9 References

1. a) Barker, J.; Kilner, M. *Coord. Chem. Rev.* **1994**, 133, 219. b) Coles, M *Dalton Trans.* **2006**, 985.
2. a) Li, C.; Wang, Y.; Zhou, L.; Sun, H.; Shen, Q. *J. Appl. Polym. Sci.* **2006**, 102, 22. b) Chivers, T.; Fedorchuk, C.; Parvez, M. *Organomet.* **2005**, 24, 580. c) Motoyama, Y.; Hanada, S.; Niibayashi, S.; Shimamoto, K.; Takaoka, N.; Nagashima, H. *Tetrahedron*, **2005**, 61, 10216. d) Chen, C.-T.; Rees, L. H.; Cowley, A. R.; Green, M. L. H. *J. Chem. Soc. Dalton Trans.* **2001**, 1761. e) Meier, R. J.; Koglin, E. *J. Phys. Chem. A* **2001**, 105, 3867.
3. a) Lu, Z.; Hill, N. J.; Findlater, M.; Cowley, A. H. *Inorg. Chim. Acta* **2007**, 360, 1316. b) Bai, S.-D.; Guo, J.-P.; Liu, D.-S. *Dalt. Trans.* **2006**, 2244. c) Jones, C.; Baker, R. J. *J. Organomet. Chem.* **2006**, 691, 65. d) McNevin, M. J.; Hagadorn, J. R. *Inorg. Chem.* **2004**, 43, 8547. e) Hagadorn, J. R.; McNevin, M. J.; Wiedenfeld, G.; Shoemaker, R. *Organomet.* **2003**, 22, 4818. f) Grundy, J.; Coles, M. P.; Hitchcock, P. B. *J. Organomet. Chem.* **2002**, 662, 178. g) Jenkins, H. A.; Abeysekera, D.; Dickie, D. A.; Clyburne, J. A. C. *J. Chem. Soc. Dalton. Trans.* **2002**, 3919.
4. See, for example, Kraft, A. *J. Chem. Soc. Perkin Trans. 1* **1999**, 705.
5. a) Bertogg, A.; Togni, A. *Organomet.* **2006**, 25, 622. b) Manowitz, M.; Virgilio, J. A. *Ger. Offen.* **1978**, 19.
6. a) Cotton, F.A.; Walton, R. A. *Multiple Bonds Between Metal Atoms*, 3rd, ed., Wiley, New York, **1994**. b) Casas, J. M.; Cayton, R. H.; Chisholm, M. H. *Inorg. Chem.* **1991**, 30, 359.
7. See, for example, a)Grätzel, M. *Inorg. Chem.* **2005**, 44, 6841. b) Alstrum-Acevedo, J. H.; Brennaman, M. K.; Meyer, T. J. *Inorg. Chem.* **2005**, 44, 6802. c) Meyer, G. J. *Inorg. Chem.* **2005**, 44, 6852. d) Polo, A. S.; Itokazu, M. K.; Yukie, N.; Iha, M. *Coord. Chem. Rev.* **2004**, 248, 1343.
8. a) Galoppini, E. *Coord. Chem. Rev.* **2004**, 248, 1283. b) Gregg, B. A. *Coord. Chem. Rev.* **2004**, 248, 1215. c) Katoh, R.; Furube, A.; Barzykin, A. V.; Arakawa, H.; Tachiya, M. *Coord. Chem. Rev.* **2004**, 248, 1195.

9. See, for example, Whitener, G. D.; Hagadorn, J. R.; Arnold, J. *J. Chem. Soc. Dalton Trans.* **1999**, 1249.
10. Greene, T. W.; Wuts, P. G. M. *Protective Groups in Organic Synthesis*, 3rd ed. Wiley-Interscience, Wiley and Sons, **1999**.
11. Raczynska, E. D.; Laurence, C.; Berthelot, M. *Analyst*, **1994**, 119, 683.
12. See, for example, a) Polson, M. I. J.; Medlycott, E. A.; Hanan, G. S.; Mikelsons, L.; Taylor, N. J.; Watanabe, M.; Tanaka, Y.; Loiseau, F.; Passalacqua, R.; Campagna, S. *Chem. Eur. J.* **2004**, 10, 3640. b) Sun, L.; Hammarstrom, L.; Akermark, B.; Styring, S. *Chem. Soc. Rev.* **2001**, 30, 36. c) Barigelletti, F.; Flamigni, L. *Chem. Soc. Rev.* **2000**, 29, 1. d) Hagfeldt, A.; Graetzel, M. *Acc. Chem. Res.* **2000**, 33, 269. e) Sauvage, J.-P.; Collin, J.-P.; Chambron, J.-C.; Guillerez, S.; Coudret, C. ; Balzani, V. ; Barigelletti, F. ; De Cola, L. ; Flamigni, L. *Chem. Rev.* **1994**, 94, 993.
13. See, for example a) Montalti, M.; Wadhwa, S.; Kim, W. Y.; Kipp, R. A.; Schmehl, R. H. *Inorg. Chem.* **2000**, 39, 76. b) Nazeeruddin, M. K.; Zakeeruddin, S. M.; Humphry-Baker, R.; Kaden, T. A.; Grätzel, M. *Inorg. Chem.* **2000**, 39, 4542. c) Nazeeruddin, M. K.; Zakeeruddin, S. M.; Humphry-Baker, R.; Jirousek, M.; Liska, P.; Vlachopoulos, N.; Shklover, V.; Fischer, C.-H.; Grätzel, M. *Inorg. Chem.* **1999**, 38, 6298. d) Lay, P.A.; Sasse, W. H. F. *Inorg. Chem.* **1984**, 23, 4123.
14. Barigelletti, F.; Flamigni, L.; Guardigli, M.; Sauvage, J.-P.; Collin, J.-P. *Chem. Comm.* **1996**, 1329.
15. Nazeeruddin, M. K.; Kalyanasundaram, K. *Inorg. Chem.* **1989**, 28, 4251 and references therein.
16. Raczynska, E.; Oszczapowicz, J. *Tetrahedron* **1985**, 41, 5175.
17. Daoust, B.; Lessard, J. *Can. J. Chem.* **1995**, 73, 362.
18. Boyd, G. V. *The Chemistry of Amidines and Imidates* vol.2, **1991**, John Wiley and Sons.
19. Ng, W. Y.; Gong, X.; Chan, W. K. *Chem. Mater.* **1999**, 11, 1165.
20. Grundmann, C.; Kreutzberger, A. *J. Am. Chem. Soc.* **1955**, 77, 6559.
21. March, J.; Smith, M. B. *Adv. Org. Chem.: Reactions, Mechanism, and Structure* 5th ed., Wiley-Interscience, John Wiley and Sons, Inc., **2001**.

22. See, for example, a) Tadashi, H.; Hiroki, T.; Hiroshi, Y. *Synlett.* **2006**, 13, 2075. b) McLaughlin, M.; Mohareb, R.; Rapaport, H. *J. Org. Chem.* **2003**, 68, 50.
23. Spectral information for *N*-phenylformamide is available from the *Spectral Database for Organic Compounds* (SDBS). SDBS No:3422. CAS Registry No: 103-70-8.
24. See, for example, a) Dequeant, M. Q.; Bradley, P. M.; Xu, G.-L.; Lutterman, D. A.; Turro, C.; Ren, T. *Inorg. Chem.* **2004**, 43, 7887. b) Ren, T.; Lin, C.; Valente, E. J.; Zubkowski, J. D. *Inorg. Chim. Acta.* **2000**, 297, 283.
25. Cooke, M. W.; Wang, J.; Theobald, I.; Hanan, G.S. *Synthetic Commun.* **2006**, 36, 1721.
26. Sullivan, B. P.; Calvert, J. M.; Meyer, T. J.; *Inorg. Chem.* **1980**, 19, 1404.
27. Rempel, G. A.; Legzdins, P.; Smith, H.; Wilkinson, G. *Inorg. Synth.* **1972**, 13, 90.
28. Storrier, G. D.; Colbran, S. B. *Inorg. Chim. Acta* **1999**, 284, 76.

Chapter 5: Rh_2^{4+} building blocks for the divergent synthesis of multinuclear arrays

5.1 Introduction

The kinetic and thermodynamic advantages of utilizing amidinates in place of carboxylates are well known with regard to ligand displacement in metal dimers. However, as we have seen already regarding the formation of dimetal paddlewheel complexes, the consequence of this is usually more elaborated synthetic protocols relative to those employing carboxylates. Regardless, these methods are all convergent in approach and are, more importantly, quite ineffective when utilizing various amidine-derivatized $Ru(tpy)_2^{2+}$ complexes. This prompted us to investigate the feasibility of a divergent synthetic strategy utilizing covalent bond formation.

In this vein, Ren and co-workers have recently capitalized upon a series of paramagnetic diruthenium complexes of the type $Ru_2(O_2CMe)_{4-n}(DArF)_nCl$ (where DArF = *N,N'*-diarylformamidinate) first described for the purposes of creating, via self-assembly, higher-order paramagnetic supramolecular architectures with rich electrochemistry.[1] It was recognized that replacement of the relatively labile carboxylates in these precursor complexes with *N,N'*-dimethyl-4'-iodobenzamidinate ligands gave access to acetylenic functionality using conventional Pd-catalyzed coupling conditions.[2] More recently, such peripheral ligand modification has been extended to include olefin cross-metathesis and Suzuki cross-coupling reactions.[3, 4] So far, the extent to which higher-order diruthenium systems have been investigated has been limited to dimerized diruthenium complexes formed by olefin cross-metathesis and Pd-catalyzed cross-coupling of acetylenic and iodo bearing diruthenium complexes.[3, 5] Notably, Ren and co-workers have also utilized such diruthenium acetylenic complexes as templates for covalent attachment, via Cu(I) catalyzed 1,3-cycloaddition, of azido(poly)benzylether dendrons,[6] an idea which was preceded earlier using dimolybdenum units.[7]

It is only very recently that dimeric units have been prepared and modified for the purpose of synthetic transformations, the noted references above constituting the scope of reported examples. Although not entirely prerequisite,[7] it is no coincidence that the most

promising and resilient diruthenium complexes mentioned above possess amidinate chelates, as this imparts added thermodynamic and kinetic stability relative to their purely carboxylate counterparts.[8] Given the large body of known dimetal complexes, we sought, then, a dimetal paddlewheel motif that would be suitably robust and amenable to synthetic manipulation.

Over twenty years ago, Kadish and co-workers reported the dirhodium(II,II) tetra-amidinate complex Rh_2(*N,N'*-diphenylbenzamidinate)$_4$ (Figure 5.1a).[9] This complex possesses two quasi-reversible one-electron oxidations corresponding to the redox couples $Rh_2^{5+/4+}$ and $Rh_2^{6+/5+}$ at 0.05 and 1.08 V (vs SCE), respectively. The presence of two quasi-reversible Rh_2-based oxidations is also characteristic of tetra-amidates (Figure 5.1b),[10, 11] and stands in stark contrast to the single $Rh_2^{5+/4+}$ process observed in $Rh_2(O_2CR)_4$ type complexes. This is attributable to enhanced donor capacity for both amidates and amidinates over carboxylates in general, which results in stabilization of such higher oxidation states. The first and second oxidation processes of Rh_2(*N,N'*-diphenyl-benzamidinate)$_4$ are shifted to lower potential by 0.29 and 0.46 V (vs SCE), respectively, relative to those for the related tetra-amidate complex Rh_2(*N*-phenyl acetamidate)$_4$ (Figure 5.1b). This is not surprising since the amidine is expected to be more basic. The importance of this tetra-amidinate was that it possessed a chemically reversible and electrochemically quasi-reversible (ΔE_p = 90 mV) one-electron reduction process corresponding to the couple $Rh_2^{4+/3+}$ at -1.52 V (vs SCE). That this occurred was a surprise considering such large negative displacement of the oxidation potentials and the fact that the tetra-amidate did not possess this couple. This reduction was previously observed only as an irreversible process during electrochemical reduction of some $Rh_2(O_2CR)_4$ complexes.[12] The electrochemically generated Rh_2^{3+} reduced species proved to be stable at an applied potential of -1.7 V (vs SCE) and provided experimental insight into the nature of the LUMO by EPR analysis, which suggested it to be of Rh_2-σ^* parentage based on previous predictions for an electron in a $\sigma_{M\text{-}M}$ type orbital. [13] This is also consistent with $Rh_2(O_2CR)_4L_2$ complexes where the axial ligand is either absent or weak (e.g. L = H_2O).[14] Soon after this report, it was realized that complexes of the type $Rh_2(DArF)_4$ (where DArF = *N,N'*-diarylformamidinate) possessed similar electrochemistry, which indicates a stabilizing effect imparted by the presence of *N*-aryl

groups.[15] However, in the presence of donors such as CH_3CN or CO, the reduction process $Rh_2^{4+/3+}$ was found to be irreversible for $Rh_2(DArF)_4$ type complexes [15] but completely reversible for Rh_2(*N,N'*-diphenylbenzamidinate)$_4$.[9, 16] This is rationalized considering that axial ligation serves to destabilize the Rh_2-σ^* LUMO and that the *N*-aryl groups impose steric encumbrance for axial ligation in both cases. However, such encumbrance is more pronounced when accommodating the central aromatic ring of the benzamidinate ligand.

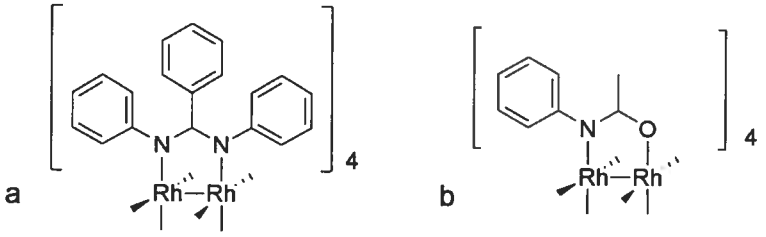

Figure 5.1. Representation of dirhodium(II,II) tetra(*N,N'*-diphenylbenzamidinate) (**a**) and dirhodium(II,II) tetra(*N*-phenyl acetamidate) (**b**).

The Rh_2(*N,N'*-diphenylbenzamidinate)$_4$ motif is an attractive candidate for synthetic modification considering the usual integrity afforded by amidinate ligands, the rich and reversible electrochemistry, the diamagnetic nature, and the presence of a central aromatic ring upon which to perform such synthetic transformations. As we will see, another crucial attribute is simplicity and efficacy of preparation. The first step, then, was to prepare potentially reactive analogues of Rh_2(*N,N'*-diphenyl-benzamidinate)$_4$.

5.2 Synthesis, Solid-State, and Solution NMR Characterization of Rh_2(*N,N'*-diphenyl-4-bromobenzamidinate)$_4$ (V-1) and Rh_2(*N,N'*-diphenyl-3,5-dibromobenzamidinate)$_4$ (V-2) (refer to pages LXXVI and LXXXII of Appendix 5 for X-ray data and parameters of complexes **V-1** and **V-2**, respectively)

As first entries in the creation of a potential library of useful building blocks, it was decided to make use of the commercially available 4-bromobenzoic and 3,5-dibromobenzoic acids as substrates in a traditional amidine synthesis (Scheme 5.1) for subsequent formation of the corresponding halogenated tetra-amidinate dirhodium(II,II)

complexes. This required the formation of the *N*-phenyl amide which was subsequently chlorinated and reacted with a second equivalent of aniline to yield the symmetric amidine ligand. With these ligands in hand, a melt protocol was used that is typical for formation of both tetra-amidinates and tetra-amidates from tetracarboxylates. Such reactions require an amidine melting point below 180°C, considering that $Rh_2(O_2CR)_4$ complexes are known to decompose close to 180°C. In this case, significant changes were made to the standard protocol encountered for formation of dirhodium(II,II) tetra-amidinates.[9]

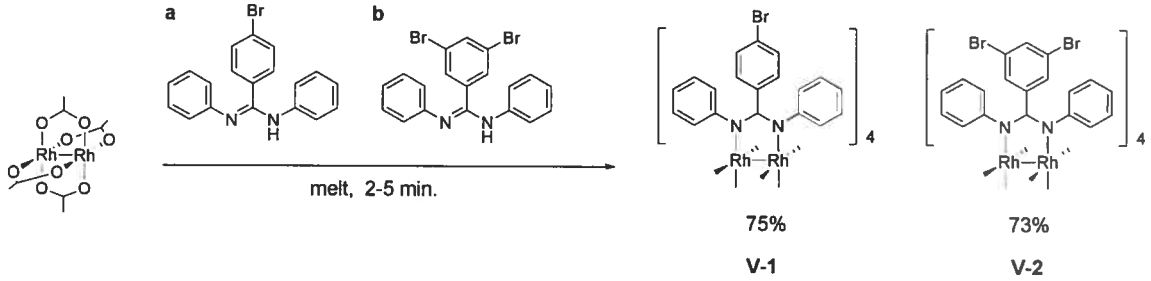

Scheme 5.1. Melt reaction to form Rh_2(*N,N'*-diphenyl-4-bromobenzamidinate)$_4$ (**V-1**), (**a**) and Rh_2(*N,N*-diphenyl-3,5-dibromobenzamidinate)$_4$ (**V-2**), (**b**). Yields reported upon crystallization.

Such a melt protocol, using $Rh_2(OAc)_4$, is typically performed for 8-10 h under an inert atmosphere. However, considering the relatively high melting point for *N,N'*-diphenyl-4-bromobenzamidinte (170°C), it is risky to extend the reaction over such a long period considering the likely decomposition of $Rh_2(O_2C_2H_3)_4$. Fortunately, it was found that the duration of the reaction may be minimized to only several minutes at temperatures equal to, or even exceeding, the amidine melt temperature. In fact, the melt temperature was often in excess of 200°C upon addition of $Rh_2(O_2C_2H_3)_4$. The decomposition temperatures for Rh_2(*N,N'*-diphenyl-4-bromobenzamidinate)$_4$ and Rh_2(*N,N*-diphenyl-3,5-dibromobenzamidinte)$_4$ were found to be 396°C and 362°C, respectively, and so it is likely that their rapid formation precludes decomposition under such reaction conditions. These complexes are quite stable and amenable to column purification, but surprisingly they were found to be sparingly soluble in DCM. This permitted rapid preliminary purification of the crude reaction mixture by removing the bulk of the excess amidine ligand upon washing with DCM.

Diffusion of DCM into a chloroform solution and slow evaporation from a chloroform / methanol solution gave single crystals suitable for structure determination by X-ray diffraction for Rh_2(*N,N'*-diphenyl-4-bromobenzamidinate)$_4$ and Rh_2(*N,N'*-diphenyl-3,5-dibromobenzamidinte)$_4$, respectively. The vast majority of dimetal paddlewheel complexes possess, ideally, D_{4h} molecular symmetry. However, as with the previously reported complex Rh_2(*N,N'*-diphenylbenzamidinate)$_4$,[9, 16] this symmetry is reduced to D_4 for both Rh_2(*N,N'*-diphenyl-4-bromobenzamidinte)$_4$ and Rh_2(*N,N'*-diphenyl-3,5-dibromobenzamidinte)$_4$ (Figures 5.2 and 5.3, respectively) by a N-Rh-Rh-N torsion angle of 12.0 ° and 16.0 °, respectively. Such twisting is not uncommon for dimetal paddlewheel complexes in general, particularly for those based upon rhodium(II).[8] In the case of Rh_2(*N,N'*-diphenylbenzamidinate)$_4$, this twist angle was found to be 17.3 °.

There is essentially no deviation in Rh-Rh bond length upon installation of bromine atoms to the central phenyl ring of the amidine ligand, as both Rh_2(*N,N'*-diphenyl-4-bromobenzamidinte)$_4$ and Rh_2(*N,N'*-diphenyl-3,5-dibromobenzamidinte)$_4$ possess bond lengths (2.4017(6) Å and 2.3980(6) Å, respectively) that are essentially identical to that of Rh_2(*N,N*-diphenylbenzamidinate)$_4$ (2.389(1) Å), considering that packing effects may also lead to deviations of 0.01 Å.[8] The same may be said of the Rh-N distances, which were found to be 2.042(4) Å and 2.052(2) Å for Rh_2(*N,N'*-diphenyl-4-bromobenzamidinte)$_4$ and Rh_2(*N,N*-diphenyl-3,5-dibromobenzamidinte)$_4$, respectively, which are nearly identical to that reported for Rh_2(*N,N'*-diphenylbenzamidinate)$_4$ (2.056(2) Å). All these bond distances are, moreover, in quite good agreement with those reported for dirhodium(II,II) tetra-amidinates in general.

The crystal structure of *N,N'*-diphenylbenzamidine has been reported and provides an interesting commentary on the effect of complexation.[17] Firstly, the C=N and C-N bond distances of this free amidine are, respectively, 1.302(7) Å and 1.360(8) Å but are essentially equal and intermediate for both Rh_2(*N,N'*-diphenyl-4-bromobenzamidinte)$_4$ (1.333(7), 1.327(7) Å) and Rh_2(*N,N'*-diphenyl-3,5-dibromobenzamidinte)$_4$ (1.333(4), 1.332(4) Å), as anticipated for a formally anionic chelate. Secondly, and more interestingly, the mean C-C bond distance from the amidine carbon to the central phenyl ring is 1.485 Å for *N,N'*-diphenylbenzamidine. This distance

is slightly, but consistently, longer for the reference complex Rh_2(*N,N'*-diphenyl-4-bromobenzamidinte)$_4$ (1.502(4) Å) as it is for both Rh_2(*N,N'*-diphenyl-4-bromobenzamidinte)$_4$ (1.497(5) Å) and Rh_2(*N,N'*-diphenyl-3,5-dibromobenzamidinte)$_4$ (1.494(4) Å). Such lengthening has been suggested to be a consequence of reduced conjugation to the central phenyl ring in favour of delocalization about the M-N-C-N-M fragment.[18]

Apart from Rh_2(*N,N'*-diphenylbenzamidinate)$_4$, complexes of the type M_2(*N,N'*-diphenylbenzamidinate)$_4$ have been reported previously for M = Cu(II),[18] Mo(II),[19] Pd(II),[20] and Co(II).[16] However, only where M = Cu(II), Co(II) are paddlewheel complexes obtained which are iso-structural to those where M = Rh(II). In the case of M = Mo(II), there is only two-fold molecular symmetry (C_2) about an axis perpendicular to the Mo-Mo bond direction, while where M = Pd(II), the two metal atoms are spanned by only two amidinate ligands with the other two each chelated to a single palladium(II) center. This latter case is clearly a consequence of the steric bulk imposed by such a ligand, considering that there is no formal bond-order for Pd_2(II,II) dimetal complexes.

To accommodate such steric encumbrance, the aryl rings are located in positions that are markedly non-planar relative to the delocalized Rh-N-C-N-Rh moiety (Figures 5.2 and 5.3, below). Firstly, the central aryl ring is twisted out of the N-C-N plane by ~ 50° for Rh_2(*N,N'*-diphenyl-4-bromobenzamidinate)$_4$ and by ~ 61° for Rh_2(*N,N'*-diphenyl-3,5-dibromobenzamidinate)$_4$. Secondly, and most notably, the aryl rings appended to the nitrogen atoms of the ligand occur in a regular edge-to face arrangement wherein the 2,6 protons of the phenyl rings are located in very different environments (see Figure 5.4 below). One of these protons, highlighted in green in Figure 5.4, is within 2.8 Å of the plane of the ring which is orthogonal to it. The other proton, highlighted in yellow, is within 2.6 Å of the edge of the nearest phenyl ring. The dynamic solution behaviour of these aryl rings, earmarked by these 2,6 phenyl protons, will be discussed in the next section. As expected, the structures for both the tetra-bromo and tetra-dibromo complexes are void of any axial ligation, as this has been shown to be exclusive to nitriles and CO.[16]

It is worthy to note that both Rh_2(*N,N'*-diphenyl-4-bromobenzamidinate)$_4$ and Rh_2(*N,N'*-diphenyl-3,5-dibromobenzamidinate)$_4$ are chiral, a point which has eluded

mention in all previous reports of related complexes.[16, 18, 19] This point may have also gone unnoticed here if not for the fact that crystals of Rh_2(*N,N'*-diphenyl-4-bromobenzamidinte)$_4$ were found to be enantiopure, which is in accord with the tetragonal space in which it crystallizes (I_4) being devoid of symmetry elements possessing mirror planes. On the other hand, Rh_2(*N,N'*-diphenyl-3,5-dibromobenzamidinte)$_4$ was found to crystallize in $P_{4/nnc}$, and as such one finds both enantiomers in the crystal structure (Figure 5.3).

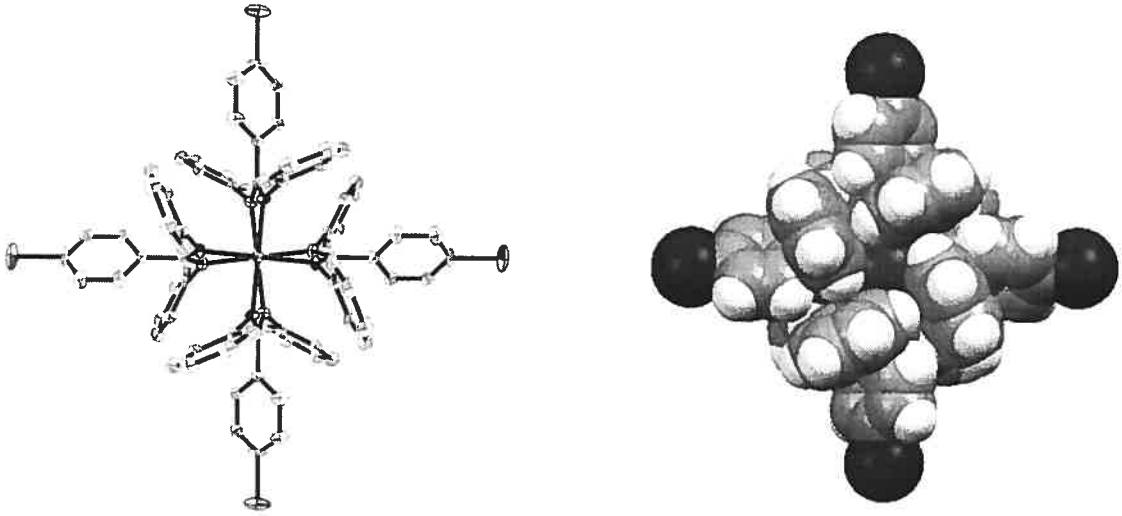

Figure 5.2. X-ray crystal structure of **V-1** viewed along the Rh-Rh bond-axis. At left, a representation with 50 % thermal ellipsoids where hydrogen atoms have been omitted for clarity. At right, a space-filling representation. Solvent has been omitted for clarity.

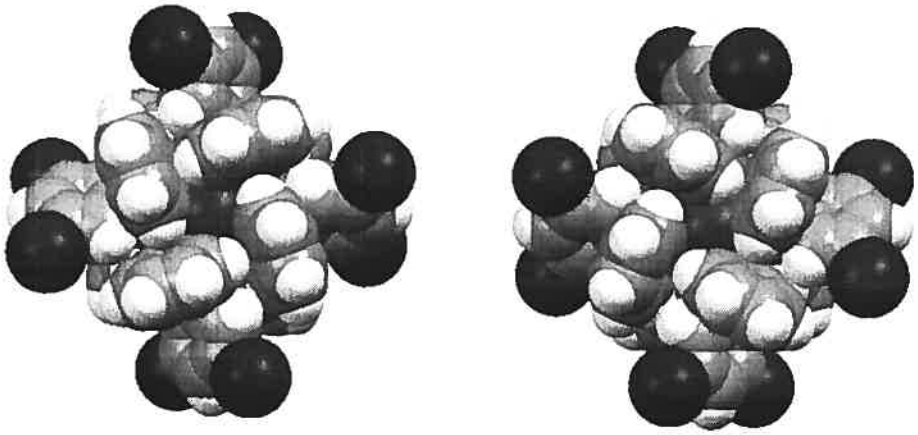

Figure 5.3. Space-filling representation for enantiomers of **V-2** found in the solid state structure.

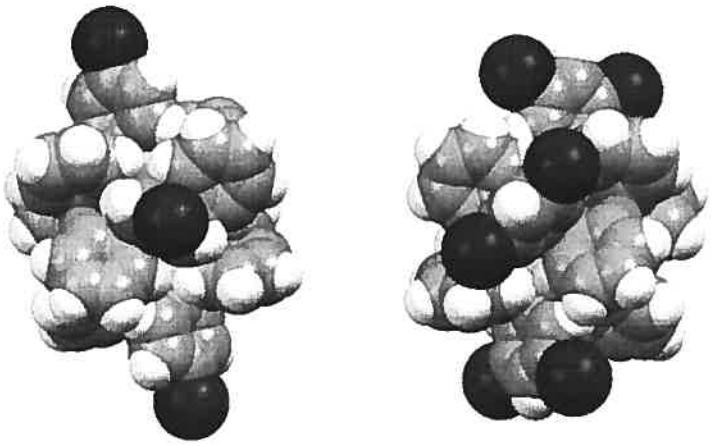

Figure 5.4. Side-on view of space-filling representations of **V-1** (left) and **V-2** (right) highlighting the 2,6 protons of the amidine phenyl ring.

The ^{1}H NMR spectra of both the tetra-bromo and tetra-dibromo amidinate complexes in $CDCl_3$ are depicted in Figures 5.5 and 5.6, respectively. The ^{1}H NMR spectra of Rh_2(*N,N'*-diphenyl-benzamidinate)$_4$ has not been reported, but the analysis here should apply to it nonetheless. At room temperature, the spectra of both complexes are characterized by broad features comprised solely of proton resonances of the phenyl rings bound to the nitrogen atoms. Of these, that which is located most downfield is comprised of the 3,5-phenyl protons and is, in the case of the dibromo analogue, resolved into a distinct multiplet. The remaining two broad features are largely invariant between the two complexes but are quite well separated ($\Delta\delta \approx 0.8$-0.9 ppm). The proton which is intimately directed toward the plane of its neighbor in an edge-to-face fashion should experience a strong shielding effect and is therefore assigned as the broad resonance which is located most upfield. To further support these assignments, and to shed some light on the solution dynamics of these compounds, variable temperature ^{1}H NMR was performed on a d_6-DMSO solution of Rh_2(*N,N'*-diphenyl-4-bromobenzamidinte)$_4$ in the high-temperature regime between 298-393 K. These spectra are shown in Figures 5.7 and 5.8 below.

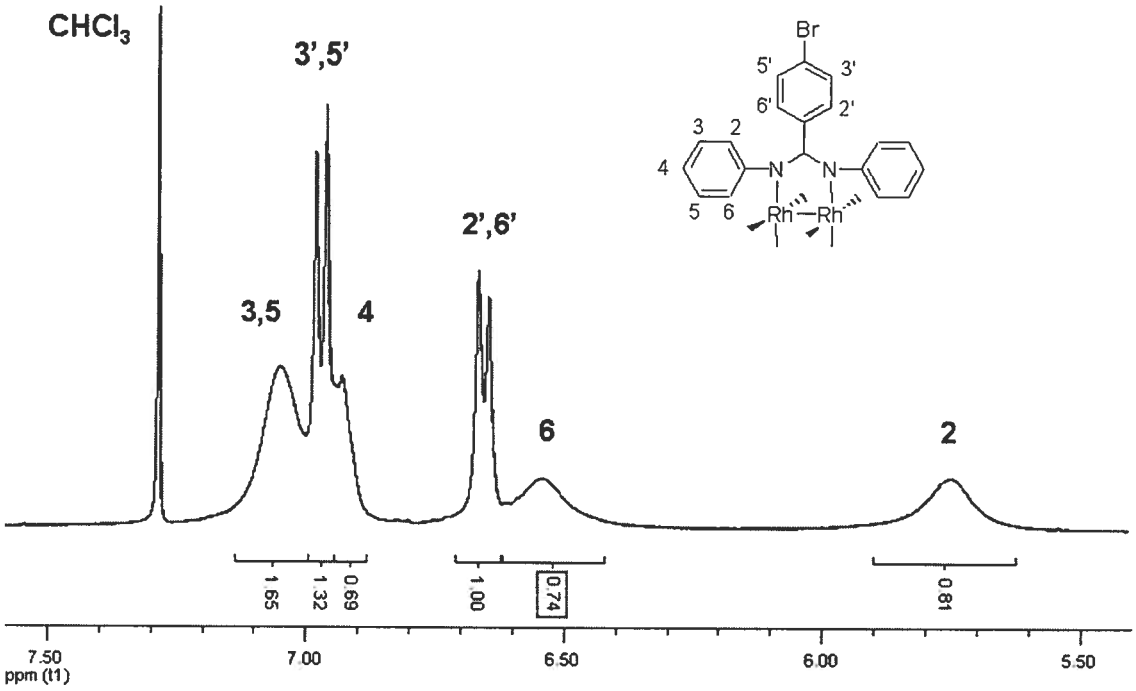

Figure 5.5. ^{1}H NMR of Rh_2(*N,N'*-diphenyl-4-bromobenzamidinate)$_4$ in $CDCl_3$ at r.t.

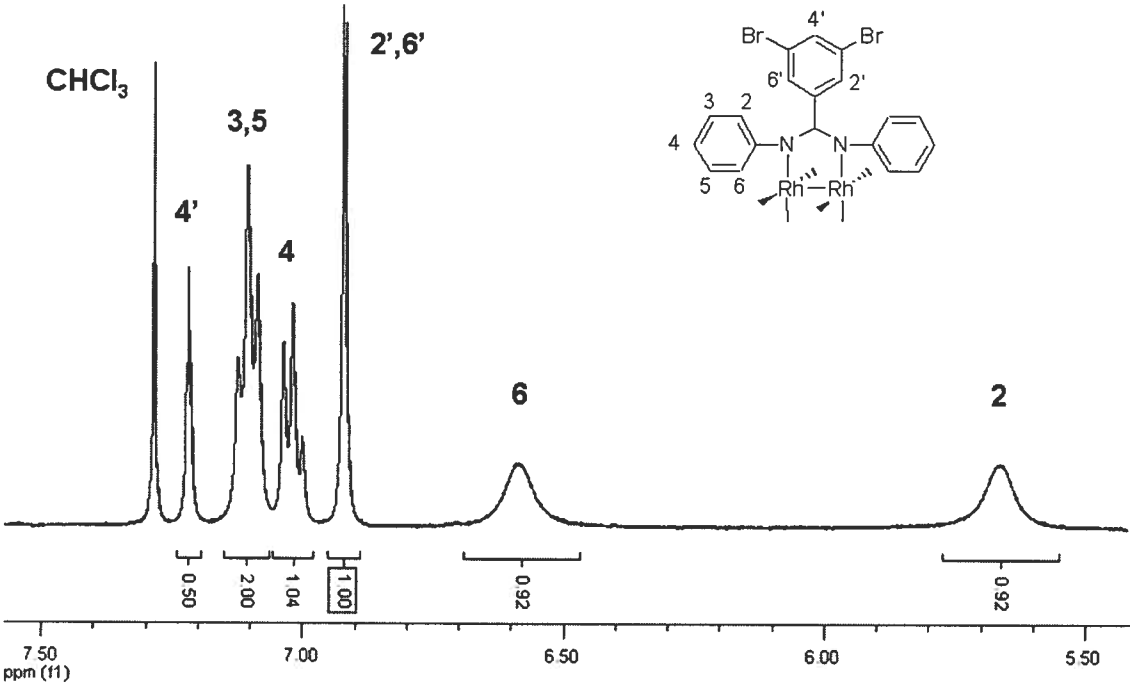

Figure 5.6. ^{1}H NMR of Rh_2(*N,N'*-diphenyl-3,5-dibromobenzamidinate)$_4$ in $CDCl_3$ at r.t.

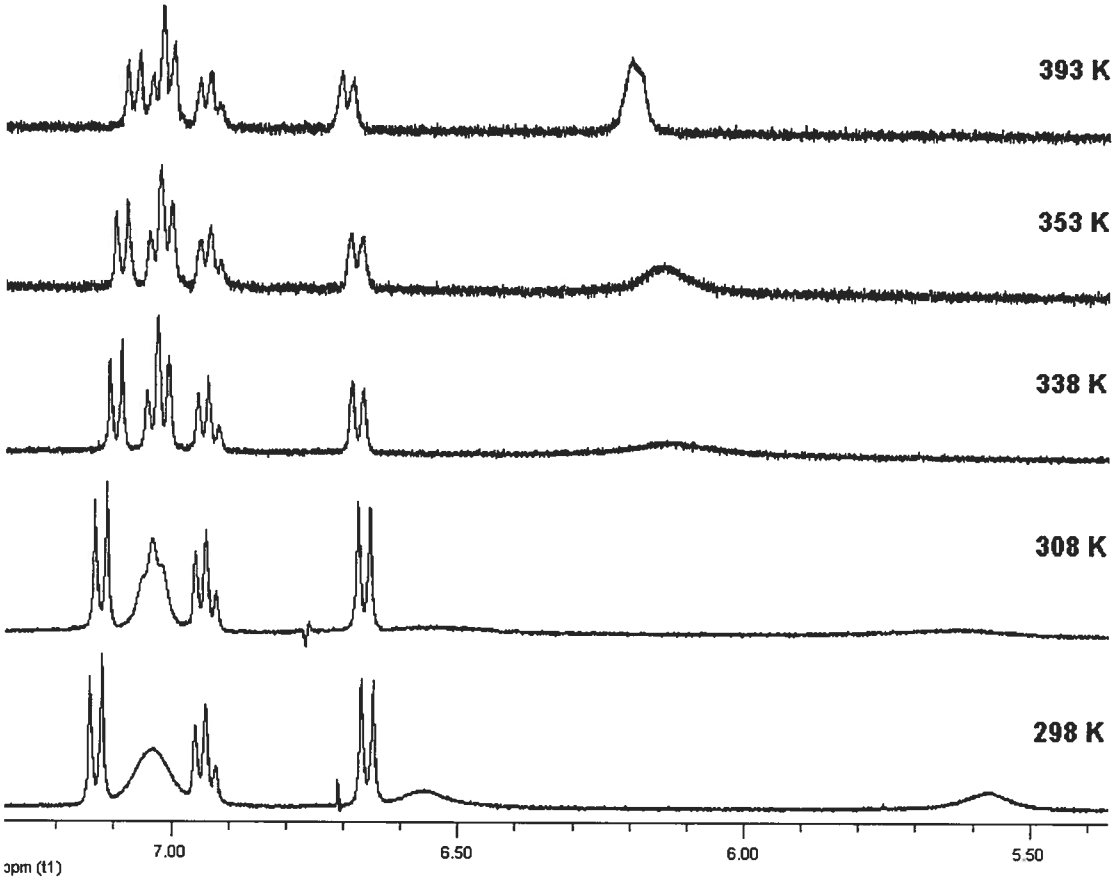

Figure 5.7. Variable-temperature ^{1}H NMR spectra of Rh_2(*N,N'*-diphenyl-4-bromobenzamidinate)$_4$ in d_6-DMSO.

The complex Rh_2(*N,N'*-diphenyl-4-bromobenzamidinte)$_4$ was found to be sparingly soluble in DMSO solution, which contributed to the rough character of these spectra. However, it provided for greatly improved resolution of the 3,5, 3',5', and 4 resonances by shifting the 3',5' phenyl doublet by ~ 0.15 ppm relative to that found in $CDCl_3$. Increasing the temperature resulted in distinctly different effects for the broad resonances associated with the *N*-bound phenyl groups. Firstly, the broad resonance at 7.2 ppm becomes a clear multiplet at ~ 313 K whose integration supports its assignment as the 3,5 phenyl protons. However, the broad resonances between 6.6 and 5.5 ppm continue to broaden until they effectively become unobservable at 318 K. This is characteristic of exchange broadening effects observed by chemically unique protons that are interchanging environments but which still show distinct resonances.[21] This is

commonly referred to as the slow-exchange region,[22] and may be contextualized by the following relationship:

$$\tau = \sqrt{2} / 2\pi\Delta\nu \qquad \textbf{(Eqn. 5.1)}$$

where τ is the lifetime of the two sites and $\Delta\nu$ is the difference in their frequencies. If we consider two interchanging spins, the lifetime of each must be greater than that described in the relation above for their resonances to be distinguishable at a given temperature. These lifetimes will of course vary inversely with temperature. The broadening effect in this slow-exchange region occurs because not all of the nuclei are being exchanged. The nuclei which do exchange begin to precess at another frequency but are then returned to their original frequency. This creates phase errors with the spins that did not exchange and leads to deconstructive interference, the end result of which is a rapidly decaying FID signal. In the slow-exchange region, the more frequently the spins interchange sites, the greater will be the loss of phase coherence and hence broadening. To complicate matters further, tumbling of such a symmetric molecule in solution should also contribute to line broadening.

Conversely, a temperature will be reached in such a system where site exchange is too rapid for separate resonances to be distinguished.[22] At this temperature, the environment is averaged for both spins and is indicated experimentally by the emergence of a single broad resonance. This is the coalescence temperature (T_c), determined to be ~323 K in the case here for Rh_2(*N,N*-diphenyl-4-bromobenzamidinte)$_4$ in d_6-DMSO (see Figure 8). Beyond this point, one enters the fast exchange region where line broadening effects are reduced due to this averaging effect. With T_c in hand, one may determine the exchange rate constant (k_c) at T_c according to the relationship below

$$k_c = \pi\Delta\nu / \sqrt{2} \qquad \textbf{(Eqn. 5.2)}$$

where $\Delta\nu$ is the chemical shift (Hz) between the two resonances at T_c. Since this is not possible to observe directly, it is usually calculated by extrapolation of chemical shift differences obtained at low temperatures according to a linear relationship. With this

information in hand, one may then use the expression below to arrive at the free-energy of activation (ΔG^*) for site interchange of the spins in question.[22]

$$\Delta G^* = 4.57\ T_c\ \{9.97 + \log\ (T_c / \Delta v)\ \text{(cal/mol)} \quad \text{(Eqn. 3)}$$

Use of this expression to calculate ΔG^* is strictly limited to cases where the populations of the two spin environments are equal. Where this is not the case is when there exists an equilibrium distribution between the species produced upon site exchange, such that one of the sites is more populated on the basis that it is associated with a more thermodynamically stable species. Such cannot be the case here, and so application of the above relation applies.

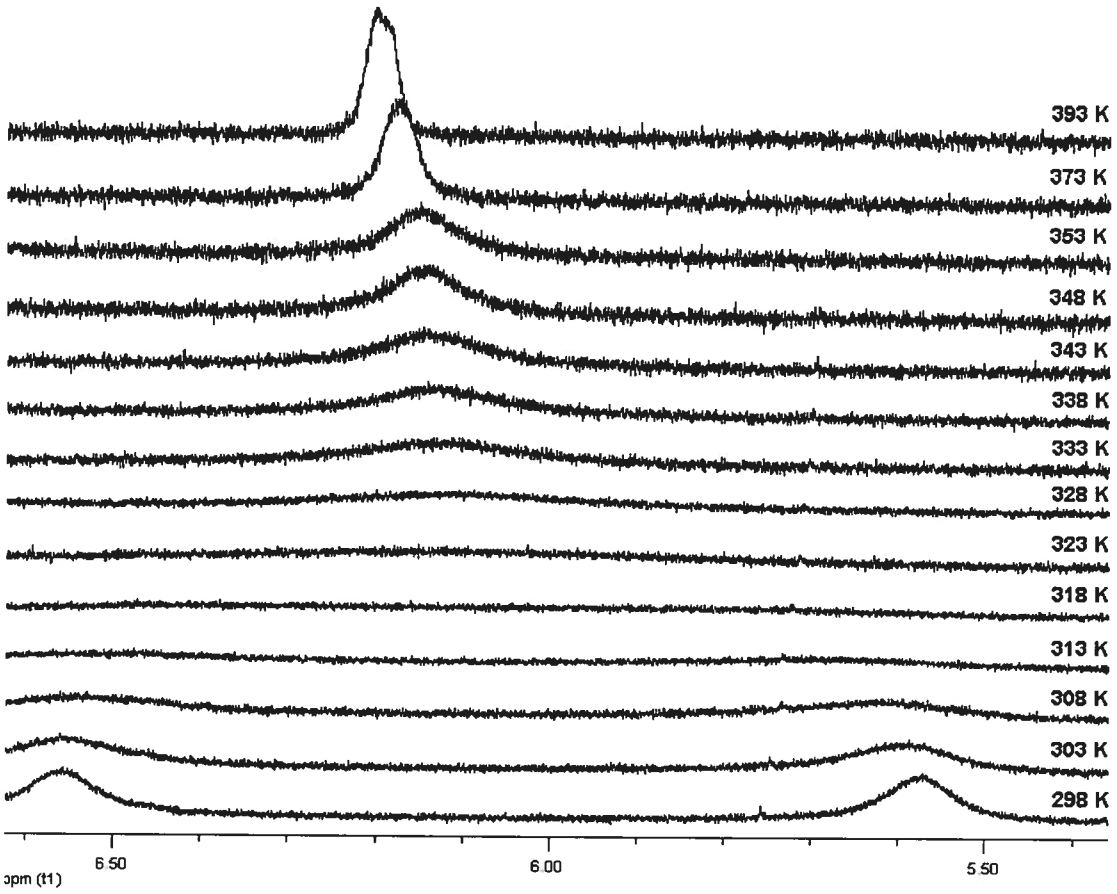

Figure 5.8. Coalescence phenomenon of the 2,6-phenyl protons of Rh_2(*N,N'*-diphenyl-4-bromobenzamidinate)$_4$ in d_6-DMSO.

Although the chemical shift is most often arrived at through linear extrapolation,[22] a polynomial fitting of the slow-exchange data (Figure 5.9) was found to be more suitable. Still, both linear and polynomial expressions were used to arrive at chemical shifts of 191 and 282 Hz, respectively.

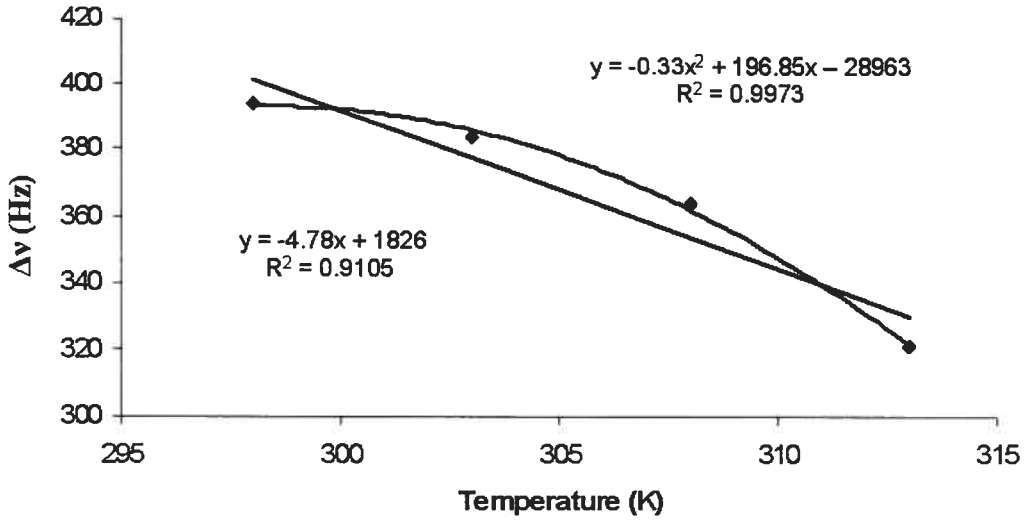

Figure 5.9. Linear and polynomial fits of chemical shifts as a function of temperature in the slow-exchange region for Rh_2(*N,N'*-diphenyl-4-bromobenzamidinate)$_4$ in d_6-DMSO.

Application of equation 5.3 gives ΔG^* = 15.0 kcal/mol employing $\Delta\nu$ = 191 Hz, while ΔG^* = 14.8 kcal/mol when employing $\Delta\nu$ = 282 Hz. Since error in determination of the chemical shift at T_c must be considered, it is best to consider the average of the two, ΔG^* = 14.9 kcal/mol, as being a more representative value. Another source of error that must be noted is the determination of the actual coalescence temperature. In this case, increments of 5 K were used (Figure 8) which has apparently captured the early onset of coalescence. Some brief mention of other methods for determining such thermodynamic parameters must be made, since these are often reported either alone or in support of analysis of the sort performed herein.[21, 22] The temperature dependence of exchange broadening effects may be utilized to extract exchange constants (k_c) by line-width analysis at half peak-height for a given temperature. From this, Arrhenius plots of ln(k_c) vs 1/T may be used to extract enthalpic and entropic parameters of activation. However, this is limited to the slow-exchange region and relies on accurate determination of line-

widths of the resonances in question. Here, owing to the rough nature of the spectrum traces and the extreme broadness of the resonances, such error would be particularly problematic. For these reasons, this method has been, for the most part, replaced with full line-shape analysis wherein the variable temperature spectra are calculated. Those which provide the best fit to the experimental data are used to extract such thermodynamic parameters. Such calculation could be useful to support the analysis given here.

The coalescence behaviour discussed above supports the previous assignment of these spins and is understood by the unique environments depicted in the solid state structure. It is interesting to note that, as expected, the high temperature limit of 393 K reveals that the 2,6-phenyl protons are beginning to display the profile of a true doublet. However, it remains to interpret these results so as to visualize the solution dynamics that are taking place. To this point, it can be said with certainty only that the 2,6 phenyl protons are exchanging, and that this involves a four-fold concerted effort since there are four such edge-to-face interactions. Whether this concerted exchange results in conversion between enantiomers or occurs within the context of each enantiomer is uncertain at this point, but the addition of an appropriate chiral shift reagent under such temperature variation may shed some light on this question.

5.3 'Chemistry on the Complex': Synthesis, Solid-State, and Solution NMR Characterization of Peripherally Modified Analogues of Rh_2(*N,N'*-diphenyl-4-bromobenzamidinate)$_4$ (refer to pages LXXXIX, CIV, CXIX, CXXXVIII, and CLI of Appendix 5 for X-ray data and parameters of complexes **V-5**, **V-6**, **V-7**, ***cis*-V-8**, and **V-10**, respectively)

A wide variety of chemistry may be attempted on these halogenated substrates. Toward creating systems of high nuclearity based upon photoactive units, we desire to create linkage that is efficient, robust, and conducive to energy and / or electron transfer processes. With regard to polypyridyl systems, transition metal-catalyzed C-C bond formation has played a very important role in creating polytopic ligands capable of supporting multiple metal centers.[23] More recently, focus has shifted to performing such transformations on the complex as this can significantly simplify synthesis and

purification.[24] To this end, Suzuki-Miyaura coupling reactions are particularly attractive considering that the required conditions are generally mild and high yielding for a wide range of substrates due to constant advancement in catalyst technology.[25] In the context of $Ru(tpy)_2^{2+}$ units, Williams and co-workers have adopted current methodology to create such complexes appended with boron ester functionality, which is readily hydrolyzed to the requisite boronic acid (Scheme 5.2).[26] With this complex in hand, Williams and co-workers were able to couple other polypyridyl complexes possessing secondary halide functionality. More recently, Buchwald and co-workers reported that using the supporting ligand 2-(2',6'-dimethoxybiphenyl)-dicyclohexylphosphine (SPhos, Scheme 5.2) enabled the efficient coupling of both deactivated and sterically hindered aryl halides and boronic acids at low catalyst loadings.[27] Adopting such a protocol, however, was unsuccessful in cross-coupling the boronic acid complex to the Rh_2(*N,N'*-diphenyl-4-bromobenzamidinate)$_4$ substrate.

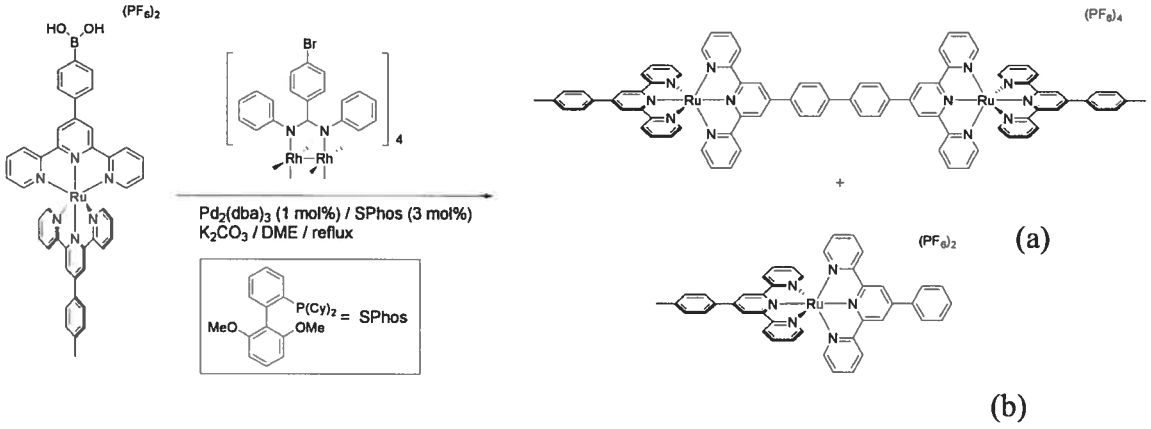

Scheme 5.2. Attempted Suzuki coupling on Rh_2(*N,N'*-diphenyl-4-bromobenzamidinate)$_4$ in degassed 1,2-dimethoxyethane.

The major products recovered from this reaction were determined to be the homocoupled dinuclear complex (Scheme 5.2, a) and the hydrolyzed mononuclear complex (Scheme 5.2, b). Conversely, installation of boron ester functionality on the tetrabromo-amidinate using an appropriate diboron ester was abandoned as this was found to give a complicated mix which, upon treatment with dilute HCl, did not yield any apparent boronic acid functionality.

Formylation of the peripheral bromides of these tetra-amidinate complexes is highly-desirable as this makes available a wide range of transformations such as, for instance, the synthesis of porphyrins.[28] Formylation of aryl halides is most commonly accomplished by lithiation followed by electrophilic addition of DMF. Unfortunately, despite using various lithiating reagents under a wide range of temperatures in THF, lithiation of Rh_2(*N,N'*-diphenyl-4-bromobenzamidinate) was found to be very inefficient. Moreover, it appeared that any lithiated material was slow to react with DMF as evidenced by ^{1}H NMR and mass spectrometry which showed only trace amounts of formylated product along with a relatively larger amount of hydrolysed material and a very large amount of the starting material. As such, formylation was attempted on the ligand *N,N'*-diphenyl-4-bromobenzamidinate in the hope that the product would be sufficiently stable under the melt conditions employed to form these tetra-amidinates.

We desire selective lithiation of *N,N'*-diphenyl-4-bromobenzamidine, but clearly lithiation of the amidine is competitive and could potentially lead to its alkylation in the presence of a bromo-alkyl species generated upon lithiation of the bromide. To circumvent this occurrence, it is desired to first protect the amidine. Surprisingly, there are relatively few reports in the literature regarding amidine protection.[29] Previous experience in protecting the related amidine 4'-(*N,N'*-diphenylbenzamidine)-tpy using Me_3SiCl proved to be inefficient. However, acetylation of the amidine could be accomplished quantitatively by simply refluxing in the acetic anhydride. De-protection was easily accomplished by hydrolysis in acidic media on the ligand itself, but once it was complexed to Ru(II) it became exceedingly difficult to remove. For this reason, shortened reaction times were employed to improve the yield of complex formation (see Chapter 4). Here, refluxing *N,N'*-diphenyl-4-bromobenzamidine in acetic anhydride produced spot-to-spot conversion, and this material was used in subsequent lithiations using n-BuLi according to Scheme 5.3 below.

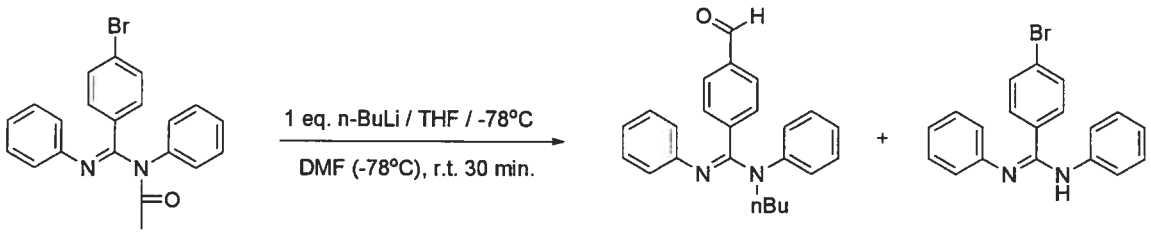

Scheme 5.3. Attempted lithiation of acetylated *N,N'*-diphenyl-4-bromobenzamidine.

Unfortunately, however, the principle constituents of this reaction were the *N*-butylated species along with the de-protected ligand. Forgoing protection and using 2 equivalents of n-BuLi was then focused upon with systematic variation of reaction time and temperature, for which the conditions outlined in Scheme 5.4 were found to be optimal.

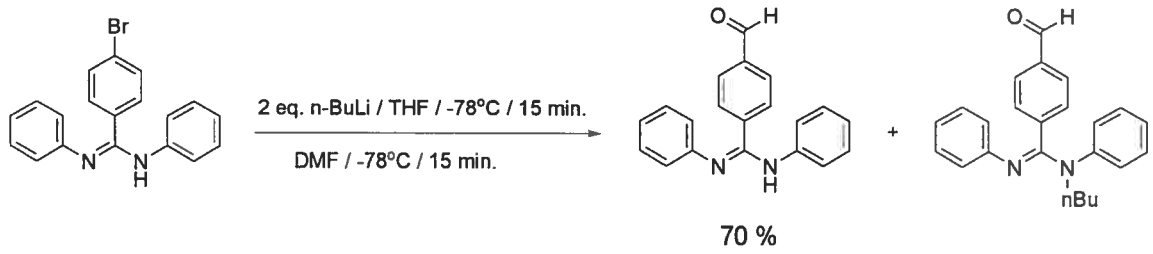

Scheme 5.4. Optimized lithiation of *N,N'*-diphenyl-4-bromobenzamidine. Yield obtained of pure product after chromatographic purification.

The melting point of the *N,N'*-diphenyl-4-formyl-benzamidine (m.p. = 149°C) was found to be suitable for the melt protocol outlined previously with $Rh_2(O_2CCH_3)_4$. Pure Rh_2 (*N,N'*-diphenyl-4-formyl-benzamidinate)$_4$ (**V-3**) was then obtained by chromatography on silica. The ^{1}H NMR spectrum is depicted below in Figure 5.10.

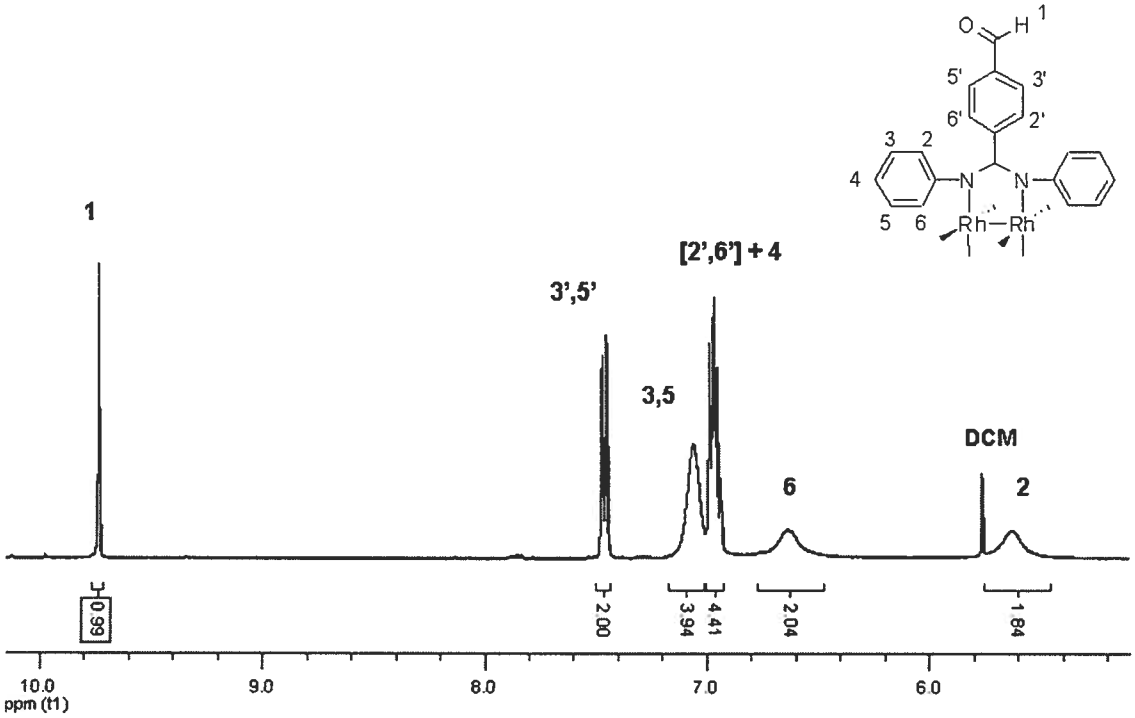

Figure 5.10. ^{1}H NMR of Rh_2(*N,N'*-diphenyl-4-formyl-benzamidinate)$_4$ in d_6-DMSO.

Direct oxidation of this tetra-aldehyde complex using common oxidizing agents such as $KMnO_4$ was complicated by the formation of intractable, unidentified material. However, mild oxidation to the tetra-methylcarboxy dimer complex (**V-4**, Scheme 5.5) could be carried out in high yield, after chromatographic purification, using iodine in methanolic potassium hydroxide.[30]

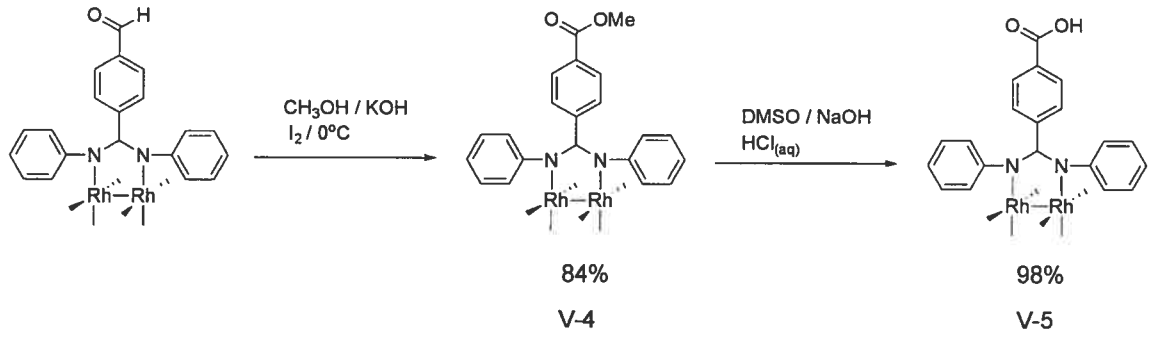

Scheme 5.5. Synthesis of Rh_2(*N,N'*-diphenyl-4-carboxy-benzamidinate)$_4$ (**V-5**). Indicated yields are before crystallization.

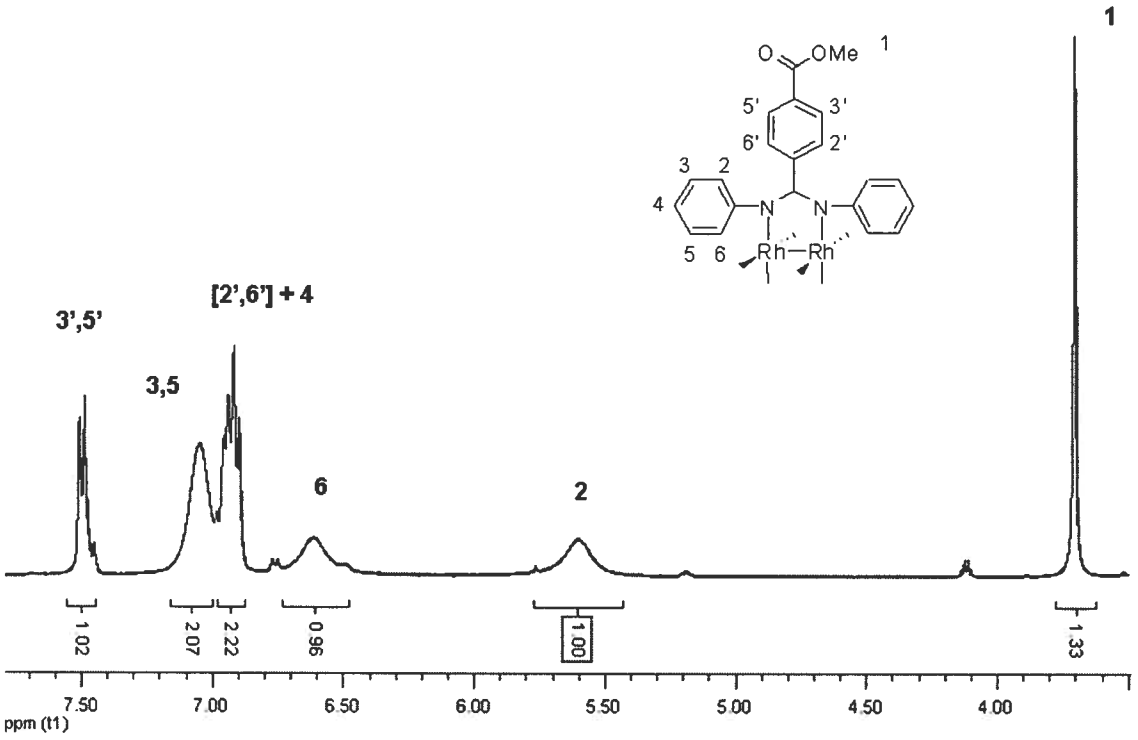

Figure 5.11. ^{1}H NMR of Rh_2(*N,N'*-diphenyl-4-methylcarboxy-benzamidinate)$_4$ in d_6-DMSO.

Saponification of the methylcarboxy analogue in DMSO afforded the tetra-carboxylate dimer, which was precipitated in near quantitative yield as the tetra-carboxylic acid dimer upon acidification of the solution with $HCl_{(aq)}$ (see Scheme 5.5).As expected, Rh_2(*N,N'*-diphenyl-4-carboxy-benzamidinate)$_4$ moves only under very polar conditions (e.g. methanol) on silica substrate. The tendency of this compound to diffuse strongly and adsorb irreversibly to some extent on both silica and alumina substrate preclude its chromatographic purification, although simple trituration with solvents such as DCM suffices to remove any residual starting materials. While the ^{1}H NMR spectrum could be recorded in DMSO (see Figure 5.12), it is notably featureless relative to that for both the tetra-formyl and tetra-methylcarboxy dimeric complexes. This is likely a consequence of the carboxylates, which could effectively alter the tumbling rate of the dimeric species through association with the solvent media and/or through intermolecular association. The nature of this association is likely hydrogen bonding, as noted also in its crystal structure with DMSO.

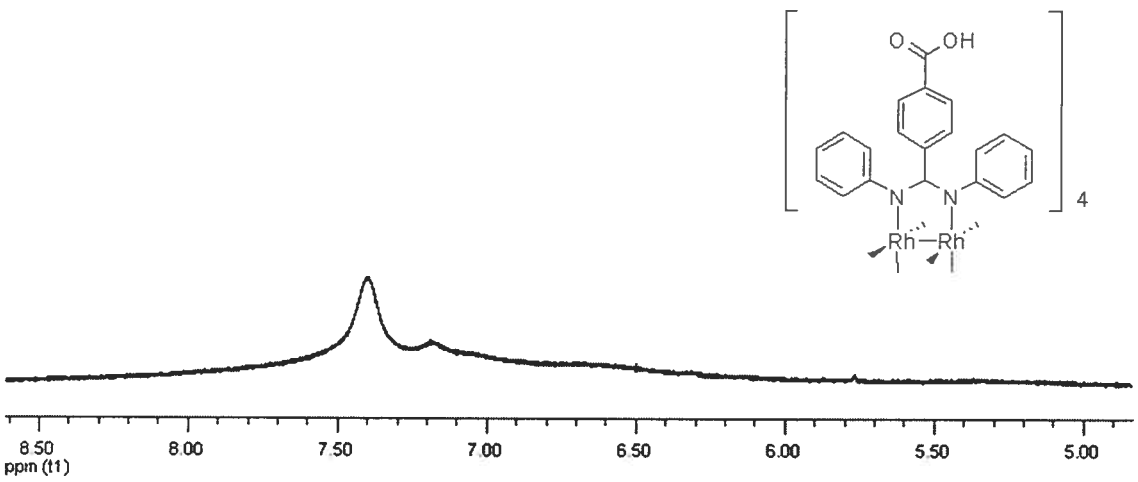

Figure 5.12. ^{1}H NMR of **V-5** in d_6-DMSO.

Single crystals suitable for structure determination could be grown upon standing of a DMSO solution, owing to the slow absorption of water over time. However, this does not afford efficient crystallization, as the complex is also somewhat water-soluble. The structure is depicted in Figure 5.13.

Figure 5.13. X-ray crystal structure of **V-5** with thermal ellipsoids at 50 % probability. Solvent and aromatic protons have been omitted for clarity.

This complex crystallizes in $P2_1/n$ space, and so one finds both enantiomers in the crystal structure. As expected, no axial association to potential donor atoms is observed. While the presence of four carboxylic acid groups holds potential for creating porous networks, the packing is actually quite dense owing to hydrogen bonding between each carboxy group and a DMSO acceptor ($O_{(COOH)}$ --- $O_{(DMSO)}$ < 2.7 Å). In fact, roughly 30% of the unit cell volume is attributable to these DMSO molecules. With regard to the structural parameters of the dimetal complex itself, they are invariant relative to those noted already for both Rh_2(*N,N'*-diphenyl-4-bromobenzamidinate)$_4$ and Rh_2(*N,N'*-diphenyl-3,5-dibromobenzamidinate)$_4$.

To the best of our knowledge, this is the first example of a dimetal paddlewheel complex possessing uncomplexed tetracarboxylate functionality. The nearest example to this was reported by Yaghi, wherein an extended structure possessing 1-D channels was formed upon self-assembly of $Zn(NO_3)_2{\cdot}(H_2O)_6$ and 1,4-benzenedicarboxylic acid in the

presence of triethylamine.[31] Here, the repeating unit was found to be $Zn_2(O_2C\text{-}ph\text{-}CO_2)_4(H_2O)_2$. However, it does not exist as a discrete molecular unit, which makes our example here unique. The rigidity, stability, and potential applications afforded by porous metal-organic frameworks have made such systems an area of intense focus.[32] In this context, the tetra-carboxylate dimer prepared here holds much potential toward the formation of various architectures directed by the addition of complementary bridging ligands, considering in particular its rich electrochemistry, thermal stability, and rigidity.

Another desirable secondary functionality to possess on the exterior of the Rh_2(*N,N'*-diphenylbenzamidinate)$_4$ unit is amino functionality, as this makes available amide bond formation as a means to create connectivity that is robust, high yielding, and conducive to both energy and electron transfer processes.[33] It has been noted that benzophenone imine can serve as a convenient ammonia equivalent in the palladium-catalyzed amination of aryl halides and triflates (Scheme 5.6).[34] The resulting benzophenone imine adducts were reported to be quite robust as they were stable to chromatographic purification on silica and, in the case of benzophenone imine protected 4-bromoaniline, could even tolerate halogen-metal exchange (n-BuLi, THF, -78°C) without significant addition to the imine.

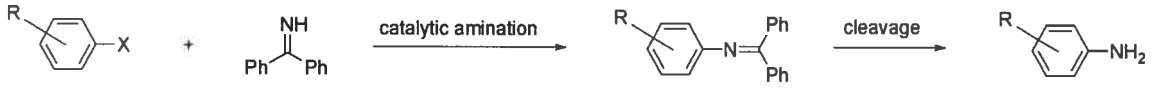

Scheme 5.6. Strategy for the formation of unsubstituted primary aniline derivatives.

Given the straightforward nature of this protocol and the integrity of the installed benzophenone imine, we opted to apply such an approach to the Rh_2(*N,N'*-diphenyl-4-bromobenzamidinate)$_4$ substrate. Reaction conditions for such amination reactions typically employ a palladium source along with a supporting ligand, most commonly BINAP (racemic mix), along with either Cs_2CO_3 or NaO*t*Bu as base in either THF or toluene at a temperature and duration that depends on the reactivity of the aryl halide substrate.[34]

Considering our previous success with S-PHOS as supporting ligand and also its ease of preparation and stability to air and moisture, we chose to optimize systems based upon this ligand. It was found initially that using Cs_2CO_3 as base and THF as solvent provided superior reaction progression at reflux temperature (i.e. 65 °C). However, even in the presence of an excess of benzophenone imine, this reaction required about 4-5 days to give exclusively the tetra-aminated product (Scheme 5.7). Fortunately, this reaction time was found to be dramatically shortened to 12 h at elevated temperature and pressure (THF at 140°C) using a sealed pressure vessel. Purification of the Rh_2(*N,N'*-diphenyl-4-diphenylketimine-benzamidinate)$_4$ **(V-6)** product entailed column chromatography on silica gel using DCM / 0.5% Et_3N as eluent, after which the recovered residue could be crystallized on a large scale from a chlorobenzene / methanol solution.

During the course of the reaction to form Rh_2(*N,N'*-diphenyl-4-diphenylketimine-benzamidinate)$_4$, the formation and consumption of the mono, bis, and tris-aminated intermediates could be observed by TLC. Targeting these intermediates could be accomplished using an appropriate number of equivalents of benzophenone imine, but in all cases produced a range of products. It was found that, like with the tetra-aminated species, the tris-aminated species was produced most efficiently at elevated temperature and pressure. This may be indicative of reduced reaction rates as the substrate becomes larger with each successive coupling to the imine.

The mono and bis-aminated species, on the other hand, were best arrived at by conventional reflux at 65°C. Quite often, for instance, targeting the bis-aminated product at 140°C led to a product distribution that was weighted in favour of the tris-aminated species. Perhaps this is because slower reaction rates are more forgiving to experimental error in measuring and transferring the quantities of substrate and benzophenone imine used. In the end, a 24 h conventional reflux was found to suffice.

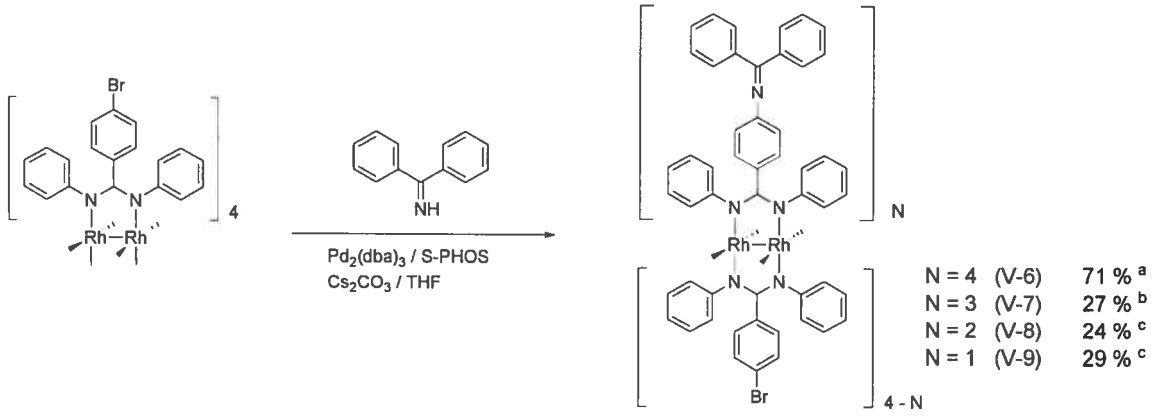

Scheme 5.7. Amination of Rh_2(*N,N'*-diphenyl-4-bromobenzamidinate)$_4$ using benzophenone imine.(a) 1.5 mol % $Pd_2(dba)_3$, 4.8 mol % S-PHOS, 2.0 eq. Cs_2CO_3, 4.8 eq. imine, THF, 140°C, 12 h. Yield obtained after crystallization. (b) 1.3 mol % $Pd_2(dba)_3$, 4.0 mol % S-PHOS, 2.0 eq Cs_2CO_3, 3.0 eq. imine, THF, 140°C, 8 h. Yield obtained after crystallization. (c) 1.5 mol % $Pd_2(dba)_3$, 4.8 mol % S-PHOS, 1.0 eq. Cs_2CO_3, 1.2 eq. imine, THF, 65°C, 24 h. Yield obtained before crystallization.

All intermediate species could be purified by column chromatography in the same manner as for the tetra-aminated compound. However, the tris and tetra-aminated products often contained trace amounts of what appeared to be either S-PHOS or a decomposition by-product thereof. Fortunately, both species could be efficiently crystallized to yield pure material. Also, the bis-aminated material was found to be resolved into its *cis* and *trans* components upon further column chromatography using silica gel and chloroform as eluent. The relative *cis* / *trans* composition was found to be 2.7:1.0, weighted in favour of the *cis* isomer, as expected.

Initial inspection of the ^{1}H NMR spectra for this series of aminated tetra-amidinate complexes appears to be complex, but it is readily interpreted given the spectra for Rh_2(*N,N'*-diphenyl-4-diphenylketimine-benzamidinate)$_4$ and Rh_2(*N,N'*-diphenyl-4-bromobenzamidinate)$_4$, 2-D COSY NMR, and single crystal X-ray structures. These spectra are depicted below, along with their respective assignments, in Figures 5.14-5.18.

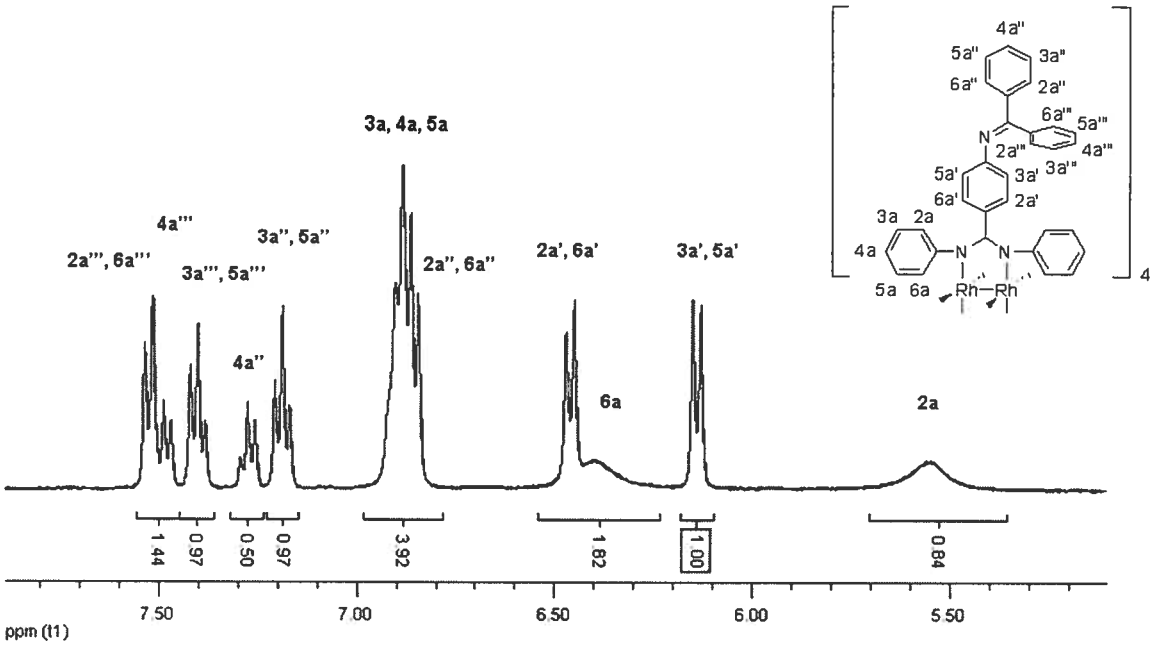

Figure 5.14. ^{1}H NMR of **V-6** in d_6-DMSO.

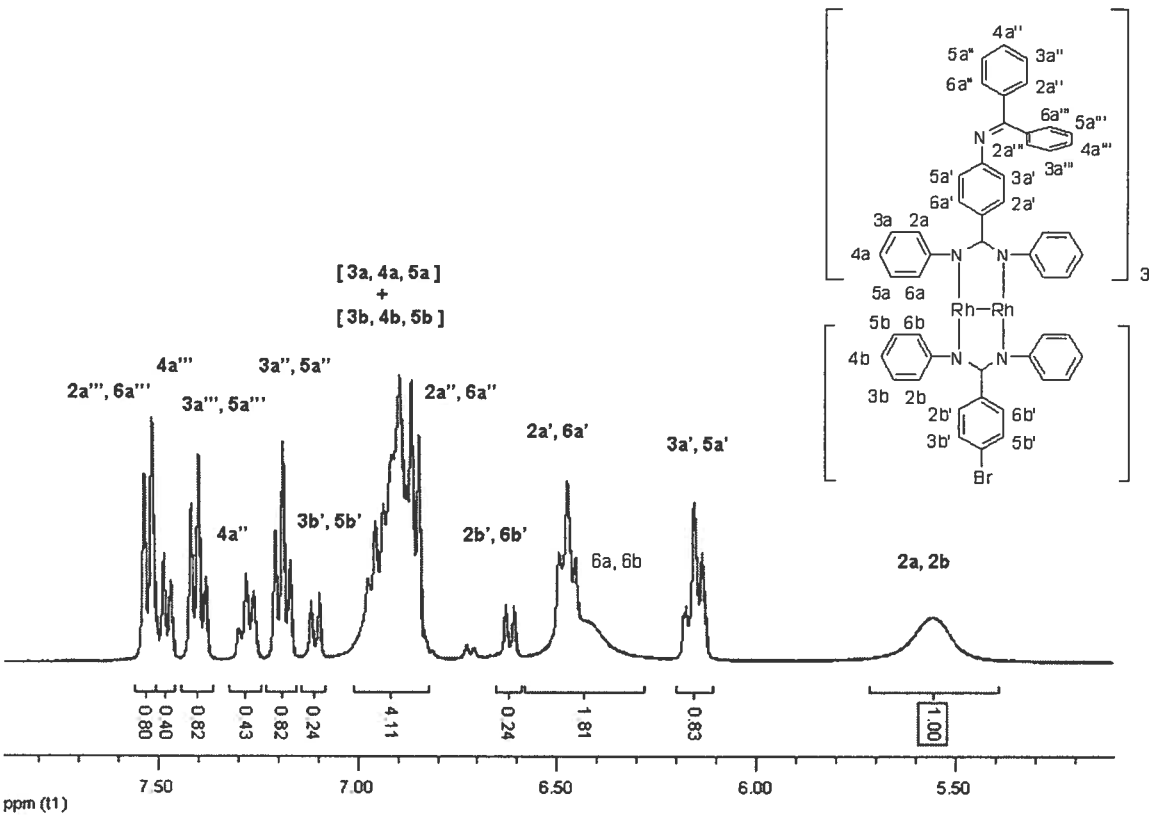

Figure 5.15. ^{1}H NMR of **V-7** in d_6-DMSO.

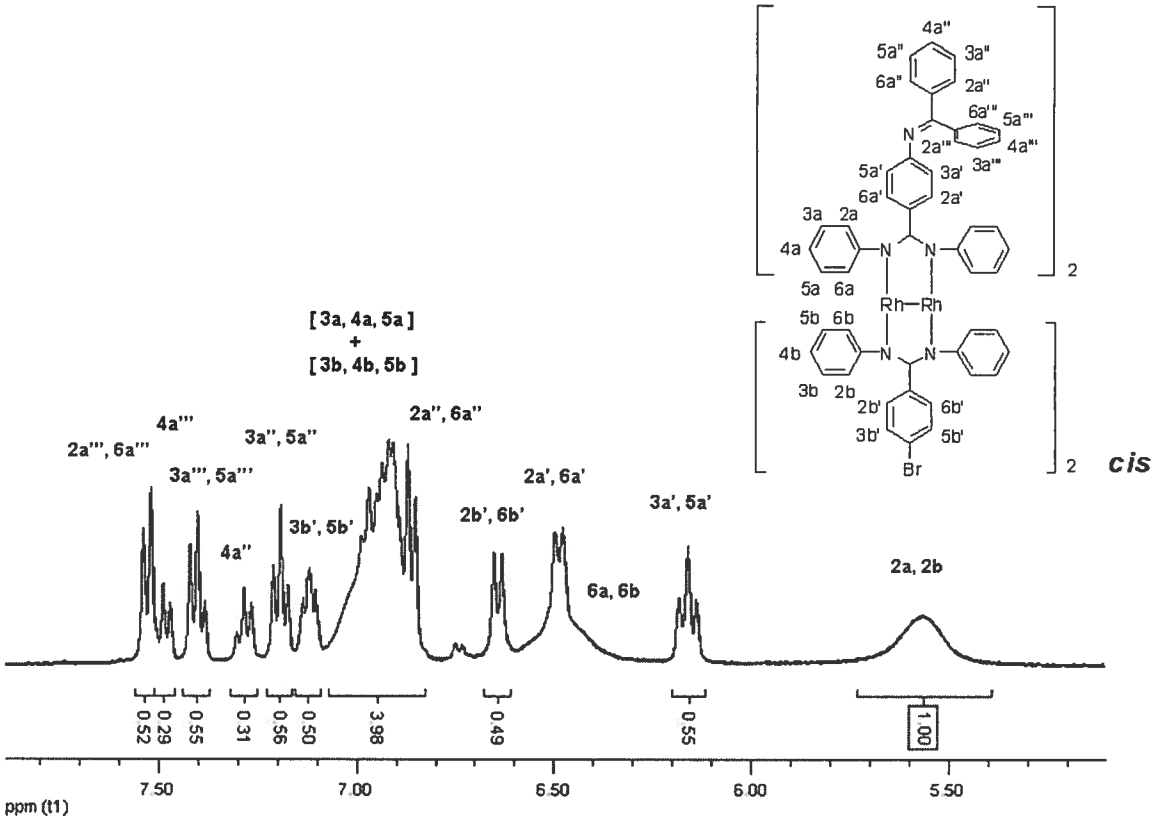

Figure 5.16. ^{1}H NMR of ***cis*-V-8** in d_6-DMSO.

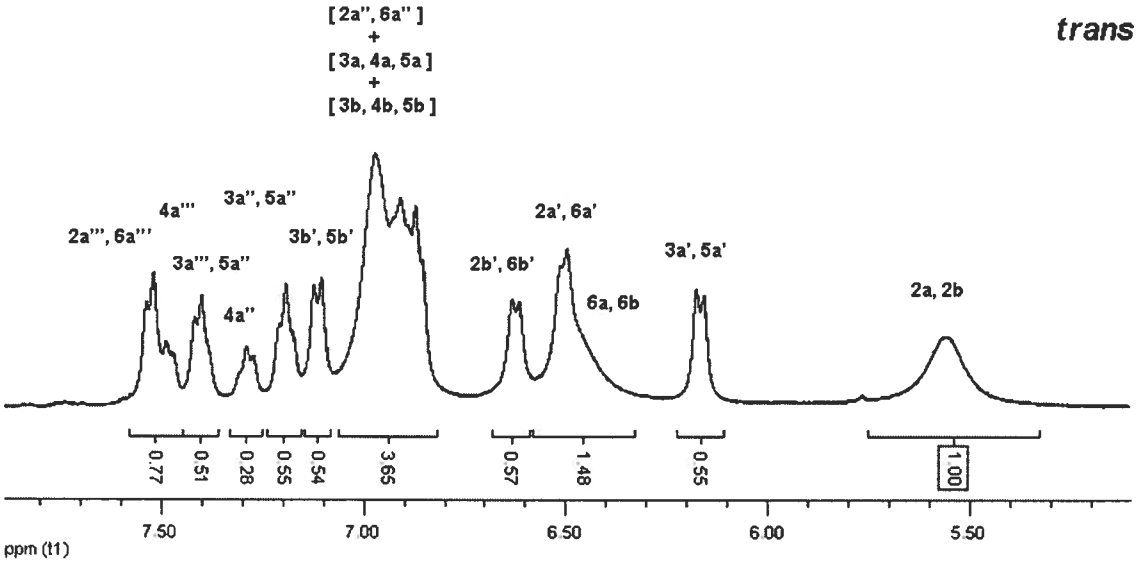

Figure 5.17. ^{1}H NMR of ***trans*-V-8** in d_6-DMSO.

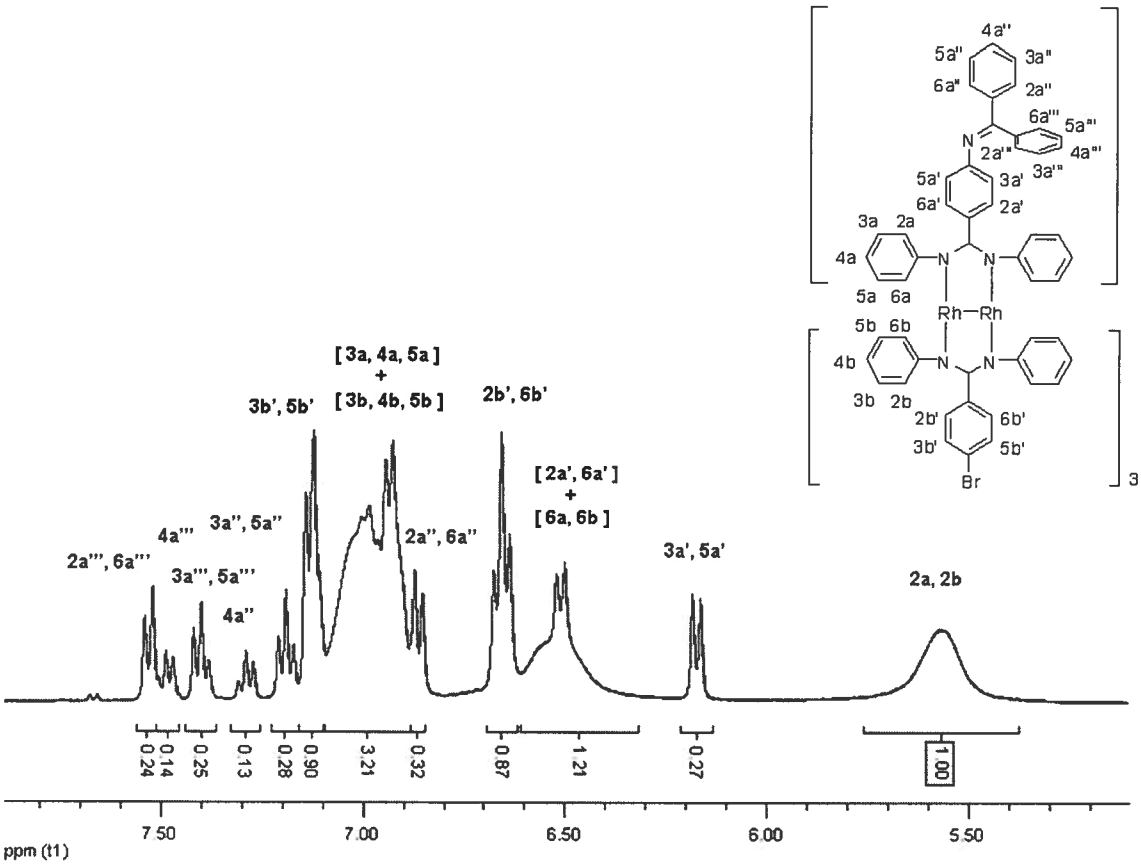

Figure 5.18. ^{1}H NMR of **V-9** in d_6-DMSO.

As with the tetra-brominated complexes Rh_2(*N,N'*-diphenyl-4-bromobenzamidinate)$_4$ and Rh_2(*N,N'*-diphenyl-3,5-dibromobenzamidinate)$_4$, there exists characteristically broad resonances between 7 and 5 ppm owing to the phenyl rings directly connected to the amidine nitrogen atoms. The remaining resonances, those associated with the diphenyl ketimine moieties and the central phenyl ring of the amidinate ligand are, for the most part, well-separated. As such, their relative integration offers unambiguous support for the identity of these complexes. Interestingly, the distribution of these resonances indicates a lower symmetry than what one may otherwise anticipate. That this occurs for the resonances of the central phenyl ring of the amidinate ligand is anticipated on the basis of the substituent in the 4'-position (i.e. bromo or diphenyl ketimine). The phenyl doublets of the ring bearing the diphenyl ketimine moiety occur at ~ 6.2 and ~ 6.5 ppm, while those of the bromo-substituted ring occur at ~ 6.7 and ~ 7.1 ppm. This reflects a relative electron releasing effect of the diphenyl ketimine

group. More importantly, these resonances serve as excellent diagnostic markers for interpretation of these spectra.

The asymmetry of the resonances stemming from the phenyl rings of the ketimine substituent may be interpreted with the aid of the solid-state structures, in particular that for Rh_2(*N,N'*-diphenyl-4-diphenylketimine-benzamidinate)$_4$ depicted in Figure 5.19. These rings are distinct owing to the angular connection imposed by the ketimine nitrogen atom and their mutually orthogonal disposition. However, there are only a total of six resonances attributable to these phenyl rings, occurring in three pairs. It is likely that rotation of these phenyl rings in solution creates equivalency between the proton resonances within each ring, and so differentiation occurs solely because of the angular nature of the ketimine connection. The separation between related resonances 4a'' and 4a''' and between 3a'',5a'' and 3a''',5a''' is consistent and modest at $\Delta\ \delta = 0.2$ ppm. However, the separation between 2a'',6a'' and 2a''',6a''' is $\Delta\ \delta = 0.7$ ppm, as judged most accurately from the spectra for the mono-aminated complex (Figure 5.18). A plausible explanation is that the 2,6 protons of one of these rings experiences an averaged environment which is more shielding due to a significant π-interaction contribution. This may be understood considering the space-filling illustration in Figure 5.19 below for the phenyl rings of the ketimine in relation to the central phenyl ring of the amidinate ligand. Here, the orange and yellow-highlighted protons are offset with respect to their nearest phenyl ring counterparts, with distances of ~ 2.8 Å and ~ 2.6 Å, respectively, to the nearest carbon atom of the neighboring phenyl ring. It is not likely that these constitute significant aromatic ring-shielding interactions. However, the green-highlighted proton is within 2.5 Å of the carbon-nitrogen double bond of the ketimine moiety. More importantly, the ketimine double bond is reasonably within the plane of the phenyl ring containing the green-highlighted proton (torsion angle ~ 27 °), and so this likely constitutes a stronger π interaction, leading to an exchange environment that is relatively more shielding.

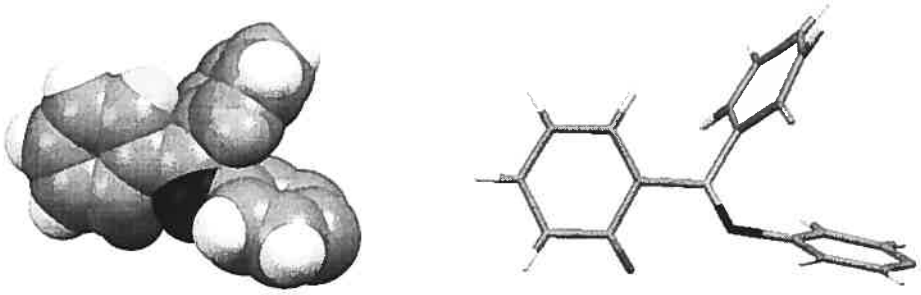

Figure 5.19. Space-filling representation of phenyl rings about ketimine moiety for Rh_2(*N,N'*-diphenyl-4-diphenylketimine-benzamidinate)$_4$.

Single crystals suitable for structure determination by X-ray diffraction could be obtained for most of these aminated complexes (Figures 5.20-5.22), with the exception of the mono-aminated species which proved challenging to crystallize. Both enantiomers of each complex are found within their respective solid-state structures. In all cases, the tetra-amidinate core is structurally analogous to that discussed already for the tetra-bromo complexes, with no evidence for axial ligation.

With regard to the structure of complex Rh_2(*N,N'*-diphenyl-4-diphenylketimine-benzamidinate)$_4$ depicted in Figure 5.20, the diphenyl ketimine groups do not occur in a regular orientation, but rather in symmetrically equivalent pairs which serves to lower the ideal symmetry of the molecule from D_4 to D_2. These diphenyl ketimine groups are in general well-defined, with the exception of one ketimine ring for which anisotropic refinement proved problematic. Consequently, refinement for this ring is left isotropic. For the tris- and bis-aminated structures (Figures 5.21 and 5.22, respectively), all atoms were refined anisotropically. Both the tris- and bis-aminated complexes possess a two-fold symmetry axis. Hence, the structures depicted in Figures 5.21 and 5.22 describe one unique orientation of these diphenylketimine substituents, which have been modeled based on partial occupancy Idealized molecular symmetry (i.e. that excluding the peripheral diphenylketimines) is reduced to C_2 for both the tris and bis-aminated products.

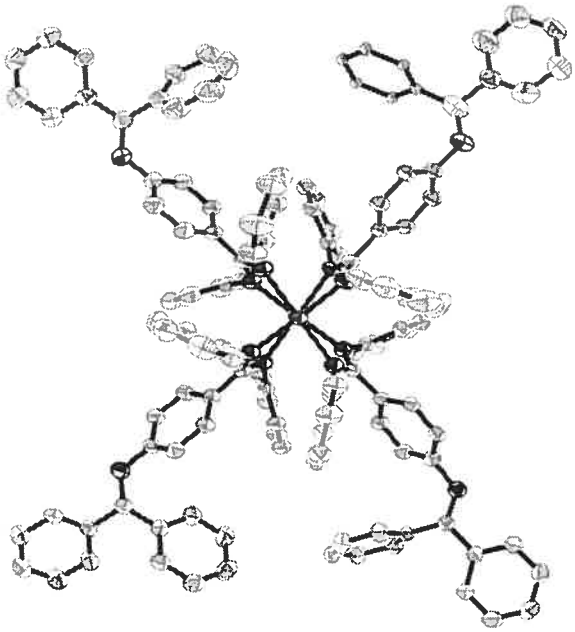

Figure 5.20. X-ray crystal structure of **V-6** with thermal ellipsoids at 50 % probability. Protons and solvent molecules have been omitted for clarity.

Figure 5.21. X-ray crystal structure of **V-7** (one representation of two) with thermal ellipsoids at 50 % probability. Protons and solvent molecules have been omitted for clarity.

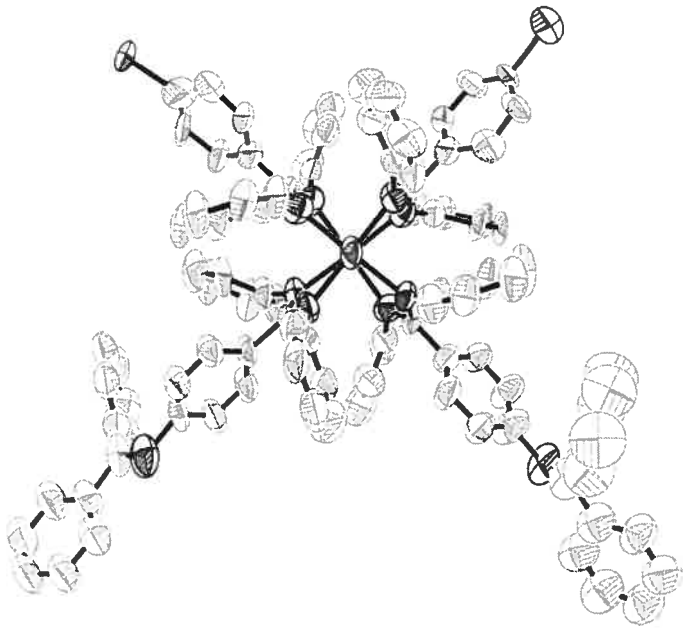

Figure 5.22. X-ray crystal structure of ***cis*-V-8** (one representation of two) with thermal ellipsoids at 50 % probability. Protons and solvent molecules have been omitted for clarity.

Considering the lasting appeal in the literature toward formation of squares, rectangles, and various other geometric motifs using metal complex building blocks,[35] it is easy to envision many potential assemblies based upon this self-complementary family of complexes. However, to this end one should look toward efficient means of creating linkage. As such, the potential utility of this family as building blocks is predicated on the efficiency to convert the appended diphenyl ketimine to its ammonia equivalent. This was found to be efficiently carried out according to the acid-promoted hydrolysis depicted in Scheme 5.8. Here, a mix of THF / $HCl_{(aq)}$ suffices to cleave the ketimine group at room temperature, the free base of which is recovered efficiently and quickly without need for chromatographic purification owing to the insolubility of the compound as the hydrochloride salt in solvents such as DCM.

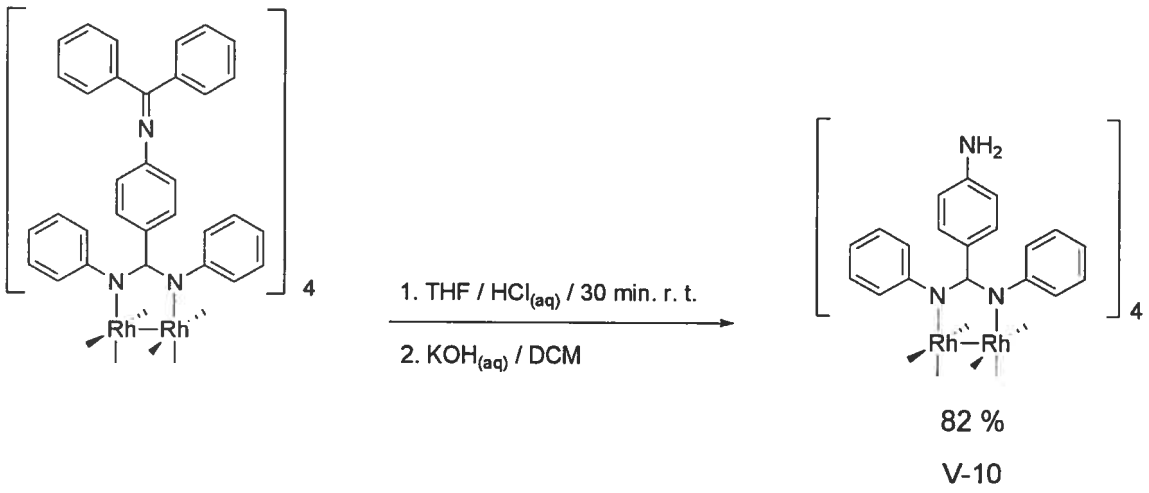

Scheme 5.8. Acid-promoted hydrolysis of Rh_2(*N,N'*-diphenyl-4-diphenylketimine-benzamidinate)$_4$ **(V-10)**.

The ^{1}H NMR spectra of the tetra-amino complex is shown below in Figure 5.23. It bears a strong resemblance to those of the tetra-bromo analogues, with two notable exceptions. The first, and most obvious, is the appearance of a singlet resonance at ~ 5 ppm for the amino protons. The second is an inverted assignment of the phenyl doublets, with the 3',5' doublet occuring upfield relative to that for the 2',6' resonance. The justification for this assignment was made by comparison to the corresponding doublets in the diphenyl ketimine complexes (Figures 5.14-5.18). Hydrolysis of the ketimine to the amino should have a slightly increased electron releasing effect on the phenyl ring, and this should be more pronounced for the 3',5' protons. The phenyl doublets bearing the ketimine moiety appear at ~ 6.5 ppm and ~ 6.2 ppm, while those of the phenyl ring bearing an amino substituent appear at ~ 6.4 ppm and ~ 6.0 ppm. Since one anticipates a general upfield shift for both resonances, the doublet at 6.5 ppm must correspond to that at 6.4 ppm, and that at 6.2 ppm to that at 6.0 ppm. This gives, respectively, $\Delta\delta$ = 0.1 ppm and 0.2 ppm, and so the resonance set occurring at ~ 6.5 ppm (ketimine complex) and at 6.4 ppm (amino complex) corresponds to the 2',6' phenyl protons while the resonance set occurring at ~ 6.2 ppm (ketimine complex) and at ~ 6.0 ppm (amino complex) corresponds to the 3',5' phenyl protons.

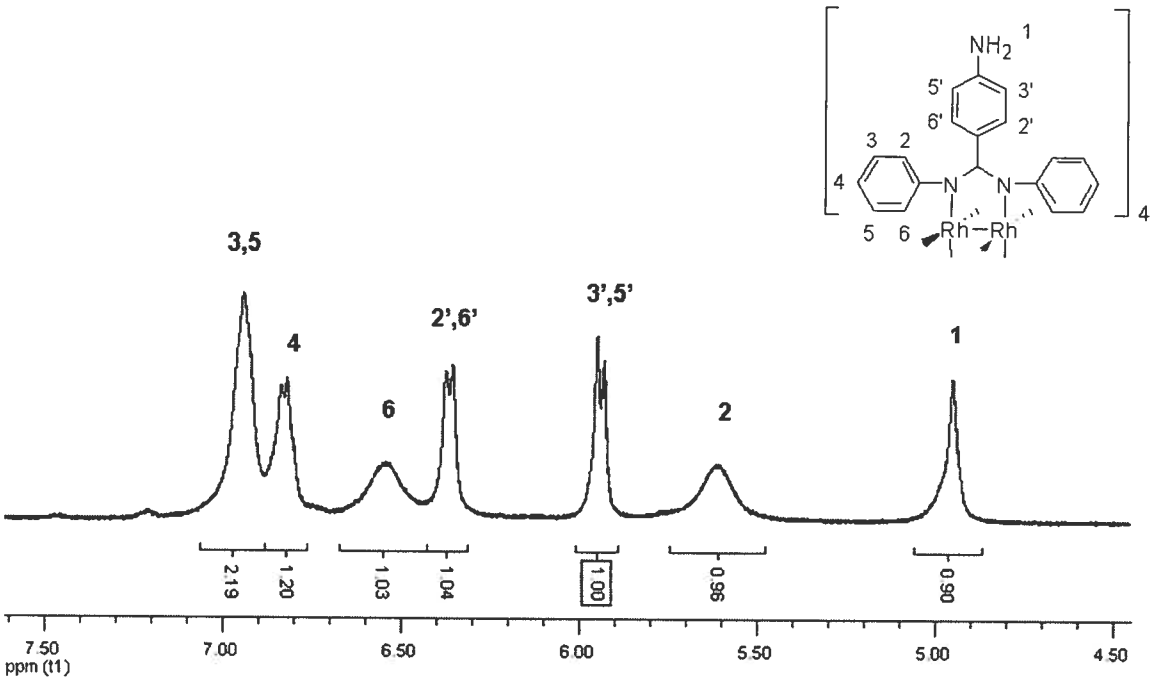

Figure 5.23. ^{1}H NMR of **V-10** in d_6-DMSO.

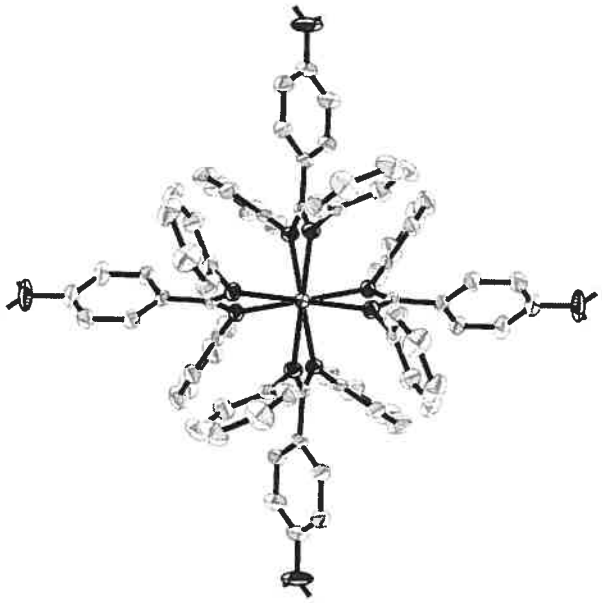

Figure 5.24. X-ray crystal structure of **V-10** with thermal ellipsoids at 50 % probability. Protons and solvent molecules have been omitted for clarity.

Single crystals suitable for structure determination by X-ray diffraction were grown upon standing of a DMSO solution of the tetra-amino complex. Like the tetra-carboxylate complex (Figure 5.13), this method was the only one capable of yielding crystalline material. This compound was found to crystallize in P_4/n space, and one finds both enantiomers within the unit cell (see Figure 5.24). Like the tetra-carboxylate structure, a large portion of unit cell volume is attributable to solvent, in this case ~ 22 %. However, unlike the tetra-carboxylate structure, this solvent was disordered enough to prompt the use of the 'squeeze' function in PLATON to account for this missing electronic density in place of their actual refinement. Concerning the molecule itself, the structural parameters again reflect those of the tetra-bromo complexes, with again an absence of axial ligation.

As an initial foray into the feasibility of using these tetra-amidinate complexes as robust templates, the tetra-amino complex is the most straightforward owing to its symmetry. It is also a good assessment of the efficiency for the method of connection chosen, as this must be performed four-fold. The chosen means of creating connectivity here is amide bond formation, the advantages of which have been mentioned previously. However, an equally important appeal to using this mode of connection is the ease with which carboxylate functionality may be incorporated into polypyridyl ligands, as evidenced by their prolific occurrence in current literature.[36] This makes readily available a wide range of potentially interesting photoactive subunits.

It was desired to connect, in this manner, both a tpy ligand and its corresponding ruthenium(II) complex to determine the general applicability of the protocol. Chlorination of 4-carboxytpy (Scheme 5.9) followed by addition of the tetra-amino complex in the presence of a strong base led to a reaction mixture that could be purified without chromatography in a reasonable yield. The ^{1}H NMR spectrum of the tetra-tpy complex is shown in Figure 5.25 (below). It is essentially the summation of the spectra for the individual components, with the exception of a characteristic N-H resonance from the amide functionality at 10.75 ppm. Interestingly, single crystals could be grown from slow evaporation from a mixture of chloroform and methanol but did not diffract sufficiently for satisfactory structural refinement.

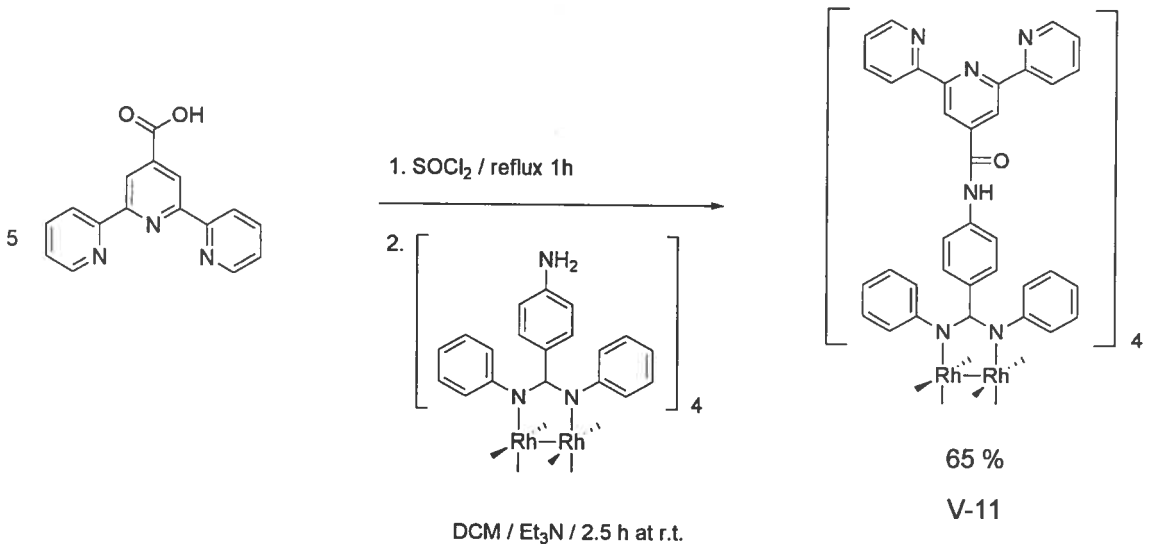

Scheme 5. 9. Synthesis of Rh_2(*N,N'*-diphenyl-4-amidotpy-benzamidinate)$_4$ **(V-11)**.

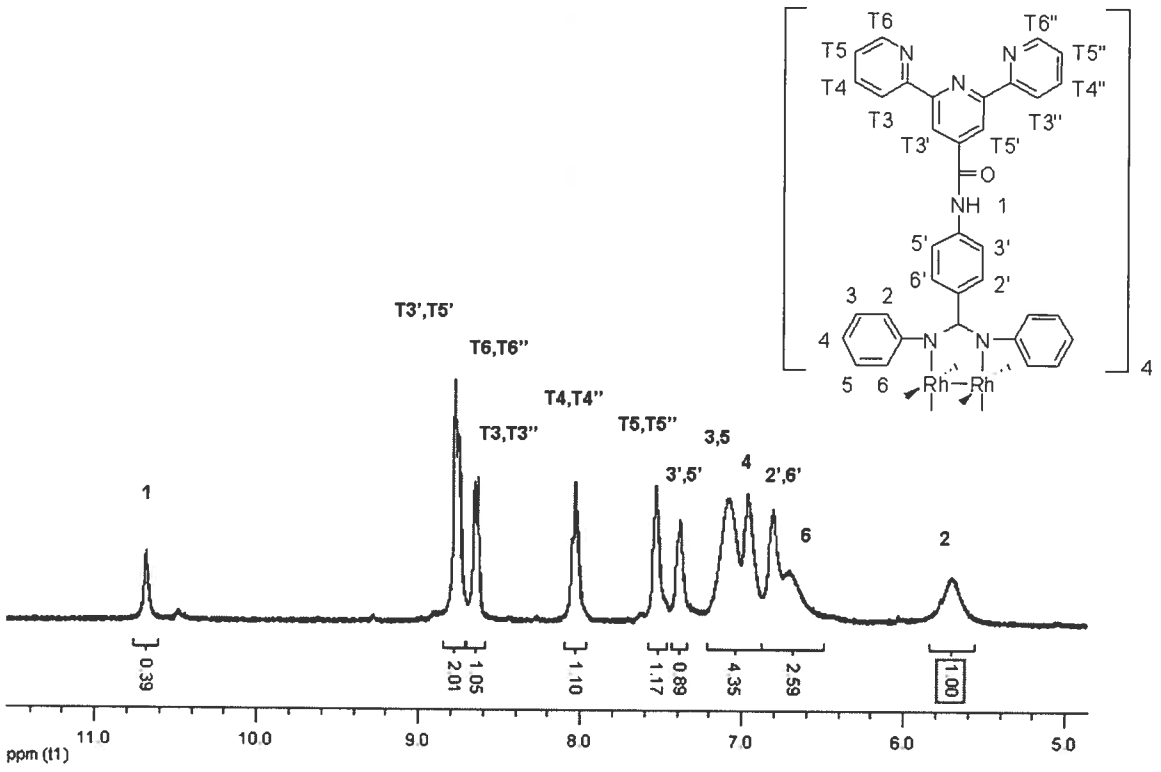

Figure 5.25. ^{1}H NMR of **V-11** in d_6-DMSO.

With 4'-carboxytpy in hand, the heteroleptic complex [(4'-carboxytpy)(4'-tolyltpy)Ru]$(PF_6)_2$ was synthesized (Scheme 5.10) owing to the facile and expedient synthesis of 4'-tolyltpy and its corresponding ruthenium(III) trichloride complex. Although similar complexes have been prepared, this is the first known report for this particular compound. The ^{1}H NMR spectrum is shown in Figure 5.26.

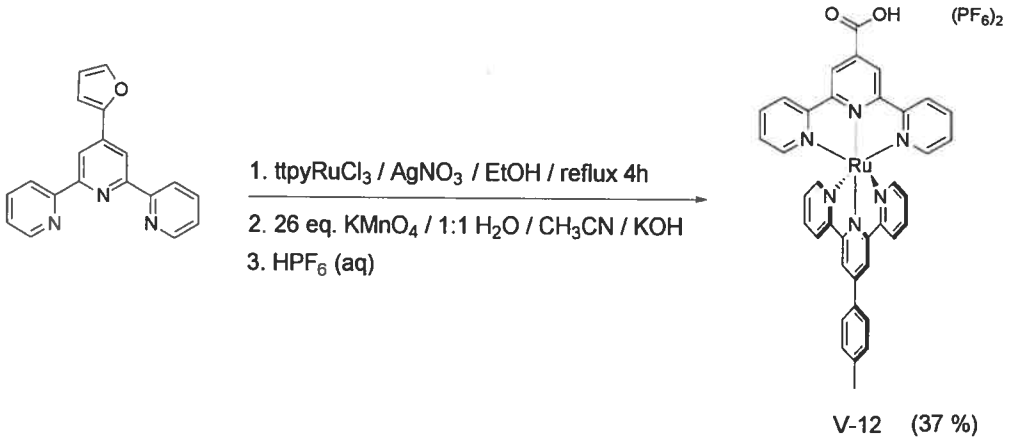

Scheme 5.10. Synthesis of [(4'-carboxytpy)(4'-tolyltpy)Ru]$(PF_6)_2$ (**V-12**). Yield obtained after column chromatography.

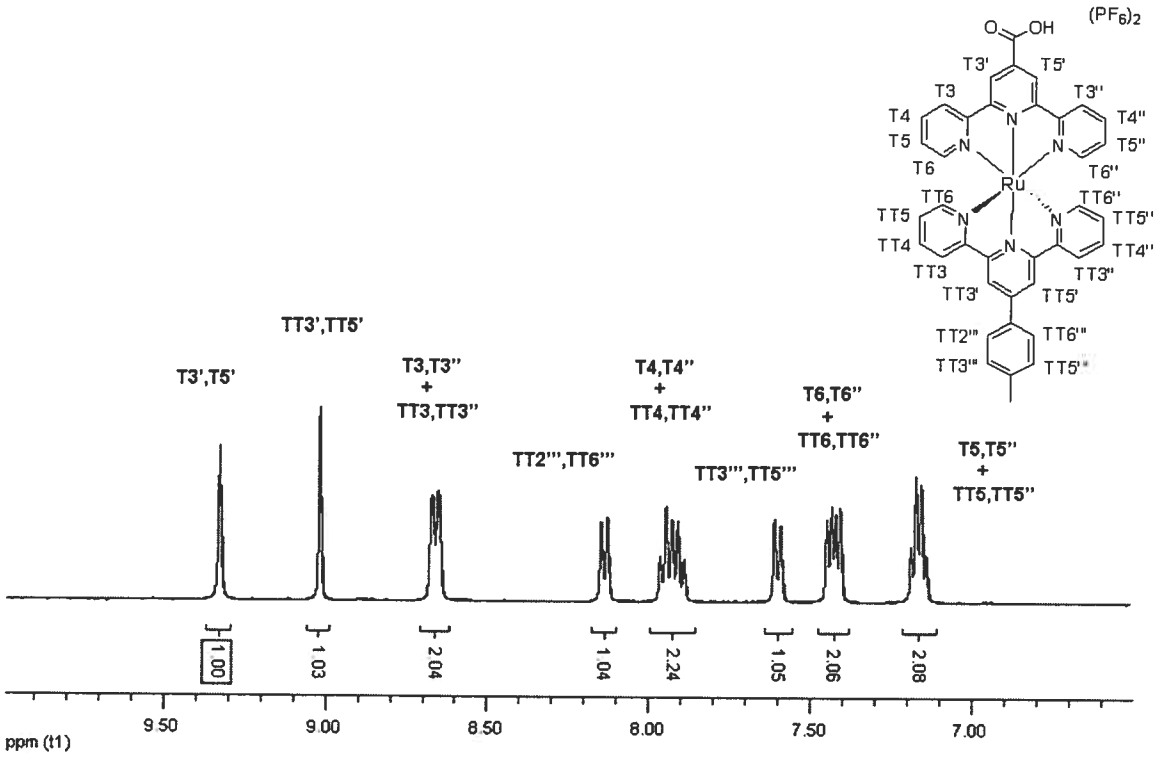

Figure 5.26. ^{1}H NMR of **V-12** in CD_3CN. Methyl resonance occurs at 2.57 ppm (not shown).

With this complex in hand, a similar protocol to that used for appendage of 4'-carboxytpy was employed (Scheme 5.11) with the exception that it was necessary to use acetonitrile as solvent to fully dissolve the starting materials. Chlorination of a two-fold excess of [(4'-carboxytpy)(4'-tolyltpy)Ru]$(PF_6)_2$ gave, after brief reflux with (*N,N'*-diphenyl-4-amino-benzamidinate)$_4$, a solution whose colour was markedly more intense than initially observed.

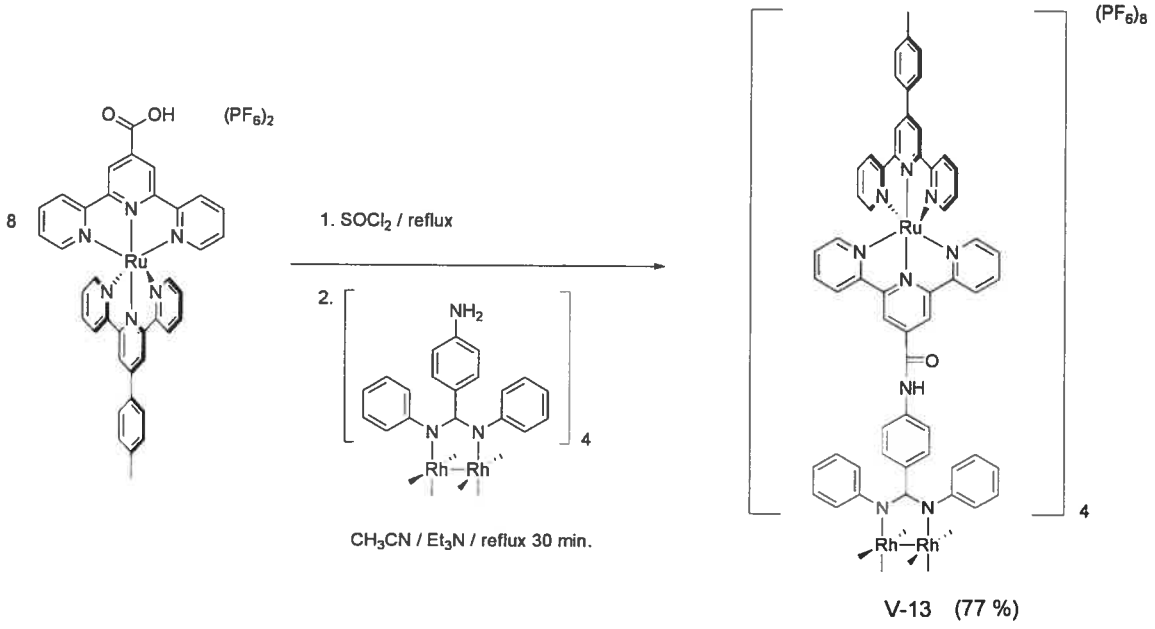

Scheme 5.11. Synthesis of Rh_2(*N,N'*-diphenyl-{(4'-amidotpy)(4'-tolyltpy)Ru]$(PF_6)_2$}-benzamidinate)$_4$ **(V-13).** Yield obtained after column chromatography.

Chromatographic separation of this reaction mixture on silica substrate gave an intense band that moved reasonably well (R_f = 0.32, using 7:1 CH_3CN / $KNO_{3(sat,\ aq)}$). This material, following anion exchange using NH_4PF_6, was shown by ^{1}H NMR (Figure 5.27) and ESI-MS to be the desired tetra-amido product. The features of this spectrum are strikingly similar to those for the parent complex in Figure 5.26, with the exception that the multiplets stemming from overlapped resonances of protons T6,T6'' / TT6, TT6'' and T5,T5'' / TT5,TT5'' are resolved into their individual components, along with the appearance of a characteristic N-H resonance from the amide moiety at 9.5 ppm. Evidence for the tetra-amidinate core is provided by the characteristically broad resonances for the 6 and 2 protons of the N-bound amidinate protons (refer to Figures 5.5

and 5.6) at 6.1 ppm and 5.6 ppm, respectively. Interestingly, the resonances of the 3, 5, and 4 protons of the N-bound phenyl and the 2',6' / 3',5' protons of the central phenyl of the amidinate ligand are not resolved but are likely severely broadened. Broadening is also observed, although to a lesser extent, for both the N-H amide and the T3',T5' resonances at 9.5 and 9.2 ppm, respectively, the latter of which occurs as a doublet, perhaps differentiated by the chiral nature and enantiomeric occurrence of the central dimeric unit. Such broadening may be the consequence of tumbling rates for such a large and symmetric structure in solution. An excellent frame of reference in support of this notion is the ^{1}H NMR spectrum for the tetra-amidotpy complex (Figure 5.25) for which the resonances of the tetra-amidinate core, along with the N-H amide resonance, are readily discernable and notably sharper. This could be a consequence of the smaller size of the tetra-amidotpy complex. However, it must be noted that the tetra-amidotpy complex is also charge neutral compared to the highly charged (8+) tetra-Ru(II) complex here. To clarify this matter, variable temperature ^{1}H NMR should be helpful as it was for elucidating the solution dynamics of Rh_2(*N,N*-diphenyl-4-bromobenzamidinate)$_4$ and should be included in further characterization of this compound.

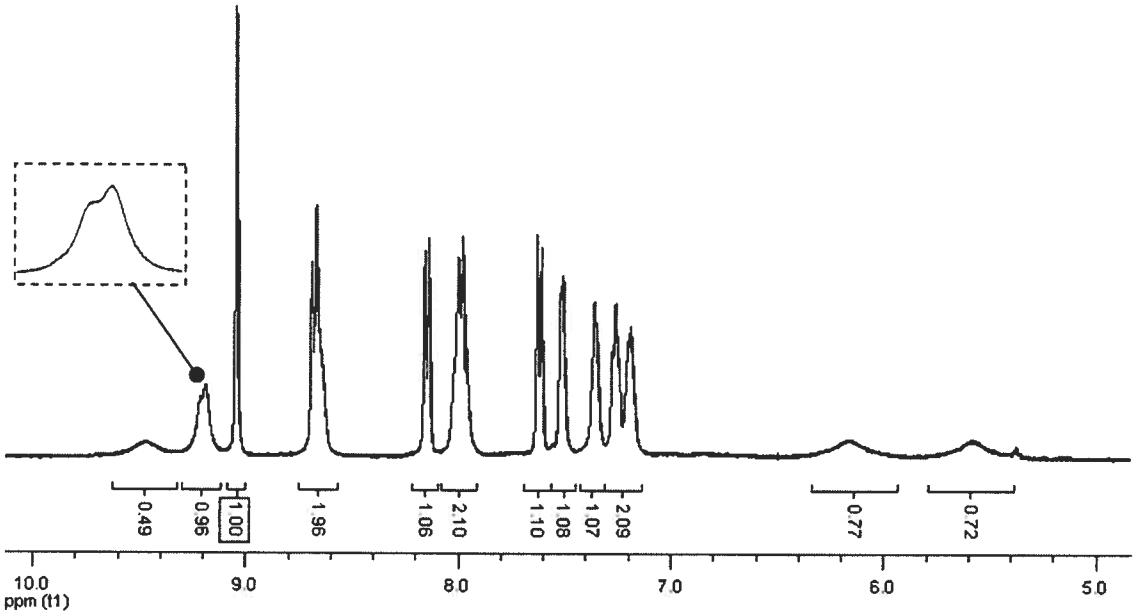

Figure 5.27. ^{1}H NMR of **V-13** in CD_3CN. Methyl resonance occurs at 2.57 ppm (not shown).

The major motivation for pursuing such tetra-amidinate complexes was to create robust templates bearing suitable functionality so as to efficiently connect polypyridyl-based photoactive unit(s) in light of problems associated with the kinetic lability of carboxylate-derived $Ru(tpy)_2^{2+}$ units appended to the dimetallic core (Chapter 2). To this end, as anticipated, the complex Rh_2(*N,N'*-diphenyl-{(4'-amidotpy)(4'-tolyltpy)Ru]$(PF_6)_2$}-benzamidinate)$_4$ is indefinitely stable in the presence of competing donors, such as other carboxylates and in neat pyridine itself. Lastly, this compound could be crystallized by vapour diffusion of isopropyl ether into an acetonitrile solution to give apparently good quality crystals which, as with the tetra-amidotpy complex, did not diffract sufficiently. This may be due in part, perhaps, to poor packing in the solid state owing to the large, spherical nature of these compounds and the presence of many counter-anions.

Further illustration of the amenability of these complexes toward synthetic manipulation is provided by the alkynylation of Rh_2(*N,N'*-diphenyl-4-diphenylketimine-benzamidinate)$_3$(*N,N*-diphenyl-4-bromobenzamidinate), according to Scheme 5.12 below. The installation of terminal alkynyl functionality into these tetra-amidinate complexes expands upon the library of reactive tetra-amidinate building-blocks created thus far, making available a wide range of coupling partners.

The most popular method for creating $C(sp^2)$-C(sp) bonds has been the Sonagashira protocol whereby a copper (I) co-catalyst is used in conjunction with a palladium source in the presence of a suitable base. Much modification upon the original coupling conditions have been made toward improving the scope and efficiency of the reaction so as to include unactivated and sterically demanding substrates and to suppress deleterious dimerization and oligomerization processes.[37] Among the family of mixed bromo / diphenyl ketimine substrates here, the mono-bromo complex Rh_2(*N,N'*-diphenyl-4-diphenylketimine-benzamidinate)$_3$(*N,N*-diphenyl-4-bromobenzamidinate) is naturally preferred toward reaction optimization.

Initial coupling attempts with trimethylsilyl acetylene were performed according to the most common protocol encountered in the literature, whereby the substrate was heated to reflux in neat, degassed *N,N*-diisopropyl ethylamine in the presence of $PdCl_2(PPh_3)_2$ and CuI (Scheme 5.12, a). This protocol, however, produced only small

quantities of the desired product after column chromatography along with a large amount of intractable material.

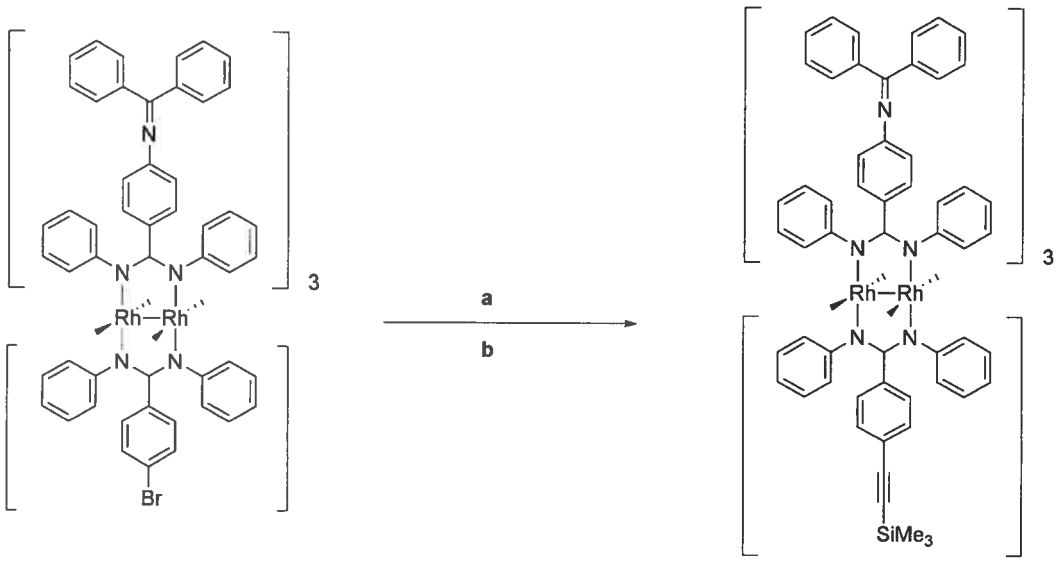

V-14

10 % [a] 67 % [b]

Scheme 5.12. Synthesis of Rh_2(*N,N'*-diphenyl-4-diphenylketimine-benzamidinate)$_3$(*N,N*-diphenyl-4-trimethylsilylethynyl-benzamidinate) (**V-14**). (a) 10 mol % $PdCl_2(PPh_3)_2$, 10 mol % CuI, 20 mol % PPh_3, 1.5 eq Me_3Si-CCH, 18 h at 70°C under argon atmosphere. (b) 5 mol % $Pd_2(dba)_3$, 16 mol % S-PHOS, 3 eq Cs_2CO_3, 1.5 eq Me_3Si-CCH, THF (degassed), 120°C, 1 h. Yield based on pure material recovered from column chromatography.

In search of efficient catalytic systems for the coupling of activated and de-activated aryl chlorides with terminal alkynes, Buchwald and co-workers explored the use of bulky, electron-rich phosphines closely related to S-PHOS.[37c] Surprisingly, it was found that the presence of a copper (I) co-catalyst suppressed the cross-coupling reaction and invariantly led to consumption of the added terminal alkyne and recovery of unreacted chloro-substrate. When the copper (I) source was omitted, the reaction progressed in modest to high yield within 1-3 h in acetonitrile at elevated temperature (70-95°C) using cesium carbonate as base. These conditions comprise a simple method for such coupling reactions, the scope of which has been further extended by more recent

reports from Buchwald,[37d] and others, who have made slight modifications to address the needs of particularly demanding substrates.[37e] Similarly, we too have found that copper-free conditions employing $Pd_2(dba)_3$ / S-PHOS in THF at elevated temperatures were required to couple Rh_2(*N,N'*-diphenyl-4-diphenylketimine-benzamidinate)$_3$(*N,N*-diphenyl-4-trimethylsilylacetylenyl-benzamidinate) in acceptable yield (Scheme 5.12, b).

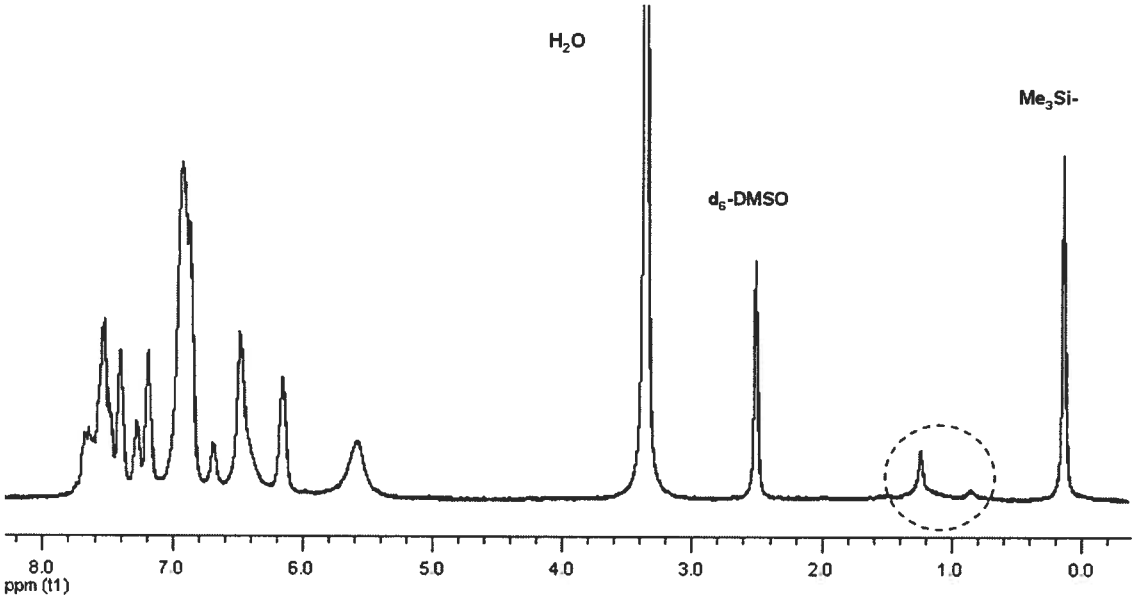

Figure 5.28. ^{1}H NMR of **V-14** in d_6-DMSO. Circled region represents resonances from S-PHOS (or related) impurity.

The ^{1}H NMR depicted above in Figure 5.28 of material recovered from column chromatography is remarkably similar to that for Rh_2(*N,N'*-diphenyl-4-diphenylketimine-benzamidinate)$_3$(*N,N*-diphenyl-4-bromobenzamidinate) (refer to Figure 5.15). However, it is readily distinguished by a strong singlet resonance at 0.14 ppm attributable to the Me_3Si- moiety. Less noticeable is that the small doublet at 7.1 ppm arising from the 3b', 5b' phenyl protons for the phenyl ring bearing the bromo-substituent in the parent complex, i.e. Rh_2(*N,N'*-diphenyl-4-diphenylketimine-benzamidinate)$_3$(*N,N*-diphenyl-4-bromobenzamidinate) (see Figure 5.15), has been displaced enough that it is no longer resolved upon installation of the trimethylsilyl acetylene group. However, the 2b', 6b' protons of the same ring remain resolved, being displaced upfield by ~ 0.1 ppm upon acetylation. Lastly, the circled region depicted in the spectra likely arises from contamination of the S-PHOS ligand (or a decomposition product thereof). This was

found to be a problem in general for compounds which move relatively slowly on silica ($R_f < \sim 0.4$) and can only be eliminated upon crystallization of the compound. Notably, column chromatography sufficed to purify the mono-aminated complex Rh_2(*N,N'*-diphenyl-4-diphenylketimine-benzamidinate)(*N,N*-diphenyl-4-bromobenzamidinate)$_3$ ($R_f = 0.47$, refer to Figure 5.18). In this case, the enhanced solubility afforded by the trimethylsilyl acetylene group made crystallization inefficient. However, such impurity is inconsequential considering that subsequent steps will either use S-PHOS or eliminate it completely through work-up and crystallization.

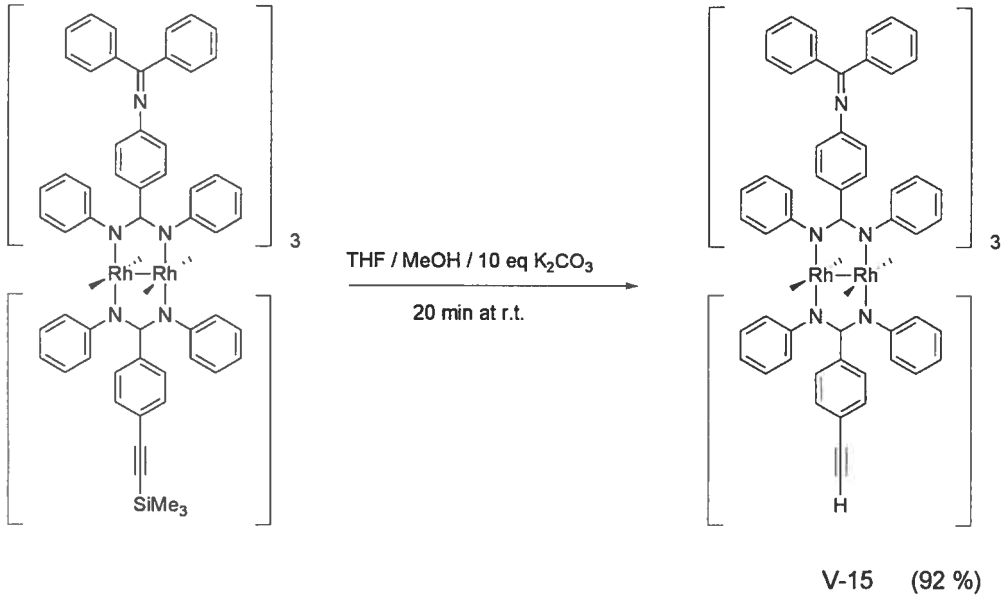

V-15 (92 %)

Scheme 5.13. Removal of trimethylsilyl to give Rh_2(*N,N'*-diphenyl-4-diphenylketimine-benzamidinate)$_3$(*N,N'*-diphenyl-4-ethynylbenzamidinate) (**V-15**).

Removal of the trimethylsilyl group could be performed in excellent yield using a methanolic solution of potassium carbonate (Scheme 5.13). Conversion proceeds cleanly, although the persistence of small amounts of S-PHOS can be discerned from the ^{1}H NMR spectra in Figure 5.29. More importantly, the strong singlet resonance characteristic of the trimethylsilyl group is no longer present while a resonance at 4.1 ppm attributable to the naked acetylene moiety is now evident. For both the trimethylsilyl and naked acetylene analogues, IR spectroscopy showed characteristic frequencies for the –CC- stretching mode corresponding to 2156 cm^{-1} and 2359 cm^{-1}, respectively.

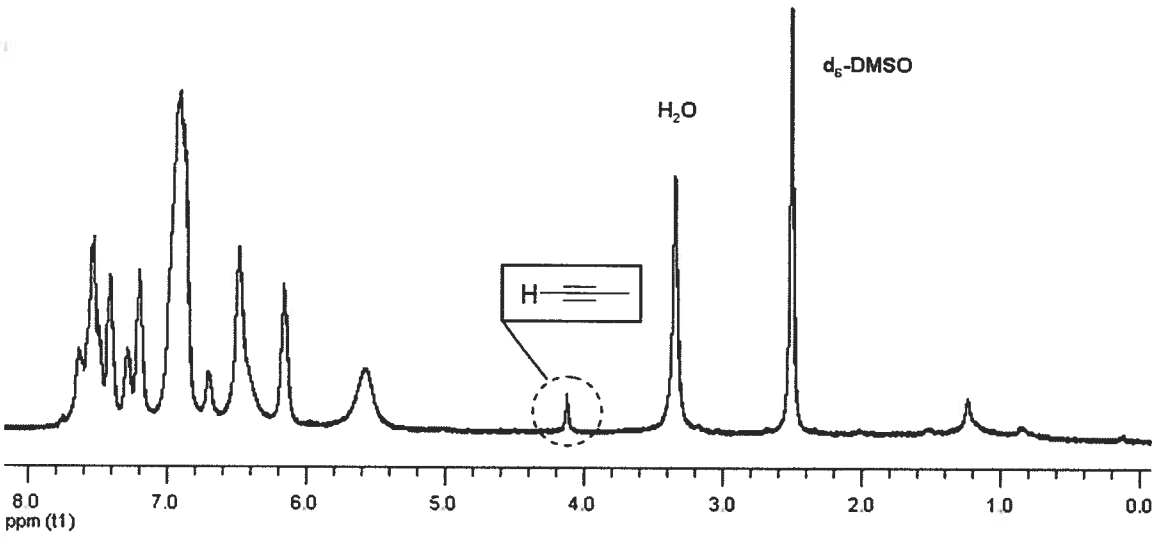

Figure 5.29. ^{1}H NMR of **V-15** in d_6-DMSO.

5.4 Electronic Absorption

The electronic configuration of the metal-based molecular orbitals in Rh_2^{4+} paddlewheel-type complexes depends on the nature of both the axial and equatorially bound ligands. For instance, those with weakly π-donating chelates, such as sulfonates and carboxylates, in combination with weak axial σ-donors, such as water or nitriles, possess an electronic configuration of the order $\sigma^2 \pi^4 \delta^2 \delta^{*2} \pi^{*4}$.[14] However, exchanging the axial donor for strong σ-donors such as phosphines or phosphites results in the ordering $\pi^4 \delta^2 \pi^{*4} \delta^{*2} \sigma^2$, where the HOMO is of σ-Rh-P character.[38] Conversely, relatively stronger π-donating chelates such as amidates and amidinates with either weak or absent axial σ-donors possess an electronic configuration of the order $\sigma^2 \pi^4 \delta^2 \pi^{*4} \delta^{*2}$.[39] This bears resemblance to that for complexes of weakly π-donating chelates (e.g. $Rh_2(O_2CCH_3)_4(CH_3CN)_2$), but differs significantly in two respects. If we compare tetra-amidinate complexes of the form $Rh_2(RN\text{-}CR'\text{-}NR)_4$ with tetra-carboxylate complexes of the form $Rh_2(O_2CR)_4$, both with weak axial donors, replacement of the oxygen atoms with eight nitrogen donors effectively increases the one-electron metal-based orbital energies by ~ 2 eV.[39c] However, this increase is not proportionate for all orbitals, as the

Rh_2-δ^* based orbital is significantly mixed with pπ-N orbitals of the chelate, placing it significantly higher in energy than that of the Rh_2-π^* orbital. Interestingly, no cases of such tetra-amidinate complexes bearing strong axial σ-donors have been reported to date. This may be due to the fact that most such complexes bear aryl groups on the nitrogen atoms, which impose steric encumbrance to axial ligation. Moreover, it has been suggested that the higher energy of the metal-based orbitals for tetra-amidinate complexes relative to those of more weakly donating chelates may lead to an energetic mismatch between Rh_2-σ/σ^* orbitals and the lone-pairs of the axial donor in general.[39c] This stands in contrast to dirhodium(II,II) complexes bearing more weakly donating chelates such as carboxylates, which show a high affinity toward axial ligation.[40]

The visible spectra of dirhodium(II,II) tetracarboxylates contain two bands attributed to a higher energy π (Rh-O) $\rightarrow$ σ^* (Rh-O) transition (~ 440 nm) and a lower energy π^* (Rh_2) $\rightarrow$ σ^* (Rh_2) transition (~ 500-600 nm), the latter of which varies according to the donor capacity of the solvent, reflecting the metal-metal σ-bond component of the transition.[41] However, no precise assignment of the bands observed in the electronic spectra of either tetra-amidato or tetra-amidinato dirhodium(II,II) complexes has been made despite numerous theoretical and experimental investigations into their electronic structure. Generally, where comment to this end has been made, those bands in the visible whose energy varies directly with the σ-donor capacity of the solvent have been implicated to possess a strong σ^* (Rh_2) component. Kadish and co-workers have made this analogy for several tetra-amidate dirhodium(II,II) complexes, attributing a general blue-shift of this solvent dependent band and a more complex visible spectra to, respectively, the increasing basicity and asymmetry of the amide ligands compared to those of carboxylates.[42] Extrapolation to tetra-amidinate analogues is tempting and one may predict a further blue-shift for related bands along with relatively simplified visible spectra, where symmetric amidinates are concerned. However, Kadish and co-workers have noted a visible spectrum for Rh_2(*N,N'*-diphenylbenzamidinate)$_4$ that contains two high-intensity bands at 518 nm ($\varepsilon = 6.1 \times 10^3$ $M^{-1}cm^{-1}$) and 847 nm ($\varepsilon = 2.9 \times 10^3$ $M^{-1}cm^{-1}$), a weak band at 590 nm ($\varepsilon = 3.0 \times 10^2$ $M^{-1}cm^{-1}$), and a shoulder at 440 nm.[16] Not surprisingly, these bands were invariant in solvents such as dichloromethane, acetone, tetrahydrofuran, dimethyl sulfoxide, and pyridine, owing to restricted interaction

with the Rh-Rh axis imposed by the four *N*-phenyl rings. However, in solvents such as acetonitrile and benzonitrile, the intensity of the bands at 518 and 847 nm were found to diminish while a new, broad band of equal intensity appeared at 547 nm. Moreover, these bands were found to disappear completely in the presence of an excess of CN^-. These observations clearly indicate a significant axial interaction with nitriles and suggest σ^* (Rh_2) contribution to the bands observed at 518 nm and 847 nm. When this complex was oxidized to give the remarkably stable mixed-valent complex [Rh_2(*N,N'*-diphenylbenzamidinate)$_4$]Cl, the visible spectrum (in toluene) was characterized by similar overlapping bands at 520 nm ($\varepsilon = 2.5 \times 10^3$ $M^{-1}cm^{-1}$) and 445 nm ($\varepsilon = 2.4 \times 10^3$ $M^{-1}cm^{-1}$), but with a shoulder at 650 nm and a broad, relatively intense near-IR band at 1030 nm ($\varepsilon = 3.6 \times 10^3$ $M^{-1}cm^{-1}$) with a shoulder at 830 nm. The intensity and energy of this near-IR band was found to vary with the nature of the counter-anion, while axial coordination of CO or various nitriles gives rise to two near-IR bands. Although not explicitly stated, it is very likely that this band is attributable to a LMCT transition involving the nitrogen non-bonding π MO's and the partially-filled Rh_2-based HOMO of δ^* symmetry, as this has been noted previously for Rh_2^{5+} complexes based on related nitrogen chelates.[43]

The dirhodium(II,II) tetra-amidinate complexes prepared here (Table 5.1) exhibit a nearly identical spectral profile in their respective visible spectra as that discussed above for Rh_2(*N,N'*-diphenylbenzamidinate)$_4$, with the exception that we also note a weak band at ~ 750 nm. Within this series, the bands do not vary significantly with the changing functionality of the amidine ligand, with the exception of the tetra-amino derivative for which the higher intensity bands centered at 862 nm and 506 nm have been displaced by ~ 20 nm to lower and higher energy, respectively, relative to that for the tetra-bromo complex. Presumably this is a function of the relatively electron releasing amino group.

The spectral data in Table 5.1 was recorded for freshly prepared and crystallized material, with one exception. The tetra-dibromo analogue, although crystalline and initially very pure, sat in a vial for over 8 months under an aerobic atmosphere. The consequence of this is seen in the near-IR region of the spectra, shown below in Figure 5.30, where a broad band at 1080 nm ($\varepsilon = 1150$ $M^{-1}cm^{-1}$) has appeared. Considering the

previous discussion, it is very likely that this is due to a mixed-valent Rh_2^{5+} species. In fact, since the molar absorptivities for the bands at 533 nm and 438 nm are very similar to those of the aforementioned [Rh_2(*N,N'*-diphenylbenzamidinate)$_4$]Cl, it is reasonable to conclude that about one-third of the sample has been oxidized during this time by comparison of the molar absorptivities for their mutual near-IR bands. That this occurs even in the solid-state is testament to the stability of this mixed-valent species.

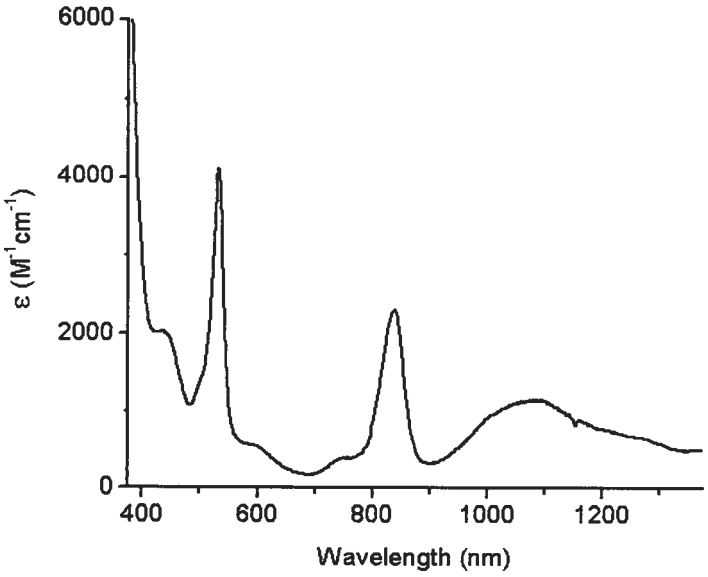

Figure 5.30. Absorption spectrum for Rh_2(*N,N*-diphenyl-3,5-dibromobenzamidinate)$_4$ in air-equilibrated chloroform.

Table 5.1. Electronic absorption data (general).[a]

Compound	λ_{max} (nm), ε ($M^{-1}cm^{-1}$)				
$Rh_2(L\text{-}Br)_4$	846 (2720)	753_{sh} (320)	596_{sh} (432)	523 (4720)	430_{sh} (1991)
$Rh_2(L\text{-}Br_2)_4$	838 (2260)	754_{sh} (200)	589_{sh} (320)	533 (3965)	438_{sh} (1696)
$Rh_2(L\text{-}CO_2H)_4$ [b]	832 (1150)	-	-	548 (1990)	440_{sh} (1350)
$Rh_2(L\text{-}NH_2)_4$ [b]	862 (2160)	785_{sh} (470)	-	506 (3180)	-
$Rh_2(L\text{-}Br)_3(L_1)$	847 (2870)	761_{sh} (370)	587_{sh} (420)	525 (4670)	435_{sh} (2190)
cis-$Rh_2(L\text{-}Br)_2(L_1)_2$	849 (3130)	765_{sh} (390	588_{sh} (450)	526 (4540)	-
trans-$Rh_2(L\text{-}Br)_2(L_1)_2$	849 (2960)	765_{sh} (410)	588_{sh} (460)	526 (4290)	-
$Rh_2(L\text{-}Br)(L_1)_3$	851 (2910)	765_{sh} (460)	599_{sh} (410)	527 (3880)	377_{sh} (17200)
$Rh_2(L_1)_4$	853 (2680)	760_{sh} (460)	600_{sh} (380)	529 (3060)	377_{sh} (16900)
$Rh_2(L_1)_3(L\text{-}C_2SiMe_3)$	851 (1800)	765_{sh} (280)	598_{sh} (280)	534 (2440)	376_{sh} (13300)
$Rh_2(L_1)_3(L\text{-}C_2H)$	851 (2270)	764_{sh} (550)	593_{sh} (450)	533 (2820)	376_{sh} (11100)
$Rh_2(L\text{-}tpy)_4$	845 (1700)	759 (1960)	573 (3720)	530_{sh} (3100)	-

a) All spectra recorded in air-equilibrated $CHCl_3$, unless otherwise indicated.

b) Recorded in DMSO.

Key:

L = 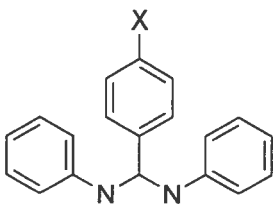

L_1 = 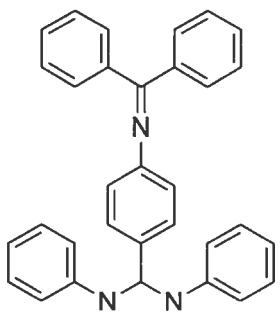

5.5 Electrochemistry

The progression from carboxylate-based chelates to nitrogen-based analogues has introduced a second reversible Rh_2-based oxidation not observed with dirhodium(II,II) tetracarboxylates.[42] This is also shared by amidinato analogues, but there is an added bonus if the amidinate ligand bears *N*-aryl groups in that a (quasi)reversible reduction ($Rh_2^{4+/3+}$) is made accessible. The cationic mixed-valent Rh_2^{5+} species is remarkably stable,[44] being separated and purified by column chromatography after initial bulk electrolysis while the Rh_2^{3+} species is exceptionally reactive to molecular oxygen.[9] All redox processes have been determined to be metal-centered on the basis of EPR measurements for both the cationic (Rh_2^{5+}) and anionic (Rh_2^{3+}) radical complexes.[9,16,44] A representative voltammogram is depicted below in Figure 5.31 for the tetra-diphenylketimine analogue.

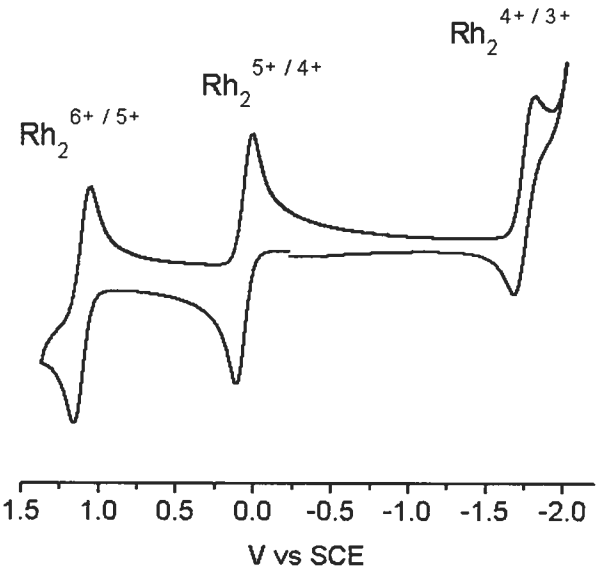

Figure 5.31. Cyclic voltammogram of Rh_2(*N,N'*-diphenyl-4-diphenylketimine-benzamidinate)$_4$ in 0.1 M $TBAPF_6$ DCM solution at 100 mVs^{-1}.

The origin of the $Rh_2^{4+/3+}$ couple is thought to be due to the steric encumbrance afforded by the *N*-aryl groups of the amidinate ligand and its effective capacity to frustrate axial coordination. The σ^* (Rh_2) orbital becomes occupied to form the SOMO upon reduction to the Rh_2^{3+} species. However, this orbital is also sensitive to axial

ligation, becoming destabilized as a direct function of the σ-donor capacity of the ligand, and so exclusion of axial coordination serves to facilitate reduction. These redox processes are a trait of both *N,N'*-diaryl formamidinate and *N,N'*-diaryl benzamidinate dirhodium(II,II) complexes, the latter providing more *N*-phenyl steric encumbrance owing to accommodation of the central phenyl ring. As a reflection of the thermodynamic stability of the mixed-valent Rh_2^{5+} species, Piraino and co-workers determined its comproportionation constant (K_c) to be 5 x 10^{13} for the case of Rh_2(*N,N'*-di-*p*-tolylformamidinate)$_4$ and 1 x 10^{17} for Rh_2(*N,N'*-diphenylbenzamidinate)$_4$,[15] making it a completely delocalized species ($Rh^{2.5+}$-$Rh^{2.5+}$) according to the Robin and Day classification in both cases,[45] in good agreement with EPR measurements for their respective cationic radical complexes. Notably, these results indicate an added stabilization effect afforded by the central aromatic ring of the benzamidinate ligand.

The redox potentials of the Rh_2-based processes of tetra-*N,N'*-diaryl amidinates have been shown to be influenced through substitution of the *N*-aryl groups [46] and / or by axial coordination.[15, 16, 44] Here, examination of the Rh_2-based redox couples in Table 5.2 shows that this may also occur through substitution of the central aromatic ring of the benzamidinate ligand. This is best exemplified by comparing the oxidation and reduction potentials of the tetra-bromo, tetra-dibromo, and tetra-amino analogues. The first oxidation and reduction potentials of the tetra-bromo complex shift anodically by 160 mV and 130 mV, respectively, upon incorporation of a second bromine, the second oxidation potential lying outside the THF solvent window in both cases. This reflects an electron withdrawing effect of the bromine atoms. Despite axial crowding in such complexes, Kadish and co-workers found that the first and second oxidation potentials of Rh_2(*N,N'*-diphenylbenzamidinate)$_4$ are shifted cathodically in the presence of donors such as CH_3CN, CN^-, SCN^-, and Cl^- relative to that recorded in CH_2Cl_2, indicating a stabilization of the Rh_2(*N,N'*-diphenylbenzamidinate)$_4^+$ intermediate, while the reduction process was displaced cathodically, reflecting a destabilization of the σ^* (Rh_2) MO.[16] As such, inference of any electronic effect from the amino substituent of Rh_2(*N,N*-diphenyl-4-aminobenzamidinate)$_4$ is best made by comparison to data recorded for Rh_2(*N,N'*-diphenylbenzamidinate)$_4$ in the same solvent (CH_3CN, see Table 5.2). A strong cathodic displacement of 180 mV, 150 mV, and 120 mV for the first and second oxidation and

reduction processes, respectively, clearly indicates a strong electron releasing effect of the amino group. Likewise, the metal-based redox processes show a gradual but consistent cathodic shift as the number of diphenylketimine groups increases from one to four along the mixed bromo-diphenylketimine species. This is expected as one progressively replaces the electron withdrawing bromo-substituents, but the Rh_2-based potentials for the tetra-diphenylketimine complex (Table 5.2) are cathodically displaced by ~ 150 mV relative to those of Rh_2(*N,N'*-diphenylbenzamidinate)$_4$ (1.24 V ($Rh_2^{6+/5+}$), 0.23 V ($Rh_2^{5+/4+}$), -1.58 V ($Rh_2^{4+/3+}$) vs SCE) for the same solvent (DCM),[9] which suggests an electron releasing effect of these diphenylketimine groups.

Lastly, it is interesting to note that the current response of the $Rh_2^{4+/3+}$ couple, at times, lags behind that of the two oxidation processes in the cyclic voltammogram (Figure 5.31). Ren and co-workers have noted a similar occurrence for a series of dirhodium(II,II) tetra-formamidinate complexes, although for the second Rh_2-based oxidation process (DCM, 100 mVs^{-1}).[46] This was found to be an artifact of using a platinum working electrode, as glassy carbon gave an approximate ratio of 1:1:1 as expected for three (quasi)reversible one-electron processes. Here, however, it was found that the use of a glassy-carbon working electrode resulted in a chemically irreversible $Rh_2^{4+/3+}$ couple exhibiting a severely diminished, or non-existent, return oxidation wave at scan rates ranging from 0.05 to 3 Vs^{-1} in dichloromethane. Such chemical irreversibility has been observed for Rh_2(*N,N'*-di-p-tolylformamidinate)$_4$ (Pt working electrode) and has been attributed to, upon generation of the reduced Rh_2^{3+} species, an irreversible reduction of the halogenated solvent that becomes chemically reversible at higher scan rates (> 2 Vs^{-1}).[15, 44] Irreversibility of the $Rh_2^{4+/3+}$ couple is also generally found for dirhodium(II,II) (tetra) *N,N'*-diaryl formamidinates in the presence of axial donors. [44] This stands in contrast to dirhodium(II,II) (tetra) *N,N'*-diaryl benzamidinates for which reduction is consistently reversible. For now, no satisfactory explanation can be given, although interestingly the current responses are much more agreeable in the square-wave voltammograms and when acetonitrile is used as solvent for the cyclic voltammogram, such as for Rh_2(*N,N'*-diphenyl-4-amino-benzamidinate)$_4$ where the current ratios are almost exactly 1:1:1 for the $Rh_2^{6+/5+}$ / $Rh_2^{5+/4+}$ / $Rh_2^{4+/3+}$ redox couples, respectively.

Table 5.2. Electrochemical data (general).

Compound	Potential [V] vs SCE, ΔE_p (mV) [a]		
	$Rh_2^{6+/5+}$	$Rh_2^{5+/4+}$	$Rh_2^{4+/3+}$
$Rh_2(L\text{-}Br)_4$ [b]	-	0.30 (110)	-1.57 (140)
$Rh_2(L\text{-}Br_2)_4$ [b]	-	0.46 (160)	-1.44 (190)
$Rh_2(L\text{-}CO_2H)_4$ [c]	-	0.29 (95)	-1.66 (irr)
$Rh_2(L\text{-}NH_2)_4$ [d]	0.90 (93)	-0.10 (83)	-1.64 (80)
$Rh_2(L\text{-}Br)_3(L_1)$	1.21 (94)	0.19 (92)	-1.64 (110)
cis-$Rh_2(L\text{-}Br)_2(L_1)_2$	1.18 (88)	0.15 (74)	-1.66 (110)
trans-$Rh_2(L\text{-}Br)_2(L_1)_2$	1.18 (80)	0.15 (74)	-1.66 (100)
$Rh_2(L\text{-}Br)(L_1)_3$	1.14 (79)	0.11 (78)	-1.68 (90)
$Rh_2(L_1)_4$	1.10 (88)	0.05 (89)	-1.76 (120)
$Rh_2(L_1)_3(L\text{-}C_2SiMe_3)$	1.13 (100)	0.09 (83)	-1.70 (120)
$Rh_2(L_1)_3(L\text{-}C_2H)$	1.15 (86)	0.10 (79)	-1.71 (100)
$Rh_2(dpb)_4$ [e]	1.08 (60)	0.05 (60)	-1.52 (90)

a) Cyclic voltammogram scan rate is 100 mV s^{-1}. $E_{1/2}$ = ½ (E_{pa} + E_{pc}), where E_{pa} and E_{pc} are the anodic and cathodic peak potential, respectively. $\Delta E_p = E_{pa} - E_{pc}$. Reported values for irreversible processes, labeled irr, are peak potentials. Potentials are corrected by internal reference to ferrocene (395 mV vs SCE). Data recorded in solutions of 0.1 M $TBAPF_6$ in DCM, unless otherwise indicated.

b) Recorded in THF, c) DMSO, d) CH_3CN. e) Ref. [9]. Recorded in CH_3CN at 50 mVs^{-1}.

Key:

L = 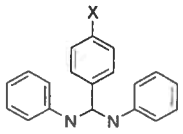

L_1 = 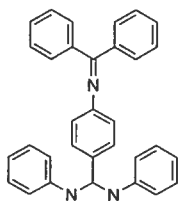

dpb = *N,N'*-diphenylbenzamidinate

5.6 Electronic Absorption and Electrochemistry of Terpyridyl Analogues

The ultimate purpose of these dirhodium(II,II) complexes is to facilitate multinuclear growth of photoactive units. As such, the electronic spectra and electrochemical behaviour of Rh_2(*N,N'*-diphenyl-4-amidotpy-benzamidinate)$_4$ and Rh_2(*N,N'*-diphenyl-4-{(4'-amidotpy)(4'-tolyltpy)Ru]$(PF_6)_2$-benzamidinate)$_4$ warrant separate discussion. All data pertaining to their electronic absorption is summarized in Table 5.3, with the exception of that for Rh_2(*N,N'*-diphenyl-4-amidotpy-benzamidinate)$_4$ which is found in Table 5.1. All electrochemical data for these complexes is provided in Table 5.4.

With regard to Rh_2(*N,N'*-diphenyl-4-amidotpy-benzamidinate)$_4$, both the electronic absorption and electrochemical data are not particularly noteworthy with the exception that the introduction of the terpyridine ligands has resulted in a chemically irreversible $Rh_2^{4+/3+}$ couple whose return oxidation wave is severely diminished relative to that of the cathodic wave.

On the other hand, Rh_2(*N,N'*-diphenyl-{(4'-amidotpy)(4'-tolyltpy)Ru]$(PF_6)_2$-benzamidinate)$_4$ displays interesting behaviour on both fronts. The absorption spectrum is shown in Figure 5.32 and, as expected, is dominated by bands associated with the Ru(II) complex. While the band maxima do not vary significantly with those of the mononuclear Ru(II) complex, there is a dramatic increase in their molar absorptivities well in excess (6-8 times) of that anticipated by simple summation of the individual components. Regardless, such large absorption supports the high nuclearity of this complex. A second notable feature is a broad, low energy band centered at 950 nm and is attributed to the central dirhodium(II,II) tetra(*N,N'*-diphenylbenzamidinate)$_4$ core. It was discussed previously (Section 5.4) that the absorption spectra of dirhodium(II,II) tetra(*N,N'*-diphenylbenzamidinate)$_4$ possesses a low energy transition centered at 847 nm in CH_2Cl_2. By comparison, the low energy band for dirhodium(II,II) tetra(*N,N'*-diphenyl-4-aminobenzamidinate)$_4$ in acetonitrile occurs at 860 nm (ε = 1260 $M^{-1}cm^{-1}$) and has a much sharper profile than the band here at 950 nm, and so they are likely not related. However, as discussed previously, the mixed-valent species [Rh_2(*N,N'*-diphenylbenzamidinate)$_4$]$^+$ possesses a broad near-IR band of LMCT origin whose

energy depends on the nature of the counter-anion. For chloride counter-anion, this band occurs at 1030 nm. Considering that the effect of PF_6^- counter-anion has not been studied in this regard, it is reasonable to attribute the low energy band of Rh_2(*N,N'*-diphenyl-{(4'-amidotpy)(4'-tolyltpy)Ru]$(PF_6)_2$-benzamidinate)$_4$ to the presence of mixed-valent Rh_2^{5+} species. Moreover, because the intensity of the band here at 950 nm (ε = 3100 $M^{-1}cm^{-1}$) agrees quite well with that for [Rh_2(*N,N'*-diphenylbenzamidinate)$_4$]Cl at 1030 nm (ε = 3600 $M^{-1}cm^{-1}$), it is likely that nearly all of this complex has been oxidized to the Rh_2^{5+} form over the course of five months that it was sitting in a vial under ambient conditions. Such oxidation has been observed previously for Rh_2(*N,N*-diphenyl-3,5-dibromobenzamidinate)$_4$ under similar conditions. Notably, the paramagnetic nature of the Rh_2^{5+} species may lend to the broadened features associated with the resonances of the dirhodium(II,II) core of the Rh_2(*N,N'*-diphenyl-{(4'-amidotpy)(4'-tolyltpy)Ru]$(PF_6)_2$-benzamidinate)$_4$ complex (Figure 5.27) in the ^{1}H NMR spectrum, although this was recorded soon after its preparation.

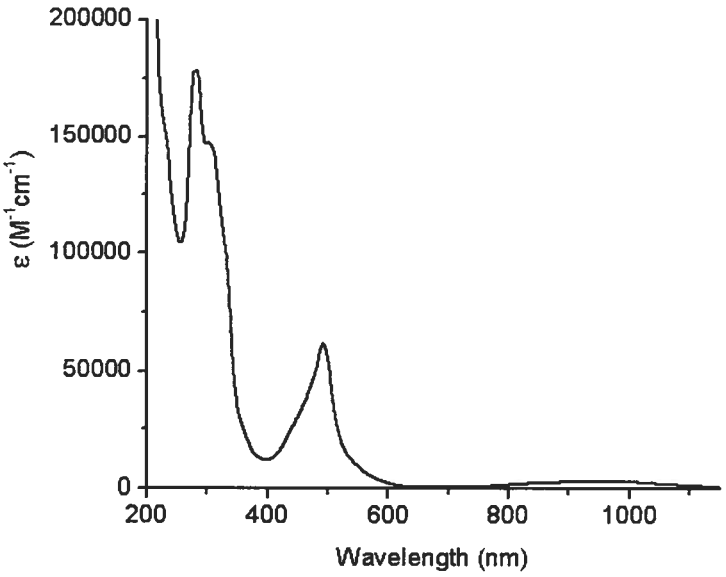

Figure 5.32. Absorption spectrum for Rh_2(*N,N'*-diphenyl-{(4'-amidotpy)(4'-tolyltpy)Ru]$(PF_6)_2$-benzamidinate)$_4$ in air-equilibrated acetonitrile.

Emission spectra were also recorded in air-equilibrated acetonitrile solutions for both the mononuclear Ru(II) complex and the multinuclear species upon excitation of the

MLCT transition, the respective traces of which are depicted below in Figure 5.33. Although this experiment is strictly qualitative in nature, it is interesting to note that the multinuclear species is still emissive, displaying a 12 nm blue shift of its emission maxima relative to the mononuclear complex. Moreover, if we use the artifact common to both traces (at ~550 nm) as a crude means of normalization, it appears that emission in this multinuclear complex has been severely diminished relative to its mononuclear subunit. Whether emission would be observed at all if not for partial or complete oxidation to the mixed-valent Rh_2^{5+} species merits investigation, as it is certainly feasible that such facile oxidation of the dirhodium(II,II) could quench the emissive state of the Ru(II) complex.

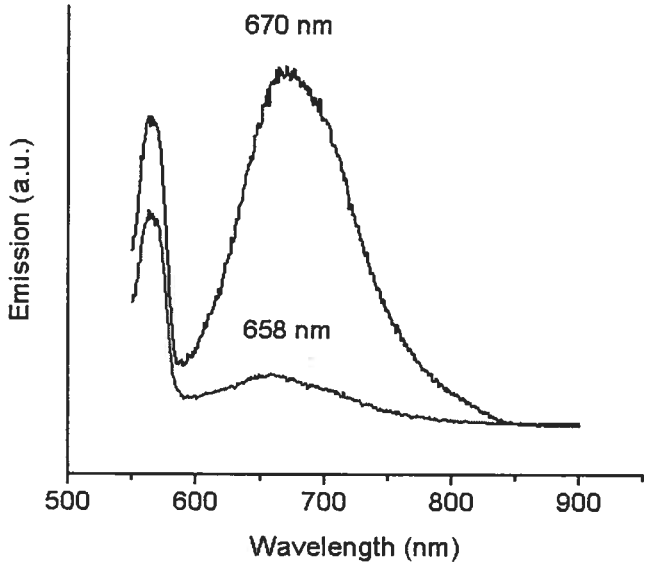

Figure 5.33. Room temperature emission spectra in air-equilibrated acetonitrile solutions of [(4'-carboxytpy)(4'-tolyltpy)Ru]$(PF_6)_2$ (black trace) and Rh_2(*N,N'*-diphenyl-{(4'-amidotpy)(4'-tolyltpy)Ru]$(PF_6)_2$-benzamidinate)$_4$ (red trace) upon excitation at 485 nm.

The cyclic voltammogram of Rh_2(*N,N'*-diphenyl-{(4'-amidotpy)(4'-tolyltpy)Ru]$(PF_6)_2$-benzamidinate)$_4$ is shown in Figure 5.34. On the basis of the characteristically reversible Rh_2-based redox processes observed to this point, one expects a total of four metal-centered couples in the absence of significant electronic coupling between Ru(II) subunits. The $Ru^{3+/2+}$ couple here is simply the superposition of

four simultaneous one-electron processes. Relative to the $Ru^{3+/2+}$ couple of the mononuclear complex, this couple has been anodically displaced by 110 mV, likely due to the high cationic charge of the complex. Between -0.1 V and 1.5 V one finds three weak but reversible couples. The number and reversibility of these couples suggests they are of dirhodium parentage. This is particularly true for the most anodically displaced couple at 1.06 V, which is within the ranges observed for the $Rh_2^{6+/5+}$ redox process (see Table 5.2 and Table 5.4). Assignment of the couples at 0.83 V and 0.05 V to the $Rh_2^{5+/4+}$ and $Rh_2^{4+/3+}$ processes, respectively, would constitute an enormous anodic shift relative to the range of potentials typically found for these processes (see Table 5.2 and Table 5.4). Such a shift may be explained by the high charge of the complex, making oxidation more difficult and reduction more facile, although assignment of the most anodic potential here to $Rh_2^{6+/5+}$ would seem to contradict this trend. Comparison of the current responses for these three smaller redox couples with each other and with that for the $Ru^{3+/2+}$ couple by integration of the current waves in the square-wave voltammogram is justified by their chemical reversibility (i.e. $i_{pc} / i_{pa} \sim 1$). Integration of the redox waves for these three smaller couples in the square-wave voltammogram gives essentially a 1:1:1 ratio, which is consistent with three dirhodium-based one-electron processes. However, the $Ru^{3+/2+}$ couple has a current response ten-fold that of these three smaller couples, much greater than that anticipated for four superimposed one-electron $Ru^{3+/2+}$ processes. For now, we cautiously assign these three smaller couples to dirhodium-based processes, their diminished current response perhaps being a consequence of high charge and/or the protected nature of the dirhodium core. Unfortunately, no related precedence could be found in the literature with regard to the second point.

Lastly, at negatively applied potentials there are two dominant terpyridine reduction processes. That which occurs at less negative potential has a sharp return oxidation profile (Figure 5.34) that is indicative of a current response that is not diffusion limited. Typically this is the result of insoluble species generated during the course of the potential sweep that adsorb to the working electrode surface. Here, it was found that this irreversible process was shifted anodically as the potential sweep was extended to more negative potentials, indicating that the nature of the chemically irreversible species generated depends on the magnitude of the cathodic potential. Moreover, its displacement

revealed the return oxidation wave for the first terpyridine-based reduction, scanning to - 1.9 V, but was made irreversible on scanning to -2.0 V (Figure 5.35).

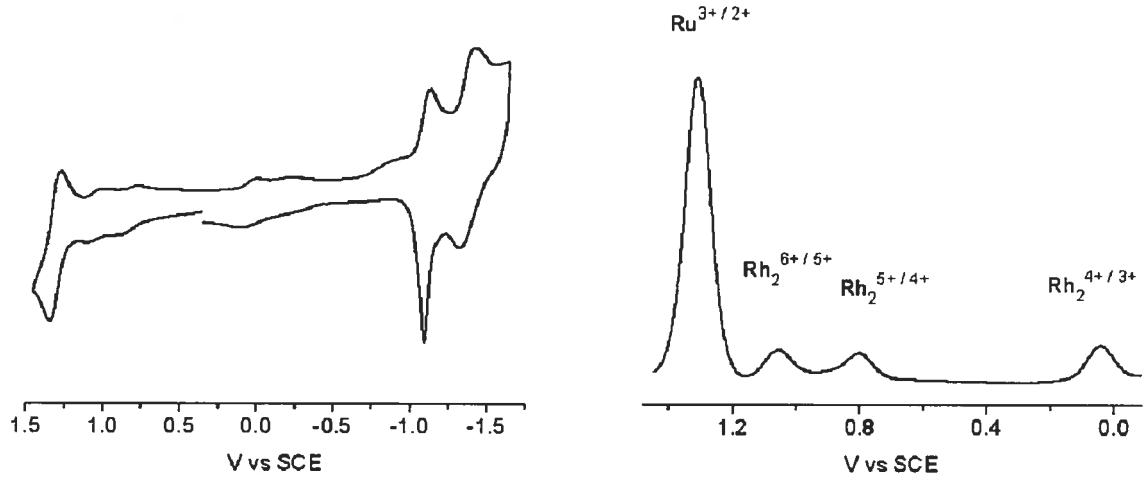

Figure 5.34. Cyclic voltammogram (positive initial scan direction from 0 mV) of Rh_2(*N,N'*-diphenyl-{(4'-amidotpy)(4'-tolyltpy)Ru]$(PF_6)_2$-benzamidinate)$_4$ in 0.1 M $TBAPF_6$ CH_3CN solution at 100 mVs^{-1} over the potential range of 1.4 to -1.8 V (left). Square-wave voltammogram of metal-centered processes (right), scanning from high to low potential.

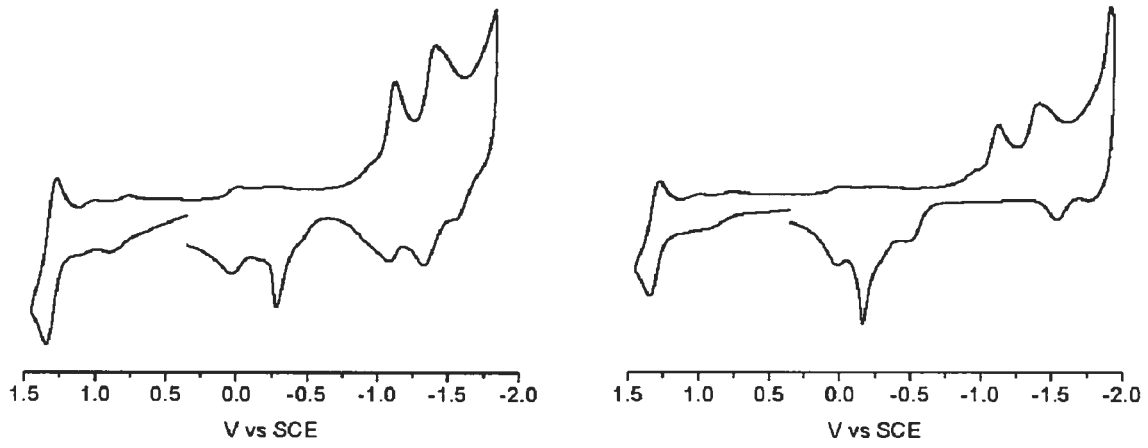

Figure 5.35. Cyclic voltammogram (positive initial scan direction from 0 mV) of Rh_2(*N,N'*-diphenyl-{(4'-amidotpy)(4'-tolyltpy)Ru]$(PF_6)_2$-benzamidinate)$_4$ in 0.1 M $TBAPF_6$ CH_3CN solution at 100 mVs^{-1} over the potential ranges 1.4 to -1.9 V (left) and 1.4 to -2.0 V (right).

Table 5.3. Electronic absorption data for terpyridyl analogues.

Compound	^{1}MLCT λ_{max} (nm) ε ($M^{-1}cm^{-1}$)	LC transitions λ_{max} (nm), ε ($M^{-1}cm^{-1}$)			
[Ru]	487 (8320)	329_{sh} (13500)	305 (22300)	275 (25200)	228_{sh} (20500)
Rh_2(L-[Ru])$_4$	492 (61700)	332_{sh} (86900)	-	275_{sh} (181400)	229_{sh} (179700)

All spectra recorded in air-equilibrated CH_3CN.

Table 5.4. Electrochemical data for terpyridyl analogues.

Cmpd	Potential [V] vs SCE, ΔE_p (mV) [a]					
	$Ru^{3+/2+}$	$Rh_2^{6+/5+}$	$Rh_2^{5+/4+}$	$Rh_2^{4+/3+}$	tpy	
Rh_2(L-tpy)$_4$[b]	-	1.15 (61)	0.14 (65)	-1.79 (irr)	-	-
Rh_2(L-[Ru])$_4$[c]	1.31 (70)	1.06 (80)	0.83 (100)	0.05 (100)	-1.13 [e]	-1.38 (90)
Rh_2(L-[Ru])$_4$[d]	1.31 (70)	1.07 (100)	0.83 (120)	0.02 (60)	-1.10 (60)	-1.37 (90)
[Ru]	1.20 (100)	-	-	-	-1.28 (60)	-1.56 (80)

a) Cyclic voltammogram scan rate is 100 mV s^{-1}. $E_{1/2}$ = ½ (E_{pa} + E_{pc}), where E_{pa} and E_{pc} are the anodic and cathodic peak potential, respectively. $\Delta E_p = E_{pa} - E_{pc}$. Potentials are corrected by internal reference to ferrocene (395 mV vs SCE). Data recorded in solutions of 0.1 M $TBAPF_6$ in CH_3CN, unless otherwise noted.

b) Recorded in DCM.

c) Recorded over potential range of 1.4 V to -1.7 V.

d) Recorded over potential range of 1.4 V to -1.9 V.

e) Cathodic peak potential.

Key:

L = 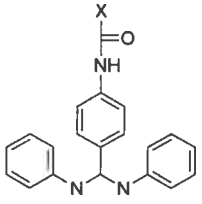

X = 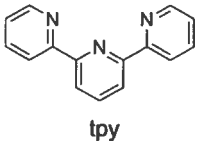

[Ru] = 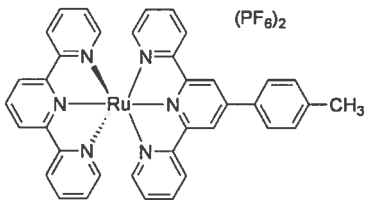

5.7 Proof of Principle

A tetra-nuclear Ru(II) polypyridyl complex templated from a dirhodium(II,II) center of the type discussed above serves as an excellent assessment of the efficacy of the synthetic strategy employed and the compatibility of the dirhodium(II,II) template. Moreover, its preliminary characterization offers insight into physical and photophysical attributes that may guide future work. However, it is also a dead end. If we endeavour to develop a viable strategy toward creating polynuclear transition-metal polypyridyl complexes, we should show that the family of building blocks herein described is indeed suitable to template design, from which the nuclearity, structure, symmetry, and even potential physical properties will be dictated.

To this point, we have introduced three classes of reactive functionality to the periphery of the dirhodium(II,II) tetra(*N,N'*-diphenylbenzamidine)$_4$ core, namely: 1.) bromine, 2.) amine, and 3.) acetylene groups. We have shown already, through installation of amino and acetylenic functionality, that the bromo-analogues are amenable to carbon (sp^2)-nitrogen and carbon (sp^2)-carbon (sp) bond formation, respectively. However, it remains to be seen if such reactivity extends to substrates based exclusively upon the dirhodium(II,II) tetra(*N,N'*-diphenylbenzamidine)$_4$ unit. To this end we have selected two multinuclear dirhodium targets to prove the self-complementary nature of the reactive building blocks developed thus far.

5.7.1 Dirhodium(II,II) Tetra(*N,N'*-diphenylbenzamidinate)$_4$: A Penta-dinuclear First Generation Dendrimer

Using the amination conditions outlined previously, Rh_2(*N,N'*-diphenyl-4-diphenylketimine-benzamidinate)$_3$(*N,N*-diphenyl-4-bromobenzamidinate) was reacted with Rh_2(*N,N'*-diphenyl-4-amino-benzamidinate)$_4$ to give the desired penta-dinuclear compound (**V-16**, Scheme 5.14) in moderate yield (51 %). The reaction mixture after 40h is surprisingly simple, revealing only a relatively broad and intense band in addition to a small remaining excess of the bromo-substrate, both of which could be effectively separated on silica substrate using a 10:0.15 $CHCl_3$ / Et_2O eluent mix. The identity of this new material was suggested to be the desired dendritic compound by MALDI-TOF mass

spectrometry (see section 5.9.3). The ^{1}H NMR spectrum of this material is shown in Figure 5.36 and is expectedly complex. However, it bears strong resemblance the other mixed diphenylketimine/bromine tetra-benzamidinate complexes described in Figures 5.14-5.18. Most significant is the appearance of a distinct N-H resonance at ~ 9.8 ppm, characteristic for an aryl-NH-aryl fragment. Interestingly, this resonance occurs as a doublet, reminiscent of the multinuclear complex Rh_2(*N,N'*-diphenyl-4-{(4'-amidotpy)(4'-tolyltpy)Ru][$(PF_6)_2$}-benzamidinate)$_4$ (see Figure 5.27), and may be due to the enantiomeric occurrence of the central dimeric unit.

To help further support the identity of this complex, this material was hydrolysed as outlined previously (see Scheme 5.8) to generate the dodeca-amino analogue (**V-17**, Figure 37) in 86 % yield. Doing so simplifies the ^{1}H NMR spectrum (Figure 5.37), which displays a spectral profile remarkably similar to that of Rh_2(*N,N'*-diphenyl-4-aminobenzamidinate)$_4$ (see Figure 5.23), though notably with more rounded features and an absent N-H resonance.

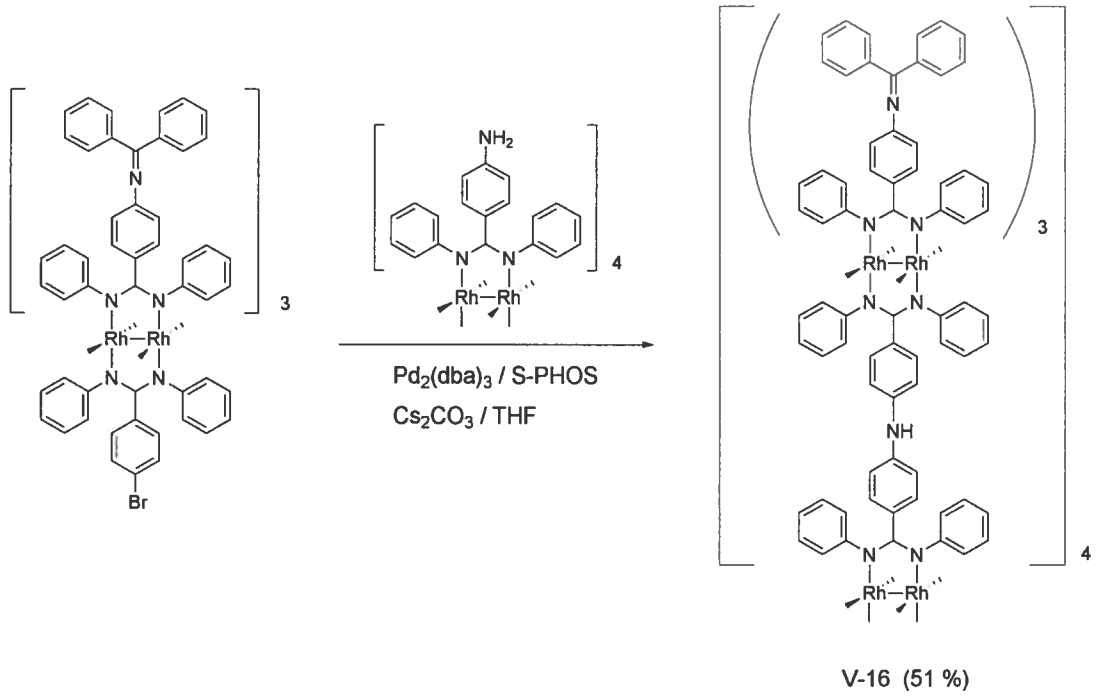

Scheme 5.14. Synthesis of **V-16** using 1.25 eq Br-substrate, 1.5 mol % $Pd_2(dba)_3$, 4.8 mol % S-PHOS, 2.0 eq. Cs_2CO_3, THF, 110°C, 40 h. Yield obtained after chromatographic separation.

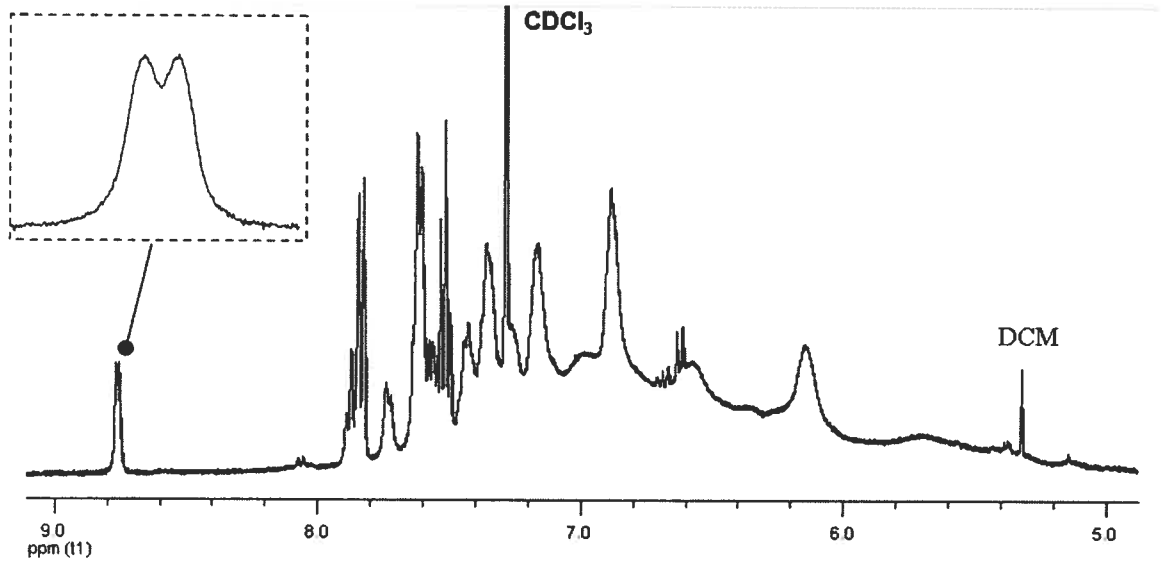

Figure 5.36. ^{1} H NMR of **V-16** in $CDCl_3$.

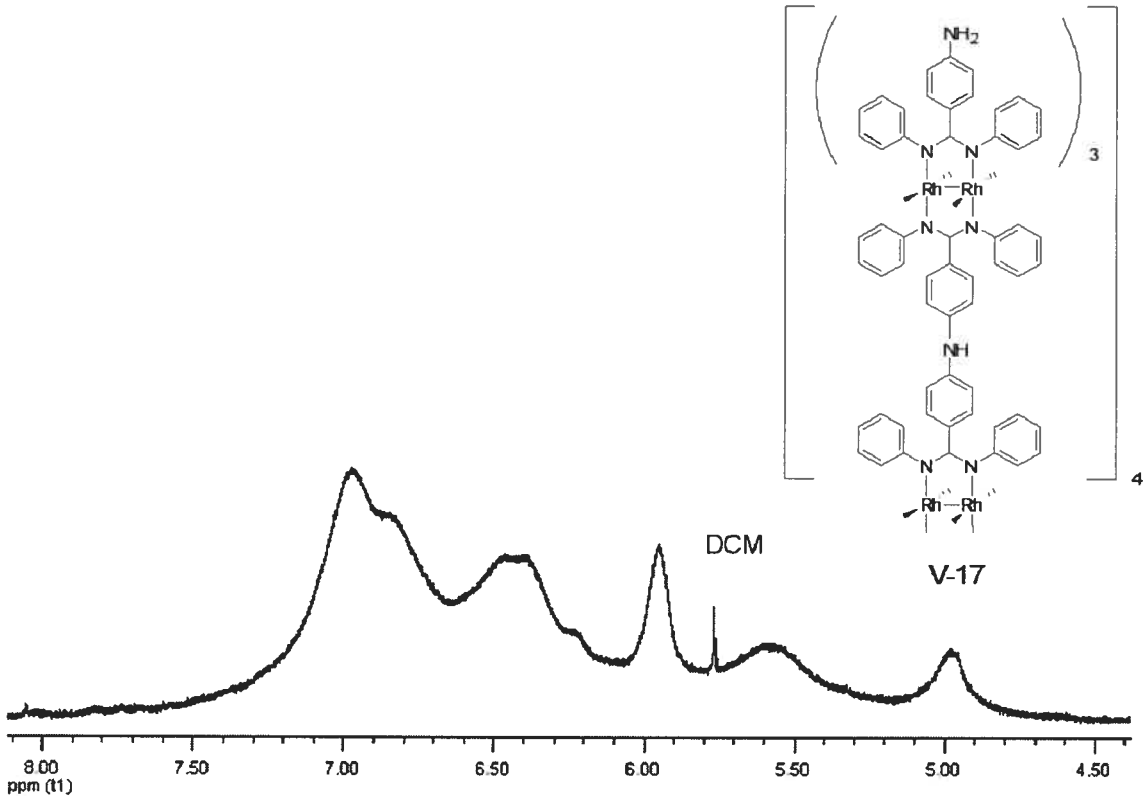

Figure 5. 37. ^{1}H NMR of **V-17** in d_6-DMSO.

Conversion of **V-16** to **V-17** also reduces the molecular mass dramatically and makes available ESI-MS analysis, which revealed exact masses for the $[M]^{3+}$, $[M]^{4+}$, and $[M]^{5+}$ molecular ions. This reflects not only the facile oxidation of the dirhodium subunit but also the multi-nuclearity of the complex, considering that all mononuclear dirhodium(II,II) tetra(*N,N'*-diphenylbenzamidinate)$_4$ complexes prepared herein exhibit exclusively $[M]^+$ molecular ions (see section 5.9 for experimental).

The electronic spectrum of **V-17**, recorded in DMSO, shows two characteristically intense bands at 858 nm (ε = 12100 $M^{-1}cm^{-1}$) and 514 nm (ε = 16800 $M^{-1}cm^{-1}$), along with a weak shoulder at ~ 600 nm (ε = 3100 M^{-1} cm^{-1}). The spectral profile resembles those of the mononuclear dirhodium complexes in Table 5.1, but is much more intense. For instance, the bands at 858 nm and 506 nm are, respectively, 6 and 5 times the intensity of those for Rh_2(*N,N'*-diphenyl-4-aminobenzamidinate)$_4$ in DMSO, which supports the nuclearity of the complex.

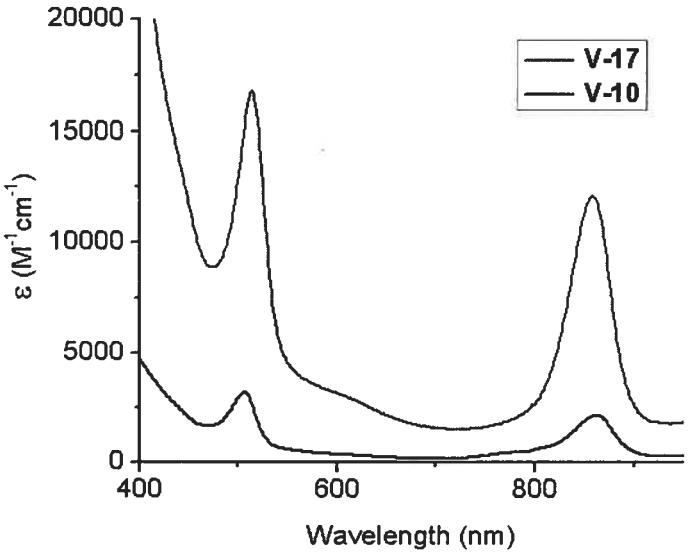

Figure 5.38. Electronic absorption spectra of **V-17** and **V-10** in air-equilibrated DMSO.

While the electrochemistry of mononuclear dirhodium(II,II) tetra(*N,N'*-diphenylbenzamidinate)$_4$ complexes is characteristically reversible (refer to Figure 5.31 and Table 5.2), that of the dendritic complex **V-17** is notably irreversible (see Figure 5.39). In addition, there is an additional oxidation process (see Table 5.5). Considering

that the relative anodic current ratio for the oxidation processes at 0.8, 1.22, and -0.04 V is, respectively, 2:1:6 and also the redox potentials for Rh_2(*N,N'*-diphenyl-4-aminobenzamidinate)$_4$ (refer to Table 5.2), we postulate that the irreversible oxidation at 0.8 V is due to a second oxidation ($Rh_2^{6+/5+}$) of the central dirhodium unit.

Table 5.5. Electrochemical Data for V-17.

Potential [V] vs SCE, ΔE_p (mV) [a] (i_c / i_a)[b]		
$Rh_2^{6+/5+}$	$Rh_2^{5+/4+}$	$Rh_2^{4+/3+}$
1.22 (irr), 0.8 (irr)	-0.04 (80) (0.3)	-1.63 (140) (5.2)

a) Cyclic voltammogram scan rate is 100 mV s^{-1}. $E_{1/2}$ = ½ (E_{pa} + E_{pc}), where E_{pa} and E_{pc} are the anodic and cathodic peak potential, respectively. $\Delta E_p = E_{pa} - E_{pc}$. Potentials are corrected by internal reference to ferrocene (395 mV vs SCE). Anodic peak potentials are given for irreversible (irr) oxidation processes. Data recorded in 0.1 M $TBAPF_6$ CH_3CN solution.

b) Cathodic to anodic current ratio.

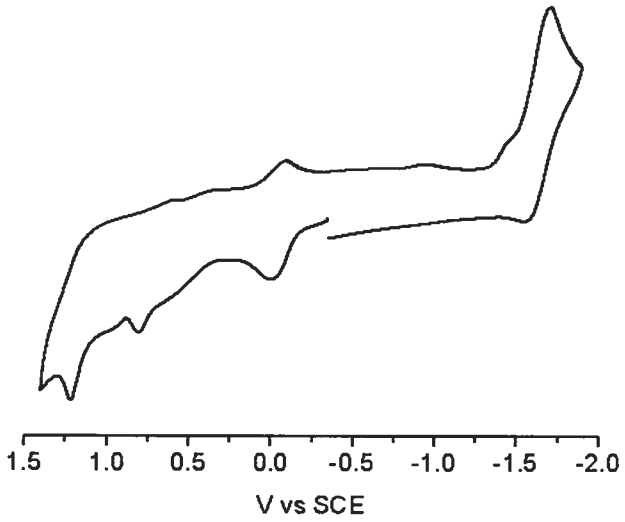

Figure 5.39. Cyclic voltammogram of **V-17** in 0.1 M $TBAPF_6$ CH_3CN solution at 100 mVs^{-1}.

To put these dendritic complexes into context, it must be noted that the highest nuclearity of a *molecular* species obtained to date, based on the dimetal paddlewheel motif, has been achieved by Yaghi and co-workers for a cage network comprising 12 Cu_2(II,II) paddlewheel units using the bridging ligand 1,3-benzenedicarboxylate.[47] Cotton and co-workers have also demonstrated discrete square,[48] triangular,[49] and cage [50] species based upon the dirhodium(II,II) paddlewheel motif, achieving a maximal nuclearity of 6 dimetal units in the latter case. Beyond molecular species, extended structures have also been prepared from dimeric paddlewheel units, of which those based upon dirhodium(II,II) carboxylates are most prominent. This may be done in one of two ways, through either connection along the equatorial [51] or axial [52] binding sites of the dimer. However, common amongst all the above noted examples is reliance upon self-assembly. The formation of **V-16** and **V-17** represent unprecedented examples of high-nuclearity dimetal complexes through covalent bond formation. Moreover, **V-17** is truly a first-generation dendrimer with potential for much greater nuclearity.

The importance of dimetal nuclearity must be stressed. Creating templates like **V-17** ensures the assembly of high-nuclearity complexes based upon photoactive units such as $Ru(tpy)_2^{2+}$. As mentioned previously in Chapter 2, this is important considering that the conversion of incident photons to electrical equivalents (for use in eventual application) is inherently inefficient and thus requires a high input of light energy. However, a recent publication from Turro and co-workers places the same consideration on multinuclear molecules composed exclusively of dirhodium(II,II) tetra(*N,N'*-diarylamidinate) complexes, such as **V-17**.[53] This is due to the discovery that irradiation of such mononuclear dirhodium complexes (λ_{irr} >795 nm) leads to the reduction and dimerization of alkyl halides. Such characteristics may lead to potential catalytic applications for a molecule such as **V-17**.

5.7.2 *Bis*(Rh_2(*N,N'*-diphenyl-4-diphenylketimine-benzamidinate)$_3$(*N,N*-diphenyl-4-ethynylbenzamidinate) (V-18): A Covalently Assembled 'Dimer-Bridge-Dimer' Complex

Using the alkynylation conditions outlined in Scheme 5.12b, the ethynyl-appended complex **V-15** was reacted with one equivalent of **V-7** for 16 h in THF to form the acetylene bridged 'dimer of dimer' complex (Figure 5.40 below) in 37 % yield after column purification. This yield was found to be acceptable for now, but should be improved greatly based on observations by Buchwald and co-workers concerning the rate of addition of the acetylene and also based on the presence of material that did not move under the separation conditions used.[37c] With regard to the latter point, it is expected that this material will be the mono-oxidized Rh_2^{4+}-bridge-Rh_2^{5+} and / or the bis-oxidized Rh_2^{5+}-bridge-Rh_2^{5+} mixed-valent complexes.

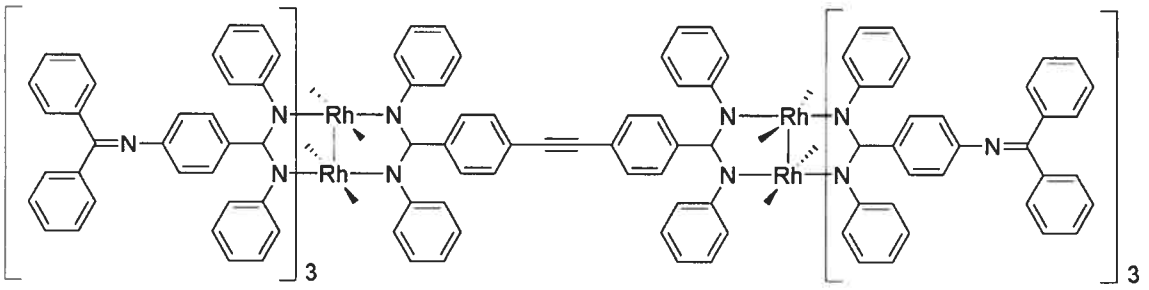

Figure 5.40. Illustration of *Bis*(Rh_2(*N,N'*-diphenyl-4-diphenylketimine-benzamidinate)$_3$(*N,N'*-diphenyl-4-ethynylbenzamidinate) (**V-18**).

Single crystals could be grown upon vapour diffusion of hexanes into a 1,2 dimethoxyethane solution of this material but, unfortunately, did not diffract well enough for structure determination. However, these crystallization conditions were found to be effective at removing any trace S-PHOS impurity. The ^{1}H NMR spectrum is shown below in Figure 5.41 and, as expected, is nearly identical to that of the starting material **V-15**) (see Figure 29) but with the important exception that the acetylene resonance at ~ 4.2 ppm is no longer present. As with the previous acetylene complexes, this compound displays a characteristic –CC- stretch at 2342 cm^{-1} in the IR spectrum and has been

identified by ESI-MS for the $[M]^{2+}$ molecular ion. Further verification was provided by acid-promoted hydrolysis of a small sample (refer to Scheme 5.8), for which ESI-MS showed clearly the $[M]^{2+}$ molecular ion of the hexa-amino complex.

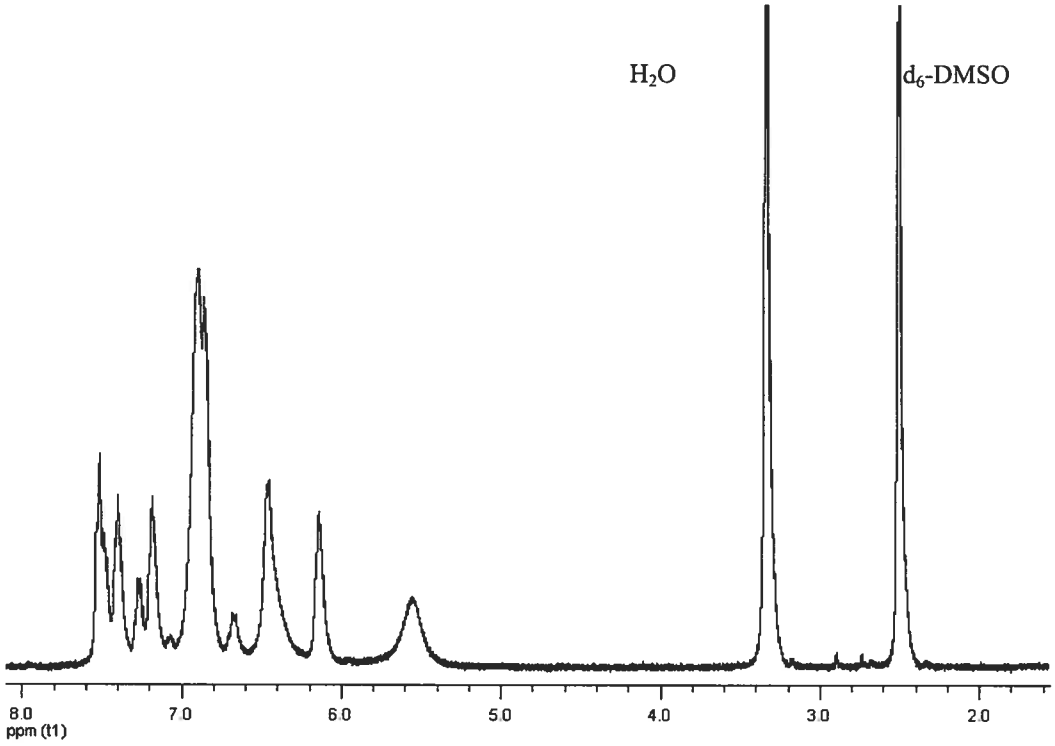

Figure 5.41. ^{1}H NMR of **V-18** (crystalline sample) in d_6-DMSO.

The electronic absorption spectrum of **V-18** is shown below in Figure 5.42 and displays two characteristically intense bands centered at 851 nm (ε = 4850 $M^{-1}cm^{-1}$) and 537 nm (ε = 4840 $M^{-1}cm^{-1}$) along with two weak shoulders at ~762 nm (ε = 760 $M^{-1}cm^{-1}$) and ~ 597 nm (ε = 870 $M^{-1}cm^{-1}$). The number and energy of these bands is nearly identical to that for the parent acetylenic complex **V-15**; however, they are double the intensity which is consistent with the proposed formulation.

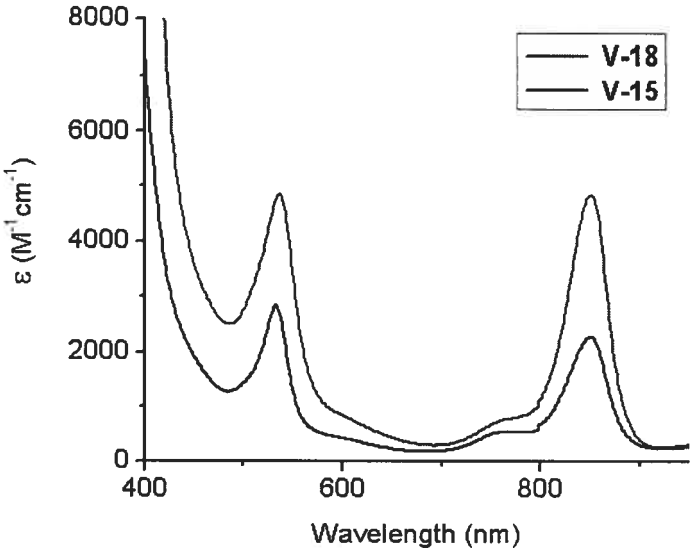

Figure 5.42. Electronic absorption spectrum of **V-18** and **V-15**.

As discussed previously (Chapter 4), 'dimer-bridge-dimer' complexes are invariably based upon Mo_2(II,II) or W_2(II,II) paddlewheel motifs since their nature permits the use of various techniques toward assessment of electronic delocalization in their mixed-valent forms.[54] For instance, the electron count of these dimers is such that the HOMO is of Rh_2-δ parentage. Since this metal-based δ MO is primarily responsible for electronically coupling dimeric units through interaction with the π and π^* orbitals of the bridge, electrochemistry becomes the most straight-forward means of interpreting significant electronic mixing. However, in the case of Rh_2(II,II) tetra-carboxylates and tetra-amidinates, the HOMO is of Rh_2-π^* and Rh_2-δ^* parentage, respectively. Also, one must bear in mind that, in the case of tetra-amidinates, the metal-based MO's are displaced to significantly higher energy relative to their tetra-carboxylate counterparts (Section 5.4). This latter point does not, in itself, appear to deter electronic mixing considering that Cotton and co-workers have reported various mixed amidinate / carboxylate complexes of the form $[Mo_2]$-O_2-R-O_2-$[Mo_2]$ (where $[Mo_2]$ = [*(N,N'*-diarylformamidinate)$_3Mo_2$]$^+$) that display significant inter-dimer electronic communication comparable to their purely carboxylate analogues for a given bridging ligand.[55]

The cyclic voltammogram (Figure 5.43, below) shows three characteristically (quasi)reversible metal-centered processes. Notably, the chemical reversibility of this bis-dimeric complex stands in contrast to the irreversibility displayed by the penta-dimeric complex (**V-17**). In the absence of any apparent resolution of these coincident redox processes, one may say that the π^* LUMO is not significantly mixed with the π system of the acetylene bridge. In fact, the similarity in energy and a strict doubling of absorption intensity for the bands observed in the electronic absorption spectra relative to those of its precursor complexes suggests a general absence of any significant electronic mixing between the Rh_2 centers.

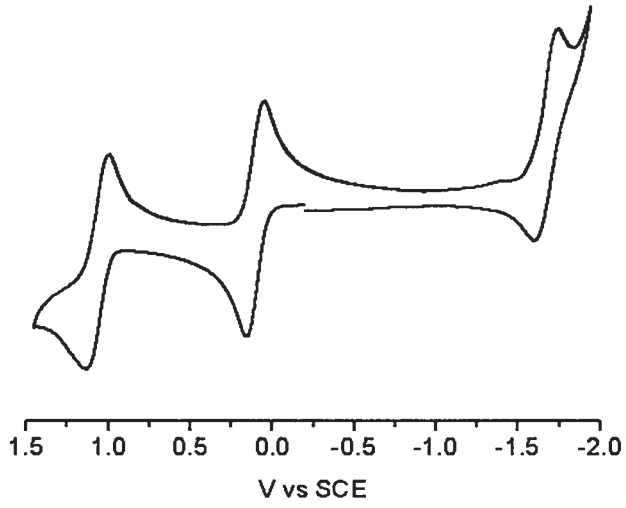

Figure 5.43. Cyclic voltammogram of **V-18** in 0.1 M $TBAPF_6$ DCM solution at 100 mVs^{-1}.

Table 5.6. Electrochemical data for V-18.

Potential [V] vs SCE, ΔE_p (mV) [a]		
$Rh_2^{6+/5+}$	$Rh_2^{5+/4+}$	$Rh_2^{4+/3+}$
1.06 (140)	0.10 (110)	1.67 (140)

a) Cyclic voltammogram scan rate is 100 mV s^{-1}. $E_{1/2}$ = ½ (E_{pa} + E_{pc}), where E_{pa} and E_{pc} are the anodic and cathodic peak potential, respectively. $\Delta E_p = E_{pa} - E_{pc}$. Potentials are corrected by internal reference to ferrocene (395 mV vs SCE). Data recorded in 0.1 M $TBAPF_6$ DCM solution.

The 'M_2-bridge-M_2' complex described here is unique in that it is the first *based on dirhodium units* to be comprised exclusively of *N*-chelates. In fact, it is only the second such complex to be assembled on the basis of covalent bond formation. The first,[5] depicted below in Figure 5.44, was reported recently by Ren and co-workers based on cross coupling of reactive Ru_2^{5+} complexes bearing peripheral iodo and acetylene functionality. Unlike the bis-Rh_2 complex assembled here, the bis-Ru_2 complex in Figure 5.44 displayed significant stabilization of redox intermediates, with ~ 0.5 V separation between successive one-electron processes of the same type, strongly suggesting significant inter-dimer electronic communication.

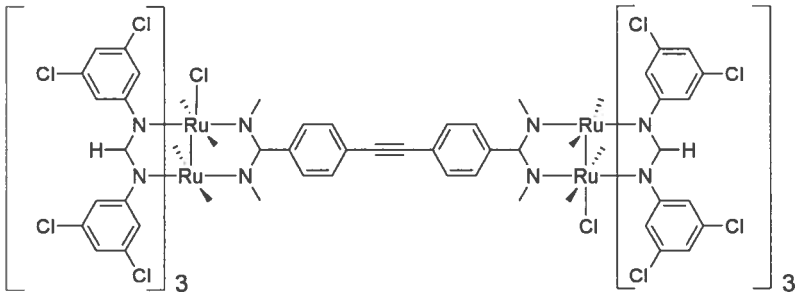

Figure 5.44. First covalently assembled 'M_2-bridge-M_2' complex, based on Ru_2^{5+} units.

Inter-dimer connectivity of dirhodium paddlewheel complexes has invariably entailed axial coordination.[56] The use of acetylides has been of interest where 'molecular wire' applications are concerned, of which those based on the Ru_2 unit have been most popular.[57] In particular, Bear and co-workers have prepared (*bis*)dirhodium complexes according to Scheme 5.15, below, where both a diethynyl and diisocyano linker was used to bridge two mixed-valent Rh_2^{5+} units.[56a] Interestingly, modest resolution of only the two one-electron reduction processes ($\Delta E_{1/2}$ = 130 mV) was observed in the former case. The latter case exhibited no resolution of the overlapped rhodium-centered redox processes with nearly identical potential values to that of the $Rh_2(dpf)_4$ precursor, much like that found here. More recently, both polymeric and trimeric complexes of $Rh_2(form)_4$ (where form = *N,N'*-di-p-tolylformamidinate) have also been prepared using 1,4-diisocyanobenzene, although no electrochemistry was reported.[56b]

a)

$$(ap)_4Rh_2(C{\equiv}C)_2Li + (ap)_4Rh_2Cl \longrightarrow (ap)_4Rh_2(C{\equiv}C)_2Rh_2(ap)_4 + LiCl_{(s)}$$

b)

$$2\,(dpf)_4Rh_2 + CN\text{-}C_6H_4\text{-}NC \longrightarrow (dpf)_4Rh_2(CN\text{-}C_6H_4\text{-}NC)Rh_2(dpf)_4$$

Scheme 5.15. Synthesis of axially-connected Rh_2(II,II) complexes. a) Ethynyl-bridged Rh_2^{5+} complexes (where ap = 2-anilinopyridinate) formed by metathesis reaction. b) 1,4-diisocyanobenzene-bridged Rh_2^{4+} complexes (where dpf = *N,N'*-diphenylformamidinate).

5.8 Concluding Remarks

Limitations arising from the reversibility of the dative bond, made most prevalent in Chapter 2, have been addressed in this chapter with the development of a reactive series of Rh_2-amidinate complexes. The nature of this reactivity has been, and should absolutely remain, conducive to simple and efficient organic transformations en route to creating linkage amenable to both energy and electron transfer. The capacity for these complexes to act as structural templates for photo-active units (here, $(tpy)_2Ru^{2+}$) bearing complimentary functionality has been demonstrated in good yield by straightforward means. Moreover, and perhaps most importantly, the versatility of these building blocks toward designing structural templates capable of supporting a large quantity of photo-active units has been demonstrated. The components described to this point have the potential to give rise to an extraordinary variety of such high-nuclearity templates. Simply expanding the range of reactive functionality and the type of dimetal unit employed should provide architectures limited primarily by imagination.

5.9 Experimental

5.9.1 Materials and Methods All reaction solvents used were dried using a solvent purification system. Both triethylamine and aniline were distilled over anhydrous Na_2SO_4 and stored over activated 3 Å molecular sieves. Where noted, 'degassed solutions' entailed three freeze-pump-thaw cycles. Unless otherwise indicated, all manipulations were performed under an argon atmosphere using standard Schlenk techniques.

5.9.2 Physical Measurements All ^1H NMR spectra were recorded using a Bruker 400RG at 400 MHz. Electrochemical data was recorded using a BAS Epsilon potentiostat using argon-degassed, spectroscopic grade acetonitrile solutions of 0.1 M tetrabutylammonium hexafluorophosphate ($TBAPF_6$) as supporting electrolyte. A three electrode set-up was employed using a working Pt button electrode, a Pt wire auxiliary electrode, and a Ag wire pseudo-reference electrode with addition of ferrocene as an internal reference. All data is corrected to the Fc/Fc^+ couple vs SCE. Single crystal X-ray diffraction data were collected on a Microstar Apex 2 at 100 K using Cu-Kα radiation (λ= 1.54178 Å). X-ray data collection and refinement were performed by Marie-Pierre Santoni. Mass spectrometry was performed by direct injection using a LC-MSD TOF (Agilent) spectrometer with electrospray ionization. An AutoFlex MALDI TOF (Bruker Daltronics) was used for compound **V-16**.

5.9.3 Synthesis and Purification

***N*-phenyl-4-bromobenzamide** In a typical preparation, 4-bromo-benzoic acid (6.0 g, 30 mmol) is refluxed in neat thionyl chloride (30 mL) for 16 h, after which excess thionyl chloride is removed by distillation and the residue dried under vacuum for 2h. The solid residue is then charged with DCM (60 mL) followed by triethylamine (8.7 g, 86 mmol). The solution is cooled to -10°C and aniline (15.3 g, 165 mmol) is added slowly, giving a heavy precipitate. The solution is allowed to reach room temperature, at which point it is transferred to a reflux condenser equipped with a drying tube and heated to reflux for 12h. After distillation of DCM, the residue is dissolved in hot methanol (200 mL) and an equal volume of water is added to give a heavy precipitate which is removed by filtration. The solid is triturated in methanol (20 mL), re-filtered, and dried under vacuum to give

7.6 g of pure product in 92 % yield. R_f = 0.50 (SiO_2 substrate, 5:2 hexanes/ethyl acetate as eluent). ^{1}H NMR (400 MHz, d_6-DMSO) δ ppm 10.33 (s, 1H), 7.92 (d, J = 8.4 Hz, 2H), 7.78 (d, J = 8.4 Hz, 2H), 7.75 (d, J = 8.4 Hz, 2H), 7.36 (m, 2H), 7.12 (m, 1H). ^{13}C NMR (300 MHz, d_6-DMSO) δ ppm 165.89, 140.21, 135.29, 132.69, 131.09, 129.94, 126.63, 125.16, 121.73. ESI-MS: $[M + H]^+$ cald. for $C_{13}H_{11}BrNO$, 276.00241; found, 276.00064.

***N,N'*-diphenyl-4-bromobenzamidine** In a typical preparation, PCl_5 (9.0 g, 43 mmol) is stirred in DCM (60 mL) for 10 min at room temperature. The solution is then cooled to -10°C and *N*-phenyl-4-bromobenzamide (7.1 g, 26 mmol) is added portion wise. The mixture is brought to room temperature and stirred for an additional 3 h, giving a clear yellow solution. The solution is cooled to -40°C and aniline (20.4 g, 219 mmol) is then added slowly over the course of 5 min. The reaction mixture is slowly brought to room temperature and stirred an additional 1h. The resultant heavy precipitate is removed by filtration and washed with copious amounts of DCM, then triturated in a 2:1 CH_3OH/H_2O mixture (200 mL) made basic (pH = 12) with $KOH_{(s)}$. The solid suspension is filtered and dissolved in DCM, then washed several times with 200 mL portions of H_2O. The DCM solution is dried over Na_2SO_4, filtered, and the filtrate dried to give 8.2 g of pure product in 90 % yield. R_f = 0.68 (SiO_2 substrate, 5:2 hexanes/ethyl acetate as eluent). ^{1}H NMR (400 MHz, d_6-DMSO) δ ppm 9.25 (s, 1H), 7.86 (d, J = 8.0 Hz, 2H), 7.53 (d, J = 8.4 Hz, 2H), 7.29 (m, 2H), 7.24 (d, J = 8.3 Hz, 2H), 7.07 (m, 2H), 6.99 (t, J = 7.3 Hz, 1H), 6.78 (t, J = 7.3 Hz, 1H), 6.59 (d, J = 7.6 Hz, 2H). ^{13}C NMR (300 MHz, d_6-DMSO) δ ppm 155.01, 151.64, 149.85, 142.43, 135.19, 132.31, 130.10, 129.70, 123.63, 123.49, 122.49, 120.80, 116.97, 115.18. ESI-MS: $[M + H]^+$ cald. for $C_{19}H_{16}BrN_2$, 351.04969; found, 351.04849. m.p. = 170°C.

***N*-phenyl-3,5-dibromobenzamide** In a typical preparation, 3,5-dibromobenzoic acid (6.0 g, 21 mmol) is refluxed in neat thionyl chloride (30 mL) for 20 h, after which excess thionyl chloride is remove by distillation and the residue dried under vacuum for 2 h. To the round-bottom flask containing the residue is charged DCM (50mL), and the mixture is stirred briefly to completely dissolve the residue. Triethylamine (8.7 g, 86 mmol) is added at once and the solution is cooled to -10°C. Aniline (20.4 g, 219 mmol) is then

added slowly, giving a heavy precipitate. The reaction mixture is brought to room temperature and transferred to a reflux condenser equipped with a drying tube. After heating at reflux for 20 h, the DCM is removed by distillation and the residue is dissolved in hot methanol (200 mL). An equal volume of water is added to give a heavy precipitate which is removed by filtration. The solid is triturated in methanol (20 mL), re-filtered, and dried under vacuum to give 6.8 g of pure product in 89 % yield. R_f = 0.49 (SiO_2 substrate, 15:1 toluene/ethyl acetate as eluent). ^{1}H NMR (400 MHz, d_6-DMSO) δ ppm 10.43 (s, 1H), 8.15 (d, J = 1.6 Hz, 2H), 8.09 (t, J = 1.6 Hz, 1H), 7.76 (d, J = 7.8 Hz, 2H), 7.37 (m, 2H), 7.14 (m, 1H). ^{13}C NMR (300 MHz, d_6-DMSO) δ ppm 163.82, 139.85, 139.69, 137.50, 130.93, 129.99, 125.48, 123.91, 121.79. ESI-MS: $[M + H]^+$ cald. for $C_{13}H_{10}Br_2NO$, 353.91292; found, 353.91124.

***N,N'*-diphenyl-3,5-dibromobenzamidine** In a typical preparation, PCl_5 (2.1 g, 10 mmol) is stirred in DCM (60 mL) for 10 min at room temperature. The solution is then cooled to -10°C and *N*-phenyl-3,5-dibromobenzamide (2.4 g, 6.8 mmol) is added portion wise. The solution is brought to room temperature and stirred for an additional 20 h, giving a clear orange solution. The solution is cooled to -40°C and aniline (6.6 g, 71 mmol) is added slowly over the course of 5 min. The solution is brought to room temperature and stirred for an additional 20 h, forming a heavy precipitate. After concentrating the solution (~ 40 mL), the precipitate is removed by filtration and discarded. The filtrate is dried under vacuum to give a residual oil that is dissolved in a minimal amount of methanol and precipitated in water. The precipitate is collected by filtration and re-dissolved in methanol, then made strongly acidic (pH < 1) with the addition of $HCl_{(conc)}$. The mixture is dry-loaded onto silica substrate and dried under vacuum to assure complete removal of methanol. The silica mix is then triturated in ethyl acetate and filtered. After discarding the ethyl acetate washings, the silica is washed on the frit with methanol. After reducing the methanol washings to dryness, the residue is triturated in an aqueous solution made basic (pH = 12) with $KOH_{(s)}$. The aqueous mixture is then washed twice with 200 mL portions of DCM, which are combined, dried over Na_2SO_4, filtered and dried under vacuum to give 1.5 g of pure product in 51 % yield. R_f = 0.50 (SiO_2 substrate, 15:1 toluene/ethyl acetate as eluent). ^{1}H NMR (400 MHz, d_6-DMSO) δ ppm 9.34 (s, 1H), 7.86

(d, J = 7.5 Hz, 2H), 7.81 (s, 1H), 7.52 (s, 2H), 7.30 (m, 2H), 7.11 (m, 2H), 7.00 (t, J = 6.8 Hz, 1H), 6.82 (t, J = 6.8 Hz, 1H), 6.65 (d, J = 7.2 Hz, 2H). ^{13}C NMR (300 MHz, d_6-DMSO) δ ppm 152.82, 151.22, 142.23, 139.59, 135.12, 132.04, 129.72, 123.47, 123.37, 122.82, 120.79. ESI-MS: $[M + H]^+$ cald. for $C_{19}H_{15}Br_2N_2$, 428.96020; found, 428.95877. m.p. = 140°C.

***N,N'*-diphenyl-4-formyl-benzamidine** In a typical preparation, *N,N'*-diphenyl-4-bromobenzamidine (1.0 g, 2.8 mmol) is charged to a flask containing THF (50 mL). After dissolution of the substrate, the solution is cooled to -78°C and 2 equivalents of n-BuLi (1.6 M soln. in hexanes, 5.6 mmol) are added drop wise over the course of 5 min. The solution is allowed to stir for 15 min at -78°C, at which point DMF (7.60 g, 104 mmol) is added at once. The solution is stirred for an additional 15 min at -78°C, at which point the reaction is quenched with addition of water. The reaction mixture is then distilled to give an orange oily residue that is taken up in a 5:2 mix of hexanes/ethyl acetate and eluted on a silica column. Drying the desired fractions gave 0.6 g of pure product in 70 % yield. R_f = 0.33 (SiO_2 substrate, 5:2 hexanes/ethyl acetate as eluent). ^{1}H NMR (400 MHz, d_6-DMSO) δ ppm 9.98 (s, 1H), 9.35 (s, 1H), 7.88 (d, J = 8.0 Hz, 2H), 7.85 (d, J = 8.0 Hz, 2H), 7.52 (d, J = 8.0 Hz, 2H), 7.30 (m, 2H), 7.05 (m, 2H), 7.00 (t, J = 7.2 Hz, 1H), 6.77 (t, J = 7.2 Hz, 1H), 6.61 (d, J = 7.6 Hz, 2H). ^{13}C NMR (300 MHz, d_6-DMSO) δ ppm 194.10, 155.08, 142.38, 141.70, 137.28, 131.00, 130.35, 129.69, 123.51, 123.45, 122.57, 120.81. ESI-MS: $[M + H]^+$ cald. for $C_{20}H_{17}N_2O$, 300.12626; found, 301.13354. m.p. = 149°C.

Dirhodium(II,II) tetra(*N,N'*-diphenyl-4-bromobenzamidinate) (V-1) Typically, *N,N'*-diphenyl-4-bromobenzamidine (7.5 g, 21 mmol) is heated to melting in an open flask, upon which $Rh_2(O_2C_2H_3)_4(CH_3OH)_2$ (0.42 g, 0.83 mol) is added at once, producing a dark red solution. The melt is stirred until it solidifies, which occurs within several minutes. The solid residue is heated to 100°C under vacuum to remove residual acetic acid, after which it is cooled. The crude solid is triturated in 100 mL DCM and filtered. This is repeated three times, the washings of which are combined and saved for recuperation of the excess amidine ligand. The red-brown solid which remains is

dissolved in chloroform and crystallized en mass via diffusion with DCM to give 0.99 g of pure product in 75 % yield. R_f = 0.58 (SiO_2 substrate, 5:1 hexanes/ethyl acetate as eluent). ^{1}H NMR (400 MHz, d_6-DMSO, 20°C) δ ppm 7.14 (d, J = 8.4 Hz, 2H), 7.04 (br, 4H), 6.95 (t, J = 7.2 Hz, 2H), 6.66 (d, J = 8.4 Hz, 2H), 6.57 (br, 2H), 5.58 (br, 2H). ESI-MS: $[M]^+$ cald. for $C_{76}H_{56}N_8Br_4Rh_2$, 1601.94713; found, 1601.94026.

Dirhodium(II,II) tetra(*N,N'*-diphenyl-3,5-dibromobenzamidinate) (V-2) Identical procedure as that described previously for **V-1**, but using *N,N'*-diphenyl-3,5-dibromobenzamidine (1.14 g, 2.65 mmol) and $Rh_2(O_2C_2H_3)_4(CH_3OH)_2$ (0.056 g, 0.110 mmol). The compound was crystallized by slow evaporation from a 4:1 $CHCl_3/CH_3OH$ mix to give 0.16 g of pure product in 73 % yield. R_f = 0.61 (SiO_2 substrate, 5:1 hexanes/ethyl acetate a eluent. ^{1}H NMR (400 MHz, $CDCl_3$, 20°C) δ ppm 7.22 (t, J = 1.8 Hz, 1H), 7.10 (m, 4H), 7.02 (t, J = 7.2 Hz, 2H), 6.92 (d, J = 1.8 Hz, 2H), 6.59 (br, 2H), 5.68 (br, 2H). ESI-MS: $[M]^+$ cald. for $C_{76}H_{52}Br_8N_8Rh_2$, 1913.58918; found, 1913.58305.

Dirhodium(II,II) tetra(*N,N'*-diphenyl-4-formyl-benzamidinate) (V-3) Identical procedure as that described previously for **V-1**, but using *N,N'*-diphenyl-4-formyl-benzamidinate (2.9 g, 9.6 mmol) and $Rh_2(O_2C_2H_3)_4(CH_3OH)_2$ (0.20 g, 0.39 mmol). The compound was purified by column chromatography using silica and a 2:1 hexanes/ethyl acetate mix as eluent. Drying of the desired fractions gave 0.34 g of pure product in 62 % yield. Single crystals suitable for structure determination by X-ray diffraction were obtained on standing from a DMSO solution. R_f = 0.27 (SiO_2 substrate, 2:1 hexanes/ethyl acetate as eluent). ^{1}H NMR (400 MHz, d_6-DMSO, 20°C) δ ppm 9.74 (s, 1H), 7.47 (d, J = 8.2 Hz, 2H), 7.07 (br, 4H), 6.99 (d, J = 8.2 Hz, 2H), 6.95 (t, J = 7.2 Hz, 2H), 6.64 (br, 2H), 5.63 (br, 2H). ESI-MS: $[M]^+$ cald for $C_{80}H_{60}N_8O_4Rh_2$, 1402.28474; found 1402.28890.

Dirhodium(II,II) tetra(*N,N'*-diphenyl-4-methylcarboxy-benzamidinate) (V-4) Typically, **V-3** (0.06 g, 0.04 mmol) is charged to a flask containing methanol (20 mL). The solution is cooled to 0°C and $KOH_{(s)}$ (0.023 g, 0.410 mmol) is then added, followed

by iodine (0.052 g, 0.210 mmol). The solution is stirred cold for 1h, reduced to dryness, and the residue is purified by column chromatography using silica and 2:1 hexanes/ethyl acetate as eluent. Drying the desired fractions gave 0.050 g of pure product in 84 % yield. R_f = 0.80 (SiO_2 substrate, 2:1 hexanes/ethyl acetate as eluent). ^1H NMR (400 MHz, d_6-DMSO, 20°C) δ ppm 7.50 (d, J = 8.2 Hz, 2H), 7.05 (br, 4H), 6.93 (m, 4H), 6.62 (br, 2H), 5.60 (br, 2H), 3.71 (s, 3H). ESI-MS: $[M]^+$ cald for $C_{84}H_{68}N_8O_8Rh_2$, 1522.32700; found, 1522.30407.

Dirhodium(II,II) tetra(*N,N'*-diphenyl-4-carboxy-benzamidinate) (V-5) Typically, $NaOH_{(s)}$ (0.2 g, 5.0 mmol) is dissolved in a 4:1 DMSO/H_2O mix (30 mL). To this is charged **V-4** (0.050 g, 0.033 mmol), and the solution is stirred at room temperature for 1h. The solution is then made acidic (pH < 1) with addition of $HCl_{(conc)}$ to give a precipitate which is removed by filtration and washed on the frit with water. Drying of the solid under vacuum gave 0.047 g of product in 98 % yield. Single crystals suitable for structure determination by X-ray diffraction were grown upon standing from a DMSO solution. ESI-MS: $[M]^+$ cald for $C_{80}H_{60}N_8O_8Rh_2$, 1466.26440; found, 1466.26473.

Protocol *A* :

To a dry reaction flask equipped with stir-bar is charged THF (30 mL) followed by $Pd_2(dba)_3$ (0.005 g, 0.005 mmol), S-PHOS (0.006 g, 0.015 mmol), Cs_2CO_3 (0.40 g, 1.2 mmol), **V-1** (0.50 g, 0.31 mmol) and benzophenone imine (0.056 g, 0.370 mmol, 1.2 eq.). The mix is triturated briefly and then refluxed under an argon atmosphere for 24 h. After cooling, the reaction mix is filtered over a plug of celite to remove Cs_2CO_3. The filtrate is reduced to dryness and applied to a silica column for elution with a DCM / 0.5 % Et_3N mix. Drying the recovered fractions gave 0.110 g of the tetra-bromo starting material along with 0.185 g of the mono-ketimine product, 0.082 g of the bis-ketimine product, and 0.060 g of the tris-ketimine product (after crystallization) in 29 %, 24 %, and 25 % yield, respectively, based upon benzophenone imine.

Protocol *B* :

To a dry 35 mL pressure vessel, equipped with a Viton O-ring and stir-bar, is charged THF (25 mL) followed by $Pd_2(dba)_3$ (0.005 g, 0.005 mmol), S-PHOS (0.006 g, 0.015 mmol), Cs_2CO_3 (0.96 g, 2.9 mmol), **V-1** (0.60 g, 0.37 mmol), and benzophenone imine (0.20 g, 1.1 mmol, 3.0 eq.). The reaction mix is triturated briefly and then heated to 140°C for 8 h, after which it is cooled and treated as in protocol A giving 0.050 g of the mono-ketimine product, 0.114 g of the bis-ketimine product, 0.191 g of the tris-ketimine product (after crystallization), and 0.140 g of the tetra-ketimine product (after crystallization) in 3 %, 11 %, 27 %, and 25 % yield, respectively, based upon benzophenone imine.

Rh_2(*N,N'*-diphenyl-4-diphenylketimine-benzamidinate)$_4$ (V-6) As with protocol B but using $Pd_2(dba)_3$ (0.005 g, 0.005 mmol), S-PHOS (0.006 g, 0.015 mmol), Cs_2CO_3 (0.81 g, 2.5 mmol), **V-1** (0.50 g, 0.31 mmol), and benzophenone imine (0.27g, 1.5 mmol, 4.8 eq.). The mix is triturated briefly and then heated to reflux at 140°C for 12 h in an oil bath, after which it is treated as in protocol A. The material recovered from the column could be crystallized *en masse* by dissolving it in chlorobenzene (60 mL) and adding an equal volume of methanol, giving 0.450 g of pure product in 71% yield. Single crystals suitable for structure determination by X-ray diffraction were grown by slow evaporation from a 2:1 $CHCl_3$ / CH_3OH solution. R_f = 0.21 (SiO_2 substrate, 4:1 hexanes/ethyl acetate as eluent). ^{1}H NMR (400 MHz, d_6-DMSO) δ ppm 7.53 (d, J = 7.3 Hz, 8H), 7.49 (t, J = 7.3 Hz, 4H), 7.40 (m, 8H), 7.28 (t, J = 7.3 Hz, 4H), 7.19 (m, 8H), 6.88 (m, 32 H), 6.46 (d, J = 8.2 Hz, 8H), 6.40 (br, 8H), 6.14 (d, J = 8.2 Hz, 8H), 5.56 (br, 8H). ESI-MS: $[M]^+$ cald for $C_{128}H_{96}N_{12}Rh_2$, 2006.59908; found, 2006.60144.

Rh_2(*N,N'*-diphenyl-4-diphenylketimine-benzamidinate)$_3$(*N,N'*-diphenyl-4-bromobenzamidinate) (V-7) This material, recovered from either protocol A or B, could be crystallized *en masse* upon cooling to -10°C of a saturated solution in CH_3NO_2. Single crystals suitable for structure determination by X-ray diffraction could be grown by slow evaporation from 2-ethoxyethanol. R_f = 0.28 (SiO_2 substrate, 4:1 hexanes/ethyl acetate as eluent). ^{1}H NMR (400 MHz, d_6-DMSO) δ ppm 7.53 (d, J = 7.4 Hz, 6H), 7.49 (t, J = 7.4

Hz, 3H), 7.40 (m, 6H), 7.28 (t, J = 7.6 Hz, 3H), 7.19 (m, 6H), 7.11 (d, J = 8.3 Hz, 2H), 6.90 (m, 24H), 6.85 (d, J = 7.6 Hz, 6H), 6.62 (d, J = 8.3 Hz, 2H), 6.48 (m, 6H), 6.43 (br, 8H), 6.15 (m, 6H), 5.56 (br, 8H). ESI-MS: $[M]^+$ cald for $C_{115}H_{86}BrN_{11}Rh_2$, 1905.43609; found, 1905.43635.

***Cis*-Rh$_2$(*N,N'*-diphenyl-4-diphenylketimine-benzamidinate)$_2$(*N,N'*-diphenyl-4-bromobenzamidinate)$_2$ (*cis*-V-8) and *trans*-Rh$_2$(*N,N'*-diphenyl-4-diphenylketimine-benzamidinate)$_2$(*N,N'*-diphenyl-4-bromobenzamidinate)$_2$ (*trans*-V-8)** Bis-ketimine material recovered from either protocol A or B (R_f = 0.37, SiO_2 substrate, 4:1 hexanes/ethyl acetate as eluent) could be resolved into the *cis* and *trans* components upon elution with $CHCl_3$ on silica substrate. For instance, the 0.082 g recovered from protocol A was resolved into 0.055 g and 0.020 g of the *cis* and *trans* isomers, respectively. For the *cis*-isomer, single crystals suitable for structure determination by X-ray diffraction were grown by vapour diffusion of hexanes into a 1,2-dimethoxyethane solution. ***Cis*:** R_f = 0.20 (SiO_2 substrate, $CHCl_3$ as eluent). ^{1}H NMR (400 MHz, d_6-DMSO) δ ppm 7.53 (d, J = 7.4 Hz, 4H), 7.49 (t, J = 7.2 Hz, 2H), 7.40 (m, 4H), 7.28 (t, J = 7.3 Hz, 2H), 7.19 (m, 4H), 7.12 (m, 4H), 6.92 (m, 24H), 6.86 (d, J = 7.5 Hz, 4H), 6.64 (d, J = 8.1 Hz, 4H), 6.49 (d, J = 7.9 Hz, 4H), 6.46 (br, 8H), 6.16 (m, 4H), 5.57 (br, 8H). ESI-MS: $[M]^+$ cald for $C_{102}H_{76}Br_2N_{10}Rh_2$, 1804.27311; found, 1804.27378. ***Trans*:** R_f = 0.45 (SiO_2 substrate, $CHCl_3$ as eluent). ^{1}H NMR (400 MHz, d_6-DMSO) δ ppm 7.53 (d, J = 7.0 Hz, 4H), 7.49 (t, J = 7.0 Hz, 2H), 7.40 (m, 4H), 7.29 (t, J = 7.0 Hz, 2H), 7.20 (m, 4H), 7.12 (d, J = 7.5 Hz, 4H), 6.92 (m, 28 H), 6.63 (d, J = 7.5 Hz, 4H), 6.51 (d, J = 7.4 Hz, 4H), 6.48 (br, 8H), 6.17 (d, J = 7.4 Hz, 4H), 5.56 (br, 8H). ESI-MS: $[M]^+$ cald for $C_{102}H_{76}Br_2N_{10}Rh_2$, 1804.27311; found, 1804.27539.

Rh$_2$(*N,N'*-diphenyl-4-diphenylketimine-benzamidinate)(*N,N'*-diphenyl-4-bromobenzamidinate)$_3$ (V-9) This material, recovered from either protocol A or B, was found to be sufficiently pure after column chromatography. R_f = 0.47 (SiO_2 substrate, 4:1 hexanes / ethyl acetate as eluent). ^{1}H NMR (400 MHz, d_6-DMSO) δ ppm 7.53 (d, J = 7.9 Hz, 2H), 7.49 (t, J = 7.0 Hz, 1H), 7.40 (m, 2H), 7.29 (t, J = 7.4 Hz, 1H), 7.19 (m, 2H), 7.13 (m, 6H), 6.98 (m, 24 H), 6.86 (d, J = 7.9 Hz, 2H), 6.66 (m, 6H), 6.53 (br, 8H), 6.51

(d, J = 8.0 Hz, 2H), 6.17 (d, J = 8.0 Hz, 2H), 5.57 (br, 8H). ESI-MS: $[M]^+$ cald for $C_{89}H_{66}Br_3N_9Rh_2$, 1703.11012; found, 1703.10715.

Rh_2(*N,N'*-diphenyl-4-aminobenzamidinate)$_4$ (V-10) In a typical preparation, **V-6** (0.50 g, 0.25 mmol) is stirred under ambient conditions in THF (50 mL) made acidic (pH < 2) with addition of $HCl_{(conc, aq)}$ for 30 min. The solvent was then concentrated under vacuum and the precipitate was removed by filtration and washed with a copious amount of DCM. The solid was then re-dissolved in a 5:1 THF / H_2O mix. A phase separation was effected upon addition of $KOH_{(aq)}$ solution (100 mL, pH ~ 14) with which the organic layer was washed. The organic layer was removed and dried to give a residue that was taken up in DCM, washed with water, and dried over Na_2SO_4. Filtration and removal of the solvent gave 0.28 g of pure product in 82 % yield. Single crystals suitable for structure determination by X-ray diffraction were grown upon standing of a DMSO solution containing the complex. R_f = 0.31 (SiO_2 substrate, 10:1 Et_2O / CH_3OH as eluent). ^1H NMR (400 MHz, d_6-DMSO) δ ppm 6.94 (br, 16H), 6.83 (m, 8H), 6.55 (br, 8H), 6.37 (d, J = 8.0 Hz, 8H), 5.94 (d, J = 8.0 Hz, 8H), 5.61 (br, 8H), 4.95 (s, 8H). ESI-MS: $[M]^+$ cald for $C_{76}H_{64}N_{12}Rh_2$, 1350.34868; found, 1350.35192.

Rh_2(*N,N'*-diphenyl-4-amidotpy-benzamidinate)$_4$ (V-11) Typically, 4'-carboxytpy (0.10 g, 0.36 mmol, 5 eq) is heated to reflux in thionyl chloride for 1h. Excess thionyl chloride is removed by vacuum distillation and the residue is dried under vacuum. To the residue is charged DCM (20 mL) followed by triethylamine (0.36 g, 3.6 mmol) and **V-10** (0.097 g, 0.072 mmol). The reaction mix is then stirred at room temperature under an inert atmosphere for 2.5 h, during which time a fine precipitate forms. The precipitate is removed by filtration and the filtrate is dried under vacuum to give a residue that is triturated in a methanolic solution made basic (pH ~ 12) with $KOH_{(s)}$. The solid is re-filtered and taken up in DCM, washed with H_2O and dried over Na_2SO_4. Filtration and removal of the solvent gave 0.112 g of pure product in 65 % yield. ^1H NMR (400 MHz, d_6-DMSO) δ ppm 10.69 (s, 1H), 8.79 (s, 2H), 8.75 (d, J = 3.0 Hz, 2H), 8.65 (d, J = 7.6 Hz, 2H), 8.04 (m, 2H), 7.54 (m, 2H), 7.39 (d, J = 6.6 Hz, 2H), 7.09 (br, 16H), 6.96 (m, 8H), 6.82 (d, J = 6.6 Hz, 8H), 6.71 (br, 8H), 5.70 (br, 8H). ESI-MS: $[M + 2H]^{2+}$ cald for

$C_{140}H_{102}N_{24}O_4Rh_2$, 1194.33129; found, 1194.33536. $[M + 3H]^{3+}$ cald for $C_{140}H_{103}N_{24}O_4Rh_2$, 796.55681; found, 796.55897.

[(4'-Carboxytpy)(4'-tolyl-tpy)Ru](PF$_6$)$_2$ (V-12) In a typical preparation, 4'-(2-furyl)-tpy (0.38 g, 1.3 mmol), (4'-tolyl-tpy)$RuCl_3$ (0.67 g, 1.3 mmol), and $AgNO_3$ (0.65 g, 3.8 mmol, 3 eq) are combined and heated to reflux in ethanol (50 mL) for 4h, after which $AgCl_{(s)}$ is removed by filtration over celite. The filtrate is dried and the resulting residue is taken up in a 1:1 mix of H_2O / CH_3CN and made basic (pH ~ 12) with addition of $KOH_{(s)}$. To this is added $KMnO_4$ (2.60 g, 16.5 mmol, 13 eq) and the solution is stirred at room temperature for 2.5 h, after which the same quantity of $KMnO_4$ is added again and the solution stirred for an additional 8 h. A solution of $Na_2S_2O_{3\,(aq)}$ (10 %) is added until a consistently red-coloured solution persists, at which point the reaction mix is filtered over celite. The filtrate is concentrated and then made acidic (pH ~ 2) with addition of $HPF_{6(aq)}$ (60 %). The resulting precipitate is collected by filtration and washed with a copious amount of water, then taken up in a minimal amount of CH_3CN and purified by column chromatography (SiO_2, 7:2 CH_3CN / $KNO_{3\,(aq,\,sat)}$ as eluent). The desired fractions were combined, reduced in volume, and then precipitated from $KPF_{6\,(aq,\,sat)}$ solution. The resulting precipitate was taken up in CH_3CN and precipitated from H_2O, filtered and dried to give 0.46 g of pure product in 37 % yield. R_f = 0.41 (SiO_2 substrate, 7:2 CH_3CN / $KNO_{3\,(aq,\,sat)}$ as eluent). ^{1}H NMR (400 MHz, CD_3CN) δ ppm 9.33 (s, 2H), 9.02 (s, 2H), 8.66 (d, J = 7.7 Hz, 4H), 8.14 (d, J = 8.0 Hz, 2H), 7.93 (m, 4H), 7.60 (d, J = 8.0 Hz, 2H), 7.44 (d, J = 5.6 Hz, 2H), 7.41 (d, J = 5.6 Hz, 2H), 7.17 (m, 4H), 2.57 (s, 3H). ESI-MS: $[M]^{2+}$ cald. for $C_{38}H_{28}N_6O_2Ru$, 351.06586; found, 351.06447.

Rh$_2$(*N,N'*-diphenyl-4-{(4'-amidotpy)(4'-tolyltpy)Ru](PF$_6$)$_2$}-benzamidinate)$_4$ (V-13) In a typical preparation, **V-12** (0.29 g, 0.30 mmol) is heated to reflux in thionyl chloride for 3 h. Excess thionyl chloride is removed by vacuum distillation and the residue is dried under vacuum. To this residue is charged acetonitrile (40 mL) and triethylamine (0.30 g, 3.0 mmol). **V-10** (0.050 g, 0.004 mmol) is then added portion wise as an acetonitrile solution (5 mL) and the reaction mix is heated to reflux unde an inert atmosphere for 30 min. The intensely dark red solution is then concentrated for purification by column

chromatography using silica and 7:2 CH_3CN / $KNO_{3\ (aq,\ sat)}$. The desired fractions are concentrated and precipitated from $KPF_{6\ (aq,\ sat)}$ solution. The resulting precipitate was taken up in CH_3CN and precipitated from H_2O, filtered and dried to give 0.149 g of product in 77 % yield. R_f = 0.48 (SiO_2 substrate, 7:2 CH_3CN / $KNO_{3\ (aq,\ sat)}$ as eluent). ^1H NMR (400 MHz, CD_3CN) δ ppm 9.47 (br, 4H), 9.20 (m, 8H), 9.05 (s, 8H), 8.67 (m, 16H), 8.15 (d, J = 8.0 Hz, 8H), 8.00 (m, 16H), 7.62 (d, J = 8.0 Hz, 8H), 7.51 (d, J = 4.7 Hz, 8H), 7.36 (d, J = 4.7 Hz, 8H), 7.26 (m, 8H), 7.19 (m, 8H), 6.16 (br, 8H), 5.58 (br, 8H). ESI-MS: $[M]^{8+}$ cald for $C_{228}H_{168}N_{36}O_4Rh_2Ru_4$, 510.85416; found, 510.85434. $[M(PF_6)]^{7+}$ 604.402, $[M(PF_6)_2]^{6+}$ 729.461, $[M(PF_6)_3]^{5+}$ 904.348, $[M(PF_6)_4]^{4+}$ 1166.674, $[M(PF_6)_5]^{3+}$ 1603.900.

Rh_2(*N,N'*-diphenyl-4-diphenylketimine-benzamidinate)$_3$(*N,N'*-diphenyl-4-trimethylsilylethynyl-benzamidinate) (V-14) To a dry 35 mL pressure vessel, equipped with a Viton O-ring and stir-bar, is charged THF (25 mL, degassed) followed by $Pd_2(dba)_3$ (0.0027 g, 0.0026 mmol), S-PHOS (0.0033 g, 0.0084 mmol), Cs_2CO_3 (0.050 g, 0.157 mmol, 3 eq.), **V-7** (0.100 g, 0.052 mmol), and trimethylsilyl acetylene (0.008 g, 0.079 mmol, 1.5 eq.). The reaction mix is triturated briefly and then heated to 120°C for 1 h, after which it is cooled and filtered over a plug of celite. The filtrate is dried and the residue purified by column chromatography on silica gel using 2:1 hexanes / ethyl acetate as eluent. The desired fractions are combined and dried to give 0.068 g of the desired product in 67 % yield. R_f = 0.46 (SiO_2 substrate, 3:1 hexanes / ethyl acetate as eluent). ^1H NMR (400 MHz, d_6-DMSO) δ ppm 7.62 (d, J = 6.0 Hz, 2H), 7.54 (d, J = 7.0 Hz, 6H), 7.49 (t, J = 7.0 Hz, 3H), 7.40 (m, 6H), 7.28 (t, J = 7.0 Hz, 3H), 7.19 (m, 6H), 6.90 (m, 30 H), 6.69 (d, J = 6.0 Hz, 2H), 6.48 (m, 6H), 6.43 (br, 8H), 6.15 (m, 6H), 5.58 (br, 8H), 0.14 (s, 9H). IR (KBr pellet): 2156 cm^{-1} [ν (-CC-)]. ESI-MS: $[M]^+$ cald for $C_{120}H_{95}N_{11}SiRh_2$, 1923.56511; found, 1923.55671.

Rh_2(*N,N'*-diphenyl-4-diphenylketimine-benzamidinate)$_3$(*N,N'*-diphenyl-4-ethynylbenzamidinate) (V-15) Typically, **V-14** (0.100 g, 0.052 mmol) is stirred in a 1:1 THF / CH_3OH solution (10 mL) containing K_2CO_3 (0.072 g, 0.518 mmol) at room temperature for 20 min. The reaction mix is then dried and the residue is triturated in

DCM and filtered. Drying the filtrate gave a residue that was purified by column chromatography on silica gel using 2:1 hexanes / ethyl acetate as eluent. The desired fractions are combined and dried to give 0.089 g of the desired product in 92 % yield. R_f = 0.33 (SiO_2 substrate, 3:1 hexanes / ethyl acetate as eluent). ^1H NMR (400 MHz, d_6-DMSO) δ ppm 7.62 (d, J = 6.0 Hz, 2H), 7.53 (d, J = 7.0 Hz, 6H), 7.49 (t, J = 7.0 Hz, 3H), 7.40 (m, 6H), 7.28 (t, J = 6.0 Hz, 3H), 7.19 (m, 6H), 6.90 (m, 30 H), 6.69 (d, J = 7.0 Hz, 2H), 6.48 (m, 6H), 6.43 (br, 8H), 6.15 (m, 6H), 5.57 (br, 8H), 4.12 (s, 1H). IR (KBr pellet): 2359 cm^{-1} [ν (-CC-)]. ESI-MS: $[M]^+$ cald. for $C_{117}H_{87}N_{11}Rh_2$, 1851.52558; found, 1851.51766.

Tetrakis[(*N,N'*-diphenyl-4-diphenylketimine-benzamidinate)$_3$Rh$_2$(*N,N'*-diphenylbenzamidinate)-NH-(*N,N'*-diphenylbenzamidinate)] Rh$_2$ (V-16) To a dry 35 mL pressure vessel, equipped with a Viton O-ring and stir-bar, is charged THF (25 mL) followed by $Pd_2(dba)_3$ (0.0008 g, 0.0008 mmol), S-PHOS (0.0010 g, 0.0025 mmol), Cs_2CO_3 (0.140 g, 0.432 mmol), **V-7** (0.100 g, 0.052 mmol), and **V-10** (0.014 g, 0.010 mmol). The reaction mix is triturated briefly and then heated to 110°C for 40 h, after which it is cooled and filtered over a plug of celite. The filtrate is then dried and purified by column chromatography using silica gel and 10:0.15 $CHCl_3$ / Et_2O. The desired fractions are combined and dried to give 0.045 g of the desired product in 51 % yield. R_f = 0.39 (SiO_2 substrate, 10:0.15 $CHCl_3$ / Et_2O as eluent). MALDI-TOF-MS: $[M]^+$ cald. for $C_{536}H_{404}N_{56}Rh_{10}$, 8652.4; found, 8672.7.

Tetrakis[(*N,N'*-diphenyl-4-aminobenzamidinate)$_3$Rh$_2$(*N,N'*-diphenylbenzamidinate)-NH-(*N,N'*-diphenylbenzamidinate)] Rh$_2$ (V-17) **V-16** (0.0300 g, 0.0035 mmol) was stirred under ambient conditions in THF (10 mL) made acidic (pH < 2) with addition of $HCl_{(conc, aq)}$ for 1 h. The reaction mix was then dried and the residue washed with a copious amount of DCM. The solid was then filtered and taken up in a 5:1 THF / H_2O mix. A phase separation was effected upon addition of a $KOH_{(aq)}$ solution (20 mL, pH ~ 14) with which the organic layer was washed. The organic layer was removed and dried to give a residue that was taken up in DCM, washed with water, and dried over Na_2SO_4. Filtration and removal of the solvent gave 0.020 g of product in

86 % yield. ^{1}H NMR (400 MHz, d_6-DMSO) δ ppm 6.97 (br, 80H), 6.83 (br, 40H), 6.47 (br, 40H), 6.38 (br, 40H), 5.95 (br, 40H), 5.59 (br, 40H), 4.97 (br, 24H). ESI-MS: $[M]^{3+}$ cald for $C_{380}H_{308}N_{56}Rh_{10}$, 2227.87910; found, 2227.87521. $[M]^{4+}$ 1671.910, $[M]^{5+}$ 1337.331.

Bis(Rh_2(*N,N'*-diphenyl-4-diphenylketimine-benzamidinate)$_3$(*N,N'*-diphenyl-4-ethynylbenzamidinate) (V-18) To a dry 35 mL pressure vessel, equipped with a Viton O-ring and stir-bar, is charged THF (25 mL, degassed) followed by $Pd_2(dba)_3$ (0.0017 g, 0.0016 mmol), S-PHOS (0.0021 g, 0.0052 mmol), Cs_2CO_3 (0.0314 g, 0.0097 mmol), **V-15** (0.0600 g, 0.0032 mmol), and **V-7** (0.0616 g, 0.0032 mmol). The reaction mix is triturated briefly and then heated to 120°C for 16 h, after which it is cooled and filtered over a plug of celite. The filtrate is dried and the residue purified by column chromatography on silica gel using 2:1 hexanes / ethyl acetate as eluent. The desired fractions are combined and dried to give 0.0440 g of the desired product in 37 % yield. This sample can be crystallized from a 1,2-dimethoxyethane solution upon vapour diffusion with hexanes. R_f = 0.10 (SiO_2 substrate, 3:1 hexanes / ethyl acetate as eluent). ^{1}H NMR (400 MHz, d_6-DMSO) δ ppm 7.53 (d, J = 7.0 Hz, 12H), 7.49 (t, J = 7.0 Hz, 6H), 7.40 (m, 12H), 7.27 (t, J = 7.0 Hz, 6H), 7.08 (br, 4H), 6.90 (br, 48H), 6.85 (d, J = 7.0 Hz, 12H), 6.67 (d, J = 8.0 Hz, 4H), 6.47 (d, J = 6.0 Hz, 12H), 6.43 (br, 16H), 6.14 (br, 12H), 5.56 (br, 16H). ESI-MS: $[M]^{2+}$ cald for $C_{232}H_{172}N_{22}Rh_4$, 1838.51778; found, 1838.51442. Bis(Rh_2(N,N'-diphenyl-4-aminobenzamidinate)$_3$(N,N-diphenyl-4-ethynylbenzamidinate) ESI-MS: $[M]^{2+}$ cald for $C_{154}H_{124}N_{22}Rh_4$, 1346.32997; found, 1346.32766.

5.10 References

1. a) Angaridis, P.; Cotton, F.A.; Murillo, C. A.; Villagran, D.; Wang, X. *Inorg. Chem.* **2004**, 43, 8290. b) Angaridis, P.; Berry, J. F.; Cotton, F.A.; Lei, P.; Lin, C.; Murillo, C.A.; Villagran, D. *Inorg. Chem. Comm.* **2004**, 7, 9. c) Barral, M.C.; Herrero, S.; Jimenez-Aparicio, R.; Torres, M.R.; Urbanos, F.A. *Inorg. Chem. Comm.* **2004**, 7, 42.
2. a) Chen, W.-Z.; Ren, T. *Organomet.* **2004**, 23, 3766. b) Chen, W.-Z.; Ren, T. *Organomet.* **2005**, 24, 2660. c) Chen, W.-Z.; Ren, T. *Inorg. Chem.* **2006**, 45, 8156.
3. Chen, W.-Z.; Protasiewicz, J.D.; Shirar, A.J.; Ren, T. *Eur. J. Inorg. Chem.* **2006**, 4737.
4. Xu, G.-L.; Ren, T.; *Inorg. Chem.* **2006**, 45, 10449.
5. Chen, W.-Z. ; Ren, T. *Inorg. Chem.* **2006**, 45, 9175.
6. Chen, W.-Z.; Fanwick, P.E.; Ren, T. *Inorg. Chem.* **2007**, 46, 3429.
7. Liwporncharoenvong, T.; Luck, R.L. *J. Am. Chem. Soc.* **2001**, 123, 3615.
8. Cotton, F.A.; Walton, R. A. *Multiple Bonds Between Metal Atoms*, 3rd, ed., Wiley, New York, **1994**.
9. Le, J.C.; Chavan, M.Y.; Chau, L.K.; Bear, J.L.; Kadish, K.M. *J. Am. Chem. Soc.* **1985**, 107, 7195.
10. Bear, J.L.; Zhu, T.P.; Malinski, T.; Dennis, A.M.; Kadish, K.M. *Inorg. Chem.* **1984**, 23, 674.
11. Amidates suffer from the occurrence of a statistical distribution of geometrical isomers upon formation of the dimetal paddlewheel complex, owing to the inherent asymmetry of the ligand.
12. Das, K.; Kadish, K.M.; Bear, J.L. *Inorg. Chem.* **1978**, 17, 930 and references therein.
13. Kawamura, T.; Fukamachi, K.; Haysashida, S.; Yonezawa, T. *J. Am. Chem. Soc.* **1981**, 103, 364.
14. a) Miskowski, V.M.; Schaefer, W.P.; Sadeghi, B.; Santarsiero, B.D.; Gray, H.B. *Inorg. Chem.* **1984**, 23, 1154. b) Sowa, T.; Kawamura, T.; Shida, T.; Yonezawa, T. *Inorg. Chem.* **1983**, 22, 56. c) Norman, J. G. Jr.; Renzoni, G. E.; Case, D. A. *J. Am. Chem. Soc.* **1979**, 101, 5256. d) Norman, J. G. Jr.; Kolari, H. J. *J. Am. Chem. Soc.* **1978**, 100, 791.

15. Piraino. P.; Bruno, G.; Lo Schiavo, S.; Laschi, F.; Zanello, P. *Inorg. Chem.* **1987**, 26, 2205.

16. He, L.-P.; Yao, C.-L.; Naris, M.; Lee, J. C.; Korp, J. D.; Bear, J. L. *Inorg. Chem.* **1992**, 31, 620.

17. Alcock, N.W.; Barker, J.; *Acta Cryst.* **1988**, C44, 712.

18. Halfpenny, J. *Acta Cryst.* **1995**, C51, 2542.

19. Cotton, F.A.; Inglis, T.; Kilner, M.; Webb, T.R. *Inorg. Chem.* **1975**, 14, 2023.

20. Yao, C.-L.; He, L.-P.; Korp, J.D.; Bear, J.L. *Inorg. Chem.* **1988**, 27, 4389.

21. see, for example, Dickson, P.M.; McGowan, M.A.D.; Yearwood, B.; Heeg, M.J.; Oliver, J.P. *J. Organomet. Chem.* **1999**, 588, 42.

22. a) Oki, Michinori *Methods in Stereochemical Analysis 4:Applications of Dynamic NMR Spectroscopy to Organic Chemistry*, VCH, Inc., Deerfield Beach, Florida, **1985**. b) Sanders, J.K.M.; Hunter, B.K. *Modern NMR Spectroscopy: A Guide for Chemists* 2nd ed., Oxford University Press, **1993**.

23. see, for example, a) Denti, G.; Campagna, S.; Sabatino, L.; Serroni, S.; Ciano, M.; Balzani, V. *J. Am. Chem. Soc.* **1992**, 114, 2944. (b) Campagna, S.; Denti, G.; Serroni, S.; Juris, A.; Venturi, M.; Ricevuto, V.; Balzani, V. *Chem. Eur. J.* **1995**, *1*, 211. c) Denti, G.; Campagna, S.; Sabatino, L.; Serroni, S.; Ciano, M.; Balzani, V. *Inorg. Chem.* **1990**, 29, 4750.

24. see, for example, a) Polson, M.I.J.; Loiseau, F.; Campagna, S.; Hanan, G.S. *Chem Comm.* **2006**, 1301. b) Fang, F.-Q.; Polson, M.I.J.; Hanan, G.S. *Inorg. Chem.* **2003**, 42, 5. c) Constable, E.C. *Chem. Commun.* **1997**, 1073.

25. a) Phan, N.T.S.; Van Der Sluys, M.; Jones, C.W. *Adv. Synth. Catal.* **2006**, 348, 609. b) Bellina, F.; Carpita, A.; Rossi, R. *Synthesis* **2004**, 2419. c) Miura, M.; *Angew. Chem. Intl. Ed.* **2004**, 43, 2201.

26. Aspley, C.J.; Williams, J.A.G. *New J. Chem.* **2001**, 25, 1136.

27. Barder, T. E.; Walker, S.D.; Martinelli, J.R.; Buchwald, S.L. *J. Am. Chem. Soc.* **2005**, 127, 4685.

28. see, for example, Cheng, K. F.; Thai, N.A.; Grohmann, K.; Teague, L.C.; Drain, C.M. *Inorg. Chem.*, 2006, **45**, 6928 and references therein.

29. Grubbs, R.H.; Despagnet-Ayoub, E. *J. Am. Chem. Soc.* **2004**, 126, 10198.

30. Yamada, S.; Morizono, D.; Yamamoto, K. *Tet. Lett.* **1992**, 33, 4329.

31. Li, H.; Eddaoudi, M.; Groy, T.L.; Yaghi, O.M. *J. Am. Chem. Soc.* **1998**, 120, 8571.

32. see, for example a) Kitagawa, S.; Uemura, K. *Chem. Soc. Rev.* **2005**, 34, 109. b) Lu, J.; Mondal, A.; Moulton, B.; Zaworotko, M.J. *Angew. Chem. Intl. Ed.* **2001**, 40, 2113. c) Eddaoudi, M.; Li, H.; Yaghi, O.M. *J. Am. Chem. Soc.* **2000**, 122, 1391 and references therein.

33. Huynh, M.H.V.; Dattelbaum, D.M.; Meyer, T.J. *Coord. Chem. Rev.* **2005**, 249, 457 and references therein.

34. Wolfe, J.P.; Ahman, J.; Sadighi, J.P.; Singer, R.A.; Buchwald, S.L. *Tetrahedron Lett.* **1997**, 38, 6367.

35. a) Thanasekaran, P.; Liao, R.-T.; Liu, Y.-H.; Rajendran, T.; Rajagopal, S.; Lu, K.-L. Coord. Chem. Rev. 2005, 249, 1085. b) Wurthner, F.; You, C.-C.; Saha-Moller, C.R. *Chem. Soc. Rev.* **2004**, 33, 133.

36. see, for example a) Cooke, M.W.; Hanan, G.S.; Loiseau, F.; Campagna, S.; Watanabe, M.; Tanaka, Y. *Angew. Chem. Intl. Ed.* **2005**, 44, 4881. b) Krebs, F.C.; Duprez, V. *Tetrahedron Lett.* **2006**, 47, 3785.

37. a) Tykwinski, R.R. *Angew. Chem. Intl. Ed.* **2003**, 42, 1566. b) Méry, D.; Heuzé, K.; Astruc, D. *Chem. Comm.* **2003**, 1934. c) Gelman, D.; Buchwald, S.L. *Angew. Intl. Ed.* **2003**, 42, 5993. d) Anderson, K.W.; Buchwald, S.L. *Angew. Intl. Ed.* **2005**, 44, 6173. e) McLaughlin, M.; Palucki, M.; Davies, I.W. *Org. Lett.* **2006**, 8, 3307.

38. a) Clark, R. J. H.; West, D. J.; Withnall, R. *Inorg. Chem.* **1992**, 31, 456. b) Bursten, B. E.; Cotton, F. A. *Inorg. Chem.* **1981**, 20, 3042.

39. a) Kawamura, T.; Maeda, M.; Miyamoto, M.; Usami, H.; Imaeda, K.; Ebihara, M. *J. Am. Chem. Soc.* **1998**, 120, 8136. b) Cotton, F. A.; Feng, X. *Inorg. Chem.* **1989**, 28, 1180. c) Rizzi, G. A.; Casarin, M.; Tondello, E.; Piraino, P.; Granozzi, G. *Inorg. Chem.* **1987**, 26, 3406.

40. see, for example a) Drago, R. S.; Long, J. R.; Cosmano, R. *Inorg. Chem.* **1982**, 21, 2196. b) Koh, Y. B.; Christoph, G. G. *Inorg. Chem.* **1978**, 17, 2590. c) Cotton, F.A.; Walton, R. A. *Multiple Bonds Between Metal Atoms*, 3rd, ed., Wiley, New York, **1994**.

41. a) Trexler, J. W. Jr.; Schreiner, A. F. ; Cotton, F. A. *Inorg. Chem.* **1988**, 27, 3265. b) Miskowski, V. M.; Schaefer, W. P.; Sadeghi, B.; Santarsiero, B. D.; Gray, H. B. *Inorg. Chem.* **1984**, 23, 1154.

42. a) Ahsan, M. Q.; Bernal, I.; Bear, J. L. *Inorg. Chem.* **1986**, 25, 260. b) Bear, J. L.; Zhu, T. P.; Malinski, T.; Dennis, A. M.; Kadish, K. M. *Inorg. Chem.* **1984**, 23, 674. c) Kadish, K. M.; Lancon, D.; Dennis, A. M.; Bear, J. L. *Inorg. Chem.* **1982**, 21, 2987.

43. Bear, J. L.; Yao, C.-L.; Liu, L.-M.; Capdevielle, F. J. ; Korp, J. D.; Albright, T. A.; Kang, S.-K.; Kadish, K. M. *Inorg. Chem.* **1989**, 28, 1254.

44. Bear, J. L.; Yao, C.-L.; Lifsey, R. S.; Korp, J. D., Kadish, K. M. *Inorg. Chem.* **1991**, 30, 336.

45. Robin, M. B.; Day, P. *Adv. Inorg. Chem. Radiochem.* **1967**, 10, 247.

46. Ren, T.; Lin, C.; Valente, E. J.; Zubkowski, J. D. *Inorg. Chim. Acta.* **2000**, 297, 283.

47. Eddaoudi, M.; Kim, J.; Wachter, J. B.; Chae, H. K.; O'Keefe, M.; Yaghi, O. M. *J. Am. Chem. Soc.* **2001**, 123, 4368.

48. see, for example, Cotton, F. A.; Daniels, L. M.; Lin, C.; Murillo, C. A.; Yu, S.-Y. *J. Chem. Soc. Dalton Trans.* **2001**, 502.

49. a) Cotton, F. A.; Murillo, C. A.; Stiriba, S.-E.; Wang, X.; Yu, R. *Inorg. Chem.* **2005**, 44, 8223. b)Cotton, F. A.; Daniels, L. M.; Lin, C.; Murillo, C. A. *J. Am. Chem. Soc.* **1999**, 121, 4538.

50. Cotton, F. A.; Lin, C.; Murillo, C. A. *Inorg. Chem.* **2001**, 40, 6413.

51. Naito, S.; Tanibe, T.; Saito, E.; Miyao, T.; Mori, W. *Chem. Lett.* **2001**, 1178.

52. a) Cotton, F.A.; Dikarev, E. V.; Petrukhina, M. A.; Schmitz, M.; Stang, P. J. *Inorg. Chem.* **2002**, 41, 2903. b) Cotton, F. A.; Dikarev, E. V.; Petrukhina, M. A.; *J. Chem. Soc. Dalton Trans.* **2000**, 4241.

53. Lutterman, D. A.; Degtyareva, N. N.; Johnston, D. H.; Gallucci, J. C.; Eglin, J. L.; Turro, C. *Inorg. Chem.* **2005**, 44, 5388.

54. Chisholm, M. H.; Patmore, N. J. *Acc. Chem. Res.* **2007**, 40, 19, and references therein.

55. a) Cotton, F. A.; Donahue, J. P.; Murillo, C. A. *J. Am. Chem. Soc.* **2003**, 125, 5436. b) Cotton, F. A.; Lin, C.; Murillo, C. A. *Inorg. Chem.* **2001**, 40, 1234. c) Cotton, F. A.; Lin, C.; Murillo, C. A. *J. Chem. Soc. Dalt. Trans.* **1998**, 19, 3151.

56. a) Bear, J. L.; Han, B.; Wu, Z.; Caemelbecke, E.V.; Kadish, K.M. *Inorg. Chem.* **2001**, 40, 2275. b) Handa, M.; Yasuda, M.; Muraki, Y.; Yoshioka, D.; Mikuriya, M.; Kasuga, K. *Chem. Lett.* **2004**, 32, 946.

57. a) Xu, G.-L.; DeRosa, M.C.; Crutchley, R.; Ren, T. *J. Am. Chem. Soc.* **2004**, 126, 3728. b) Zuo, J.-L.; Herdtweck, E.; Kühn, F.E. *J. Chem. Soc. Dalton Trans.* **2002**, 1244.

Chapter 6: Future Work

There are many avenues that may be pursued from the foundations that have been established to this point. Some of these are outlined herein, addressed systematically according to the order of their appearance in this thesis.

6.1. Chapter 2

With respect to the convergent synthesis of polynuclear $(tpy)_2Ru^{2+}$ systems outlined in Chapter 2, the reversibility of the appended carboxy-derived Ru(II) complexes limits their use as building blocks for continued growth via coordination chemistry. The best approach to this end is to take advantage of the high-affinity of $Rh_2(II,II)$ units for axial ligation, whereby bis-monodentate ligands may be used to bridge $Rh_2(II,II)$ units about which carboxy-functionalized Ru(II) photoactive complexes have already been convergently assembled. Where rigid, linear bis-monodentate ligands are concerned, uncontrolled polymer formation typically encountered via one-pot self-assembly of neutral dimetal units will likely be precluded by the charged nature of the $Rh_2(II,II)$/Ru(II) adducts,[1] in the same way that the charged nature of the Ru(II) complex afforded control over the replacement of the acetates of $Rh_2(OAc)_4$. In addition, depending on the angular nature of the bidentate ligand, various photo-active architectures can be self-assembled to produce systems of extremely high nuclearity. The potential porosity of these assemblies may be used to advantage, particularly with regard to sensory applications.[2]

Potential problems may arise given the relative fragility of μ-bidentate binding in the presence of competing donors such as pyridine (see Chapter 2, Figure 2.20), and it is conceivable that synthesis of a higher-order target by axial ligation will be compromised and complicated by competing equatorial ligation. The nature of this dative competition has been ascribed to an electrostatic origin, the most compelling evidence of which has been the surprisingly short $Rh\text{-}O_{(acetate)}$ bond length. A related phenomenon has been demonstrated for dimetal complexes in general, whereby reducing the basicity of the equatorial bidentate (e.g. trifluoroacetate vs acetate) actually strengthens the axial bonding interaction.[3] Considering this, it is reasonable to assume that sufficiently strong

axial donor ligands will help to stabilize the highly charged $Rh_2(II,II)/Ru(II)$ adducts described in Chapter 2, thereby reducing the tendency for the appended carboxy-Ru(II) complexes to be displaced. En route to axial ligation by such ligands, it is conceivable that some competition will take place with the equatorially bound chelates. However, the most stable dimetal motifs are formed by μ-bidentate ligands which possess a significant π-donor/acceptor quality in addition to σ-donor capacity.[4] Thus, utilization of a strictly σ-donor axial connector (and, moreover, a rigid one incapable of μ-bidentate coordination) should inherently disfavour displacement of carboxylates. Regardless, competition for equatorial ligation may be suppressed even further using axial connectors which impose a degree of steric encumbrance, since it is well known that equatorial displacement is slowed using relatively bulky incoming chelates.[4] To fit the criteria outlined to this point, polytopic phosphines could potentially exert a stabilizing influence en route to creating higher order assemblies from these $Rh_2(II,II)/Ru(II)$ adducts, particularly since they are known to form very strong axial interactions with $Rh_2(O_2CR)_4$ complexes.[5]

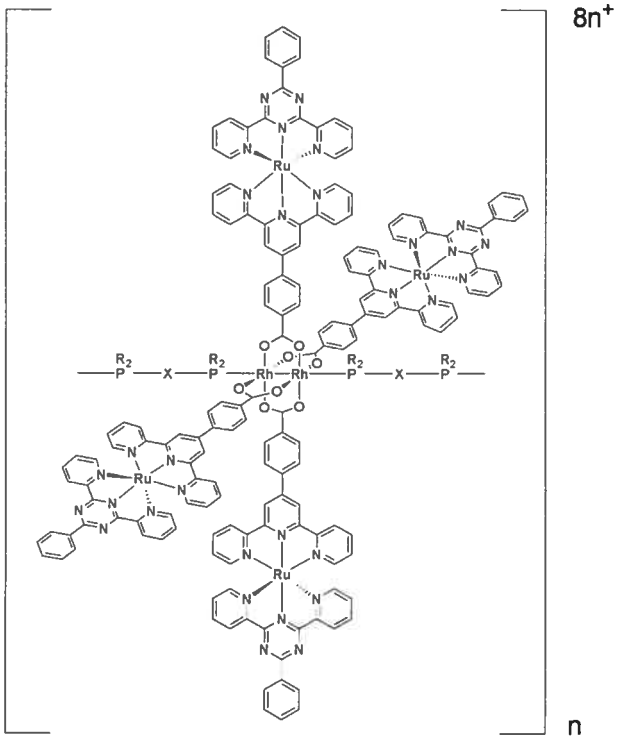

Figure 6.1. Proposed axial connection of the tetranuclear photo-active complex **II-4b** using linear bis-monodentate phosphines.

Dimetal paddlewheel complexes have only very recently received attention regarding their potential photo-excited states.[6] In particular, those with quadruple metal-metal bonding have been shown to possess long-lived ^{3}MLCT. Complexes of the form $Mo_2(O_2CAr)_4$ have been shown, by transient absorption measurements, to possess a long-lived, non-emissive state ranging from 40-76 μs depending on the nature of the aryl group (Ar), originating from a $\delta_{Mo\text{-}Mo} \rightarrow \pi^*_{(-CO2)}$ transition.[6b] In addition, complexes of the form Re_2(*N,N'*-dialkylbenzamidinate)$_4Cl_2$ have been shown to be strongly emissive, the origin of which has been attributed to a metal-based $\delta_{Re\text{-}Re} \rightarrow \delta^*_{Re\text{-}Re}$ transition.[6c] The creation of adducts analogous to complexes **II-1a-II-3a** and **II-1b-II-4b** based on these dimetal motifs should be ideal models for study of energy transfer processes.

6.2. Chapter 3

The controlled symmetric and asymmetric appendage of $Rh_2(OAc)_3^+$ fragments to a series of linearly bridging dicarboxylate Ru(II) complexes was shown to be straightforward. The electronic absorption data is suggestive of electronic mixing between the Ru(II) bridge complex and the attached Rh_2(II,II) fragments, but the question remains if these Ru(II) bridge complexes are capable of electronically coupling the two appended dimetal centers, and if so, to what extent. To this end, the creation of symmetrically substituted analogues of both $Mo_2(O_2CR)^+$ and $W_2(O_2CR)_3^+$ fragments (**A**, Figure 6.2) makes electrochemical assessment possible and very straightforward. If electronic coupling is demonstrated, it would be remarkable considering the relative scarcity of reports demonstrating significant electronic coupling over such long distances. Moreover, the potential for correlation of such long-range coupling to systematic variation of the bridging Ru(II) complexes (in terms of length and planarity) offers more insight as to the governing factors involved. Such information is invaluable toward incorporating these assemblies into higher-order networks and for potential applications.

In addition, the asymmetric complexes containing one $Rh_2(OAc)_3^+$ fragment offer easy access to mixed dimetallic species. This is particularly appealing considering the recently elucidated emissive and non-emissive states of several quadruple metal-metal

bonded paddlewheel complexes, mentioned previously. Such complexes (**B**, Figure 6.2) should likely serve as ideal models for study of energy transfer processes.

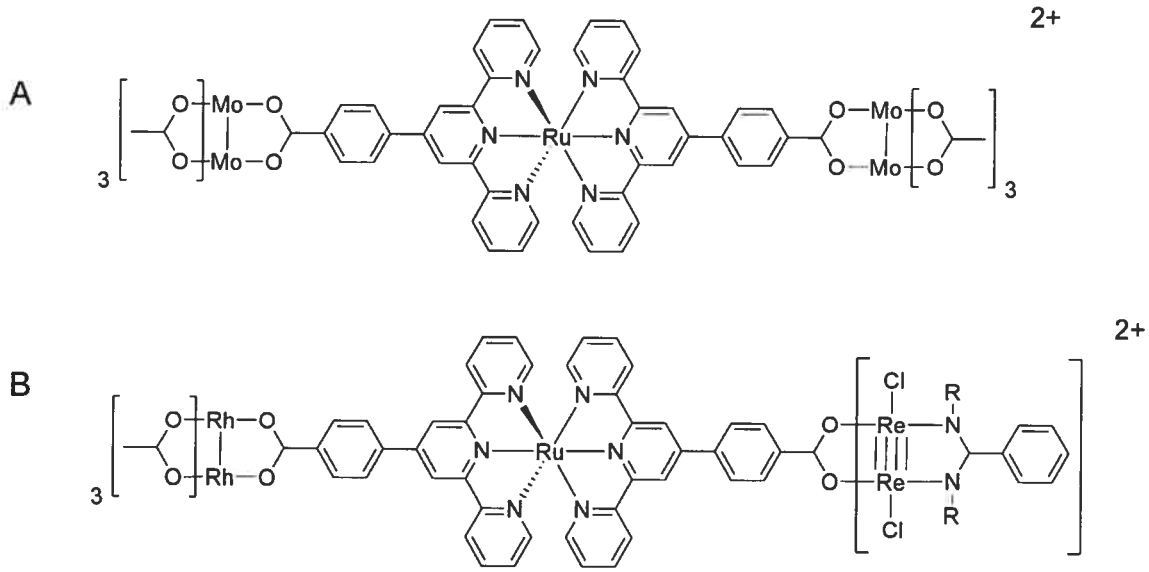

Figure 6.2. Proposed homo-dimetallic (**A**) and hetero-dimetallic (**B**) complexes.

6.3 Chapter 4

Much of the future direction with regard to the compounds prepared in this chapter has been alluded to already, and so will be reiterated here only briefly. The *N,N'*-dipropylbenzamidine and *N,N'*-diphenylbenzamidine appended $(tpy)_2Ru^{2+}$ complexes described in this chapter emphasize the degree to which the basicity (and hence donor capacity) of the amidinate fragment may be modified depending on the nature of the *N*-substituent. This is particularly appealing with regard to sensitization of semi-conductor substrates for solar cell applications. Studies of this nature have focused on carboxylate and phosphonate groups as means to anchor the dye molecule to such surfaces. It would therefore be instructive to see how such amidine-bearing complexes compare to structurally similar carboxylate and / or phosphonate analogues in terms of photo-current production and stability in device applications. The degree and ease with which such parameters can be optimized may be much more accessible for these amidine-bearing sensitizers, considering the wide range of *N*-substituents available. Moreover, such

amidine-bearing dye sensitizers may help to shed more light on the complex nature of dye-substrate binding interactions.[7]

6.4 Chapter 5

Unfortunately, time constraints have abbreviated complete photophysical characterization of the Rh_2 and Ru-appended Rh_2 complexes described in this chapter. It will prove most interesting to see to what, if any, degree the emissive state of the appended $(tpy)_2Ru^{2+}$ complexes has been attenuated by the Rh_2(*N,N'*-diphenylbenzamidinate)$_4$ template, and how this compares to the carboxylate adducts described in Chapter 2. Moreover, the potential photo-excited state(s) of the Rh_2 complexes themselves warrant elaboration. To both ends, both 298 K and 77 K emission will be necessary, along with transient absorption measurements if possible.

The range of functionality (and, moreover, its periodicity and orientation) installed on the periphery of the Rh_2(*N,N'*-diphenylbenzamidinate)$_4$ complex makes available an enormous array of potential targets. Of these, the most intriguing may be those of high-nuclearity based on the Rh_2(*N,N'*-diphenylbenzamidinate)$_4$ unit, considering that: 1) such templates offer many reactive sites for covalent connection to complimentarily functionalized $(tpy)_2Ru^{2+}$ complexes and 2) related complexes to Rh_2(*N,N'*-diphenylbenzamidinate)$_4$ have been shown to serve as photo-activated reductive catalysts. [8] To this end, both open and closed structures may be constructed, of which the latter has been demonstrated through the preparation of both dendritic pentakis-Rh_2 and linear bis-Rh_2 assemblies (refer to Sections 5.7.1 and 5.7.2, respectively). Open structures bearing orthogonal corner units are accessible via the *cis*-Rh_2(*N,N'*-diphenyl-4-bromobenzamidinate)$_2$(*N,N'*-diphenyl-4-diphenylketimine-benzamidinate)$_2$ complex and rigid bridging ligands bearing mutually opposed, two-fold functionality capable of forming linear covalent linkage to the Rh_2-subunit.

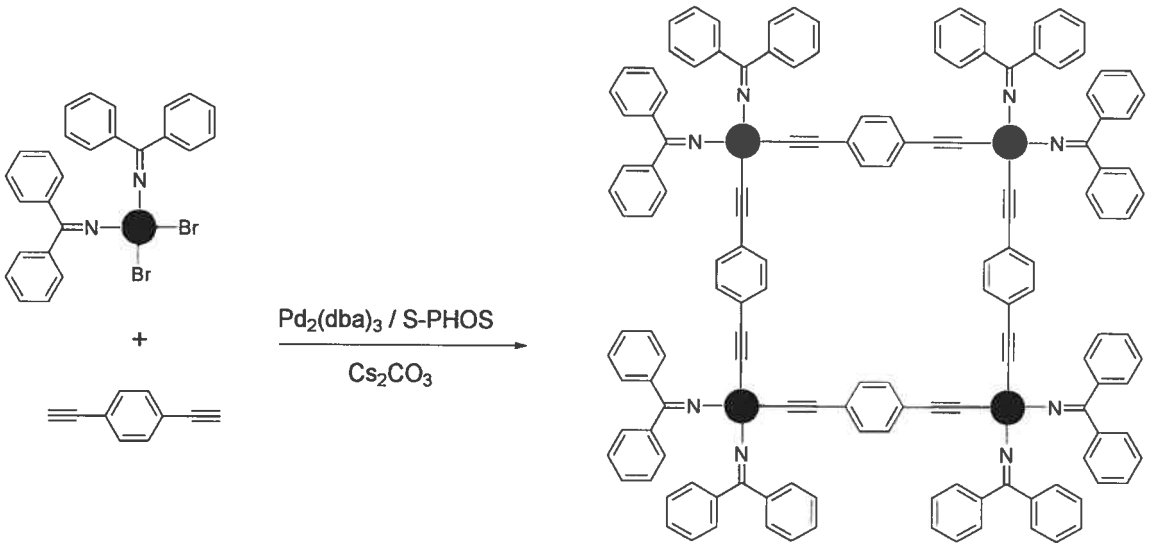

Scheme 6.1. Proposed 'one-pot' square formation from *cis*-Rh_2(*N,N'*-diphenyl-4-bromobenzamidinate)$_2$(*N,N'*-diphenyl-4-diphenylketimine-benzamidinate)$_2$.

The example illustrated in Scheme 6.1 should be attainable in a 'one-pot' synthesis using the optimized Sonogashira coupling procedure described in Scheme 5.12 (Chapter 5). This resembles strongly the synthetic protocol followed for the covalent assembly of the Pt(II)-based square and triangular structures depicted in Figure 1.5 (Chapter 1). Once formed, the peripheral ketimine groups of the square assembly in Figure 6.3 can be converted to their amine equivalents for coupling to carboxy-functionalized $(tpy)_2Ru^{2+}$ units via amide bond formation, as outlined in Chapter 5. The porous nature is promising for sensory applications subsequent to guest-molecule binding, but like other charged photoactive assemblies, this will likely depend on the occurrence of counter-anions within the cavity of the structure.

The accessibility of such porous structures as that depicted in Scheme 6.1 above can be made much more efficient through the preparation of mixed amidinate/carboxylate Rh_2 complexes. To this end, a synthetic protocol according to Scheme 6.2, whereby labile carboxylates are displaced via salt metathesis, is a well-known method for formation of tetra-μ-amidinate dimetal complexes and, in particular, this approach has been used to successfully prepare such complexes from *N,N'*-diphenylbenzamidine.[9] Given the amenability of the Rh_2 amidinate complexes described in Chapter 5 to chromatographic

purification, it should then be possible to separate these mixed ligand products, the distribution of which can be directed to favour a particular target by the stoichiometric quantity of amidine ligand employed. However, this approach has a serious flaw, and it stems from the strong *trans*-influence of the amidinate ligands. The development of open structures relies on efficiently producing the *cis*-Rh_2(amidinate)$_2$(carboylate)$_2$ subunit, but such a synthetic approach will yield predominantly the *trans* isomer, owing to the *trans*-labilizing effect exerted by the relatively more basic amidinate ligands.[10] The way around this is typically to form first the M_2(amidinate)$_4$ complex, then use strong acids in refluxing acetonitrile solutions to form solvent adducts of the form $[M_2(\text{amidinate})_{4-n}(CH_3CN)_{2n}]^+$, of which the *cis*-adduct can be isolated in good yield. The problem with this approach is the harsh reaction conditions, which may not be suitable for all reactive functionalities. This is particularly true for the diphenyl ketimine groups which undergo rapid acid-promoted hydrolysis to their amine equivalents. These amino groups could potentially complicate subsequent complexation steps en route to higher-order assemblies.

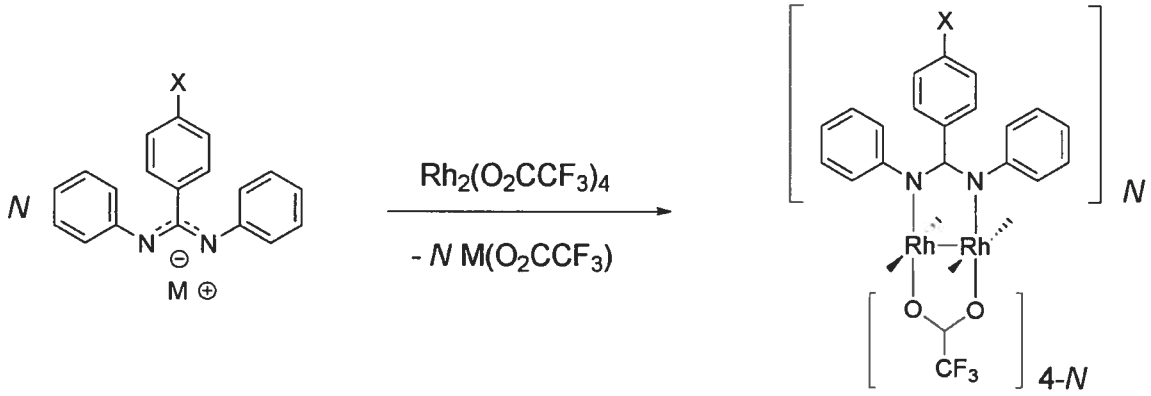

Scheme 6.2. Proposed formation of mixed amidinate / carboxylate Rh_2 complexes.

Alternatively, preparation of a dimeric complex of the form [Rh(COD)(amidinate)]$_2$ (where COD = cycloocta-1,5-diene) provides access to a mild and selective protocol for the preparation of *cis*-Rh_2(amidinate)$_2$(carboxylate)$_2$ complexes (Scheme 6.3).[11] The preparation of this precursor typically proceeds in a straightforward manner by reacting [Rh(COD)Cl]$_2$ with 2 equivalents of the amidinate salt.[12] Subsequent oxidation of this dimeric Rh(I) complex with an appropriate silver(I) salt yields the cis-

$Rh_2(amidinate)_2(carboxylate)_2$ complex in yields ranging from 50-60 % upon crystallization from the crude reaction mix. Considering that *N,N'*-diarylformamidines are most often utilized with this approach,[14] it is very likely that the *N,N'*-diphenylbenzamidine-based ligands described in Chapter 5 will be amenable to forming the desired *cis*-Rh_2 subunit (Scheme 6.3).

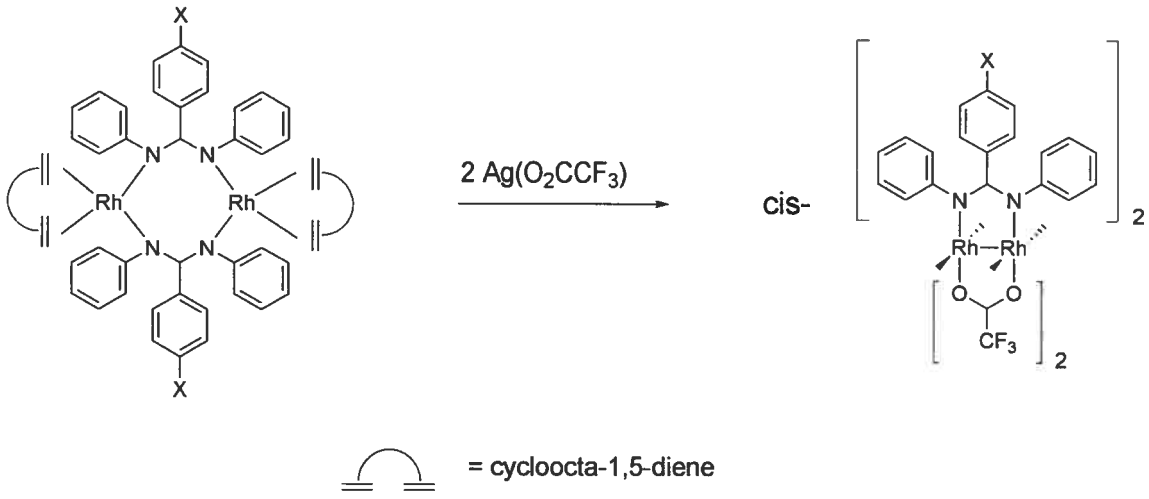

Scheme 6.3. Proposed route to selective *cis*-Rh_2 formation.

With such a *cis*-Rh_2 complex in hand, a true self-assembly approach can be used to arrive at structures analogous to those postulated by purely covalent means (Scheme 6.1). A wide range of conventional bridging ligands may be used, but we can take advantage of the dicarboxylate-Ru(II) complexes described in Chapter 3. An example is illustrated in Scheme 6.4, utilizing the triazine based complex **III-2b $(PF_6)_2$**. In addition, a wide variety of reactive functionality (X) may be incorporated via the amidinate ligands to the exterior of such an assembly. Particularly appealing are diphenyl ketimine groups, as this gives easy access to coupling photoactive units via amide bond formation, as demonstrated in Chapter 5. This gives an assembly with very high nuclearity and rigidity, the photophysical properties of which may be manipulated simply by selection of the photoactive groups incorporated.

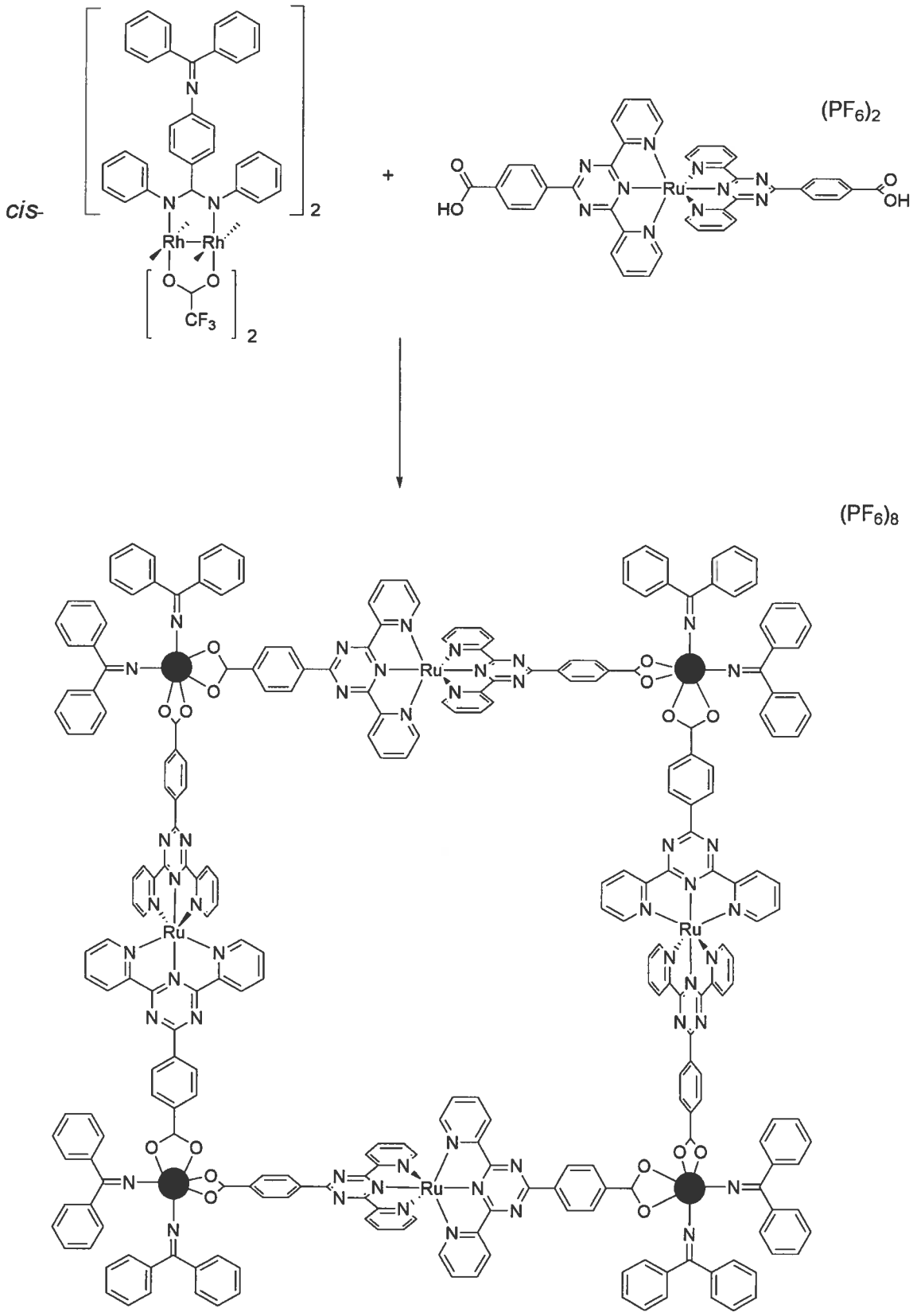

Scheme 6.4. Proposed self-assembly of a photoactive molecular square architecture.

6.5 References

1. Cayton, R. H.; Chisholm, M. H.; Huffman, J. C.; Lobkovsky, E. *J. Am. Chem. Soc.* **1991**, 113, 8709.
2. see, for example, Mines, G. A.; Tzeng, B.C.; Stevenson, K.J.; Li, J.; Hupp, J.T. *Angew. Chem. Intl. Ed.* **2002**, 41, 154.
3. a) Cotton, F. A.; Hillard, E. A.; Liu, C. Y.; Murillo, C. A.; Wang, W.; Wang, X. *Inorg. Chim. Acta* **2002**, 337, 233. b) Cotton, F. A.; Felthouse, T. R. *Inorg. Chem.* **1980**, 19, 323.
4. Cotton, F.A.; Walton, R. A. *Multiple Bonds Between Metal Atoms*, 3rd, ed., Wiley, New York, **1994**.
5. a) Clark, R. J. H.; West, D. J.; Withnall, R. *Inorg. Chem.* **1992**, 31, 456. b) Kawamura, T.; Fukamachi, K.; Sowa, T.; Hayashida, S.; Yonezawa, T. *J. Am. Chem. Soc.* **1981**, 103, 364.
6. a) Burdzinski, G. T.; Ramnauth, R.; Chisholm, M. H.; Gustafson, T. L. *J. Am. Chem. Soc.* **2006**, 128, 6776. b) Byrnes, M. J.; Chisholm, M. H.; Gallucci, J. A.; Liu, Y.; Ramnauth, R.; Turro, C. *J. Am. Chem. Soc.* **2005**, 127, 17344. c) Dequeant, M. Q.; Bradley, P. M.; Xu, G.-L.; Lutterman, D. A.; Turro, C.; Ren, T. *Inorg. Chem.* **2004**, 43, 7887.
7. a) Galoppini, E. *Coord. Chem. Rev.* **2004**, 248, 1283. b) Katoh, R.; Furube, A.; Barzykin, A. V.; Arakawa, H.; Tachiya, M. *Coord. Chem. Rev.* **2004**, 248, 1195. c) Durrant, J. R.; Haque, S. A.; Palomares, E. *Coord. Chem. Rev.* **2004**, 248, 1247.
8. Lutterman, D. A. ; Degtyareva, N. N. ; Johnston, D. H. ; Gallucci, J. C. ; Eglin, J. L. ; Turro, C. *Inorg. Chem.* **2005**, 44, 5388.
9. He, L.-P.; Yao, C.-L., Naris, M.; Lee, J. C.; Korp, J. D.; Bear, J. L. *Inorg. Chem.* **1992**, 31, 620.
10. see, for example, Cotton, F. A.; Liu, C. Y.; Murillo, C. A. *Inorg. Chem.* **2004**, 43, 2267.
11. Piraino, P.; Bruno, G.; Tresoldi, G.; Schiavo, S. L.; Zanello, P. *Inorg. Chem.* **1987**, 26, 91.
12. Piraino, P.; Tresoldi, G.; Faraone, F. *J. Organomet. Chem.* **1982**, 224, 305.

Appendix

Appendix 1: CCDC N°'s for compounds in chapter II.

The crystallographic reports and cif files of the structures listed below are available from the Cambridge Crystallographic Data Centre (CCDC) and may be downloaded electronically from the internet site: www.ccdc.cam.ac.uk/data_request/cif. Alternatively, requests can be made by email at the following address: data_request@ccdc.cam.ac.uk.

Chapter	Complex	CCDC N°
II	II-5a $\{C_{85}H_{66}B_2N_6O_2Ru\}$	653532
	II-5b $\{C_{69}H_{54}BF_6PN_{10}O_2Ru\}$	653531
	trans-II-2a $\{C_{130}H_{102}B_4F_8N_{14}O_8Rh_2Ru_2\}$	252629

Appendix 2: Supplementary information for chapter II

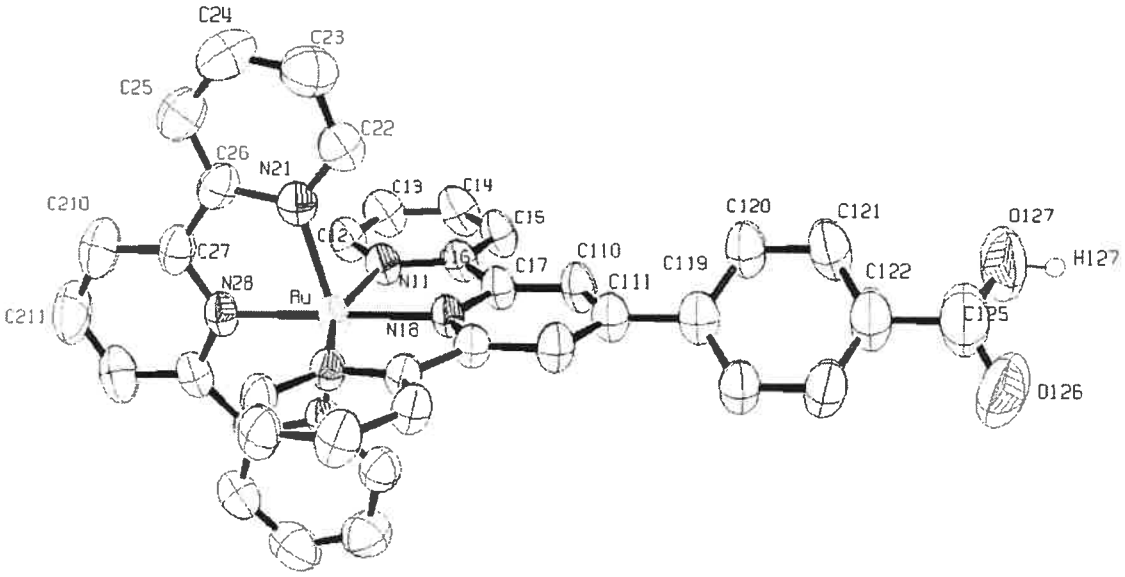

Table 1. Crystal data and structure refinement for **II-5a.**

Empirical formula	C85 H66 B2 N6 O2 Ru
Formula weight	1326.13
Temperature	220(2)K
Wavelength	1.54178 Å
Crystal system	Monoclinic
Space group	C2/c
Unit cell dimensions	a = 21.3875(6) Å α = 90° b = 22.6852(5) Å β = 91.494(2)° c = 18.1795(5) Å γ = 90°
Volume	8817.3(4)Å^3
Z	4
Density (calculated)	0.999 g/cm^3
Absorption coefficient	1.765 mm^{-1}
F(000)	2752
Crystal size	0.30 x 0.28 x 0.23 mm

Theta range for data collection	2.84 to 72.88°
Index ranges	$-26 \leq h \leq 26$, $-28 \leq k \leq 27$, $-22 \leq \ell \leq 22$
Reflections collected	53589
Independent reflections	8738 [R_{int} = 0.041]
Absorption correction	Semi-empirical from equivalents
Max. and min. transmission	0.6900 and 0.5000
Refinement method	Full-matrix least-squares on F^2
Data / restraints / parameters	8738 / 338 / 446
Goodness-of-fit on F^2	0.954
Final R indices [I>2sigma(I)]	R_1 = 0.0466, wR_2 = 0.1136
R indices (all data)	R_1 = 0.0549, wR_2 = 0.1163
Largest diff. peak and hole	1.305 and -0.384 e/Å^3

Table 2. Bond lengths [Å] and angles [°]for **II-5a**.

Ru-N(18)	1.979(2)	C(22)-C(23)	1.373(4)
Ru-N(28)	1.989(2)	C(22)-H(22)	0.94
Ru-N(21)#1	2.065(2)	C(23)-C(24)	1.387(4)
Ru-N(21)	2.065(2)	C(23)-H(23)	0.94
Ru-N(11)	2.0755(17)	C(24)-C(25)	1.363(4)
Ru-N(11)#1	2.0755(17)	C(24)-H(24)	0.94
N(11)-C(12)	1.337(3)	C(25)-C(26)	1.374(4)
N(11)-C(16)	1.368(3)	C(25)-H(25)	0.94
N(18)-C(17)	1.348(2)	C(26)-C(27)	1.472(3)
N(18)-C(17)#1	1.348(2)	C(27)-C(210)	1.388(3)
N(21)-C(22)	1.344(3)	C(110)-C(111)	1.403(3)
N(21)-C(26)	1.368(3)	C(110)-H(110)	0.94
N(28)-C(27)#1	1.339(3)	C(111)-C(110)#1	1.403(3)
N(28)-C(27)	1.339(3)	C(111)-C(119)	1.466(5)
C(12)-C(13)	1.375(3)	C(119)-C(120)	1.399(3)
C(12)-H(12)	0.94	C(119)-C(120)#1	1.399(3)
C(13)-C(14)	1.381(3)	C(120)-C(121)	1.379(4)
C(13)-H(13)	0.94	C(120)-H(120)	0.94
C(14)-C(15)	1.376(3)	C(121)-C(122)	1.388(4)
C(14)-H(14)	0.94	C(121)-H(121)	0.94
C(15)-C(16)	1.387(3)	C(122)-C(121)#1	1.388(4)
C(15)-H(15)	0.94	C(122)-C(125)	1.482(6)
C(16)-C(17)	1.468(3)	C(125)-O(126)#1	1.280(4)
C(17)-C(110)	1.386(3)	C(125)-O(126)	1.280(4)
		C(125)-O(127)	1.405(4)

C(125)-O(127)#1	1.405(4)
O(127)-H(127)	0.83
C(210)-C(211)	1.368(4)
C(210)-H(210)	0.94
C(211)-C(210)#1	1.368(4)
C(211)-H(211)	0.94
B(3)-C(51)	1.641(3)
B(3)-C(31)	1.650(3)
B(3)-C(61)	1.650(4)
B(3)-C(41)	1.652(3)
C(31)-C(36)	1.390(3)
C(31)-C(32)	1.393(4)
C(32)-C(33)	1.391(4)
C(32)-H(32)	0.94
C(33)-C(34)	1.366(5)
C(33)-H(33)	0.94
C(34)-C(35)	1.374(5)
C(34)-H(34)	0.94
C(35)-C(36)	1.384(4)
C(35)-H(35)	0.94
C(36)-H(36)	0.94
C(41)-C(46)	1.393(4)
C(41)-C(42)	1.395(4)
C(42)-C(43)	1.402(4)
C(42)-H(42)	0.94
C(43)-C(44)	1.359(5)
C(43)-H(43)	0.94
C(44)-C(45)	1.376(6)
C(44)-H(44)	0.94
C(45)-C(46)	1.396(4)
C(45)-H(45)	0.94
C(46)-H(46)	0.94
C(51)-C(56)	1.399(3)
C(51)-C(52)	1.401(3)
C(52)-C(53)	1.386(3)
C(52)-H(52)	0.94
C(53)-C(54)	1.380(4)
C(53)-H(53)	0.94
C(54)-C(55)	1.361(4)
C(54)-H(54)	0.94
C(55)-C(56)	1.384(4)
C(55)-H(55)	0.94
C(56)-H(56)	0.94
C(61)-C(66)	1.396(3)
C(61)-C(62)	1.407(3)
C(62)-C(63)	1.372(4)
C(62)-H(62)	0.94
C(63)-C(64)	1.359(5)
C(63)-H(63)	0.94
C(64)-C(65)	1.385(5)
C(64)-H(64)	0.94
C(65)-C(66)	1.372(4)
C(65)-H(65)	0.94
C(66)-H(66)	0.94
N(18)-RU-N(28)	180
N(18)-RU-N(21)#1	101.16(5)
N(28)-RU-N(21)#1	78.84(5)
N(18)-RU-N(21)	101.16(5)
N(28)-RU-N(21)	78.84(5)
N(21)#1-RU-N(21)	157.68(11)
N(18)-RU-N(11)	78.88(5)
N(28)-RU-N(11)	101.12(5)
N(21)#1-RU-N(11)	92.92(7)
N(21)-RU-N(11)	91.36(7)
N(18)-RU-N(11)#1	78.88(5)
N(28)-RU-N(11)#1	101.12(5)
N(21)#1-RU-N(11)#1	91.36(7)
N(21)-RU-N(11)#1	92.92(7)
N(11)-RU-N(11)#1	157.76(10)
C(12)-N(11)-C(16)	118.90(19)
C(12)-N(11)-RU	127.25(16)
C(16)-N(11)-RU	113.81(13)
C(17)-N(18)-C(17)#1	121.9(2)
C(17)-N(18)-RU	119.03(12)
C(17)#1-N(18)-RU	119.03(12)
C(22)-N(21)-C(26)	117.4(2)
C(22)-N(21)-RU	127.92(18)
C(26)-N(21)-RU	114.62(17)
C(27)#1-N(28)-C(27)	123.0(3)
C(27)#1-N(28)-RU	118.49(14)
C(27)-N(28)-RU	118.49(14)
N(11)-C(12)-C(13)	122.3(2)
N(11)-C(12)-H(12)	118.9
C(13)-C(12)-H(12)	118.9
C(12)-C(13)-C(14)	119.2(2)
C(12)-C(13)-H(13)	120.4
C(14)-C(13)-H(13)	120.4
C(15)-C(14)-C(13)	119.3(2)
C(15)-C(14)-H(14)	120.4
C(13)-C(14)-H(14)	120.4
C(14)-C(15)-C(16)	119.4(2)
C(14)-C(15)-H(15)	120.3
C(16)-C(15)-H(15)	120.3
N(11)-C(16)-C(15)	120.88(19)
N(11)-C(16)-C(17)	114.96(17)
C(15)-C(16)-C(17)	124.15(19)
N(18)-C(17)-C(110)	119.97(19)
N(18)-C(17)-C(16)	113.17(18)
C(110)-C(17)-C(16)	126.85(18)
N(21)-C(22)-C(23)	122.6(3)
N(21)-C(22)-H(22)	118.7
C(23)-C(22)-H(22)	118.7
C(22)-C(23)-C(24)	119.2(3)
C(22)-C(23)-H(23)	120.4
C(24)-C(23)-H(23)	120.4
C(25)-C(24)-C(23)	118.9(3)
C(25)-C(24)-H(24)	120.5
C(23)-C(24)-H(24)	120.5
C(24)-C(25)-C(26)	119.7(3)
C(24)-C(25)-H(25)	120.2
C(26)-C(25)-H(25)	120.2
N(21)-C(26)-C(25)	122.1(3)
N(21)-C(26)-C(27)	114.1(2)

C(25)-C(26)-C(27)	123.9(2)
N(28)-C(27)-C(210)	118.8(3)
N(28)-C(27)-C(26)	113.9(2)
C(210)-C(27)-C(26)	127.3(3)
C(17)-C(110)-C(111)	120.1(2)
C(17)-C(110)-H(110)	119.9
C(111)-C(110)-H(110)	119.9
C(110)#1-C(111)-C(110)	117.9(3)
C(110)#1-C(111)-C(119)	121.07(15)
C(110)-C(111)-C(119)	121.07(15)
C(120)-C(119)-C(120)#1	117.9(3)
C(120)-C(119)-C(111)	121.03(17)
C(120)#1-C(119)-C(111)	121.03(17)
C(121)-C(120)-C(119)	121.3(3)
C(121)-C(120)-H(120)	119.4
C(119)-C(120)-H(120)	119.4
C(120)-C(121)-C(122)	119.6(3)
C(120)-C(121)-H(121)	120.2
C(122)-C(121)-H(121)	120.2
C(121)#1-C(122)-C(121)	120.4(4)
C(121)#1-C(122)-C(125)	119.81(19)
C(121)-C(122)-C(125)	119.81(19)
O(126)-C(125)-O(127)	109.5(5)
O(126)#1-C(125)-O(127)#	109.5(5)
O(126)#1-C(125)-C(122)	118.7(4)
O(126)-C(125)-C(122)	118.7(4)
O(127)-C(125)-C(122)	115.0(4)
O(127)#1-C(125)-C(122)	115.0(4)
C(125)-O(127)-H(127)	109.5
C(211)-C(210)-C(27)	119.8(3)
C(211)-C(210)-H(210)	120.1
C(27)-C(210)-H(210)	120.1
C(210)-C(211)-C(210)#1	119.9(4)
C(210)-C(211)-H(211)	120.1
C(210)#1-C(211)-H(211)	120.1
C(51)-B(3)-C(31)	111.1(2)
C(51)-B(3)-C(61)	104.58(18)
C(31)-B(3)-C(61)	113.9(2)
C(51)-B(3)-C(41)	112.8(2)
C(31)-B(3)-C(41)	103.85(18)
C(61)-B(3)-C(41)	110.9(2)
C(36)-C(31)-C(32)	114.5(2)
C(36)-C(31)-B(3)	124.2(2)
C(32)-C(31)-B(3)	121.2(2)
C(33)-C(32)-C(31)	123.0(3)
C(33)-C(32)-H(32)	118.5
C(31)-C(32)-H(32)	118.5
C(34)-C(33)-C(32)	120.5(3)
C(34)-C(33)-H(33)	119.8
C(32)-C(33)-H(33)	119.8
C(33)-C(34)-C(35)	118.4(3)
C(33)-C(34)-H(34)	120.8
C(35)-C(34)-H(34)	120.8
C(34)-C(35)-C(36)	120.6(3)
C(34)-C(35)-H(35)	119.7
C(36)-C(35)-H(35)	119.7
C(35)-C(36)-C(31)	123.1(3)
C(35)-C(36)-H(36)	118.5
C(31)-C(36)-H(36)	118.5
C(46)-C(41)-C(42)	115.3(3)
C(46)-C(41)-B(3)	121.9(3)
C(42)-C(41)-B(3)	122.6(2)
C(41)-C(42)-C(43)	122.3(3)
C(41)-C(42)-H(42)	118.9
C(43)-C(42)-H(42)	118.9
C(44)-C(43)-C(42)	120.3(4)
C(44)-C(43)-H(43)	119.9
C(42)-C(43)-H(43)	119.9
C(43)-C(44)-C(45)	119.6(3)
C(43)-C(44)-H(44)	120.2
C(45)-C(44)-H(44)	120.2
C(44)-C(45)-C(46)	119.7(4)
C(44)-C(45)-H(45)	120.1
C(46)-C(45)-H(45)	120.1
C(41)-C(46)-C(45)	122.8(3)
C(41)-C(46)-H(46)	118.6
C(45)-C(46)-H(46)	118.6
C(56)-C(51)-C(52)	114.7(2)
C(56)-C(51)-B(3)	124.2(2)
C(52)-C(51)-B(3)	120.9(2)
C(53)-C(52)-C(51)	122.9(2)
C(53)-C(52)-H(52)	118.5
C(51)-C(52)-H(52)	118.5
C(54)-C(53)-C(52)	120.0(3)
C(54)-C(53)-H(53)	120
C(52)-C(53)-H(53)	120
C(55)-C(54)-C(53)	119.0(3)
C(55)-C(54)-H(54)	120.5
C(53)-C(54)-H(54)	120.5
C(54)-C(55)-C(56)	120.9(3)
C(54)-C(55)-H(55)	119.6
C(56)-C(55)-H(55)	119.6
C(55)-C(56)-C(51)	122.6(3)
C(55)-C(56)-H(56)	118.7
C(51)-C(56)-H(56)	118.7
C(66)-C(61)-C(62)	114.4(3)
C(66)-C(61)-B(3)	122.3(2)
C(62)-C(61)-B(3)	123.0(2)
C(63)-C(62)-C(61)	122.5(3)
C(63)-C(62)-H(62)	118.7
C(61)-C(62)-H(62)	118.7
C(64)-C(63)-C(62)	121.2(3)
C(64)-C(63)-H(63)	119.4
C(62)-C(63)-H(63)	119.4
C(63)-C(64)-C(65)	118.4(3)
C(63)-C(64)-H(64)	120.8
C(65)-C(64)-H(64)	120.8
C(66)-C(65)-C(64)	120.3(3)
C(66)-C(65)-H(65)	119.9
C(64)-C(65)-H(65)	119.9
C(65)-C(66)-C(61)	123.1(3)
C(65)-C(66)-H(66)	118.4
C(61)-C(66)-H(66)	118.4

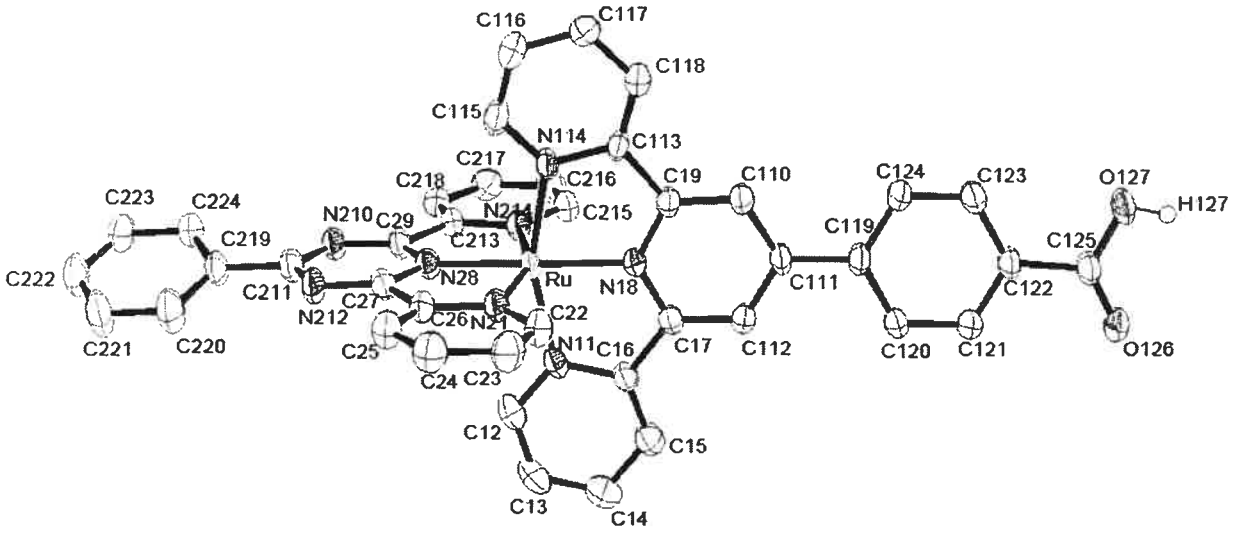

Table 1. Crystal data and structure refinement for **II-5b**.

Empirical formula	C69 H54 B F6 N10 O2 P Ru
Formula weight	1312.07
Temperature	220(2)K
Wavelength	1.54178 Å
Crystal system	Triclinic
Space group	P-1
Unit cell dimensions	a = 12.9474(3) Å α = 90.348(2)° b = 13.3066(3) Å β = 93.154(1)° c = 19.1280(4) Å γ = 110.644(1)°
Volume	3078.06(12)Å^3
Z	2
Density (calculated)	1.416 g/cm^3
Absorption coefficient	2.923 mm^{-1}
F(000)	1344
Crystal size	0.55 x 0.36 x 0.24 mm
Theta range for data collection	2.31 to 72.89°

Index ranges	$-16 \leq h \leq 15$, $-16 \leq k \leq 16$, $-23 \leq \ell \leq 23$
Reflections collected	37359
Independent reflections	11773 [R_{int} = 0.041]
Absorption correction	Semi-empirical from equivalents
Max. and min. transmission	0.6200 and 0.3800
Refinement method	Full-matrix least-squares on F^2
Data / restraints / parameters	11773 / 14 / 813
Goodness-of-fit on F^2	0.990
Final R indices [I>2sigma(I)]	R_1 = 0.0536, wR_2 = 0.1361
R indices (all data)	R_1 = 0.0662, wR_2 = 0.1437
Largest diff. peak and hole	1.304 and -0.642 e/Å^3

Table 2. Bond lengths [Å] and angles [°] for **II-5b**.

Ru-N(28)	1.975(3)	C(113)-N(114)	1.384(4)
Ru-N(18)	1.980(2)	N(114)-C(115)	1.345(4)
Ru-N(114)	2.063(3)	C(115)-C(116)	1.360(5)
Ru-N(11)	2.085(3)	C(115)-H(115)	0.94
Ru-N(214)	2.089(3)	C(116)-C(117)	1.388(5)
Ru-N(21)	2.092(3)	C(116)-H(116)	0.94
N(11)-C(12)	1.341(4)	C(117)-C(118)	1.381(5)
N(11)-C(16)	1.368(4)	C(117)-H(117)	0.94
C(12)-C(13)	1.369(5)	C(118)-H(118)	0.94
C(12)-H(12)	0.94	C(119)-C(120)	1.393(5)
C(13)-C(14)	1.374(6)	C(119)-C(124)	1.399(5)
C(13)-H(13)	0.94	C(120)-C(121)	1.381(4)
C(14)-C(15)	1.393(5)	C(120)-H(120)	0.94
C(14)-H(14)	0.94	C(121)-C(122)	1.377(5)
C(15)-C(16)	1.373(5)	C(121)-H(121)	0.94
C(15)-H(15)	0.94	C(122)-C(123)	1.386(5)
C(16)-C(17)	1.476(4)	C(122)-C(125)	1.487(4)
C(17)-N(18)	1.352(4)	C(123)-C(124)	1.386(4)
C(17)-C(112)	1.385(4)	C(123)-H(123)	0.94
N(18)-C(19)	1.356(4)	C(124)-H(124)	0.94
C(19)-C(110)	1.384(4)	C(125)-O(126)	1.2125(10)
C(19)-C(113)	1.475(4)	C(125)-O(127)	1.3083(10)
C(110)-C(111)	1.402(4)	O(127)-H(127)	0.83
C(110)-H(110)	0.94	N(21)-C(22)	1.339(4)
C(111)-C(112)	1.405(4)	N(21)-C(26)	1.378(4)
C(111)-C(119)	1.481(4)	C(22)-C(23)	1.371(5)
C(112)-H(112)	0.94	C(22)-H(22)	0.94
C(113)-C(118)	1.376(5)	C(23)-C(24)	1.373(5)

C(23)-H(23)	0.94	C(44)-H(44)	0.94
C(24)-C(25)	1.394(5)	C(45)-C(46)	1.382(5)
C(24)-H(24)	0.94	C(45)-H(45)	0.94
C(25)-C(26)	1.372(5)	C(46)-H(46)	0.94
C(25)-H(25)	0.94	C(51)-C(56)	1.398(5)
C(26)-C(27)	1.469(5)	C(51)-C(52)	1.399(5)
C(27)-N(212)	1.313(4)	C(52)-C(53)	1.374(6)
C(27)-N(28)	1.348(4)	C(52)-H(52)	0.94
N(28)-C(29)	1.337(4)	C(53)-C(54)	1.384(8)
C(29)-N(210)	1.316(4)	C(53)-H(53)	0.94
C(29)-C(213)	1.475(4)	C(54)-C(55)	1.369(7)
N(210)-C(211)	1.357(4)	C(54)-H(54)	0.94
C(211)-N(212)	1.359(4)	C(55)-C(56)	1.404(5)
C(211)-C(219)	1.471(4)	C(55)-H(55)	0.94
C(213)-N(214)	1.371(4)	C(56)-H(56)	0.94
C(213)-C(218)	1.373(5)	C(61)-C(66)	1.401(5)
N(214)-C(215)	1.346(4)	C(61)-C(62)	1.405(5)
C(215)-C(216)	1.380(5)	C(62)-C(63)	1.399(5)
C(215)-H(215)	0.94	C(62)-H(62)	0.94
C(216)-C(217)	1.380(5)	C(63)-C(64)	1.372(6)
C(216)-H(216)	0.94	C(63)-H(63)	0.94
C(217)-C(218)	1.391(5)	C(64)-C(65)	1.376(6)
C(217)-H(217)	0.94	C(64)-H(64)	0.94
C(218)-H(218)	0.94	C(65)-C(66)	1.390(5)
C(219)-C(224)	1.382(5)	C(65)-H(65)	0.94
C(219)-C(220)	1.387(5)	C(66)-H(66)	0.94
C(220)-C(221)	1.381(5)	P-F(6)	1.541(3)
C(220)-H(220)	0.94	P-F(2)	1.565(3)
C(221)-C(222)	1.372(6)	P-F(3)	1.566(3)
C(221)-H(221)	0.94	P-F(4)	1.566(3)
C(222)-C(223)	1.369(5)	P-F(5)	1.571(3)
C(222)-H(222)	0.94	P-F(1)	1.592(3)
C(223)-C(224)	1.387(4)	N(71)-C(72)	1.111(6)
C(223)-H(223)	0.94	C(72)-C(73)	1.459(8)
C(224)-H(224)	0.94	C(73)-H(73a)	0.97
B(3)-C(61)	1.641(5)	C(73)-H(73b)	0.97
B(3)-C(31)	1.649(5)	C(73)-H(73c)	0.97
B(3)-C(41)	1.653(5)	N(81)-C(82)	1.104(6)
B(3)-C(51)	1.655(5)	C(82)-C(83)	1.461(7)
C(31)-C(32)	1.382(5)	C(83)-H(83a)	0.97
C(31)-C(36)	1.401(5)	C(83)-H(83b)	0.97
C(32)-C(33)	1.384(5)	C(83)-H(83c)	0.97
C(32)-H(32)	0.94		
C(33)-C(34)	1.370(6)	N(28)-RU-N(18)	178.18(11)
C(33)-H(33)	0.94	N(28)-RU-N(114)	100.89(10)
C(34)-C(35)	1.385(6)	N(18)-RU-N(114)	78.81(10)
C(34)-H(34)	0.94	N(28)-RU-N(11)	101.43(11)
C(35)-C(36)	1.384(5)	N(18)-RU-N(11)	78.98(10)
C(35)-H(35)	0.94	N(114)-RU-N(11)	157.48(10)
C(36)-H(36)	0.94	N(28)-RU-N(214)	77.74(10)
C(41)-C(46)	1.386(5)	N(18)-RU-N(214)	100.48(10)
C(41)-C(42)	1.396(5)	N(114)-RU-N(214)	94.48(11)
C(42)-C(43)	1.396(6)	N(11)-RU-N(214)	93.11(11)
C(42)-H(42)	0.94	N(28)-RU-N(21)	78.08(10)
C(43)-C(44)	1.365(6)	N(18)-RU-N(21)	103.69(10)
C(43)-H(43)	0.94	N(114)-RU-N(21)	89.95(11)
C(44)-C(45)	1.377(6)	N(11)-RU-N(21)	91.74(11)

N(214)-RU-N(21)	155.83(10)	C(124)-C(119)-C(111)	122.0(3)
C(12)-N(11)-C(16)	118.7(3)	C(121)-C(120)-C(119)	121.0(3)
C(12)-N(11)-RU	127.5(2)	C(121)-C(120)-H(120)	119.5
C(16)-N(11)-RU	113.6(2)	C(119)-C(120)-H(120)	119.5
N(11)-C(12)-C(13)	122.1(3)	C(122)-C(121)-C(120)	121.0(3)
N(11)-C(12)-H(12)	118.9	C(122)-C(121)-H(121)	119.5
C(13)-C(12)-H(12)	118.9	C(120)-C(121)-H(121)	119.5
C(12)-C(13)-C(14)	119.9(3)	C(121)-C(122)-C(123)	118.9(3)
C(12)-C(13)-H(13)	120	C(121)-C(122)-C(125)	118.1(3)
C(14)-C(13)-H(13)	120	C(123)-C(122)-C(125)	123.0(3)
C(13)-C(14)-C(15)	118.5(4)	C(124)-C(123)-C(122)	120.7(3)
C(13)-C(14)-H(14)	120.8	C(124)-C(123)-H(123)	119.7
C(15)-C(14)-H(14)	120.8	C(122)-C(123)-H(123)	119.7
C(16)-C(15)-C(14)	119.6(3)	C(123)-C(124)-C(119)	120.7(3)
C(16)-C(15)-H(15)	120.2	C(123)-C(124)-H(124)	119.7
C(14)-C(15)-H(15)	120.2	C(119)-C(124)-H(124)	119.7
N(11)-C(16)-C(15)	121.1(3)	O(126)-C(125)-O(127)	124.0(3)
N(11)-C(16)-C(17)	115.2(3)	O(126)-C(125)-C(122)	120.5(2)
C(15)-C(16)-C(17)	123.7(3)	O(127)-C(125)-C(122)	115.4(2)
N(18)-C(17)-C(112)	120.0(3)	C(125)-O(127)-H(127)	109.5
N(18)-C(17)-C(16)	112.9(3)	C(22)-N(21)-C(26)	118.0(3)
C(112)-C(17)-C(16)	127.0(3)	C(22)-N(21)-RU	128.0(2)
C(17)-N(18)-C(19)	121.5(3)	C(26)-N(21)-RU	113.9(2)
C(17)-N(18)-RU	119.1(2)	N(21)-C(22)-C(23)	122.1(3)
C(19)-N(18)-RU	119.3(2)	N(21)-C(22)-H(22)	118.9
N(18)-C(19)-C(110)	120.0(3)	C(23)-C(22)-H(22)	118.9
N(18)-C(19)-C(113)	113.0(3)	C(22)-C(23)-C(24)	120.3(3)
C(110)-C(19)-C(113)	127.0(3)	C(22)-C(23)-H(23)	119.8
C(19)-C(110)-C(111)	120.3(3)	C(24)-C(23)-H(23)	119.8
C(19)-C(110)-H(110)	119.8	C(23)-C(24)-C(25)	118.5(3)
C(111)-C(110)-H(110)	119.8	C(23)-C(24)-H(24)	120.7
C(110)-C(111)-C(112)	117.7(3)	C(25)-C(24)-H(24)	120.7
C(110)-C(111)-C(119)	122.1(3)	C(26)-C(25)-C(24)	119.1(3)
C(112)-C(111)-C(119)	120.2(3)	C(26)-C(25)-H(25)	120.5
C(17)-C(112)-C(111)	120.3(3)	C(24)-C(25)-H(25)	120.5
C(17)-C(112)-H(112)	119.8	C(25)-C(26)-N(21)	121.9(3)
C(111)-C(112)-H(112)	119.8	C(25)-C(26)-C(27)	123.3(3)
C(118)-C(113)-N(114)	120.7(3)	N(21)-C(26)-C(27)	114.8(3)
C(118)-C(113)-C(19)	125.2(3)	N(212)-C(27)-N(28)	123.1(3)
N(114)-C(113)-C(19)	114.0(3)	N(212)-C(27)-C(26)	124.4(3)
C(115)-N(114)-C(113)	117.9(3)	N(28)-C(27)-C(26)	112.5(3)
C(115)-N(114)-RU	127.2(2)	C(29)-N(28)-C(27)	118.4(3)
C(113)-N(114)-RU	114.8(2)	C(29)-N(28)-RU	121.0(2)
N(114)-C(115)-C(116)	123.2(3)	C(27)-N(28)-RU	120.6(2)
N(114)-C(115)-H(115)	118.4	N(210)-C(29)-N(28)	122.9(3)
C(116)-C(115)-H(115)	118.4	N(210)-C(29)-C(213)	124.8(3)
C(115)-C(116)-C(117)	119.3(3)	N(28)-C(29)-C(213)	112.4(3)
C(115)-C(116)-H(116)	120.3	C(29)-N(210)-C(211)	115.4(3)
C(117)-C(116)-H(116)	120.3	N(210)-C(211)-N(212)	125.0(3)
C(118)-C(117)-C(116)	118.7(3)	N(210)-C(211)-C(219)	117.6(3)
C(118)-C(117)-H(117)	120.7	N(212)-C(211)-C(219)	117.4(3)
C(116)-C(117)-H(117)	120.7	C(27)-N(212)-C(211)	115.1(3)
C(113)-C(118)-C(117)	120.1(3)	N(214)-C(213)-C(218)	122.3(3)
C(113)-C(118)-H(118)	119.9	N(214)-C(213)-C(29)	114.5(3)
C(117)-C(118)-H(118)	119.9	C(218)-C(213)-C(29)	123.2(3)
C(120)-C(119)-C(124)	117.8(3)	C(215)-N(214)-C(213)	117.7(3)
C(120)-C(119)-C(111)	120.2(3)	C(215)-N(214)-RU	127.9(2)

C(213)-N(214)-RU	114.4(2)
N(214)-C(215)-C(216)	122.3(3)
N(214)-C(215)-H(215)	118.8
C(216)-C(215)-H(215)	118.8
C(215)-C(216)-C(217)	120.0(3)
C(215)-C(216)-H(216)	120
C(217)-C(216)-H(216)	120
C(216)-C(217)-C(218)	118.4(3)
C(216)-C(217)-H(217)	120.8
C(218)-C(217)-H(217)	120.8
C(213)-C(218)-C(217)	119.4(3)
C(213)-C(218)-H(218)	120.3
C(217)-C(218)-H(218)	120.3
C(224)-C(219)-C(220)	119.6(3)
C(224)-C(219)-C(211)	120.0(3)
C(220)-C(219)-C(211)	120.4(3)
C(221)-C(220)-C(219)	119.8(4)
C(221)-C(220)-H(220)	120.1
C(219)-C(220)-H(220)	120.1
C(222)-C(221)-C(220)	120.2(4)
C(222)-C(221)-H(221)	119.9
C(220)-C(221)-H(221)	119.9
C(223)-C(222)-C(221)	120.3(3)
C(223)-C(222)-H(222)	119.8
C(221)-C(222)-H(222)	119.8
C(222)-C(223)-C(224)	120.1(4)
C(222)-C(223)-H(223)	120
C(224)-C(223)-H(223)	120
C(219)-C(224)-C(223)	119.9(3)
C(219)-C(224)-H(224)	120
C(223)-C(224)-H(224)	120
C(61)-B(3)-C(31)	110.1(3)
C(61)-B(3)-C(41)	110.7(3)
C(31)-B(3)-C(41)	108.6(3)
C(61)-B(3)-C(51)	109.6(3)
C(31)-B(3)-C(51)	109.2(3)
C(41)-B(3)-C(51)	108.6(3)
C(32)-C(31)-C(36)	114.7(3)
C(32)-C(31)-B(3)	123.4(3)
C(36)-C(31)-B(3)	121.8(3)
C(31)-C(32)-C(33)	123.0(4)
C(31)-C(32)-H(32)	118.5
C(33)-C(32)-H(32)	118.5
C(34)-C(33)-C(32)	120.8(4)
C(34)-C(33)-H(33)	119.6
C(32)-C(33)-H(33)	119.6
C(33)-C(34)-C(35)	118.5(4)
C(33)-C(34)-H(34)	120.8
C(35)-C(34)-H(34)	120.8
C(36)-C(35)-C(34)	119.8(4)
C(36)-C(35)-H(35)	120.1
C(34)-C(35)-H(35)	120.1
C(35)-C(36)-C(31)	123.2(4)
C(35)-C(36)-H(36)	118.4
C(31)-C(36)-H(36)	118.4
C(46)-C(41)-C(42)	114.4(4)
C(46)-C(41)-B(3)	124.4(3)
C(42)-C(41)-B(3)	121.2(3)
C(41)-C(42)-C(43)	122.6(4)
C(41)-C(42)-H(42)	118.7
C(43)-C(42)-H(42)	118.7
C(44)-C(43)-C(42)	120.4(4)
C(44)-C(43)-H(43)	119.8
C(42)-C(43)-H(43)	119.8
C(43)-C(44)-C(45)	118.8(4)
C(43)-C(44)-H(44)	120.6
C(45)-C(44)-H(44)	120.6
C(44)-C(45)-C(46)	119.9(4)
C(44)-C(45)-H(45)	120.1
C(46)-C(45)-H(45)	120.1
C(45)-C(46)-C(41)	123.8(4)
C(45)-C(46)-H(46)	118.1
C(41)-C(46)-H(46)	118.1
C(56)-C(51)-C(52)	115.1(4)
C(56)-C(51)-B(3)	124.0(3)
C(52)-C(51)-B(3)	120.8(4)
C(53)-C(52)-C(51)	122.9(5)
C(53)-C(52)-H(52)	118.6
C(51)-C(52)-H(52)	118.6
C(52)-C(53)-C(54)	120.6(5)
C(52)-C(53)-H(53)	119.7
C(54)-C(53)-H(53)	119.7
C(55)-C(54)-C(53)	118.9(5)
C(55)-C(54)-H(54)	120.5
C(53)-C(54)-H(54)	120.5
C(54)-C(55)-C(56)	120.0(5)
C(54)-C(55)-H(55)	120
C(56)-C(55)-H(55)	120
C(51)-C(56)-C(55)	122.4(4)
C(51)-C(56)-H(56)	118.8
C(55)-C(56)-H(56)	118.8
C(66)-C(61)-C(62)	114.1(3)
C(66)-C(61)-B(3)	123.7(3)
C(62)-C(61)-B(3)	122.1(3)
C(63)-C(62)-C(61)	123.3(4)
C(63)-C(62)-H(62)	118.3
C(61)-C(62)-H(62)	118.3
C(64)-C(63)-C(62)	119.6(4)
C(64)-C(63)-H(63)	120.2
C(62)-C(63)-H(63)	120.2
C(63)-C(64)-C(65)	119.5(4)
C(63)-C(64)-H(64)	120.2
C(65)-C(64)-H(64)	120.2
C(64)-C(65)-C(66)	120.1(4)
C(64)-C(65)-H(65)	119.9
C(66)-C(65)-H(65)	119.9
C(65)-C(66)-C(61)	123.3(4)
C(65)-C(66)-H(66)	118.3
C(61)-C(66)-H(66)	118.3
F(6)-P-F(2)	90.3(2)
F(6)-P-F(3)	92.1(2)
F(2)-P-F(3)	89.8(2)
F(6)-P-F(4)	92.1(2)
F(2)-P-F(4)	177.6(2)

F(3)-P-F(4)	89.6(2)
F(6)-P-F(5)	91.2(2)
F(2)-P-F(5)	89.6(2)
F(3)-P-F(5)	176.7(2)
F(4)-P-F(5)	90.8(2)
F(6)-P-F(1)	177.2(2)
F(2)-P-F(1)	92.3(2)
F(3)-P-F(1)	88.9(2)
F(4)-P-F(1)	85.4(2)
F(5)-P-F(1)	87.9(2)
N(71)-C(72)-C(73)	177.9(9)
C(72)-C(73)-H(73A)	109.5
C(72)-C(73)-H(73B)	109.5
H(73A)-C(73)-H(73B)	109.5
C(72)-C(73)-H(73C)	109.5
H(73A)-C(73)-H(73C)	109.5
H(73B)-C(73)-H(73C)	109.5
N(81)-C(82)-C(83)	178.9(8)
C(82)-C(83)-H(83A)	109.5
C(82)-C(83)-H(83B)	109.5
H(83A)-C(83)-H(83B)	109.5
C(82)-C(83)-H(83C)	109.5
H(83A)-C(83)-H(83C)	109.5
H(83B)-C(83)-H(83C)	109.5

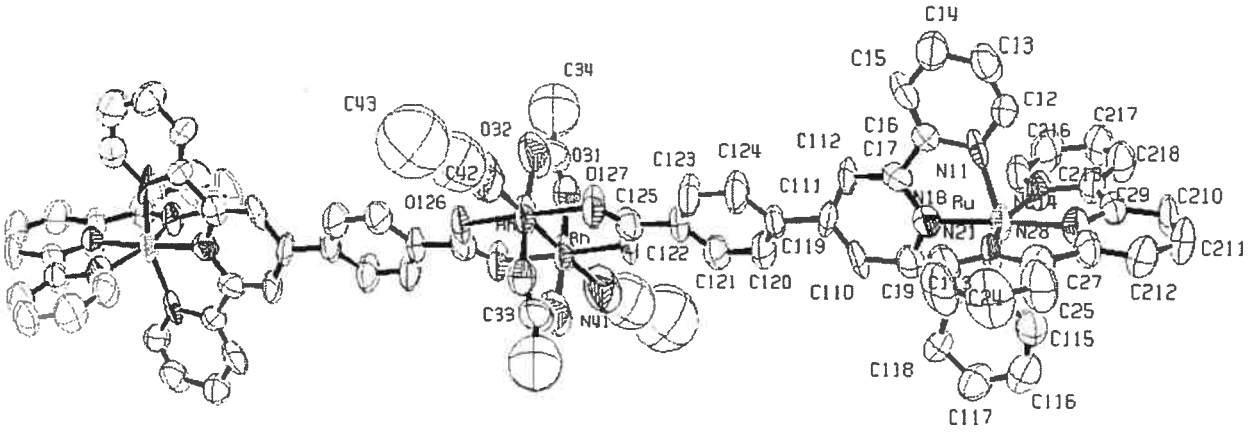

Table 1. Crystal data and structure refinement for ***trans*-II-2a**.

Empirical formula	C130 H102 B4 F8 N14 O8 Rh2 Ru2
Formula weight	2591.46
Temperature	220(2)K
Wavelength	1.54178 Å
Crystal system	Triclinic
Space group	P-1
Unit cell dimensions	a = 9.5166(7) Å α = 89.659(4)° b = 13.4933(10) Å β = 82.213(4)° c = 26.5103(17) Å γ = 71.513(4)°
Volume	3196.3(4)Å^3
Z	1
Density (calculated)	1.346 g/cm^3
Absorption coefficient	4.516 mm^{-1}
F(000)	1314
Crystal size	0.14 x 0.08 x 0.06 mm
Theta range for data collection	1.68 to 55.10°
Index ranges	$-10 \leq h \leq 10$, $-13 \leq k \leq 13$, $-28 \leq \ell \leq 28$
Reflections collected	39731

Independent reflections	7673 [R_{int} = 0.044]
Absorption correction	Semi-empirical from equivalents
Max. and min. transmission	0.8200 and 0.6000
Refinement method	Full-matrix least-squares on F^2
Data / restraints / parameters	7673 / 246 / 711
Goodness-of-fit on F^2	0.852
Final R indices [I>2sigma(I)]	R_1 = 0.0708, wR_2 = 0.1656
R indices (all data)	R_1 = 0.1616, wR_2 = 0.1905
Largest diff. peak and hole	1.749 and -0.331 e

Table 2. Bond lengths [Å] and angles [°] for ***trans*-II-2a**.

Ru-N(28)	1.975(8)	C(111)-C(119)	1.490(14)
Ru-N(21)	1.978(12)	C(112)-H(112)	0.94
Ru-N(18)	1.987(8)	C(113)-N(114)	1.365(13)
Ru-N(114)	2.001(11)	C(113)-C(118)	1.368(13)
Ru-N(214)	2.032(10)	N(114)-C(115)	1.336(13)
Ru-N(11)	2.055(10)	C(115)-C(116)	1.392(14)
Rh-O(31)	1.86(1)	C(115)-H(115)	0.94
Rh-O(32)#1	1.936(11)	C(116)-C(117)	1.377(15)
Rh-O(127)#1	2.051(7)	C(116)-H(116)	0.94
Rh-O(126)	2.052(7)	C(117)-C(118)	1.356(13)
Rh-N(41)	2.200(15)	C(117)-H(117)	0.94
Rh-Rh#1	2.367(2)	C(118)-H(118)	0.94
N(11)-C(12)	1.330(12)	C(119)-C(120)	1.348(14)
N(11)-C(16)	1.394(12)	C(119)-C(124)	1.380(14)
C(12)-C(13)	1.303(13)	C(120)-C(121)	1.379(14)
C(12)-H(12)	0.94	C(120)-H(120)	0.94
C(13)-C(14)	1.436(13)	C(121)-C(122)	1.387(14)
C(13)-H(13)	0.94	C(121)-H(121)	0.94
C(14)-C(15)	1.391(14)	C(122)-C(123)	1.325(14)
C(14)-H(14)	0.94	C(122)-C(125)	1.505(16)
C(15)-C(16)	1.334(14)	C(123)-C(124)	1.365(13)
C(15)-H(15)	0.94	C(123)-H(123)	0.94
C(16)-C(17)	1.445(14)	C(124)-H(124)	0.94
C(17)-C(112)	1.375(13)	C(125)-O(127)	1.213(12)
C(17)-N(18)	1.386(12)	C(125)-O(126)	1.286(12)
N(18)-C(19)	1.347(12)	O(127)-Rh#1	2.051(7)
C(19)-C(110)	1.417(13)	N(21)-C(26)	1.374(13)
C(19)-C(113)	1.468(14)	N(21)-C(22)	1.391(15)
C(110)-C(111)	1.365(13)	C(22)-C(23)	1.291(15)
C(110)-H(110)	0.94	C(22)-H(22)	0.94
C(111)-C(112)	1.389(13)	C(23)-C(24)	1.445(18)

C(23)-H(23)	0.94	C(523)-C(524)	1.39
C(24)-C(25)	1.373(17)	C(523)-H(523)	0.94
C(24)-H(24)	0.94	C(524)-C(525)	1.39
C(25)-C(26)	1.378(15)	C(524)-H(524)	0.94
C(25)-H(25)	0.94	C(525)-C(526)	1.39
C(26)-C(27)	1.478(15)	C(525)-H(525)	0.94
C(27)-N(28)	1.333(13)	C(526)-H(526)	0.94
C(27)-C(212)	1.391(14)	C(531)-C(532)	1.39
N(28)-C(29)	1.329(12)	C(531)-C(536)	1.39
C(29)-C(210)	1.405(13)	C(532)-C(533)	1.39
C(29)-C(213)	1.456(14)	C(532)-H(532)	0.94
C(210)-C(211)	1.387(14)	C(533)-C(534)	1.39
C(210)-H(210)	0.94	C(533)-H(533)	0.94
C(211)-C(212)	1.353(15)	C(534)-C(535)	1.39
C(211)-H(211)	0.94	C(534)-H(534)	0.94
C(212)-H(212)	0.94	C(535)-C(536)	1.39
C(213)-N(214)	1.369(12)	C(535)-H(535)	0.94
C(213)-C(218)	1.373(14)	C(536)-H(536)	0.94
N(214)-C(215)	1.340(13)	C(541)-C(542)	1.39
C(215)-C(216)	1.371(15)	C(541)-C(546)	1.39
C(215)-H(215)	0.94	C(542)-C(543)	1.39
C(216)-C(217)	1.386(15)	C(542)-H(542)	0.94
C(216)-H(216)	0.94	C(543)-C(544)	1.39
C(217)-C(218)	1.353(14)	C(543)-H(543)	0.94
C(217)-H(217)	0.94	C(544)-C(545)	1.39
C(218)-H(218)	0.94	C(544)-H(544)	0.94
O(31)-C(33)	1.184(16)	C(545)-C(546)	1.39
O(32)-C(33)	1.296(16)	C(545)-H(545)	0.94
O(32)-Rh#1	1.936(11)	C(546)-H(546)	0.94
C(33)-C(34)	1.477(19)	B(6)-F(63)	1.330(13)
C(34)-H(34a)	0.97	B(6)-F(62)	1.350(13)
C(34)-H(34b)	0.97	B(6)-F(64)	1.352(13)
C(34)-H(34c)	0.97	B(6)-F(61)	1.365(13)
N(41)-C(42)	1.1299(11)		
C(42)-C(43)	1.4381(11)	N(28)-RU-N(21)	78.9(5)
C(43)-H(43a)	0.97	N(28)-RU-N(18)	177.8(5)
C(43)-H(43b)	0.97	N(21)-RU-N(18)	100.1(4)
C(43)-H(43c)	0.97	N(28)-RU-N(114)	99.2(4)
B(5)-C(511)	1.641(14)	N(21)-RU-N(114)	91.0(4)
B(5)-C(541)	1.681(14)	N(18)-RU-N(114)	78.8(4)
B(5)-C(531)	1.695(14)	N(28)-RU-N(214)	78.5(5)
B(5)-C(521)	1.724(14)	N(21)-RU-N(214)	157.4(4)
C(511)-C(512)	1.39	N(18)-RU-N(214)	102.5(4)
C(511)-C(516)	1.39	N(114)-RU-N(214)	93.5(4)
C(512)-C(513)	1.39	N(28)-RU-N(11)	102.2(4)
C(512)-H(512)	0.94	N(21)-RU-N(11)	92.4(4)
C(513)-C(514)	1.39	N(18)-RU-N(11)	79.8(4)
C(513)-H(513)	0.94	N(114)-RU-N(11)	158.6(4)
C(514)-C(515)	1.39	N(214)-RU-N(11)	91.4(3)
C(514)-H(514)	0.94	O(31)-RH-O(32)#1	171.3(5)
C(515)-C(516)	1.39	O(31)-RH-O(127)#1	88.3(3)
C(515)-H(515)	0.94	O(32)#1-RH-O(127)#1	91.0(3)
C(516)-H(516)	0.94	O(31)-RH-O(126)	91.8(3)
C(521)-C(522)	1.39	O(32)#1-RH-O(126)	88.4(3)
C(521)-C(526)	1.39	O(127)#1-RH-O(126)	176.3(3)
C(522)-C(523)	1.39	O(31)-RH-N(41)	96.4(5)
C(522)-H(522)	0.94	O(32)#1-RH-N(41)	92.3(5)

O(127)#1-RH-N(41)	95.1(4)
O(126)-RH-N(41)	88.5(4)
O(31)-RH-RH#1	84.7(4)
O(32)#1-RH-RH#1	86.7(4)
O(127)#1-RH-RH#1	88.9(3)
O(126)-RH-RH#1	87.5(3)
N(41)-RH-RH#1	175.9(3)
C(12)-N(11)-C(16)	117.0(1)
C(12)-N(11)-RU	130.1(8)
C(16)-N(11)-RU	112.8(9)
C(13)-C(12)-N(11)	125.50(11)
C(13)-C(12)-H(12)	117.2
N(11)-C(12)-H(12)	117.2
C(12)-C(13)-C(14)	119.50(12)
C(12)-C(13)-H(13)	120.3
C(14)-C(13)-H(13)	120.3
C(15)-C(14)-C(13)	115.10(12)
C(15)-C(14)-H(14)	122.5
C(13)-C(14)-H(14)	122.5
C(16)-C(15)-C(14)	122.70(12)
C(16)-C(15)-H(15)	118.6
C(14)-C(15)-H(15)	118.6
C(15)-C(16)-N(11)	120.20(11)
C(15)-C(16)-C(17)	122.70(12)
N(11)-C(16)-C(17)	117.20(12)
C(112)-C(17)-N(18)	118.6(1)
C(112)-C(17)-C(16)	129.70(12)
N(18)-C(17)-C(16)	111.60(11)
C(19)-N(18)-C(17)	123.0(1)
C(19)-N(18)-RU	118.2(8)
C(17)-N(18)-RU	118.5(8)
N(18)-C(19)-C(110)	116.10(11)
N(18)-C(19)-C(113)	112.70(11)
C(110)-C(19)-C(113)	130.90(13)
C(111)-C(110)-C(19)	123.20(11)
C(111)-C(110)-H(110)	118.4
C(19)-C(110)-H(110)	118.4
C(110)-C(111)-C(112)	117.4(1)
C(110)-C(111)-C(119)	118.30(12)
C(112)-C(111)-C(119)	124.30(11)
C(17)-C(112)-C(111)	121.20(11)
C(17)-C(112)-H(112)	119.4
C(111)-C(112)-H(112)	119.4
N(114)-C(113)-C(118)	124.70(11)
N(114)-C(113)-C(19)	113.40(12)
C(118)-C(113)-C(19)	121.90(12)
C(115)-N(114)-C(113)	113.40(11)
C(115)-N(114)-RU	130.0(9)
C(113)-N(114)-RU	116.7(8)
N(114)-C(115)-C(116)	126.10(12)
N(114)-C(115)-H(115)	117
C(116)-C(115)-H(115)	117
C(117)-C(116)-C(115)	117.20(13)
C(117)-C(116)-H(116)	121.4
C(115)-C(116)-H(116)	121.4
C(118)-C(117)-C(116)	119.20(13)
C(118)-C(117)-H(117)	120.4
C(116)-C(117)-H(117)	120.4
C(117)-C(118)-C(113)	119.50(12)
C(117)-C(118)-H(118)	120.3
C(113)-C(118)-H(118)	120.3
C(120)-C(119)-C(124)	117.3(1)
C(120)-C(119)-C(111)	122.40(12)
C(124)-C(119)-C(111)	120.30(13)
C(119)-C(120)-C(121)	123.10(12)
C(119)-C(120)-H(120)	118.4
C(121)-C(120)-H(120)	118.4
C(120)-C(121)-C(122)	117.70(12)
C(120)-C(121)-H(121)	121.2
C(122)-C(121)-H(121)	121.2
C(123)-C(122)-C(121)	119.80(11)
C(123)-C(122)-C(125)	120.20(13)
C(121)-C(122)-C(125)	119.90(13)
C(122)-C(123)-C(124)	121.80(12)
C(122)-C(123)-H(123)	119.1
C(124)-C(123)-H(123)	119.1
C(123)-C(124)-C(119)	120.30(12)
C(123)-C(124)-H(124)	119.8
C(119)-C(124)-H(124)	119.8
O(127)-C(125)-O(126)	127.00(13)
O(127)-C(125)-C(122)	120.20(13)
O(126)-C(125)-C(122)	112.80(12)
C(125)-O(126)-RH	118.2(8)
C(125)-O(127)-RH#1	118.4(9)
C(26)-N(21)-C(22)	113.30(12)
C(26)-N(21)-RU	117.0(9)
C(22)-N(21)-RU	129.6(1)
C(23)-C(22)-N(21)	125.90(14)
C(23)-C(22)-H(22)	117.1
N(21)-C(22)-H(22)	117.1
C(22)-C(23)-C(24)	119.80(14)
C(22)-C(23)-H(23)	120.1
C(24)-C(23)-H(23)	120.1
C(25)-C(24)-C(23)	117.00(13)
C(25)-C(24)-H(24)	121.5
C(23)-C(24)-H(24)	121.5
C(24)-C(25)-C(26)	119.10(14)
C(24)-C(25)-H(25)	120.5
C(26)-C(25)-H(25)	120.5
N(21)-C(26)-C(25)	124.70(12)
N(21)-C(26)-C(27)	112.70(12)
C(25)-C(26)-C(27)	122.60(14)
N(28)-C(27)-C(212)	119.00(11)
N(28)-C(27)-C(26)	112.10(12)
C(212)-C(27)-C(26)	128.80(15)
C(29)-N(28)-C(27)	122.0(1)
C(29)-N(28)-RU	118.8(9)
C(27)-N(28)-RU	119.0(9)
N(28)-C(29)-C(210)	120.40(12)
N(28)-C(29)-C(213)	113.70(11)
C(210)-C(29)-C(213)	125.90(13)
C(211)-C(210)-C(29)	118.30(11)
C(211)-C(210)-H(210)	120.9
C(29)-C(210)-H(210)	120.9

C(212)-C(211)-C(210)	119.20(11)
C(212)-C(211)-H(211)	120.4
C(210)-C(211)-H(211)	120.4
C(211)-C(212)-C(27)	121.10(13)
C(211)-C(212)-H(212)	119.5
C(27)-C(212)-H(212)	119.5
N(214)-C(213)-C(218)	120.80(11)
N(214)-C(213)-C(29)	113.30(12)
C(218)-C(213)-C(29)	125.90(12)
C(215)-N(214)-C(213)	116.50(11)
C(215)-N(214)-RU	128.2(8)
C(213)-N(214)-RU	115.3(9)
N(214)-C(215)-C(216)	124.10(11)
N(214)-C(215)-H(215)	118
C(216)-C(215)-H(215)	118
C(215)-C(216)-C(217)	119.00(12)
C(215)-C(216)-H(216)	120.5
C(217)-C(216)-H(216)	120.5
C(218)-C(217)-C(216)	117.30(12)
C(218)-C(217)-H(217)	121.3
C(216)-C(217)-H(217)	121.3
C(217)-C(218)-C(213)	122.20(11)
C(217)-C(218)-H(218)	118.9
C(213)-C(218)-H(218)	118.9
C(33)-O(31)-RH	132.10(13)
C(33)-O(32)-RH#1	122.30(11)
O(31)-C(33)-O(32)	114.10(15)
O(31)-C(33)-C(34)	128(2)
O(32)-C(33)-C(34)	118.20(18)
C(33)-C(34)-H(34A)	109.5
C(33)-C(34)-H(34B)	109.5
H(34A)-C(34)-H(34B)	109.5
C(33)-C(34)-H(34C)	109.5
H(34A)-C(34)-H(34C)	109.5
H(34B)-C(34)-H(34C)	109.5
C(42)-N(41)-RH	168.90(17)
N(41)-C(42)-C(43)	169(3)
C(42)-C(43)-H(43A)	109.5
C(42)-C(43)-H(43B)	109.5
H(43A)-C(43)-H(43B)	109.5
C(42)-C(43)-H(43C)	109.5
H(43A)-C(43)-H(43C)	109.5
H(43B)-C(43)-H(43C)	109.5
C(511)-B(5)-C(541)	112.9(9)
C(511)-B(5)-C(531)	106.6(8)
C(541)-B(5)-C(531)	111.9(8)
C(511)-B(5)-C(521)	111.0(9)
C(541)-B(5)-C(521)	109.1(8)
C(531)-B(5)-C(521)	105.0(9)
C(512)-C(511)-C(516)	120
C(512)-C(511)-B(5)	124.2(9)
C(516)-C(511)-B(5)	115.7(9)
C(513)-C(512)-C(511)	120
C(513)-C(512)-H(512)	120
C(511)-C(512)-H(512)	120
C(512)-C(513)-C(514)	120
C(512)-C(513)-H(513)	120
C(514)-C(513)-H(513)	120
C(515)-C(514)-C(513)	120
C(515)-C(514)-H(514)	120
C(513)-C(514)-H(514)	120
C(514)-C(515)-C(516)	120
C(514)-C(515)-H(515)	120
C(516)-C(515)-H(515)	120
C(515)-C(516)-C(511)	120
C(515)-C(516)-H(516)	120
C(511)-C(516)-H(516)	120
C(522)-C(521)-C(526)	120
C(522)-C(521)-B(5)	117.2(9)
C(526)-C(521)-B(5)	122.8(9)
C(523)-C(522)-C(521)	120
C(523)-C(522)-H(522)	120
C(521)-C(522)-H(522)	120
C(522)-C(523)-C(524)	120
C(522)-C(523)-H(523)	120
C(524)-C(523)-H(523)	120
C(525)-C(524)-C(523)	120
C(525)-C(524)-H(524)	120
C(523)-C(524)-H(524)	120
C(524)-C(525)-C(526)	120
C(524)-C(525)-H(525)	120
C(526)-C(525)-H(525)	120
C(525)-C(526)-C(521)	120
C(525)-C(526)-H(526)	120
C(521)-C(526)-H(526)	120
C(532)-C(531)-C(536)	120
C(532)-C(531)-B(5)	115.9(8)
C(536)-C(531)-B(5)	124.1(8)
C(531)-C(532)-C(533)	120
C(531)-C(532)-H(532)	120
C(533)-C(532)-H(532)	120
C(532)-C(533)-C(534)	120
C(532)-C(533)-H(533)	120
C(534)-C(533)-H(533)	120
C(535)-C(534)-C(533)	120
C(535)-C(534)-H(534)	120
C(533)-C(534)-H(534)	120
C(534)-C(535)-C(536)	120
C(534)-C(535)-H(535)	120
C(536)-C(535)-H(535)	120
C(535)-C(536)-C(531)	120
C(535)-C(536)-H(536)	120
C(531)-C(536)-H(536)	120
C(542)-C(541)-C(546)	120
C(542)-C(541)-B(5)	121.7(8)
C(546)-C(541)-B(5)	118.3(8)
C(541)-C(542)-C(543)	120
C(541)-C(542)-H(542)	120
C(543)-C(542)-H(542)	120
C(544)-C(543)-C(542)	120
C(544)-C(543)-H(543)	120
C(542)-C(543)-H(543)	120
C(543)-C(544)-C(545)	120
C(543)-C(544)-H(544)	120

C(545)-C(544)-H(544)	120
C(546)-C(545)-C(544)	120
C(546)-C(545)-H(545)	120
C(544)-C(545)-H(545)	120
C(545)-C(546)-C(541)	120
C(545)-C(546)-H(546)	120
C(541)-C(546)-H(546)	120
F(63)-B(6)-F(62)	108.00(11)
F(63)-B(6)-F(64)	112.00(12)
F(62)-B(6)-F(64)	108.90(11)
F(63)-B(6)-F(61)	109.80(11)
F(62)-B(6)-F(61)	109.50(11)
F(64)-B(6)-F(61)	108.60(11)

Appendix 3: Supplementary information for chapter III.

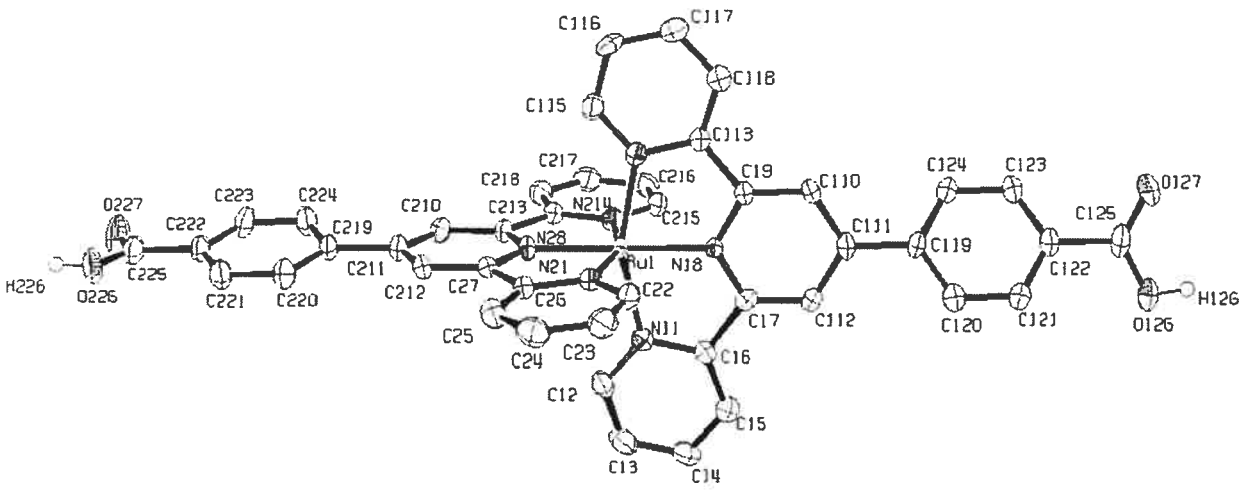

Table 1. Crystal data and structure refinement for **III-1b**.

Empirical formula	C44 H29 F6 N6 O4 P Ru
Formula weight	951.77
Temperature	220(2)K
Wavelength	1.54178 Å
Crystal system	Triclinic
Space group	P-1
Unit cell dimensions	a = 8.8964(2) Å α = 78.175(2)° b = 11.1630(3) Å β = 87.671(2)° c = 24.7288(5) Å γ = 78.603(2)°
Volume	2356.32(10)Å^3
Z	2
Density (calculated)	1.341 Mg/m^3
Absorption coefficient	3.616 mm^{-1}
F(000)	960
Crystal size	0.20 x 0.04 x 0.03 mm
Theta range for data collection	1.83 to 72.92°

Index ranges	$-10 \leq h \leq 11$, $-13 \leq k \leq 13$, $-30 \leq \ell \leq 30$
Reflections collected	28632
Independent reflections	8989 [R_{int} = 0.037]
Absorption correction	Semi-empirical from equivalents
Max. and min. transmission	0.9400 and 0.7200
Refinement method	Full-matrix least-squares on F^2
Data / restraints / parameters	8989 / 0 / 561
Goodness-of-fit on F^2	0.953
Final R indices [I>2sigma(I)]	R_1 = 0.0532, wR_2 = 0.1247
R indices (all data)	R_1 = 0.0698, wR_2 = 0.1293
Largest diff. peak and hole	2.259 and -0.462 e/Å^3

Table 2. Atomic coordinates (x 10^4) and equivalent isotropic displacement parameters (Å^2 x 10^3) for **III-1b**.

U_{eq} is defined as one third of the trace of the orthogonalized Uij tensor.

	Occ.	x	y	z	U_{eq}
Ru(1)	1	5101(1)	1942(1)	1932(1)	23(1)
N(11)	1	7033(4)	2658(3)	2042(1)	25(1)
C(12)	1	7980(5)	3111(4)	1653(2)	32(1)
C(13)	1	9187(6)	3610(5)	1776(2)	40(1)
C(14)	1	9437(5)	3664(5)	2320(2)	43(1)
C(15)	1	8479(5)	3188(5)	2723(2)	38(1)
C(16)	1	7282(5)	2694(4)	2579(2)	28(1)
C(17)	1	6185(5)	2180(4)	2982(2)	28(1)
N(18)	1	5091(4)	1790(3)	2743(1)	24(1)
C(19)	1	3939(5)	1327(4)	3043(2)	26(1)
C(110)	1	3878(5)	1261(5)	3613(2)	33(1)
C(111)	1	5001(5)	1672(5)	3871(2)	34(1)
C(112)	1	6163(5)	2127(4)	3545(2)	33(1)
C(113)	1	2851(5)	984(4)	2702(2)	28(1)
N(114)	1	3131(4)	1212(3)	2145(1)	25(1)
C(115)	1	2139(5)	970(4)	1810(2)	29(1)
C(116)	1	868(5)	478(4)	2004(2)	36(1)
C(117)	1	593(5)	221(5)	2567(2)	39(1)
C(118)	1	1603(5)	481(5)	2914(2)	36(1)
C(119)	1	4920(5)	1682(5)	4468(2)	36(1)

C(120)	1	6236(6)	1459(5)	4783(2)	43(1)
C(121)	1	6144(6)	1524(5)	5334(2)	44(1)
C(122)	1	4728(6)	1805(5)	5588(2)	38(1)
C(123)	1	3426(6)	2008(5)	5278(2)	48(1)
C(124)	1	3508(6)	1962(5)	4724(2)	46(1)
C(125)	1	4629(6)	1884(5)	6190(2)	43(1)
O(126)	1	5846(4)	2030(4)	6404(1)	55(1)
O(127)	1	3421(4)	1796(4)	6441(1)	62(1)
N(21)	1	6448(4)	252(3)	1838(1)	24(1)
C(22)	1	7119(5)	-682(4)	2236(2)	32(1)
C(23)	1	8087(5)	-1731(5)	2125(2)	37(1)
C(24)	1	8351(5)	-1825(4)	1580(2)	38(1)
C(25)	1	7667(5)	-886(4)	1162(2)	36(1)
C(26)	1	6711(5)	143(4)	1298(2)	27(1)
C(27)	1	5904(5)	1196(4)	885(2)	25(1)
N(28)	1	5102(4)	2125(3)	1117(1)	26(1)
C(29)	1	4323(5)	3185(4)	803(2)	24(1)
C(210)	1	4299(5)	3322(4)	238(2)	29(1)
C(211)	1	5087(5)	2387(4)	-19(2)	30(1)
C(212)	1	5901(5)	1300(4)	320(2)	27(1)
C(213)	1	3532(5)	4077(4)	1141(2)	27(1)
N(214)	1	3772(4)	3706(3)	1697(1)	26(1)
C(215)	1	3094(5)	4481(4)	2025(2)	30(1)
C(216)	1	2184(5)	5627(4)	1825(2)	35(1)
C(217)	1	1941(5)	5988(5)	1260(2)	37(1)
C(218)	1	2611(5)	5210(4)	918(2)	33(1)
C(219)	1	5071(5)	2523(4)	-633(2)	29(1)
C(220)	1	6026(6)	1675(4)	-895(2)	34(1)
C(221)	1	6030(5)	1824(4)	-1461(2)	35(1)
C(222)	1	5086(5)	2813(4)	-1783(2)	31(1)
C(223)	1	4116(6)	3664(5)	-1529(2)	37(1)
C(224)	1	4099(5)	3508(4)	-961(2)	35(1)
C(225)	1	5097(6)	3001(5)	-2398(2)	38(1)
O(226)	1	5839(4)	2053(3)	-2591(1)	46(1)
O(227)	1	4461(5)	3971(4)	-2693(1)	62(1)
P(1)	1	196(2)	2251(1)	239(1)	41(1)
F(11)	1	-1396(4)	3201(3)	280(1)	65(1)
F(12)	1	709(4)	3226(3)	-259(1)	69(1)
F(13)	1	-552(4)	1654(4)	-187(1)	73(1)
F(14)	1	-324(4)	1286(3)	742(1)	62(1)
F(15)	1	937(3)	2864(3)	665(1)	59(1)
F(16)	1	1781(4)	1309(3)	208(1)	68(1)

Table 3. Hydrogen coordinates (x 10^4) and isotropic displacement parameters ($Å^2$ x 10^3) for **III-1b**.

	Occ.	x	y	z	U_{eq}
H(12)	1	7813	3086	1282	39
H(13)	1	9838	3912	1494	48
H(14)	1	10243	4018	2412	52

H(15)	1	8639	3199	3095	45
H(110)	1	3087	943	3823	39
H(112)	1	6935	2398	3709	39
H(115)	1	2313	1142	1427	35
H(116)	1	195	318	1756	43
H(117)	1	-260	-123	2708	47
H(118)	1	1440	315	3298	43
H(120)	1	7202	1263	4619	51
H(121)	1	7048	1376	5542	53
H(123)	1	2461	2181	5445	57
H(124)	1	2601	2122	4518	56
H(126)	0.50	5704	2019	6739	83
H(22)	1	6922	-620	2606	38
H(23)	1	8555	-2366	2413	44
H(24)	1	9001	-2534	1494	46
H(25)	1	7848	-944	790	43
H(210)	1	3743	4058	23	35
H(212)	1	6443	646	161	32
H(215)	1	3248	4229	2409	36
H(216)	1	1740	6150	2066	42
H(217)	1	1320	6762	1112	45
H(218)	1	2447	5445	534	39
H(220)	1	6679	989	-682	40
H(221)	1	6689	1240	-1630	42
H(223)	1	3468	4349	-1744	45
H(224)	1	3416	4080	-793	42
H(226)	0.50	5769	2208	-2933	69

Table 4. Anisotropic parameters ($Å^2$ x 10^3) for **III-1b**.
The anisotropic displacement factor exponent takes the form:

$$-2\,\pi^2\,[\,h^2\,a^{*2}\,U_{11} + \ldots + 2\,h\,k\,a^*\,b^*\,U_{12}\,]$$

	U11	U22	U33	U23	U13	U12
Ru(1)	23(1)	33(1)	12(1)	-6(1)	0(1)	-6(1)
N(11)	23(2)	31(2)	24(2)	-8(2)	3(2)	-8(2)
C(12)	32(2)	39(3)	23(2)	-5(2)	7(2)	-2(2)
C(13)	38(3)	46(3)	40(3)	-12(2)	14(2)	-15(2)
C(14)	31(3)	63(4)	43(3)	-16(3)	10(2)	-23(3)
C(15)	36(3)	54(3)	29(2)	-15(2)	2(2)	-16(2)
C(16)	23(2)	41(3)	22(2)	-9(2)	4(2)	-6(2)
C(17)	25(2)	37(3)	24(2)	-8(2)	-2(2)	-9(2)
N(18)	17(2)	40(2)	15(2)	-8(2)	0(1)	-5(2)
C(19)	28(2)	37(3)	16(2)	-6(2)	2(2)	-10(2)
C(110)	31(2)	55(3)	16(2)	-7(2)	6(2)	-18(2)
C(111)	38(3)	51(3)	16(2)	-11(2)	3(2)	-14(2)
C(112)	28(2)	52(3)	21(2)	-10(2)	-2(2)	-14(2)
C(113)	25(2)	38(3)	21(2)	-9(2)	2(2)	-8(2)
N(114)	26(2)	30(2)	19(2)	-5(2)	-1(2)	-9(2)
C(115)	29(2)	35(3)	21(2)	-7(2)	-2(2)	-2(2)

C(116)	26(2)	49(3)	35(3)	-11(2)	-12(2)	-9(2)
C(117)	34(3)	51(3)	36(3)	-9(2)	-3(2)	-18(2)
C(118)	33(3)	52(3)	26(2)	-8(2)	2(2)	-16(2)
C(119)	37(3)	59(3)	16(2)	-11(2)	-2(2)	-19(2)
C(120)	37(3)	70(4)	24(2)	-15(2)	4(2)	-14(3)
C(121)	35(3)	76(4)	22(2)	-10(2)	-2(2)	-14(3)
C(122)	41(3)	61(3)	18(2)	-11(2)	2(2)	-17(3)
C(123)	35(3)	91(4)	19(2)	-14(3)	5(2)	-17(3)
C(124)	31(3)	91(4)	21(2)	-16(3)	-1(2)	-17(3)
C(125)	54(3)	59(4)	18(2)	-8(2)	-4(2)	-14(3)
O(126)	57(2)	97(3)	20(2)	-21(2)	2(2)	-24(2)
O(127)	55(2)	116(4)	23(2)	-20(2)	14(2)	-35(2)
N(21)	24(2)	29(2)	21(2)	-5(2)	0(2)	-8(2)
C(22)	33(3)	44(3)	21(2)	-4(2)	-2(2)	-15(2)
C(23)	34(3)	39(3)	33(3)	-1(2)	-5(2)	-3(2)
C(24)	31(3)	35(3)	45(3)	-9(2)	2(2)	0(2)
C(25)	37(3)	44(3)	28(2)	-9(2)	4(2)	-7(2)
C(26)	23(2)	40(3)	19(2)	-7(2)	1(2)	-7(2)
C(27)	20(2)	36(3)	20(2)	-9(2)	1(2)	-7(2)
N(28)	28(2)	37(2)	15(2)	-9(2)	1(2)	-7(2)
C(29)	26(2)	32(2)	14(2)	-3(2)	-2(2)	-8(2)
C(210)	30(2)	37(3)	19(2)	-3(2)	-4(2)	-5(2)
C(211)	34(3)	40(3)	17(2)	-8(2)	0(2)	-10(2)
C(212)	27(2)	37(3)	18(2)	-10(2)	4(2)	-7(2)
C(213)	25(2)	38(3)	22(2)	-11(2)	1(2)	-9(2)
N(214)	29(2)	28(2)	23(2)	-8(2)	2(2)	-8(2)
C(215)	32(2)	43(3)	23(2)	-16(2)	3(2)	-13(2)
C(216)	29(2)	38(3)	41(3)	-16(2)	9(2)	-5(2)
C(217)	27(2)	41(3)	42(3)	-10(2)	0(2)	0(2)
C(218)	30(2)	38(3)	27(2)	-3(2)	-1(2)	-3(2)
C(219)	34(2)	38(3)	15(2)	-6(2)	2(2)	-11(2)
C(220)	43(3)	35(3)	21(2)	-4(2)	-1(2)	-6(2)
C(221)	40(3)	41(3)	24(2)	-11(2)	2(2)	-3(2)
C(222)	38(3)	43(3)	15(2)	-4(2)	0(2)	-13(2)
C(223)	45(3)	44(3)	22(2)	-10(2)	-10(2)	-2(2)
C(224)	41(3)	42(3)	23(2)	-10(2)	3(2)	-5(2)
C(225)	44(3)	51(3)	22(2)	-7(2)	-1(2)	-18(3)
O(226)	57(2)	61(2)	20(2)	-13(2)	3(2)	-6(2)
O(227)	97(3)	59(3)	21(2)	-2(2)	-7(2)	-1(2)
P(1)	36(1)	61(1)	24(1)	-6(1)	0(1)	-10(1)
F(11)	49(2)	92(3)	42(2)	-1(2)	-1(2)	3(2)
F(12)	65(2)	97(3)	41(2)	3(2)	10(2)	-26(2)
F(13)	73(2)	107(3)	52(2)	-28(2)	-7(2)	-31(2)
F(14)	67(2)	76(2)	40(2)	5(2)	3(2)	-25(2)
F(15)	55(2)	79(2)	47(2)	-18(2)	-10(2)	-17(2)
F(16)	57(2)	80(3)	62(2)	-22(2)	3(2)	6(2)

Table 5. Bond lengths [Å] and angles [°] for **III-1b**.

		Ru(1)-N(11)	2.084(3)
Ru(1)-N(18)	1.978(3)	N(11)-C(12)	1.340(5)
Ru(1)-N(28)	1.983(3)	N(11)-C(16)	1.365(5)
Ru(1)-N(214)	2.068(4)	C(12)-C(13)	1.375(6)
Ru(1)-N(21)	2.077(3)	C(13)-C(14)	1.388(7)
Ru(1)-N(114)	2.080(3)	C(14)-C(15)	1.376(6)

C(15)-C(16)	1.381(6)	P(1)-F(14)	1.588(3)
C(16)-C(17)	1.478(6)	P(1)-F(16)	1.593(3)
C(17)-N(18)	1.345(5)	P(1)-F(15)	1.594(3)
C(17)-C(112)	1.379(5)	P(1)-F(11)	1.606(3)
N(18)-C(19)	1.363(5)		
C(19)-C(110)	1.396(5)	N(18)-RU1-N(28)	179.06(15)
C(19)-C(113)	1.463(6)	N(18)-RU1-N(214)	100.12(14)
C(110)-C(111)	1.403(6)	N(28)-RU1-N(214)	79.01(14)
C(111)-C(112)	1.396(6)	N(18)-RU1-N(21)	102.11(14)
C(111)-C(119)	1.479(5)	N(28)-RU1-N(21)	78.76(14)
C(113)-N(114)	1.371(5)	N(214)-RU1-N(21)	157.77(13)
C(113)-C(118)	1.378(6)	N(18)-RU1-N(114)	79.11(13)
N(114)-C(115)	1.335(5)	N(28)-RU1-N(114)	101.20(14)
C(115)-C(116)	1.379(6)	N(214)-RU1-N(114)	90.06(13)
C(116)-C(117)	1.384(6)	N(21)-RU1-N(114)	94.63(13)
C(117)-C(118)	1.378(6)	N(18)-RU1-N(11)	78.85(13)
C(119)-C(120)	1.386(6)	N(28)-RU1-N(11)	100.82(14)
C(119)-C(124)	1.392(6)	N(214)-RU1-N(11)	92.31(13)
C(120)-C(121)	1.378(6)	N(21)-RU1-N(11)	91.44(13)
C(121)-C(122)	1.393(6)	N(114)-RU1-N(11)	157.91(13)
C(122)-C(123)	1.371(6)	C(12)-N(11)-C(16)	118.7(4)
C(122)-C(125)	1.507(6)	C(12)-N(11)-RU1	127.6(3)
C(123)-C(124)	1.379(6)	C(16)-N(11)-RU1	113.6(3)
C(125)-O(127)	1.229(6)	N(11)-C(12)-C(13)	122.1(4)
C(125)-O(126)	1.277(6)	C(12)-C(13)-C(14)	119.5(5)
N(21)-C(22)	1.339(5)	C(15)-C(14)-C(13)	118.5(5)
N(21)-C(26)	1.372(5)	C(14)-C(15)-C(16)	119.9(4)
C(22)-C(23)	1.379(6)	N(11)-C(16)-C(15)	121.1(4)
C(23)-C(24)	1.379(6)	N(11)-C(16)-C(17)	115.2(4)
C(24)-C(25)	1.377(6)	C(15)-C(16)-C(17)	123.6(4)
C(25)-C(26)	1.380(6)	N(18)-C(17)-C(112)	120.4(4)
C(26)-C(27)	1.474(6)	N(18)-C(17)-C(16)	112.8(4)
C(27)-N(28)	1.354(5)	C(112)-C(17)-C(16)	126.8(4)
C(27)-C(212)	1.377(5)	C(17)-N(18)-C(19)	121.7(3)
N(28)-C(29)	1.350(5)	C(17)-N(18)-RU1	119.5(3)
C(29)-C(210)	1.376(5)	C(19)-N(18)-RU1	118.8(3)
C(29)-C(213)	1.484(5)	N(18)-C(19)-C(110)	119.6(4)
C(210)-C(211)	1.389(6)	N(18)-C(19)-C(113)	113.0(3)
C(211)-C(212)	1.409(6)	C(110)-C(19)-C(113)	127.4(4)
C(211)-C(219)	1.495(5)	C(19)-C(110)-C(111)	119.7(4)
C(213)-N(214)	1.364(5)	C(112)-C(111)-C(110)	118.4(4)
C(213)-C(218)	1.385(6)	C(112)-C(111)-C(119)	120.5(4)
N(214)-C(215)	1.346(5)	C(110)-C(111)-C(119)	121.0(4)
C(215)-C(216)	1.379(6)	C(17)-C(112)-C(111)	120.3(4)
C(216)-C(217)	1.386(6)	N(114)-C(113)-C(118)	121.0(4)
C(217)-C(218)	1.371(6)	N(114)-C(113)-C(19)	115.5(4)
C(219)-C(220)	1.389(6)	C(118)-C(113)-C(19)	123.5(4)
C(219)-C(224)	1.390(6)	C(115)-N(114)-C(113)	118.3(4)
C(220)-C(221)	1.376(6)	C(115)-N(114)-RU1	128.2(3)
C(221)-C(222)	1.374(6)	C(113)-N(114)-RU1	113.6(3)
C(222)-C(223)	1.386(6)	N(114)-C(115)-C(116)	122.7(4)
C(222)-C(225)	1.491(6)	C(115)-C(116)-C(117)	119.5(4)
C(223)-C(224)	1.379(6)	C(118)-C(117)-C(116)	118.2(4)
C(225)-O(227)	1.222(6)	C(117)-C(118)-C(113)	120.5(4)
C(225)-O(226)	1.299(6)	C(120)-C(119)-C(124)	118.3(4)
P(1)-F(12)	1.584(3)	C(120)-C(119)-C(111)	121.3(4)
P(1)-F(13)	1.586(3)	C(124)-C(119)-C(111)	120.4(4)

C(121)-C(120)-C(119)	120.6(5)		C(215)-N(214)-C(213)	118.0(4)	
C(120)-C(121)-C(122)	120.9(5)		C(215)-N(214)-RU1	127.8(3)	
C(123)-C(122)-C(121)	118.4(4)		C(213)-N(214)-RU1	114.1(3)	
C(123)-C(122)-C(125)	120.8(4)		N(214)-C(215)-C(216)	123.0(4)	
C(121)-C(122)-C(125)	120.8(4)		C(215)-C(216)-C(217)	118.3(4)	
C(122)-C(123)-C(124)	121.1(5)		C(218)-C(217)-C(216)	119.7(5)	
C(123)-C(124)-C(119)	120.7(4)		C(217)-C(218)-C(213)	119.5(4)	
O(127)-C(125)-O(126)	124.7(4)		C(220)-C(219)-C(224)	117.7(4)	
O(127)-C(125)-C(122)	119.3(5)		C(220)-C(219)-C(211)	121.3(4)	
O(126)-C(125)-C(122)	116.1(5)		C(224)-C(219)-C(211)	121.0(4)	
C(22)-N(21)-C(26)	118.4(4)		C(221)-C(220)-C(219)	120.9(4)	
C(22)-N(21)-RU1	127.6(3)		C(222)-C(221)-C(220)	121.0(4)	
C(26)-N(21)-RU1	114.0(3)		C(221)-C(222)-C(223)	118.9(4)	
N(21)-C(22)-C(23)	122.7(4)		C(221)-C(222)-C(225)	121.6(4)	
C(24)-C(23)-C(22)	118.3(4)		C(223)-C(222)-C(225)	119.4(4)	
C(25)-C(24)-C(23)	120.3(5)		C(224)-C(223)-C(222)	120.2(4)	
C(24)-C(25)-C(26)	118.8(4)		C(223)-C(224)-C(219)	121.3(4)	
N(21)-C(26)-C(25)	121.4(4)		O(227)-C(225)-O(226)	123.2(4)	
N(21)-C(26)-C(27)	115.1(4)		O(227)-C(225)-C(222)	122.4(5)	
C(25)-C(26)-C(27)	123.5(4)		O(226)-C(225)-C(222)	114.5(4)	
N(28)-C(27)-C(212)	120.2(4)		F(12)-P(1)-F(13)	89.70(19)	
N(28)-C(27)-C(26)	112.6(3)		F(12)-P(1)-F(14)	179.4(2)	
C(212)-C(27)-C(26)	127.2(4)		F(13)-P(1)-F(14)	90.73(19)	
C(29)-N(28)-C(27)	121.3(4)		F(12)-P(1)-F(16)	90.53(19)	
C(29)-N(28)-RU1	119.3(3)		F(13)-P(1)-F(16)	90.6(2)	
C(27)-N(28)-RU1	119.4(3)		F(14)-P(1)-F(16)	89.93(19)	
N(28)-C(29)-C(210)	120.1(4)		F(12)-P(1)-F(15)	90.01(18)	
N(28)-C(29)-C(213)	112.3(3)		F(13)-P(1)-F(15)	179.4(2)	
C(210)-C(29)-C(213)	127.6(4)		F(14)-P(1)-F(15)	89.55(18)	
C(29)-C(210)-C(211)	120.8(4)		F(16)-P(1)-F(15)	89.95(18)	
C(210)-C(211)-C(212)	117.7(4)		F(12)-P(1)-F(11)	89.93(19)	
C(210)-C(211)-C(219)	121.4(4)		F(13)-P(1)-F(11)	90.12(19)	
C(212)-C(211)-C(219)	120.9(4)		F(14)-P(1)-F(11)	89.61(18)	
C(27)-C(212)-C(211)	120.0(4)		F(16)-P(1)-F(11)	179.16(18)	
N(214)-C(213)-C(218)	121.5(4)		F(15)-P(1)-F(11)	89.35(18)	
N(214)-C(213)-C(29)	115.2(4)				
C(218)-C(213)-C(29)	123.3(4)				

Table 6. Bond lengths [Å] and angles [°] related to the hydrogen bonding for **III-1b**.

D-H	..A	d(D-H)	d(H..A)	d(D..A)	<DHA
O(126)-H(126)	O(226)#1	0.83	1.68	2.491(4)	166.6
O(226)-H(226)	O(126)#2	0.83	1.69	2.491(4)	161.7

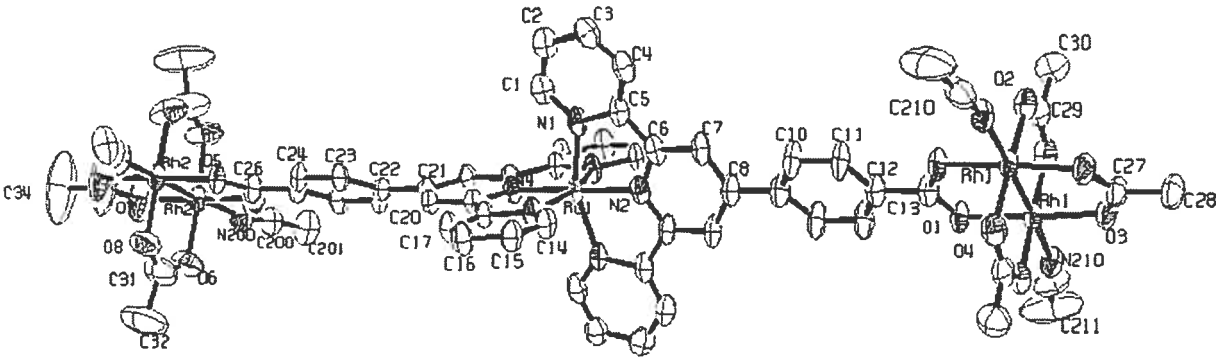

Table 1. Crystal data and structure refinement for **III-5b**.

Identification code	$gar_1 44$
Empirical formula	C83 H77 F12 N12 O16 P2 Rh4 Ru
Formula weight	2301.22
Temperature	100(2)K
Wavelength	1.54178 Å
Crystal system	Orthorhombic
Space group	Pnna
Unit cell dimensions	a = 18.9022(3) Å α = 90° b = 14.4179(2) Å β = 90° c = 37.8184(5) Å γ = 90°
Volume	10306.6(3)Å^3
Z	4
Density (calculated)	1.483 g/cm^3
Absorption coefficient	7.253 mm^{-1}
F(000)	4596
Crystal size	0.20 x 0.08 x 0.08 mm
Theta range for data collection	2.34 to 67.90°
Index ranges	$-19 \leq h \leq 17$, $-17 \leq k \leq 17$, $-45 \leq \ell \leq 45$
Reflections collected	107415

Independent reflections	8483 [R_{int} = 0.046]
Absorption correction	Semi-empirical from equivalents
Max. and min. transmission	0.560 and 0.368
Refinement method	Full-matrix least-squares on F^2
Data / restraints / parameters	8483 / 0 / 605
Goodness-of-fit on F^2	1.074
Final R indices [I>2sigma(I)]	R1 = 0.0760, wR_2 = 0.2335
R indices (all data)	R1 = 0.0963, wR_2 = 0.2531
Largest diff. peak and hole	3.043 and -1.247 e/Å^3

Table 2. Atomic coordinates (x 10^4) and equivalent isotropic displacement parameters (Å^2 x 10^3) for **III-5b**.

U_{eq} is defined as one third of the trace of the orthogonalized Uij tensor.

	Occ.	x	y	z	U_{eq}
Rh(1)	1	6953(1)	-418(1)	1324(1)	45(1)
Rh(2)	1	6879(1)	-156(1)	8257(1)	47(1)
Ru(1)	1	7500	0	4792(1)	39(1)
N(1)	1	7956(4)	1273(5)	4692(1)	42(2)
N(2)	1	7500	0	4265(2)	44(2)
N(3)	1	8488(4)	-548(5)	4897(1)	42(2)
N(4)	1	7500	0	5315(2)	44(2)
O(1)	1	7002(3)	-436(4)	1861(1)	50(2)
O(2)	1	7522(4)	-1615(4)	1313(1)	53(2)
O(3)	1	6972(4)	-353(4)	786(2)	59(2)
O(4)	1	6451(4)	827(5)	1332(1)	57(2)
O(5)	1	6914(3)	-124(4)	7722(1)	47(2)
O(6)	1	7120(5)	-1534(5)	8257(2)	89(2)
O(7)	1	6913(5)	-162(8)	8793(2)	108(4)
O(8)	1	6721(5)	1221(5)	8283(2)	83(2)
C(1)	1	8214(5)	1877(6)	4924(2)	51(2)
C(2)	1	8559(5)	2690(6)	4830(2)	52(2)
C(3)	1	8647(5)	2864(6)	4468(2)	55(2)
C(4)	1	8386(5)	2263(7)	4227(2)	56(2)
C(5)	1	8047(4)	1466(6)	4333(2)	44(2)
C(6)	1	7771(5)	741(6)	4095(2)	44(2)
C(7)	1	7765(5)	768(7)	3730(2)	48(2)

C(8)	1	7500	0	3540(3)	46(3)
C(9)	1	7500	0	3149(3)	56(3)
C(10)	1	8006(5)	516(8)	2958(2)	62(3)
C(11)	1	7997(5)	504(8)	2592(2)	64(3)
C(12)	1	7500	0	2411(3)	51(3)
C(13)	1	7500	0	2011(3)	49(3)
C(14)	1	8997(5)	-816(6)	4658(2)	47(2)
C(15)	1	9645(5)	-1126(6)	4760(2)	49(2)
C(16)	1	9796(5)	-1199(7)	5120(2)	54(2)
C(17)	1	9301(4)	-939(6)	5364(2)	46(2)
C(18)	1	8645(5)	-618(5)	5248(2)	39(2)
C(19)	1	8085(4)	-316(6)	5490(2)	39(2)
C(20)	1	8091(4)	-317(5)	5855(2)	37(2)
C(21)	1	7500	0	6046(2)	37(3)
C(22)	1	7500	0	6433(2)	34(2)
C(23)	1	8123(4)	164(6)	6625(2)	39(2)
C(24)	1	8125(5)	162(6)	6988(2)	46(2)
C(25)	1	7500	0	7174(3)	46(3)
C(26)	1	7500	0	7575(3)	46(3)
C(27)	1	7500	0	633(3)	54(3)
C(28)	1	7500	0	235(3)	71(5)
C(29)	1	6812(7)	1561(7)	1320(2)	53(3)
C(30)	1	6407(6)	2461(8)	1307(3)	75(3)
C(31)	1	7235(9)	1746(9)	8293(5)	105(5)
C(32)	1	7108(10)	2755(10)	8381(7)	179(11)
C(33)	1	7500	0	8939(4)	143(12)
C(34)	1	7500	0	9352(6)	250(20)
C(200)	1	5147(6)	-443(7)	8098(2)	54(2)
C(201)	1	4478(6)	-506(9)	7958(3)	81(3)
N(200)	1	5708(5)	-389(6)	8213(2)	61(2)
N(210)	1	5929(4)	-1171(6)	1348(2)	51(2)
C(210)	1	5438(7)	-1513(8)	1426(3)	74(3)
C(211)	1	4753(9)	-1940(10)	1535(6)	156(8)
P(1)	1	9790(1)	207(2)	3706(1)	52(1)
F(1)	1	9499(3)	658(4)	4065(1)	63(1)
F(2)	1	10100(3)	-239(5)	3358(2)	91(2)
F(3)	1	10249(3)	-504(4)	3944(2)	69(2)
F(4)	1	9346(3)	952(4)	3486(1)	71(2)
F(5)	1	9139(4)	-493(5)	3710(2)	85(2)
F(6)	1	10445(3)	912(4)	3721(1)	57(1)
C(300)	1	5146(10)	7500	7500	83(5)
C(301)	1	4900(13)	8008(12)	7257(3)	128(7)
C(312)	1	4265(15)	8147(18)	7206(6)	159(8)
C(322)	1	3784(10)	7744(12)	7372(3)	106(5)
C(303)	1	5967(17)	7500	7500	226(19)
C(400)	1	4054(13)	7500	2500	110(7)
C(401)	1	4483(11)	6655(14)	2415(4)	130(6)
C(402)	1	5135(13)	6656(19)	2370(9)	235(15)
C(403)	1	5525(15)	7500	2500	230(20)
C(404)	1	3212(17)	7500	2500	370(40)
N(600)	1	6721(14)	7219(12)	9231(4)	209(10)
C(600)	1	6295(12)	7425(10)	9018(3)	128(7)
C(601)	1	5839(10)	7623(11)	8731(4)	127(6)

Table 3. Hydrogen coordinates ($\times 10^4$) and isotropic displacement parameters ($Å^2 \times 10^3$) for **III-5b**.

	Occ.	x	y	z	U_{eq}
H(1)	1	8160	1744	5169	61
H(2)	1	8728	3112	5004	62
H(3)	1	8891	3405	4392	66
H(4)	1	8437	2392	3982	67
H(7)	1	7936	1298	3607	58
H(10)	1	8351	871	3080	74
H(11)	1	8340	851	2465	77
H(14)	1	8892	-784	4412	56
H(15)	1	9990	-1290	4589	59
H(16)	1	10241	-1430	5196	64
H(17)	1	9402	-976	5610	55
H(20)	1	8497	-533	5978	44
H(23)	1	8552	279	6501	47
H(24)	1	8553	271	7112	55
H(28A)	0.50	7727	-568	148	106
H(28B)	0.50	7761	542	148	106
H(28C)	0.50	7012	26	148	106
H(30A)	1	6465	2748	1074	112
H(30B)	1	6588	2882	1490	112
H(30C)	1	5904	2339	1350	112
H(32A)	1	7370	2918	8596	268
H(32B)	1	6601	2857	8420	268
H(32C)	1	7270	3143	8184	268
H(34A)	0.50	7169	471	9438	373
H(34B)	0.50	7977	140	9438	373
H(34C)	0.50	7354	-612	9438	373
H(20A)	1	4185	0	8050	121
H(20B)	1	4267	-1103	8024	121
H(20C)	1	4504	-461	7700	121
H(21A)	1	4847	-2490	1680	234
H(21B)	1	4485	-2119	1324	234
H(21C)	1	4479	-1490	1673	234
H(322)	1	3326	7845	7275	127
H(30D)	0.50	6140	8129	7454	339
H(30E)	0.50	6140	7080	7315	339
H(30F)	0.50	6140	7291	7731	339
H(401)	1	4241	6080	2395	156
H(402)	1	5373	6153	2259	282
H(403)	1	6027	7500	2500	273
H(40A)	0.50	3039	7548	2256	551
H(40B)	0.50	3039	8030	2638	551
H(40C)	0.50	3039	6923	2606	551
H(60A)	1	6121	7769	8521	190
H(60B)	1	5539	8154	8791	190
H(60C)	1	5540	7081	8683	190

Table 4. Anisotropic parameters ($Å^2$ x 10^3) for **III-5b**.
The anisotropic displacement factor exponent takes the form:

$$-2\pi^2 [h^2 a^{*2} U_{11} + ... + 2 h k a^* b^* U_{12}]$$

	U11	U22	U33	U23	U13	U12
Rh(1)	50(1)	65(1)	21(1)	0(1)	-1(1)	-5(1)
Rh(2)	53(1)	65(1)	24(1)	2(1)	3(1)	-2(1)
Ru(1)	36(1)	66(1)	17(1)	0	0	14(1)
N(1)	33(5)	67(4)	27(3)	4(3)	3(3)	13(3)
N(2)	36(7)	66(6)	31(4)	0	0	20(5)
N(3)	29(5)	72(4)	24(3)	-3(3)	2(3)	19(3)
N(4)	48(8)	60(5)	23(4)	0	0	18(5)
O(1)	47(4)	79(4)	22(2)	0(2)	1(2)	-5(3)
O(2)	57(6)	69(4)	34(3)	3(2)	-1(2)	2(3)
O(3)	76(6)	73(4)	27(3)	0(2)	-4(3)	-14(3)
O(4)	60(5)	71(4)	39(3)	-2(2)	-6(3)	3(4)
O(5)	34(5)	85(4)	23(3)	1(2)	3(2)	4(3)
O(6)	72(7)	60(4)	136(7)	29(4)	-11(5)	-3(4)
O(7)	81(8)	214(11)	30(4)	1(5)	7(3)	-34(6)
O(8)	68(6)	55(4)	125(6)	-18(4)	27(5)	2(4)
C(1)	47(6)	71(6)	36(4)	-3(4)	5(3)	25(4)
C(2)	46(7)	64(5)	45(4)	-1(4)	3(4)	10(4)
C(3)	51(7)	62(5)	53(4)	11(4)	0(4)	12(5)
C(4)	49(7)	81(6)	36(4)	12(4)	6(4)	15(5)
C(5)	27(6)	75(5)	31(3)	3(3)	2(3)	16(4)
C(6)	29(6)	73(5)	30(3)	8(3)	6(3)	18(4)
C(7)	32(6)	88(6)	24(3)	5(4)	2(3)	9(4)
C(8)	24(8)	85(8)	30(5)	0	0	6(6)
C(9)	45(10)	92(9)	30(6)	0	0	-3(7)
C(10)	41(7)	121(9)	23(4)	0(4)	-3(3)	-19(5)
C(11)	51(7)	119(9)	22(4)	-4(4)	-6(3)	-7(6)
C(12)	41(9)	83(9)	30(6)	0	0	5(6)
C(13)	39(9)	75(8)	31(5)	0	0	1(6)
C(14)	45(6)	72(5)	23(3)	-6(3)	9(3)	14(4)
C(15)	41(6)	76(5)	30(3)	-5(3)	6(3)	11(4)
C(16)	43(6)	82(6)	36(4)	-1(4)	-1(4)	22(5)
C(17)	35(6)	75(5)	27(3)	-3(3)	0(3)	19(4)
C(18)	35(6)	59(4)	22(3)	-2(3)	4(3)	7(4)
C(19)	30(6)	56(4)	31(4)	-2(3)	1(3)	11(3)
C(20)	35(6)	49(4)	25(3)	0(3)	-2(3)	9(3)
C(21)	39(8)	49(6)	24(5)	0	0	3(5)
C(22)	30(8)	46(5)	26(5)	0	0	1(5)
C(23)	28(6)	66(5)	25(3)	3(3)	2(3)	6(4)
C(24)	38(6)	75(5)	24(4)	-4(3)	-7(3)	5(4)
C(25)	35(9)	75(8)	26(5)	0	0	1(6)
C(26)	35(9)	74(8)	29(5)	0	0	0(6)
C(27)	62(11)	71(8)	28(5)	0	0	-17(7)
C(28)	82(14)	97(11)	33(7)	0	0	-23(9)
C(29)	63(9)	66(6)	30(4)	-1(3)	-3(4)	2(5)
C(30)	67(9)	73(7)	85(7)	-7(5)	3(6)	2(6)
C(31)	65(11)	71(8)	178(15)	-29(8)	44(9)	4(7)

C(32)	116(15)	69(9)	350(30)	-47(14)	70(18)	6(9)
C(33)	81(18)	310(40)	35(8)	0	0	-51(19)
C(34)	180(40)	530(80)	40(11)	0	0	-50(40)
C(200)	45(8)	77(6)	41(4)	0(4)	6(4)	2(5)
C(201)	58(9)	122(10)	61(6)	-15(6)	6(5)	10(7)
N(200)	61(7)	85(5)	38(4)	12(3)	13(4)	-1(5)
N(210)	39(6)	75(5)	37(3)	-5(3)	3(3)	-10(4)
C(210)	67(9)	67(6)	88(7)	-27(5)	23(6)	-4(6)
C(211)	96(14)	87(9)	290(20)	-40(12)	80(14)	-38(9)
P(1)	38(2)	73(1)	46(1)	-7(1)	-2(1)	5(1)
F(1)	46(4)	98(4)	46(2)	-3(2)	1(2)	17(3)
F(2)	51(4)	146(6)	74(4)	-59(4)	1(3)	-2(4)
F(3)	52(4)	73(3)	83(4)	9(3)	5(3)	10(3)
F(4)	48(4)	113(4)	50(3)	9(3)	-12(2)	8(3)
F(5)	50(5)	92(4)	112(5)	-24(3)	4(3)	-6(3)
F(6)	42(4)	81(3)	48(2)	6(2)	-13(2)	4(3)
C(300)	72(15)	80(11)	97(12)	-25(9)	0	0
C(301)	210(20)	109(11)	69(7)	-6(7)	-38(11)	35(13)
C(312)	190(30)	160(20)	131(17)	-35(15)	-41(17)	-1(18)
C(322)	99(13)	140(14)	79(9)	6(8)	-12(7)	-17(10)
C(303)	140(30)	160(30)	380(50)	-180(30)	0	0
C(400)	110(20)	109(16)	113(14)	-4(12)	0	0
C(401)	83(14)	152(16)	157(15)	-1(12)	-13(10)	4(12)
C(402)	62(18)	180(20)	470(50)	40(30)	10(20)	16(15)
C(403)	40(20)	220(40)	420(60)	-130(40)	0	0
C(404)	70(20)	230(40)	810(120)	230(60)	0	0
N(600)	400(30)	147(13)	82(8)	19(9)	-72(13)	43(17)
C(600)	220(20)	103(10)	60(7)	32(7)	-13(9)	-7(11)
C(601)	138(15)	114(12)	128(12)	45(9)	-9(10)	-30(11)

Table 5. Bond lengths [Å] and angles [°] for **III-5b**.

Rh(1)-O(1)	2.033(5)	N(2)-C(6)#1	1.348(9)
Rh(1)-O(4)	2.030(7)	N(2)-C(6)	1.349(9)
Rh(1)-O(3)	2.036(6)	N(3)-C(14)	1.377(9)
Rh(1)-O(2)	2.035(7)	N(3)-C(18)	1.364(8)
Rh(1)-N(210)	2.222(8)	N(4)-C(19)#1	1.367(9)
Rh(1)-Rh(1)#1	2.3934(14)	N(4)-C(19)	1.367(9)
Rh(2)-O(8)	2.010(7)	O(1)-C(13)	1.266(7)
Rh(2)-O(6)	2.038(8)	O(2)-C(29)#1	1.260(12)
Rh(2)-O(5)	2.022(5)	O(3)-C(27)	1.260(8)
Rh(2)-O(7)	2.029(7)	O(4)-C(29)	1.261(12)
Rh(2)-N(200)	2.244(10)	O(5)-C(26)	1.253(7)
Rh(2)-Rh(2)#1	2.3907(14)	O(6)-C(31)#1	1.264(17)
Ru(1)-N(4)	1.977(8)	O(7)-C(33)	1.262(10)
Ru(1)-N(2)	1.994(9)	O(8)-C(31)	1.231(16)
Ru(1)-N(1)#1	2.062(7)	C(1)-C(2)	1.388(13)
Ru(1)-N(1)	2.062(7)	C(1)-H(1)	0.95
Ru(1)-N(3)#1	2.066(6)	C(2)-C(3)	1.401(11)
Ru(1)-N(3)	2.066(6)	C(2)-H(2)	0.95
N(1)-C(1)	1.329(11)	C(3)-C(4)	1.351(13)
N(1)-C(5)	1.396(9)	C(3)-H(3)	0.95

C(4)-C(5)	1.376(13)	C(33)-O(7)#1	1.262(10)
C(4)-H(4)	0.95	C(33)-C(34)	1.56(3)
C(5)-C(6)	1.477(12)	C(34)-H(34a)	1.0437
C(6)-C(7)	1.382(10)	C(34)-H(34b)	1.0437
C(7)-C(8)	1.410(11)	C(34)-H(34c)	1.0437
C(7)-H(7)	0.95	C(200)-N(200)	1.149(13)
C(8)-C(7)#1	1.410(11)	C(200)-C(201)	1.376(16)
C(8)-C(9)	1.478(15)	C(201)-H(20a)	0.98
C(9)-C(10)#1	1.411(11)	C(201)-H(20b)	0.98
C(9)-C(10)	1.411(11)	C(201)-H(20c)	0.98
C(10)-C(11)	1.383(11)	N(210)-C(210)	1.091(13)
C(10)-H(10)	0.95	C(210)-C(211)	1.490(18)
C(11)-C(12)	1.371(11)	C(211)-H(21a)	0.9849
C(11)-H(11)	0.95	C(211)-H(21b)	0.9849
		C(211)-H(21c)	0.9849
		P(1)-F(2)	1.579(6)
C(12)-C(11)#1	1.371(11)	P(1)-F(5)	1.591(7)
C(12)-C(13)	1.510(14)	P(1)-F(6)	1.604(6)
C(13)-O(1)#1	1.266(7)	P(1)-F(4)	1.597(6)
C(14)-C(15)	1.360(12)	P(1)-F(1)	1.601(5)
C(14)-H(14)	0.95	P(1)-F(3)	1.616(6)
C(15)-C(16)	1.397(10)	C(300)-C(301)#2	1.264(16)
C(15)-H(15)	0.95	C(300)-C(301)	1.264(16)
C(16)-C(17)	1.366(11)	C(300)-C(303)	1.55(4)
C(16)-H(16)	0.95	C(301)-C(312)	1.23(3)
C(17)-C(18)	1.393(11)	C(312)-C(322)	1.25(3)
C(17)-H(17)	0.95	C(322)-C(322)#2	1.20(3)
C(18)-C(19)	1.468(10)	C(322)-H(322)	0.95
C(19)-C(20)	1.379(10)	C(303)-H(30d)	1.0128
C(20)-C(21)	1.406(9)	C(303)-H(30e)	1.0128
C(20)-H(20)	0.95	C(303)-H(30f)	1.0128
C(21)-C(20)#1	1.406(9)	C(400)-C(401)#3	1.50(2)
C(21)-C(22)	1.464(13)	C(400)-C(401)	1.50(2)
C(22)-C(23)#1	1.404(10)	C(400)-C(404)	1.59(4)
C(22)-C(23)	1.404(10)	C(401)-C(402)	1.24(2)
C(23)-C(24)	1.372(10)	C(401)-H(401)	0.95
C(23)-H(23)	0.95	C(402)-C(403)	1.51(3)
C(24)-C(25)	1.395(10)	C(402)-H(402)	0.95
C(24)-H(24)	0.95	C(403)-C(402)#3	1.51(3)
C(25)-C(24)#1	1.395(10)	C(403)-H(403)	0.95
C(25)-C(26)	1.517(14)	C(404)-H(40a)	1.0245
C(26)-O(5)#1	1.253(7)	C(404)-H(40b)	1.0245
C(27)-O(3)#1	1.260(8)	C(404)-H(40c)	1.0245
C(27)-C(28)	1.508(15)	N(600)-C(600)	1.17(2)
C(28)-H(28a)	0.98	C(600)-C(601)	1.42(2)
C(28)-H(28b)	0.98	C(601)-H(60a)	0.98
C(28)-H(28c)	0.98	C(601)-H(60b)	0.98
C(29)-O(2)#1	1.260(12)	C(601)-H(60c)	0.98
C(29)-C(30)	1.508(15)		
C(30)-H(30a)	0.98	O(1)-RH1-O(4)	91.0(2)
C(30)-H(30b)	0.98	O(1)-RH1-O(3)	175.9(3)
C(30)-H(30c)	0.98	O(4)-RH1-O(3)	89.1(2)
C(31)-O(6)#1	1.265(17)	O(1)-RH1-O(2)	89.1(2)
C(31)-C(32)	1.511(19)	O(4)-RH1-O(2)	175.9(3)
C(32)-H(32a)	0.9801	O(3)-RH1-O(2)	90.5(2)
C(32)-H(32b)	0.98	O(1)-RH1-N(210)	89.6(2)
C(32)-H(32c)	0.98	O(4)-RH1-N(210)	91.4(3)

O(3)-RH1-N(210)	94.5(2)	N(1)-C(1)-C(2)	123.9(7)
O(2)-RH1-N(210)	92.7(3)	N(1)-C(1)-H(1)	118.1
O(1)-RH1-RH1#1	88.09(17)	C(2)-C(1)-H(1)	118.1
O(4)-RH1-RH1#1	87.7(2)	C(3)-C(2)-C(1)	117.2(8)
O(3)-RH1-RH1#1	87.79(18)	C(3)-C(2)-H(2)	121.4
O(2)-RH1-RH1#1	88.3(2)	C(1)-C(2)-H(2)	121.4
N(210)-RH1-RH1#1	177.48(16)	C(4)-C(3)-C(2)	120.1(9)
O(8)-RH2-O(6)	174.8(4)	C(4)-C(3)-H(3)	119.9
O(8)-RH2-O(5)	91.7(3)	C(2)-C(3)-H(3)	119.9
O(6)-RH2-O(5)	90.9(3)	C(5)-C(4)-C(3)	120.5(7)
O(8)-RH2-O(7)	87.8(4)	C(5)-C(4)-H(4)	119.8
O(6)-RH2-O(7)	89.3(4)	C(3)-C(4)-H(4)	119.8
O(5)-RH2-O(7)	176.2(3)	C(4)-C(5)-N(1)	120.6(8)
O(8)-RH2-N(200)	90.3(3)	C(4)-C(5)-C(6)	125.2(7)
O(6)-RH2-N(200)	94.3(3)	N(1)-C(5)-C(6)	114.1(7)
O(5)-RH2-N(200)	87.9(2)	N(2)-C(6)-C(7)	119.8(8)
O(7)-RH2-N(200)	95.9(3)	N(2)-C(6)-C(5)	113.8(6)
O(8)-RH2-RH2#1	87.7(3)	C(7)-C(6)-C(5)	126.5(8)
O(6)-RH2-RH2#1	87.9(3)	C(6)-C(7)-C(8)	119.3(9)
O(5)-RH2-RH2#1	87.91(16)	C(6)-C(7)-H(7)	120.4
O(7)-RH2-RH2#1	88.3(2)	C(8)-C(7)-H(7)	120.3
N(200)-RH2-RH2#1	175.27(18)	C(7)#1-C(8)-C(7)	118.9(1)
N(4)-RU1-N(2)	180.000(1)	C(7)#1-C(8)-C(9)	120.6(5)
N(4)-RU1-N(1)#1	100.59(16)	C(7)-C(8)-C(9)	120.6(5)
N(2)-RU1-N(1)#1	79.41(16)	C(10)#1-C(9)-C(10)	118.2(1)
N(4)-RU1-N(1)	100.59(16)	C(10)#1-C(9)-C(8)	120.9(5)
N(2)-RU1-N(1)	79.41(16)	C(10)-C(9)-C(8)	120.9(5)
N(1)#1-RU1-N(1)	158.8(3)	C(11)-C(10)-C(9)	119.9(9)
N(4)-RU1-N(3)#1	78.93(15)	C(11)-C(10)-H(10)	120
N(2)-RU1-N(3)#1	101.07(15)	C(9)-C(10)-H(10)	120.1
N(1)#1-RU1-N(3)#1	89.9(3)	C(10)-C(11)-C(12)	121.0(9)
N(1)-RU1-N(3)#1	94.2(3)	C(10)-C(11)-H(11)	119.5
N(4)-RU1-N(3)	78.94(15)	C(12)-C(11)-H(11)	119.5
N(2)-RU1-N(3)	101.06(15)	C(11)#1-C(12)-C(11)	120.00(11)
N(1)#1-RU1-N(3)	94.2(3)	C(11)#1-C(12)-C(13)	120.0(6)
N(1)-RU1-N(3)	89.9(3)	C(11)-C(12)-C(13)	120.0(6)
N(3)#1-RU1-N(3)	157.9(3)	O(1)-C(13)-O(1)#1	126.6(1)
C(1)-N(1)-C(5)	117.7(8)	O(1)-C(13)-C(12)	116.7(5)
C(1)-N(1)-RU1	128.0(5)	O(1)#1-C(13)-C(12)	116.7(5)
C(5)-N(1)-RU1	114.1(6)	C(15)-C(14)-N(3)	122.3(6)
C(6)#1-N(2)-C(6)	122.9(9)	C(15)-C(14)-H(14)	118.8
C(6)#1-N(2)-RU1	118.5(5)	N(3)-C(14)-H(14)	118.8
C(6)-N(2)-RU1	118.5(5)	C(14)-C(15)-C(16)	119.1(7)
C(14)-N(3)-C(18)	117.8(7)	C(14)-C(15)-H(15)	120.4
C(14)-N(3)-RU1	127.8(5)	C(16)-C(15)-H(15)	120.5
C(18)-N(3)-RU1	114.4(5)	C(17)-C(16)-C(15)	119.8(8)
C(19)#1-N(4)-C(19)	121.9(9)	C(17)-C(16)-H(16)	120.1
C(19)#1-N(4)-RU1	119.0(4)	C(15)-C(16)-H(16)	120.1
C(19)-N(4)-RU1	119.0(4)	C(16)-C(17)-C(18)	119.2(7)
C(13)-O(1)-RH1	118.5(6)	C(16)-C(17)-H(17)	120.4
C(29)#1-O(2)-RH1	118.3(6)	C(18)-C(17)-H(17)	120.4
C(27)-O(3)-RH1	119.4(6)	N(3)-C(18)-C(17)	121.7(6)
C(29)-O(4)-RH1	119.2(7)	N(3)-C(18)-C(19)	115.4(7)
C(26)-O(5)-RH2	118.5(6)	C(17)-C(18)-C(19)	122.9(6)
C(31)#1-O(6)-RH2	116.8(8)	N(4)-C(19)-C(20)	119.5(7)
C(33)-O(7)-RH2	117.7(9)	N(4)-C(19)-C(18)	112.3(6)
C(31)-O(8)-RH2	119.4(9)	C(20)-C(19)-C(18)	128.2(7)

C(19)-C(20)-C(21)	120.3(7)
C(19)-C(20)-H(20)	119.8
C(21)-C(20)-H(20)	119.8
C(20)#1-C(21)-C(20)	118.3(9)
C(20)#1-C(21)-C(22)	120.8(4)
C(20)-C(21)-C(22)	120.8(4)
C(23)#1-C(22)-C(23)	117.6(9)
C(23)#1-C(22)-C(21)	121.2(5)
C(23)-C(22)-C(21)	121.2(5)
C(24)-C(23)-C(22)	121.3(8)
C(24)-C(23)-H(23)	119.4
C(22)-C(23)-H(23)	119.4
C(23)-C(24)-C(25)	120.3(8)
C(23)-C(24)-H(24)	119.9
C(25)-C(24)-H(24)	119.9
C(24)#1-C(25)-C(24)	119.3(1)
C(24)#1-C(25)-C(26)	120.4(5)
C(24)-C(25)-C(26)	120.4(5)
O(5)#1-C(26)-O(5)	127.2(1)
O(5)#1-C(26)-C(25)	116.4(5)
O(5)-C(26)-C(25)	116.4(5)
O(3)-C(27)-O(3)#1	125.4(1)
O(3)-C(27)-C(28)	117.3(5)
O(3)#1-C(27)-C(28)	117.3(5)
C(27)-C(28)-H(28A)	109.5
C(27)-C(28)-H(28B)	109.5
H(28A)-C(28)-H(28B)	109.5
C(27)-C(28)-H(28C)	109.5
H(28A)-C(28)-H(28C)	109.5
H(28B)-C(28)-H(28C)	109.5
O(4)-C(29)-O(2)#1	126.4(9)
O(4)-C(29)-C(30)	116.6(1)
O(2)#1-C(29)-C(30)	117.0(9)
C(29)-C(30)-H(30A)	109.4
C(29)-C(30)-H(30B)	109.5
H(30A)-C(30)-H(30B)	109.5
C(29)-C(30)-H(30C)	109.4
H(30A)-C(30)-H(30C)	109.5
H(30B)-C(30)-H(30C)	109.5
O(6)#1-C(31)-O(8)	127.50(12)
O(6)#1-C(31)-C(32)	114.20(14)
O(8)-C(31)-C(32)	118.20(13)
C(31)-C(32)-H(32A)	110.4
C(31)-C(32)-H(32B)	109.2
H(32A)-C(32)-H(32B)	109.5
C(31)-C(32)-H(32C)	108.9
H(32A)-C(32)-H(32C)	109.5
H(32B)-C(32)-H(32C)	109.5
O(7)-C(33)-O(7)#1	128.10(15)
O(7)-C(33)-C(34)	115.9(8)
O(7)#1-C(33)-C(34)	115.9(8)
C(33)-C(34)-H(34A)	115.6
C(33)-C(34)-H(34B)	115.6
H(34A)-C(34)-H(34B)	102.7
C(33)-C(34)-H(34C)	115.6
H(34A)-C(34)-H(34C)	102.7
H(34B)-C(34)-H(34C)	102.7
N(200)-C(200)-C(201)	179.50(11)
C(200)-C(201)-H(20A)	109.4
C(200)-C(201)-H(20B)	109.5
H(20A)-C(201)-H(20B)	109.5
C(200)-C(201)-H(20C)	109.5
H(20A)-C(201)-H(20C)	109.5
H(20B)-C(201)-H(20C)	109.5
C(200)-N(200)-RH2	161.4(7)
C(210)-N(210)-RH1	166.6(8)
N(210)-C(210)-C(211)	177.60(12)
C(210)-C(211)-H(21A)	110
C(210)-C(211)-H(21B)	109.9
H(21A)-C(211)-H(21B)	109
C(210)-C(211)-H(21C)	110
H(21A)-C(211)-H(21C)	109
H(21B)-C(211)-H(21C)	109
F(2)-P(1)-F(5)	92.1(4)
F(2)-P(1)-F(6)	90.0(3)
F(5)-P(1)-F(6)	177.5(3)
F(2)-P(1)-F(4)	92.0(3)
F(5)-P(1)-F(4)	91.5(4)
F(6)-P(1)-F(4)	89.8(3)
F(2)-P(1)-F(1)	178.3(4)
F(5)-P(1)-F(1)	89.1(3)
F(6)-P(1)-F(1)	88.8(3)
F(4)-P(1)-F(1)	89.3(3)
F(2)-P(1)-F(3)	90.4(4)
F(5)-P(1)-F(3)	90.4(4)
F(6)-P(1)-F(3)	88.2(3)
F(4)-P(1)-F(3)	176.9(3)
F(1)-P(1)-F(3)	88.3(3)
C(301)#2-C(300)-C(301)	137(3)
C(301)#2-C(300)-C(303)	111.60(14)
C(301)-C(300)-C(303)	111.60(14)
C(312)-C(301)-C(300)	125(3)
C(301)-C(312)-C(322)	124(3)
C(312)-C(322)-C(322)#2	132.80(15)
C(312)-C(322)-H(322)	113.7
C(322)#2-C(322)-H(322)	113.5
C(300)-C(303)-H(30D)	112.6
C(300)-C(303)-H(30E)	112.6
H(30D)-C(303)-H(30E)	106.1
C(300)-C(303)-H(30F)	112.6
H(30D)-C(303)-H(30F)	106.1
H(30E)-C(303)-H(30F)	106.1
C(401)#3-C(400)-C(401)	115(2)
C(401)#3-C(400)-C(404)	122.70(11)
C(401)-C(400)-C(404)	122.70(11)
C(402)-C(401)-C(400)	124(2)
C(402)-C(401)-H(401)	117.9
C(400)-C(401)-H(401)	117.7
C(401)-C(402)-C(403)	116(3)
C(401)-C(402)-H(402)	121.8
C(403)-C(402)-H(402)	122.1
C(402)#3-C(403)-C(402)	121(3)
C(402)#3-C(403)-H(403)	119.3
C(402)-C(403)-H(403)	119.3

C(400)-C(404)-H(40A)	113.6
C(400)-C(404)-H(40B)	113.6
H(40A)-C(404)-H(40B)	105
C(400)-C(404)-H(40C)	113.6
H(40A)-C(404)-H(40C)	105
H(40B)-C(404)-H(40C)	105
N(600)-C(600)-C(601)	173(2)
C(600)-C(601)-H(60A)	109.5
C(600)-C(601)-H(60B)	109.5
H(60A)-C(601)-H(60B)	109.5
C(600)-C(601)-H(60C)	109.4
H(60A)-C(601)-H(60C)	109.5
H(60B)-C(601)-H(60C)	109.5

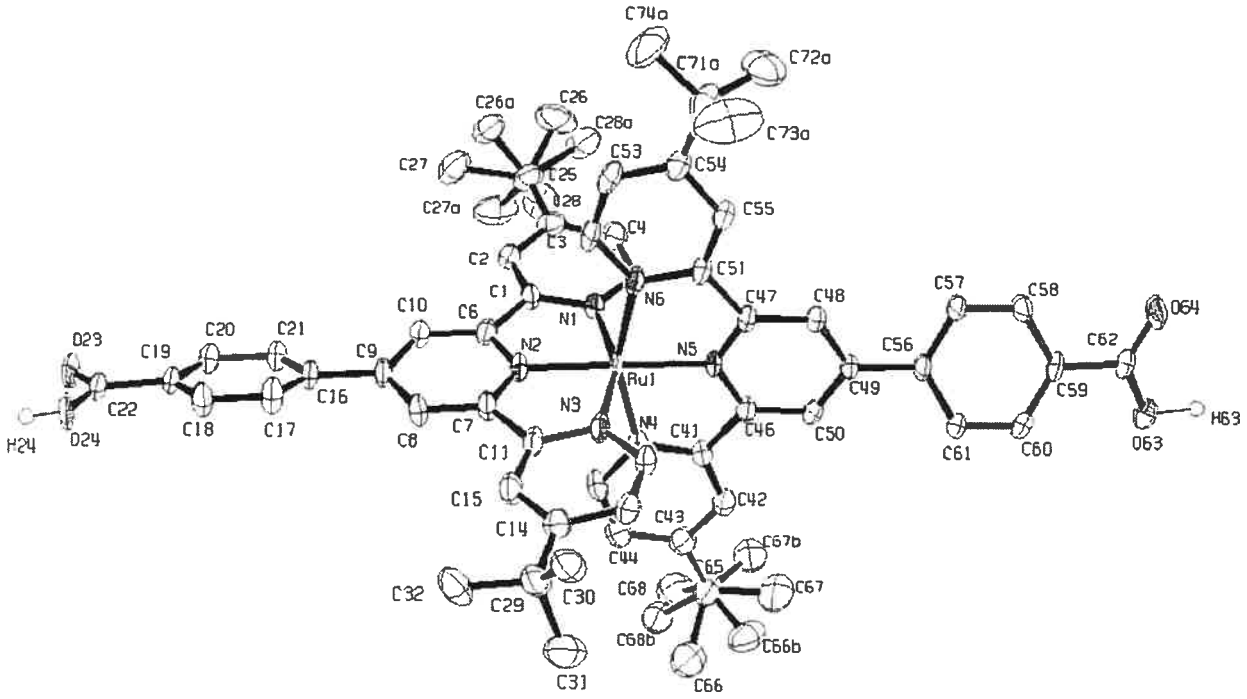

Table 1. Crystal data and structure refinement for **III-4**.

Empirical formula	C67 H77 F9 N6.50 O5 P1.50 Ru
Formula weight	1372.03
Temperature	293(2)K
Wavelength	1.54178 Å
Crystal system	Monoclinic
Space group	C2/c
Unit cell dimensions	a = 36.4372(4) Å α = 90° b = 16.9548(2) Å β = 119.8360(10)° c = 26.0003(3) Å γ = 90°
Volume	13933.5(3)Å^3
Z	8
Density (calculated)	1.309 g/cm^3
Absorption coefficient	2.786 mm^{-1}
F(000)	5701
Crystal size	0.67 x 0.31 x 0.23 mm
Theta range for data collection	2.80 to 72.99°
Index ranges	$-45 \leq h \leq 45$, $-21 \leq k \leq 20$, $-28 \leq \ell \leq 31$

Reflections collected	56953
Independent reflections	13729 [R_{int} = 0.036]
Absorption correction	Semi-empirical from equivalents
Max. and min. transmission	0.6800 and 0.4200
Refinement method	Full-matrix least-squares on F^2
Data / restraints / parameters	13729 / 292 / 1038
Goodness-of-fit on F^2	0.980
Final R indices [I>2sigma(I)]	R_1 = 0.0544, wR_2 = 0.1453
R indices (all data)	R_1 = 0.0784, wR_2 = 0.1560
Largest diff. peak and hole	1.105 and -0.441 e/Å^3

Table 2. Atomic coordinates (x 10^4) and equivalent isotropic displacement parameters (Å^2 x 10^3) for **III-4**.

U_{eq} is defined as one third of the trace of the orthogonalized Uij tensor.

	Occ.	x	y	z	U_{eq}
Ru(1)	1	2013(1)	3632(1)	7729(1)	27(1)
N(1)	1	1760(1)	4519(2)	8013(1)	26(1)
C(1)	1	1428(1)	4916(2)	7559(2)	28(1)
C(2)	1	1202(1)	5471(3)	7670(2)	32(1)
C(3)	1	1294(1)	5639(3)	8250(2)	35(1)
C(4)	1	1641(1)	5256(3)	8699(2)	35(1)
C(5)	1	1863(1)	4715(3)	8567(2)	31(1)
C(6)	1	1334(1)	4690(2)	6958(2)	28(1)
N(2)	1	1583(1)	4095(2)	6963(1)	27(1)
C(7)	1	1550(1)	3805(2)	6457(2)	29(1)
C(8)	1	1260(1)	4127(3)	5917(2)	33(1)
C(9)	1	990(1)	4731(3)	5889(2)	30(1)
C(10)	1	1032(1)	5008(3)	6423(2)	29(1)
C(11)	1	1846(1)	3148(2)	6557(2)	29(1)
N(3)	1	2098(1)	2943(2)	7140(1)	29(1)
C(12)	1	2378(1)	2356(3)	7257(2)	36(1)
C(13)	1	2421(1)	1972(3)	6823(2)	39(1)
C(14)	1	2166(1)	2174(3)	6224(2)	36(1)
C(15)	1	1875(1)	2771(3)	6107(2)	33(1)
C(16)	1	664(1)	5048(3)	5305(2)	32(1)
C(17)	1	532(2)	4607(3)	4791(2)	42(1)
C(18)	1	235(1)	4903(3)	4241(2)	44(1)
C(19)	1	59(1)	5632(3)	4199(2)	39(1)
C(20)	1	178(1)	6063(3)	4705(2)	40(1)
C(21)	1	481(1)	5780(3)	5255(2)	36(1)
C(22)	1	-250(1)	5978(4)	3609(2)	46(1)

O(23)	1	-410(1)	6623(3)	3558(2)	59(1)
O(24)	1	-322(1)	5500(2)	3165(1)	49(1)
C(25)	1	1015(2)	6205(3)	8367(2)	42(1)
C(26)	0.315(9)	856(7)	5762(12)	8694(9)	65(7)
C(27)	0.315(9)	598(5)	6443(13)	7736(8)	62(7)
C(28)	0.315(9)	1258(7)	6913(12)	8651(9)	60(6)
C(26A)	0.685(9)	560(2)	5929(5)	8045(4)	49(2)
C(27A)	0.685(9)	1067(3)	7034(5)	8203(5)	66(3)
C(28A)	0.685(9)	1150(3)	6227(5)	9050(3)	56(3)
C(29)	1	2227(2)	1776(3)	5745(2)	42(1)
C(30)	1	2197(2)	875(3)	5780(2)	46(1)
C(31)	1	2669(2)	1998(3)	5857(3)	59(2)
C(32)	1	1902(2)	2050(3)	5123(2)	51(1)
N(4)	1	2540(1)	4299(2)	7905(1)	30(1)
C(41)	1	2897(1)	4091(3)	8425(2)	29(1)
C(42)	1	3274(1)	4479(3)	8622(2)	35(1)
C(43)	1	3313(1)	5100(3)	8304(2)	39(1)
C(44)	1	2952(2)	5275(3)	7766(2)	43(1)
C(45)	1	2583(2)	4873(3)	7584(2)	38(1)
C(46)	1	2845(1)	3422(2)	8745(2)	25(1)
N(5)	1	2446(1)	3141(2)	8480(1)	25(1)
C(47)	1	2342(1)	2510(2)	8698(2)	26(1)
C(48)	1	2650(1)	2137(2)	9210(2)	26(1)
C(49)	1	3064(1)	2427(2)	9496(2)	25(1)
C(50)	1	3158(1)	3074(2)	9253(2)	27(1)
C(51)	1	1889(1)	2308(2)	8349(2)	27(1)
N(6)	1	1657(1)	2791(2)	7867(1)	29(1)
C(52)	1	1237(1)	2685(3)	7566(2)	34(1)
C(53)	1	1033(1)	2119(3)	7720(2)	36(1)
C(54)	1	1261(1)	1610(3)	8194(2)	32(1)
C(55)	1	1701(1)	1724(3)	8504(2)	31(1)
C(56)	1	3395(1)	2090(2)	10063(2)	26(1)
C(57)	1	3297(1)	1842(2)	10490(2)	28(1)
C(58)	1	3613(1)	1614(2)	11043(2)	29(1)
C(59)	1	4036(1)	1633(2)	11189(2)	26(1)
C(60)	1	4134(1)	1852(3)	10758(2)	32(1)
C(61)	1	3817(1)	2072(3)	10199(2)	33(1)
C(62)	1	4368(1)	1441(2)	11811(2)	28(1)
O(63)	1	4737(1)	1691(2)	11970(1)	40(1)
O(64)	1	4258(1)	1083(2)	12125(1)	43(1)
C(65)	1	3735(2)	5522(3)	8539(3)	54(2)
C(66)	0.279(10)	3876(7)	5236(12)	8020(10)	64(7)
C(67)	0.279(10)	4085(6)	5223(14)	9105(11)	69(8)
C(68)	0.279(10)	3690(9)	6351(16)	8498(14)	67(7)
C(66B)	0.721(10)	4059(3)	4976(5)	8577(5)	65(3)
C(67B)	0.721(10)	3876(2)	5827(5)	9190(3)	56(2)
C(68B)	0.721(10)	3692(3)	6259(5)	8190(4)	52(2)
C(71A)	1	1062(1)	966(3)	8385(2)	41(1)
C(72A)	1	1220(2)	986(4)	9041(2)	69(2)
C(73A)	1	1162(2)	171(3)	8217(4)	98(3)
C(74A)	1	589(2)	1072(4)	8065(3)	92(3)
C(91)	0.50	4441(2)	3809(4)	10091(3)	280(30)
C(92)	0.50	4834(5)	3298(11)	10369(9)	109(6)
C(93)	0.50	5091(8)	3240(20)	11041(10)	168(12)
O(94)	0.50	5100(4)	3540(9)	10152(7)	146(6)
C(95)	0.50	4992(9)	3395(15)	9530(10)	172(10)
C(96)	0.50	5122(7)	4020(15)	9211(12)	200(12)
C(97)	0.50	5197(10)	2624(16)	9468(14)	226(14)
C(101)	0.50	4885(5)	3448(12)	11005(7)	92(6)
C(102)	0.50	4529(3)	3670(8)	10420(6)	60(3)
N(103)	0.50	4244(4)	3799(7)	9986(5)	79(4)
C(111)	0.50	4723(5)	2927(10)	9217(7)	96(5)

C(112)	0.50	4535(4)	2707(9)	8581(6)	75(4)
C(113)	0.50	4844(6)	2266(12)	8471(9)	140(8)
O(114)	0.50	4189(5)	2186(7)	8445(8)	68(4)
C(115)	0.50	3800(12)	2580(20)	8388(16)	205(15)
C(116)	0.50	3504(6)	1853(13)	8388(9)	72(5)
C(117)	0.50	3545(6)	2945(10)	7765(6)	86(5)
P(1)	0.60	2665(3)	9742(3)	9321(3)	71(3)
F(11)	0.60	3068(3)	9236(5)	9775(4)	110(3)
F(12)	0.60	2975(4)	10245(9)	9208(6)	177(7)
F(13)	0.60	2734(3)	10278(5)	9849(4)	98(3)
F(14)	0.60	2374(4)	9173(6)	9418(5)	129(4)
F(15)	0.60	2554(4)	9163(6)	8773(4)	116(4)
F(16)	0.60	2297(3)	10290(7)	8881(5)	99(4)
P(11)	0.40	2603(4)	9762(6)	9272(5)	71(4)
F(111)	0.40	2788(4)	9138(6)	9791(5)	90(4)
F(112)	0.40	3017(3)	10323(7)	9503(6)	89(4)
F(113)	0.40	2484(5)	10335(7)	9652(6)	94(4)
F(114)	0.40	2176(4)	9338(9)	9079(7)	142(7)
F(115)	0.40	2764(4)	9330(9)	8889(6)	82(4)
F(116)	0.40	2374(5)	10369(9)	8752(6)	73(4)
P(2)	0.50	3750(1)	2410(3)	8316(2)	52(1)
F(21)	0.50	3937(3)	2817(6)	8937(4)	119(3)
F(22)	0.50	3587(6)	1772(11)	8608(7)	156(7)
F(23)	0.50	3333(2)	2899(5)	8109(4)	91(3)
F(24)	0.50	3929(4)	3036(6)	8077(6)	121(4)
F(25)	0.50	4151(4)	1864(6)	8508(6)	71(3)
F(26)	0.50	3524(3)	1935(6)	7721(4)	126(4)

Table 3. Hydrogen coordinates (x 10^4) and isotropic displacement parameters (Å^2 x 10^3) for **III-4**.

	Occ.	x	y	z	U_{eq}
H(2)	1	983	5740	7354	39
H(4)	1	1725	5366	9093	42
H(5)	1	2097	4473	8878	38
H(8)	1	1244	3940	5571	39
H(10)	1	856	5408	6419	34
H(12)	1	2551	2203	7649	43
H(13)	1	2621	1574	6928	47
H(15)	1	1695	2921	5716	40
H(17)	1	644	4106	4816	50
H(18)	1	154	4606	3901	53
H(20)	1	54	6552	4679	48
H(21)	1	561	6083	5593	43
H(24)	1	-477	5720	2849	73
H(26A)	0.315(9)	692	6104	8797	97
H(26B)	0.315(9)	1090	5553	9049	97
H(26C)	0.315(9)	681	5337	8453	97
H(27A)	0.315(9)	503	5991	7480	93
H(27B)	0.315(9)	671	6858	7551	93
H(27C)	0.315(9)	377	6620	7806	93
H(28A)	0.315(9)	1080	7287	8702	90
H(28B)	0.315(9)	1360	7140	8407	90
H(28C)	0.315(9)	1493	6779	9031	90
H(26D)	0.685(9)	542	5417	8188	73

H(26E)	0.685(9)	462	5901	7627	73
H(26F)	0.685(9)	388	6295	8114	73
H(27D)	0.685(9)	889	7385	8272	98
H(27E)	0.685(9)	988	7051	7792	98
H(27F)	0.685(9)	1357	7194	8441	98
H(28D)	0.685(9)	1438	6404	9277	83
H(28E)	0.685(9)	1126	5708	9177	83
H(28F)	0.685(9)	969	6583	9108	83
H(30A)	1	2386	703	6178	69
H(30B)	1	2274	629	5515	69
H(30C)	1	1912	732	5670	69
H(31A)	1	2684	2558	5818	88
H(31B)	1	2721	1736	5573	88
H(31C)	1	2877	1838	6250	88
H(32A)	1	1623	1924	5048	77
H(32B)	1	1953	1789	4837	77
H(32C)	1	1926	2610	5094	77
H(42)	1	3508	4323	8976	42
H(44)	1	2963	5672	7526	52
H(45)	1	2350	5003	7221	45
H(48)	1	2580	1699	9360	31
H(50)	1	3433	3272	9434	32
H(52)	1	1074	3006	7240	41
H(53)	1	740	2079	7503	44
H(55)	1	1869	1395	8821	37
H(57)	1	3016	1829	10401	33
H(58)	1	3544	1445	11323	35
H(60)	1	4414	1851	10846	38
H(61)	1	3886	2209	9911	39
H(63)	1	5000	1670(40)	12500	60
H(66A)	0.279(10)	4164	5388	8155	96
H(66B)	0.279(10)	3693	5488	7648	96
H(66C)	0.279(10)	3850	4674	7970	96
H(67A)	0.279(10)	4335	5528	9215	103
H(67B)	0.279(10)	4138	4680	9059	103
H(67C)	0.279(10)	4009	5267	9408	103
H(68A)	0.279(10)	3962	6589	8628	100
H(68B)	0.279(10)	3579	6529	8744	100
H(68C)	0.279(10)	3500	6497	8093	100
H(66D)	0.721(10)	4324	5249	8731	97
H(66E)	0.721(10)	3977	4774	8190	97
H(66F)	0.721(10)	4089	4547	8836	97
H(67D)	0.721(10)	3901	5386	9437	83
H(67E)	0.721(10)	3668	6188	9175	83
H(67F)	0.721(10)	4144	6090	9351	83
H(68D)	0.721(10)	3958	6533	8369	79
H(68E)	0.721(10)	3479	6593	8188	79
H(68F)	0.721(10)	3613	6119	7790	79
H(72A)	1	1068	606	9136	104
H(72B)	1	1176	1503	9151	104
H(72C)	1	1516	863	9253	104
H(73A)	1	997	101	7796	148
H(73B)	1	1096	-240	8412	148
H(73C)	1	1458	147	8338	148
H(74A)	1	484	1091	7645	138
H(74B)	1	521	1555	8191	138
H(74C)	1	462	637	8154	138
H(91A)	0.50	4569	4304	10268	420
H(91B)	0.50	4197	3723	10133	420
H(91C)	0.50	4357	3817	9678	420
H(92)	0.50	4741	2762	10220	131
H(93A)	0.50	5353	2971	11155	252

H(93B)	0.50	4933	2942	11183	252
H(93C)	0.50	5148	3755	11211	252
H(95)	0.50	4685	3330	9295	206
H(96A)	0.50	4885	4357	8974	299
H(96B)	0.50	5208	3757	8961	299
H(96C)	0.50	5353	4330	9501	299
H(97A)	0.50	5061	2177	9528	339
H(97B)	0.50	5493	2619	9759	339
H(97C)	0.50	5164	2598	9078	339
H(10A)	0.50	4781	3141	11216	138
H(10B)	0.50	5019	3917	11228	138
H(10C)	0.50	5086	3143	10954	138
H(11A)	0.50	4522	3229	9271	145
H(11B)	0.50	4973	3237	9336	145
H(11C)	0.50	4795	2458	9454	145
H(112)	0.50	4435	3178	8331	89
H(11D)	0.50	4719	2154	8055	211
H(11E)	0.50	4919	1780	8689	211
H(11F)	0.50	5094	2580	8597	211
H(115)	0.50	3866	2959	8705	246
H(11G)	0.50	3654	1563	8752	108
H(11H)	0.50	3437	1509	8059	108
H(11I)	0.50	3248	2062	8352	108
H(11J)	0.50	3710	3352	7720	129
H(11K)	0.50	3288	3167	7717	129
H(11L)	0.50	3479	2545	7470	129

Table 4. Anisotropic parameters ($Å^2$ x 10^3) for **III-4**.
The anisotropic displacement factor exponent takes the form:

$$-2\pi^2 [h^2 a^{*2} U_{11} + ... + 2 h k a^* b^* U_{12}]$$

	U11	U22	U33	U23	U13	U12
Ru(1)	20(1)	33(1)	16(1)	8(1)	1(1)	6(1)
N(1)	20(2)	33(2)	19(2)	4(1)	5(1)	1(1)
C(1)	23(2)	35(2)	18(2)	6(2)	5(2)	0(2)
C(2)	22(2)	39(2)	31(2)	9(2)	10(2)	3(2)
C(3)	31(2)	38(3)	37(2)	-5(2)	18(2)	-6(2)
C(4)	30(2)	46(3)	25(2)	-4(2)	9(2)	-8(2)
C(5)	23(2)	42(2)	17(2)	4(2)	1(2)	-7(2)
C(6)	22(2)	30(2)	26(2)	6(2)	7(2)	3(2)
N(2)	24(2)	32(2)	17(2)	7(1)	3(1)	6(1)
C(7)	27(2)	33(2)	19(2)	7(2)	5(2)	6(2)
C(8)	32(2)	38(2)	17(2)	5(2)	4(2)	5(2)
C(9)	24(2)	35(2)	20(2)	10(2)	2(2)	5(2)
C(10)	22(2)	34(2)	23(2)	8(2)	6(2)	5(2)
C(11)	23(2)	29(2)	24(2)	7(2)	5(2)	5(2)
N(3)	24(2)	32(2)	22(2)	8(1)	4(1)	5(1)
C(12)	27(2)	42(3)	31(2)	17(2)	9(2)	11(2)
C(13)	32(2)	41(3)	41(3)	16(2)	16(2)	16(2)
C(14)	36(2)	33(2)	38(2)	9(2)	19(2)	6(2)
C(15)	32(2)	33(2)	28(2)	10(2)	10(2)	7(2)
C(16)	22(2)	43(3)	21(2)	12(2)	2(2)	6(2)

C(17)	36(3)	46(3)	27(2)	9(2)	4(2)	10(2)
C(18)	34(3)	61(3)	23(2)	12(2)	3(2)	2(2)
C(19)	19(2)	61(3)	26(2)	21(2)	4(2)	7(2)
C(20)	28(2)	52(3)	32(2)	18(2)	9(2)	14(2)
C(21)	28(2)	46(3)	25(2)	13(2)	7(2)	11(2)
C(22)	19(2)	76(4)	28(2)	26(3)	2(2)	5(2)
O(23)	36(2)	95(3)	32(2)	32(2)	7(2)	34(2)
O(24)	32(2)	69(2)	21(2)	22(2)	-5(1)	-4(2)
C(25)	33(3)	52(3)	44(3)	-8(2)	21(2)	2(2)
C(26)	84(16)	73(14)	71(14)	3(11)	66(13)	13(11)
C(27)	35(9)	107(18)	38(10)	-18(10)	14(8)	11(10)
C(28)	68(14)	61(13)	46(11)	-21(10)	26(10)	-4(10)
C(26A)	31(4)	73(6)	40(4)	-14(4)	16(3)	1(4)
C(27A)	71(7)	47(5)	105(9)	-6(5)	64(7)	10(5)
C(28A)	39(4)	81(7)	43(4)	-23(4)	17(4)	0(4)
C(29)	51(3)	43(3)	41(3)	13(2)	29(2)	15(2)
C(30)	58(3)	43(3)	49(3)	8(2)	35(3)	13(2)
C(31)	67(4)	55(3)	77(4)	11(3)	52(4)	10(3)
C(32)	78(4)	48(3)	38(3)	8(2)	36(3)	18(3)
N(4)	26(2)	36(2)	23(2)	9(1)	8(1)	7(2)
C(41)	28(2)	35(2)	23(2)	8(2)	11(2)	6(2)
C(42)	27(2)	38(2)	34(2)	10(2)	11(2)	5(2)
C(43)	34(2)	36(3)	48(3)	14(2)	20(2)	3(2)
C(44)	46(3)	40(3)	46(3)	20(2)	24(2)	9(2)
C(45)	40(3)	41(3)	29(2)	17(2)	14(2)	11(2)
C(46)	22(2)	28(2)	21(2)	2(2)	7(2)	2(2)
N(5)	18(2)	33(2)	15(2)	7(1)	3(1)	5(1)
C(47)	19(2)	30(2)	19(2)	3(2)	4(2)	4(2)
C(48)	19(2)	33(2)	19(2)	4(2)	5(2)	2(2)
C(49)	19(2)	34(2)	16(2)	5(2)	5(2)	6(2)
C(50)	15(2)	36(2)	22(2)	3(2)	4(2)	-1(2)
C(51)	18(2)	31(2)	21(2)	3(2)	1(2)	3(2)
N(6)	19(2)	34(2)	22(2)	7(1)	2(1)	2(1)
C(52)	20(2)	42(3)	21(2)	1(2)	-3(2)	6(2)
C(53)	17(2)	46(3)	29(2)	-4(2)	-1(2)	0(2)
C(54)	23(2)	33(2)	31(2)	-1(2)	6(2)	-1(2)
C(55)	21(2)	32(2)	26(2)	3(2)	3(2)	3(2)
C(56)	18(2)	32(2)	17(2)	5(2)	2(2)	2(2)
C(57)	15(2)	37(2)	22(2)	7(2)	3(2)	-2(2)
C(58)	22(2)	38(2)	18(2)	6(2)	4(2)	-4(2)
C(59)	17(2)	26(2)	20(2)	3(2)	-1(2)	3(2)
C(60)	16(2)	46(3)	27(2)	8(2)	6(2)	7(2)
C(61)	20(2)	50(3)	24(2)	10(2)	8(2)	7(2)
C(62)	19(2)	30(2)	20(2)	1(2)	0(2)	4(2)
O(63)	18(2)	61(2)	26(2)	6(1)	-1(1)	0(1)
O(64)	28(2)	60(2)	23(2)	18(2)	-1(1)	0(2)
C(65)	38(3)	46(3)	73(4)	28(3)	23(3)	1(2)
C(66)	57(14)	52(13)	86(17)	26(12)	39(13)	5(10)
C(67)	41(12)	66(16)	84(18)	18(13)	20(12)	-18(11)
C(68)	68(16)	63(15)	80(20)	8(16)	44(16)	7(12)
C(66B)	47(5)	53(5)	107(8)	27(5)	48(5)	8(4)
C(67B)	42(4)	56(5)	59(5)	5(4)	18(4)	-19(4)
C(68B)	40(4)	48(5)	68(6)	22(5)	26(5)	-3(3)
C(71A)	25(2)	36(3)	50(3)	-1(2)	10(2)	-4(2)
C(72A)	64(4)	83(5)	62(4)	2(3)	32(3)	-32(4)
C(73A)	106(6)	44(4)	179(9)	-40(5)	97(6)	-33(4)
C(74A)	32(3)	94(5)	128(7)	43(5)	23(4)	-9(3)
C(91)	250(30)	290(30)	290(30)	50(20)	130(20)	40(20)
C(92)	77(10)	125(13)	135(14)	24(11)	59(10)	-2(9)
C(93)	150(20)	200(20)	157(19)	46(16)	84(16)	-3(16)
O(94)	102(9)	187(13)	166(13)	33(10)	79(9)	-7(8)
C(95)	153(18)	210(20)	133(17)	-26(16)	58(14)	-14(16)

C(96)	128(16)	230(20)	230(20)	66(17)	84(15)	-34(15)
C(97)	220(20)	200(20)	250(20)	-21(17)	106(17)	37(17)
C(101)	66(10)	92(12)	81(11)	-7(8)	9(8)	-7(9)
C(102)	30(5)	72(8)	70(8)	-20(7)	20(5)	-5(5)
N(103)	67(7)	86(8)	86(8)	19(7)	39(7)	-3(6)
C(111)	93(11)	82(10)	87(10)	-18(8)	24(8)	-33(9)
C(112)	66(8)	80(9)	58(7)	-16(7)	17(6)	-7(7)
C(113)	86(11)	181(16)	141(14)	-72(12)	46(10)	10(11)
O(114)	60(6)	54(7)	93(9)	-21(7)	40(6)	-1(6)
C(115)	220(20)	220(20)	210(20)	-10(18)	127(19)	36(18)
C(116)	48(8)	91(11)	67(9)	8(8)	22(7)	3(7)
C(117)	84(10)	92(11)	67(9)	1(8)	27(8)	15(9)
P(1)	106(5)	35(3)	71(4)	-8(2)	43(3)	16(3)
F(11)	110(6)	86(5)	90(5)	-8(4)	16(5)	36(5)
F(12)	159(9)	228(11)	194(11)	1(8)	125(8)	6(7)
F(13)	104(6)	63(4)	92(5)	-33(4)	22(5)	16(4)
F(14)	179(9)	96(6)	140(8)	-7(6)	99(7)	-44(6)
F(15)	161(9)	88(6)	86(6)	6(4)	50(6)	61(6)
F(16)	82(5)	61(5)	130(8)	9(5)	35(5)	32(4)
P(11)	81(5)	70(7)	67(5)	28(4)	41(4)	42(4)
F(111)	91(7)	62(6)	70(6)	23(5)	5(6)	9(6)
F(112)	48(5)	71(6)	104(8)	-8(6)	5(5)	8(5)
F(113)	141(9)	78(7)	87(7)	5(6)	74(7)	16(7)
F(114)	112(9)	118(9)	133(10)	26(8)	13(7)	-36(7)
F(115)	97(8)	78(7)	88(8)	3(6)	58(6)	34(6)
F(116)	107(9)	57(7)	52(5)	-1(4)	38(6)	21(6)
P(2)	54(2)	58(2)	41(2)	3(1)	21(1)	22(2)
F(21)	106(6)	168(8)	73(5)	-35(5)	38(5)	26(6)
F(22)	173(11)	172(11)	174(12)	13(8)	124(9)	21(8)
F(23)	71(5)	97(6)	93(5)	-27(4)	31(4)	22(4)
F(24)	120(7)	102(7)	162(8)	44(6)	86(6)	26(6)
F(25)	66(6)	68(7)	61(5)	2(5)	19(4)	11(5)
F(26)	90(6)	135(7)	118(7)	-52(6)	25(5)	43(5)

Table 5. Bond lengths [Å] and angles [°] for **III-4**.

Ru(1)-N(5)	1.982(3)	C(8)-C(9)	1.396(6)
Ru(1)-N(2)	1.984(3)	C(8)-H(8)	0.93
Ru(1)-N(3)	2.069(4)	C(9)-C(10)	1.400(6)
Ru(1)-N(4)	2.074(4)	C(9)-C(16)	1.488(5)
Ru(1)-N(6)	2.075(3)	C(10)-H(10)	0.93
Ru(1)-N(1)	2.083(3)	C(11)-N(3)	1.369(5)
N(1)-C(5)	1.335(5)	C(11)-C(15)	1.382(6)
N(1)-C(1)	1.374(5)	N(3)-C(12)	1.347(5)
C(1)-C(2)	1.373(6)	C(12)-C(13)	1.376(6)
C(1)-C(6)	1.475(5)	C(12)-H(12)	0.93
C(2)-C(3)	1.402(6)	C(13)-C(14)	1.401(6)
C(2)-H(2)	0.93	C(13)-H(13)	0.93
C(3)-C(4)	1.383(6)	C(14)-C(15)	1.384(6)
C(3)-C(25)	1.535(6)	C(14)-C(29)	1.530(6)
C(4)-C(5)	1.376(6)	C(15)-H(15)	0.93
C(4)-H(4)	0.93	C(16)-C(21)	1.384(6)
C(5)-H(5)	0.93	C(16)-C(17)	1.391(6)
C(6)-N(2)	1.351(5)	C(17)-C(18)	1.389(6)
C(6)-C(10)	1.383(5)	C(17)-H(17)	0.93
N(2)-C(7)	1.353(5)	C(18)-C(19)	1.371(7)
C(7)-C(8)	1.382(5)	C(18)-H(18)	0.93
C(7)-C(11)	1.481(6)	C(19)-C(20)	1.374(7)
		C(19)-C(22)	1.497(5)

C(20)-C(21)	1.387(5)	C(47)-C(51)	1.473(5)
C(20)-H(20)	0.93	C(48)-C(49)	1.399(5)
C(21)-H(21)	0.93	C(48)-H(48)	0.93
C(22)-O(23)	1.215(7)	C(49)-C(50)	1.392(5)
C(22)-O(24)	1.327(6)	C(49)-C(56)	1.479(5)
O(24)-H(24)	0.82	C(50)-H(50)	0.93
C(25)-C(26)	1.452(17)	C(51)-C(55)	1.374(6)
C(25)-C(28)	1.456(19)	C(51)-N(6)	1.379(5)
C(25)-C(27a)	1.508(10)	N(6)-C(52)	1.341(5)
C(25)-C(26a)	1.511(8)	C(52)-C(53)	1.388(6)
C(25)-C(28a)	1.588(9)	C(52)-H(52)	0.93
C(25)-C(27)	1.638(18)	C(53)-C(54)	1.391(6)
C(26)-H(26a)	0.96	C(53)-H(53)	0.93
C(26)-H(26b)	0.96	C(54)-C(55)	1.404(6)
C(26)-H(26c)	0.96	C(54)-C(71a)	1.522(6)
C(27)-H(27a)	0.96	C(55)-H(55)	0.93
C(27)-H(27b)	0.96	C(56)-C(57)	1.391(5)
C(27)-H(27c)	0.96	C(56)-C(61)	1.397(5)
C(28)-H(28a)	0.96	C(57)-C(58)	1.377(5)
C(28)-H(28b)	0.96	C(57)-H(57)	0.93
C(28)-H(28c)	0.96	C(58)-C(59)	1.390(5)
C(26a)-H(26d)	0.96	C(58)-H(58)	0.93
C(26a)-H(26e)	0.96	C(59)-C(60)	1.383(6)
C(26a)-H(26f)	0.96	C(59)-C(62)	1.498(5)
C(27a)-H(27d)	0.96	C(60)-C(61)	1.384(5)
C(27a)-H(27e)	0.96	C(60)-H(60)	0.93
C(27a)-H(27f)	0.96	C(61)-H(61)	0.93
C(28a)-H(28d)	0.96	C(62)-O(64)	1.233(5)
C(28a)-H(28e)	0.96	C(62)-O(63)	1.267(5)
C(28a)-H(28f)	0.96	O(63)-H(63)	1.226(4)
C(29)-C(32)	1.525(6)	C(65)-C(68)	1.41(3)
C(29)-C(31)	1.532(7)	C(65)-C(66b)	1.464(9)
C(29)-C(30)	1.536(7)	C(65)-C(67)	1.48(2)
C(30)-H(30a)	0.96	C(65)-C(68b)	1.506(9)
C(30)-H(30b)	0.96	C(65)-C(67b)	1.591(10)
C(30)-H(30c)	0.96	C(65)-C(66)	1.74(2)
C(31)-H(31a)	0.96	C(66)-H(66a)	0.96
C(31)-H(31b)	0.96	C(66)-H(66b)	0.96
C(31)-H(31c)	0.96	C(66)-H(66c)	0.96
C(32)-H(32a)	0.96	C(67)-H(67a)	0.96
C(32)-H(32b)	0.96	C(67)-H(67b)	0.96
C(32)-H(32c)	0.96	C(67)-H(67c)	0.96
N(4)-C(45)	1.339(5)	C(68)-H(68a)	0.96
N(4)-C(41)	1.376(5)	C(68)-H(68b)	0.96
C(41)-C(42)	1.372(6)	C(68)-H(68c)	0.96
C(41)-C(46)	1.474(5)	C(66b)-H(66d)	0.96
C(42)-C(43)	1.389(6)	C(66b)-H(66e)	0.96
C(42)-H(42)	0.93	C(66b)-H(66f)	0.96
C(43)-C(44)	1.395(6)	C(67b)-H(67d)	0.96
C(43)-C(65)	1.521(7)	C(67b)-H(67e)	0.96
C(44)-C(45)	1.367(6)	C(67b)-H(67f)	0.96
C(44)-H(44)	0.93	C(68b)-H(68d)	0.96
C(45)-H(45)	0.93	C(68b)-H(68e)	0.96
C(46)-N(5)	1.347(5)	C(68b)-H(68f)	0.96
C(46)-C(50)	1.377(5)	C(71a)-C(72a)	1.504(7)
N(5)-C(47)	1.352(5)	C(71a)-C(74a)	1.505(6)
C(47)-C(48)	1.395(5)	C(71a)-C(73a)	1.517(7)

C(72a)-H(72a)	0.96	C(117)-H(11k)	0.96
C(72a)-H(72b)	0.96	C(117)-H(11l)	0.96
C(72a)-H(72c)	0.96	P(1)-F(14)	1.543(9)
C(73a)-H(73a)	0.96	P(1)-F(12)	1.555(11)
C(73a)-H(73b)	0.96	P(1)-F(13)	1.559(8)
C(73a)-H(73c)	0.96	P(1)-F(16)	1.562(9)
C(74a)-H(74a)	0.96	P(1)-F(11)	1.600(9)
C(74a)-H(74b)	0.96	P(1)-F(15)	1.608(9)
C(74a)-H(74c)	0.96	P(11)-F(114)	1.553(13)
C(91)-C(92)	1.514(15)	P(11)-F(115)	1.565(12)
C(91)-H(91a)	0.96	P(11)-F(116)	1.568(12)
C(91)-H(91b)	0.96	P(11)-F(111)	1.579(12)
C(91)-H(91c)	0.9598	P(11)-F(113)	1.592(12)
C(92)-O(94)	1.404(14)	P(11)-F(112)	1.626(12)
C(92)-C(93)	1.522(19)	P(2)-F(24)	1.53(1)
C(92)-H(92)	0.98	P(2)-F(26)	1.565(9)
C(93)-H(93a)	0.96	P(2)-F(21)	1.568(9)
C(93)-H(93b)	0.96	P(2)-F(23)	1.572(8)
C(93)-H(93c)	0.96	P(2)-F(25)	1.586(11)
O(94)-C(95)	1.481(17)	P(2)-F(22)	1.596(14)
C(95)-C(97)	1.554(19)		
C(95)-C(96)	1.558(19)	N(5)-RU1-N(2)	178.08(14)
C(95)-H(95)	0.98	N(5)-RU1-N(3)	98.78(13)
C(96)-H(96a)	0.96	N(2)-RU1-N(3)	79.31(13)
C(96)-H(96b)	0.96	N(5)-RU1-N(4)	79.37(13)
C(96)-H(96c)	0.96	N(2)-RU1-N(4)	100.81(13)
C(97)-H(97a)	0.96	N(3)-RU1-N(4)	90.48(14)
C(97)-H(97b)	0.96	N(5)-RU1-N(6)	78.52(13)
C(97)-H(97c)	0.96	N(2)-RU1-N(6)	101.35(13)
C(101)-C(102)	1.475(14)	N(3)-RU1-N(6)	94.40(14)
C(101)-H(10a)	0.96	N(4)-RU1-N(6)	157.83(13)
C(101)-H(10b)	0.96	N(5)-RU1-N(1)	103.31(13)
C(101)-H(10c)	0.96	N(2)-RU1-N(1)	78.59(13)
C(102)-N(103)	1.112(14)	N(3)-RU1-N(1)	157.89(12)
C(102)-H(91a)	1.1782	N(4)-RU1-N(1)	92.98(13)
C(102)-H(91b)	1.0639	N(6)-RU1-N(1)	90.59(13)
N(103)-H(91a)	1.3455	C(5)-N(1)-C(1)	117.4(4)
N(103)-H(91b)	0.5076	C(5)-N(1)-RU1	128.7(3)
N(103)-H(91c)	1.0694	C(1)-N(1)-RU1	113.8(3)
C(111)-C(112)	1.488(18)	C(2)-C(1)-N(1)	121.2(4)
C(111)-H(11a)	0.96	C(2)-C(1)-C(6)	123.6(4)
C(111)-H(11b)	0.96	N(1)-C(1)-C(6)	115.1(4)
C(111)-H(11c)	0.96	C(1)-C(2)-C(3)	121.2(4)
C(112)-O(114)	1.430(18)	C(1)-C(2)-H(2)	119.4
C(112)-C(113)	1.494(19)	C(3)-C(2)-H(2)	119.4
C(112)-H(112)	0.98	C(4)-C(3)-C(2)	116.1(4)
C(113)-H(11d)	0.96	C(4)-C(3)-C(25)	122.9(4)
C(113)-H(11e)	0.96	C(2)-C(3)-C(25)	120.9(4)
C(113)-H(11f)	0.96	C(5)-C(4)-C(3)	120.5(4)
O(114)-C(115)	1.50(4)	C(5)-C(4)-H(4)	119.8
C(115)-C(117)	1.54(4)	C(3)-C(4)-H(4)	119.8
C(115)-C(116)	1.63(4)	N(1)-C(5)-C(4)	123.4(4)
C(115)-H(115)	0.98	N(1)-C(5)-H(5)	118.3
C(116)-H(11g)	0.96	C(4)-C(5)-H(5)	118.3
C(116)-H(11h)	0.96	N(2)-C(6)-C(10)	119.7(4)
C(116)-H(11i)	0.96	N(2)-C(6)-C(1)	112.5(3)
C(117)-H(11j)	0.96	C(10)-C(6)-C(1)	127.8(4)

C(6)-N(2)-C(7)	121.9(3)	C(28)-C(25)-C(27A)	40.9(8)
C(6)-N(2)-RU1	119.7(3)	C(26)-C(25)-C(26A)	61.3(9)
C(7)-N(2)-RU1	118.4(3)	C(28)-C(25)-C(26A)	139.4(1)
N(2)-C(7)-C(8)	119.7(4)	C(27A)-C(25)-C(26A)	112.9(6)
N(2)-C(7)-C(11)	113.5(3)	C(26)-C(25)-C(3)	106.8(8)
C(8)-C(7)-C(11)	126.8(4)	C(28)-C(25)-C(3)	108.7(9)
C(7)-C(8)-C(9)	120.5(4)	C(27A)-C(25)-C(3)	109.7(5)
C(7)-C(8)-H(8)	119.8	C(26A)-C(25)-C(3)	110.3(5)
C(9)-C(8)-H(8)	119.8	C(26)-C(25)-C(28A)	49.6(9)
C(8)-C(9)-C(10)	117.8(4)	C(28)-C(25)-C(28A)	69.0(9)
C(8)-C(9)-C(16)	120.1(4)	C(27A)-C(25)-C(28A)	106.4(6)
C(10)-C(9)-C(16)	122.0(4)	C(26A)-C(25)-C(28A)	105.9(5)
C(6)-C(10)-C(9)	120.4(4)	C(3)-C(25)-C(28A)	111.6(5)
C(6)-C(10)-H(10)	119.8	C(26)-C(25)-C(27)	105.90(12)
C(9)-C(10)-H(10)	119.8	C(28)-C(25)-C(27)	109.30(12)
N(3)-C(11)-C(15)	121.9(4)	C(27A)-C(25)-C(27)	70.8(9)
N(3)-C(11)-C(7)	114.4(4)	C(26A)-C(25)-C(27)	46.1(8)
C(15)-C(11)-C(7)	123.7(4)	C(3)-C(25)-C(27)	109.3(7)
C(12)-N(3)-C(11)	116.9(4)	C(28A)-C(25)-C(27)	137.1(7)
C(12)-N(3)-RU1	128.7(3)	C(25)-C(26)-H(26A)	109.5
C(11)-N(3)-RU1	114.3(3)	C(25)-C(26)-H(26B)	109.5
N(3)-C(12)-C(13)	123.0(4)	H(26A)-C(26)-H(26B)	109.5
N(3)-C(12)-H(12)	118.5	C(25)-C(26)-H(26C)	109.5
C(13)-C(12)-H(12)	118.5	H(26A)-C(26)-H(26C)	109.5
C(12)-C(13)-C(14)	120.8(4)	H(26B)-C(26)-H(26C)	109.5
C(12)-C(13)-H(13)	119.6	C(25)-C(27)-H(27A)	109.5
C(14)-C(13)-H(13)	119.6	C(25)-C(27)-H(27B)	109.5
C(15)-C(14)-C(13)	115.8(4)	H(27A)-C(27)-H(27B)	109.5
C(15)-C(14)-C(29)	123.3(4)	C(25)-C(27)-H(27C)	109.5
C(13)-C(14)-C(29)	120.8(4)	H(27A)-C(27)-H(27C)	109.5
C(11)-C(15)-C(14)	121.5(4)	H(27B)-C(27)-H(27C)	109.5
C(11)-C(15)-H(15)	119.2	C(25)-C(28)-H(28A)	109.5
C(14)-C(15)-H(15)	119.2	C(25)-C(28)-H(28B)	109.5
C(21)-C(16)-C(17)	118.2(4)	H(28A)-C(28)-H(28B)	109.5
C(21)-C(16)-C(9)	121.5(4)	C(25)-C(28)-H(28C)	109.5
C(17)-C(16)-C(9)	120.3(4)	H(28A)-C(28)-H(28C)	109.5
C(18)-C(17)-C(16)	120.9(5)	H(28B)-C(28)-H(28C)	109.5
C(18)-C(17)-H(17)	119.6	C(25)-C(26A)-H(26D)	109.5
C(16)-C(17)-H(17)	119.6	C(25)-C(26A)-H(26E)	109.5
C(19)-C(18)-C(17)	120.2(5)	H(26D)-C(26A)-H(26E)	109.5
C(19)-C(18)-H(18)	119.9	C(25)-C(26A)-H(26F)	109.5
C(17)-C(18)-H(18)	119.9	H(26D)-C(26A)-H(26F)	109.5
C(18)-C(19)-C(20)	119.3(4)	H(26E)-C(26A)-H(26F)	109.5
C(18)-C(19)-C(22)	121.3(5)	C(25)-C(27A)-H(27D)	109.5
C(20)-C(19)-C(22)	119.4(5)	C(25)-C(27A)-H(27E)	109.5
C(19)-C(20)-C(21)	120.9(5)	H(27D)-C(27A)-H(27E)	109.5
C(19)-C(20)-H(20)	119.6	C(25)-C(27A)-H(27F)	109.5
C(21)-C(20)-H(20)	119.6	H(27D)-C(27A)-H(27F)	109.5
C(16)-C(21)-C(20)	120.4(4)	H(27E)-C(27A)-H(27F)	109.5
C(16)-C(21)-H(21)	119.8	C(25)-C(28A)-H(28D)	109.5
C(20)-C(21)-H(21)	119.8	C(25)-C(28A)-H(28E)	109.5
O(23)-C(22)-O(24)	125.3(4)	H(28D)-C(28A)-H(28E)	109.5
O(23)-C(22)-C(19)	122.7(5)	C(25)-C(28A)-H(28F)	109.5
O(24)-C(22)-C(19)	112.0(5)	H(28D)-C(28A)-H(28F)	109.5
C(22)-O(24)-H(24)	109.5	H(28E)-C(28A)-H(28F)	109.5
C(26)-C(25)-C(28)	116.70(12)	C(32)-C(29)-C(14)	112.1(4)
C(26)-C(25)-C(27A)	142.2(9)	C(32)-C(29)-C(31)	108.4(4)

C(14)-C(29)-C(31)	107.6(4)
C(32)-C(29)-C(30)	109.0(4)
C(14)-C(29)-C(30)	110.2(4)
C(31)-C(29)-C(30)	109.5(4)
C(29)-C(30)-H(30A)	109.5
C(29)-C(30)-H(30B)	109.5
H(30A)-C(30)-H(30B)	109.5
C(29)-C(30)-H(30C)	109.5
H(30A)-C(30)-H(30C)	109.5
H(30B)-C(30)-H(30C)	109.5
C(29)-C(31)-H(31A)	109.5
C(29)-C(31)-H(31B)	109.5
H(31A)-C(31)-H(31B)	109.5
C(29)-C(31)-H(31C)	109.5
H(31A)-C(31)-H(31C)	109.5
H(31B)-C(31)-H(31C)	109.5
C(29)-C(32)-H(32A)	109.5
C(29)-C(32)-H(32B)	109.5
H(32A)-C(32)-H(32B)	109.5
C(29)-C(32)-H(32C)	109.5
H(32A)-C(32)-H(32C)	109.5
H(32B)-C(32)-H(32C)	109.5
C(45)-N(4)-C(41)	116.9(4)
C(45)-N(4)-RU1	129.8(3)
C(41)-N(4)-RU1	113.3(3)
C(42)-C(41)-N(4)	121.7(4)
C(42)-C(41)-C(46)	123.0(4)
N(4)-C(41)-C(46)	115.3(4)
C(41)-C(42)-C(43)	121.5(4)
C(41)-C(42)-H(42)	119.3
C(43)-C(42)-H(42)	119.3
C(42)-C(43)-C(44)	115.7(4)
C(42)-C(43)-C(65)	120.0(4)
C(44)-C(43)-C(65)	124.3(4)
C(45)-C(44)-C(43)	121.0(4)
C(45)-C(44)-H(44)	119.5
C(43)-C(44)-H(44)	119.5
N(4)-C(45)-C(44)	123.2(4)
N(4)-C(45)-H(45)	118.4
C(44)-C(45)-H(45)	118.4
N(5)-C(46)-C(50)	120.5(4)
N(5)-C(46)-C(41)	113.1(3)
C(50)-C(46)-C(41)	126.3(4)
C(46)-N(5)-C(47)	121.5(3)
C(46)-N(5)-RU1	118.9(3)
C(47)-N(5)-RU1	119.6(3)
N(5)-C(47)-C(48)	119.9(4)
N(5)-C(47)-C(51)	112.8(3)
C(48)-C(47)-C(51)	127.2(4)
C(47)-C(48)-C(49)	119.4(4)
C(47)-C(48)-H(48)	120.3
C(49)-C(48)-H(48)	120.3
C(50)-C(49)-C(48)	118.8(3)
C(50)-C(49)-C(56)	119.5(3)
C(48)-C(49)-C(56)	121.6(4)
C(46)-C(50)-C(49)	119.9(4)
C(46)-C(50)-H(50)	120
C(49)-C(50)-H(50)	120
C(55)-C(51)-N(6)	121.6(4)
C(55)-C(51)-C(47)	123.8(4)
N(6)-C(51)-C(47)	114.4(3)
C(52)-N(6)-C(51)	117.2(4)
C(52)-N(6)-RU1	128.4(3)
C(51)-N(6)-RU1	114.3(3)
N(6)-C(52)-C(53)	122.8(4)
N(6)-C(52)-H(52)	118.6
C(53)-C(52)-H(52)	118.6
C(52)-C(53)-C(54)	121.1(4)
C(52)-C(53)-H(53)	119.4
C(54)-C(53)-H(53)	119.4
C(53)-C(54)-C(55)	115.4(4)
C(53)-C(54)-C(71A)	124.3(4)
C(55)-C(54)-C(71A)	120.3(4)
C(51)-C(55)-C(54)	121.7(4)
C(51)-C(55)-H(55)	119.2
C(54)-C(55)-H(55)	119.2
C(57)-C(56)-C(61)	118.8(3)
C(57)-C(56)-C(49)	120.4(3)
C(61)-C(56)-C(49)	120.7(4)
C(58)-C(57)-C(56)	120.1(4)
C(58)-C(57)-H(57)	119.9
C(56)-C(57)-H(57)	119.9
C(57)-C(58)-C(59)	121.2(4)
C(57)-C(58)-H(58)	119.4
C(59)-C(58)-H(58)	119.4
C(60)-C(59)-C(58)	118.7(3)
C(60)-C(59)-C(62)	122.5(4)
C(58)-C(59)-C(62)	118.7(4)
C(59)-C(60)-C(61)	120.5(4)
C(59)-C(60)-H(60)	119.7
C(61)-C(60)-H(60)	119.7
C(60)-C(61)-C(56)	120.5(4)
C(60)-C(61)-H(61)	119.8
C(56)-C(61)-H(61)	119.8
O(64)-C(62)-O(63)	126.2(4)
O(64)-C(62)-C(59)	117.9(4)
O(63)-C(62)-C(59)	115.9(4)
C(62)-O(63)-H(63)	117.60(14)
C(68)-C(65)-C(66B)	133.90(12)
C(68)-C(65)-C(67)	115.30(17)
C(66B)-C(65)-C(67)	56.50(11)
C(68)-C(65)-C(68B)	32.40(11)
C(66B)-C(65)-C(68B)	113.8(6)
C(67)-C(65)-C(68B)	131.6(9)
C(68)-C(65)-C(43)	112.50(12)
C(66B)-C(65)-C(43)	110.4(5)
C(67)-C(65)-C(43)	116.0(8)
C(68B)-C(65)-C(43)	111.5(5)
C(68)-C(65)-C(67B)	73.80(13)
C(66B)-C(65)-C(67B)	108.1(6)
C(67)-C(65)-C(67B)	52.40(11)
C(68B)-C(65)-C(67B)	104.7(6)
C(43)-C(65)-C(67B)	107.9(5)
C(68)-C(65)-C(66)	106.70(14)

C(66B)-C(65)-C(66)	48.3(8)	H(73A)-C(73A)-H(73C)	109.5
C(67)-C(65)-C(66)	103.60(14)	H(73B)-C(73A)-H(73C)	109.5
C(68B)-C(65)-C(66)	75.2(8)	C(71A)-C(74A)-H(74A)	109.5
C(43)-C(65)-C(66)	100.8(8)	C(71A)-C(74A)-H(74B)	109.5
C(67B)-C(65)-C(66)	148.7(9)	H(74A)-C(74A)-H(74B)	109.5
C(65)-C(66)-H(66A)	109.5	C(71A)-C(74A)-H(74C)	109.5
C(65)-C(66)-H(66B)	109.5	H(74A)-C(74A)-H(74C)	109.5
H(66A)-C(66)-H(66B)	109.5	H(74B)-C(74A)-H(74C)	109.5
C(65)-C(66)-H(66C)	109.5	C(92)-C(91)-H(91A)	98.9
H(66A)-C(66)-H(66C)	109.5	C(92)-C(91)-H(91B)	124.7
H(66B)-C(66)-H(66C)	109.5	H(91A)-C(91)-H(91B)	109.5
C(65)-C(67)-H(67A)	109.5	C(92)-C(91)-H(91C)	103.9
C(65)-C(67)-H(67B)	109.5	H(91A)-C(91)-H(91C)	109.5
H(67A)-C(67)-H(67B)	109.5	H(91B)-C(91)-H(91C)	109.5
C(65)-C(67)-H(67C)	109.5	O(94)-C(92)-C(91)	108.60(12)
H(67A)-C(67)-H(67C)	109.5	O(94)-C(92)-C(93)	109.30(17)
H(67B)-C(67)-H(67C)	109.5	C(91)-C(92)-C(93)	118.80(17)
C(65)-C(68)-H(68A)	109.5	O(94)-C(92)-H(92)	106.5
C(65)-C(68)-H(68B)	109.5	C(91)-C(92)-H(92)	106.5
H(68A)-C(68)-H(68B)	109.5	C(93)-C(92)-H(92)	106.5
C(65)-C(68)-H(68C)	109.5	C(92)-C(93)-H(93A)	109.5
H(68A)-C(68)-H(68C)	109.5	C(92)-C(93)-H(93B)	109.5
H(68B)-C(68)-H(68C)	109.5	H(93A)-C(93)-H(93B)	109.5
C(65)-C(66B)-H(66D)	109.5	C(92)-C(93)-H(93C)	109.5
C(65)-C(66B)-H(66E)	109.5	H(93A)-C(93)-H(93C)	109.5
H(66D)-C(66B)-H(66E)	109.5	H(93B)-C(93)-H(93C)	109.5
C(65)-C(66B)-H(66F)	109.5	C(92)-O(94)-C(95)	121.90(18)
H(66D)-C(66B)-H(66F)	109.5	O(94)-C(95)-C(97)	112(2)
H(66E)-C(66B)-H(66F)	109.5	O(94)-C(95)-C(96)	119(2)
C(65)-C(67B)-H(67D)	109.5	C(97)-C(95)-C(96)	103(2)
C(65)-C(67B)-H(67E)	109.5	O(94)-C(95)-H(95)	107.5
H(67D)-C(67B)-H(67E)	109.5	C(97)-C(95)-H(95)	107.5
C(65)-C(67B)-H(67F)	109.5	C(96)-C(95)-H(95)	107.5
H(67D)-C(67B)-H(67F)	109.5	C(95)-C(96)-H(96A)	109.5
H(67E)-C(67B)-H(67F)	109.5	C(95)-C(96)-H(96B)	109.5
C(65)-C(68B)-H(68D)	109.5	H(96A)-C(96)-H(96B)	109.5
C(65)-C(68B)-H(68E)	109.5	C(95)-C(96)-H(96C)	109.5
H(68D)-C(68B)-H(68E)	109.5	H(96A)-C(96)-H(96C)	109.5
C(65)-C(68B)-H(68F)	109.5	H(96B)-C(96)-H(96C)	109.5
H(68D)-C(68B)-H(68F)	109.5	C(95)-C(97)-H(97A)	109.5
H(68E)-C(68B)-H(68F)	109.5	C(95)-C(97)-H(97B)	109.5
C(72A)-C(71A)-C(74A)	108.1(5)	H(97A)-C(97)-H(97B)	109.5
C(72A)-C(71A)-C(73A)	109.6(5)	C(95)-C(97)-H(97C)	109.5
C(74A)-C(71A)-C(73A)	108.6(5)	H(97A)-C(97)-H(97C)	109.5
C(72A)-C(71A)-C(54)	112.2(4)	H(97B)-C(97)-H(97C)	109.5
C(74A)-C(71A)-C(54)	109.5(4)	N(103)-C(102)-C(101)	174.90(16)
C(73A)-C(71A)-C(54)	108.8(4)	N(103)-C(102)-H(91A)	71.9
C(71A)-C(72A)-H(72A)	109.5	C(101)-C(102)-H(91A)	112.7
C(71A)-C(72A)-H(72B)	109.5	N(103)-C(102)-H(91B)	26.9
H(72A)-C(72A)-H(72B)	109.5	C(101)-C(102)-H(91B)	148.6
C(71A)-C(72A)-H(72C)	109.5	H(91A)-C(102)-H(91B)	88.6
H(72A)-C(72A)-H(72C)	109.5	C(102)-N(103)-H(91A)	56.3
H(72B)-C(72A)-H(72C)	109.5	C(102)-N(103)-H(91B)	71.3
C(71A)-C(73A)-H(73A)	109.5	H(91A)-N(103)-H(91B)	106.6
C(71A)-C(73A)-H(73B)	109.5	C(102)-N(103)-H(91C)	104.4
H(73A)-C(73A)-H(73B)	109.5	H(91A)-N(103)-H(91C)	80.1
C(71A)-C(73A)-H(73C)	109.5	H(91B)-N(103)-H(91C)	166.6

C(112)-C(111)-H(11A)	109.5	F(12)-P(1)-F(16)	88.6(7)
C(112)-C(111)-H(11B)	109.5	F(13)-P(1)-F(16)	90.1(6)
H(11A)-C(111)-H(11B)	109.5	F(14)-P(1)-F(11)	89.8(7)
C(112)-C(111)-H(11C)	109.5	F(12)-P(1)-F(11)	86.9(8)
H(11A)-C(111)-H(11C)	109.5	F(13)-P(1)-F(11)	88.6(6)
H(11B)-C(111)-H(11C)	109.5	F(16)-P(1)-F(11)	175.3(8)
O(114)-C(112)-C(111)	107.00(13)	F(14)-P(1)-F(15)	82.7(7)
O(114)-C(112)-C(113)	107.40(13)	F(12)-P(1)-F(15)	93.1(8)
C(111)-C(112)-C(113)	111.40(14)	F(13)-P(1)-F(15)	174.7(9)
O(114)-C(112)-H(112)	110.3	F(16)-P(1)-F(15)	88.2(7)
C(111)-C(112)-H(112)	110.3	F(11)-P(1)-F(15)	93.5(6)
C(113)-C(112)-H(112)	110.3	F(114)-P(11)-F(115)	102.10(11)
C(112)-C(113)-H(11D)	109.5	F(114)-P(11)-F(116)	90.4(1)
C(112)-C(113)-H(11E)	109.5	F(115)-P(11)-F(116)	88.2(9)
H(11D)-C(113)-H(11E)	109.5	F(114)-P(11)-F(111)	84.1(8)
C(112)-C(113)-H(11F)	109.5	F(115)-P(11)-F(111)	95.4(9)
H(11D)-C(113)-H(11F)	109.5	F(116)-P(11)-F(111)	174.00(12)
H(11E)-C(113)-H(11F)	109.5	F(114)-P(11)-F(113)	86.9(1)
C(112)-O(114)-C(115)	115.10(19)	F(115)-P(11)-F(113)	169.70(11)
O(114)-C(115)-C(117)	109(2)	F(116)-P(11)-F(113)	86.6(8)
O(114)-C(115)-C(116)	105(2)	F(111)-P(11)-F(113)	90.6(8)
C(117)-C(115)-C(116)	105(3)	F(114)-P(11)-F(112)	170.80(11)
O(114)-C(115)-H(115)	112.5	F(115)-P(11)-F(112)	86.3(9)
C(117)-C(115)-H(115)	112.5	F(116)-P(11)-F(112)	86.2(9)
C(116)-C(115)-H(115)	112.5	F(111)-P(11)-F(112)	98.8(1)
C(115)-C(116)-H(11G)	109.5	F(113)-P(11)-F(112)	84.4(9)
C(115)-C(116)-H(11H)	109.5	F(24)-P(2)-F(26)	94.4(7)
H(11G)-C(116)-H(11H)	109.5	F(24)-P(2)-F(21)	93.4(7)
C(115)-C(116)-H(11I)	109.5	F(26)-P(2)-F(21)	172.0(7)
H(11G)-C(116)-H(11I)	109.5	F(24)-P(2)-F(23)	91.8(5)
H(11H)-C(116)-H(11I)	109.5	F(26)-P(2)-F(23)	89.5(4)
C(115)-C(117)-H(11J)	109.5	F(21)-P(2)-F(23)	88.3(5)
C(115)-C(117)-H(11K)	109.5	F(24)-P(2)-F(25)	91.2(6)
H(11J)-C(117)-H(11K)	109.5	F(26)-P(2)-F(25)	87.7(6)
C(115)-C(117)-H(11L)	109.5	F(21)-P(2)-F(25)	94.1(6)
H(11J)-C(117)-H(11L)	109.5	F(23)-P(2)-F(25)	176.1(6)
H(11K)-C(117)-H(11L)	109.5	F(24)-P(2)-F(22)	176.1(9)
F(14)-P(1)-F(12)	174.5(8)	F(26)-P(2)-F(22)	89.2(8)
F(14)-P(1)-F(13)	92.5(7)	F(21)-P(2)-F(22)	83.1(8)
F(12)-P(1)-F(13)	91.9(7)	F(23)-P(2)-F(22)	89.8(8)
F(14)-P(1)-F(16)	94.8(8)	F(25)-P(2)-F(22)	87.5(8)

Appendix 4: Supplementary information for chapter IV.

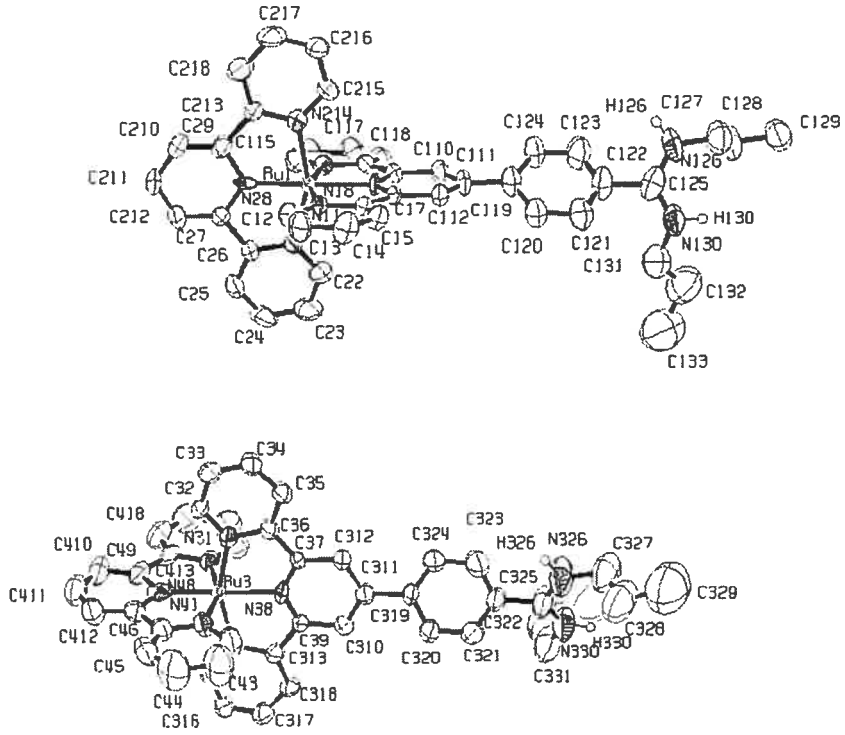

Table 1. Crystal data and structure refinement for **IV-1**.

Empirical formula	C182 H162 B4 F12 N16 P2 Ru2
Formula weight	3108.60
Temperature	220(2)K
Wavelength	1.54178 Å
Crystal system	Monoclinic
Space group	P21
Unit cell dimensions	a = 18.6928(8) Å α = 90° b = 22.4646(7) Å β = 94.336(3)° c = 21.6484(8) Å γ = 90°
Volume	9064.7(6)Å^3
Z	2
Density (calculated)	1.139 Mg/m^3

Absorption coefficient	2.033 mm^{-1}
F(000)	3224
Crystal size	0.54 x 0.48 x 0.20 mm
Theta range for data collection	2.05 to 72.81°
Index ranges	$-23 \leq h \leq 23$, $-27 \leq k \leq 27$, $-26 \leq \ell \leq 26$
Reflections collected	72843
Independent reflections	33931 [R_{int} = 0.027]
Absorption correction	Semi-empirical from equivalents
Max. and min. transmission	0.7400 and 0.5700
Refinement method	Full-matrix least-squares on F^2
Data / restraints / parameters	33931 / 1344 / 1965
Goodness-of-fit on F^2	0.874
Final R indices [I>2sigma(I)]	R_1 = 0.0707, wR_2 = 0.1634
R indices (all data)	R_1 = 0.1117, wR_2 = 0.1794
Absolute structure parameter	0.549(8)
Largest diff. peak and hole	1.813 and -0.580 e/Å^3

Table 2. Atomic coordinates (x 10^4) and equivalent isotropic displacement parameters (Å^2 x 10^3) for **IV-1**.

U_{eq} is defined as one third of the trace of the orthogonalized Uij tensor.

	x	y	z	U_{eq}
Ru(1)	4954(1)	1315(1)	2495(1)	36(1)
N(11)	4167(3)	1481(2)	3105(3)	45(2)
C(12)	3789(4)	1093(3)	3397(4)	51(2)
C(13)	3255(4)	1261(4)	3761(4)	66(2)
C(14)	3093(5)	1859(4)	3826(4)	71(2)
C(15)	3492(4)	2273(3)	3520(3)	53(2)
C(16)	4018(4)	2085(3)	3163(3)	43(2)
C(17)	4481(4)	2473(3)	2821(3)	37(2)
N(18)	4947(3)	2222(2)	2484(2)	35(2)
C(19)	5384(4)	2483(3)	2139(3)	37(2)

C(110)	5357(4)	3117(3)	2117(3)	42(2)
C(111)	4891(4)	3428(3)	2459(3)	49(2)
C(112)	4444(4)	3103(3)	2816(3)	44(2)
C(113)	5872(4)	2099(3)	1829(3)	42(2)
N(114)	5747(3)	1493(3)	1904(3)	48(2)
C(115)	6180(4)	1114(4)	1670(4)	60(2)
C(116)	6773(4)	1283(4)	1335(4)	71(2)
C(117)	6909(4)	1891(4)	1260(4)	70(2)
C(118)	6444(4)	2295(3)	1522(3)	50(2)
C(119)	4850(4)	4084(3)	2441(4)	62(2)
C(120)	4726(4)	4411(3)	2983(4)	68(2)
C(121)	4706(4)	5018(4)	2998(5)	81(2)
C(122)	4848(5)	5322(3)	2450(5)	79(3)
C(123)	5010(5)	5016(4)	1924(4)	84(3)
C(124)	4991(4)	4409(3)	1923(4)	66(2)
C(125)	4855(5)	6012(4)	2442(4)	85(3)
N(126)	4528(4)	6264(3)	1952(3)	84(2)
C(127)	4517(4)	6898(3)	1832(4)	92(3)
C(128)	5198(4)	7121(3)	1655(5)	93(3)
C(129)	5215(5)	7791(3)	1517(4)	95(3)
N(130)	5158(4)	6314(3)	2914(3)	85(2)
C(131)	5654(5)	6104(4)	3406(4)	104(3)
C(132)	6231(6)	6524(5)	3574(6)	149(5)
C(133)	6728(7)	6253(6)	4130(6)	189(6)
N(21)	5763(3)	1107(2)	3171(3)	37(1)
C(22)	6222(4)	1489(4)	3469(4)	55(2)
C(23)	6783(4)	1313(5)	3872(4)	72(3)
C(24)	6910(4)	687(4)	3955(4)	66(3)
C(25)	6434(4)	297(3)	3642(4)	56(2)
C(26)	5876(4)	511(3)	3255(3)	42(2)
C(27)	5356(4)	115(3)	2894(3)	46(2)
N(28)	4906(3)	453(3)	2506(2)	42(2)
C(29)	4392(4)	149(4)	2135(4)	53(2)
C(210)	4321(5)	-441(3)	2163(4)	67(3)
C(211)	4769(5)	-782(4)	2562(4)	72(3)
C(212)	5304(4)	-479(3)	2929(4)	63(2)
C(213)	3956(4)	578(3)	1745(3)	42(2)
N(214)	4148(3)	1163(3)	1808(3)	43(2)
C(215)	3778(4)	1573(3)	1462(3)	52(2)
C(216)	3228(4)	1429(4)	1036(4)	59(2)
C(217)	3031(5)	827(4)	959(4)	72(3)
C(218)	3401(5)	409(4)	1317(4)	64(3)
Ru(3)	10077(1)	61(1)	7499(1)	42(1)
N(31)	9263(3)	208(2)	6824(3)	45(2)
C(32)	8890(4)	-194(3)	6481(3)	48(2)
C(33)	8340(4)	-39(4)	6062(4)	63(2)
C(34)	8162(4)	541(3)	5966(4)	56(2)
C(35)	8546(4)	974(3)	6303(4)	52(2)
C(36)	9115(4)	790(3)	6726(3)	44(2)
C(37)	9544(4)	1198(3)	7095(3)	36(2)
N(38)	10044(3)	967(3)	7487(3)	48(2)
C(39)	10506(4)	1234(3)	7879(3)	38(2)
C(310)	10473(4)	1870(3)	7907(3)	51(2)
C(311)	9960(4)	2164(4)	7507(3)	50(2)
C(312)	9509(4)	1833(3)	7087(3)	49(2)
C(313)	10993(4)	866(3)	8266(3)	44(2)
N(314)	10901(3)	267(2)	8172(3)	40(2)

C(315)	11320(4)	-108(3)	8514(3)	51(2)
C(316)	11877(4)	105(4)	8930(3)	51(2)
C(317)	11969(5)	682(4)	9006(4)	64(2)
C(318)	11542(4)	1078(3)	8676(3)	46(2)
C(319)	9917(3)	2823(3)	7516(3)	49(2)
C(320)	9873(4)	3098(3)	8092(4)	66(2)
C(321)	9803(4)	3710(3)	8130(4)	72(2)
C(322)	9817(4)	4047(3)	7598(4)	70(2)
C(323)	9865(5)	3778(4)	7032(4)	88(3)
C(324)	9920(4)	3157(3)	6984(4)	64(2)
C(325)	9744(5)	4710(3)	7645(5)	103(3)
N(326)	9159(4)	4947(3)	7373(5)	138(4)
C(327)	8999(6)	5576(4)	7340(6)	144(5)
C(328)	8582(8)	5732(5)	7868(6)	177(6)
C(329)	8284(9)	6382(6)	7721(8)	272(9)
N(330)	10285(4)	5044(4)	7878(4)	119(3)
C(331)	11009(5)	4844(4)	8046(6)	127(4)
C(332)	11529(8)	4928(8)	7600(8)	252(10)
C(333)	11450(13)	5487(9)	7184(10)	338(14)
N(41)	9344(3)	-105(3)	8168(3)	53(2)
C(42)	9029(5)	301(4)	8489(4)	79(3)
C(43)	8597(7)	162(6)	8922(6)	127(4)
C(44)	8450(7)	-453(6)	9035(6)	124(4)
C(45)	8799(5)	-860(4)	8703(5)	79(3)
C(46)	9254(5)	-688(4)	8272(4)	58(2)
C(47)	9642(5)	-1104(4)	7914(4)	57(2)
N(48)	10075(3)	-797(4)	7511(3)	52(2)
C(49)	10476(4)	-1127(4)	7129(4)	55(2)
C(410)	10449(5)	-1722(4)	7107(5)	75(3)
C(411)	10062(5)	-2004(6)	7504(5)	92(4)
C(412)	9650(5)	-1701(4)	7924(5)	78(3)
C(413)	10876(4)	-722(3)	6741(4)	50(2)
N(414)	10797(3)	-128(3)	6845(3)	48(2)
C(415)	11152(5)	251(4)	6517(4)	63(2)
C(416)	11589(5)	73(5)	6076(4)	85(3)
C(417)	11677(5)	-542(5)	5957(5)	87(3)
C(418)	11307(5)	-926(4)	6317(4)	75(3)
B(5)	3574(4)	8832(3)	9948(4)	40(2)
C(511)	3085(4)	8799(3)	9272(3)	43(2)
C(512)	2439(4)	8477(3)	9217(4)	51(2)
C(513)	2053(4)	8386(3)	8654(4)	61(2)
C(514)	2311(5)	8635(4)	8107(4)	69(3)
C(515)	2929(5)	8953(4)	8142(4)	73(3)
C(516)	3324(4)	9023(3)	8742(3)	50(2)
C(521)	3069(4)	8806(3)	10529(4)	47(2)
C(522)	3294(5)	8482(4)	11102(4)	58(2)
C(523)	2888(5)	8514(4)	11584(4)	77(3)
C(524)	2246(6)	8838(5)	11602(5)	85(3)
C(525)	2054(5)	9163(4)	11064(5)	75(3)
C(526)	2434(4)	9148(4)	10539(4)	55(2)
C(531)	4039(4)	9462(3)	10050(4)	49(2)
C(532)	4593(4)	9495(4)	10501(4)	58(2)
C(533)	4963(5)	10005(5)	10642(4)	74(3)
C(534)	4807(5)	10536(5)	10303(5)	82(3)
C(535)	4274(5)	10521(4)	9854(4)	74(3)
C(536)	3886(4)	9988(4)	9740(4)	58(2)
C(541)	4140(4)	8268(3)	9913(3)	50(2)

C(542)	4821(4)	8330(3)	9699(4)	57(2)
C(543)	5271(5)	7848(4)	9643(5)	80(3)
C(544)	5071(6)	7269(4)	9772(5)	78(3)
C(545)	4373(5)	7196(3)	9967(4)	73(3)
C(546)	3925(4)	7686(3)	10039(3)	52(2)
B(6)	6444(4)	8790(3)	5084(4)	39(2)
C(611)	6049(4)	9443(3)	5067(4)	52(2)
C(612)	6314(5)	9946(4)	5367(4)	76(3)
C(613)	5958(6)	10502(5)	5295(6)	101(4)
C(614)	5346(6)	10559(5)	4922(6)	94(4)
C(615)	5073(5)	10066(5)	4603(5)	92(3)
C(616)	5417(5)	9527(4)	4682(4)	66(3)
C(621)	6851(4)	8762(3)	4453(4)	51(2)
C(622)	7494(5)	9055(4)	4380(4)	66(2)
C(623)	7816(6)	9092(5)	3821(5)	90(3)
C(624)	7498(8)	8802(6)	3313(5)	114(4)
C(625)	6849(6)	8497(4)	3369(5)	94(3)
C(626)	6549(5)	8491(3)	3896(4)	61(2)
C(631)	7037(4)	8694(3)	5705(4)	50(2)
C(632)	6903(5)	8928(4)	6264(4)	65(2)
C(633)	7388(7)	8804(5)	6811(5)	97(4)
C(634)	7961(6)	8417(6)	6735(7)	113(5)
C(635)	8096(5)	8204(5)	6175(5)	93(4)
C(636)	7622(4)	8342(4)	5669(4)	62(2)
C(641)	5861(4)	8250(3)	5166(3)	50(2)
C(642)	5962(4)	7668(3)	4964(3)	59(2)
C(643)	5483(5)	7207(3)	5061(4)	75(3)
C(644)	4894(5)	7300(4)	5375(4)	80(3)
C(645)	4791(5)	7866(4)	5615(4)	76(3)
C(646)	5264(4)	8331(4)	5497(4)	62(2)
B(7)	8565(5)	7680(4)	59(5)	56(3)
C(711)	8111(4)	7656(3)	660(4)	52(2)
C(712)	7479(5)	7343(4)	654(4)	60(2)
C(713)	7077(5)	7262(4)	1163(5)	77(3)
C(714)	7360(6)	7488(5)	1711(5)	84(3)
C(715)	7936(6)	7799(4)	1752(5)	77(3)
C(716)	8312(5)	7874(4)	1216(5)	71(3)
C(721)	9168(4)	8206(3)	54(4)	56(2)
C(722)	9064(5)	8774(4)	298(4)	77(3)
C(723)	9563(6)	9243(4)	253(5)	95(3)
C(724)	10175(6)	9147(5)	-29(5)	96(4)
C(725)	10304(5)	8616(4)	-304(5)	81(3)
C(726)	9799(5)	8154(4)	-244(4)	72(3)
C(731)	8056(5)	7779(4)	-580(4)	68(3)
C(732)	7458(5)	8152(5)	-588(5)	101(4)
C(733)	7020(6)	8321(5)	-1112(6)	110(4)
C(734)	7215(7)	8039(7)	-1642(7)	120(5)
C(735)	7801(6)	7714(5)	-1719(5)	105(4)
C(736)	8201(6)	7581(4)	-1153(5)	92(3)
C(741)	8979(4)	7015(3)	62(3)	47(2)
C(742)	8698(5)	6507(4)	-253(4)	69(3)
C(743)	9027(6)	5971(4)	-195(5)	85(3)
C(744)	9670(6)	5889(4)	181(5)	84(3)
C(745)	9960(5)	6369(4)	493(4)	67(2)
C(746)	9606(5)	6924(4)	433(4)	56(2)
B(8)	8568(5)	2472(4)	4972(5)	54(3)
C(811)	9034(4)	1852(3)	5020(4)	48(2)

C(812)	8800(4)	1325(4)	4728(4)	57(2)
C(813)	9186(5)	801(4)	4798(5)	81(3)
C(814)	9807(6)	777(4)	5205(5)	80(3)
C(815)	10039(5)	1276(4)	5489(4)	70(2)
C(816)	9657(4)	1803(4)	5413(4)	54(2)
C(821)	8108(4)	2558(3)	4328(4)	53(2)
C(822)	7468(5)	2895(4)	4251(4)	70(3)
C(823)	7100(5)	3008(4)	3672(5)	82(3)
C(824)	7324(6)	2768(5)	3169(5)	87(3)
C(825)	7949(5)	2417(5)	3180(5)	85(3)
C(826)	8327(5)	2320(4)	3759(5)	78(3)
C(831)	9120(4)	3060(3)	5013(4)	55(2)
C(832)	9769(5)	3065(4)	4754(4)	70(3)
C(833)	10233(5)	3553(4)	4752(5)	90(3)
C(834)	10039(6)	4058(5)	5031(6)	93(3)
C(835)	9405(6)	4095(4)	5278(5)	86(3)
C(836)	8937(4)	3605(3)	5292(4)	64(2)
C(841)	8050(4)	2436(3)	5545(4)	51(2)
C(842)	7440(4)	2102(4)	5510(4)	61(2)
C(843)	7007(5)	1996(4)	5984(4)	76(3)
C(844)	7212(5)	2255(4)	6568(5)	74(3)
C(845)	7804(5)	2607(4)	6641(4)	68(2)
C(846)	8221(4)	2675(3)	6136(4)	56(2)
P(1)	2663(1)	9481(1)	3520(2)	101(1)
F(11)	3065(3)	8997(3)	3110(3)	129(2)
F(12)	2676(3)	9024(2)	4078(3)	111(2)
F(13)	3427(3)	9735(2)	3770(3)	133(2)
F(14)	2660(4)	9944(3)	2969(4)	181(3)
F(15)	1907(3)	9224(2)	3262(3)	140(2)
F(16)	2280(4)	9941(3)	3906(4)	165(3)
P(2)	790(2)	6599(2)	8548(2)	133(1)
F(21)	474(4)	6395(3)	7886(4)	168(3)
F(22)	1496(4)	6209(4)	8502(4)	196(3)
F(23)	1166(5)	7139(4)	8223(5)	211(4)
F(24)	101(5)	6982(4)	8607(5)	221(4)
F(25)	412(5)	6038(3)	8807(4)	204(4)
F(26)	1138(6)	6765(4)	9237(4)	226(4)

Table 3. Hydrogen coordinates (x 10^4) and isotropic displacement parameters ($Å^2$ x 10^3) for **IV-1**.

	x	y	z	U_{eq}
H(12)	3889	685	3354	61
H(13)	2999	970	3966	80
H(14)	2724	1980	4070	85
H(15)	3399	2682	3560	64
H(110)	5661	3325	1866	50
H(112)	4117	3301	3054	53
H(115)	6097	705	1727	72
H(116)	7066	994	1167	85

H(117)	7296	2023	1043	84
H(118)	6527	2706	1487	60
H(120)	4654	4200	3348	81
H(121)	4602	5225	3358	97
H(123)	5132	5225	1571	101
H(124)	5077	4206	1556	79
H(126)	4301	6033	1680	101
H(12A)	4146	6985	1500	110
H(12B)	4389	7108	2205	110
H(12C)	5326	6904	1287	111
H(12D)	5566	7033	1990	111
H(12E)	4856	7884	1183	143
H(12F)	5686	7900	1394	143
H(12G)	5113	8012	1885	143
H(130)	5044	6689	2929	102
H(13A)	5864	5728	3279	125
H(13B)	5391	6024	3772	125
H(13C)	6030	6905	3699	179
H(13D)	6514	6596	3218	179
H(13E)	6926	6572	4391	283
H(13F)	7115	6029	3967	283
H(13G)	6446	5991	4372	283
H(22)	6155	1898	3398	66
H(23)	7077	1595	4088	87
H(24)	7301	546	4212	79
H(25)	6493	-116	3695	68
H(210)	3961	-630	1907	80
H(211)	4717	-1197	2587	86
H(212)	5627	-693	3199	75
H(215)	3903	1976	1517	62
H(216)	2986	1728	798	70
H(217)	2654	715	670	86
H(218)	3280	5	1272	77
H(32)	9009	-599	6530	58
H(33)	8081	-337	5837	76
H(34)	7785	647	5675	67
H(35)	8431	1379	6252	63
H(310)	10786	2085	8185	61
H(312)	9186	2028	6802	59
H(315)	11241	-520	8477	61
H(316)	12183	-164	9153	62
H(317)	12334	823	9291	77
H(318)	11617	1490	8725	55
H(320)	9892	2866	8454	79
H(321)	9747	3893	8514	87
H(323)	9862	4013	6672	106
H(324)	9957	2974	6598	77
H(326)	8842	4705	7198	166
H(32A)	8721	5668	6949	173
H(32B)	9445	5807	7357	173
H(32C)	8889	5728	8256	212
H(32D)	8187	5451	7904	212
H(32E)	8664	6627	7577	407
H(32F)	8114	6554	8093	407
H(32G)	7891	6360	7402	407
H(330)	10195	5419	7935	142
H(33A)	11182	5050	8428	153

H(33B)	10991	4418	8141	153
H(33C)	11517	4578	7331	302
H(33D)	12005	4941	7824	302
H(33E)	10948	5548	7052	507
H(33F)	11721	5432	6823	507
H(33G)	11632	5832	7415	507
H(42)	9114	705	8408	95
H(43)	8389	462	9153	152
H(44)	8127	-570	9325	149
H(45)	8725	-1267	8771	95
H(410)	10698	-1935	6817	89
H(411)	10063	-2422	7506	110
H(412)	9388	-1913	8205	93
H(415)	11102	661	6591	76
H(416)	11831	357	5851	102
H(417)	11968	-680	5652	105
H(418)	11358	-1339	6265	90
H(512)	2262	8317	9577	61
H(513)	1627	8163	8633	74
H(514)	2052	8578	7722	83
H(515)	3098	9125	7785	88
H(516)	3761	9231	8764	60
H(522)	3718	8256	11129	70
H(523)	3045	8300	11942	92
H(524)	1969	8836	11947	102
H(525)	1644	9406	11059	90
H(526)	2268	9367	10187	66
H(532)	4723	9147	10724	70
H(533)	5326	10006	10967	88
H(534)	5069	10887	10390	98
H(535)	4158	10863	9616	88
H(536)	3501	9992	9434	70
H(542)	4979	8711	9590	69
H(543)	5733	7916	9512	97
H(544)	5382	6945	9732	93
H(545)	4206	6811	10049	88
H(546)	3466	7623	10177	62
H(612)	6741	9920	5625	91
H(613)	6150	10837	5509	122
H(614)	5110	10928	4881	113
H(615)	4656	10099	4335	110
H(616)	5219	9196	4465	79
H(622)	7727	9239	4729	80
H(623)	8240	9312	3792	108
H(624)	7712	8806	2934	137
H(625)	6628	8296	3025	113
H(626)	6106	8296	3909	73
H(632)	6498	9169	6300	78
H(633)	7317	8977	7197	116
H(634)	8259	8304	7084	136
H(635)	8502	7967	6127	111
H(636)	7712	8183	5281	75
H(642)	6372	7583	4754	71
H(643)	5571	6826	4904	91
H(644)	4565	6992	5431	96
H(645)	4403	7938	5856	91
H(646)	5171	8712	5649	74

H(712)	7305	7170	277	72
H(713)	6634	7062	1130	92
H(714)	7125	7414	2072	101
H(715)	8105	7972	2130	92
H(716)	8738	8097	1257	85
H(722)	8645	8847	500	92
H(723)	9470	9620	418	114
H(724)	10518	9453	-35	115
H(725)	10712	8559	-525	97
H(726)	9898	7783	-419	86
H(732)	7337	8304	-205	121
H(733)	6639	8593	-1105	133
H(734)	6893	8081	-1994	144
H(735)	7935	7588	-2108	126
H(736)	8604	7333	-1175	110
H(742)	8272	6542	-511	82
H(743)	8821	5643	-412	102
H(744)	9891	5514	215	101
H(745)	10389	6331	745	81
H(746)	9807	7250	657	67
H(812)	8368	1327	4477	68
H(813)	9031	460	4574	97
H(814)	10056	417	5275	96
H(815)	10469	1270	5745	84
H(816)	9825	2141	5635	65
H(822)	7278	3051	4607	84
H(823)	6693	3256	3645	99
H(824)	7059	2833	2788	105
H(825)	8108	2253	2815	102
H(826)	8745	2087	3772	94
H(832)	9912	2713	4563	84
H(833)	10667	3530	4561	108
H(834)	10351	4387	5054	111
H(835)	9268	4459	5446	104
H(836)	8506	3639	5486	77
H(842)	7302	1927	5125	73
H(843)	6592	1761	5923	91
H(844)	6937	2182	6906	89
H(845)	7929	2799	7019	82
H(846)	8647	2897	6197	68

Table 4. Anisotropic parameters ($Å^2$ x 10^3) for **IV-1**.

The anisotropic displacement factor exponent takes the form:

$$-2\pi^2 [h^2 a^{*2} U_{11} + ... + 2 h k a^* b^* U_{12}]$$

	U11	U22	U33	U23	U13	U12
Ru(1)	47(1)	22(1)	39(1)	1(1)	-9(1)	-4(1)
N(11)	62(4)	29(3)	41(3)	5(2)	-9(3)	-12(3)

C(12)	52(5)	43(4)	58(5)	2(3)	6(4)	-9(3)
C(13)	72(5)	47(4)	81(6)	11(4)	16(4)	-18(4)
C(14)	75(6)	60(5)	81(6)	-11(4)	34(5)	-6(4)
C(15)	62(5)	41(4)	57(5)	-5(3)	14(4)	-6(3)
C(16)	54(4)	30(3)	45(4)	1(3)	-9(4)	-6(3)
C(17)	52(4)	24(3)	34(4)	4(3)	1(3)	-13(3)
N(18)	54(4)	11(2)	42(4)	-1(2)	8(3)	1(2)
C(19)	45(4)	30(4)	35(4)	5(3)	1(3)	0(3)
C(110)	41(4)	30(4)	54(4)	7(3)	1(4)	-7(3)
C(111)	58(5)	21(3)	67(5)	6(3)	5(4)	-2(3)
C(112)	52(4)	27(3)	52(4)	0(3)	0(4)	2(3)
C(113)	47(4)	38(4)	40(4)	9(3)	-4(3)	-2(3)
N(114)	55(4)	38(3)	50(4)	-7(3)	-12(3)	5(3)
C(115)	56(4)	50(4)	72(6)	-2(4)	-10(4)	5(3)
C(116)	68(5)	62(5)	83(6)	1(5)	9(4)	9(4)
C(117)	60(5)	66(5)	85(6)	18(4)	17(4)	-5(4)
C(118)	46(4)	49(4)	54(4)	9(3)	0(4)	-5(3)
C(119)	72(5)	37(3)	81(5)	6(4)	22(4)	-2(3)
C(120)	79(5)	44(4)	82(6)	6(4)	23(5)	1(4)
C(121)	84(5)	53(4)	108(7)	9(5)	14(5)	-5(4)
C(122)	97(6)	42(4)	100(7)	-6(5)	30(6)	8(4)
C(123)	105(6)	55(5)	95(6)	2(5)	22(5)	-12(5)
C(124)	78(5)	40(4)	82(6)	8(4)	30(4)	1(3)
C(125)	92(7)	59(5)	105(7)	-25(5)	20(6)	4(5)
N(126)	107(6)	40(3)	106(6)	23(4)	6(5)	8(4)
C(127)	94(6)	59(5)	121(8)	7(5)	-4(6)	-6(5)
C(128)	79(6)	52(5)	146(8)	17(5)	-2(6)	1(4)
C(129)	93(6)	67(5)	121(8)	11(5)	-23(6)	-1(5)
N(130)	114(6)	41(4)	100(6)	8(4)	11(5)	0(4)
C(131)	122(8)	77(6)	113(8)	5(6)	5(7)	-13(6)
C(132)	148(10)	127(9)	168(11)	-28(9)	-16(9)	-13(8)
C(133)	165(11)	212(13)	186(12)	-35(11)	-2(10)	29(11)
N(21)	36(3)	33(3)	41(3)	6(2)	-5(3)	-3(2)
C(22)	56(5)	54(5)	54(5)	0(4)	-4(4)	-7(3)
C(23)	59(5)	87(6)	68(5)	9(5)	-21(4)	-20(5)
C(24)	54(5)	80(6)	61(5)	28(5)	-19(4)	-8(4)
C(25)	66(5)	39(4)	63(5)	14(4)	-6(4)	-3(3)
C(26)	50(4)	31(4)	44(4)	5(3)	-2(4)	1(3)
C(27)	49(4)	36(4)	50(4)	0(3)	-12(3)	-8(3)
N(28)	38(4)	53(4)	31(3)	4(3)	-21(3)	3(3)
C(29)	49(4)	43(4)	66(5)	-10(4)	-7(4)	-14(4)
C(210)	89(6)	38(4)	69(5)	-14(4)	-17(5)	-12(4)
C(211)	119(7)	22(4)	71(6)	3(3)	-11(5)	-16(4)
C(212)	77(5)	30(4)	77(6)	8(4)	-15(5)	6(4)
C(213)	47(4)	32(4)	46(4)	-4(3)	-9(4)	-3(3)
N(214)	49(4)	38(4)	43(4)	-3(3)	2(3)	1(3)
C(215)	58(5)	44(4)	51(5)	5(3)	-12(4)	12(3)
C(216)	63(5)	54(5)	55(5)	-6(4)	-19(4)	13(4)
C(217)	64(5)	78(6)	69(6)	-17(5)	-29(5)	23(5)
C(218)	66(6)	64(5)	59(5)	-16(4)	-7(5)	3(4)
Ru(3)	50(1)	28(1)	46(1)	-3(1)	-10(1)	5(1)
N(31)	55(4)	30(3)	48(4)	-3(3)	-5(3)	4(3)
C(32)	53(4)	33(4)	54(5)	-3(3)	-17(4)	-9(3)
C(33)	65(5)	60(5)	60(5)	2(4)	-23(4)	-24(4)
C(34)	49(4)	46(4)	70(5)	7(4)	-21(4)	-2(3)
C(35)	50(4)	42(4)	61(5)	11(3)	-15(4)	-1(3)
C(36)	45(4)	38(4)	46(4)	5(3)	-6(4)	-7(3)

C(37)	47(4)	24(3)	36(4)	3(3)	-8(3)	6(3)
N(38)	61(4)	20(3)	62(4)	-8(3)	8(4)	-5(3)
C(39)	48(4)	28(4)	37(4)	-2(3)	-1(3)	4(3)
C(310)	61(5)	41(4)	47(4)	-1(3)	-8(4)	8(3)
C(311)	53(4)	35(4)	59(5)	4(3)	-9(4)	-1(3)
C(312)	61(4)	33(4)	52(4)	0(3)	-11(4)	-1(3)
C(313)	50(4)	39(4)	45(4)	-9(3)	7(4)	3(3)
N(314)	42(3)	38(3)	39(3)	-3(3)	-9(3)	5(2)
C(315)	60(5)	37(4)	55(5)	-2(3)	-7(4)	20(3)
C(316)	55(4)	44(4)	54(4)	1(4)	-5(4)	15(4)
C(317)	71(6)	57(5)	62(5)	-9(4)	-22(5)	2(4)
C(318)	43(4)	48(4)	44(4)	-7(3)	-17(4)	2(3)
C(319)	62(4)	26(3)	57(4)	-1(3)	-8(3)	-7(3)
C(320)	77(5)	42(4)	73(5)	-3(3)	-27(4)	1(3)
C(321)	86(6)	58(5)	68(5)	-12(4)	-25(5)	21(4)
C(322)	81(5)	39(4)	84(6)	-12(4)	-32(5)	11(3)
C(323)	105(7)	60(5)	95(7)	13(5)	-27(6)	-12(5)
C(324)	72(5)	52(4)	65(5)	2(4)	-19(4)	-3(4)
C(325)	101(6)	45(4)	155(9)	-23(5)	-53(6)	8(4)
N(326)	114(6)	58(5)	228(10)	-15(6)	-87(7)	19(4)
C(327)	128(9)	99(8)	198(12)	-45(8)	-33(9)	44(7)
C(328)	196(12)	133(10)	199(13)	-62(10)	1(11)	28(9)
C(329)	288(16)	215(15)	305(17)	-52(14)	-24(14)	51(13)
N(330)	119(6)	55(4)	170(8)	-14(5)	-68(6)	13(5)
C(331)	108(8)	82(7)	185(11)	-32(7)	-38(8)	8(6)
C(332)	254(16)	263(17)	240(16)	-50(14)	34(14)	37(14)
C(333)	350(20)	330(20)	340(20)	-44(17)	26(16)	14(16)
N(41)	63(4)	41(4)	56(4)	7(3)	18(3)	8(3)
C(42)	112(8)	50(5)	81(6)	8(4)	34(6)	4(5)
C(43)	155(10)	90(8)	144(10)	6(7)	71(8)	-8(7)
C(44)	136(9)	109(9)	137(10)	12(8)	72(8)	-21(7)
C(45)	84(6)	62(5)	89(7)	22(5)	-3(6)	-1(5)
C(46)	61(5)	52(5)	60(5)	9(4)	-4(4)	-8(4)
C(47)	53(5)	49(5)	66(6)	6(4)	-21(5)	3(4)
N(48)	38(4)	66(5)	47(4)	-2(3)	-25(4)	3(3)
C(49)	45(4)	48(5)	70(6)	-18(4)	-18(4)	14(4)
C(410)	81(6)	45(5)	97(7)	-12(5)	1(6)	-8(4)
C(411)	106(9)	50(6)	118(10)	-10(6)	-3(8)	13(5)
C(412)	90(7)	53(5)	88(7)	12(5)	-9(6)	2(5)
C(413)	51(4)	47(4)	51(5)	-18(3)	-5(4)	15(3)
N(414)	46(4)	38(3)	58(4)	-6(3)	-16(3)	3(3)
C(415)	66(6)	52(5)	70(6)	-8(4)	2(5)	8(4)
C(416)	77(6)	96(7)	82(6)	-10(6)	12(5)	-3(6)
C(417)	78(6)	95(7)	91(7)	-21(6)	20(5)	4(5)
C(418)	65(5)	72(5)	88(7)	-31(5)	-1(5)	10(4)
B(5)	47(4)	24(3)	49(5)	-4(3)	4(4)	1(3)
C(511)	46(4)	39(4)	45(4)	-6(3)	0(3)	4(3)
C(512)	53(4)	40(4)	59(5)	-16(3)	-6(4)	3(3)
C(513)	45(4)	54(5)	84(6)	-24(4)	0(4)	7(3)
C(514)	73(6)	74(6)	58(5)	-31(4)	-8(5)	24(4)
C(515)	102(7)	67(5)	52(5)	0(4)	17(5)	32(5)
C(516)	57(4)	50(4)	43(4)	1(3)	-2(4)	9(3)
C(521)	46(4)	48(4)	46(4)	-14(3)	-4(4)	-8(3)
C(522)	54(5)	62(5)	58(5)	-15(4)	2(4)	-4(4)
C(523)	75(6)	88(7)	66(6)	5(5)	1(5)	-11(5)
C(524)	79(6)	110(8)	67(6)	-14(6)	5(6)	-24(6)
C(525)	80(7)	75(6)	69(6)	-14(5)	6(5)	-5(5)

C(526)	54(5)	56(4)	56(5)	-13(4)	-2(4)	-3(4)
C(531)	53(5)	30(3)	65(5)	-12(3)	3(4)	7(3)
C(532)	57(5)	42(4)	74(6)	-8(4)	-6(5)	0(4)
C(533)	61(5)	64(5)	94(7)	-6(5)	-5(5)	-2(5)
C(534)	78(6)	63(6)	103(8)	-19(5)	1(6)	-21(5)
C(535)	98(7)	35(4)	86(6)	4(4)	-8(6)	-12(4)
C(536)	56(4)	46(4)	71(5)	-3(4)	4(4)	1(4)
C(541)	58(5)	38(4)	53(4)	-7(3)	-7(4)	4(3)
C(542)	55(5)	36(4)	83(6)	6(4)	17(4)	7(3)
C(543)	60(6)	67(6)	115(8)	-5(5)	10(6)	23(5)
C(544)	91(7)	40(4)	102(7)	-1(4)	4(6)	22(4)
C(545)	88(6)	40(4)	89(6)	4(4)	-11(5)	2(4)
C(546)	57(4)	37(3)	61(5)	-3(3)	1(4)	-8(3)
B(6)	43(4)	31(4)	44(5)	-3(3)	5(4)	-2(3)
C(611)	53(4)	43(4)	60(5)	7(4)	5(4)	-4(3)
C(612)	75(5)	47(5)	106(7)	1(5)	11(5)	-3(4)
C(613)	111(8)	53(5)	140(10)	-20(6)	15(7)	-7(5)
C(614)	91(8)	53(6)	142(10)	4(6)	23(7)	13(5)
C(615)	73(6)	81(7)	124(8)	36(7)	16(6)	17(6)
C(616)	67(6)	48(5)	81(6)	10(4)	2(5)	-2(4)
C(621)	56(4)	40(4)	57(5)	-1(3)	2(4)	5(3)
C(622)	80(6)	59(5)	61(6)	10(4)	15(5)	5(4)
C(623)	91(7)	86(7)	98(8)	15(6)	35(7)	5(5)
C(624)	168(11)	113(9)	66(7)	4(6)	32(8)	-11(8)
C(625)	123(8)	77(6)	81(7)	-5(6)	-6(7)	15(6)
C(626)	69(5)	54(5)	60(5)	-2(4)	2(4)	10(4)
C(631)	49(4)	48(4)	51(4)	19(3)	-5(4)	-12(3)
C(632)	82(6)	66(5)	46(5)	11(4)	-2(4)	-24(4)
C(633)	141(10)	93(7)	55(5)	5(5)	1(7)	-52(7)
C(634)	89(8)	128(9)	117(10)	63(8)	-34(8)	-33(7)
C(635)	59(5)	114(8)	104(8)	51(7)	-8(6)	-14(5)
C(636)	50(4)	68(5)	68(5)	25(4)	-2(4)	-4(4)
C(641)	59(5)	37(4)	52(4)	-3(3)	-10(4)	-5(3)
C(642)	66(5)	41(4)	72(5)	-3(4)	6(4)	-4(3)
C(643)	95(7)	41(4)	90(6)	5(4)	-2(6)	-22(4)
C(644)	86(6)	61(5)	92(7)	-4(5)	10(6)	-26(5)
C(645)	68(5)	76(6)	86(6)	5(5)	18(5)	-17(4)
C(646)	59(5)	54(4)	72(5)	-1(4)	5(4)	-14(4)
B(7)	58(5)	45(5)	63(6)	6(4)	-14(5)	3(4)
C(711)	65(5)	39(4)	52(5)	13(3)	-2(4)	3(3)
C(712)	72(6)	53(5)	54(5)	9(4)	5(5)	-4(4)
C(713)	64(6)	74(6)	94(8)	18(6)	13(6)	0(5)
C(714)	93(7)	85(7)	77(7)	18(6)	31(6)	31(6)
C(715)	86(7)	83(7)	60(6)	-7(5)	0(5)	23(5)
C(716)	68(6)	67(6)	76(6)	-1(5)	-3(5)	18(5)
C(721)	56(5)	44(4)	66(5)	17(4)	-12(4)	-6(3)
C(722)	76(5)	54(5)	99(7)	25(5)	-5(5)	-10(4)
C(723)	105(7)	48(5)	132(9)	6(5)	4(7)	-3(5)
C(724)	90(7)	82(7)	114(8)	24(6)	4(7)	-19(6)
C(725)	59(6)	69(6)	114(8)	25(6)	3(6)	-1(5)
C(726)	72(6)	52(5)	88(6)	16(4)	-13(5)	-1(4)
C(731)	67(5)	73(6)	63(5)	29(5)	-5(5)	-23(4)
C(732)	75(6)	106(8)	120(8)	76(7)	-6(6)	-10(5)
C(733)	81(7)	126(9)	121(9)	70(8)	-15(7)	-6(6)
C(734)	96(9)	157(11)	103(9)	66(9)	-18(8)	-48(8)
C(735)	105(8)	136(9)	71(7)	36(6)	-14(7)	-35(7)
C(736)	89(7)	85(7)	98(8)	44(6)	-11(6)	-38(5)

C(741)	58(5)	44(4)	38(4)	4(3)	-5(4)	-6(3)
C(742)	78(6)	67(6)	59(5)	2(4)	-3(5)	-16(4)
C(743)	105(7)	65(6)	82(7)	-7(5)	-5(6)	-17(5)
C(744)	116(8)	39(5)	102(8)	3(5)	44(7)	7(5)
C(745)	71(5)	52(5)	79(6)	13(4)	10(4)	13(5)
C(746)	66(6)	44(4)	57(5)	1(4)	0(4)	-2(4)
B(8)	56(5)	38(4)	65(6)	-2(4)	-13(5)	-6(4)
C(811)	49(4)	39(4)	56(5)	-6(3)	1(4)	-3(3)
C(812)	58(4)	37(4)	74(5)	-11(4)	-3(4)	-2(4)
C(813)	95(7)	49(5)	99(7)	-10(5)	6(6)	-13(5)
C(814)	90(7)	46(5)	105(7)	5(5)	9(6)	8(5)
C(815)	64(5)	53(5)	91(6)	12(5)	-1(5)	6(4)
C(816)	50(5)	48(4)	63(5)	-1(4)	-7(4)	1(4)
C(821)	53(4)	44(4)	60(5)	16(4)	-6(4)	-12(3)
C(822)	67(6)	61(5)	78(6)	19(4)	-13(5)	-3(4)
C(823)	76(6)	76(6)	90(7)	43(6)	-22(6)	-23(5)
C(824)	107(8)	89(7)	62(6)	23(6)	-15(6)	-36(6)
C(825)	91(7)	90(7)	76(7)	17(5)	10(6)	-40(5)
C(826)	92(7)	70(6)	72(6)	20(5)	-2(5)	-19(5)
C(831)	51(4)	38(4)	73(6)	2(4)	-3(4)	2(3)
C(832)	66(5)	48(5)	98(7)	11(5)	7(5)	4(4)
C(833)	68(6)	62(6)	138(9)	13(6)	3(6)	-10(5)
C(834)	73(6)	64(6)	138(9)	17(6)	-15(6)	-20(5)
C(835)	109(7)	45(5)	100(7)	10(5)	-26(6)	-2(5)
C(836)	74(5)	49(4)	66(5)	11(4)	-12(4)	-9(4)
C(841)	47(4)	49(4)	57(5)	10(3)	-2(4)	7(3)
C(842)	63(5)	60(5)	62(5)	0(4)	13(4)	-2(4)
C(843)	70(5)	77(6)	79(6)	-1(5)	2(5)	-11(4)
C(844)	79(6)	62(5)	84(7)	19(5)	25(5)	20(4)
C(845)	87(6)	59(5)	57(5)	9(4)	-5(5)	17(4)
C(846)	56(5)	49(4)	62(5)	4(4)	-11(4)	-1(3)
P(1)	83(2)	60(1)	154(3)	27(2)	-31(2)	-18(1)
F(11)	150(5)	105(4)	128(5)	9(4)	-12(4)	8(4)
F(12)	115(4)	82(3)	134(5)	25(3)	-2(4)	-34(3)
F(13)	140(5)	81(3)	171(6)	25(4)	-46(4)	-54(3)
F(14)	161(6)	152(6)	217(7)	89(5)	-80(5)	-44(5)
F(15)	110(4)	90(4)	208(7)	29(4)	-64(4)	-29(3)
F(16)	141(5)	107(5)	249(8)	-25(5)	32(5)	20(4)
P(2)	129(3)	80(2)	195(4)	-52(2)	43(3)	-24(2)
F(21)	181(6)	135(6)	180(7)	-43(5)	-44(6)	-26(5)
F(22)	135(6)	193(7)	261(9)	-28(7)	23(6)	-1(6)
F(23)	186(7)	152(7)	293(10)	31(7)	11(7)	-68(6)
F(24)	215(8)	155(7)	301(10)	-61(7)	75(8)	35(6)
F(25)	251(9)	142(6)	229(9)	-42(6)	92(7)	-68(6)
F(26)	291(10)	209(8)	177(7)	-87(7)	2(7)	-60(7)

Table 5. Bond lengths [Å] and angles [°] for **IV-1**.

		N(11)-C(12)	1.313(8)
Ru(1)-N(28)	1.938(7)	N(11)-C(16)	1.392(8)
Ru(1)-N(18)	2.038(5)		
Ru(1)-N(214)	2.063(6)		
Ru(1)-N(114)	2.069(7)	C(12)-C(13)	1.371(10)
Ru(1)-N(21)	2.076(5)	C(13)-C(14)	1.387(11)
Ru(1)-N(11)	2.083(6)	C(14)-C(15)	1.392(10)

C(15)-C(16)	1.364(10)	N(31)-C(32)	1.332(7)
C(16)-C(17)	1.467(9)	N(31)-C(36)	1.350(8)
C(17)-N(18)	1.307(8)	C(32)-C(33)	1.365(9)
C(17)-C(112)	1.417(8)	C(33)-C(34)	1.356(11)
N(18)-C(19)	1.288(8)	C(34)-C(35)	1.383(10)
C(19)-C(110)	1.426(9)	C(35)-C(36)	1.412(9)
C(19)-C(113)	1.456(9)	C(36)-C(37)	1.424(9)
C(110)-C(111)	1.377(9)	C(37)-N(38)	1.320(8)
C(111)-C(112)	1.387(9)	C(37)-C(312)	1.426(9)
C(111)-C(119)	1.475(10)	N(38)-C(39)	1.311(8)
C(113)-C(118)	1.372(9)	C(39)-C(310)	1.431(9)
C(113)-N(114)	1.394(8)	C(39)-C(313)	1.448(9)
N(114)-C(115)	1.305(9)	C(310)-C(311)	1.408(9)
C(115)-C(116)	1.421(11)	C(311)-C(312)	1.405(9)
C(116)-C(117)	1.401(11)	C(311)-C(319)	1.483(10)
C(117)-C(118)	1.405(10)	C(313)-N(314)	1.370(8)
C(119)-C(124)	1.381(9)	C(313)-C(318)	1.390(9)
C(119)-C(120)	1.418(10)	N(314)-C(315)	1.336(8)
C(120)-C(121)	1.365(9)	C(315)-C(316)	1.409(9)
C(121)-C(122)	1.411(11)	C(316)-C(317)	1.316(11)
C(122)-C(123)	1.383(10)	C(317)-C(318)	1.36(1)
C(122)-C(125)	1.548(11)	C(319)-C(324)	1.374(9)
C(123)-C(124)	1.364(9)	C(319)-C(320)	1.398(9)
C(125)-N(126)	1.313(8)	C(320)-C(321)	1.384(9)
C(125)-N(130)	1.318(8)	C(321)-C(322)	1.381(10)
N(126)-C(127)	1.449(7)	C(322)-C(323)	1.375(11)
C(127)-C(128)	1.446(8)	C(322)-C(325)	1.501(10)
C(128)-C(129)	1.536(7)	C(323)-C(324)	1.402(10)
N(130)-C(131)	1.439(7)	C(325)-N(326)	1.314(8)
C(131)-C(132)	1.459(9)	C(325)-N(330)	1.327(9)
C(132)-C(133)	1.585(9)	N(326)-C(327)	1.445(8)
N(21)-C(22)	1.344(8)	C(327)-C(328)	1.474(9)
N(21)-C(26)	1.366(8)	C(328)-C(329)	1.586(10)
C(22)-C(23)	1.37(1)	N(330)-C(331)	1.446(7)
C(23)-C(24)	1.435(13)	C(331)-C(332)	1.432(9)
C(24)-C(25)	1.389(10)	C(332)-C(333)	1.546(10)
C(25)-C(26)	1.374(9)	N(41)-C(42)	1.314(10)
C(26)-C(27)	1.493(9)	N(41)-C(46)	1.341(9)
C(27)-C(212)	1.339(10)	C(42)-C(43)	1.318(12)
C(27)-N(28)	1.373(8)	C(43)-C(44)	1.435(15)
N(28)-C(29)	1.384(8)	C(44)-C(45)	1.358(13)
C(29)-C(210)	1.335(11)	C(45)-C(46)	1.366(11)
C(29)-C(213)	1.483(10)	C(46)-C(47)	1.445(11)
C(210)-C(211)	1.388(10)	C(47)-C(412)	1.341(12)
C(211)-C(212)	1.406(10)	C(47)-N(48)	1.413(10)
C(213)-N(214)	1.365(8)	N(48)-C(49)	1.374(9)
C(213)-C(218)	1.392(10)	C(49)-C(410)	1.338(11)
N(214)-C(215)	1.346(8)	C(49)-C(413)	1.479(11)
C(215)-C(216)	1.368(10)	C(410)-C(411)	1.325(13)
C(216)-C(217)	1.409(12)	C(411)-C(412)	1.409(13)
C(217)-C(218)	1.371(11)	C(413)-C(418)	1.346(11)
Ru(3)-N(48)	1.930(8)	C(413)-N(414)	1.362(9)
Ru(3)-N(38)	2.035(6)	N(414)-C(415)	1.321(10)
Ru(3)-N(31)	2.055(6)	C(415)-C(416)	1.362(11)
Ru(3)-N(414)	2.070(7)	C(416)-C(417)	1.417(13)
Ru(3)-N(314)	2.090(5)	C(417)-C(418)	1.383(12)
Ru(3)-N(41)	2.100(6)	B(5)-C(521)	1.629(11)

B(5)-C(541)	1.656(10)	B(7)-C(721)	1.635(11)
B(5)-C(531)	1.667(10)	B(7)-C(741)	1.683(11)
B(5)-C(511)	1.667(10)	C(711)-C(716)	1.328(11)
C(511)-C(516)	1.359(9)	C(711)-C(712)	1.375(10)
C(511)-C(512)	1.406(9)	C(712)-C(713)	1.392(11)
C(512)-C(513)	1.383(10)	C(713)-C(714)	1.360(13)
C(513)-C(514)	1.426(11)	C(714)-C(715)	1.280(12)
C(514)-C(515)	1.355(11)	C(715)-C(716)	1.410(12)
C(515)-C(516)	1.454(10)	C(721)-C(726)	1.391(12)
C(521)-C(526)	1.417(10)	C(721)-C(722)	1.400(11)
C(521)-C(522)	1.471(10)	C(722)-C(723)	1.415(11)
C(522)-C(523)	1.338(11)	C(723)-C(724)	1.354(14)
C(523)-C(524)	1.408(12)	C(724)-C(725)	1.363(14)
C(524)-C(525)	1.398(12)	C(725)-C(726)	1.416(12)
C(525)-C(526)	1.385(11)	C(731)-C(736)	1.365(13)
C(531)-C(532)	1.37(1)	C(731)-C(732)	1.397(12)
C(531)-C(536)	1.378(10)	C(732)-C(733)	1.401(12)
C(532)-C(533)	1.363(11)	C(733)-C(734)	1.382(16)
C(533)-C(534)	1.420(13)	C(734)-C(735)	1.338(16)
C(534)-C(535)	1.339(12)	C(735)-C(736)	1.418(12)
C(535)-C(536)	1.411(11)	C(741)-C(746)	1.384(10)
C(541)-C(542)	1.395(10)	C(741)-C(742)	1.411(10)
C(541)-C(546)	1.401(9)	C(742)-C(743)	1.353(12)
C(542)-C(543)	1.383(11)	C(743)-C(744)	1.412(13)
C(543)-C(544)	1.389(12)	C(744)-C(745)	1.363(13)
C(544)-C(545)	1.410(12)	C(745)-C(746)	1.414(11)
C(545)-C(546)	1.40(1)	B(8)-C(821)	1.595(11)
B(6)-C(621)	1.615(11)	B(8)-C(841)	1.632(12)
B(6)-C(611)	1.64(1)	B(8)-C(811)	1.641(11)
B(6)-C(641)	1.65(1)	B(8)-C(831)	1.674(11)
B(6)-C(631)	1.69(1)	C(811)-C(816)	1.393(10)
C(611)-C(612)	1.376(11)	C(811)-C(812)	1.396(10)
C(611)-C(616)	1.406(11)	C(812)-C(813)	1.384(11)
C(612)-C(613)	1.420(13)	C(813)-C(814)	1.404(13)
C(613)-C(614)	1.355(14)	C(814)-C(815)	1.335(13)
C(614)-C(615)	1.381(14)	C(815)-C(816)	1.386(11)
C(615)-C(616)	1.375(12)	C(821)-C(822)	1.414(10)
C(621)-C(622)	1.389(10)	C(821)-C(826)	1.430(12)
C(621)-C(626)	1.428(10)	C(822)-C(823)	1.407(11)
C(622)-C(623)	1.394(12)	C(823)-C(824)	1.312(13)
C(623)-C(624)	1.373(14)	C(824)-C(825)	1.408(13)
C(624)-C(625)	1.406(14)	C(825)-C(826)	1.408(12)
C(625)-C(626)	1.307(12)	C(831)-C(832)	1.376(11)
C(631)-C(636)	1.357(10)	C(831)-C(836)	1.418(10)
C(631)-C(632)	1.36(1)	C(832)-C(833)	1.399(11)
C(632)-C(633)	1.461(12)	C(833)-C(834)	1.348(14)
C(633)-C(634)	1.400(15)	C(834)-C(835)	1.338(14)
C(634)-C(635)	1.345(15)	C(835)-C(836)	1.407(11)
C(635)-C(636)	1.391(11)	C(841)-C(842)	1.363(10)
C(641)-C(646)	1.381(10)	C(841)-C(846)	1.402(10)
C(641)-C(642)	1.397(9)	C(842)-C(843)	1.373(11)
C(642)-C(643)	1.394(10)	C(843)-C(844)	1.417(12)
C(643)-C(644)	1.355(12)	C(844)-C(845)	1.361(12)
C(644)-C(645)	1.392(12)	C(845)-C(846)	1.397(11)
C(645)-C(646)	1.402(10)	P(1)-F(16)	1.539(7)
B(7)-C(711)	1.606(12)	P(1)-F(14)	1.582(7)
B(7)-C(731)	1.633(11)	P(1)-F(12)	1.583(6)

P(1)-F(15)	1.587(5)
P(1)-F(13)	1.596(5)
P(1)-F(11)	1.622(7)
P(2)-F(24)	1.561(9)
P(2)-F(25)	1.569(8)
P(2)-F(21)	1.578(7)
P(2)-F(23)	1.594(8)
P(2)-F(22)	1.594(8)
P(2)-F(26)	1.625(8)
N(28)-RU1-N(18)	177.0(2)
N(28)-RU1-N(214)	79.1(2)
N(18)-RU1-N(214)	98.8(2)
N(28)-RU1-N(114)	103.7(2)
N(18)-RU1-N(114)	78.6(2)
N(214)-RU1-N(114)	96.0(2)
N(28)-RU1-N(21)	78.4(2)
N(18)-RU1-N(21)	103.6(2)
N(214)-RU1-N(21)	157.5(2)
N(114)-RU1-N(21)	87.8(2)
N(28)-RU1-N(11)	97.8(2)
N(18)-RU1-N(11)	79.9(2)
N(214)-RU1-N(11)	88.6(2)
N(114)-RU1-N(11)	158.5(2)
N(21)-RU1-N(11)	96.1(2)
C(12)-N(11)-C(16)	119.0(7)
C(12)-N(11)-RU1	128.1(5)
C(16)-N(11)-RU1	112.8(5)
N(11)-C(12)-C(13)	122.4(7)
C(12)-C(13)-C(14)	120.0(8)
C(13)-C(14)-C(15)	118.0(8)
C(16)-C(15)-C(14)	119.8(7)
C(15)-C(16)-N(11)	120.7(7)
C(15)-C(16)-C(17)	125.4(6)
N(11)-C(16)-C(17)	113.9(7)
N(18)-C(17)-C(112)	117.5(6)
N(18)-C(17)-C(16)	117.9(6)
C(112)-C(17)-C(16)	124.6(7)
C(19)-N(18)-C(17)	127.3(6)
C(19)-N(18)-RU1	117.3(5)
C(17)-N(18)-RU1	115.4(4)
N(18)-C(19)-C(110)	116.9(7)
N(18)-C(19)-C(113)	116.4(6)
C(110)-C(19)-C(113)	126.7(7)
C(111)-C(110)-C(19)	120.8(7)
C(110)-C(111)-C(112)	117.7(7)
C(110)-C(111)-C(119)	121.7(7)
C(112)-C(111)-C(119)	120.6(7)
C(111)-C(112)-C(17)	119.9(7)
C(118)-C(113)-N(114)	120.9(7)
C(118)-C(113)-C(19)	124.9(7)
N(114)-C(113)-C(19)	114.0(7)
C(115)-N(114)-C(113)	118.5(7)
C(115)-N(114)-RU1	127.5(6)
C(113)-N(114)-RU1	113.3(5)
N(114)-C(115)-C(116)	123.7(8)
C(117)-C(116)-C(115)	118.4(8)
C(116)-C(117)-C(118)	117.3(8)
C(113)-C(118)-C(117)	121.1(7)
C(124)-C(119)-C(120)	116.8(7)
C(124)-C(119)-C(111)	122.6(7)
C(120)-C(119)-C(111)	120.4(7)
C(121)-C(120)-C(119)	122.9(8)
C(120)-C(121)-C(122)	117.2(8)
C(123)-C(122)-C(121)	121.2(8)
C(123)-C(122)-C(125)	119.0(8)
C(121)-C(122)-C(125)	119.7(8)
C(124)-C(123)-C(122)	119.4(8)
C(123)-C(124)-C(119)	122.3(8)
N(126)-C(125)-N(130)	123.4(8)
N(126)-C(125)-C(122)	115.9(7)
N(130)-C(125)-C(122)	120.7(8)
C(125)-N(126)-C(127)	124.7(7)
C(128)-C(127)-N(126)	112.8(7)
C(127)-C(128)-C(129)	115.0(7)
C(125)-N(130)-C(131)	128.3(8)
N(130)-C(131)-C(132)	113.3(7)
C(131)-C(132)-C(133)	108.6(8)
C(22)-N(21)-C(26)	118.4(6)
C(22)-N(21)-RU1	126.9(5)
C(26)-N(21)-RU1	114.3(4)
N(21)-C(22)-C(23)	123.6(8)
C(22)-C(23)-C(24)	118.2(8)
C(25)-C(24)-C(23)	117.7(7)
C(26)-C(25)-C(24)	120.4(7)
N(21)-C(26)-C(25)	121.7(7)
N(21)-C(26)-C(27)	115.3(6)
C(25)-C(26)-C(27)	123.0(7)
C(212)-C(27)-N(28)	122.8(7)
C(212)-C(27)-C(26)	127.6(7)
N(28)-C(27)-C(26)	109.5(7)
C(27)-N(28)-C(29)	116.7(7)
C(27)-N(28)-RU1	122.2(5)
C(29)-N(28)-RU1	121.1(5)
C(210)-C(29)-N(28)	122.1(8)
C(210)-C(29)-C(213)	128.2(7)
N(28)-C(29)-C(213)	109.7(7)
C(29)-C(210)-C(211)	121.2(7)
C(210)-C(211)-C(212)	117.1(7)
C(27)-C(212)-C(211)	120.1(7)
N(214)-C(213)-C(218)	120.4(7)
N(214)-C(213)-C(29)	116.1(6)
C(218)-C(213)-C(29)	123.5(7)
C(215)-N(214)-C(213)	118.9(6)
C(215)-N(214)-RU1	127.2(5)
C(213)-N(214)-RU1	113.7(5)
N(214)-C(215)-C(216)	122.8(7)
C(215)-C(216)-C(217)	118.9(8)
C(218)-C(217)-C(216)	118.3(8)
C(217)-C(218)-C(213)	120.6(8)
N(48)-RU3-N(38)	178.2(2)
N(48)-RU3-N(31)	99.6(2)
N(38)-RU3-N(31)	79.1(2)
N(48)-RU3-N(414)	78.7(3)
N(38)-RU3-N(414)	102.6(2)

N(31)-RU3-N(414)	91.8(2)	C(325)-N(326)-C(327)	125.5(8)
N(48)-RU3-N(314)	102.3(2)	N(326)-C(327)-C(328)	108.3(9)
N(38)-RU3-N(314)	78.9(2)	C(327)-C(328)-C(329)	105.1(9)
N(31)-RU3-N(314)	158.0(3)	C(325)-N(330)-C(331)	126.3(8)
N(414)-RU3-N(314)	92.2(2)	C(332)-C(331)-N(330)	117.4(9)
N(48)-RU3-N(41)	79.1(3)	C(331)-C(332)-C(333)	117.40(11)
N(38)-RU3-N(41)	99.6(2)	C(42)-N(41)-C(46)	121.4(8)
N(31)-RU3-N(41)	91.9(2)	C(42)-N(41)-RU3	125.7(6)
N(414)-RU3-N(41)	157.9(3)	C(46)-N(41)-RU3	112.7(6)
N(314)-RU3-N(41)	92.5(2)	N(41)-C(42)-C(43)	122.4(9)
C(32)-N(31)-C(36)	118.5(6)	C(42)-C(43)-C(44)	119.00(11)
C(32)-N(31)-RU3	128.0(5)	C(45)-C(44)-C(43)	116.9(1)
C(36)-N(31)-RU3	113.5(5)	C(44)-C(45)-C(46)	121.3(9)
N(31)-C(32)-C(33)	122.2(7)	N(41)-C(46)-C(45)	118.9(9)
C(34)-C(33)-C(32)	120.7(7)	N(41)-C(46)-C(47)	117.9(8)
C(33)-C(34)-C(35)	118.9(7)	C(45)-C(46)-C(47)	123.2(8)
C(34)-C(35)-C(36)	118.2(7)	C(412)-C(47)-N(48)	119.5(1)
N(31)-C(36)-C(35)	121.3(7)	C(412)-C(47)-C(46)	130.1(1)
N(31)-C(36)-C(37)	115.8(6)	N(48)-C(47)-C(46)	110.4(8)
C(35)-C(36)-C(37)	122.7(7)	C(49)-N(48)-C(47)	118.2(9)
N(38)-C(37)-C(36)	116.6(6)	C(49)-N(48)-RU3	121.9(6)
N(38)-C(37)-C(312)	115.6(6)	C(47)-N(48)-RU3	119.9(6)
C(36)-C(37)-C(312)	127.8(6)	C(410)-C(49)-N(48)	122.6(1)
C(39)-N(38)-C(37)	129.4(7)	C(410)-C(49)-C(413)	127.8(9)
C(39)-N(38)-RU3	115.6(5)	N(48)-C(49)-C(413)	109.5(7)
C(37)-N(38)-RU3	114.9(4)	C(411)-C(410)-C(49)	118.40(11)
N(38)-C(39)-C(310)	117.1(6)	C(410)-C(411)-C(412)	122.70(12)
N(38)-C(39)-C(313)	117.8(7)	C(47)-C(412)-C(411)	118.50(11)
C(310)-C(39)-C(313)	125.0(7)	C(418)-C(413)-N(414)	121.7(9)
C(311)-C(310)-C(39)	118.2(7)	C(418)-C(413)-C(49)	122.1(8)
C(312)-C(311)-C(310)	119.7(8)	N(414)-C(413)-C(49)	116.2(7)
C(312)-C(311)-C(319)	120.5(6)	C(415)-N(414)-C(413)	118.5(8)
C(310)-C(311)-C(319)	119.7(7)	C(415)-N(414)-RU3	127.9(5)
C(311)-C(312)-C(37)	119.8(7)	C(413)-N(414)-RU3	113.6(6)
N(314)-C(313)-C(318)	120.7(7)	N(414)-C(415)-C(416)	122.7(9)
N(314)-C(313)-C(39)	114.1(6)	C(415)-C(416)-C(417)	119.9(1)
C(318)-C(313)-C(39)	125.1(7)	C(418)-C(417)-C(416)	115.9(9)
C(315)-N(314)-C(313)	118.3(6)	C(413)-C(418)-C(417)	121.4(9)
C(315)-N(314)-RU3	128.1(5)	C(521)-B(5)-C(541)	114.6(6)
C(313)-N(314)-RU3	113.5(5)	C(521)-B(5)-C(531)	104.8(6)
N(314)-C(315)-C(316)	121.0(7)	C(541)-B(5)-C(531)	109.1(6)
C(317)-C(316)-C(315)	119.8(7)	C(521)-B(5)-C(511)	111.5(6)
C(316)-C(317)-C(318)	120.9(8)	C(541)-B(5)-C(511)	103.6(6)
C(317)-C(318)-C(313)	119.1(7)	C(531)-B(5)-C(511)	113.5(6)
C(324)-C(319)-C(320)	120.6(6)	C(516)-C(511)-C(512)	117.0(7)
C(324)-C(319)-C(311)	122.0(7)	C(516)-C(511)-B(5)	122.1(6)
C(320)-C(319)-C(311)	117.4(6)	C(512)-C(511)-B(5)	120.5(7)
C(321)-C(320)-C(319)	120.3(7)	C(513)-C(512)-C(511)	122.6(8)
C(322)-C(321)-C(320)	119.1(8)	C(512)-C(513)-C(514)	119.2(8)
C(323)-C(322)-C(321)	120.6(7)	C(515)-C(514)-C(513)	120.0(8)
C(323)-C(322)-C(325)	120.6(8)	C(514)-C(515)-C(516)	118.7(8)
C(321)-C(322)-C(325)	118.7(8)	C(511)-C(516)-C(515)	122.5(8)
C(322)-C(323)-C(324)	120.8(8)	C(526)-C(521)-C(522)	116.2(8)
C(319)-C(324)-C(323)	118.4(7)	C(526)-C(521)-B(5)	121.8(7)
N(326)-C(325)-N(330)	121.7(8)	C(522)-C(521)-B(5)	121.6(7)
N(326)-C(325)-C(322)	116.7(7)	C(523)-C(522)-C(521)	119.2(8)
N(330)-C(325)-C(322)	121.1(8)	C(522)-C(523)-C(524)	125.8(1)

C(525)-C(524)-C(523)	114.3(1)	C(711)-B(7)-C(731)	112.5(7)
C(526)-C(525)-C(524)	123.8(1)	C(711)-B(7)-C(721)	115.8(7)
C(525)-C(526)-C(521)	120.5(9)	C(731)-B(7)-C(721)	104.7(7)
C(532)-C(531)-C(536)	114.8(7)	C(711)-B(7)-C(741)	103.7(6)
C(532)-C(531)-B(5)	119.9(7)	C(731)-B(7)-C(741)	111.3(7)
C(536)-C(531)-B(5)	125.2(7)	C(721)-B(7)-C(741)	108.9(7)
C(533)-C(532)-C(531)	123.3(8)	C(716)-C(711)-C(712)	112.3(9)
C(532)-C(533)-C(534)	120.7(9)	C(716)-C(711)-B(7)	126.4(8)
C(535)-C(534)-C(533)	117.8(9)	C(712)-C(711)-B(7)	121.0(8)
C(534)-C(535)-C(536)	119.6(9)	C(711)-C(712)-C(713)	125.1(9)
C(531)-C(536)-C(535)	123.9(8)	C(714)-C(713)-C(712)	116.4(1)
C(542)-C(541)-C(546)	116.1(7)	C(715)-C(714)-C(713)	122.20(11)
C(542)-C(541)-B(5)	122.8(7)	C(714)-C(715)-C(716)	118.5(1)
C(546)-C(541)-B(5)	120.8(7)	C(711)-C(716)-C(715)	125.3(1)
C(543)-C(542)-C(541)	121.9(8)	C(726)-C(721)-C(722)	113.6(8)
C(542)-C(543)-C(544)	122.8(1)	C(726)-C(721)-B(7)	123.4(8)
C(543)-C(544)-C(545)	116.0(8)	C(722)-C(721)-B(7)	122.7(8)
C(546)-C(545)-C(544)	121.1(7)	C(721)-C(722)-C(723)	122.7(9)
C(545)-C(546)-C(541)	122.0(8)	C(724)-C(723)-C(722)	119.8(1)
C(621)-B(6)-C(611)	104.9(6)	C(723)-C(724)-C(725)	121.30(11)
C(621)-B(6)-C(641)	114.8(6)	C(724)-C(725)-C(726)	117.50(11)
C(611)-B(6)-C(641)	111.1(6)	C(721)-C(726)-C(725)	125.0(9)
C(621)-B(6)-C(631)	110.2(6)	C(736)-C(731)-C(732)	113.5(9)
C(611)-B(6)-C(631)	113.5(6)	C(736)-C(731)-B(7)	125.6(9)
C(641)-B(6)-C(631)	102.7(6)	C(732)-C(731)-B(7)	120.4(9)
C(612)-C(611)-C(616)	115.2(8)	C(731)-C(732)-C(733)	126.10(12)
C(612)-C(611)-B(6)	125.3(7)	C(734)-C(733)-C(732)	111.90(12)
C(616)-C(611)-B(6)	119.4(7)	C(735)-C(734)-C(733)	128.60(13)
C(611)-C(612)-C(613)	121.4(9)	C(734)-C(735)-C(736)	113.00(12)
C(614)-C(613)-C(612)	121.10(11)	C(731)-C(736)-C(735)	126.00(11)
C(613)-C(614)-C(615)	119.0(1)	C(746)-C(741)-C(742)	115.4(7)
C(616)-C(615)-C(614)	119.5(1)	C(746)-C(741)-B(7)	120.1(7)
C(615)-C(616)-C(611)	123.8(9)	C(742)-C(741)-B(7)	124.2(7)
C(622)-C(621)-C(626)	113.2(8)	C(743)-C(742)-C(741)	121.7(9)
C(622)-C(621)-B(6)	123.0(7)	C(742)-C(743)-C(744)	122.0(9)
C(626)-C(621)-B(6)	123.4(7)	C(745)-C(744)-C(743)	118.2(9)
C(621)-C(622)-C(623)	124.2(9)	C(744)-C(745)-C(746)	119.1(9)
C(624)-C(623)-C(622)	118.50(11)	C(741)-C(746)-C(745)	123.6(8)
C(623)-C(624)-C(625)	119.10(11)	C(821)-B(8)-C(841)	111.1(7)
C(626)-C(625)-C(624)	120.60(11)	C(821)-B(8)-C(811)	114.0(7)
C(625)-C(626)-C(621)	124.3(9)	C(841)-B(8)-C(811)	104.7(6)
C(636)-C(631)-C(632)	118.6(8)	C(821)-B(8)-C(831)	103.8(6)
C(636)-C(631)-B(6)	120.8(7)	C(841)-B(8)-C(831)	113.4(7)
C(632)-C(631)-B(6)	120.4(7)	C(811)-B(8)-C(831)	110.1(7)
C(631)-C(632)-C(633)	120.2(9)	C(816)-C(811)-C(812)	115.4(7)
C(634)-C(633)-C(632)	117.10(11)	C(816)-C(811)-B(8)	121.4(7)
C(635)-C(634)-C(633)	121.70(11)	C(812)-C(811)-B(8)	122.9(7)
C(634)-C(635)-C(636)	118.50(11)	C(813)-C(812)-C(811)	121.9(7)
C(631)-C(636)-C(635)	123.6(1)	C(812)-C(813)-C(814)	120.0(9)
C(646)-C(641)-C(642)	114.7(7)	C(815)-C(814)-C(813)	118.8(9)
C(646)-C(641)-B(6)	121.7(7)	C(814)-C(815)-C(816)	121.0(8)
C(642)-C(641)-B(6)	123.3(7)	C(815)-C(816)-C(811)	122.7(8)
C(643)-C(642)-C(641)	123.0(8)	C(822)-C(821)-C(826)	113.2(8)
C(644)-C(643)-C(642)	121.1(8)	C(822)-C(821)-B(8)	124.3(8)
C(643)-C(644)-C(645)	117.9(9)	C(826)-C(821)-B(8)	122.5(8)
C(644)-C(645)-C(646)	120.3(9)	C(823)-C(822)-C(821)	123.6(1)
C(641)-C(646)-C(645)	122.8(8)	C(824)-C(823)-C(822)	120.00(11)

C(823)-C(824)-C(825)	122.10(11)	F(14)-P(1)-F(13)	88.4(3)
C(824)-C(825)-C(826)	117.50(11)	F(12)-P(1)-F(13)	90.6(3)
C(825)-C(826)-C(821)	123.5(1)	F(15)-P(1)-F(13)	179.1(5)
C(832)-C(831)-C(836)	114.5(8)	F(16)-P(1)-F(11)	179.7(5)
C(832)-C(831)-B(8)	122.9(8)	F(14)-P(1)-F(11)	90.2(4)
C(836)-C(831)-B(8)	122.5(7)	F(12)-P(1)-F(11)	90.1(3)
C(831)-C(832)-C(833)	125.0(9)	F(15)-P(1)-F(11)	90.1(4)
C(834)-C(833)-C(832)	118.1(1)	F(13)-P(1)-F(11)	89.1(4)
C(835)-C(834)-C(833)	120.4(1)	F(24)-P(2)-F(25)	91.0(5)
C(834)-C(835)-C(836)	122.1(9)	F(24)-P(2)-F(21)	88.9(5)
C(835)-C(836)-C(831)	119.7(9)	F(25)-P(2)-F(21)	86.8(4)
C(842)-C(841)-C(846)	113.1(8)	F(24)-P(2)-F(23)	90.6(5)
C(842)-C(841)-B(8)	121.9(7)	F(25)-P(2)-F(23)	174.7(6)
C(846)-C(841)-B(8)	124.6(7)	F(21)-P(2)-F(23)	88.2(5)
C(841)-C(842)-C(843)	126.3(8)	F(24)-P(2)-F(22)	178.9(6)
C(842)-C(843)-C(844)	117.4(8)	F(25)-P(2)-F(22)	88.8(5)
C(845)-C(844)-C(843)	120.2(9)	F(21)-P(2)-F(22)	92.2(5)
C(844)-C(845)-C(846)	118.0(9)	F(23)-P(2)-F(22)	89.7(5)
C(845)-C(846)-C(841)	124.7(8)	F(24)-P(2)-F(26)	94.3(5)
F(16)-P(1)-F(14)	89.6(4)	F(25)-P(2)-F(26)	90.9(5)
F(16)-P(1)-F(12)	90.1(4)	F(21)-P(2)-F(26)	176.1(5)
F(14)-P(1)-F(12)	179.0(4)	F(23)-P(2)-F(26)	94.1(5)
F(16)-P(1)-F(15)	89.9(4)	F(22)-P(2)-F(26)	84.7(5)
F(14)-P(1)-F(15)	91.3(3)		
F(12)-P(1)-F(15)	89.7(3)		
F(16)-P(1)-F(13)	90.9(4)		

Table 6. Bond lengths [Å] and angles [°] related to the hydrogen bonding for **IV-1**.

D-H	..A	d(D-H)	d(H..A)	d(D..A)	<DHA
N(326)-H(326)	F(15)#1	0.87	1.98	2.845(9)	173.9
N(330)-H(330)	F(21)#2	0.87	2.26	3.055(11)	152.4
N(330)-H(330)	F(25)#2	0.87	2.36	3.004(11)	131.5

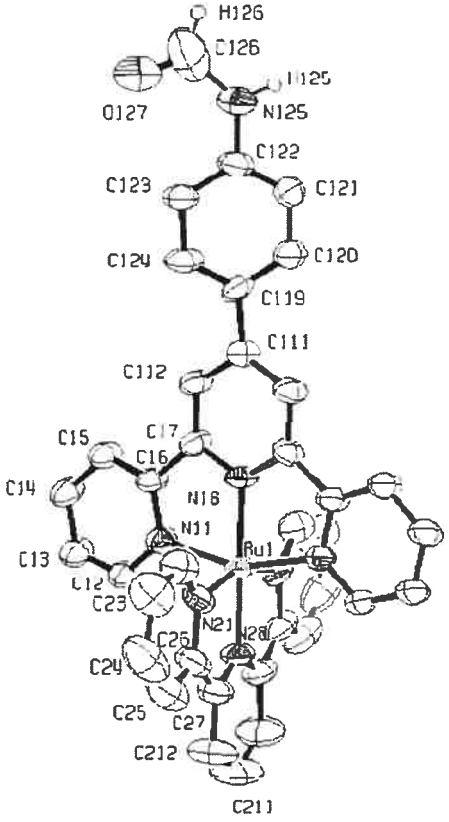

Table 1. Crystal data and structure refinement for **IV-3**.

Empirical formula	C85 H67 B2 N7 O Ru	
Formula weight	1325.15	
Temperature	100(2)K	
Wavelength	1.54178 Å	
Crystal system	Monoclinic	
Space group	C2/c	
Unit cell dimensions	a = 21.4989(6) Å	$\alpha = 90^\circ$
	b = 22.1518(5) Å	$\beta = 90.8620(10)^\circ$
	c = 18.1137(4) Å	$\gamma = 90^\circ$
Volume	8625.5(4)Å^3	
Z	4	

Density (calculated)	1.020 g/cm^3
Absorption coefficient	1.799 mm^{-1}
F(000)	2752
Crystal size	0.10 x 0.05 x 0.05 mm
Theta range for data collection	2.86 to 68.30°
Index ranges	$-25 \leq h \leq 24$, $-26 \leq k \leq 26$, $-21 \leq \ell \leq 21$
Reflections collected	45834
Independent reflections	7814 [R_{int} = 0.031]
Absorption correction	Semi-empirical from equivalents
Max. and min. transmission	0.9400 and 0.7100
Refinement method	Full-matrix least-squares on F^2
Data / restraints / parameters	7814 / 49 / 422
Goodness-of-fit on F^2	1.125
Final R indices [I>2sigma(I)]	R_1 = 0.0751, wR_2 = 0.2093
R indices (all data)	R_1 = 0.0972, wR_2 = 0.2327
Extinction coefficient	y
Largest diff. peak and hole	1.262 and -2.410 $e/Å^3$

Table 2. Atomic coordinates (x 10^4) and equivalent isotropic displacement parameters ($Å^2$ x 10^3) for **IV-3**.

U_{eq} is defined as one third of the trace of the orthogonalized Uij tensor.

	Occ.	x	y	z	U_{eq}
Ru(1)	1	5000	1956(1)	2500	46(1)
N(11)	1	4373(2)	2137(2)	1653(2)	48(1)
C(12)	1	4069(2)	1736(2)	1222(3)	56(1)
C(13)	1	3693(3)	1904(2)	645(3)	64(2)
C(14)	1	3630(3)	2513(2)	475(3)	66(2)
C(15)	1	3939(3)	2932(2)	906(3)	54(1)
C(16)	1	4303(2)	2736(2)	1492(2)	46(1)

C(17)	1	4639(2)	3150(2)	1995(2)	45(1)
N(18)	1	5000	2857(2)	2500	43(1)
C(111)	1	5000	4104(2)	2500	40(1)
C(112)	1	4635(2)	3770(2)	1989(2)	48(1)
C(119)	0.50	4916(2)	4764(2)	2543(2)	53(2)
C(120)	0.50	5441(2)	5110(2)	2697(2)	57(5)
C(121)	0.50	5393(6)	5740(5)	2767(6)	58(3)
C(122)	0.50	4820(6)	6016(4)	2708(6)	60(3)
C(123)	0.50	4276(6)	5677(4)	2535(6)	57(3)
C(124)	0.50	4341(8)	5044(5)	2474(7)	58(3)
N(125)	0.50	4775(5)	6648(3)	2836(5)	74(3)
C(126)	0.50	4266(6)	7080(7)	2772(9)	112(5)
O(127)	0.50	3786(6)	6894(4)	2549(7)	117(4)
N(21)	1	4313(2)	1778(2)	3265(2)	52(1)
C(22)	1	3977(3)	2166(3)	3658(3)	66(1)
C(23)	1	3546(4)	1993(3)	4163(3)	86(2)
C(24)	1	3455(3)	1376(4)	4282(3)	98(2)
C(25)	1	3805(3)	970(3)	3890(3)	84(2)
C(26)	1	4227(3)	1164(2)	3391(3)	65(1)
C(27)	1	4614(3)	768(2)	2941(3)	70(2)
N(28)	1	5000	1055(2)	2500	55(1)
C(211)	1	5000	-164(4)	2500	140(5)
C(212)	1	4595(4)	145(3)	2932(5)	113(3)
B(3)	1	2479(3)	4364(2)	1017(3)	60(2)
C(31)	1	3080(2)	4364(1)	439(2)	58(1)
C(32)	1	3646(2)	4618(1)	654(2)	61(1)
C(33)	1	4159(2)	4565(2)	202(2)	77(2)
C(34)	1	4108(2)	4258(2)	-466(2)	88(2)
C(35)	1	3542(2)	4004(2)	-681(2)	78(2)
C(36)	1	3028(2)	4057(1)	-229(2)	68(2)
C(41)	1	2567(2)	3715(1)	1479(2)	57(1)
C(42)	1	2939(2)	3706(1)	2114(2)	56(1)
C(43)	1	3048(2)	3165(1)	2482(2)	68(2)
C(44)	1	2786(2)	2633(1)	2216(2)	83(2)
C(45)	1	2415(2)	2641(1)	1581(2)	88(2)
C(46)	1	2306(2)	3182(2)	1213(2)	75(2)
C(51)	1	1787(2)	4413(2)	562(2)	74(2)
C(52)	1	1264(2)	4140(2)	854(2)	100(2)
C(53)	1	688(2)	4210(2)	506(3)	130(3)
C(54)	1	635(2)	4553(3)	-135(3)	134(3)
C(55)	1	1159(3)	4827(2)	-427(2)	121(3)
C(56)	1	1735(2)	4757(2)	-79(2)	90(2)
C(61)	1	2465(2)	4961(1)	1605(2)	63(1)
C(62)	1	2143(2)	4889(1)	2259(2)	78(2)
C(63)	1	2092(2)	5370(2)	2747(2)	96(2)
C(64)	1	2363(2)	5923(1)	2582(2)	96(2)
C(65)	1	2685(2)	5994(1)	1928(2)	92(2)
C(66)	1	2736(2)	5513(1)	1439(2)	73(2)

Table 3. Hydrogen coordinates (x 10^4) and isotropic displacement parameters ($Å^2$ x 10^3) for **IV-3**.

	Occ.	x	y	z	U_{eq}
H(12)	1	4120	1318	1324	67
H(13)	1	3475	1608	363	77
H(14)	1	3378	2638	68	79
H(15)	1	3901	3350	801	64
H(112)	1	4384	3977	1636	58
H(120)	0.50	5835	4919	2755	68
H(121)	0.50	5756	5976	2855	70
H(123)	0.50	3884	5867	2463	69
H(124)	0.50	3982	4804	2384	70
H(125)	0.50	5128	6812	2984	89
H(126)	0.50	4320	7493	2903	134
H(22)	1	4041	2586	3582	79
H(23)	1	3314	2285	4427	103
H(24)	1	3158	1239	4626	117
H(25)	1	3752	549	3969	101
H(211)	1	5000	-593	2500	168
H(212)	1	4302	-67	3223	136
H(32)	1	3681	4828	1110	73
H(33)	1	4546	4738	349	92
H(34)	1	4459	4222	-775	105
H(35)	1	3507	3794	-1137	93
H(36)	1	2642	3884	-376	82
H(42)	1	3118	4070	2296	67
H(43)	1	3302	3159	2916	82
H(44)	1	2861	2263	2468	99
H(45)	1	2236	2278	1399	106
H(46)	1	2052	3188	779	90
H(52)	1	1300	3905	1291	120
H(53)	1	330	4023	705	156
H(54)	1	242	4601	-372	161
H(55)	1	1123	5061	-864	145
H(56)	1	2093	4943	-278	108
H(62)	1	1957	4512	2372	93
H(63)	1	1872	5321	3194	115
H(64)	1	2328	6251	2916	115
H(65)	1	2870	6372	1815	110
H(66)	1	2956	5562	992	87

Table 4. Anisotropic parameters ($Å^2$ x 10^3) for **IV-3**.

The anisotropic displacement factor exponent takes the form:

$$-2\pi^2 [h^2 a^{*2} U_{11} + ... + 2 h k a^* b^* U_{12}]$$

	U11	U22	U33	U23	U13	U12
Ru(1)	62(1)	24(1)	51(1)	0	-14(1)	0
N(11)	59(3)	32(2)	53(2)	-6(2)	-12(2)	6(2)
C(12)	67(3)	33(2)	68(3)	-13(2)	-24(3)	6(2)
C(13)	81(4)	37(2)	73(3)	-18(2)	-27(3)	12(2)
C(14)	90(4)	42(2)	64(3)	-14(2)	-33(3)	18(3)
C(15)	77(4)	34(2)	49(3)	-6(2)	-16(2)	8(2)
C(16)	62(3)	29(2)	47(2)	-5(2)	-4(2)	6(2)
C(17)	63(3)	34(2)	38(2)	4(2)	-9(2)	9(2)
N(18)	61(3)	23(2)	44(3)	0	0(3)	0
C(111)	60(4)	34(3)	25(3)	0	1(3)	0
C(112)	71(3)	33(2)	41(2)	5(2)	-10(2)	5(2)
C(119)	74(7)	35(3)	49(4)	2(7)	-20(4)	19(6)
C(120)	77(10)	43(7)	50(8)	0(5)	-21(7)	2(6)
C(121)	66(8)	46(6)	62(7)	-9(5)	-22(6)	1(6)
C(122)	89(10)	32(4)	60(8)	-2(4)	-20(6)	-7(5)
C(123)	75(9)	30(5)	66(7)	-3(5)	-8(6)	1(5)
C(124)	98(10)	28(5)	49(6)	-7(4)	-16(8)	4(6)
N(125)	90(7)	35(4)	97(7)	-10(4)	-18(5)	-1(4)
C(126)	100(8)	133(9)	102(8)	3(7)	-20(7)	-35(8)
O(127)	117(7)	61(5)	171(8)	2(5)	-12(7)	1(5)
N(21)	59(3)	45(2)	53(2)	7(2)	-8(2)	-18(2)
C(22)	82(4)	60(3)	56(3)	1(2)	-4(3)	-5(3)
C(23)	98(5)	99(5)	61(4)	1(3)	9(4)	-17(4)
C(24)	112(6)	115(6)	67(4)	9(4)	-4(4)	-55(5)
C(25)	105(5)	73(4)	73(4)	10(3)	-15(4)	-36(4)
C(26)	78(4)	49(3)	68(3)	13(2)	-16(3)	-29(3)
C(27)	92(4)	35(2)	80(4)	6(2)	-31(3)	-13(3)
N(28)	75(4)	23(2)	65(3)	0	-15(3)	0
C(211)	159(12)	32(4)	230(15)	0	1(11)	0
C(212)	144(7)	36(3)	159(7)	17(4)	-10(6)	-15(4)
B(3)	74(4)	38(3)	67(3)	-14(2)	-27(3)	14(3)
C(31)	87(4)	37(2)	49(3)	0(2)	-21(3)	13(2)
C(32)	88(4)	45(2)	48(3)	10(2)	-13(3)	5(3)
C(33)	107(5)	61(3)	62(3)	19(3)	-17(3)	-3(3)
C(34)	120(6)	78(4)	65(4)	14(3)	17(4)	26(4)
C(35)	105(5)	68(4)	60(3)	-3(3)	-13(4)	8(3)
C(36)	96(4)	50(3)	59(3)	-8(2)	-16(3)	19(3)
C(41)	68(3)	35(2)	68(3)	-13(2)	-5(3)	7(2)
C(42)	76(4)	32(2)	58(3)	-4(2)	-3(3)	2(2)
C(43)	91(5)	45(3)	68(3)	5(2)	6(3)	5(3)
C(44)	113(5)	33(2)	103(5)	15(3)	24(4)	-1(3)
C(45)	122(6)	36(3)	106(5)	-6(3)	-7(4)	-16(3)
C(46)	84(4)	49(3)	91(4)	-15(3)	-17(3)	5(3)
C(51)	86(4)	57(3)	79(3)	-34(3)	-20(3)	29(3)
C(52)	71(4)	98(4)	130(5)	-55(4)	-24(4)	18(4)

C(53)	94(5)	138(6)	159(7)	-69(5)	-8(5)	23(5)
C(54)	116(6)	140(6)	145(6)	-83(5)	-41(5)	65(5)
C(55)	144(6)	118(5)	101(5)	-50(4)	-45(5)	64(5)
C(56)	106(5)	84(4)	78(4)	-34(3)	-41(3)	51(3)
C(61)	87(4)	40(2)	61(3)	-6(2)	-30(3)	19(2)
C(62)	116(5)	50(3)	67(3)	-10(2)	-7(3)	23(3)
C(63)	156(7)	64(4)	68(4)	-19(3)	-19(4)	46(4)
C(64)	146(7)	55(3)	86(4)	-34(3)	-49(4)	37(4)
C(65)	131(6)	41(3)	103(5)	-13(3)	-38(4)	19(3)
C(66)	102(5)	37(2)	78(3)	-6(2)	-31(3)	12(3)

Table 5. Bond lengths [Å] and angles [°] for **IV-3**.

Ru(1)-N(18)	1.995(5)	N(21)-C(26)	1.392(6)
Ru(1)-N(28)	1.996(5)	C(22)-C(23)	1.368(8)
Ru(1)-N(11)#1	2.066(4)	C(22)-H(22)	0.95
Ru(1)-N(11)	2.066(4)	C(23)-C(24)	1.397(9)
Ru(1)-N(21)#1	2.078(4)	C(23)-H(23)	0.95
Ru(1)-N(21)	2.078(4)	C(24)-C(25)	1.377(9)
N(11)-C(12)	1.345(6)	C(24)-H(24)	0.95
N(11)-C(16)	1.366(5)	C(25)-C(26)	1.359(8)
C(12)-C(13)	1.364(7)	C(25)-H(25)	0.95
C(12)-H(12)	0.95	C(26)-C(27)	1.466(8)
C(13)-C(14)	1.388(6)	C(27)-N(28)	1.323(6)
C(13)-H(13)	0.95	C(27)-C(212)	1.381(7)
C(14)-C(15)	1.376(6)	N(28)-C(27)#1	1.323(6)
C(14)-H(14)	0.95	C(211)-C(212)#1	1.364(8)
C(15)-C(16)	1.380(6)	C(211)-C(212)	1.364(8)
C(15)-H(15)	0.95	C(211)-H(211)	0.95
C(16)-C(17)	1.474(6)	C(212)-H(212)	0.95
C(17)-N(18)	1.356(5)	B(3)-C(41)	1.673(6)
C(17)-C(112)	1.373(5)	B(3)-C(31)	1.676(7)
N(18)-C(17)#1	1.356(5)	B(3)-C(51)	1.692(7)
C(111)-C(112)	1.413(5)	B(3)-C(61)	1.699(5)
C(111)-C(112)#1	1.413(5)	C(31)-C(32)	1.39
C(111)-C(119)#1	1.475(6)	C(31)-C(36)	1.39
C(111)-C(119)	1.475(6)	C(32)-C(33)	1.39
C(112)-H(112)	0.95	C(32)-H(32)	0.95
C(119)-C(124)	1.387(15)	C(33)-C(34)	1.39
C(119)-C(120)	1.39	C(33)-H(33)	0.95
C(120)-C(121)	1.407(11)	C(34)-C(35)	1.39
C(120)-H(120)	0.95	C(34)-H(34)	0.95
C(121)-C(122)	1.378(16)	C(35)-C(36)	1.39
C(121)-H(121)	0.95	C(35)-H(35)	0.95
C(122)-C(123)	1.421(16)	C(36)-H(36)	0.95
C(122)-N(125)	1.423(11)	C(41)-C(42)	1.39
C(123)-C(124)	1.413(14)	C(41)-C(46)	1.39
C(123)-H(123)	0.95	C(42)-C(43)	1.39
C(124)-H(124)	0.95	C(42)-H(42)	0.95
N(125)-C(126)	1.457(9)	C(43)-C(44)	1.39
N(125)-H(125)	0.88	C(43)-H(43)	0.95
C(126)-O(127)	1.179(16)	C(44)-C(45)	1.39
C(126)-H(126)	0.95	C(44)-H(44)	0.95
N(21)-C(22)	1.335(7)	C(45)-C(46)	1.39

C(45)-H(45)	0.95
C(46)-H(46)	0.95
C(51)-C(52)	1.39
C(51)-C(56)	1.39
C(52)-C(53)	1.39
C(52)-H(52)	0.95
C(53)-C(54)	1.39
C(53)-H(53)	0.95
C(54)-C(55)	1.39
C(54)-H(54)	0.95
C(55)-C(56)	1.39
C(55)-H(55)	0.95
C(56)-H(56)	0.95
C(61)-C(62)	1.39
C(61)-C(66)	1.39
C(62)-C(63)	1.39
C(62)-H(62)	0.95
C(63)-C(64)	1.39
C(63)-H(63)	0.95
C(64)-C(65)	1.39
C(64)-H(64)	0.95
C(65)-C(66)	1.39
C(65)-H(65)	0.95
C(66)-H(66)	0.95

N(18)-RU1-N(28)	180
N(18)-RU1-N(11)#1	78.81(10)
N(28)-RU1-N(11)#1	101.19(10)
N(18)-RU1-N(11)	78.81(10)
N(28)-RU1-N(11)	101.19(10)
N(11)#1-RU1-N(11)	157.6(2)
N(18)-RU1-N(21)#1	100.92(11)
N(28)-RU1-N(21)#1	79.08(11)
N(11)#1-RU1-N(21)#1	94.00(15)
N(11)-RU1-N(21)#1	90.22(15)
N(18)-RU1-N(21)	100.92(11)
N(28)-RU1-N(21)	79.08(11)
N(11)#1-RU1-N(21)	90.22(15)
N(11)-RU1-N(21)	94.00(15)
N(21)#1-RU1-N(21)	158.2(2)
C(12)-N(11)-C(16)	117.8(4)
C(12)-N(11)-RU1	127.5(3)
C(16)-N(11)-RU1	114.5(3)
N(11)-C(12)-C(13)	122.8(4)
N(11)-C(12)-H(12)	118.6
C(13)-C(12)-H(12)	118.6
C(12)-C(13)-C(14)	119.3(5)
C(12)-C(13)-H(13)	120.4
C(14)-C(13)-H(13)	120.4
C(15)-C(14)-C(13)	119.0(5)
C(15)-C(14)-H(14)	120.5
C(13)-C(14)-H(14)	120.5
C(14)-C(15)-C(16)	119.2(4)
C(14)-C(15)-H(15)	120.4
C(16)-C(15)-H(15)	120.4
N(11)-C(16)-C(15)	121.9(4)
N(11)-C(16)-C(17)	114.9(4)
C(15)-C(16)-C(17)	123.2(4)
N(18)-C(17)-C(112)	119.2(4)
N(18)-C(17)-C(16)	112.9(4)
C(112)-C(17)-C(16)	127.9(4)
C(17)#1-N(18)-C(17)	122.7(5)
C(17)#1-N(18)-RU1	118.6(2)
C(17)-N(18)-RU1	118.6(2)
C(112)-C(111)-C(112)#1	116.8(5)
C(112)-C(111)-C(119)#1	123.5(2)
C(112)#1-C(111)-C(119)#1	119.1(3)
C(112)-C(111)-C(119)	119.1(3)
C(112)#1-C(111)-C(119)	123.5(2)
C(119)#1-C(111)-C(119)	15.4(4)
C(17)-C(112)-C(111)	121.0(4)
C(17)-C(112)-H(112)	119.5
C(111)-C(112)-H(112)	119.5
C(124)-C(119)-C(120)	119.4(6)
C(124)-C(119)-C(111)	123.3(6)
C(120)-C(119)-C(111)	117.21(18)
C(119)-C(120)-C(121)	120.3(5)
C(119)-C(120)-H(120)	119.8
C(121)-C(120)-H(120)	119.8
C(122)-C(121)-C(120)	120.0(1)
C(122)-C(121)-H(121)	120
C(120)-C(121)-H(121)	120
C(121)-C(122)-C(123)	121.0(8)
C(121)-C(122)-N(125)	119.0(1)
C(123)-C(122)-N(125)	120.0(1)
C(124)-C(123)-C(122)	117.30(12)
C(124)-C(123)-H(123)	121.3
C(122)-C(123)-H(123)	121.3
C(119)-C(124)-C(123)	121.80(13)
C(119)-C(124)-H(124)	119.1
C(123)-C(124)-H(124)	119.1
C(122)-N(125)-C(126)	133.30(12)
C(122)-N(125)-H(125)	113.3
C(126)-N(125)-H(125)	113.3
O(127)-C(126)-N(125)	116.80(14)
O(127)-C(126)-H(126)	121.6
N(125)-C(126)-H(126)	121.6
C(22)-N(21)-C(26)	117.9(5)
C(22)-N(21)-RU1	129.0(3)
C(26)-N(21)-RU1	113.1(4)
N(21)-C(22)-C(23)	123.6(5)
N(21)-C(22)-H(22)	118.2
C(23)-C(22)-H(22)	118.2
C(22)-C(23)-C(24)	118.4(6)
C(22)-C(23)-H(23)	120.8
C(24)-C(23)-H(23)	120.8
C(25)-C(24)-C(23)	118.8(6)
C(25)-C(24)-H(24)	120.6
C(23)-C(24)-H(24)	120.6
C(26)-C(25)-C(24)	120.7(6)
C(26)-C(25)-H(25)	119.6
C(24)-C(25)-H(25)	119.6
C(25)-C(26)-N(21)	120.6(5)

C(25)-C(26)-C(27)	124.7(5)
N(21)-C(26)-C(27)	114.6(4)
N(28)-C(27)-C(212)	119.5(6)
N(28)-C(27)-C(26)	114.5(4)
C(212)-C(27)-C(26)	126.0(6)
C(27)#1-N(28)-C(27)	122.6(6)
C(27)#1-N(28)-RU1	118.7(3)
C(27)-N(28)-RU1	118.7(3)
C(212)#1-C(211)-C(212)	119.8(9)
C(212)#1-C(211)-H(211)	120.1
C(212)-C(211)-H(211)	120.1
C(211)-C(212)-C(27)	119.3(8)
C(211)-C(212)-H(212)	120.4
C(27)-C(212)-H(212)	120.4
C(41)-B(3)-C(31)	103.3(3)
C(41)-B(3)-C(51)	113.1(4)
C(31)-B(3)-C(51)	112.1(4)
C(41)-B(3)-C(61)	111.0(4)
C(31)-B(3)-C(61)	114.4(4)
C(51)-B(3)-C(61)	103.4(3)
C(32)-C(31)-C(36)	120
C(32)-C(31)-B(3)	120.3(3)
C(36)-C(31)-B(3)	119.4(3)
C(31)-C(32)-C(33)	120
C(31)-C(32)-H(32)	120
C(33)-C(32)-H(32)	120
C(34)-C(33)-C(32)	120
C(34)-C(33)-H(33)	120
C(32)-C(33)-H(33)	120
C(35)-C(34)-C(33)	120
C(35)-C(34)-H(34)	120
C(33)-C(34)-H(34)	120
C(34)-C(35)-C(36)	120
C(34)-C(35)-H(35)	120
C(36)-C(35)-H(35)	120
C(35)-C(36)-C(31)	120
C(35)-C(36)-H(36)	120
C(31)-C(36)-H(36)	120
C(42)-C(41)-C(46)	120
C(42)-C(41)-B(3)	119.0(3)
C(46)-C(41)-B(3)	120.8(3)
C(43)-C(42)-C(41)	120
C(43)-C(42)-H(42)	120
C(41)-C(42)-H(42)	120
C(42)-C(43)-C(44)	120
C(42)-C(43)-H(43)	120
C(44)-C(43)-H(43)	120
C(45)-C(44)-C(43)	120
C(45)-C(44)-H(44)	120
C(43)-C(44)-H(44)	120
C(46)-C(45)-C(44)	120
C(46)-C(45)-H(45)	120
C(44)-C(45)-H(45)	120
C(45)-C(46)-C(41)	120
C(45)-C(46)-H(46)	120
C(41)-C(46)-H(46)	120
C(52)-C(51)-C(56)	120
C(52)-C(51)-B(3)	119.8(4)
C(56)-C(51)-B(3)	120.1(4)
C(53)-C(52)-C(51)	120
C(53)-C(52)-H(52)	120
C(51)-C(52)-H(52)	120
C(52)-C(53)-C(54)	120
C(52)-C(53)-H(53)	120
C(54)-C(53)-H(53)	120
C(55)-C(54)-C(53)	120
C(55)-C(54)-H(54)	120
C(53)-C(54)-H(54)	120
C(54)-C(55)-C(56)	120
C(54)-C(55)-H(55)	120
C(56)-C(55)-H(55)	120
C(55)-C(56)-C(51)	120
C(55)-C(56)-H(56)	120
C(51)-C(56)-H(56)	120
C(62)-C(61)-C(66)	120
C(62)-C(61)-B(3)	117.3(3)
C(66)-C(61)-B(3)	122.6(3)
C(63)-C(62)-C(61)	120
C(63)-C(62)-H(62)	120
C(61)-C(62)-H(62)	120
C(62)-C(63)-C(64)	120
C(62)-C(63)-H(63)	120
C(64)-C(63)-H(63)	120
C(65)-C(64)-C(63)	120
C(65)-C(64)-H(64)	120
C(63)-C(64)-H(64)	120
C(66)-C(65)-C(64)	120
C(66)-C(65)-H(65)	120
C(64)-C(65)-H(65)	120
C(65)-C(66)-C(61)	120
C(65)-C(66)-H(66)	120
C(61)-C(66)-H(66)	120

Appendix 5: Supplementary information for chapter V.

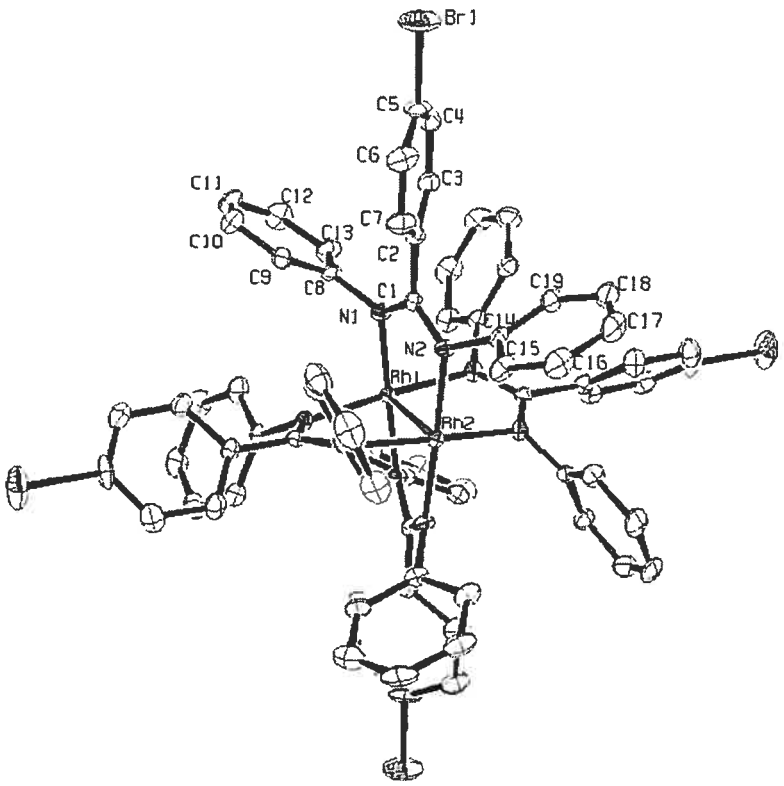

Table 1. Crystal data and structure refinement for **V-1**.

Empirical formula	C79 H62 Br4 Cl6 N8 Rh2
Formula weight	1861.53
Temperature	150(2)K
Wavelength	1.54178 Å
Crystal system	Tetragonal
Space group	I4
Unit cell dimensions	a = 14.84650(10) Å α = 90° b = 14.84650(10) Å β = 90° c = 17.3717(2) Å γ = 90°
Volume	3829.04(6)Å^3
Z	2

Density (calculated)	1.615 g/cm^3
Absorption coefficient	8.241 mm^{-1}
F(000)	1848
Crystal size	0.20 x 0.20 x 0.20 mm
Theta range for data collection	3.92 to 71.94°
Index ranges	$-16 \leq h \leq 17$, $-18 \leq k \leq 18$, $-21 \leq \ell \leq 21$
Reflections collected	31119
Independent reflections	3727 [R_{int} = 0.042]
Absorption correction	Semi-empirical from equivalents
Max. and min. transmission	0.192 and 0.154
Refinement method	Full-matrix least-squares on F^2
Data / restraints / parameters	3727 / 9 / 247
Goodness-of-fit on F^2	1.082
Final R indices [I>2sigma(I)]	R_1 = 0.0479, wR_2 = 0.1230
R indices (all data)	R_1 = 0.0513, wR_2 = 0.1344
Absolute structure parameter	0.471(11)
Largest diff. peak and hole	1.199 and -0.642 e/Å^3

Table 2. Atomic coordinates (x 10^4) and equivalent isotropic displacement parameters (Å^2 x 10^3) for **V-1**.

U_{eq} is defined as one third of the trace of the orthogonalized Uij tensor.

	Occ.	x	y	z	U_{eq}
Rh(1)	1	5000	5000	1680(1)	12(1)
Rh(2)	1	5000	5000	3062(1)	12(1)
N(1)	1	3763(3)	4400(3)	1728(2)	16(1)
N(2)	1	3664(3)	4671(3)	3029(3)	17(1)
Br(1)	1	-638(1)	3021(1)	2351(1)	53(1)
C(1)	1	3288(2)	4388(2)	2375(4)	15(1)
C(2)	1	2334(3)	4063(3)	2371(4)	18(1)

C(3)	1	1714(3)	4381(3)	1821(3)	23(1)
C(4)	1	842(3)	4071(4)	1816(3)	27(1)
C(5)	1	578(3)	3443(3)	2354(5)	29(1)
C(6)	1	1162(4)	3102(4)	2897(3)	31(1)
C(7)	1	2048(4)	3409(4)	2897(3)	27(1)
C(8)	1	3528(3)	3814(3)	1109(2)	17(1)
C(9)	1	3418(3)	2884(3)	1225(3)	21(1)
C(10)	1	3228(4)	2334(4)	607(3)	31(1)
C(11)	1	3171(4)	2664(4)	-121(3)	34(1)
C(12)	1	3285(4)	3587(4)	-255(3)	33(1)
C(13)	1	3460(4)	4162(4)	364(3)	26(1)
C(14)	1	3132(3)	4973(3)	3656(3)	19(1)
C(15)	1	3306(4)	4631(4)	4390(3)	25(1)
C(16)	1	2865(4)	4978(4)	5023(3)	33(1)
C(17)	1	2244(4)	5682(4)	4941(3)	35(1)
C(18)	1	2056(4)	6011(4)	4208(4)	33(1)
C(19)	1	2493(3)	5665(3)	3572(3)	24(1)
C(100)	1	5000	0	9103(6)	47(2)
C(101)	0.25	9500(30)	170(70)	2287(19)	210(50)
Cl(1)	1	4732(1)	939(1)	9686(1)	56(1)
Cl(2)	0.25	9594(19)	0(90)	3294(9)	151(14)
Cl(3)	0.25	10449(14)	678(17)	1850(18)	173(11)

Table 3. Hydrogen coordinates (x 10^4) and isotropic displacement parameters ($Å^2$ x 10^3) for **V-1**.

	Occ.	x	y	z	U_{eq}
H(3)	1	1896	4805	1459	28
H(4)	1	435	4282	1451	32
H(6)	1	970	2677	3254	38
H(7)	1	2455	3175	3251	32
H(9)	1	3472	2641	1716	25
H(10)	1	3136	1722	691	37
H(11)	1	3058	2277	-531	41
H(12)	1	3245	3816	-752	40
H(13)	1	3531	4776	280	31
H(15)	1	3721	4168	4452	30
H(16)	1	2981	4743	5509	40
H(17)	1	1961	5926	5370	42
H(18)	1	1633	6467	4146	40
H(19)	1	2364	5891	3085	28
H(10A)	0.50	4491	-145	8775	56
H(10B)	0.50	5509	145	8775	56
H(10C)	0.25	8972	542	2190	252
H(10D)	0.25	9389	-411	2042	252

Table 4. Anisotropic parameters ($Å^2$ x 10^3) for **V-1**.

The anisotropic displacement factor exponent takes the form:

$$-2\pi^2 [h^2 a^{*2} U_{11} + ... + 2 h k a^* b^* U_{12}]$$

	U11	U22	U33	U23	U13	U12
Rh(1)	15(1)	15(1)	6(1)	0	0	0
Rh(2)	15(1)	15(1)	6(1)	0	0	0
N(1)	16(2)	24(2)	10(2)	1(2)	-1(1)	-2(1)
N(2)	14(2)	23(2)	13(2)	2(2)	2(2)	-4(1)
Br(1)	21(1)	86(1)	51(1)	-8(1)	0(1)	-19(1)
C(1)	19(2)	12(2)	12(2)	0(2)	1(2)	0(1)
C(2)	18(2)	23(2)	13(2)	-3(2)	-1(2)	0(1)
C(3)	24(2)	24(2)	21(2)	-2(2)	-6(2)	2(2)
C(4)	23(2)	31(3)	27(2)	-6(2)	-6(2)	7(2)
C(5)	10(2)	47(3)	30(2)	-14(3)	6(3)	-11(2)
C(6)	31(3)	42(3)	21(2)	1(2)	1(2)	-11(2)
C(7)	24(2)	40(3)	16(2)	2(2)	-3(2)	-6(2)
C(8)	16(2)	25(2)	12(2)	-5(2)	-3(2)	-2(2)
C(9)	20(2)	25(2)	18(2)	-5(2)	0(2)	2(2)
C(10)	31(3)	28(3)	34(3)	-10(2)	-3(2)	-3(2)
C(11)	35(3)	41(3)	25(3)	-18(2)	-8(2)	-2(2)
C(12)	40(3)	47(3)	13(2)	-3(2)	-2(2)	2(2)
C(13)	28(3)	36(3)	14(2)	-3(2)	-4(2)	-2(2)
C(14)	22(2)	20(2)	14(2)	-5(2)	2(2)	-5(2)
C(15)	33(3)	29(3)	13(2)	-2(2)	2(2)	-6(2)
C(16)	38(3)	45(3)	16(2)	-2(2)	9(2)	-10(2)
C(17)	35(3)	46(3)	24(3)	-17(2)	17(2)	-9(2)
C(18)	29(3)	30(3)	41(3)	-14(2)	6(2)	-4(2)
C(19)	23(2)	27(2)	20(2)	-4(2)	4(2)	-2(2)
C(100)	52(6)	38(5)	50(5)	0	0	-4(4)
C(101)	250(90)	330(100)	50(20)	10(80)	0(40)	50(70)
Cl(1)	44(1)	53(1)	72(1)	-7(1)	6(1)	14(1)
Cl(2)	117(14)	220(30)	110(10)	-20(40)	33(12)	-30(20)
Cl(3)	116(13)	176(19)	230(30)	99(18)	70(15)	36(11)

Table 5. Bond lengths [Å] and angles [°] for **V-1**.

Rh(1)-N(1)#1	2.042(4)	N(1)-C(8)	1.427(6)
Rh(1)-N(1)	2.042(4)	N(2)-C(1)	1.333(7)
Rh(1)-N(1)#2	2.042(4)	N(2)-C(14)	1.419(6)
Rh(1)-N(1)#3	2.042(4)	Br(1)-C(5)	1.911(4)
Rh(1)-Rh(2)	2.4017(6)	C(1)-C(2)	1.497(5)
Rh(2)-N(2)#3	2.043(4)	C(2)-C(7)	1.400(7)
Rh(2)-N(2)#1	2.043(4)	C(2)-C(3)	1.408(7)
Rh(2)-N(2)	2.044(4)	C(3)-C(4)	1.374(7)
Rh(2)-N(2)#2	2.044(4)	C(3)-H(3)	0.93
N(1)-C(1)	1.327(7)	C(4)-C(5)	1.377(9)

C(4)-H(4)	0.93	C(8)-N(1)-RH1	117.1(3)
C(5)-C(6)	1.379(9)	C(1)-N(2)-C(14)	121.4(4)
C(6)-C(7)	1.391(7)	C(1)-N(2)-RH2	120.4(3)
C(6)-H(6)	0.93	C(14)-N(2)-RH2	116.3(3)
C(7)-H(7)	0.93	N(1)-C(1)-N(2)	119.7(3)
C(8)-C(13)	1.398(7)	N(1)-C(1)-C(2)	120.2(5)
C(8)-C(9)	1.404(7)	N(2)-C(1)-C(2)	120.1(5)
C(9)-C(10)	1.377(7)	C(7)-C(2)-C(3)	118.5(4)
C(9)-H(9)	0.93	C(7)-C(2)-C(1)	120.5(4)
C(10)-C(11)	1.360(8)	C(3)-C(2)-C(1)	120.9(4)
C(10)-H(10)	0.93	C(4)-C(3)-C(2)	120.5(5)
C(11)-C(12)	1.400(9)	C(4)-C(3)-H(3)	119.7
C(11)-H(11)	0.93	C(2)-C(3)-H(3)	119.7
C(12)-C(13)	1.397(7)	C(3)-C(4)-C(5)	119.4(5)
C(12)-H(12)	0.93	C(3)-C(4)-H(4)	120.3
C(13)-H(13)	0.93	C(5)-C(4)-H(4)	120.3
C(14)-C(15)	1.396(7)	C(4)-C(5)-C(6)	122.3(4)
C(14)-C(19)	1.406(7)	C(4)-C(5)-BR1	119.3(5)
C(15)-C(16)	1.379(7)	C(6)-C(5)-BR1	118.4(5)
C(15)-H(15)	0.93	C(5)-C(6)-C(7)	118.3(5)
C(16)-C(17)	1.40(1)	C(5)-C(6)-H(6)	120.8
C(16)-H(16)	0.93	C(7)-C(6)-H(6)	120.8
C(17)-C(18)	1.392(9)	C(6)-C(7)-C(2)	120.9(5)
C(17)-H(17)	0.93	C(6)-C(7)-H(7)	119.5
C(18)-C(19)	1.380(7)	C(2)-C(7)-H(7)	119.5
C(18)-H(18)	0.93	C(13)-C(8)-C(9)	119.1(4)
C(19)-H(19)	0.93	C(13)-C(8)-N(1)	119.3(4)
C(100)-Cl(1)#4	1.768(6)	C(9)-C(8)-N(1)	121.4(4)
C(100)-Cl(1)	1.768(6)	C(10)-C(9)-C(8)	119.7(5)
C(100)-H(10a)	0.97	C(10)-C(9)-H(9)	120.1
C(100)-H(10b)	0.97	C(8)-C(9)-H(9)	120.1
C(101)-Cl(2)	1.77(2)	C(11)-C(10)-C(9)	121.6(5)
C(101)-Cl(3)	1.78(2)	C(11)-C(10)-H(10)	119.2
C(101)-H(10c)	0.97	C(9)-C(10)-H(10)	119.2
C(101)-H(10d)	0.97	C(10)-C(11)-C(12)	119.9(5)
N(1)#1-RH1-N(1)	89.903(10)	C(10)-C(11)-H(11)	120
N(1)#1-RH1-N(1)#2	175.3(2)	C(12)-C(11)-H(11)	120
N(1)-RH1-N(1)#2	89.901(10)	C(13)-C(12)-C(11)	119.6(5)
N(1)#1-RH1-N(1)#3	89.902(10)	C(13)-C(12)-H(12)	120.2
N(1)-RH1-N(1)#3	175.3(2)	C(11)-C(12)-H(12)	120.2
N(1)#2-RH1-N(1)#3	89.902(10)	C(12)-C(13)-C(8)	120.0(5)
N(1)#1-RH1-RH2	87.63(12)	C(12)-C(13)-H(13)	120
N(1)-RH1-RH2	87.63(12)	C(8)-C(13)-H(13)	120
N(1)#2-RH1-RH2	87.63(12)	C(15)-C(14)-C(19)	119.1(4)
N(1)#3-RH1-RH2	87.63(12)	C(15)-C(14)-N(2)	118.9(4)
N(2)#3-RH2-N(2)#1	89.958(7)	C(19)-C(14)-N(2)	121.8(4)
N(2)#3-RH2-N(2)	176.8(2)	C(16)-C(15)-C(14)	120.3(5)
N(2)#1-RH2-N(2)	89.953(8)	C(16)-C(15)-H(15)	119.9
N(2)#3-RH2-N(2)#2	89.953(7)	C(14)-C(15)-H(15)	119.9
N(2)#1-RH2-N(2)#2	176.8(2)	C(15)-C(16)-C(17)	120.6(5)
N(2)-RH2-N(2)#2	89.957(7)	C(15)-C(16)-H(16)	119.7
N(2)#3-RH2-RH1	88.39(13)	C(17)-C(16)-H(16)	119.7
N(2)#1-RH2-RH1	88.39(13)	C(18)-C(17)-C(16)	119.2(5)
N(2)-RH2-RH1	88.39(13)	C(18)-C(17)-H(17)	120.4
N(2)#2-RH2-RH1	88.39(13)	C(16)-C(17)-H(17)	120.4
C(1)-N(1)-C(8)	120.0(4)	C(19)-C(18)-C(17)	120.5(6)
C(1)-N(1)-RH1	121.2(3)	C(19)-C(18)-H(18)	119.8

C(17)-C(18)-H(18)	119.8
C(18)-C(19)-C(14)	120.4(5)
C(18)-C(19)-H(19)	119.8
C(14)-C(19)-H(19)	119.8
CL1#4-C(100)-CL1	110.1(6)
CL1#4-C(100)-H(10A)	109.6
CL1-C(100)-H(10A)	109.6
CL1#4-C(100)-H(10B)	109.6
CL1-C(100)-H(10B)	109.6
H(10A)-C(100)-H(10B)	108.1
CL2-C(101)-CL3	115(3)
CL2-C(101)-H(10C)	108.4
CL3-C(101)-H(10C)	108.6
CL2-C(101)-H(10D)	108.8
CL3-C(101)-H(10D)	108.7
H(10C)-C(101)-H(10D)	107.6

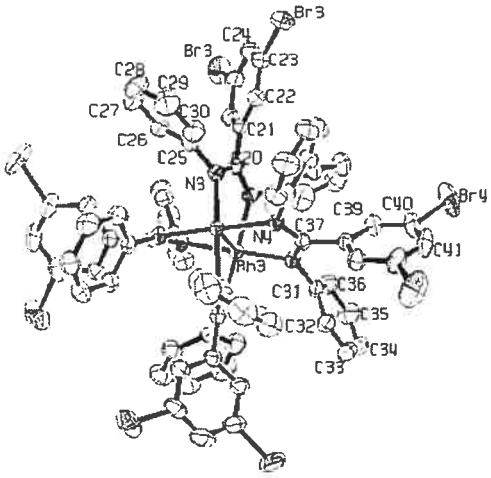

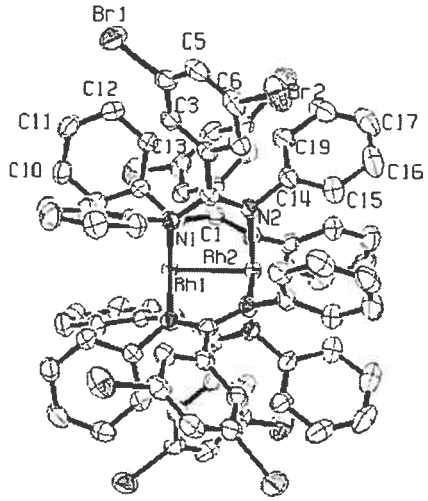

Table 1. Crystal data and structure refinement for **V-2**.

Empirical formula	C76 H52 Br8 N8 Rh2
Formula weight	1922.36
Temperature	200(2)K
Wavelength	1.54178 Å
Crystal system	Tetragonal
Space group	P4/nnc
Unit cell dimensions	a = 20.3414(5) Å α = 90° b = 20.3414(5) Å β = 90° c = 36.6224(12) Å γ = 90°
Volume	15153.3(7)Å^3
Z	8
Density (calculated)	1.685 g/cm^3
Absorption coefficient	8.830 mm^{-1}
F(000)	7472
Crystal size	0.12 x 0.09 x 0.06 mm
Theta range for data collection	2.41 to 69.07°

Index ranges	$-24 \leq h \leq 24$, $-24 \leq k \leq 24$, $-43 \leq \ell \leq 43$
Reflections collected	206124
Independent reflections	7051 [R_{int} = 0.041]
Absorption correction	Semi-empirical from equivalents
Max. and min. transmission	0.590 and 0.445
Refinement method	Full-matrix least-squares on F^2
Data / restraints / parameters	7051 / 0 / 430
Goodness-of-fit on F^2	1.088
Final R indices [I>2sigma(I)]	R_1 = 0.0354, wR_2 = 0.1063
R indices (all data)	R_1 = 0.0373, wR_2 = 0.1081
Largest diff. peak and hole	1.150 and -1.456 e/Å^3

Table 2. Atomic coordinates (x 10^4) and equivalent isotropic displacement parameters (Å^2 x 10^3) for **V-2**.

U_{eq} is defined as one third of the trace of the orthogonalized Uij tensor.

	Occ.	x	y	z	U_{eq}
Rh(1)	1	7500	7500	387(1)	25(1)
Rh(2)	1	7500	7500	-268(1)	28(1)
Rh(3)	1	3092(1)	7500	7500	27(1)
N(1)	1	7110(1)	8430(1)	363(1)	30(1)
N(2)	1	6714(1)	6870(1)	-247(1)	32(1)
N(3)	1	3052(1)	8499(1)	7576(1)	32(1)
N(4)	1	3054(1)	7368(1)	8054(1)	32(1)
Br(1)	1	5073(1)	10065(1)	788(1)	58(1)
Br(2)	1	6352(1)	11030(1)	-476(1)	67(1)
Br(3)	1	1412(1)	11022(1)	7990(1)	81(1)
Br(4)	1	1625(1)	6417(1)	9457(1)	100(1)
C(1)	1	6812(1)	8633(1)	60(1)	31(1)
C(2)	1	6417(2)	9252(1)	72(1)	33(1)
C(3)	1	5973(2)	9341(2)	356(1)	35(1)
C(4)	1	5637(2)	9929(2)	383(1)	40(1)
C(5)	1	5724(2)	10432(2)	132(1)	47(1)
C(6)	1	6171(2)	10333(2)	-146(1)	44(1)
C(7)	1	6520(2)	9751(2)	-183(1)	39(1)

C(8)	1	7255(1)	8874(1)	652(1)	30(1)
C(9)	1	7075(2)	8724(2)	1008(1)	38(1)
C(10)	1	7238(2)	9135(2)	1293(1)	47(1)
C(11)	1	7583(2)	9709(2)	1231(1)	50(1)
C(12)	1	7762(2)	9869(2)	878(1)	48(1)
C(13)	1	7607(2)	9455(2)	591(1)	39(1)
C(14)	1	6647(2)	6419(2)	-541(1)	36(1)
C(15)	1	6499(2)	6662(2)	-889(1)	49(1)
C(16)	1	6489(2)	6240(3)	-1185(1)	61(1)
C(17)	1	6632(2)	5580(2)	-1142(1)	59(1)
C(18)	1	6774(2)	5338(2)	-799(1)	57(1)
C(19)	1	6784(2)	5758(2)	-499(1)	42(1)
C(20)	1	2500	8819(2)	7500	32(1)
C(21)	1	2500	9555(2)	7500	35(1)
C(22)	1	2037(2)	9894(2)	7704(1)	42(1)
C(23)	1	2049(2)	10574(2)	7704(1)	52(1)
C(24)	1	2500	10929(3)	7500	55(1)
C(25)	1	3578(2)	8815(2)	7760(1)	36(1)
C(26)	1	3488(2)	9131(2)	8091(1)	46(1)
C(27)	1	4006(2)	9424(2)	8271(1)	64(1)
C(28)	1	4633(2)	9398(2)	8126(1)	74(1)
C(29)	1	4729(2)	9077(3)	7797(1)	72(1)
C(30)	1	4210(2)	8783(2)	7613(1)	53(1)
C(31)	1	3583(2)	7032(2)	8228(1)	34(1)
C(32)	1	3498(2)	6407(2)	8372(1)	41(1)
C(33)	1	4026(2)	6062(2)	8520(1)	50(1)
C(34)	1	4636(2)	6346(2)	8526(1)	53(1)
C(35)	1	4727(2)	6968(2)	8383(1)	58(1)
C(36)	1	4205(2)	7309(2)	8232(1)	46(1)
C(37)	1	2500	7500	8233(1)	33(1)
C(38)	1	2500	7500	8640(1)	34(1)
C(39)	1	2104(2)	7061(2)	8827(1)	43(1)
C(40)	1	2126(2)	7062(2)	9203(1)	55(1)
C(41)	1	2500	7500	9396(2)	64(2)

Table 3. Hydrogen coordinates (x 10^4) and isotropic displacement parameters (Å^2 x 10^3) for **V-2**.

	Occ.	x	y	z	U_{eq}
H(3)	1	5901	9002	530	42
H(5)	1	5485	10831	151	56
H(7)	1	6823	9693	-378	47
H(9)	1	6836	8332	1056	46
H(10)	1	7111	9023	1535	56
H(11)	1	7696	9990	1428	60
H(12)	1	7993	10266	833	58
H(13)	1	7740	9566	350	47
H(15)	1	6405	7115	-922	59
H(16)	1	6383	6406	-1420	73
H(17)	1	6632	5295	-1348	71

H(18)	1	6866	4883	-767	68
H(19)	1	6886	5589	-264	51
H(22)	1	1716	9662	7842	50
H(24)	1	2500	11396	7500	66
H(26)	1	3061	9147	8197	55
H(27)	1	3932	9645	8495	76
H(28)	1	4991	9598	8250	89
H(29)	1	5158	9058	7695	87
H(30)	1	4284	8560	7389	64
H(32)	1	3073	6211	8370	49
H(33)	1	3964	5632	8616	60
H(34)	1	4997	6115	8629	64
H(35)	1	5151	7163	8389	69
H(36)	1	4273	7733	8131	55
H(39)	1	1823	6767	8699	51
H(41)	1	2500	7500	9656	76

Table 4. Anisotropic parameters ($Å^2$ x 10^3) for **V-2**.

The anisotropic displacement factor exponent takes the form:

$$-2\pi^2 [h^2 a^{*2} U_{11} + ... + 2 h k a^* b^* U_{12}]$$

	U11	U22	U33	U23	U13	U12
Rh(1)	27(1)	27(1)	23(1)	0	0	0
Rh(2)	30(1)	30(1)	23(1)	0	0	0
Rh(3)	29(1)	30(1)	24(1)	1(1)	0	0
N(1)	33(1)	30(1)	28(1)	-1(1)	-2(1)	2(1)
N(2)	34(1)	34(1)	28(1)	-4(1)	-1(1)	-3(1)
N(3)	34(1)	32(1)	30(1)	0(1)	0(1)	-2(1)
N(4)	33(1)	38(1)	26(1)	2(1)	-1(1)	1(1)
Br(1)	47(1)	67(1)	60(1)	-17(1)	2(1)	14(1)
Br(2)	105(1)	41(1)	55(1)	15(1)	-22(1)	-2(1)
Br(3)	111(1)	63(1)	68(1)	-15(1)	-5(1)	43(1)
Br(4)	92(1)	137(1)	72(1)	52(1)	19(1)	-25(1)
C(1)	30(1)	30(1)	32(1)	2(1)	-2(1)	-2(1)
C(2)	34(2)	32(1)	34(2)	-2(1)	-10(1)	1(1)
C(3)	33(2)	37(2)	35(2)	-2(1)	-7(1)	2(1)
C(4)	36(2)	43(2)	43(2)	-8(1)	-11(1)	6(1)
C(5)	52(2)	36(2)	52(2)	-7(1)	-21(2)	10(1)
C(6)	58(2)	33(2)	41(2)	2(1)	-19(2)	0(1)
C(7)	46(2)	37(2)	36(2)	-1(1)	-10(1)	1(1)
C(8)	29(1)	30(1)	32(1)	-2(1)	-3(1)	3(1)
C(9)	41(2)	38(2)	35(2)	0(1)	1(1)	-5(1)
C(10)	53(2)	55(2)	32(2)	-5(1)	4(1)	-6(2)
C(11)	58(2)	49(2)	42(2)	-16(2)	-4(2)	-5(2)
C(12)	55(2)	38(2)	52(2)	-3(2)	-5(2)	-12(2)
C(13)	44(2)	38(2)	35(2)	0(1)	0(1)	-6(1)
C(14)	33(2)	42(2)	32(2)	-8(1)	1(1)	-5(1)
C(15)	51(2)	62(2)	34(2)	-5(2)	-3(2)	4(2)

C(16)	56(2)	90(3)	35(2)	-15(2)	-3(2)	-2(2)
C(17)	49(2)	78(3)	51(2)	-33(2)	7(2)	-9(2)
C(18)	52(2)	51(2)	67(3)	-24(2)	9(2)	-10(2)
C(19)	41(2)	43(2)	43(2)	-9(1)	4(1)	-7(1)
C(20)	37(2)	31(2)	27(2)	0	2(2)	0
C(21)	39(2)	33(2)	34(2)	0	-7(2)	0
C(22)	49(2)	36(2)	40(2)	-2(1)	-8(1)	4(1)
C(23)	67(2)	39(2)	51(2)	-8(2)	-17(2)	15(2)
C(24)	74(4)	31(2)	60(3)	0	-25(3)	0
C(25)	38(2)	34(2)	37(2)	6(1)	-6(1)	-6(1)
C(26)	50(2)	45(2)	42(2)	-3(1)	-8(2)	-2(2)
C(27)	73(3)	62(2)	56(2)	-10(2)	-22(2)	-9(2)
C(28)	69(3)	75(3)	78(3)	0(2)	-31(2)	-23(2)
C(29)	42(2)	95(4)	80(3)	9(3)	-4(2)	-17(2)
C(30)	42(2)	66(2)	52(2)	1(2)	1(2)	-6(2)
C(31)	38(2)	40(2)	25(1)	-1(1)	-3(1)	2(1)
C(32)	41(2)	43(2)	39(2)	4(1)	-5(1)	-1(1)
C(33)	57(2)	46(2)	47(2)	11(2)	-6(2)	5(2)
C(34)	47(2)	58(2)	54(2)	8(2)	-13(2)	11(2)
C(35)	37(2)	61(2)	75(3)	2(2)	-13(2)	-1(2)
C(36)	40(2)	45(2)	53(2)	6(2)	-5(2)	-2(2)
C(37)	39(2)	32(2)	28(2)	0	0	-5(2)
C(38)	35(2)	39(2)	28(2)	0	0	1(2)
C(39)	44(2)	49(2)	36(2)	4(1)	1(1)	-7(2)
C(40)	49(2)	78(3)	37(2)	16(2)	8(2)	-2(2)
C(41)	59(4)	106(5)	26(2)	0	0	5(3)

Table 5. Bond lengths [Å] and angles [°] for **V-2**.

Rh(1)-N(1)#1	2.052(2)	Br(4)-C(40)	1.903(4)
Rh(1)-N(1)	2.052(2)	C(1)-N(2)#1	1.333(4)
Rh(1)-N(1)#2	2.052(2)	C(1)-C(2)	1.494(4)
Rh(1)-N(1)#3	2.052(2)	C(2)-C(3)	1.390(4)
Rh(1)-Rh(2)	2.3980(6)	C(2)-C(7)	1.394(4)
Rh(2)-N(2)	2.050(3)	C(3)-C(4)	1.381(4)
Rh(2)-N(2)#2	2.050(3)	C(3)-H(3)	0.95
Rh(2)-N(2)#1	2.050(3)	C(4)-C(5)	1.385(5)
Rh(2)-N(2)#3	2.050(3)	C(5)-C(6)	1.380(5)
Rh(3)-N(4)	2.046(2)	C(5)-H(5)	0.95
Rh(3)-N(4)#4	2.046(2)	C(6)-C(7)	1.388(5)
Rh(3)-N(3)	2.052(2)	C(7)-H(7)	0.95
Rh(3)-N(3)#4	2.052(2)	C(8)-C(9)	1.387(4)
Rh(3)-Rh(3)#5	2.4090(6)	C(8)-C(13)	1.399(4)
N(1)-C(1)	1.332(4)	C(9)-C(10)	1.379(5)
N(1)-C(8)	1.422(4)	C(9)-H(9)	0.95
N(2)-C(1)#3	1.333(4)	C(10)-C(11)	1.380(5)
N(2)-C(14)	1.421(4)	C(10)-H(10)	0.95
N(3)-C(20)	1.328(3)	C(11)-C(12)	1.381(5)
N(3)-C(25)	1.419(4)	C(11)-H(11)	0.95
N(4)-C(37)	1.332(3)	C(12)-C(13)	1.386(5)
N(4)-C(31)	1.425(4)	C(12)-H(12)	0.95
Br(1)-C(4)	1.897(3)	C(13)-H(13)	0.95
Br(2)-C(6)	1.899(3)	C(14)-C(19)	1.383(5)
Br(3)-C(23)	1.898(4)	C(14)-C(15)	1.401(5)

C(15)-C(16)	1.381(5)
C(15)-H(15)	0.95
C(16)-C(17)	1.383(7)
C(16)-H(16)	0.95
C(17)-C(18)	1.382(6)
C(17)-H(17)	0.95
C(18)-C(19)	1.389(5)
C(18)-H(18)	0.95
C(19)-H(19)	0.95
C(20)-N(3)#6	1.328(3)
C(20)-C(21)	1.497(6)
C(21)-C(22)	1.386(4)
C(21)-C(22)#6	1.386(4)
C(22)-C(23)	1.384(5)
C(22)-H(22)	0.95
C(23)-C(24)	1.386(5)
C(24)-C(23)#6	1.387(5)
C(24)-H(24)	0.95
C(25)-C(26)	1.386(5)
C(25)-C(30)	1.394(5)
C(26)-C(27)	1.378(5)
C(26)-H(26)	0.95
C(27)-C(28)	1.382(7)
C(27)-H(27)	0.95
C(28)-C(29)	1.384(7)
C(28)-H(28)	0.95
C(29)-C(30)	1.389(6)
C(29)-H(29)	0.95
C(30)-H(30)	0.95
C(31)-C(36)	1.385(5)
C(31)-C(32)	1.388(5)
C(32)-C(33)	1.394(5)
C(32)-H(32)	0.95
C(33)-C(34)	1.368(6)
C(33)-H(33)	0.95
C(34)-C(35)	1.382(6)
C(34)-H(34)	0.95
C(35)-C(36)	1.384(5)
C(35)-H(35)	0.95
C(36)-H(36)	0.95
C(37)-N(4)#5	1.332(3)
C(37)-C(38)	1.489(6)
C(38)-C(39)#5	1.385(4)
C(38)-C(39)	1.385(4)
C(39)-C(40)	1.378(5)
C(39)-H(39)	0.95
C(40)-C(41)	1.368(5)
C(41)-C(40)#5	1.368(5)
C(41)-H(41)	0.95

N(1)#1-RH1-N(1)	89.904(6)
N(1)#1-RH1-N(1)#2	89.903(6)
N(1)-RH1-N(1)#2	175.27(13)
N(1)#1-RH1-N(1)#3	175.27(13)
N(1)-RH1-N(1)#3	89.903(6)
N(1)#2-RH1-N(1)#3	89.900(6)
N(1)#1-RH1-RH2	87.64(7)
N(1)-RH1-RH2	87.64(7)
N(1)#2-RH1-RH2	87.64(7)
N(1)#3-RH1-RH2	87.64(7)
N(2)-RH2-N(2)#2	175.60(14)
N(2)-RH2-N(2)#1	89.914(6)
N(2)#2-RH2-N(2)#1	89.918(5)
N(2)-RH2-N(2)#3	89.914(5)
N(2)#2-RH2-N(2)#3	89.917(6)
N(2)#1-RH2-N(2)#3	175.60(14)
N(2)-RH2-RH1	87.80(7)
N(2)#2-RH2-RH1	87.80(7)
N(2)#1-RH2-RH1	87.80(7)
N(2)#3-RH2-RH1	87.80(7)
N(4)-RH3-N(4)#4	175.68(14)
N(4)-RH3-N(3)	89.66(10)
N(4)#4-RH3-N(3)	90.17(10)
N(4)-RH3-N(3)#4	90.17(10)
N(4)#4-RH3-N(3)#4	89.66(10)
N(3)-RH3-N(3)#4	175.48(14)
N(4)-RH3-RH3#5	87.85(7)
N(4)#4-RH3-RH3#5	87.84(7)
N(3)-RH3-RH3#5	87.74(7)
N(3)#4-RH3-RH3#5	87.74(7)
C(1)-N(1)-C(8)	121.1(2)
C(1)-N(1)-RH1	119.80(19)
C(8)-N(1)-RH1	118.39(17)
C(1)#3-N(2)-C(14)	122.1(3)
C(1)#3-N(2)-RH2	120.0(2)
C(14)-N(2)-RH2	116.70(19)
C(20)-N(3)-C(25)	121.0(3)
C(20)-N(3)-RH3	119.4(2)
C(25)-N(3)-RH3	118.9(2)
C(37)-N(4)-C(31)	121.0(3)
C(37)-N(4)-RH3	119.6(2)
C(31)-N(4)-RH3	118.51(19)
N(1)-C(1)-N(2)#1	119.9(3)
N(1)-C(1)-C(2)	118.9(2)
N(2)#1-C(1)-C(2)	121.2(3)
C(3)-C(2)-C(7)	120.3(3)
C(3)-C(2)-C(1)	118.7(3)
C(7)-C(2)-C(1)	120.9(3)
C(4)-C(3)-C(2)	119.2(3)
C(4)-C(3)-H(3)	120.4
C(2)-C(3)-H(3)	120.4
C(3)-C(4)-C(5)	121.9(3)
C(3)-C(4)-BR1	118.7(3)
C(5)-C(4)-BR1	119.3(3)
C(6)-C(5)-C(4)	117.8(3)
C(6)-C(5)-H(5)	121.1
C(4)-C(5)-H(5)	121.1
C(5)-C(6)-C(7)	122.3(3)
C(5)-C(6)-BR2	119.2(3)
C(7)-C(6)-BR2	118.4(3)
C(6)-C(7)-C(2)	118.5(3)
C(6)-C(7)-H(7)	120.7
C(2)-C(7)-H(7)	120.7
C(9)-C(8)-C(13)	118.2(3)

C(9)-C(8)-N(1)	120.3(3)
C(13)-C(8)-N(1)	121.5(3)
C(10)-C(9)-C(8)	121.0(3)
C(10)-C(9)-H(9)	119.5
C(8)-C(9)-H(9)	119.5
C(9)-C(10)-C(11)	120.7(3)
C(9)-C(10)-H(10)	119.7
C(11)-C(10)-H(10)	119.7
C(10)-C(11)-C(12)	119.2(3)
C(10)-C(11)-H(11)	120.4
C(12)-C(11)-H(11)	120.4
C(11)-C(12)-C(13)	120.5(3)
C(11)-C(12)-H(12)	119.7
C(13)-C(12)-H(12)	119.7
C(12)-C(13)-C(8)	120.5(3)
C(12)-C(13)-H(13)	119.8
C(8)-C(13)-H(13)	119.8
C(19)-C(14)-C(15)	119.1(3)
C(19)-C(14)-N(2)	121.7(3)
C(15)-C(14)-N(2)	119.0(3)
C(16)-C(15)-C(14)	119.9(4)
C(16)-C(15)-H(15)	120
C(14)-C(15)-H(15)	120
C(15)-C(16)-C(17)	120.7(4)
C(15)-C(16)-H(16)	119.6
C(17)-C(16)-H(16)	119.6
C(18)-C(17)-C(16)	119.6(3)
C(18)-C(17)-H(17)	120.2
C(16)-C(17)-H(17)	120.2
C(17)-C(18)-C(19)	120.1(4)
C(17)-C(18)-H(18)	119.9
C(19)-C(18)-H(18)	119.9
C(14)-C(19)-C(18)	120.6(4)
C(14)-C(19)-H(19)	119.7
C(18)-C(19)-H(19)	119.7
N(3)-C(20)-N(3)#6	121.3(4)
N(3)-C(20)-C(21)	119.4(2)
N(3)#6-C(20)-C(21)	119.4(2)
C(22)-C(21)-C(22)#6	120.3(4)
C(22)-C(21)-C(20)	119.8(2)
C(22)#6-C(21)-C(20)	119.8(2)
C(23)-C(22)-C(21)	119.1(4)
C(23)-C(22)-H(22)	120.5
C(21)-C(22)-H(22)	120.5
C(22)-C(23)-C(24)	122.1(4)
C(22)-C(23)-BR3	117.9(3)
C(24)-C(23)-BR3	120.0(3)
C(23)-C(24)-C(23)#6	117.3(5)
C(23)-C(24)-H(24)	121.4
C(23)#6-C(24)-H(24)	121.4
C(26)-C(25)-C(30)	118.8(3)
C(26)-C(25)-N(3)	121.8(3)
C(30)-C(25)-N(3)	119.3(3)
C(27)-C(26)-C(25)	121.1(4)
C(27)-C(26)-H(26)	119.5
C(25)-C(26)-H(26)	119.5
C(26)-C(27)-C(28)	120.5(4)
C(26)-C(27)-H(27)	119.8
C(28)-C(27)-H(27)	119.8
C(27)-C(28)-C(29)	118.8(4)
C(27)-C(28)-H(28)	120.6
C(29)-C(28)-H(28)	120.6
C(28)-C(29)-C(30)	121.2(4)
C(28)-C(29)-H(29)	119.4
C(30)-C(29)-H(29)	119.4
C(29)-C(30)-C(25)	119.6(4)
C(29)-C(30)-H(30)	120.2
C(25)-C(30)-H(30)	120.2
C(36)-C(31)-C(32)	118.8(3)
C(36)-C(31)-N(4)	119.9(3)
C(32)-C(31)-N(4)	121.1(3)
C(31)-C(32)-C(33)	120.9(3)
C(31)-C(32)-H(32)	119.6
C(33)-C(32)-H(32)	119.6
C(34)-C(33)-C(32)	119.5(3)
C(34)-C(33)-H(33)	120.2
C(32)-C(33)-H(33)	120.2
C(33)-C(34)-C(35)	120.1(3)
C(33)-C(34)-H(34)	119.9
C(35)-C(34)-H(34)	119.9
C(34)-C(35)-C(36)	120.5(4)
C(34)-C(35)-H(35)	119.7
C(36)-C(35)-H(35)	119.7
C(35)-C(36)-C(31)	120.1(3)
C(35)-C(36)-H(36)	120
C(31)-C(36)-H(36)	120
N(4)-C(37)-N(4)#5	120.9(4)
N(4)-C(37)-C(38)	119.6(2)
N(4)#5-C(37)-C(38)	119.6(2)
C(39)#5-C(38)-C(39)	120.6(4)
C(39)#5-C(38)-C(37)	119.7(2)
C(39)-C(38)-C(37)	119.7(2)
C(40)-C(39)-C(38)	118.4(4)
C(40)-C(39)-H(39)	120.8
C(38)-C(39)-H(39)	120.8
C(41)-C(40)-C(39)	122.4(4)
C(41)-C(40)-BR4	119.6(3)
C(39)-C(40)-BR4	118.0(3)
C(40)-C(41)-C(40)#5	117.8(5)
C(40)-C(41)-H(41)	121.1
C(40)#5-C(41)-H(41)	121.1

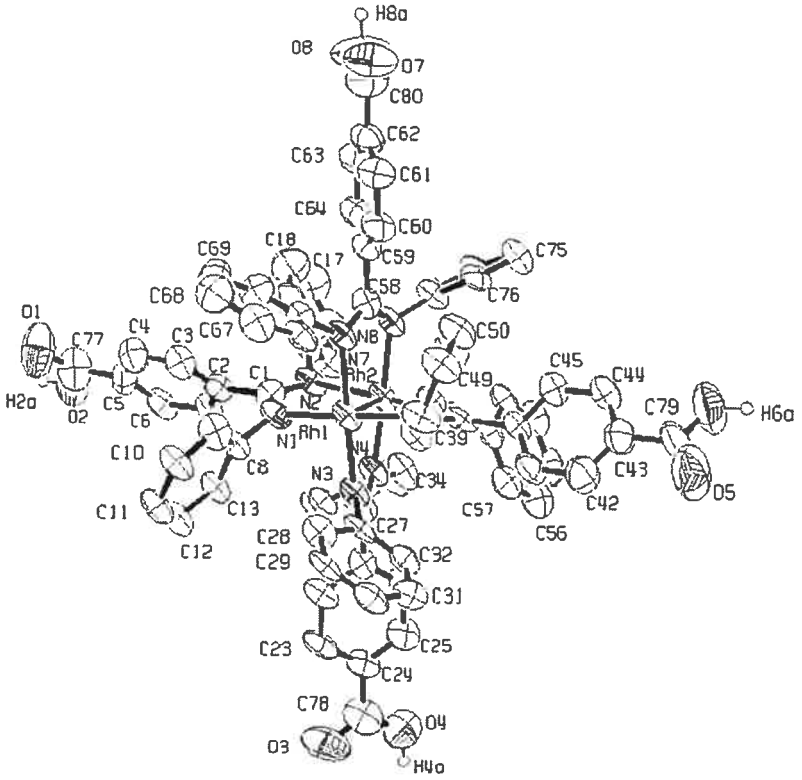

Table 1. Crystal data and structure refinement for **V-5**.

Empirical formula	C90 H90 N8 O13 Rh2 S5
Formula weight	1857.82
Temperature	100(2)K
Wavelength	1.54178 Å
Crystal system	Monoclinic
Space group	P21/n
Unit cell dimensions	a = 13.4351(6) Å α = 90° b = 21.1663(11) Å β = 101.958(2)° c = 31.3538(15) Å γ = 90°
Volume	8722.6(7)Å^3
Z	4
Density (calculated)	1.415 g/cm^3
Absorption coefficient	4.720 mm^{-1}

F(000)	3840
Crystal size	0.24 x 0.10 x 0.10 mm
Theta range for data collection	2.54 to 56.15°
Index ranges	$-14 \leq h \leq 14$, $-16 \leq k \leq 21$, $-33 \leq \ell \leq 33$
Reflections collected	79792
Independent reflections	10701 [R_{int} = 0.063]
Absorption correction	Semi-empirical from equivalents
Max. and min. transmission	0.625 and 0.435
Refinement method	Full-matrix least-squares on F^2
Data / restraints / parameters	10701 / 816 / 1042
Goodness-of-fit on F^2	1.080
Final R indices [I>2sigma(I)]	R1 = 0.1259, wR_2 = 0.3228
R indices (all data)	R1 = 0.1569, wR_2 = 0.3457
Largest diff. peak and hole	2.930 and -1.667 e/Å^3

Table 2. Atomic coordinates (x 10^4) and equivalent isotropic displacement parameters (Å^2 x 10^3) for **V-5**.

U_{eq} is defined as one third of the trace of the orthogonalized Uij tensor.

	Occ.	x	y	z	U_{eq}
Rh(1)	1	5988(1)	5800(1)	2434(1)	46(1)
Rh(2)	1	4901(1)	6616(1)	2613(1)	47(1)
N(1)	1	6341(9)	6395(6)	1975(4)	54(4)
N(2)	1	5084(9)	7088(5)	2063(4)	47(3)
N(3)	1	7139(9)	6167(6)	2896(4)	46(3)
N(4)	1	6168(9)	7032(6)	2956(4)	48(3)
N(5)	1	5552(9)	5277(5)	2903(4)	48(3)
N(6)	1	4805(8)	6124(6)	3161(4)	44(3)
N(7)	1	4763(9)	5472(6)	1979(4)	51(3)
N(8)	1	3693(9)	6127(7)	2252(5)	56(4)
O(1)	1	6664(17)	8123(9)	58(6)	137(7)

O(2)	1	6590(12)	8989(7)	466(5)	95(4)
O(3)	1	11245(12)	7981(8)	4118(6)	119(6)
O(4)	1	10207(13)	8165(7)	4588(5)	104(5)
O(5)	1	4904(16)	3652(13)	4817(7)	189(10)
O(6)	1	3355(13)	4059(10)	4670(6)	146(7)
O(7)	1	410(13)	3951(10)	734(6)	126(6)
O(8)	1	-283(15)	4907(10)	631(7)	159(8)
C(1)	1	5791(12)	6916(8)	1850(5)	51(4)
C(2)	1	5995(11)	7289(8)	1474(5)	50(4)
C(3)	1	6015(13)	7031(9)	1081(6)	62(5)
C(4)	1	6181(14)	7352(10)	735(6)	72(5)
C(5)	1	6383(14)	8016(11)	790(6)	73(6)
C(6)	1	6384(12)	8304(8)	1189(6)	60(5)
C(7)	1	6173(11)	7943(8)	1533(6)	56(4)
C(8)	1	7314(11)	6319(7)	1859(5)	48(4)
C(9)	1	7501(14)	5784(8)	1654(6)	66(5)
C(10)	1	8460(12)	5657(8)	1565(6)	61(5)
C(11)	1	9220(12)	6098(8)	1671(6)	64(5)
C(12)	1	9027(13)	6673(8)	1871(6)	64(5)
C(13)	1	8075(11)	6764(8)	1969(5)	54(4)
C(14)	1	4251(12)	7487(8)	1860(6)	55(4)
C(15)	1	4064(13)	8023(9)	2095(7)	74(6)
C(16)	1	3205(16)	8403(10)	1929(8)	86(6)
C(17)	1	2611(19)	8257(13)	1551(9)	111(8)
C(18)	1	2782(19)	7714(13)	1311(8)	106(8)
C(19)	1	3634(14)	7351(11)	1475(7)	80(6)
C(20)	1	7053(12)	6746(7)	3066(5)	47(4)
C(21)	1	7962(12)	7043(7)	3363(5)	49(4)
C(22)	1	8853(11)	7130(7)	3243(6)	55(4)
C(23)	1	9671(13)	7404(8)	3516(7)	67(5)
C(24)	1	9550(13)	7621(8)	3922(6)	60(5)
C(25)	1	8648(15)	7542(8)	4040(6)	68(5)
C(26)	1	7838(14)	7280(8)	3763(6)	65(5)
C(27)	1	7917(10)	5743(7)	3095(6)	50(4)
C(28)	1	8482(12)	5422(8)	2828(6)	59(5)
C(29)	1	9190(10)	4985(8)	3008(6)	56(5)
C(30)	1	9390(12)	4843(9)	3443(7)	65(5)
C(31)	1	8851(12)	5156(8)	3703(6)	62(5)
C(32)	1	8122(12)	5587(8)	3533(6)	55(4)
C(33)	1	6117(11)	7716(8)	3001(5)	51(4)
C(34)	1	5434(13)	7970(8)	3216(7)	69(5)
C(35)	1	5284(16)	8621(10)	3231(7)	83(6)
C(36)	1	5872(15)	9020(9)	3045(7)	78(6)
C(37)	1	6582(13)	8789(8)	2844(7)	67(5)
C(38)	1	6733(12)	8135(8)	2825(6)	59(5)
C(39)	1	5114(9)	5501(7)	3202(5)	44(4)
C(40)	1	4913(11)	5122(7)	3575(5)	43(4)
C(41)	1	5691(13)	4829(9)	3851(6)	69(5)
C(42)	1	5506(16)	4472(11)	4192(7)	90(7)
C(43)	1	4510(16)	4407(11)	4248(7)	82(6)
C(44)	1	3722(14)	4686(9)	3967(6)	67(5)
C(45)	1	3930(13)	5053(8)	3630(6)	58(5)
C(46)	1	5535(11)	4588(8)	2852(5)	52(4)
C(47)	1	6437(12)	4252(9)	2904(6)	61(5)
C(48)	1	6403(12)	3617(8)	2813(6)	59(5)
C(49)	1	5499(13)	3310(8)	2675(6)	65(5)
C(50)	1	4610(14)	3620(8)	2631(6)	67(5)

C(51)	1	4629(13)	4278(9)	2718(6)	66(5)
C(52)	1	4600(12)	6466(8)	3527(6)	54(4)
C(53)	1	3681(12)	6792(8)	3473(6)	56(4)
C(54)	1	3531(15)	7194(10)	3807(7)	75(6)
C(55)	1	4254(17)	7257(10)	4178(7)	80(6)
C(56)	1	5172(16)	6921(10)	4237(7)	76(6)
C(57)	1	5326(14)	6535(8)	3898(6)	63(5)
C(58)	1	3844(13)	5660(8)	1980(5)	55(4)
C(59)	1	2969(12)	5365(8)	1682(5)	55(4)
C(60)	1	2865(14)	4711(9)	1638(6)	67(5)
C(61)	1	2078(14)	4443(10)	1352(6)	71(5)
C(62)	1	1323(14)	4808(11)	1120(6)	73(6)
C(63)	1	1361(14)	5469(10)	1154(6)	72(5)
C(64)	1	2211(12)	5752(10)	1440(6)	68(5)
C(65)	1	4993(12)	5146(8)	1615(5)	50(4)
C(66)	1	5609(11)	4587(8)	1699(6)	56(4)
C(67)	1	5930(15)	4298(9)	1354(7)	71(5)
C(68)	1	5692(16)	4540(11)	949(7)	85(6)
C(69)	1	5125(17)	5106(12)	865(7)	87(7)
C(70)	1	4810(14)	5392(9)	1202(6)	68(5)
C(71)	1	2759(11)	6166(8)	2396(6)	54(4)
C(72)	1	2309(10)	6768(8)	2401(5)	52(4)
C(73)	1	1425(10)	6834(8)	2573(5)	52(4)
C(74)	1	1032(13)	6323(9)	2751(6)	65(5)
C(75)	1	1450(13)	5738(10)	2748(6)	72(5)
C(76)	1	2296(12)	5669(8)	2577(5)	60(5)
C(77)	1	6550(20)	8371(12)	404(8)	99(7)
C(78)	1	10418(18)	7938(11)	4229(9)	92(7)
C(79)	1	4296(16)	3998(13)	4604(8)	108(8)
C(80)	1	449(19)	4514(14)	813(8)	99(8)
S(1)	1	1264(5)	3362(3)	4938(2)	107(2)
O(9)	1	2382(10)	3189(10)	5033(6)	147(7)
C(81)	1	1251(19)	3952(10)	5290(6)	120(9)
C(82)	1	1047(18)	3777(11)	4440(6)	114(8)
S(2)	1	6821(4)	9449(3)	-671(2)	88(2)
O(10)	1	6365(12)	9589(7)	-283(5)	113(5)
C(83)	1	7973(12)	9127(11)	-455(7)	103(8)
C(84)	1	6191(17)	8778(9)	-924(8)	118(9)
S(3A)	0.574(9)	11647(10)	9490(7)	5083(4)	135(4)
O(11A)	0.574(9)	10950(20)	8934(14)	5078(11)	177(12)
C(85A)	0.574(9)	12160(20)	9400(20)	4648(8)	97(10)
C(86A)	0.574(9)	12710(30)	9350(30)	5509(12)	250(30)
S(3B)	0.426(9)	12946(13)	9014(9)	4886(6)	135(4)
O(11B)	0.426(9)	12790(40)	8337(12)	4738(13)	177(12)
C(85B)	0.426(9)	12400(30)	9070(20)	5316(10)	97(10)
C(86B)	0.426(9)	12090(50)	9470(30)	4504(16)	250(30)
S(4A)	0.559(10	-2275(11)	3637(7)	199(5)	135(4)
O(12A)	0.559(10	-2050(20)	4332(10)	240(11)	145(10)
C(87A)	0.559(10	-3310(20)	3560(20)	-198(12)	141(16)
C(88A)	0.559(10	-1310(20)	3278(19)	-24(13)	125(13)
S(4B)	0.441(10	-1607(13)	3743(9)	-6(5)	135(4)
O(12B)	0.441(10	-1740(30)	4431(11)	77(13)	145(10)
C(87B)	0.441(10	-2660(30)	3520(20)	-353(13)	141(16)
C(88B)	0.441(10	-1720(40)	3340(20)	476(11)	125(13)
S(5A)	0.527(12)	9447(16)	6988(10)	799(6)	195(6)
O(13A)	0.527(12	10580(20)	6920(30)	863(17)	272(17)
C(89A)	0.527(12)	9260(40)	7698(17)	1008(15)	150(17)

C(90A)	0.527(12)	8990(40)	7120(30)	238(9)	158(18)
S(5B)	0.473(12)	10147(17)	7640(12)	792(7)	195(6)
O(13B)	0.473(12)	10360(40)	6944(16)	793(19)	272(17)
C(89B)	0.473(12)	10010(40)	7830(30)	1292(10)	150(17)
C(90B)	0.473(12)	8910(30)	7750(30)	479(15)	158(18)

Table 3. Hydrogen coordinates (x 10^4) and isotropic displacement parameters ($Å^2$ x 10^3) for **V-5**.

	Occ.	x	y	z	U_{eq}
H(2A)	1	6704	9263	241	142
H(2X)	0.00	6502	9160	736	142
H(3A)	0.426(9)	11796	8194	4300	178
H(3X)	0.00	11330	7801	3850	178
H(4A)	0.574(9)	10714	8386	4790	156
H(4X)	0.00	9547	8110	4648	156
H(6A)	1	3146	3823	4894	219
H(6X)	0.00	2891	4339	4493	219
H(8A)	1	-861	4752	431	239
H(8X)	0.00	-230	5345	700	239
H(3)	1	5901	6589	1048	74
H(4)	1	6167	7149	463	86
H(6)	1	6527	8743	1227	72
H(7)	1	6150	8136	1804	67
H(9)	1	6968	5486	1569	80
H(10)	1	8583	5269	1432	74
H(11)	1	9872	6018	1611	77
H(12)	1	9538	6989	1937	77
H(13)	1	7945	7140	2113	65
H(15)	1	4509	8130	2362	89
H(16)	1	3056	8761	2088	103
H(17)	1	2051	8523	1436	134
H(18)	1	2328	7603	1047	127
H(19)	1	3786	6998	1312	96
H(22)	1	8922	6998	2961	66
H(23)	1	10305	7446	3429	81
H(25)	1	8576	7672	4322	82
H(26)	1	7194	7258	3843	78
H(28)	1	8368	5510	2524	71
H(29)	1	9559	4771	2824	68
H(30)	1	9888	4537	3561	78
H(31)	1	8987	5071	4007	74
H(32)	1	7745	5786	3720	65
H(34)	1	5049	7697	3361	83
H(35)	1	4775	8787	3370	100
H(36)	1	5777	9464	3058	94
H(37)	1	6985	9069	2714	80
H(38)	1	7256	7975	2692	71
H(41)	1	6366	4872	3808	83
H(42)	1	6050	4273	4388	108

H(44)	1	3041	4631	4002	81
H(45)	1	3391	5259	3436	69
H(47)	1	7071	4458	3001	73
H(48)	1	7021	3386	2847	71
H(49)	1	5499	2872	2609	79
H(50)	1	3982	3403	2542	80
H(51)	1	4008	4506	2684	79
H(53)	1	3172	6743	3215	67
H(54)	1	2915	7426	3775	90
H(55)	1	4136	7534	4400	96
H(56)	1	5670	6955	4499	91
H(57)	1	5952	6315	3925	75
H(60)	1	3357	4445	1812	80
H(61)	1	2055	3997	1314	86
H(63)	1	833	5723	991	86
H(64)	1	2262	6198	1466	81
H(66)	1	5794	4419	1985	67
H(67)	1	6324	3923	1404	85
H(68)	1	5908	4328	716	102
H(69)	1	4968	5281	580	105
H(70)	1	4447	5779	1149	82
H(72)	1	2599	7125	2289	62
H(73)	1	1100	7233	2566	63
H(74)	1	454	6378	2878	78
H(75)	1	1158	5385	2864	86
H(76)	1	2589	5261	2581	72
H(81A)	1	1302	3779	5584	179
H(81B)	1	615	4190	5206	179
H(81C)	1	1829	4233	5288	179
H(82A)	1	1496	4146	4467	171
H(82B)	1	336	3916	4366	171
H(82C)	1	1187	3499	4209	171
H(83A)	1	7889	8790	-251	155
H(83B)	1	8424	9454	-300	155
H(83C)	1	8270	8951	-689	155
H(84A)	1	6236	8435	-711	177
H(84B)	1	6512	8644	-1163	177
H(84C)	1	5475	8880	-1040	177
H(85A)	0.574(9)	11622	9393	4384	146
H(85B)	0.574(9)	12541	9003	4672	146
H(85C)	0.574(9)	12624	9754	4631	146
H(86A)	0.574(9)	13257	9159	5389	375
H(86B)	0.574(9)	12513	9058	5721	375
H(86C)	0.574(9)	12941	9748	5653	375
H(85D)	0.426(9)	11663	9096	5217	146
H(85E)	0.426(9)	12657	9441	5487	146
H(85F)	0.426(9)	12569	8687	5498	146
H(86D)	0.426(9)	12010	9278	4214	375
H(86E)	0.426(9)	12350	9900	4497	375
H(86F)	0.426(9)	11424	9480	4588	375
H(87A)	0.559(10-	3468	3963	-346	211
H(87B)	0.559(10-	3882	3421	-73	211
H(87C)	0.559(10-	3176	3241	-408	211
H(88A)	0.559(10)	-646	3427	132	188
H(88B)	0.559(10-	1408	3390	-333	188
H(88C)	0.559(10-	1352	2818	5	188
H(87D)	0.441(10-	3018	3887	-497	211

H(87E)	0.441(10-3111	3292	-192	211
H(87F)	0.441(10-2485	3232	-573	211
H(88D)	0.441(10-1191	3489	719	188
H(88E)	0.441(10-1630	2884	436	188
H(88F)	0.441(10-2390	3418	539	188
H(89A)	0.527(12)9586	7709	1318	225
H(89B)	0.527(12)8525	7772	976	225
H(89C)	0.527(12)9549	8028	852	225
H(90A)	0.527(12)8832	7570	188	237
H(90B)	0.527(12)8368	6871	138	237
H(90C)	0.527(12)9505	6994	77	237
H(89D)	0.473(1210676	7860	1487	225
H(89E)	0.473(12)9605	7500	1400	225
H(89F)	0.473(12)9652	8234	1283	225
H(90D)	0.473(12)8485	7962	657	237
H(90E)	0.473(12)8606	7340	382	237
H(90F)	0.473(12)8936	8012	224	237

Table 4. Anisotropic parameters ($Å^2$ x 10^3) for **V-5**.

The anisotropic displacement factor exponent takes the form:

$$-2\,\pi^2\,[\,h^2\,a^{*2}\,U_{11} + \ldots + 2\,h\,k\,a^*\,b^*\,U_{12}\,]$$

	U11	U22	U33	U23	U13	U12
Rh(1)	41(1)	20(1)	80(1)	1(1)	22(1)	1(1)
Rh(2)	43(1)	20(1)	83(1)	2(1)	24(1)	1(1)
N(1)	42(7)	38(9)	84(9)	-3(7)	19(6)	-6(6)
N(2)	42(7)	7(7)	94(9)	5(6)	17(6)	-6(5)
N(3)	41(7)	18(8)	82(9)	10(6)	20(6)	3(5)
N(4)	37(7)	27(8)	85(9)	0(6)	24(6)	8(6)
N(5)	56(7)	5(7)	94(9)	-5(6)	40(7)	1(5)
N(6)	40(7)	24(8)	73(8)	-2(6)	22(6)	-10(5)
N(7)	32(7)	46(9)	79(9)	7(7)	19(6)	3(6)
N(8)	35(7)	51(9)	85(9)	12(7)	22(6)	0(6)
O(1)	225(19)	84(13)	127(13)	12(10)	93(13)	-6(12)
O(2)	132(12)	54(10)	111(10)	7(8)	55(9)	5(8)
O(3)	81(10)	96(13)	173(15)	-52(11)	12(10)	-16(9)
O(4)	132(12)	72(11)	103(11)	0(9)	14(9)	-26(9)
O(5)	132(15)	260(20)	189(18)	143(17)	54(13)	34(16)
O(6)	114(12)	174(18)	166(15)	89(13)	64(11)	11(12)
O(7)	103(12)	99(14)	158(15)	-19(12)	-14(10)	-10(10)
O(8)	130(14)	126(16)	183(17)	-12(13)	-60(13)	-3(13)
C(1)	60(10)	33(10)	58(10)	5(7)	9(8)	14(8)
C(2)	47(9)	34(11)	70(11)	9(8)	13(7)	-1(7)
C(3)	69(11)	39(11)	82(12)	7(9)	25(9)	5(8)
C(4)	83(12)	60(14)	79(12)	-9(10)	33(10)	-5(10)
C(5)	77(12)	84(16)	63(11)	18(10)	28(9)	10(11)
C(6)	55(10)	29(10)	99(13)	16(9)	22(9)	-8(8)
C(7)	43(9)	43(12)	86(12)	6(9)	23(8)	-1(7)

C(8)	46(9)	16(9)	85(11)	1(7)	22(8)	-2(7)
C(9)	80(12)	32(11)	91(12)	1(9)	29(10)	5(9)
C(10)	53(9)	30(10)	110(13)	-12(9)	37(9)	-4(8)
C(11)	49(9)	41(12)	112(14)	2(9)	38(9)	4(8)
C(12)	58(10)	25(10)	116(14)	14(9)	34(9)	0(8)
C(13)	42(9)	39(11)	87(11)	4(8)	26(8)	1(7)
C(14)	45(9)	36(11)	88(12)	11(9)	25(8)	2(8)
C(15)	55(10)	49(13)	120(15)	8(11)	21(10)	9(9)
C(16)	82(13)	53(14)	124(17)	9(12)	23(12)	15(11)
C(17)	97(16)	102(19)	135(19)	34(16)	24(15)	44(14)
C(18)	102(16)	104(19)	108(16)	23(14)	10(13)	18(14)
C(19)	62(11)	81(15)	97(14)	19(12)	14(11)	14(11)
C(20)	56(9)	22(10)	68(10)	2(7)	22(8)	-7(7)
C(21)	60(10)	17(9)	72(10)	6(7)	20(8)	-1(7)
C(22)	41(9)	17(9)	108(13)	-2(8)	18(9)	1(7)
C(23)	45(9)	42(12)	115(15)	4(10)	16(9)	-17(8)
C(24)	58(10)	26(10)	93(13)	1(9)	6(9)	-13(8)
C(25)	83(13)	30(11)	91(13)	3(9)	17(10)	-15(9)
C(26)	66(11)	40(11)	93(13)	6(9)	25(10)	-12(9)
C(27)	25(7)	30(10)	99(12)	-4(8)	23(7)	-5(6)
C(28)	61(10)	25(10)	94(12)	0(8)	25(9)	13(8)
C(29)	25(7)	46(11)	103(13)	1(9)	24(8)	-4(7)
C(30)	38(9)	55(12)	103(14)	7(10)	17(9)	4(8)
C(31)	50(10)	47(12)	84(12)	7(9)	6(9)	1(8)
C(32)	46(9)	43(11)	78(12)	-1(8)	19(8)	-11(8)
C(33)	49(9)	30(10)	78(11)	1(8)	20(8)	-8(7)
C(34)	72(11)	25(11)	121(15)	3(9)	46(10)	-2(8)
C(35)	94(14)	47(14)	125(16)	-11(11)	60(12)	1(10)
C(36)	88(13)	23(11)	131(16)	-5(10)	40(12)	1(9)
C(37)	55(10)	21(11)	128(15)	5(9)	28(10)	-1(8)
C(38)	48(9)	45(12)	89(12)	-2(9)	24(8)	-9(8)
C(39)	19(7)	25(10)	89(11)	6(8)	13(7)	0(6)
C(40)	41(8)	20(9)	74(10)	1(7)	22(7)	0(6)
C(41)	52(10)	66(13)	92(13)	20(10)	20(9)	-12(9)
C(42)	78(13)	94(17)	98(14)	32(12)	20(11)	8(12)
C(43)	80(13)	80(15)	84(13)	22(11)	16(11)	-9(11)
C(44)	61(11)	53(12)	95(13)	7(10)	33(10)	-2(9)
C(45)	67(11)	32(11)	78(11)	4(8)	25(9)	3(8)
C(46)	37(8)	49(12)	72(10)	5(8)	18(7)	0(8)
C(47)	49(9)	54(13)	82(12)	9(9)	22(8)	-3(8)
C(48)	50(10)	25(11)	100(13)	-4(8)	12(9)	6(7)
C(49)	59(10)	29(11)	112(14)	-12(9)	26(9)	3(8)
C(50)	61(11)	31(12)	109(14)	3(9)	21(9)	-9(8)
C(51)	54(10)	54(13)	92(13)	4(10)	22(9)	12(9)
C(52)	57(10)	34(10)	77(11)	8(8)	29(9)	-11(8)
C(53)	53(9)	35(11)	90(12)	-2(8)	35(8)	-7(8)
C(54)	77(12)	59(13)	99(14)	-2(11)	38(11)	8(10)
C(55)	109(15)	64(14)	80(13)	-21(10)	50(12)	-18(12)
C(56)	89(13)	55(13)	90(13)	0(10)	32(11)	-4(11)
C(57)	67(11)	35(11)	90(13)	4(9)	26(10)	-8(8)
C(58)	61(7)	41(8)	67(7)	2(6)	20(6)	2(6)
C(59)	47(9)	50(12)	70(11)	-2(8)	18(8)	0(8)
C(60)	73(11)	36(12)	88(13)	5(9)	11(10)	-21(9)
C(61)	61(11)	60(13)	90(13)	-11(10)	8(10)	4(10)
C(62)	55(11)	82(16)	86(13)	-24(11)	23(9)	-6(10)
C(63)	58(11)	70(15)	84(13)	-3(10)	8(9)	10(10)
C(64)	50(10)	69(13)	87(12)	-7(10)	22(9)	-1(9)

C(65)	55(9)	33(10)	68(10)	-11(8)	25(8)	-1(7)
C(66)	44(9)	34(11)	95(12)	-9(9)	26(8)	-9(7)
C(67)	85(13)	33(11)	100(14)	-14(10)	33(11)	-7(9)
C(68)	93(14)	75(16)	90(14)	-27(12)	26(11)	1(12)
C(69)	107(15)	93(17)	65(12)	-9(11)	25(11)	-11(13)
C(70)	78(12)	56(13)	70(12)	-10(10)	14(9)	8(10)
C(71)	39(8)	31(10)	94(12)	-6(8)	22(8)	2(7)
C(72)	24(6)	56(8)	77(8)	-3(6)	16(6)	3(6)
C(73)	21(6)	51(8)	86(8)	-6(6)	13(6)	8(6)
C(74)	59(8)	53(8)	85(8)	5(7)	19(6)	-7(7)
C(75)	57(10)	60(13)	107(14)	9(10)	37(10)	-2(9)
C(76)	53(10)	43(11)	79(11)	13(8)	2(8)	-26(8)
C(77)	130(18)	67(17)	112(17)	3(13)	52(14)	10(13)
C(78)	85(15)	65(15)	125(18)	-14(13)	20(13)	-3(12)
C(79)	59(12)	130(20)	137(18)	79(16)	30(12)	0(12)
C(80)	96(16)	87(18)	105(16)	2(14)	-2(13)	-4(14)
S(1)	121(5)	85(5)	124(5)	14(4)	45(4)	-8(4)
O(9)	81(10)	182(18)	182(16)	69(14)	40(10)	20(11)
C(81)	170(20)	120(20)	73(13)	-22(13)	23(14)	-48(17)
C(82)	129(18)	106(19)	106(16)	2(14)	20(14)	-17(15)
S(2)	95(4)	61(4)	117(4)	17(3)	44(3)	7(3)
O(10)	167(14)	69(11)	122(11)	26(9)	76(11)	5(10)
C(83)	111(16)	89(17)	116(16)	22(13)	36(13)	15(13)
C(84)	120(18)	82(18)	150(20)	7(15)	30(16)	-10(14)

Table 5. Bond lengths [Å] and angles [°] for **V-5**.

Rh(1)-N(5)	2.022(12)	O(2)-H(2a)	0.95
Rh(1)-N(1)	2.040(13)	O(2)-H(2x)	0.95
Rh(1)-N(3)	2.040(13)	O(3)-C(78)	1.23(3)
Rh(1)-N(7)	2.064(13)	O(3)-H(3a)	0.95
Rh(1)-Rh(2)	2.4019(16)	O(3)-H(3x)	0.95
Rh(2)-N(4)	2.018(12)	O(4)-C(78)	1.31(3)
Rh(2)-N(6)	2.037(12)	O(4)-H(4a)	0.95
Rh(2)-N(8)	2.055(13)	O(4)-H(4x)	0.95
Rh(2)-N(2)	2.052(13)	O(5)-C(79)	1.19(3)
N(1)-C(1)	1.340(19)	O(6)-C(79)	1.33(3)
N(1)-C(8)	1.436(19)	O(6)-H(6a)	0.95
N(2)-C(1)	1.319(19)	O(6)-H(6x)	0.95
N(2)-C(14)	1.44(2)	O(7)-C(80)	1.22(3)
N(3)-C(20)	1.349(19)	O(8)-C(80)	1.33(3)
N(3)-C(27)	1.420(19)	O(8)-H(8a)	0.95
N(4)-C(20)	1.315(19)	O(8)-H(8x)	0.95
N(4)-C(33)	1.46(2)	C(1)-C(2)	1.49(2)
N(5)-C(39)	1.296(19)	C(2)-C(3)	1.35(2)
N(5)-C(46)	1.47(2)	C(2)-C(7)	1.41(2)
N(6)-C(39)	1.379(19)	C(3)-C(4)	1.34(2)
N(6)-C(52)	1.43(2)	C(3)-H(3)	0.95
N(7)-C(58)	1.297(19)	C(4)-C(5)	1.43(3)
N(7)-C(65)	1.42(2)	C(4)-H(4)	0.95
N(8)-C(58)	1.35(2)	C(5)-C(6)	1.39(3)
N(8)-C(71)	1.422(19)	C(5)-C(77)	1.48(3)
O(1)-C(77)	1.24(3)	C(6)-C(7)	1.40(2)
O(2)-C(77)	1.32(3)	C(6)-H(6)	0.95

C(7)-H(7)	0.95	C(39)-C(40)	1.49(2)
C(8)-C(9)	1.35(2)	C(40)-C(41)	1.36(2)
C(8)-C(13)	1.38(2)	C(40)-C(45)	1.37(2)
C(9)-C(10)	1.40(2)	C(41)-C(42)	1.37(3)
C(9)-H(9)	0.95	C(41)-H(41)	0.95
C(10)-C(11)	1.37(2)	C(42)-C(43)	1.39(3)
C(10)-H(10)	0.95	C(42)-H(42)	0.95
C(11)-C(12)	1.42(2)	C(43)-C(44)	1.36(3)
C(11)-H(11)	0.95	C(43)-C(79)	1.49(3)
C(12)-C(13)	1.39(2)	C(44)-C(45)	1.38(2)
C(12)-H(12)	0.95	C(44)-H(44)	0.95
C(13)-H(13)	0.95	C(45)-H(45)	0.95
C(14)-C(19)	1.35(3)	C(46)-C(51)	1.37(2)
C(14)-C(15)	1.40(3)	C(46)-C(47)	1.39(2)
C(15)-C(16)	1.41(3)	C(47)-C(48)	1.37(2)
C(15)-H(15)	0.95	C(47)-H(47)	0.95
C(16)-C(17)	1.32(3)	C(48)-C(49)	1.37(2)
C(16)-H(16)	0.95	C(48)-H(48)	0.95
C(17)-C(18)	1.42(3)	C(49)-C(50)	1.35(2)
C(17)-H(17)	0.95	C(49)-H(49)	0.95
C(18)-C(19)	1.39(3)	C(50)-C(51)	1.42(2)
C(18)-H(18)	0.95	C(50)-H(50)	0.95
C(19)-H(19)	0.95	C(51)-H(51)	0.95
C(20)-C(21)	1.51(2)	C(52)-C(57)	1.36(2)
C(21)-C(22)	1.34(2)	C(52)-C(53)	1.39(2)
C(21)-C(26)	1.39(2)	C(53)-C(54)	1.40(2)
C(22)-C(23)	1.37(2)	C(53)-H(53)	0.95
C(22)-H(22)	0.95	C(54)-C(55)	1.36(3)
C(23)-C(24)	1.40(3)	C(54)-H(54)	0.95
C(23)-H(23)	0.95	C(55)-C(56)	1.40(3)
C(24)-C(25)	1.35(2)	C(55)-H(55)	0.95
C(24)-C(78)	1.51(3)	C(56)-C(57)	1.39(3)
C(25)-C(26)	1.36(2)	C(56)-H(56)	0.95
C(25)-H(25)	0.95	C(57)-H(57)	0.95
C(26)-H(26)	0.95	C(58)-C(59)	1.48(2)
C(27)-C(32)	1.38(2)	C(59)-C(60)	1.40(2)
C(27)-C(28)	1.42(2)	C(59)-C(64)	1.40(2)
C(28)-C(29)	1.36(2)	C(60)-C(61)	1.36(2)
C(28)-H(28)	0.95	C(60)-H(60)	0.95
C(29)-C(30)	1.37(2)	C(61)-C(62)	1.36(3)
C(29)-H(29)	0.95	C(61)-H(61)	0.95
C(30)-C(31)	1.37(2)	C(62)-C(63)	1.40(3)
C(30)-H(30)	0.95	C(62)-C(80)	1.49(3)
C(31)-C(32)	1.36(2)	C(63)-C(64)	1.43(2)
C(31)-H(31)	0.95	C(63)-H(63)	0.95
C(32)-H(32)	0.95	C(64)-H(64)	0.95
C(33)-C(34)	1.36(2)	C(65)-C(70)	1.37(2)
C(33)-C(38)	1.40(2)	C(65)-C(66)	1.44(2)
C(34)-C(35)	1.40(3)	C(66)-C(67)	1.39(2)
C(34)-H(34)	0.95	C(66)-H(66)	0.95
C(35)-C(36)	1.37(3)	C(67)-C(68)	1.34(3)
C(35)-H(35)	0.95	C(67)-H(67)	0.95
C(36)-C(37)	1.34(2)	C(68)-C(69)	1.42(3)
C(36)-H(36)	0.95	C(68)-H(68)	0.95
C(37)-C(38)	1.40(2)	C(69)-C(70)	1.36(3)
C(37)-H(37)	0.95	C(69)-H(69)	0.95
C(38)-H(38)	0.95	C(70)-H(70)	0.95

C(71)-C(76)	1.40(2)	C(87a)-H(87c)	0.98
C(71)-C(72)	1.41(2)	C(88a)-H(88a)	0.98
C(72)-C(73)	1.410(19)	C(88a)-H(88b)	0.98
C(72)-H(72)	0.95	C(88a)-H(88c)	0.98
C(73)-C(74)	1.37(2)	S(4b)-O(12b)	1.496(17)
C(73)-H(73)	0.95	S(4b)-C(87b)	1.672(18)
C(74)-C(75)	1.36(3)	S(4b)-C(88b)	1.769(19)
C(74)-H(74)	0.95	O(12b)-H(8a)	1.5931
C(75)-C(76)	1.36(2)	C(87b)-H(87d)	0.98
C(75)-H(75)	0.95	C(87b)-H(87e)	0.98
C(76)-H(76)	0.95	C(87b)-H(87f)	0.98
S(1)-O(9)	1.515(13)	C(88b)-H(88d)	0.98
S(1)-C(81)	1.668(15)	C(88b)-H(88e)	0.98
S(1)-C(82)	1.763(16)	C(88b)-H(88f)	0.98
O(9)-H(6a)	1.7983	S(5a)-O(13a)	1.502(18)
C(81)-H(81a)	0.98	S(5a)-C(89a)	1.680(19)
C(81)-H(81b)	0.98	S(5a)-C(90a)	1.761(19)
C(81)-H(81c)	0.98	C(89a)-H(89a)	0.98
C(82)-H(82a)	0.98	C(89a)-H(89b)	0.98
C(82)-H(82b)	0.98	C(89a)-H(89c)	0.98
C(82)-H(82c)	0.98	C(90a)-H(90a)	0.98
S(2)-O(10)	1.500(12)	C(90a)-H(90b)	0.98
S(2)-C(83)	1.698(15)	C(90a)-H(90c)	0.98
S(2)-C(84)	1.757(16)	S(5b)-O(13b)	1.500(18)
O(10)-H(2a)	1.7524	S(5b)-C(89b)	1.665(19)
C(83)-H(83a)	0.98	S(5b)-C(90b)	1.77(2)
C(83)-H(83b)	0.98	C(89b)-H(89d)	0.98
C(83)-H(83c)	0.98	C(89b)-H(89e)	0.98
C(84)-H(84a)	0.98	C(89b)-H(89f)	0.98
C(84)-H(84b)	0.98	C(90b)-H(90d)	0.98
C(84)-H(84c)	0.98	C(90b)-H(90e)	0.98
S(3a)-O(11a)	1.501(17)	C(90b)-H(90f)	0.98
S(3a)-C(85a)	1.663(18)		
S(3a)-C(86a)	1.76(2)	N(5)-RH1-N(1)	174.6(5)
O(11a)-H(4a)	1.4638	N(5)-RH1-N(3)	89.1(5)
C(85a)-H(85a)	0.98	N(1)-RH1-N(3)	90.8(5)
C(85a)-H(85b)	0.98	N(5)-RH1-N(7)	90.4(5)
C(85a)-H(85c)	0.98	N(1)-RH1-N(7)	89.3(5)
C(86a)-H(86a)	0.98	N(3)-RH1-N(7)	176.3(5)
C(86a)-H(86b)	0.98	N(5)-RH1-RH2	86.7(3)
C(86a)-H(86c)	0.98	N(1)-RH1-RH2	87.9(4)
S(3b)-O(11b)	1.508(17)	N(3)-RH1-RH2	88.2(3)
S(3b)-C(85b)	1.666(19)	N(7)-RH1-RH2	88.1(4)
S(3b)-C(86b)	1.77(2)	N(4)-RH2-N(6)	88.1(5)
O(11b)-H(3a)	1.734	N(4)-RH2-N(8)	174.8(5)
C(85b)-H(85d)	0.98	N(6)-RH2-N(8)	91.5(5)
C(85b)-H(85e)	0.98	N(4)-RH2-N(2)	90.0(5)
C(85b)-H(85f)	0.98	N(6)-RH2-N(2)	176.4(5)
C(86b)-H(86d)	0.98	N(8)-RH2-N(2)	90.1(5)
C(86b)-H(86e)	0.98	N(4)-RH2-RH1	87.2(3)
C(86b)-H(86f)	0.98	N(6)-RH2-RH1	88.6(3)
S(4a)-O(12a)	1.503(16)	N(8)-RH2-RH1	87.6(4)
S(4a)-C(87a)	1.669(18)	N(2)-RH2-RH1	88.2(3)
S(4a)-C(88a)	1.763(19)	C(1)-N(1)-C(8)	119.50(13)
O(12a)-H(8a)	1.8177	C(1)-N(1)-RH1	121.30(11)
C(87a)-H(87a)	0.98	C(8)-N(1)-RH1	117.8(1)
C(87a)-H(87b)	0.98	C(1)-N(2)-C(14)	120.90(13)

C(1)-N(2)-RH2	120.9(1)	C(9)-C(8)-N(1)	118.80(14)
C(14)-N(2)-RH2	116.0(1)	C(13)-C(8)-N(1)	121.80(14)
C(20)-N(3)-C(27)	121.00(13)	C(8)-C(9)-C(10)	121.80(17)
C(20)-N(3)-RH1	120.7(1)	C(8)-C(9)-H(9)	119.1
C(27)-N(3)-RH1	116.9(1)	C(10)-C(9)-H(9)	119.1
C(20)-N(4)-C(33)	119.40(13)	C(11)-C(10)-C(9)	119.30(16)
C(20)-N(4)-RH2	123.70(11)	C(11)-C(10)-H(10)	120.4
C(33)-N(4)-RH2	115.7(9)	C(9)-C(10)-H(10)	120.4
C(39)-N(5)-C(46)	116.30(12)	C(10)-C(11)-C(12)	119.80(15)
C(39)-N(5)-RH1	124.6(1)	C(10)-C(11)-H(11)	120.1
C(46)-N(5)-RH1	117.8(1)	C(12)-C(11)-H(11)	120.1
C(39)-N(6)-C(52)	120.90(13)	C(13)-C(12)-C(11)	118.50(16)
C(39)-N(6)-RH2	119.8(1)	C(13)-C(12)-H(12)	120.8
C(52)-N(6)-RH2	118.3(1)	C(11)-C(12)-H(12)	120.8
C(58)-N(7)-C(65)	121.10(14)	C(8)-C(13)-C(12)	121.30(16)
C(58)-N(7)-RH1	121.20(12)	C(8)-C(13)-H(13)	119.3
C(65)-N(7)-RH1	116.3(9)	C(12)-C(13)-H(13)	119.3
C(58)-N(8)-C(71)	120.10(14)	C(19)-C(14)-C(15)	120.00(17)
C(58)-N(8)-RH2	120.8(1)	C(19)-C(14)-N(2)	123.20(17)
C(71)-N(8)-RH2	116.40(11)	C(15)-C(14)-N(2)	116.70(16)
C(77)-O(2)-H(2A)	120	C(14)-C(15)-C(16)	119(2)
C(77)-O(2)-H(2X)	120	C(14)-C(15)-H(15)	120.4
H(2A)-O(2)-H(2X)	120	C(16)-C(15)-H(15)	120.4
C(78)-O(3)-H(3A)	120	C(17)-C(16)-C(15)	119(2)
C(78)-O(3)-H(3X)	120	C(17)-C(16)-H(16)	120.3
H(3A)-O(3)-H(3X)	120	C(15)-C(16)-H(16)	120.3
C(78)-O(4)-H(4A)	120	C(16)-C(17)-C(18)	122(2)
C(78)-O(4)-H(4X)	120	C(16)-C(17)-H(17)	118.9
H(4A)-O(4)-H(4X)	120	C(18)-C(17)-H(17)	118.9
C(79)-O(6)-H(6A)	120	C(19)-C(18)-C(17)	118(2)
C(79)-O(6)-H(6X)	120	C(19)-C(18)-H(18)	121.1
H(6A)-O(6)-H(6X)	120	C(17)-C(18)-H(18)	121.1
C(80)-O(8)-H(8A)	120	C(14)-C(19)-C(18)	121(2)
C(80)-O(8)-H(8X)	120	C(14)-C(19)-H(19)	119.3
H(8A)-O(8)-H(8X)	120	C(18)-C(19)-H(19)	119.3
N(2)-C(1)-N(1)	119.40(14)	N(4)-C(20)-N(3)	117.50(14)
N(2)-C(1)-C(2)	121.50(14)	N(4)-C(20)-C(21)	122.70(14)
N(1)-C(1)-C(2)	119.10(14)	N(3)-C(20)-C(21)	119.70(14)
C(3)-C(2)-C(7)	118.70(16)	C(22)-C(21)-C(26)	118.90(16)
C(3)-C(2)-C(1)	123.20(16)	C(22)-C(21)-C(20)	122.80(15)
C(7)-C(2)-C(1)	118.10(15)	C(26)-C(21)-C(20)	118.20(14)
C(4)-C(3)-C(2)	124.90(18)	C(21)-C(22)-C(23)	122.10(18)
C(4)-C(3)-H(3)	117.6	C(21)-C(22)-H(22)	119
C(2)-C(3)-H(3)	117.6	C(23)-C(22)-H(22)	119
C(3)-C(4)-C(5)	117.20(18)	C(22)-C(23)-C(24)	118.50(16)
C(3)-C(4)-H(4)	121.4	C(22)-C(23)-H(23)	120.7
C(5)-C(4)-H(4)	121.4	C(24)-C(23)-H(23)	120.7
C(6)-C(5)-C(4)	120.30(17)	C(25)-C(24)-C(23)	119.40(16)
C(6)-C(5)-C(77)	123(2)	C(25)-C(24)-C(78)	120.10(19)
C(4)-C(5)-C(77)	117.00(19)	C(23)-C(24)-C(78)	120.50(18)
C(7)-C(6)-C(5)	119.30(17)	C(24)-C(25)-C(26)	121.50(19)
C(7)-C(6)-H(6)	120.3	C(24)-C(25)-H(25)	119.3
C(5)-C(6)-H(6)	120.3	C(26)-C(25)-H(25)	119.3
C(6)-C(7)-C(2)	119.50(17)	C(25)-C(26)-C(21)	119.40(17)
C(6)-C(7)-H(7)	120.2	C(25)-C(26)-H(26)	120.3
C(2)-C(7)-H(7)	120.2	C(21)-C(26)-H(26)	120.3
C(9)-C(8)-C(13)	119.30(15)	C(32)-C(27)-C(28)	116.90(15)

C(32)-C(27)-N(3)	124.30(14)	C(51)-C(46)-N(5)	120.10(14)
C(28)-C(27)-N(3)	118.70(15)	C(47)-C(46)-N(5)	120.20(14)
C(29)-C(28)-C(27)	119.60(17)	C(48)-C(47)-C(46)	119.20(16)
C(29)-C(28)-H(28)	120.2	C(48)-C(47)-H(47)	120.4
C(27)-C(28)-H(28)	120.2	C(46)-C(47)-H(47)	120.4
C(28)-C(29)-C(30)	122.60(17)	C(49)-C(48)-C(47)	121.40(16)
C(28)-C(29)-H(29)	118.7	C(49)-C(48)-H(48)	119.3
C(30)-C(29)-H(29)	118.7	C(47)-C(48)-H(48)	119.3
C(31)-C(30)-C(29)	118.00(17)	C(50)-C(49)-C(48)	120.80(18)
C(31)-C(30)-H(30)	121	C(50)-C(49)-H(49)	119.6
C(29)-C(30)-H(30)	121	C(48)-C(49)-H(49)	119.6
C(32)-C(31)-C(30)	121.10(18)	C(49)-C(50)-C(51)	118.70(17)
C(32)-C(31)-H(31)	119.5	C(49)-C(50)-H(50)	120.7
C(30)-C(31)-H(31)	119.5	C(51)-C(50)-H(50)	120.7
C(31)-C(32)-C(27)	121.80(16)	C(46)-C(51)-C(50)	120.50(16)
C(31)-C(32)-H(32)	119.1	C(46)-C(51)-H(51)	119.8
C(27)-C(32)-H(32)	119.1	C(50)-C(51)-H(51)	119.8
C(34)-C(33)-C(38)	117.40(16)	C(57)-C(52)-C(53)	120.70(17)
C(34)-C(33)-N(4)	119.50(14)	C(57)-C(52)-N(6)	121.10(15)
C(38)-C(33)-N(4)	123.10(15)	C(53)-C(52)-N(6)	117.70(15)
C(33)-C(34)-C(35)	121.70(17)	C(52)-C(53)-C(54)	118.10(17)
C(33)-C(34)-H(34)	119.2	C(52)-C(53)-H(53)	120.9
C(35)-C(34)-H(34)	119.2	C(54)-C(53)-H(53)	120.9
C(36)-C(35)-C(34)	119.70(18)	C(55)-C(54)-C(53)	120.90(19)
C(36)-C(35)-H(35)	120.1	C(55)-C(54)-H(54)	119.6
C(34)-C(35)-H(35)	120.1	C(53)-C(54)-H(54)	119.6
C(37)-C(36)-C(35)	120.40(18)	C(54)-C(55)-C(56)	121.10(19)
C(37)-C(36)-H(36)	119.8	C(54)-C(55)-H(55)	119.4
C(35)-C(36)-H(36)	119.8	C(56)-C(55)-H(55)	119.4
C(36)-C(37)-C(38)	120.20(17)	C(57)-C(56)-C(55)	117.60(19)
C(36)-C(37)-H(37)	119.9	C(57)-C(56)-H(56)	121.2
C(38)-C(37)-H(37)	119.9	C(55)-C(56)-H(56)	121.2
C(37)-C(38)-C(33)	120.40(16)	C(52)-C(57)-C(56)	121.50(18)
C(37)-C(38)-H(38)	119.8	C(52)-C(57)-H(57)	119.2
C(33)-C(38)-H(38)	119.8	C(56)-C(57)-H(57)	119.2
N(5)-C(39)-N(6)	117.20(14)	N(7)-C(58)-N(8)	119.70(15)
N(5)-C(39)-C(40)	123.70(14)	N(7)-C(58)-C(59)	120.00(15)
N(6)-C(39)-C(40)	119.20(13)	N(8)-C(58)-C(59)	120.30(15)
C(41)-C(40)-C(45)	120.30(15)	C(60)-C(59)-C(64)	118.60(17)
C(41)-C(40)-C(39)	120.30(13)	C(60)-C(59)-C(58)	122.00(16)
C(45)-C(40)-C(39)	119.40(14)	C(64)-C(59)-C(58)	119.30(17)
C(40)-C(41)-C(42)	120.40(17)	C(61)-C(60)-C(59)	121.80(18)
C(40)-C(41)-H(41)	119.8	C(61)-C(60)-H(60)	119.1
C(42)-C(41)-H(41)	119.8	C(59)-C(60)-H(60)	119.1
C(41)-C(42)-C(43)	119.10(19)	C(62)-C(61)-C(60)	120(2)
C(41)-C(42)-H(42)	120.5	C(62)-C(61)-H(61)	119.8
C(43)-C(42)-H(42)	120.5	C(60)-C(61)-H(61)	119.8
C(44)-C(43)-C(42)	120.90(19)	C(61)-C(62)-C(63)	121.00(18)
C(44)-C(43)-C(79)	119.50(19)	C(61)-C(62)-C(80)	121(2)
C(42)-C(43)-C(79)	119.50(19)	C(63)-C(62)-C(80)	118(2)
C(43)-C(44)-C(45)	118.90(17)	C(62)-C(63)-C(64)	118.40(18)
C(43)-C(44)-H(44)	120.6	C(62)-C(63)-H(63)	120.8
C(45)-C(44)-H(44)	120.6	C(64)-C(63)-H(63)	120.8
C(40)-C(45)-C(44)	120.40(16)	C(59)-C(64)-C(63)	119.50(19)
C(40)-C(45)-H(45)	119.8	C(59)-C(64)-H(64)	120.3
C(44)-C(45)-H(45)	119.8	C(63)-C(64)-H(64)	120.3
C(51)-C(46)-C(47)	119.40(17)	C(70)-C(65)-N(7)	123.30(15)

C(70)-C(65)-C(66)	118.10(15)	S(1)-C(82)-H(82A)	109.5
N(7)-C(65)-C(66)	117.60(15)	S(1)-C(82)-H(82B)	109.5
C(67)-C(66)-C(65)	118.60(17)	H(82A)-C(82)-H(82B)	109.5
C(67)-C(66)-H(66)	120.7	S(1)-C(82)-H(82C)	109.5
C(65)-C(66)-H(66)	120.7	H(82A)-C(82)-H(82C)	109.5
C(68)-C(67)-C(66)	121(2)	H(82B)-C(82)-H(82C)	109.5
C(68)-C(67)-H(67)	119.4	O(10)-S(2)-C(83)	104.3(1)
C(66)-C(67)-H(67)	119.4	O(10)-S(2)-C(84)	106.8(1)
C(67)-C(68)-C(69)	120.70(19)	C(83)-S(2)-C(84)	99.8(1)
C(67)-C(68)-H(68)	119.7	S(2)-O(10)-H(2A)	127.7
C(69)-C(68)-H(68)	119.7	S(2)-C(83)-H(83A)	109.5
C(70)-C(69)-C(68)	118(2)	S(2)-C(83)-H(83B)	109.5
C(70)-C(69)-H(69)	120.8	H(83A)-C(83)-H(83B)	109.5
C(68)-C(69)-H(69)	120.8	S(2)-C(83)-H(83C)	109.5
C(69)-C(70)-C(65)	122.70(19)	H(83A)-C(83)-H(83C)	109.5
C(69)-C(70)-H(70)	118.6	H(83B)-C(83)-H(83C)	109.5
C(65)-C(70)-H(70)	118.6	S(2)-C(84)-H(84A)	109.5
C(76)-C(71)-C(72)	116.60(14)	S(2)-C(84)-H(84B)	109.5
C(76)-C(71)-N(8)	125.60(15)	H(84A)-C(84)-H(84B)	109.5
C(72)-C(71)-N(8)	117.50(14)	S(2)-C(84)-H(84C)	109.5
C(73)-C(72)-C(71)	119.20(15)	H(84A)-C(84)-H(84C)	109.5
C(73)-C(72)-H(72)	120.4	H(84B)-C(84)-H(84C)	109.5
C(71)-C(72)-H(72)	120.4	O(11A)-S(3A)-C(85A)	105.40(17)
C(74)-C(73)-C(72)	120.30(16)	O(11A)-S(3A)-C(86A)	106.20(19)
C(74)-C(73)-H(73)	119.8	C(85A)-S(3A)-C(86A)	101.20(17)
C(72)-C(73)-H(73)	119.8	H(4A)-O(11A)-S(3A)	133.1
C(75)-C(74)-C(73)	121.40(17)	S(3A)-C(85A)-H(85A)	109.5
C(75)-C(74)-H(74)	119.3	S(3A)-C(85A)-H(85B)	109.5
C(73)-C(74)-H(74)	119.3	H(85A)-C(85A)-H(85B)	109.5
C(74)-C(75)-C(76)	118.70(18)	S(3A)-C(85A)-H(85C)	109.5
C(74)-C(75)-H(75)	120.7	H(85A)-C(85A)-H(85C)	109.5
C(76)-C(75)-H(75)	120.7	H(85B)-C(85A)-H(85C)	109.5
C(75)-C(76)-C(71)	123.80(17)	S(3A)-C(86A)-H(86A)	109.5
C(75)-C(76)-H(76)	118.1	S(3A)-C(86A)-H(86B)	109.5
C(71)-C(76)-H(76)	118.1	H(86A)-C(86A)-H(86B)	109.5
O(1)-C(77)-O(2)	123(2)	S(3A)-C(86A)-H(86C)	109.5
O(1)-C(77)-C(5)	124(2)	H(86A)-C(86A)-H(86C)	109.5
O(2)-C(77)-C(5)	113(2)	H(86B)-C(86A)-H(86C)	109.5
O(3)-C(78)-O(4)	126(2)	O(11B)-S(3B)-C(85B)	104.80(18)
O(3)-C(78)-C(24)	118(2)	O(11B)-S(3B)-C(86B)	106(2)
O(4)-C(78)-C(24)	116(2)	C(85B)-S(3B)-C(86B)	100.40(18)
O(5)-C(79)-O(6)	122(2)	S(3B)-O(11B)-H(3A)	116.3
O(5)-C(79)-C(43)	124(2)	S(3B)-C(85B)-H(85D)	109.5
O(6)-C(79)-C(43)	113(2)	S(3B)-C(85B)-H(85E)	109.5
O(7)-C(80)-O(8)	122(2)	H(85D)-C(85B)-H(85E)	109.5
O(7)-C(80)-C(62)	122(2)	S(3B)-C(85B)-H(85F)	109.5
O(8)-C(80)-C(62)	116(2)	H(85D)-C(85B)-H(85F)	109.5
O(9)-S(1)-C(81)	101.40(12)	H(85E)-C(85B)-H(85F)	109.5
O(9)-S(1)-C(82)	105.6(1)	S(3B)-C(86B)-H(86D)	109.5
C(81)-S(1)-C(82)	101.10(11)	S(3B)-C(86B)-H(86E)	109.5
S(1)-O(9)-H(6A)	111.3	H(86D)-C(86B)-H(86E)	109.5
S(1)-C(81)-H(81A)	109.5	S(3B)-C(86B)-H(86F)	109.5
S(1)-C(81)-H(81B)	109.5	H(86D)-C(86B)-H(86F)	109.5
H(81A)-C(81)-H(81B)	109.5	H(86E)-C(86B)-H(86F)	109.5
S(1)-C(81)-H(81C)	109.5	O(12A)-S(4A)-C(87A)	106.50(17)
H(81A)-C(81)-H(81C)	109.5	O(12A)-S(4A)-C(88A)	107.80(17)
H(81B)-C(81)-H(81C)	109.5	C(87A)-S(4A)-C(88A)	102.90(16)

S(4A)-O(12A)-H(8A)	130.9	H(90D)-C(90B)-H(90F)	109.5
S(4A)-C(87A)-H(87A)	109.5	H(90E)-C(90B)-H(90F)	109.5
S(4A)-C(87A)-H(87B)	109.5		
H(87A)-C(87A)-H(87B)	109.5		
S(4A)-C(87A)-H(87C)	109.5		
H(87A)-C(87A)-H(87C)	109.5		
H(87B)-C(87A)-H(87C)	109.5		
S(4A)-C(88A)-H(88A)	109.5		
S(4A)-C(88A)-H(88B)	109.5		
H(88A)-C(88A)-H(88B)	109.5		
S(4A)-C(88A)-H(88C)	109.5		
H(88A)-C(88A)-H(88C)	109.5		
H(88B)-C(88A)-H(88C)	109.5		
O(12B)-S(4B)-C(87B)	106.20(18)		
O(12B)-S(4B)-C(88B)	106.80(18)		
C(87B)-S(4B)-C(88B)	101.80(17)		
S(4B)-O(12B)-H(8A)	116.1		
S(4B)-C(87B)-H(87D)	109.5		
S(4B)-C(87B)-H(87E)	109.5		
H(87D)-C(87B)-H(87E)	109.5		
S(4B)-C(87B)-H(87F)	109.5		
H(87D)-C(87B)-H(87F)	109.5		
H(87E)-C(87B)-H(87F)	109.5		
S(4B)-C(88B)-H(88D)	109.5		
S(4B)-C(88B)-H(88E)	109.5		
H(88D)-C(88B)-H(88E)	109.5		
S(4B)-C(88B)-H(88F)	109.5		
H(88D)-C(88B)-H(88F)	109.5		
H(88E)-C(88B)-H(88F)	109.5		
O(13A)-S(5A)-C(89A)	105.50(19)		
O(13A)-S(5A)-C(90A)	106.50(19)		
C(89A)-S(5A)-C(90A)	101.30(17)		
S(5A)-C(89A)-H(89A)	109.5		
S(5A)-C(89A)-H(89B)	109.5		
H(89A)-C(89A)-H(89B)	109.5		
S(5A)-C(89A)-H(89C)	109.5		
H(89A)-C(89A)-H(89C)	109.5		
H(89B)-C(89A)-H(89C)	109.5		
S(5A)-C(90A)-H(90A)	109.5		
S(5A)-C(90A)-H(90B)	109.5		
H(90A)-C(90A)-H(90B)	109.5		
S(5A)-C(90A)-H(90C)	109.5		
H(90A)-C(90A)-H(90C)	109.5		
H(90B)-C(90A)-H(90C)	109.5		
O(13B)-S(5B)-C(89B)	107(2)		
O(13B)-S(5B)-C(90B)	107(2)		
C(89B)-S(5B)-C(90B)	102.30(18)		
S(5B)-C(89B)-H(89D)	109.5		
S(5B)-C(89B)-H(89E)	109.5		
H(89D)-C(89B)-H(89E)	109.5		
S(5B)-C(89B)-H(89F)	109.5		
H(89D)-C(89B)-H(89F)	109.5		
H(89E)-C(89B)-H(89F)	109.5		
S(5B)-C(90B)-H(90D)	109.5		
S(5B)-C(90B)-H(90E)	109.5		
H(90D)-C(90B)-H(90E)	109.5		
S(5B)-C(90B)-H(90F)	109.5		

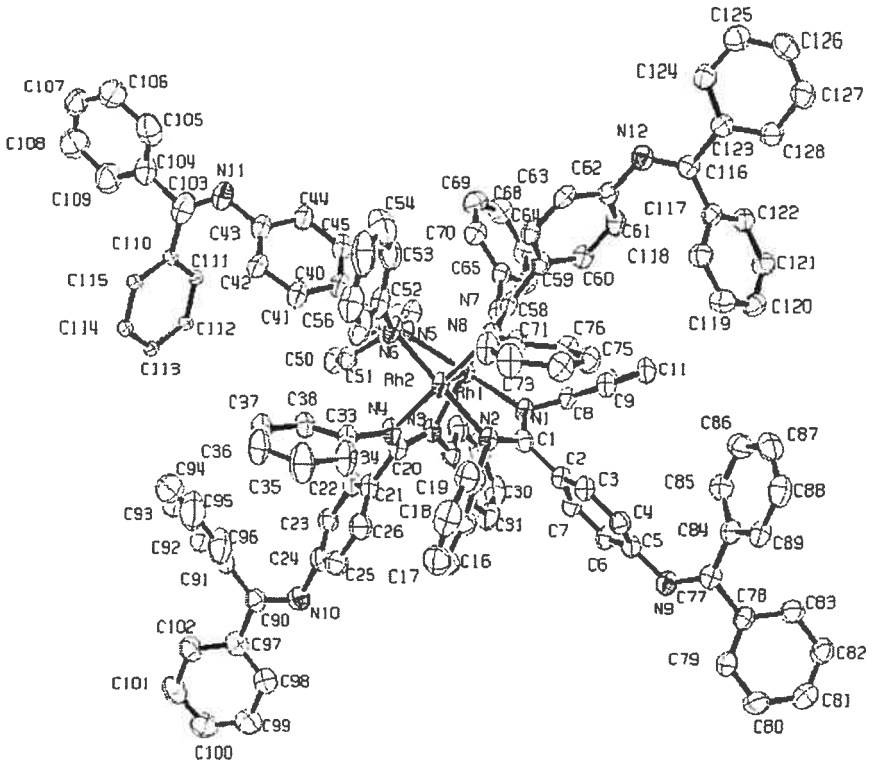

Table 1. Crystal data and structure refinement for **V-6**.

Empirical formula	C128 H96 N12 Rh2
Formula weight	2007.99
Temperature	100(2)K
Wavelength	1.54178 Å
Crystal system	Monoclinic
Space group	P21/c
Unit cell dimensions	a = 18.8013(3) Å α = 90° b = 30.6803(6) Å β = 91.8980(10)° c = 18.4655(3) Å γ = 90°
Volume	10645.6(3)Å^3
Z	4
Density (calculated)	1.253 g/cm^3
Absorption coefficient	2.940 mm^{-1}

F(000)	4152
Crystal size	0.33 x 0.24 x 0.18 mm
Theta range for data collection	2.35 to 68.97°
Index ranges	$-20 \leq h \leq 18$, $-36 \leq k \leq 36$, $-22 \leq \ell \leq 22$
Reflections collected	144520
Independent reflections	19211 [R_{int} = 0.068]
Absorption correction	
Max. and min. transmission	0.6197 and 0.4437
Refinement method	Full-matrix least-squares on F^2
Data / restraints / parameters	19211 / 1 / 1231
Goodness-of-fit on F^2	1.096
Final R indices [I>2sigma(I)]	R1 = 0.0571, wR_2 = 0.1716
R indices (all data)	R1 = 0.0750, wR_2 = 0.1799
Largest diff. peak and hole	2.475 and -0.444 e/Å^3

Table 2. Atomic coordinates (x 10^4) and equivalent isotropic displacement parameters (Å^2 x 10^3) for **V-6**.

U_{eq} is defined as one third of the trace of the orthogonalized Uij tensor.

	Occ.	x	y	z	U_{eq}
Rh(1)	1	3138(1)	4782(1)	7543(1)	31(1)
Rh(2)	1	2228(1)	5292(1)	7195(1)	34(1)
N(1)	1	3346(2)	5183(1)	8427(2)	35(1)
N(2)	1	2277(2)	5537(1)	8225(2)	36(1)
N(3)	1	2396(2)	4455(1)	8116(2)	36(1)
N(4)	1	1501(2)	4831(1)	7524(2)	41(1)
N(5)	1	2853(2)	4429(1)	6629(2)	34(1)
N(6)	1	2214(2)	5013(1)	6189(2)	39(1)
N(7)	1	3827(2)	5131(1)	6945(2)	33(1)
N(8)	1	3041(2)	5709(1)	6899(2)	34(1)
N(9)	1	3137(2)	6183(1)	11479(2)	41(1)
N(10)	1	-274(3)	3447(2)	9433(3)	55(1)
N(11)	1	1834(3)	3774(2)	3388(3)	53(1)

N(12)	1	5774(2)	6707(1)	5722(2)	39(1)
C(1)	1	2846(2)	5453(2)	8650(3)	34(1)
C(2)	1	2912(2)	5658(2)	9379(3)	36(1)
C(3)	1	2784(2)	6100(2)	9488(3)	38(1)
C(4)	1	2861(3)	6283(2)	10167(3)	39(1)
C(5)	1	3056(3)	6021(2)	10756(3)	38(1)
C(6)	1	3142(3)	5577(2)	10666(3)	40(1)
C(7)	1	3082(3)	5398(2)	9985(3)	40(1)
C(8)	1	4061(3)	5220(2)	8701(3)	35(1)
C(9)	1	4406(3)	5621(2)	8711(3)	40(1)
C(10)	1	5119(3)	5646(2)	8932(3)	45(1)
C(11)	1	5486(3)	5279(2)	9140(3)	47(1)
C(12)	1	5146(3)	4882(2)	9134(3)	46(1)
C(13)	1	4433(3)	4852(2)	8920(3)	42(1)
C(14)	1	1623(3)	5681(2)	8514(3)	44(1)
C(15)	1	1303(3)	5450(2)	9062(3)	51(1)
C(16)	1	630(3)	5567(2)	9286(4)	64(2)
C(17)	1	267(4)	5904(2)	8974(4)	67(2)
C(18)	1	576(3)	6139(2)	8435(4)	67(2)
C(19)	1	1263(3)	6035(2)	8199(3)	54(2)
C(20)	1	1702(3)	4513(2)	7968(3)	38(1)
C(21)	1	1170(3)	4228(2)	8309(3)	40(1)
C(22)	1	1266(3)	3772(2)	8336(3)	41(1)
C(23)	1	788(3)	3513(2)	8685(3)	45(1)
C(24)	1	210(3)	3692(2)	9018(3)	49(1)
C(25)	1	104(3)	4142(2)	8992(3)	54(2)
C(26)	1	578(3)	4400(2)	8632(3)	49(1)
C(27)	1	2663(3)	4224(2)	8733(3)	39(1)
C(28)	1	3221(3)	3936(2)	8640(3)	49(1)
C(29)	1	3558(3)	3736(2)	9234(4)	58(2)
C(30)	1	3332(3)	3822(2)	9931(4)	60(2)
C(31)	1	2785(4)	4098(2)	10025(3)	59(2)
C(32)	1	2439(3)	4305(2)	9433(3)	49(1)
C(33)	1	814(3)	4827(2)	7173(3)	44(1)
C(34)	1	368(3)	5191(2)	7228(4)	60(2)
C(35)	1	-283(4)	5204(2)	6856(4)	78(2)
C(36)	1	-496(3)	4852(2)	6414(4)	67(2)
C(37)	1	-67(3)	4495(2)	6377(3)	55(2)
C(38)	1	582(3)	4479(2)	6756(3)	45(1)
C(39)	1	2473(3)	4615(2)	6101(3)	36(1)
C(40)	1	2316(3)	4380(2)	5403(3)	36(1)
C(41)	1	1616(3)	4392(2)	5111(3)	41(1)
C(42)	1	1443(3)	4181(2)	4463(3)	41(1)
C(43)	1	1971(3)	3972(2)	4084(3)	41(1)
C(44)	1	2675(3)	3965(2)	4363(3)	45(1)
C(45)	1	2834(3)	4166(2)	5030(3)	43(1)
C(46)	1	2949(3)	3965(2)	6662(3)	35(1)
C(47)	1	3630(3)	3794(2)	6720(3)	43(1)
C(48)	1	3731(3)	3351(2)	6812(3)	46(1)
C(49)	1	3155(3)	3074(2)	6851(3)	46(1)
C(50)	1	2480(3)	3239(2)	6788(3)	48(1)
C(51)	1	2367(3)	3686(2)	6693(3)	40(1)
C(52)	1	2026(3)	5298(2)	5621(3)	49(1)
C(53)	1	2491(3)	5394(2)	5085(4)	62(2)
C(54)	1	2324(4)	5712(3)	4559(4)	86(3)
C(55)	1	1668(4)	5932(2)	4621(5)	86(3)
C(56)	1	1197(4)	5830(2)	5133(4)	66(2)

C(57)	1	1378(3)	5519(2)	5632(3)	57(2)
C(58)	1	3680(3)	5545(2)	6774(3)	35(1)
C(59)	1	4242(3)	5820(1)	6457(3)	35(1)
C(60)	1	4929(3)	5824(2)	6782(3)	38(1)
C(61)	1	5438(3)	6109(2)	6544(3)	39(1)
C(62)	1	5286(3)	6395(2)	5971(3)	37(1)
C(63)	1	4630(3)	6362(2)	5610(3)	37(1)
C(64)	1	4102(3)	6087(1)	5854(3)	35(1)
C(65)	1	4388(3)	4893(2)	6633(3)	36(1)
C(66)	1	4895(3)	4689(2)	7082(3)	44(1)
C(67)	1	5405(3)	4423(2)	6792(3)	55(2)
C(68)	1	5420(3)	4348(2)	6050(3)	53(1)
C(69)	1	4920(3)	4551(2)	5598(3)	48(1)
C(70)	1	4408(3)	4825(2)	5889(3)	42(1)
C(71)	1	2931(3)	6163(2)	6994(3)	38(1)
C(72)	1	2312(3)	6352(2)	6688(3)	49(1)
C(73)	1	2154(3)	6785(2)	6822(4)	56(2)
C(74)	1	2603(3)	7042(2)	7248(3)	49(1)
C(75)	1	3223(3)	6858(2)	7542(3)	46(1)
C(76)	1	3383(3)	6424(2)	7417(3)	39(1)
C(77)	1	3544(3)	6510(2)	11648(3)	38(1)
C(78)	1	3570(3)	6648(2)	12422(3)	39(1)
C(79)	1	2986(3)	6594(2)	12832(3)	57(2)
C(80)	1	2998(4)	6706(2)	13561(3)	60(2)
C(81)	1	3626(3)	6870(2)	13891(3)	51(1)
C(82)	1	4210(3)	6923(2)	13483(3)	53(1)
C(83)	1	4186(3)	6819(2)	12745(3)	48(1)
C(84)	1	3992(3)	6759(2)	11131(3)	37(1)
C(85)	1	4422(3)	6545(2)	10635(3)	45(1)
C(86)	1	4822(3)	6786(2)	10161(3)	51(1)
C(87)	1	4807(3)	7241(2)	10179(3)	56(2)
C(88)	1	4385(3)	7449(2)	10668(3)	55(2)
C(89)	1	3979(3)	7211(2)	11145(3)	45(1)
C(90)	1	-750(3)	3207(2)	9126(3)	43(1)
C(91)	1	-826(3)	3151(2)	8326(3)	51(1)
C(92)	1	-712(3)	2747(2)	8005(3)	61(2)
C(93)	1	-769(4)	2711(4)	7254(5)	97(3)
C(94)	1	-941(5)	3096(5)	6847(5)	113(4)
C(95)	1	-1044(5)	3475(4)	7194(6)	117(4)
C(96)	1	-981(4)	3507(3)	7905(4)	82(2)
C(97)	1	-1259(3)	2983(2)	9611(3)	45(1)
C(98)	1	-1224(3)	3068(2)	10356(3)	53(1)
C(99)	1	-1718(3)	2896(2)	10808(4)	60(2)
C(100)	1	-2232(3)	2628(2)	10538(4)	58(2)
C(101)	1	-2275(3)	2528(2)	9806(4)	58(2)
C(102)	1	-1802(3)	2713(2)	9335(3)	49(1)
C(103)	1	1352(3)	3507(2)	3265(3)	62(2)
C(104)	1	1244(3)	3345(2)	2486(4)	61(2)
C(105)	1	1448(3)	3616(2)	1934(4)	69(2)
C(106)	1	1316(3)	3489(3)	1193(4)	71(2)
C(107)	1	1006(3)	3097(3)	1070(4)	68(2)
C(108)	1	822(4)	2828(3)	1631(5)	88(3)
C(109)	1	925(4)	2955(3)	2346(4)	78(2)
C(110)	0.50	885(2)	3317(2)	3831(2)	20
C(111)	0.50	1227(2)	3099(2)	4404(3)	20
C(112)	0.50	830(2)	2914(2)	4947(2)	20
C(113)	0.50	93(2)	2947(2)	4917(2)	20

C(114)	0.50	-249(2)	3164(2)	4344(3)	20
C(115)	0.50	147(2)	3349(2)	3801(2)	20
C(116)	1	6151(3)	6949(2)	6155(3)	36(1)
C(117)	1	6099(3)	6958(2)	6965(3)	35(1)
C(118)	1	5473(3)	7083(2)	7285(3)	42(1)
C(119)	1	5432(3)	7087(2)	8038(3)	47(1)
C(120)	1	6011(3)	6962(2)	8476(3)	43(1)
C(121)	1	6629(3)	6832(2)	8162(3)	43(1)
C(122)	1	6684(3)	6832(2)	7413(3)	42(1)
C(123)	1	6678(3)	7251(2)	5837(3)	37(1)
C(124)	1	6845(3)	7217(2)	5111(3)	44(1)
C(125)	1	7316(3)	7507(2)	4813(3)	49(1)
C(126)	1	7628(3)	7828(2)	5226(3)	47(1)
C(127)	1	7470(3)	7863(2)	5942(3)	55(2)
C(128)	1	6997(3)	7579(2)	6246(3)	47(1)

Table 3. Hydrogen coordinates (x 10^4) and isotropic displacement parameters ($Å^2$ x 10^3) for **V-6**.

	Occ.	x	y	z	U_{eq}
H(3)	1	2642	6278	9088	45
H(4)	1	2782	6586	10233	47
H(6)	1	3243	5396	11075	48
H(7)	1	3157	5094	9924	48
H(9)	1	4155	5877	8567	48
H(10)	1	5353	5920	8939	54
H(11)	1	5974	5298	9287	57
H(12)	1	5401	4627	9278	56
H(13)	1	4200	4577	8924	50
H(15)	1	1546	5211	9285	61
H(16)	1	420	5407	9665	77
H(17)	1	-196	5977	9126	81
H(18)	1	324	6376	8217	80
H(19)	1	1477	6203	7832	65
H(22)	1	1663	3644	8111	49
H(23)	1	858	3207	8697	54
H(25)	1	-291	4270	9219	65
H(26)	1	497	4705	8606	59
H(28)	1	3375	3875	8166	58
H(29)	1	3942	3541	9165	70
H(30)	1	3563	3687	10338	72
H(31)	1	2630	4153	10500	71
H(32)	1	2056	4499	9509	59
H(34)	1	514	5430	7523	72
H(35)	1	-584	5451	6899	94
H(36)	1	-935	4862	6144	81
H(37)	1	-214	4254	6087	66
H(38)	1	870	4225	6727	54
H(41)	1	1259	4547	5358	49
H(45)	1	3306	4155	5228	51

H(47)	1	4030	3982	6695	52
H(48)	1	4200	3237	6850	55
H(49)	1	3226	2771	6921	55
H(50)	1	2084	3048	6808	57
H(51)	1	1896	3799	6651	48
H(53)	1	2932	5243	5069	74
H(54)	1	2637	5777	4180	103
H(55)	1	1554	6161	4290	103
H(56)	1	748	5972	5143	80
H(57)	1	1053	5451	5998	68
H(60)	1	5043	5629	7169	45
H(61)	1	5898	6110	6772	47
H(63)	1	4539	6532	5186	45
H(64)	1	3648	6079	5613	42
H(66)	1	4891	4732	7591	53
H(67)	1	5752	4289	7105	65
H(68)	1	5768	4161	5856	63
H(69)	1	4925	4505	5089	57
H(70)	1	4070	4966	5575	50
H(72)	1	2000	6182	6388	59
H(73)	1	1729	6908	6617	67
H(74)	1	2490	7338	7339	58
H(75)	1	3541	7031	7830	55
H(76)	1	3808	6303	7624	47
H(79)	1	2563	6478	12614	68
H(80)	1	2583	6671	13835	72
H(81)	1	3643	6943	14391	61
H(82)	1	4638	7032	13701	63
H(83)	1	4594	6865	12464	58
H(85)	1	4439	6235	10624	54
H(86)	1	5109	6641	9823	61
H(87)	1	5086	7406	9858	68
H(88)	1	4371	7758	10680	66
H(89)	1	3692	7359	11481	54
H(92)	1	-596	2500	8295	74
H(93)	1	-697	2440	7019	116
H(94)	1	-982	3084	6333	135
H(95)	1	-1165	3728	6918	140
H(96)	1	-1045	3782	8129	99
H(98)	1	-854	3248	10552	63
H(99)	1	-1698	2964	11310	72
H(100)	1	-2569	2508	10854	69
H(101)	1	-2629	2331	9627	70
H(102)	1	-1847	2656	8829	59
H(105)	1	1675	3886	2044	82
H(106)	1	1441	3674	804	85
H(107)	1	914	3004	585	81
H(108)	1	620	2551	1525	106
H(109)	1	776	2775	2730	94
H(118)	1	5072	7167	6990	51
H(119)	1	5004	7177	8254	57
H(120)	1	5980	6965	8988	51
H(121)	1	7024	6741	8459	51
H(122)	1	7117	6747	7203	50
H(124)	1	6634	6994	4820	52
H(125)	1	7425	7483	4316	59
H(126)	1	7951	8026	5018	57

H(127)	1	7689	8084	6232	66
H(128)	1	6888	7610	6742	56

Table 4. Anisotropic parameters ($Å^2$ x 10^3) for **V-6**.

The anisotropic displacement factor exponent takes the form:

$$-2\,\pi^2\,[\,h^2\,a^{*2}\,U_{11} + \ldots + 2\,h\,k\,a^*\,b^*\,U_{12}\,]$$

	U11	U22	U33	U23	U13	U12
Rh(1)	36(1)	24(1)	32(1)	1(1)	-11(1)	-2(1)
Rh(2)	37(1)	26(1)	37(1)	1(1)	-14(1)	-2(1)
N(1)	36(2)	34(2)	34(2)	-2(2)	-11(2)	-3(2)
N(2)	37(2)	32(2)	38(2)	0(2)	-8(2)	-2(2)
N(3)	35(2)	32(2)	41(2)	3(2)	-9(2)	-6(2)
N(4)	39(2)	35(2)	47(3)	5(2)	-14(2)	-7(2)
N(5)	47(2)	23(2)	33(2)	-1(2)	-12(2)	-3(2)
N(6)	55(3)	26(2)	34(2)	0(2)	-18(2)	-1(2)
N(7)	35(2)	29(2)	34(2)	3(2)	-6(2)	-3(2)
N(8)	36(2)	24(2)	40(2)	3(2)	-6(2)	0(2)
N(9)	46(3)	36(2)	39(3)	-4(2)	-3(2)	-4(2)
N(10)	54(3)	56(3)	56(3)	-9(2)	9(2)	-16(2)
N(11)	57(3)	46(3)	55(3)	-13(2)	-14(2)	0(2)
N(12)	45(3)	31(2)	40(2)	1(2)	-4(2)	-2(2)
C(1)	33(3)	29(2)	41(3)	4(2)	-5(2)	-3(2)
C(2)	35(3)	35(3)	36(3)	-2(2)	-4(2)	-2(2)
C(3)	36(3)	35(3)	42(3)	-1(2)	-8(2)	-1(2)
C(4)	40(3)	32(3)	46(3)	-3(2)	0(2)	-1(2)
C(5)	34(3)	39(3)	41(3)	-5(2)	-2(2)	-5(2)
C(6)	45(3)	33(3)	43(3)	0(2)	-6(2)	-2(2)
C(7)	46(3)	29(2)	45(3)	-1(2)	-8(2)	1(2)
C(8)	38(3)	36(3)	31(3)	-1(2)	-7(2)	-3(2)
C(9)	41(3)	35(3)	44(3)	1(2)	-8(2)	-4(2)
C(10)	44(3)	40(3)	49(3)	-2(2)	-8(2)	-11(2)
C(11)	37(3)	54(3)	50(3)	-3(3)	-15(2)	-7(2)
C(12)	42(3)	47(3)	49(3)	5(3)	-18(2)	5(2)
C(13)	40(3)	36(3)	48(3)	-5(2)	-12(2)	-3(2)
C(14)	40(3)	44(3)	47(3)	-8(2)	-10(2)	2(2)
C(15)	48(4)	50(3)	55(4)	-6(3)	2(3)	-1(2)
C(16)	49(4)	73(5)	72(5)	-7(4)	9(3)	0(3)
C(17)	53(4)	70(5)	79(5)	-18(4)	2(3)	3(3)
C(18)	61(4)	53(4)	84(5)	-18(4)	-23(3)	26(3)
C(19)	53(4)	47(3)	60(4)	-4(3)	-16(3)	8(3)
C(20)	40(3)	34(3)	39(3)	-4(2)	-9(2)	-3(2)
C(21)	42(3)	35(3)	42(3)	0(2)	-10(2)	-6(2)
C(22)	43(3)	39(3)	41(3)	1(2)	-7(2)	-7(2)
C(23)	48(3)	37(3)	50(3)	-1(2)	-4(2)	-10(2)
C(24)	53(4)	47(3)	47(3)	-4(3)	0(3)	-17(3)
C(25)	56(4)	46(3)	61(4)	-12(3)	8(3)	-9(3)
C(26)	54(4)	36(3)	58(4)	-3(3)	-2(3)	-6(2)

C(27)	42(3)	34(3)	42(3)	10(2)	-11(2)	-11(2)
C(28)	47(3)	41(3)	56(4)	11(3)	-12(3)	-8(2)
C(29)	54(4)	42(3)	76(5)	16(3)	-24(3)	1(2)
C(30)	70(4)	50(4)	57(4)	21(3)	-27(3)	-18(3)
C(31)	82(5)	52(4)	42(3)	11(3)	-15(3)	-24(3)
C(32)	54(3)	39(3)	54(4)	9(3)	-13(3)	-12(2)
C(33)	46(3)	35(3)	49(3)	1(2)	-16(2)	-6(2)
C(34)	57(4)	43(3)	79(5)	-2(3)	-29(3)	0(3)
C(35)	67(5)	56(4)	109(6)	-4(4)	-39(4)	8(3)
C(36)	54(4)	67(4)	79(5)	-7(4)	-33(3)	2(3)
C(37)	53(4)	50(3)	59(4)	1(3)	-19(3)	-10(3)
C(38)	40(3)	45(3)	48(3)	1(2)	-9(2)	-4(2)
C(39)	39(3)	28(2)	41(3)	3(2)	-11(2)	-7(2)
C(40)	47(3)	26(2)	33(3)	5(2)	-10(2)	-3(2)
C(41)	53(3)	28(2)	40(3)	2(2)	-12(2)	-1(2)
C(42)	53(3)	35(3)	35(3)	-3(2)	-8(2)	-3(2)
C(43)	50(3)	37(3)	37(3)	1(2)	-10(2)	-5(2)
C(44)	52(3)	43(3)	39(3)	2(2)	-11(2)	-9(2)
C(45)	49(3)	36(3)	42(3)	5(2)	-13(2)	-8(2)
C(46)	46(3)	27(2)	30(3)	0(2)	-8(2)	1(2)
C(47)	49(3)	35(3)	46(3)	-1(2)	-11(2)	0(2)
C(48)	54(3)	37(3)	46(3)	-3(2)	-11(2)	9(2)
C(49)	74(4)	25(2)	38(3)	1(2)	-6(3)	6(2)
C(50)	63(4)	29(3)	51(3)	-2(2)	-3(3)	-6(2)
C(51)	52(3)	29(2)	38(3)	-2(2)	-7(2)	-4(2)
C(52)	67(4)	31(3)	48(3)	2(2)	-27(3)	-8(2)
C(53)	61(4)	59(4)	65(4)	19(3)	-27(3)	-17(3)
C(54)	78(5)	90(6)	88(6)	48(5)	-27(4)	-33(4)
C(55)	93(6)	57(4)	102(6)	26(4)	-65(5)	-15(4)
C(56)	81(5)	42(3)	73(5)	4(3)	-34(4)	1(3)
C(57)	78(4)	36(3)	55(4)	-4(3)	-32(3)	10(3)
C(58)	48(3)	27(2)	30(3)	-2(2)	-11(2)	-6(2)
C(59)	43(3)	25(2)	37(3)	-2(2)	-5(2)	-3(2)
C(60)	45(3)	30(2)	37(3)	4(2)	-7(2)	-3(2)
C(61)	42(3)	30(3)	46(3)	-1(2)	-7(2)	0(2)
C(62)	43(3)	28(2)	40(3)	-3(2)	1(2)	-4(2)
C(63)	56(3)	26(2)	29(3)	-1(2)	-6(2)	3(2)
C(64)	43(3)	26(2)	35(3)	-1(2)	-9(2)	-1(2)
C(65)	44(3)	23(2)	39(3)	-1(2)	-4(2)	-4(2)
C(66)	52(3)	40(3)	41(3)	-2(2)	-9(2)	5(2)
C(67)	55(4)	45(3)	62(4)	-3(3)	-13(3)	13(3)
C(68)	55(4)	39(3)	65(4)	-5(3)	5(3)	4(2)
C(69)	65(4)	35(3)	44(3)	-2(2)	5(3)	-2(2)
C(70)	52(3)	31(3)	41(3)	3(2)	-4(2)	-1(2)
C(71)	48(3)	28(2)	38(3)	2(2)	-5(2)	-4(2)
C(72)	53(3)	33(3)	58(4)	4(2)	-19(3)	2(2)
C(73)	58(4)	33(3)	74(4)	5(3)	-18(3)	5(2)
C(74)	62(4)	27(3)	57(4)	1(2)	0(3)	4(2)
C(75)	56(3)	36(3)	45(3)	-2(2)	-4(2)	-4(2)
C(76)	48(3)	30(2)	39(3)	1(2)	-5(2)	5(2)
C(77)	41(3)	32(3)	40(3)	1(2)	-3(2)	3(2)
C(78)	46(3)	28(2)	41(3)	-4(2)	-2(2)	2(2)
C(79)	65(4)	51(3)	54(4)	-19(3)	10(3)	-21(3)
C(80)	69(4)	56(4)	56(4)	-13(3)	20(3)	-8(3)
C(81)	66(4)	44(3)	42(3)	-4(3)	-1(3)	7(3)
C(82)	45(3)	64(4)	47(4)	-6(3)	-11(3)	1(3)
C(83)	43(3)	59(4)	43(3)	-3(3)	0(2)	3(2)

C(84)	38(3)	35(3)	38(3)	2(2)	-7(2)	1(2)
C(85)	49(3)	41(3)	45(3)	6(2)	-6(2)	1(2)
C(86)	46(3)	58(4)	48(3)	8(3)	2(2)	-2(2)
C(87)	57(4)	59(4)	53(4)	17(3)	-8(3)	-14(3)
C(88)	73(4)	36(3)	55(4)	8(3)	-15(3)	-11(3)
C(89)	56(3)	37(3)	41(3)	-1(2)	-10(2)	-4(2)
C(90)	41(3)	35(3)	54(3)	-3(2)	1(2)	-2(2)
C(91)	37(3)	56(4)	59(4)	2(3)	-4(2)	-11(2)
C(92)	50(4)	80(5)	54(4)	-14(3)	-1(3)	-2(3)
C(93)	55(5)	157(9)	78(6)	-50(6)	0(4)	-15(5)
C(94)	79(6)	211(13)	47(5)	15(7)	-9(4)	-39(7)
C(95)	120(8)	145(10)	82(7)	27(7)	-36(6)	-68(7)
C(96)	93(5)	78(5)	73(5)	28(4)	-37(4)	-37(4)
C(97)	43(3)	31(3)	60(4)	1(2)	3(2)	1(2)
C(98)	49(3)	51(3)	59(4)	1(3)	-2(3)	-4(2)
C(99)	61(4)	59(4)	59(4)	11(3)	2(3)	0(3)
C(100)	60(4)	53(4)	61(4)	9(3)	11(3)	-4(3)
C(101)	47(4)	40(3)	89(5)	0(3)	4(3)	-6(2)
C(102)	45(3)	39(3)	63(4)	-4(3)	5(3)	-3(2)
C(103)	64(4)	58(4)	64(4)	-19(3)	-19(3)	14(3)
C(104)	50(4)	77(5)	55(4)	-6(3)	-10(3)	-5(3)
C(105)	43(4)	63(4)	99(6)	-30(4)	6(3)	6(3)
C(106)	50(4)	94(5)	68(5)	-16(4)	4(3)	13(3)
C(107)	44(4)	105(6)	54(4)	-38(4)	2(3)	-2(3)
C(108)	77(5)	99(6)	91(6)	-51(5)	23(4)	-10(4)
C(109)	69(5)	85(5)	82(5)	-35(4)	5(4)	-7(4)
C(116)	41(3)	28(2)	38(3)	1(2)	-1(2)	2(2)
C(117)	45(3)	26(2)	35(3)	-1(2)	-2(2)	-4(2)
C(118)	45(3)	43(3)	39(3)	4(2)	-3(2)	1(2)
C(119)	48(3)	52(3)	42(3)	6(3)	7(2)	3(2)
C(120)	58(3)	40(3)	31(3)	2(2)	2(2)	-3(2)
C(121)	46(3)	45(3)	37(3)	7(2)	-5(2)	-1(2)
C(122)	36(3)	46(3)	43(3)	-7(2)	0(2)	-4(2)
C(123)	43(3)	31(3)	37(3)	3(2)	1(2)	2(2)
C(124)	50(3)	39(3)	42(3)	-1(2)	-4(2)	-2(2)
C(125)	55(4)	50(3)	42(3)	4(3)	4(2)	1(3)
C(126)	43(3)	37(3)	62(4)	7(3)	9(3)	-1(2)
C(127)	63(4)	38(3)	65(4)	-11(3)	7(3)	-10(3)
C(128)	59(4)	37(3)	44(3)	-6(2)	7(2)	-10(2)

Table 5. Bond lengths [Å] and angles [°] for **V-6**.

Rh(1)-N(7)	2.036(4)	N(2)-C(1)	1.329(6)
Rh(1)-N(3)	2.042(4)	N(2)-C(14)	1.428(7)
Rh(1)-N(5)	2.062(4)	N(3)-C(20)	1.336(6)
Rh(1)-N(1)	2.070(4)	N(3)-C(27)	1.420(6)
Rh(1)-Rh(2)	2.3918(5)	N(4)-C(20)	1.322(6)
Rh(2)-N(2)	2.045(4)	N(4)-C(33)	1.426(6)
Rh(2)-N(6)	2.045(4)	N(5)-C(39)	1.319(6)
Rh(2)-N(4)	2.071(4)	N(5)-C(46)	1.435(6)
Rh(2)-N(8)	2.081(4)	N(6)-C(39)	1.325(6)
N(1)-C(1)	1.330(6)	N(6)-C(52)	1.402(6)
N(1)-C(8)	1.425(6)	N(7)-C(58)	1.336(6)

N(7)-C(65)	1.420(6)	C(28)-C(29)	1.391(7)
N(8)-C(58)	1.329(6)	C(28)-H(28)	0.9500
N(8)-C(71)	1.420(6)	C(29)-C(30)	1.393(9)
N(9)-C(77)	1.293(6)	C(29)-H(29)	0.9500
N(9)-C(5)	1.427(6)	C(30)-C(31)	1.348(9)
N(10)-C(90)	1.277(7)	C(30)-H(30)	0.9500
N(10)-C(24)	1.423(7)	C(31)-C(32)	1.404(8)
N(11)-C(103)	1.237(8)	C(31)-H(31)	0.9500
N(11)-C(43)	1.437(7)	C(32)-H(32)	0.9500
N(12)-C(116)	1.287(6)	C(33)-C(38)	1.378(7)
N(12)-C(62)	1.413(6)	C(33)-C(34)	1.403(8)
C(1)-C(2)	1.485(7)	C(34)-C(35)	1.384(8)
C(2)-C(7)	1.403(7)	C(34)-H(34)	0.9500
C(2)-C(3)	1.395(7)	C(35)-C(36)	1.405(9)
C(3)-C(4)	1.377(7)	C(35)-H(35)	0.9500
C(3)-H(3)	0.9500	C(36)-C(37)	1.363(9)
C(4)-C(5)	1.391(7)	C(36)-H(36)	0.9500
C(4)-H(4)	0.9500	C(37)-C(38)	1.387(7)
C(5)-C(6)	1.384(7)	C(37)-H(37)	0.9500
C(6)-C(7)	1.374(7)	C(38)-H(38)	0.9500
C(6)-H(6)	0.9500	C(39)-C(40)	1.498(7)
C(7)-H(7)	0.9500	C(40)-C(45)	1.376(7)
C(8)-C(13)	1.382(7)	C(40)-C(41)	1.407(7)
C(8)-C(9)	1.392(6)	C(41)-C(42)	1.392(7)
C(9)-C(10)	1.390(7)	C(41)-H(41)	0.9500
C(9)-H(9)	0.9500	C(42)-C(43)	1.390(7)
C(10)-C(11)	1.369(7)	C(43)-C(44)	1.404(7)
C(10)-H(10)	0.9500	C(44)-C(45)	1.402(7)
C(11)-C(12)	1.376(7)	C(45)-H(45)	0.9500
C(11)-H(11)	0.9500	C(46)-C(47)	1.384(7)
C(12)-C(13)	1.389(7)	C(46)-C(51)	1.393(7)
C(12)-H(12)	0.9500	C(47)-C(48)	1.381(7)
C(13)-H(13)	0.9500	C(47)-H(47)	0.9500
C(14)-C(15)	1.388(8)	C(48)-C(49)	1.381(8)
C(14)-C(19)	1.395(7)	C(48)-H(48)	0.9500
C(15)-C(16)	1.392(8)	C(49)-C(50)	1.366(8)
C(15)-H(15)	0.9500	C(49)-H(49)	0.9500
C(16)-C(17)	1.358(9)	C(50)-C(51)	1.397(7)
C(16)-H(16)	0.9500	C(50)-H(50)	0.9500
C(17)-C(18)	1.374(10)	C(51)-H(51)	0.9500
C(17)-H(17)	0.9500	C(52)-C(53)	1.375(9)
C(18)-C(19)	1.414(9)	C(52)-C(57)	1.396(8)
C(18)-H(18)	0.9500	C(53)-C(54)	1.404(9)
C(19)-H(19)	0.9500	C(53)-H(53)	0.9500
C(20)-C(21)	1.486(7)	C(54)-C(55)	1.414(11)
C(21)-C(26)	1.384(8)	C(54)-H(54)	0.9500
C(21)-C(22)	1.409(7)	C(55)-C(56)	1.354(11)
C(22)-C(23)	1.376(7)	C(55)-H(55)	0.9500
C(22)-H(22)	0.9500	C(56)-C(57)	1.361(8)
C(23)-C(24)	1.379(8)	C(56)-H(56)	0.9500
C(23)-H(23)	0.9500	C(57)-H(57)	0.9500
C(24)-C(25)	1.398(8)	C(58)-C(59)	1.489(7)
C(25)-C(26)	1.378(8)	C(59)-C(60)	1.406(7)
C(25)-H(25)	0.9500	C(59)-C(64)	1.399(6)
C(26)-H(26)	0.9500	C(60)-C(61)	1.379(7)
C(27)-C(28)	1.387(8)	C(60)-H(60)	0.9500
C(27)-C(32)	1.394(8)	C(61)-C(62)	1.397(7)

C(61)-H(61)	0.9500	C(93)-C(94)	1.431(14)
C(62)-C(63)	1.387(7)	C(93)-H(93)	0.9500
C(63)-C(64)	1.389(7)	C(94)-C(95)	1.346(15)
C(63)-H(63)	0.9500	C(94)-H(94)	0.9500
C(64)-H(64)	0.9500	C(95)-C(96)	1.318(12)
C(65)-C(66)	1.391(7)	C(95)-H(95)	0.9500
C(65)-C(70)	1.392(7)	C(96)-H(96)	0.9500
C(66)-C(67)	1.379(8)	C(97)-C(98)	1.400(8)
C(66)-H(66)	0.9500	C(97)-C(102)	1.399(7)
C(67)-C(68)	1.390(8)	C(98)-C(99)	1.376(8)
C(67)-H(67)	0.9500	C(98)-H(98)	0.9500
C(68)-C(69)	1.385(8)	C(99)-C(100)	1.350(9)
C(68)-H(68)	0.9500	C(99)-H(99)	0.9500
C(69)-C(70)	1.398(7)	C(100)-C(101)	1.387(9)
C(69)-H(69)	0.9500	C(100)-H(100)	0.9500
C(70)-H(70)	0.9500	C(101)-C(102)	1.386(8)
C(71)-C(76)	1.388(7)	C(101)-H(101)	0.9500
C(71)-C(72)	1.402(7)	C(102)-H(102)	0.9500
C(72)-C(73)	1.387(7)	C(103)-C(104)	1.530(8)
C(72)-H(72)	0.9500	C(103)-C(110)	1.505(7)
C(73)-C(74)	1.382(8)	C(104)-C(109)	1.358(9)
C(73)-H(73)	0.9500	C(104)-C(105)	1.378(10)
C(74)-C(75)	1.389(8)	C(105)-C(106)	1.437(9)
C(74)-H(74)	0.9500	C(105)-H(105)	0.9500
C(75)-C(76)	1.386(7)	C(106)-C(107)	1.353(10)
C(75)-H(75)	0.9500	C(106)-H(106)	0.9500
C(76)-H(76)	0.9500	C(107)-C(108)	1.377(11)
C(77)-C(78)	1.491(7)	C(107)-H(107)	0.9500
C(77)-C(84)	1.503(7)	C(108)-C(109)	1.385(10)
C(78)-C(79)	1.364(8)	C(108)-H(108)	0.9500
C(78)-C(83)	1.388(7)	C(109)-H(109)	0.9500
C(79)-C(80)	1.388(8)	C(110)-C(111)	1.3900
C(79)-H(79)	0.9500	C(110)-C(115)	1.3900
C(80)-C(81)	1.404(9)	C(111)-C(112)	1.3900
C(80)-H(80)	0.9500	C(112)-C(113)	1.3900
C(81)-C(82)	1.362(8)	C(113)-C(114)	1.3900
C(81)-H(81)	0.9500	C(114)-C(115)	1.3900
C(82)-C(83)	1.398(8)	C(116)-C(123)	1.492(7)
C(82)-H(82)	0.9500	C(116)-C(117)	1.501(7)
C(83)-H(83)	0.9500	C(117)-C(118)	1.389(7)
C(84)-C(89)	1.389(7)	C(117)-C(122)	1.407(7)
C(84)-C(85)	1.404(7)	C(118)-C(119)	1.396(7)
C(85)-C(86)	1.386(8)	C(118)-H(118)	0.9500
C(85)-H(85)	0.9500	C(119)-C(120)	1.388(7)
C(86)-C(87)	1.397(8)	C(119)-H(119)	0.9500
C(86)-H(86)	0.9500	C(120)-C(121)	1.376(7)
C(87)-C(88)	1.379(9)	C(120)-H(120)	0.9500
C(87)-H(87)	0.9500	C(121)-C(122)	1.389(7)
C(88)-C(89)	1.390(8)	C(121)-H(121)	0.9500
C(88)-H(88)	0.9500	C(122)-H(122)	0.9500
C(89)-H(89)	0.9500	C(123)-C(128)	1.382(7)
C(90)-C(91)	1.490(8)	C(123)-C(124)	1.390(7)
C(90)-C(97)	1.498(7)	C(124)-C(125)	1.384(7)
C(91)-C(96)	1.367(9)	C(124)-H(124)	0.9500
C(91)-C(92)	1.392(8)	C(125)-C(126)	1.364(8)
C(92)-C(93)	1.393(10)	C(125)-H(125)	0.9500
C(92)-H(92)	0.9500	C(126)-C(127)	1.369(8)

C(126)-H(126)	0.9500	C(7)-C(2)-C(1)	119.5(4)
C(127)-C(128)	1.376(8)	C(3)-C(2)-C(1)	122.2(4)
C(127)-H(127)	0.9500	C(4)-C(3)-C(2)	121.0(5)
C(128)-H(128)	0.9500	C(4)-C(3)-H(3)	119.5
		C(2)-C(3)-H(3)	119.5
N(7)-Rh(1)-N(3)	176.37(15)	C(3)-C(4)-C(5)	119.6(5)
N(7)-Rh(1)-N(5)	89.17(16)	C(3)-C(4)-H(4)	120.2
N(3)-Rh(1)-N(5)	90.16(16)	C(5)-C(4)-H(4)	120.2
N(7)-Rh(1)-N(1)	90.44(16)	C(6)-C(5)-C(4)	120.3(5)
N(3)-Rh(1)-N(1)	89.87(16)	C(6)-C(5)-N(9)	116.4(5)
N(5)-Rh(1)-N(1)	174.08(15)	C(4)-C(5)-N(9)	123.2(4)
N(7)-Rh(1)-Rh(2)	88.39(11)	C(7)-C(6)-C(5)	119.8(5)
N(3)-Rh(1)-Rh(2)	88.02(11)	C(7)-C(6)-H(6)	120.1
N(5)-Rh(1)-Rh(2)	87.68(11)	C(5)-C(6)-H(6)	120.1
N(1)-Rh(1)-Rh(2)	86.41(11)	C(6)-C(7)-C(2)	120.9(5)
N(2)-Rh(2)-N(6)	176.26(15)	C(6)-C(7)-H(7)	119.6
N(2)-Rh(2)-N(4)	89.30(17)	C(2)-C(7)-H(7)	119.6
N(6)-Rh(2)-N(4)	89.53(17)	C(13)-C(8)-C(9)	119.1(5)
N(2)-Rh(2)-N(8)	90.43(16)	C(13)-C(8)-N(1)	120.1(4)
N(6)-Rh(2)-N(8)	90.36(16)	C(9)-C(8)-N(1)	120.7(4)
N(4)-Rh(2)-N(8)	173.98(15)	C(10)-C(9)-C(8)	119.9(5)
N(2)-Rh(2)-Rh(1)	88.85(11)	C(10)-C(9)-H(9)	120.1
N(6)-Rh(2)-Rh(1)	87.54(11)	C(8)-C(9)-H(9)	120.1
N(4)-Rh(2)-Rh(1)	86.97(11)	C(11)-C(10)-C(9)	120.6(5)
N(8)-Rh(2)-Rh(1)	87.01(10)	C(11)-C(10)-H(10)	119.7
C(1)-N(1)-C(8)	120.5(4)	C(9)-C(10)-H(10)	119.7
C(1)-N(1)-Rh(1)	119.9(3)	C(10)-C(11)-C(12)	119.8(5)
C(8)-N(1)-Rh(1)	118.6(3)	C(10)-C(11)-H(11)	120.1
C(1)-N(2)-C(14)	121.7(4)	C(12)-C(11)-H(11)	120.1
C(1)-N(2)-Rh(2)	119.3(3)	C(11)-C(12)-C(13)	120.4(5)
C(14)-N(2)-Rh(2)	116.6(3)	C(11)-C(12)-H(12)	119.8
C(20)-N(3)-C(27)	123.2(4)	C(13)-C(12)-H(12)	119.8
C(20)-N(3)-Rh(1)	120.5(3)	C(8)-C(13)-C(12)	120.2(5)
C(27)-N(3)-Rh(1)	115.6(3)	C(8)-C(13)-H(13)	119.9
C(20)-N(4)-C(33)	120.7(4)	C(12)-C(13)-H(13)	119.9
C(20)-N(4)-Rh(2)	120.6(3)	C(15)-C(14)-C(19)	119.1(5)
C(33)-N(4)-Rh(2)	118.1(3)	C(15)-C(14)-N(2)	120.8(5)
C(39)-N(5)-C(46)	121.8(4)	C(19)-C(14)-N(2)	119.8(5)
C(39)-N(5)-Rh(1)	119.8(3)	C(14)-C(15)-C(16)	120.4(6)
C(46)-N(5)-Rh(1)	117.2(3)	C(14)-C(15)-H(15)	119.8
C(39)-N(6)-C(52)	124.6(5)	C(16)-C(15)-H(15)	119.8
C(39)-N(6)-Rh(2)	120.2(3)	C(17)-C(16)-C(15)	121.2(7)
C(52)-N(6)-Rh(2)	114.4(3)	C(17)-C(16)-H(16)	119.4
C(58)-N(7)-C(65)	123.0(4)	C(15)-C(16)-H(16)	119.4
C(58)-N(7)-Rh(1)	119.9(3)	C(16)-C(17)-C(18)	119.3(6)
C(65)-N(7)-Rh(1)	116.3(3)	C(16)-C(17)-H(17)	120.4
C(58)-N(8)-C(71)	121.9(4)	C(18)-C(17)-H(17)	120.4
C(58)-N(8)-Rh(2)	119.2(3)	C(17)-C(18)-C(19)	121.2(6)
C(71)-N(8)-Rh(2)	117.4(3)	C(17)-C(18)-H(18)	119.4
C(77)-N(9)-C(5)	122.6(4)	C(19)-C(18)-H(18)	119.4
C(90)-N(10)-C(24)	121.1(5)	C(14)-C(19)-C(18)	118.8(6)
C(103)-N(11)-C(43)	123.5(5)	C(14)-C(19)-H(19)	120.6
C(116)-N(12)-C(62)	122.5(4)	C(18)-C(19)-H(19)	120.6
N(1)-C(1)-N(2)	120.0(4)	N(4)-C(20)-N(3)	118.8(4)
N(1)-C(1)-C(2)	120.4(4)	N(4)-C(20)-C(21)	121.1(4)
N(2)-C(1)-C(2)	119.7(4)	N(3)-C(20)-C(21)	120.1(4)
C(7)-C(2)-C(3)	118.2(5)	C(26)-C(21)-C(22)	117.9(5)

C(26)-C(21)-C(20)	121.3(5)	C(45)-C(40)-C(39)	122.6(4)
C(22)-C(21)-C(20)	120.7(5)	C(41)-C(40)-C(39)	118.1(5)
C(23)-C(22)-C(21)	120.2(5)	C(42)-C(41)-C(40)	120.4(5)
C(23)-C(22)-H(22)	119.9	C(42)-C(41)-H(41)	119.8
C(21)-C(22)-H(22)	119.9	C(40)-C(41)-H(41)	119.8
C(22)-C(23)-C(24)	121.1(5)	C(41)-C(42)-C(43)	119.8(5)
C(22)-C(23)-H(23)	119.4	C(42)-C(43)-C(44)	120.2(5)
C(24)-C(23)-H(23)	119.4	C(42)-C(43)-N(11)	122.4(5)
C(23)-C(24)-C(25)	119.3(5)	C(44)-C(43)-N(11)	117.4(5)
C(23)-C(24)-N(10)	124.0(5)	C(45)-C(44)-C(43)	119.1(5)
C(25)-C(24)-N(10)	116.6(5)	C(40)-C(45)-C(44)	121.1(5)
C(26)-C(25)-C(24)	119.4(6)	C(40)-C(45)-H(45)	119.5
C(26)-C(25)-H(25)	120.3	C(44)-C(45)-H(45)	119.5
C(24)-C(25)-H(25)	120.3	C(47)-C(46)-C(51)	119.4(4)
C(25)-C(26)-C(21)	122.0(5)	C(47)-C(46)-N(5)	119.6(4)
C(25)-C(26)-H(26)	119.0	C(51)-C(46)-N(5)	120.8(4)
C(21)-C(26)-H(26)	119.0	C(46)-C(47)-C(48)	120.3(5)
C(28)-C(27)-C(32)	118.8(5)	C(46)-C(47)-H(47)	119.8
C(28)-C(27)-N(3)	117.9(5)	C(48)-C(47)-H(47)	119.8
C(32)-C(27)-N(3)	123.0(5)	C(47)-C(48)-C(49)	120.4(5)
C(27)-C(28)-C(29)	120.6(6)	C(47)-C(48)-H(48)	119.8
C(27)-C(28)-H(28)	119.7	C(49)-C(48)-H(48)	119.8
C(29)-C(28)-H(28)	119.7	C(50)-C(49)-C(48)	119.7(5)
C(30)-C(29)-C(28)	120.0(6)	C(50)-C(49)-H(49)	120.2
C(30)-C(29)-H(29)	120.0	C(48)-C(49)-H(49)	120.2
C(28)-C(29)-H(29)	120.0	C(49)-C(50)-C(51)	120.7(5)
C(31)-C(30)-C(29)	119.6(5)	C(49)-C(50)-H(50)	119.6
C(31)-C(30)-H(30)	120.2	C(51)-C(50)-H(50)	119.6
C(29)-C(30)-H(30)	120.2	C(46)-C(51)-C(50)	119.4(5)
C(30)-C(31)-C(32)	121.3(6)	C(46)-C(51)-H(51)	120.3
C(30)-C(31)-H(31)	119.3	C(50)-C(51)-H(51)	120.3
C(32)-C(31)-H(31)	119.3	C(53)-C(52)-C(57)	118.8(6)
C(27)-C(32)-C(31)	119.6(6)	C(53)-C(52)-N(6)	121.4(6)
C(27)-C(32)-H(32)	120.2	C(57)-C(52)-N(6)	119.5(6)
C(31)-C(32)-H(32)	120.2	C(52)-C(53)-C(54)	120.9(7)
C(38)-C(33)-C(34)	118.5(5)	C(52)-C(53)-H(53)	119.5
C(38)-C(33)-N(4)	121.8(5)	C(54)-C(53)-H(53)	119.5
C(34)-C(33)-N(4)	119.6(5)	C(53)-C(54)-C(55)	116.9(7)
C(35)-C(34)-C(33)	120.6(6)	C(53)-C(54)-H(54)	121.6
C(35)-C(34)-H(34)	119.7	C(55)-C(54)-H(54)	121.6
C(33)-C(34)-H(34)	119.7	C(56)-C(55)-C(54)	122.6(7)
C(34)-C(35)-C(36)	119.8(6)	C(56)-C(55)-H(55)	118.7
C(34)-C(35)-H(35)	120.1	C(54)-C(55)-H(55)	118.7
C(36)-C(35)-H(35)	120.1	C(55)-C(56)-C(57)	118.7(7)
C(37)-C(36)-C(35)	119.2(6)	C(55)-C(56)-H(56)	120.6
C(37)-C(36)-H(36)	120.4	C(57)-C(56)-H(56)	120.6
C(35)-C(36)-H(36)	120.4	C(56)-C(57)-C(52)	122.0(7)
C(36)-C(37)-C(38)	121.1(6)	C(56)-C(57)-H(57)	119.0
C(36)-C(37)-H(37)	119.4	C(52)-C(57)-H(57)	119.0
C(38)-C(37)-H(37)	119.4	N(8)-C(58)-N(7)	120.0(4)
C(33)-C(38)-C(37)	120.7(5)	N(8)-C(58)-C(59)	120.7(4)
C(33)-C(38)-H(38)	119.6	N(7)-C(58)-C(59)	119.2(4)
C(37)-C(38)-H(38)	119.6	C(60)-C(59)-C(64)	118.8(4)
N(5)-C(39)-N(6)	120.1(4)	C(60)-C(59)-C(58)	119.4(4)
N(5)-C(39)-C(40)	120.8(4)	C(64)-C(59)-C(58)	121.8(4)
N(6)-C(39)-C(40)	119.1(4)	C(61)-C(60)-C(59)	120.4(5)
C(45)-C(40)-C(41)	119.3(5)	C(61)-C(60)-H(60)	119.8

C(59)-C(60)-H(60)	119.8	C(80)-C(79)-H(79)	119.3
C(60)-C(61)-C(62)	120.9(5)	C(79)-C(80)-C(81)	119.7(6)
C(60)-C(61)-H(61)	119.5	C(79)-C(80)-H(80)	120.1
C(62)-C(61)-H(61)	119.5	C(81)-C(80)-H(80)	120.1
C(63)-C(62)-C(61)	118.3(4)	C(82)-C(81)-C(80)	119.0(6)
C(63)-C(62)-N(12)	118.1(4)	C(82)-C(81)-H(81)	120.5
C(61)-C(62)-N(12)	123.6(4)	C(80)-C(81)-H(81)	120.5
C(64)-C(63)-C(62)	121.5(5)	C(81)-C(82)-C(83)	120.8(5)
C(64)-C(63)-H(63)	119.3	C(81)-C(82)-H(82)	119.6
C(62)-C(63)-H(63)	119.3	C(83)-C(82)-H(82)	119.6
C(63)-C(64)-C(59)	119.7(4)	C(78)-C(83)-C(82)	120.3(5)
C(63)-C(64)-H(64)	120.1	C(78)-C(83)-H(83)	119.9
C(59)-C(64)-H(64)	120.1	C(82)-C(83)-H(83)	119.9
C(66)-C(65)-C(70)	118.7(5)	C(89)-C(84)-C(85)	119.3(5)
C(66)-C(65)-N(7)	119.6(5)	C(89)-C(84)-C(77)	119.1(5)
C(70)-C(65)-N(7)	121.4(4)	C(85)-C(84)-C(77)	121.6(4)
C(67)-C(66)-C(65)	120.4(5)	C(86)-C(85)-C(84)	119.9(5)
C(67)-C(66)-H(66)	119.8	C(86)-C(85)-H(85)	120.1
C(65)-C(66)-H(66)	119.8	C(84)-C(85)-H(85)	120.1
C(66)-C(67)-C(68)	121.2(5)	C(85)-C(86)-C(87)	120.5(6)
C(66)-C(67)-H(67)	119.4	C(85)-C(86)-H(86)	119.8
C(68)-C(67)-H(67)	119.4	C(87)-C(86)-H(86)	119.8
C(69)-C(68)-C(67)	119.0(5)	C(88)-C(87)-C(86)	119.3(5)
C(69)-C(68)-H(68)	120.5	C(88)-C(87)-H(87)	120.3
C(67)-C(68)-H(68)	120.5	C(86)-C(87)-H(87)	120.3
C(68)-C(69)-C(70)	120.0(5)	C(87)-C(88)-C(89)	120.8(5)
C(68)-C(69)-H(69)	120.0	C(87)-C(88)-H(88)	119.6
C(70)-C(69)-H(69)	120.0	C(89)-C(88)-H(88)	119.6
C(69)-C(70)-C(65)	120.7(5)	C(88)-C(89)-C(84)	120.1(5)
C(69)-C(70)-H(70)	119.6	C(88)-C(89)-H(89)	119.9
C(65)-C(70)-H(70)	119.6	C(84)-C(89)-H(89)	119.9
C(76)-C(71)-C(72)	118.3(5)	N(10)-C(90)-C(91)	123.3(5)
C(76)-C(71)-N(8)	123.1(4)	N(10)-C(90)-C(97)	116.8(5)
C(72)-C(71)-N(8)	118.5(4)	C(91)-C(90)-C(97)	119.8(5)
C(73)-C(72)-C(71)	120.2(5)	C(96)-C(91)-C(92)	120.1(7)
C(73)-C(72)-H(72)	119.9	C(96)-C(91)-C(90)	118.9(6)
C(71)-C(72)-H(72)	119.9	C(92)-C(91)-C(90)	120.9(6)
C(74)-C(73)-C(72)	121.1(5)	C(91)-C(92)-C(93)	119.2(8)
C(74)-C(73)-H(73)	119.4	C(91)-C(92)-H(92)	120.4
C(72)-C(73)-H(73)	119.4	C(93)-C(92)-H(92)	120.4
C(73)-C(74)-C(75)	118.7(5)	C(92)-C(93)-C(94)	117.7(9)
C(73)-C(74)-H(74)	120.6	C(92)-C(93)-H(93)	121.1
C(75)-C(74)-H(74)	120.6	C(94)-C(93)-H(93)	121.1
C(76)-C(75)-C(74)	120.6(5)	C(95)-C(94)-C(93)	119.9(9)
C(76)-C(75)-H(75)	119.7	C(95)-C(94)-H(94)	120.1
C(74)-C(75)-H(75)	119.7	C(93)-C(94)-H(94)	120.1
C(71)-C(76)-C(75)	121.0(5)	C(96)-C(95)-C(94)	121.9(11)
C(71)-C(76)-H(76)	119.5	C(96)-C(95)-H(95)	119.1
C(75)-C(76)-H(76)	119.5	C(94)-C(95)-H(95)	119.1
N(9)-C(77)-C(78)	116.9(5)	C(95)-C(96)-C(91)	121.2(9)
N(9)-C(77)-C(84)	125.5(5)	C(95)-C(96)-H(96)	119.4
C(78)-C(77)-C(84)	117.6(4)	C(91)-C(96)-H(96)	119.4
C(79)-C(78)-C(83)	118.8(5)	C(98)-C(97)-C(102)	118.6(5)
C(79)-C(78)-C(77)	119.7(5)	C(98)-C(97)-C(90)	119.4(5)
C(83)-C(78)-C(77)	121.4(5)	C(102)-C(97)-C(90)	121.8(5)
C(78)-C(79)-C(80)	121.4(6)	C(99)-C(98)-C(97)	120.9(6)
C(78)-C(79)-H(79)	119.3	C(99)-C(98)-H(98)	119.5

C(97)-C(98)-H(98)	119.5
C(100)-C(99)-C(98)	120.0(6)
C(100)-C(99)-H(99)	120.0
C(98)-C(99)-H(99)	120.0
C(99)-C(100)-C(101)	120.8(6)
C(99)-C(100)-H(100)	119.6
C(101)-C(100)-H(100)	119.6
C(100)-C(101)-C(102)	120.2(6)
C(100)-C(101)-H(101)	119.9
C(102)-C(101)-H(101)	119.9
C(101)-C(102)-C(97)	119.3(6)
C(101)-C(102)-H(102)	120.4
C(97)-C(102)-H(102)	120.4
N(11)-C(103)-C(104)	117.4(6)
N(11)-C(103)-C(110)	124.8(5)
C(104)-C(103)-C(110)	117.7(5)
C(109)-C(104)-C(105)	121.5(7)
C(109)-C(104)-C(103)	120.5(7)
C(105)-C(104)-C(103)	117.9(6)
C(104)-C(105)-C(106)	119.8(6)
C(104)-C(105)-H(105)	120.1
C(106)-C(105)-H(105)	120.1
C(107)-C(106)-C(105)	117.4(7)
C(107)-C(106)-H(106)	121.3
C(105)-C(106)-H(106)	121.3
C(106)-C(107)-C(108)	121.6(7)
C(106)-C(107)-H(107)	119.2
C(108)-C(107)-H(107)	119.2
C(107)-C(108)-C(109)	121.2(7)
C(107)-C(108)-H(108)	119.4
C(109)-C(108)-H(108)	119.4
C(104)-C(109)-C(108)	118.4(8)
C(104)-C(109)-H(109)	120.8
C(108)-C(109)-H(109)	120.8
C(111)-C(110)-C(115)	120.0
C(111)-C(110)-C(103)	116.7(4)
C(115)-C(110)-C(103)	123.3(4)
C(112)-C(111)-C(110)	120.0
C(111)-C(112)-C(113)	120.0
C(114)-C(113)-C(112)	120.0
C(113)-C(114)-C(115)	120.0
C(114)-C(115)-C(110)	120.0
N(12)-C(116)-C(123)	118.2(5)
N(12)-C(116)-C(117)	125.2(4)
C(123)-C(116)-C(117)	116.6(4)
C(118)-C(117)-C(122)	118.8(5)
C(118)-C(117)-C(116)	120.8(4)
C(122)-C(117)-C(116)	120.3(4)
C(119)-C(118)-C(117)	120.2(5)
C(119)-C(118)-H(118)	119.9
C(117)-C(118)-H(118)	119.9
C(118)-C(119)-C(120)	120.6(5)
C(118)-C(119)-H(119)	119.7
C(120)-C(119)-H(119)	119.7
C(121)-C(120)-C(119)	119.5(5)
C(121)-C(120)-H(120)	120.3
C(119)-C(120)-H(120)	120.3
C(120)-C(121)-C(122)	120.7(5)
C(120)-C(121)-H(121)	119.7
C(122)-C(121)-H(121)	119.7
C(121)-C(122)-C(117)	120.2(5)
C(121)-C(122)-H(122)	119.9
C(117)-C(122)-H(122)	119.9
C(128)-C(123)-C(124)	118.3(5)
C(128)-C(123)-C(116)	121.3(5)
C(124)-C(123)-C(116)	120.4(5)
C(125)-C(124)-C(123)	120.1(5)
C(125)-C(124)-H(124)	119.9
C(123)-C(124)-H(124)	119.9
C(126)-C(125)-C(124)	120.7(5)
C(126)-C(125)-H(125)	119.7
C(124)-C(125)-H(125)	119.7
C(127)-C(126)-C(125)	119.5(5)
C(127)-C(126)-H(126)	120.2
C(125)-C(126)-H(126)	120.2
C(126)-C(127)-C(128)	120.6(5)
C(126)-C(127)-H(127)	119.7
C(128)-C(127)-H(127)	119.7
C(127)-C(128)-C(123)	120.7(5)
C(127)-C(128)-H(128)	119.6
C(123)-C(128)-H(128)	119.6

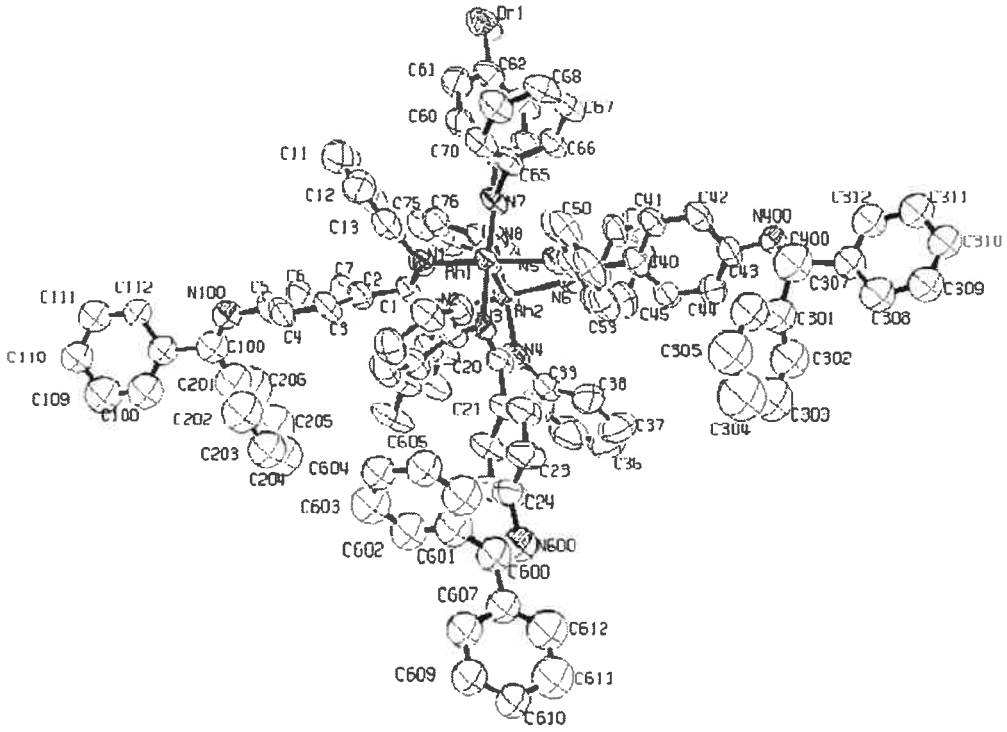

Table 1. Crystal data and structure refinement for **V-7**.

Empirical formula	C131 H126 Br N11 O8 Rh2	
Formula weight	2268.16	
Temperature	100(2)K	
Wavelength	1.54178 Å	
Crystal system	Triclinic	
Space group	P-1	
Unit cell dimensions	a = 13.5486(5) Å	α = 101.660(2)°
	b = 16.2652(6) Å	β = 100.338(2)°
	c = 27.1795(9) Å	γ = 91.572(2)°
Volume	5758.1(4)Å^3	
Z	2	
Density (calculated)	1.308 g/cm^3	
Absorption coefficient	3.216 mm^{-1}	

F(000)	2356
Crystal size	0.00 x 0.00 x 0.00 mm
Theta range for data collection	1.69 to 67.18°
Index ranges	$-16 \leq h \leq 16$, $-19 \leq k \leq 19$, $-32 \leq \ell \leq 32$
Reflections collected	51416
Independent reflections	18328 [R_{int} = 0.045]
Absorption correction	
Max. and min. transmission	0.0000 and 0.0000
Refinement method	Full-matrix least-squares on F^2
Data / restraints / parameters	18328 / 692 / 1128
Goodness-of-fit on F^2	1.019
Final R indices [I>2sigma(I)]	R1 = 0.0993, wR_2 = 0.2518
R indices (all data)	R1 = 0.1464, wR_2 = 0.2967
Extinction coefficient	0.00037(8)
Largest diff. peak and hole	1.957 and -1.571 e/Å^3

Table 2. Atomic coordinates (x 10^4) and equivalent isotropic displacement parameters (Å^2 x 10^3) for **V-7**.

U_{eq} is defined as one third of the trace of the orthogonalized Uij tensor.

	Occ.	x	y	z	U_{eq}
Rh(1)	1	7491(1)	4356(1)	2898(1)	61(1)
Rh(2)	1	6288(1)	5323(1)	2644(1)	62(1)
Br(1)	1	2874(1)	3404(1)	4723(1)	116(1)
N(1)	1	6629(5)	3421(4)	2373(2)	60(2)
N(2)	1	5732(5)	4400(4)	2018(2)	64(2)
N(3)	1	8241(4)	4616(4)	2353(2)	62(2)
N(4)	1	7283(5)	5747(4)	2262(2)	68(2)
N(5)	1	8278(5)	5331(4)	3413(2)	64(2)
N(6)	1	6919(5)	6171(4)	3284(2)	64(2)
N(7)	1	6665(5)	4174(4)	3423(2)	62(2)

N(8)	1	5360(5)	4843(4)	3045(2)	62(2)
C(1)	1	5935(5)	3596(5)	2003(2)	59(2)
C(2)	1	5397(6)	2924(5)	1577(3)	68(2)
C(3)	1	5933(7)	2325(5)	1302(3)	76(2)
C(4)	1	5437(8)	1685(6)	900(3)	87(3)
C(5)	1	4386(8)	1658(6)	767(3)	85(3)
C(6)	1	3857(7)	2232(6)	1038(3)	84(3)
C(7)	1	4368(6)	2847(5)	1440(3)	77(2)
C(8)	1	6670(6)	2600(5)	2471(3)	65(2)
C(9)	1	5807(7)	2168(6)	2534(3)	85(3)
C(10)	1	5892(9)	1376(6)	2661(4)	100(3)
C(11)	1	6816(11)	1035(7)	2720(4)	108(4)
C(12)	1	7645(8)	1451(6)	2667(4)	89(3)
C(13)	1	7573(8)	2234(6)	2536(3)	81(3)
C(14)	1	5236(6)	4661(5)	1573(3)	72(2)
C(15)	1	4434(9)	5140(6)	1590(3)	100(3)
C(16)	1	3917(10)	5374(8)	1163(4)	130(4)
C(17)	1	4233(12)	5187(9)	696(4)	144(5)
C(18)	1	5097(10)	4668(9)	684(3)	129(4)
C(19)	1	5592(8)	4439(6)	1112(3)	90(3)
C(20)	1	8079(6)	5285(5)	2159(3)	66(2)
C(21)	1	8746(6)	5571(5)	1842(3)	68(2)
C(22)	1	9778(7)	5639(6)	2013(3)	85(3)
C(23)	1	10432(7)	5858(6)	1701(3)	94(3)
C(24)	1	10042(8)	6043(7)	1239(3)	94(3)
C(25)	1	9029(8)	5988(7)	1075(3)	100(3)
C(26)	1	8379(8)	5740(6)	1354(3)	89(3)
C(27)	1	8823(6)	3997(5)	2132(3)	71(2)
C(28)	1	8643(6)	3655(5)	1606(3)	74(2)
C(29)	1	9233(8)	3030(6)	1403(3)	89(3)
C(30)	1	9992(7)	2729(6)	1703(4)	90(3)
C(31)	1	10177(6)	3053(6)	2225(3)	82(3)
C(32)	1	9602(6)	3706(5)	2440(3)	74(2)
C(33)	1	7261(7)	6589(6)	2197(3)	73(2)
C(34)	1	6432(10)	6849(7)	1921(4)	106(4)
C(35)	1	6394(13)	7675(9)	1872(4)	139(5)
C(36)	1	7164(18)	8242(9)	2094(6)	180(9)
C(37)	1	8023(15)	8009(8)	2381(6)	158(7)
C(38)	1	8052(9)	7197(6)	2428(4)	101(3)
C(39)	1	7837(6)	6072(5)	3548(3)	63(2)
C(40)	1	8381(6)	6754(5)	3977(3)	66(2)
C(41)	1	8809(6)	6552(5)	4447(3)	64(2)
C(42)	1	9339(6)	7162(5)	4831(3)	67(2)
C(43)	1	9513(6)	7970(5)	4760(3)	71(2)
C(44)	1	9072(6)	8156(5)	4298(3)	74(2)
C(45)	1	8506(6)	7557(5)	3918(3)	70(2)
C(46)	1	9327(6)	5287(5)	3557(3)	64(2)
C(47)	1	10003(6)	5850(6)	3444(3)	75(2)
C(48)	1	11036(7)	5726(6)	3537(3)	85(3)
C(49)	1	11379(7)	5072(7)	3753(3)	92(3)
C(50)	1	10693(8)	4533(6)	3876(3)	88(3)
C(51)	1	9681(7)	4637(6)	3779(3)	76(2)
C(52)	1	6318(6)	6785(5)	3499(3)	69(2)
C(53)	1	5837(7)	7296(6)	3207(4)	85(3)
C(54)	1	5153(8)	7870(6)	3390(4)	97(3)
C(55)	1	4930(8)	7887(6)	3877(4)	100(3)
C(56)	1	5381(7)	7364(7)	4163(4)	96(3)

C(57)	1	6078(7)	6797(5)	3984(3)	85(3)
C(58)	1	5713(6)	4411(5)	3395(2)	62(2)
C(59)	1	5060(6)	4176(5)	3742(3)	65(2)
C(60)	1	4887(7)	3336(6)	3766(3)	84(3)
C(61)	1	4250(7)	3093(6)	4054(3)	88(3)
C(62)	1	3795(7)	3710(6)	4341(3)	81(3)
C(63)	1	3994(6)	4553(6)	4350(3)	83(3)
C(64)	1	4609(6)	4794(6)	4036(3)	76(2)
C(65)	1	7177(6)	3957(5)	3885(3)	67(2)
C(66)	1	7306(6)	4538(5)	4346(3)	72(2)
C(67)	1	7878(7)	4351(6)	4782(3)	78(2)
C(68)	1	8325(7)	3618(6)	4765(3)	88(3)
C(69)	1	8178(8)	3006(7)	4304(3)	94(3)
C(70)	1	7606(7)	3197(6)	3869(3)	82(3)
C(71)	1	4309(6)	4841(5)	2875(3)	66(2)
C(72)	1	3842(7)	5602(6)	2885(3)	76(2)
C(73)	1	2814(7)	5593(7)	2686(3)	92(3)
C(74)	1	2267(7)	4837(7)	2482(4)	96(3)
C(75)	1	2717(6)	4091(7)	2467(3)	84(3)
C(76)	1	3752(7)	4074(6)	2661(3)	78(2)
N(100)	0.467(14)	3863(14)	1072(11)	362(5)	76(5)
C(100)	0.467(14)	3544(18)	1169(9)	-56(6)	98(7)
C(101)	0.467(14)	3601(16)	2014(9)	-190(7)	130(9)
C(102)	0.467(14)	4382(17)	2216(12)	-422(9)	130(9)
C(103)	0.467(14)	4510(19)	3023(14)	-507(11)	144(10)
C(104)	0.467(14)	3860(20)	3629(10)	-360(10)	192(13)
C(105)	0.467(14)	3075(17)	3428(11)	-127(10)	142(10)
C(106)	0.467(14)	2948(15)	2620(12)	-42(9)	183(12)
C(107)	0.467(14)	2956(11)	447(8)	-474(5)	83(6)
C(108)	0.467(14)	2825(13)	524(9)	-982(5)	122(8)
C(109)	0.467(14)	2262(14)	-96(11)	-1365(4)	129(9)
C(110)	0.467(14)	1831(12)	-794(10)	-1241(5)	96(6)
C(111)	0.467(14)	1963(12)	-871(8)	-733(6)	99(7)
C(112)	0.467(14)	2525(12)	-251(9)	-350(4)	72(5)
N(200)	0.533(14)	3904(17)	810(12)	377(6)	113(7)
C(200)	0.533(14)	3629(18)	1002(10)	-19(6)	112(8)
C(201)	0.533(14)	3742(15)	1801(9)	-205(7)	120(7)
C(202)	0.533(14)	4647(14)	2022(11)	-332(9)	159(10)
C(203)	0.533(14)	4764(15)	2771(13)	-494(10)	134(8)
C(204)	0.533(14)	3975(18)	3297(11)	-529(9)	153(9)
C(205)	0.533(14)	3069(15)	3076(12)	-402(9)	174(10)
C(206)	0.533(14)	2953(13)	2327(13)	-240(8)	195(12)
C(207)	0.533(14)	3098(12)	220(9)	-417(5)	102(6)
C(208)	0.533(14)	3101(12)	210(9)	-929(5)	133(8)
C(209)	0.533(14)	2570(12)	-436(10)	-1307(4)	104(6)
C(210)	0.533(14)	2036(12)	-1071(9)	-1172(5)	103(6)
C(211)	0.533(14)	2033(14)	-1061(10)	-659(6)	124(8)
C(212)	0.533(14)	2564(14)	-415(11)	-282(5)	152(10)
N(300)	0.662(1010074(9)		8675(9)	5176(5)	85(4)
C(300)	0.662(1010842(10)		8933(8)	5099(4)	84(4)
C(301)	0.662(1011262(9)		8826(7)	4627(4)	104(5)
C(302)	0.662(1011176(10)		9437(7)	4333(5)	130(6)
C(303)	0.662(1011565(12)		9319(10)	3886(5)	162(8)
C(304)	0.662(1012041(12)		8590(11)	3734(4)	199(10)
C(305)	0.662(1012128(12)		7980(9)	4027(6)	164(8)
C(306)	0.662(1011739(11)		8098(7)	4474(5)	119(6)
C(307)	0.662(1011484(7)		9555(6)	5568(3)	86(4)

C(308)	0.662(1012321(8)	10025(7)	5520(3)	103(5)
C(309)	0.662(1012873(7)	10576(7)	5945(4)	107(5)
C(310)	0.662(1012587(9)	10657(7)	6418(3)	95(5)
C(311)	0.662(1011750(10)	10188(7)	6466(3)	103(5)
C(312)	0.662(1011199(8)	9637(7)	6041(4)	96(5)
N(400)	0.338(1010157(13)	8437(14)	5185(8)	60(6)
C(400)	0.338(1010954(16)	8724(19)	5160(8)	132(11)
C(401)	0.338(1011476(18)	8578(17)	4714(8)	137(11)
C(402)	0.338(1011043(19)	8813(18)	4264(10)	162(12)
C(403)	0.338(1011390(30)	8510(20)	3814(8)	217(15)
C(404)	0.338(1012170(30)	7970(20)	3814(10)	200(15)
C(405)	0.338(1012600(20)	7733(17)	4264(13)	151(12)
C(406)	0.338(1012250(20)	8038(17)	4714(10)	176(15)
C(407)	0.338(1011454(17)	9381(15)	5650(7)	148(11)
C(408)	0.338(1012413(16)	9739(16)	5682(8)	149(12)
C(409)	0.338(1012861(15)	10330(15)	6116(9)	129(11)
C(410)	0.338(1012350(20)	10562(14)	6517(8)	99(9)
C(411)	0.338(1011390(20)	10204(16)	6485(8)	128(11)
C(412)	0.338(1010943(16)	9614(17)	6052(9)	116(11)
N(500)	0.557(5)10731(11)	6178(9)	894(6)	84(4)
C(500)	0.557(5)11356(12)	6739(9)	999(5)	95(5)
C(501)	0.557(5)11759(14)	7344(9)	1496(5)	142(8)
C(502)	0.557(5)12760(13)	7347(11)	1729(7)	159(10)
C(503)	0.557(5)13123(15)	7886(14)	2198(7)	228(16)
C(504)	0.557(5)12480(20)	8422(11)	2433(5)	226(14)
C(505)	0.557(5)11480(20)	8418(10)	2199(7)	224(14)
C(506)	0.557(5)11120(13)	7879(11)	1731(7)	179(11)
C(507)	0.557(5)11867(9)	6861(7)	555(4)	84(4)
C(508)	0.557(5)11949(9)	6187(6)	162(4)	76(4)
C(509)	0.557(5)12448(10)	6305(7)	-225(4)	78(4)
C(510)	0.557(5)12866(11)	7097(8)	-220(5)	103(6)
C(511)	0.557(5)12784(12)	7772(7)	173(6)	137(8)
C(512)	0.557(5)12285(11)	7654(6)	560(5)	131(7)
N(600)	0.443(5)10652(14)	6451(11)	934(8)	92(7)
C(600)	0.443(5)11121(14)	5942(8)	727(8)	100(7)
C(601)	0.443(5)11118(12)	5013(7)	700(6)	120(8)
C(602)	0.443(5)10462(12)	4464(9)	314(6)	110(7)
C(603)	0.443(5)10444(12)	3604(8)	298(6)	123(9)
C(604)	0.443(5)11081(13)	3293(7)	668(6)	92(6)
C(605)	0.443(5)11738(12)	3842(9)	1054(6)	102(7)
C(606)	0.443(5)11756(11)	4702(8)	1070(6)	128(9)
C(607)	0.443(5)11856(12)	6304(9)	431(6)	95(6)
C(608)	0.443(5)12101(13)	5751(8)	17(6)	102(7)
C(609)	0.443(5)12706(14)	6035(10)	-285(6)	103(7)
C(610)	0.443(5)13066(15)	6874(11)	-172(7)	92(7)
C(611)	0.443(5)12820(16)	7428(8)	242(8)	146(10)
C(612)	0.443(5)12215(15)	7143(9)	544(6)	134(9)
C(701)	0.96(3) 427(17)	2050(12)	3531(8)	200
C(702)	0.79(3) 1640(20)	1833(15)	2960(10)	200
C(703)	0.71(3) 2590(20)	1661(16)	2158(12)	200
C(704)	0.69(3) 1610(20)	2249(17)	3475(12)	200
C(706)	0.87(3) 4380(20)	9370(16)	1709(10)	200
C(707)	0.70(3) 2880(20)	1746(16)	2741(12)	200
C(708)	0.84(3) 4017(19)	9588(13)	864(10)	200
C(709)	0.72(3) 3480(30)	9967(17)	1511(11)	200
C(710)	0.81(3) 3764(19)	8581(15)	1734(9)	200
C(711)	0.43(3) 4810(40)	10720(30)	3670(19)	200

C(712)	0.55(4)	5260(30)	830(20)	4481(15)	200
C(713)	0.42(3)	3690(40)	780(30)	4724(18)	200
C(715)	0.58(3)	10170(30)	90(20)	2672(14)	200
C(716)	0.72(3)	1060(20)	10816(16)	771(11)	200
C(717)	0.55(3)	4400(30)	9810(20)	1401(18)	200
C(718)	0.49(3)	6060(30)	1930(20)	4693(17)	200
C(719)	0.44(3)	850(40)	1590(30)	4084(17)	200
C(720)	0.66(3)	10930(20)	2547(17)	546(11)	200
C(721)	0.58(3)	11050(40)	3800(20)	592(14)	200
C(722)	0.42(3)	9930(40)	9090(30)	1675(18)	200
C(723)	0.37(3)	11900(50)	3930(30)	550(20)	200
C(724)	0.70(3)	9250(20)	8544(17)	973(12)	200
C(725)	0.50(3)	2050(30)	9840(20)	1163(15)	200
C(726)	0.42(3)	5970(40)	1420(30)	4190(20)	200
C(727)	0.47(3)	4040(40)	710(30)	4053(18)	200
C(729)	0.46(3)	2370(40)	1210(20)	4495(16)	200
C(730)	0.47(3)	540(30)	11140(20)	336(17)	200
C(731)	0.48(3)	10270(30)	8030(20)	1208(16)	200
C(732)	0.45(3)	10160(30)	10230(20)	2134(18)	200
C(733)	0.43(3)	9670(40)	8640(30)	500(18)	200
C(734)	0.38(3)	3620(40)	9540(30)	2870(20)	200
C(735)	0.33(4)	4630(60)	1240(40)	4490(30)	200
C(736)	0.37(3)	620(40)	1170(30)	3230(20)	200
C(737)	0.38(3)	2760(40)	750(30)	2380(20)	200
C(738)	0.45(3)	13500(40)	7450(30)	2097(17)	200
C(740)	0.20(3)	3630(90)	10800(70)	3240(40)	200
C(742)	0.65(3)	3920(30)	10030(20)	3292(14)	200

Table 3. Hydrogen coordinates (x 10^4) and isotropic displacement parameters ($Å^2$ x 10^3) for **V-7**.

	Occ.	x	y	z	U_{eq}
H(3)	1	6646	2354	1391	92
H(4)	1	5808	1278	722	105
H(6)	1	3145	2209	951	100
H(7)	1	3989	3233	1628	92
H(9)	1	5174	2407	2490	102
H(10)	1	5316	1075	2707	120
H(11)	1	6865	494	2799	129
H(12)	1	8278	1212	2718	107
H(13)	1	8160	2520	2491	98
H(15)	1	4223	5320	1907	120
H(16)	1	3328	5671	1187	156
H(17)	1	3910	5382	405	172
H(18)	1	5317	4485	370	154
H(19)	1	6176	4132	1099	108
H(22)	1	10048	5537	2341	102
H(23)	1	11140	5876	1812	113
H(25)	1	8766	6126	756	120
H(26)	1	7677	5682	1221	107

H(28)	1	8116	3848	1386	89
H(29)	1	9100	2808	1044	107
H(30)	1	10386	2305	1558	108
H(31)	1	10692	2838	2441	98
H(32)	1	9755	3942	2797	88
H(34)	1	5877	6459	1761	127
H(35)	1	5810	7846	1678	167
H(36)	1	7120	8808	2054	216
H(37)	1	8573	8406	2538	189
H(38)	1	8634	7032	2626	121
H(41)	1	8728	5994	4496	76
H(42)	1	9594	7030	5153	81
H(44)	1	9164	8710	4244	88
H(45)	1	8195	7705	3609	85
H(47)	1	9767	6315	3305	89
H(48)	1	11498	6097	3450	102
H(49)	1	12078	4988	3818	110
H(50)	1	10930	4083	4031	106
H(51)	1	9223	4260	3865	91
H(53)	1	5963	7266	2871	102
H(54)	1	4849	8239	3187	117
H(55)	1	4466	8263	4004	120
H(56)	1	5227	7376	4492	115
H(57)	1	6380	6429	4189	102
H(60)	1	5226	2918	3575	100
H(61)	1	4127	2517	4057	106
H(63)	1	3710	4971	4570	100
H(64)	1	4716	5369	4025	92
H(66)	1	7004	5061	4363	86
H(67)	1	7955	4747	5098	93
H(68)	1	8740	3512	5064	106
H(69)	1	8464	2477	4292	113
H(70)	1	7509	2795	3555	99
H(72)	1	4222	6121	3027	91
H(73)	1	2496	6107	2691	110
H(74)	1	1567	4834	2350	115
H(75)	1	2325	3576	2323	101
H(76)	1	4064	3556	2648	93
H(102)	0.467(14)	4829	1802	-523	156
H(103)	0.467(14)	5044	3161	-666	173
H(104)	0.467(14)	3944	4181	-418	230
H(105)	0.467(14)	2628	3842	-26	170
H(106)	0.467(14)	2414	2483	117	220
H(108)	0.467(14)	3119	1001	-1067	146
H(109)	0.467(14)	2172	-43	-1712	155
H(110)	0.467(14)	1447	-1218	-1502	115
H(111)	0.467(14)	1668	-1348	-648	119
H(112)	0.467(14)	2615	-303	-3	86
H(202)	0.533(14)	5187	1662	-308	190
H(203)	0.533(14)	5382	2922	-581	160
H(204)	0.533(14)	4054	3809	-640	184
H(205)	0.533(14)	2530	3436	-426	208
H(206)	0.533(14)	2335	2176	-153	235
H(208)	0.533(14)	3466	644	-1021	160
H(209)	0.533(14)	2571	-443	-1657	125
H(210)	0.533(14)	1673	-1513	-1430	123
H(211)	0.533(14)	1668	-1495	-567	149

H(212)	0.533(14)2563	-408	69	182
H(302)	0.662(1010850	9935	4438	155
H(303)	0.662(1011506	9736	3685	195
H(304)	0.662(1012308	8510	3428	239
H(305)	0.662(1012454	7482	3923	197
H(306)	0.662(1011798	7680	4675	143
H(308)	0.662(1012516	9969	5197	124
H(309)	0.662(1013445	10897	5912	128
H(310)	0.662(1012964	11034	6708	114
H(311)	0.662(1011555	10244	6789	123
H(312)	0.662(1010627	9316	6073	115
H(402)	0.338(1010512	9182	4264	195
H(403)	0.338(1011092	8669	3506	260
H(404)	0.338(1012400	7760	3507	240
H(405)	0.338(1013130	7364	4265	181
H(406)	0.338(1012550	7877	5022	211
H(408)	0.338(1012763	9580	5408	178
H(409)	0.338(1013516	10574	6138	155
H(410)	0.338(1012655	10966	6813	119
H(411)	0.338(1011041	10363	6759	153
H(412)	0.338(1010287	9369	6030	139
H(502)	0.557(5)13197	6981	1568	191
H(503)	0.557(5)13807	7889	2357	274
H(504)	0.557(5)12731	8791	2753	271
H(505)	0.557(5)11046	8784	2360	268
H(506)	0.557(5)10436	7877	1571	215
H(508)	0.557(5)11663	5645	158	91
H(509)	0.557(5)12504	5843	-494	94
H(510)	0.557(5)13207	7178	-484	123
H(511)	0.557(5)13070	8314	177	164
H(512)	0.557(5)12229	8115	829	157
H(602)	0.443(5)10026	4676	61	132
H(603)	0.443(5) 9995	3228	34	148
H(604)	0.443(5)11069	2705	657	110
H(605)	0.443(5)12173	3629	1307	122
H(606)	0.443(5)12204	5077	1334	154
H(608)	0.443(5)11856	5178	-61	122
H(609)	0.443(5)12874	5657	-568	124
H(610)	0.443(5)13479	7069	-378	110
H(611)	0.443(5)13066	8001	320	175
H(612)	0.443(5)12047	7521	827	161

Table 4. Anisotropic parameters ($Å^2$ x 10^3) for **V-7**.

The anisotropic displacement factor exponent takes the form:

$$-2\pi^2 [h^2 a^{*2} U_{11} + ... + 2 h k a^* b^* U_{12}]$$

	U11	U22	U33	U23	U13	U12
Rh(1)	54(1)	86(1)	38(1)	2(1)	13(1)	-1(1)
Rh(2)	57(1)	85(1)	40(1)	3(1)	12(1)	-1(1)
Br(1)	104(1)	176(1)	72(1)	15(1)	41(1)	-11(1)
N(1)	59(4)	72(4)	47(3)	3(3)	19(3)	-2(3)
N(2)	54(4)	95(5)	38(3)	5(3)	8(3)	-4(3)
N(3)	48(4)	88(4)	48(3)	5(3)	14(3)	4(3)
N(4)	68(4)	88(5)	46(3)	9(3)	10(3)	-5(3)
N(5)	53(4)	90(4)	42(3)	4(3)	6(3)	-4(3)
N(6)	58(4)	76(4)	55(3)	4(3)	18(3)	9(3)
N(7)	56(4)	88(4)	38(3)	7(3)	4(3)	6(3)
N(8)	56(4)	86(4)	41(3)	1(3)	13(3)	3(3)
C(1)	50(4)	81(5)	40(3)	0(3)	10(3)	-1(4)
C(2)	68(5)	77(5)	55(4)	-2(3)	18(4)	-3(4)
C(3)	71(6)	105(6)	46(4)	0(4)	10(4)	-1(5)
C(4)	103(8)	97(6)	52(4)	-4(4)	15(5)	-10(5)
C(5)	92(7)	87(6)	63(5)	-7(4)	10(5)	-19(5)
C(6)	67(6)	102(7)	67(5)	3(5)	-9(5)	-11(5)
C(7)	64(5)	99(6)	60(4)	2(4)	12(4)	3(4)
C(8)	63(5)	82(5)	44(3)	0(3)	8(4)	0(4)
C(9)	80(7)	112(7)	60(4)	16(5)	9(5)	1(5)
C(10)	121(9)	86(7)	101(7)	30(5)	33(7)	-6(6)
C(11)	152(12)	84(7)	85(6)	17(5)	16(8)	12(7)
C(12)	88(7)	87(6)	90(6)	20(5)	6(6)	6(5)
C(13)	86(7)	96(6)	56(4)	6(4)	7(5)	2(5)
C(14)	62(5)	103(6)	44(4)	3(4)	4(4)	-2(4)
C(15)	115(9)	135(8)	53(4)	22(5)	15(6)	46(7)
C(16)	140(11)	193(12)	65(6)	33(7)	25(7)	67(9)
C(17)	168(15)	202(13)	74(7)	57(8)	20(8)	65(11)
C(18)	131(11)	216(13)	49(5)	42(6)	23(6)	28(9)
C(19)	95(7)	127(8)	55(4)	23(5)	26(5)	14(6)
C(20)	59(5)	91(6)	47(4)	8(4)	14(4)	-1(4)
C(21)	65(5)	95(6)	48(4)	18(4)	13(4)	9(4)
C(22)	71(6)	127(7)	58(4)	18(5)	14(4)	-5(5)
C(23)	61(6)	157(9)	71(5)	37(6)	15(5)	-11(6)
C(24)	91(7)	126(8)	71(5)	24(5)	29(5)	-10(6)
C(25)	87(7)	159(9)	66(5)	40(6)	27(5)	0(6)
C(26)	86(7)	128(8)	53(4)	21(5)	11(5)	19(6)
C(27)	55(5)	100(6)	56(4)	5(4)	17(4)	-4(4)
C(28)	63(5)	97(6)	59(4)	5(4)	15(4)	4(4)
C(29)	91(7)	110(7)	60(5)	-6(5)	27(5)	1(5)
C(30)	72(6)	106(7)	85(6)	-8(5)	28(5)	4(5)
C(31)	49(5)	127(7)	64(5)	10(5)	8(4)	-2(5)
C(32)	69(6)	86(6)	61(4)	-2(4)	21(4)	-5(4)
C(33)	67(6)	97(6)	52(4)	8(4)	12(4)	2(5)
C(34)	132(11)	98(8)	78(6)	0(5)	15(7)	12(7)

C(35)	204(17)	131(11)	89(8)	40(8)	19(9)	50(11)
C(36)	360(30)	79(9)	121(11)	32(8)	96(15)	11(13)
C(37)	270(20)	89(9)	146(12)	38(8)	98(13)	13(10)
C(38)	121(9)	94(7)	96(7)	18(5)	45(7)	-3(6)
C(39)	70(5)	71(5)	47(4)	4(3)	19(4)	-7(4)
C(40)	51(4)	91(6)	51(4)	-2(4)	15(4)	4(4)
C(41)	54(5)	86(5)	47(4)	5(3)	13(4)	2(4)
C(42)	62(5)	88(6)	47(4)	2(3)	15(4)	3(4)
C(43)	69(5)	82(5)	54(4)	-4(4)	14(4)	-1(4)
C(44)	68(6)	77(5)	70(5)	9(4)	5(4)	2(4)
C(45)	72(6)	79(5)	55(4)	5(4)	11(4)	-4(4)
C(46)	50(4)	90(5)	42(3)	-5(3)	6(3)	-2(4)
C(47)	60(5)	97(6)	60(4)	1(4)	14(4)	-1(4)
C(48)	56(5)	122(8)	63(5)	-10(5)	13(5)	-2(5)
C(49)	56(6)	149(9)	50(4)	-19(5)	2(4)	15(6)
C(50)	83(7)	120(7)	52(4)	-5(4)	10(5)	30(6)
C(51)	69(6)	98(6)	53(4)	0(4)	10(4)	19(5)
C(52)	63(5)	78(5)	61(4)	3(4)	9(4)	2(4)
C(53)	73(6)	97(7)	72(5)	0(5)	5(5)	3(5)
C(54)	91(7)	104(7)	84(6)	-11(5)	16(6)	17(6)
C(55)	83(8)	85(7)	119(8)	-2(6)	11(7)	18(5)
C(56)	75(7)	127(8)	81(6)	-5(6)	28(6)	11(6)
C(57)	88(6)	92(6)	64(5)	-19(4)	29(5)	-5(5)
C(58)	54(5)	90(5)	39(3)	3(3)	11(4)	1(4)
C(59)	59(5)	91(6)	45(3)	9(3)	14(4)	12(4)
C(60)	89(6)	94(6)	71(5)	4(4)	40(5)	1(5)
C(61)	95(7)	97(6)	81(5)	11(5)	46(5)	8(5)
C(62)	66(6)	119(7)	62(5)	21(5)	23(4)	-3(5)
C(63)	66(6)	133(8)	49(4)	6(4)	19(4)	15(5)
C(64)	64(5)	109(6)	55(4)	4(4)	26(4)	-1(4)
C(65)	56(5)	100(6)	46(4)	12(4)	15(4)	3(4)
C(66)	61(5)	105(6)	44(4)	3(4)	14(4)	-7(4)
C(67)	74(6)	115(7)	44(4)	14(4)	13(4)	7(5)
C(68)	82(7)	129(8)	57(4)	31(5)	8(5)	9(6)
C(69)	89(8)	121(8)	68(5)	18(5)	8(5)	8(6)
C(70)	82(7)	114(7)	49(4)	14(4)	10(4)	11(5)
C(71)	47(4)	104(6)	42(3)	6(4)	12(3)	-1(4)
C(72)	72(6)	97(6)	63(4)	12(4)	24(4)	7(5)
C(73)	54(5)	148(9)	78(6)	25(6)	25(5)	14(5)
C(74)	57(6)	156(10)	79(6)	33(6)	16(5)	5(6)
C(75)	48(5)	127(8)	71(5)	11(5)	8(5)	-6(5)
C(76)	77(6)	99(6)	55(4)	3(4)	21(4)	0(5)

Table 5. Bond lengths [Å] and angles [°] for **V-7**.

Rh(1)-N(5)	2.021(6)	Rh(2)-N(2)	2.040(6)
Rh(1)-N(7)	2.027(6)	Br(1)-C(62)	1.876(8)
Rh(1)-N(1)	2.035(6)	N(1)-C(1)	1.329(9)
Rh(1)-N(3)	2.043(6)	N(1)-C(8)	1.414(10)
Rh(1)-Rh(2)	2.4032(9)	N(2)-C(1)	1.337(9)
Rh(2)-N(6)	2.023(6)	N(2)-C(14)	1.423(10)
Rh(2)-N(4)	2.028(6)	N(3)-C(20)	1.309(10)
Rh(2)-N(8)	2.040(6)	N(3)-C(27)	1.402(10)

N(4)-C(20)	1.369(10)	C(26)-H(26)	0.9500
N(4)-C(33)	1.415(11)	C(27)-C(32)	1.382(12)
N(5)-C(39)	1.373(10)	C(27)-C(28)	1.399(10)
N(5)-C(46)	1.413(9)	C(28)-C(29)	1.397(11)
N(6)-C(39)	1.351(10)	C(28)-H(28)	0.9500
N(6)-C(52)	1.408(9)	C(29)-C(30)	1.361(13)
N(7)-C(58)	1.350(9)	C(29)-H(29)	0.9500
N(7)-C(65)	1.435(9)	C(30)-C(31)	1.383(11)
N(8)-C(58)	1.324(9)	C(30)-H(30)	0.9500
N(8)-C(71)	1.416(9)	C(31)-C(32)	1.428(11)
C(1)-C(2)	1.485(9)	C(31)-H(31)	0.9500
C(2)-C(7)	1.373(11)	C(32)-H(32)	0.9500
C(2)-C(3)	1.404(11)	C(33)-C(34)	1.362(14)
C(3)-C(4)	1.402(10)	C(33)-C(38)	1.405(13)
C(3)-H(3)	0.9500	C(34)-C(35)	1.378(15)
C(4)-C(5)	1.403(13)	C(34)-H(34)	0.9500
C(4)-H(4)	0.9500	C(35)-C(36)	1.34(2)
C(5)-C(6)	1.370(12)	C(35)-H(35)	0.9500
C(5)-N(100)	1.371(16)	C(36)-C(37)	1.39(2)
C(5)-N(200)	1.600(19)	C(36)-H(36)	0.9500
C(6)-C(7)	1.387(10)	C(37)-C(38)	1.353(14)
C(6)-H(6)	0.9500	C(37)-H(37)	0.9500
C(7)-H(7)	0.9500	C(38)-H(38)	0.9500
C(8)-C(13)	1.375(12)	C(39)-C(40)	1.502(10)
C(8)-C(9)	1.402(11)	C(40)-C(45)	1.357(11)
C(9)-C(10)	1.403(12)	C(40)-C(41)	1.410(10)
C(9)-H(9)	0.9500	C(41)-C(42)	1.364(10)
C(10)-C(11)	1.378(15)	C(41)-H(41)	0.9500
C(10)-H(10)	0.9500	C(42)-C(43)	1.388(11)
C(11)-C(12)	1.340(14)	C(42)-H(42)	0.9500
C(11)-H(11)	0.9500	C(43)-N(400)	1.39(2)
C(12)-C(13)	1.391(12)	C(43)-C(44)	1.384(11)
C(12)-H(12)	0.9500	C(43)-N(300)	1.513(14)
C(13)-H(13)	0.9500	C(44)-C(45)	1.368(10)
C(14)-C(15)	1.357(13)	C(44)-H(44)	0.9500
C(14)-C(19)	1.406(10)	C(45)-H(45)	0.9500
C(15)-C(16)	1.373(13)	C(46)-C(51)	1.376(11)
C(15)-H(15)	0.9500	C(46)-C(47)	1.394(10)
C(16)-C(17)	1.389(14)	C(47)-C(48)	1.405(12)
C(16)-H(16)	0.9500	C(47)-H(47)	0.9500
C(17)-C(18)	1.464(16)	C(48)-C(49)	1.370(13)
C(17)-H(17)	0.9500	C(48)-H(48)	0.9500
C(18)-C(19)	1.359(13)	C(49)-C(50)	1.389(13)
C(18)-H(18)	0.9500	C(49)-H(49)	0.9500
C(19)-H(19)	0.9500	C(50)-C(51)	1.371(12)
C(20)-C(21)	1.480(10)	C(50)-H(50)	0.9500
C(21)-C(22)	1.386(11)	C(51)-H(51)	0.9500
C(21)-C(26)	1.415(10)	C(52)-C(53)	1.362(12)
C(22)-C(23)	1.417(11)	C(52)-C(57)	1.411(11)
C(22)-H(22)	0.9500	C(53)-C(54)	1.416(12)
C(23)-C(24)	1.367(12)	C(53)-H(53)	0.9500
C(23)-H(23)	0.9500	C(54)-C(55)	1.402(14)
C(24)-C(25)	1.359(13)	C(54)-H(54)	0.9500
C(24)-N(500)	1.479(16)	C(55)-C(56)	1.353(14)
C(24)-N(600)	1.50(2)	C(55)-H(55)	0.9500
C(25)-C(26)	1.362(11)	C(56)-C(57)	1.418(12)
C(25)-H(25)	0.9500	C(56)-H(56)	0.9500

C(57)-H(57)	0.9500	C(111)-H(111)	0.9500
C(58)-C(59)	1.497(9)	C(112)-H(112)	0.9500
C(59)-C(60)	1.396(11)	N(200)-C(200)	1.182(14)
C(59)-C(64)	1.380(10)	C(200)-C(201)	1.498(13)
C(60)-C(61)	1.365(11)	C(200)-C(207)	1.555(12)
C(60)-H(60)	0.9500	C(201)-C(202)	1.3900
C(61)-C(62)	1.373(12)	C(201)-C(206)	1.3900
C(61)-H(61)	0.9500	C(202)-C(203)	1.3900
C(62)-C(63)	1.386(12)	C(202)-H(202)	0.9500
C(63)-C(64)	1.395(10)	C(203)-C(204)	1.3900
C(63)-H(63)	0.9500	C(203)-H(203)	0.9500
C(64)-H(64)	0.9500	C(204)-C(205)	1.3900
C(65)-C(70)	1.377(12)	C(204)-H(204)	0.9500
C(65)-C(66)	1.388(10)	C(205)-C(206)	1.3900
C(66)-C(67)	1.389(11)	C(205)-H(205)	0.9500
C(66)-H(66)	0.9500	C(206)-H(206)	0.9500
C(67)-C(68)	1.350(12)	C(207)-C(208)	1.3900
C(67)-H(67)	0.9500	C(207)-C(212)	1.3900
C(68)-C(69)	1.413(12)	C(208)-C(209)	1.3900
C(68)-H(68)	0.9500	C(208)-H(208)	0.9500
C(69)-C(70)	1.388(12)	C(209)-C(210)	1.3900
C(69)-H(69)	0.9500	C(209)-H(209)	0.9500
C(70)-H(70)	0.9500	C(210)-C(211)	1.3900
C(71)-C(72)	1.403(11)	C(210)-H(210)	0.9500
C(71)-C(76)	1.400(11)	C(211)-C(212)	1.3900
C(72)-C(73)	1.399(12)	C(211)-H(211)	0.9500
C(72)-H(72)	0.9500	C(212)-H(212)	0.9500
C(73)-C(74)	1.377(13)	N(300)-C(300)	1.180(11)
C(73)-H(73)	0.9500	C(300)-C(301)	1.475(11)
C(74)-C(75)	1.370(13)	C(300)-C(307)	1.561(10)
C(74)-H(74)	0.9500	C(301)-C(302)	1.3900
C(75)-C(76)	1.411(12)	C(301)-C(306)	1.3900
C(75)-H(75)	0.9500	C(302)-C(303)	1.3900
C(76)-H(76)	0.9500	C(302)-H(302)	0.9500
N(100)-C(100)	1.182(13)	C(303)-C(304)	1.3900
C(100)-C(101)	1.496(13)	C(303)-H(303)	0.9500
C(100)-C(107)	1.546(12)	C(304)-C(305)	1.3900
C(101)-C(102)	1.3900	C(304)-H(304)	0.9500
C(101)-C(106)	1.3900	C(305)-C(306)	1.3900
C(102)-C(103)	1.3900	C(305)-H(305)	0.9500
C(102)-H(102)	0.9500	C(306)-H(306)	0.9500
C(103)-C(104)	1.3900	C(307)-C(308)	1.3900
C(103)-H(103)	0.9500	C(307)-C(312)	1.3900
C(104)-C(105)	1.3900	C(308)-C(309)	1.3900
C(104)-H(104)	0.9500	C(308)-H(308)	0.9500
C(105)-C(106)	1.3900	C(309)-C(310)	1.3900
C(105)-H(105)	0.9500	C(309)-H(309)	0.9500
C(106)-H(106)	0.9500	C(310)-C(311)	1.3900
C(107)-C(108)	1.3900	C(310)-H(310)	0.9500
C(107)-C(112)	1.3900	C(311)-C(312)	1.3900
C(108)-C(109)	1.3900	C(311)-H(311)	0.9500
C(108)-H(108)	0.9500	C(312)-H(312)	0.9500
C(109)-C(110)	1.3900	N(400)-C(400)	1.183(14)
C(109)-H(109)	0.9500	C(400)-C(401)	1.493(14)
C(110)-C(111)	1.3900	C(400)-C(407)	1.561(13)
C(110)-H(110)	0.9500	C(401)-C(402)	1.3900
C(111)-C(112)	1.3900	C(401)-C(406)	1.3900

C(402)-C(403)	1.3900	C(605)-H(605)	0.9500
C(402)-H(402)	0.9500	C(606)-H(606)	0.9500
C(403)-C(404)	1.3900	C(607)-C(608)	1.3900
C(403)-H(403)	0.9500	C(607)-C(612)	1.3900
C(404)-C(405)	1.3900	C(608)-C(609)	1.3900
C(404)-H(404)	0.9500	C(608)-H(608)	0.9500
C(405)-C(406)	1.3900	C(609)-C(610)	1.3900
C(405)-H(405)	0.9500	C(609)-H(609)	0.9500
C(406)-H(406)	0.9500	C(610)-C(611)	1.3900
C(407)-C(408)	1.3900	C(610)-H(610)	0.9500
C(407)-C(412)	1.3900	C(611)-C(612)	1.3900
C(408)-C(409)	1.3900	C(611)-H(611)	0.9500
C(408)-H(408)	0.9500	C(612)-H(612)	0.9500
C(409)-C(410)	1.3900	C(701)-C(736)	1.56(5)
C(409)-H(409)	0.9500	C(701)-C(704)	1.67(3)
C(410)-C(411)	1.3900	C(701)-C(719)	1.83(5)
C(410)-H(410)	0.9500	C(702)-C(704)	1.44(3)
C(411)-C(412)	1.3900	C(702)-C(707)	1.87(4)
C(411)-H(411)	0.9500	C(703)-C(707)	1.54(3)
C(412)-H(412)	0.9500	C(703)-C(737)	1.72(5)
N(500)-C(500)	1.181(13)	C(704)-C(736)	2.11(6)
C(500)-C(501)	1.502(12)	C(706)-C(717)	1.22(4)
C(500)-C(507)	1.540(12)	C(706)-C(710)	1.53(3)
C(501)-C(502)	1.3900	C(706)-C(709)	1.65(4)
C(501)-C(506)	1.3900	C(707)-C(737)	1.71(5)
C(502)-C(503)	1.3900	C(708)-C(717)	1.43(4)
C(502)-H(502)	0.9500	C(709)-C(717)	1.35(4)
C(503)-C(504)	1.3900	C(709)-C(725)	1.99(5)
C(503)-H(503)	0.9500	C(711)-C(727)#1	1.60(5)
C(504)-C(505)	1.3900	C(711)-C(742)	1.67(5)
C(504)-H(504)	0.9500	C(711)-C(740)	1.84(12)
C(505)-C(506)	1.3900	C(711)-C(726)#1	2.06(7)
C(505)-H(505)	0.9500	C(711)-C(712)#1	2.15(6)
C(506)-H(506)	0.9500	C(712)-C(735)	1.10(7)
C(507)-C(508)	1.3900	C(712)-C(727)	1.82(6)
C(507)-C(512)	1.3900	C(712)-C(726)	1.74(5)
C(508)-C(509)	1.3900	C(712)-C(711)#2	2.15(6)
C(508)-H(508)	0.9500	C(713)-C(735)	1.73(7)
C(509)-C(510)	1.3900	C(713)-C(727)	1.94(6)
C(509)-H(509)	0.9500	C(715)-C(732)#2	1.52(5)
C(510)-C(511)	1.3900	C(716)-C(730)	1.47(4)
C(510)-H(510)	0.9500	C(718)-C(726)	1.42(5)
C(511)-C(512)	1.3900	C(719)-C(736)	2.25(7)
C(511)-H(511)	0.9500	C(720)-C(721)	2.02(4)
C(512)-H(512)	0.9500	C(721)-C(723)	1.19(6)
N(600)-C(600)	1.172(14)	C(722)-C(732)	2.01(6)
C(600)-C(601)	1.499(13)	C(724)-C(733)	1.53(5)
C(600)-C(607)	1.559(13)	C(724)-C(731)	1.73(5)
C(601)-C(602)	1.3900	C(726)-C(711)#2	2.06(7)
C(601)-C(606)	1.3900	C(727)-C(735)	1.43(7)
C(602)-C(603)	1.3900	C(727)-C(711)#2	1.60(5)
C(602)-H(602)	0.9500	C(727)-C(742)#2	2.11(6)
C(603)-C(604)	1.3900	C(732)-C(715)#1	1.52(5)
C(603)-H(603)	0.9500	C(734)-C(742)	1.25(5)
C(604)-C(605)	1.3900	C(740)-C(742)	1.36(11)
C(604)-H(604)	0.9500	C(742)-C(727)#1	2.11(6)
C(605)-C(606)	1.3900		

N(5)-Rh(1)-N(7)	89.5(2)	C(6)-C(5)-C(4)	120.0(8)
N(5)-Rh(1)-N(1)	176.5(3)	N(100)-C(5)-C(4)	121.6(11)
N(7)-Rh(1)-N(1)	89.6(2)	C(6)-C(5)-N(200)	124.9(11)
N(5)-Rh(1)-N(3)	90.0(2)	N(100)-C(5)-N(200)	14.6(10)
N(7)-Rh(1)-N(3)	175.1(3)	C(4)-C(5)-N(200)	113.6(11)
N(1)-Rh(1)-N(3)	90.6(2)	C(5)-C(6)-C(7)	119.7(9)
N(5)-Rh(1)-Rh(2)	88.5(2)	C(5)-C(6)-H(6)	120.2
N(7)-Rh(1)-Rh(2)	87.75(19)	C(7)-C(6)-H(6)	120.2
N(1)-Rh(1)-Rh(2)	88.14(19)	C(2)-C(7)-C(6)	122.9(8)
N(3)-Rh(1)-Rh(2)	87.35(19)	C(2)-C(7)-H(7)	118.5
N(6)-Rh(2)-N(4)	89.8(2)	C(6)-C(7)-H(7)	118.5
N(6)-Rh(2)-N(8)	89.9(2)	C(13)-C(8)-C(9)	118.9(9)
N(4)-Rh(2)-N(8)	176.1(3)	C(13)-C(8)-N(1)	120.2(7)
N(6)-Rh(2)-N(2)	175.4(3)	C(9)-C(8)-N(1)	120.9(8)
N(4)-Rh(2)-N(2)	90.3(2)	C(8)-C(9)-C(10)	119.0(10)
N(8)-Rh(2)-N(2)	89.7(2)	C(8)-C(9)-H(9)	120.5
N(6)-Rh(2)-Rh(1)	88.29(19)	C(10)-C(9)-H(9)	120.5
N(4)-Rh(2)-Rh(1)	88.4(2)	C(11)-C(10)-C(9)	119.7(10)
N(8)-Rh(2)-Rh(1)	87.63(19)	C(11)-C(10)-H(10)	120.2
N(2)-Rh(2)-Rh(1)	87.1(2)	C(9)-C(10)-H(10)	120.2
C(1)-N(1)-C(8)	121.0(6)	C(12)-C(11)-C(10)	121.5(10)
C(1)-N(1)-Rh(1)	120.9(5)	C(12)-C(11)-H(11)	119.2
C(8)-N(1)-Rh(1)	117.1(5)	C(10)-C(11)-H(11)	119.2
C(1)-N(2)-C(14)	120.9(6)	C(11)-C(12)-C(13)	119.6(11)
C(1)-N(2)-Rh(2)	121.5(5)	C(11)-C(12)-H(12)	120.2
C(14)-N(2)-Rh(2)	117.0(5)	C(13)-C(12)-H(12)	120.2
C(20)-N(3)-C(27)	119.6(6)	C(8)-C(13)-C(12)	121.3(9)
C(20)-N(3)-Rh(1)	121.5(5)	C(8)-C(13)-H(13)	119.4
C(27)-N(3)-Rh(1)	118.2(5)	C(12)-C(13)-H(13)	119.4
C(20)-N(4)-C(33)	120.0(7)	C(15)-C(14)-C(19)	119.2(8)
C(20)-N(4)-Rh(2)	119.9(5)	C(15)-C(14)-N(2)	120.9(7)
C(33)-N(4)-Rh(2)	118.9(5)	C(19)-C(14)-N(2)	120.0(8)
C(39)-N(5)-C(46)	120.4(6)	C(14)-C(15)-C(16)	122.1(9)
C(39)-N(5)-Rh(1)	120.3(5)	C(14)-C(15)-H(15)	119.0
C(46)-N(5)-Rh(1)	118.3(5)	C(16)-C(15)-H(15)	119.0
C(39)-N(6)-C(52)	119.7(6)	C(15)-C(16)-C(17)	121.7(12)
C(39)-N(6)-Rh(2)	121.0(5)	C(15)-C(16)-H(16)	119.1
C(52)-N(6)-Rh(2)	118.5(5)	C(17)-C(16)-H(16)	119.1
C(58)-N(7)-C(65)	119.4(6)	C(16)-C(17)-C(18)	115.2(10)
C(58)-N(7)-Rh(1)	121.3(5)	C(16)-C(17)-H(17)	122.4
C(65)-N(7)-Rh(1)	118.0(5)	C(18)-C(17)-H(17)	122.4
C(58)-N(8)-C(71)	119.6(6)	C(19)-C(18)-C(17)	121.7(10)
C(58)-N(8)-Rh(2)	121.2(5)	C(19)-C(18)-H(18)	119.1
C(71)-N(8)-Rh(2)	118.1(5)	C(17)-C(18)-H(18)	119.1
N(1)-C(1)-N(2)	118.4(6)	C(18)-C(19)-C(14)	119.7(10)
N(1)-C(1)-C(2)	121.5(7)	C(18)-C(19)-H(19)	120.1
N(2)-C(1)-C(2)	120.1(7)	C(14)-C(19)-H(19)	120.1
C(7)-C(2)-C(3)	117.0(7)	N(3)-C(20)-N(4)	119.1(7)
C(7)-C(2)-C(1)	122.3(7)	N(3)-C(20)-C(21)	122.0(7)
C(3)-C(2)-C(1)	120.6(7)	N(4)-C(20)-C(21)	118.9(7)
C(4)-C(3)-C(2)	121.4(9)	C(22)-C(21)-C(26)	117.7(8)
C(4)-C(3)-H(3)	119.3	C(22)-C(21)-C(20)	119.5(7)
C(2)-C(3)-H(3)	119.3	C(26)-C(21)-C(20)	122.7(8)
C(3)-C(4)-C(5)	118.9(9)	C(21)-C(22)-C(23)	120.4(8)
C(3)-C(4)-H(4)	120.6	C(21)-C(22)-H(22)	119.8
C(5)-C(4)-H(4)	120.6	C(23)-C(22)-H(22)	119.8
C(6)-C(5)-N(100)	118.3(12)	C(24)-C(23)-C(22)	119.8(9)

C(24)-C(23)-H(23)	120.1	C(42)-C(41)-H(41)	120.1
C(22)-C(23)-H(23)	120.1	C(40)-C(41)-H(41)	120.1
C(25)-C(24)-C(23)	119.8(8)	C(41)-C(42)-C(43)	121.3(8)
C(25)-C(24)-N(500)	120.6(10)	C(41)-C(42)-H(42)	119.4
C(23)-C(24)-N(500)	119.0(11)	C(43)-C(42)-H(42)	119.4
C(25)-C(24)-N(600)	115.8(12)	N(400)-C(43)-C(42)	109.7(12)
C(23)-C(24)-N(600)	123.6(12)	N(400)-C(43)-C(44)	132.4(12)
N(500)-C(24)-N(600)	17.5(9)	C(42)-C(43)-C(44)	117.8(7)
C(26)-C(25)-C(24)	122.0(9)	N(400)-C(43)-N(300)	15.5(12)
C(26)-C(25)-H(25)	119.0	C(42)-C(43)-N(300)	123.4(9)
C(24)-C(25)-H(25)	119.0	C(44)-C(43)-N(300)	118.5(9)
C(25)-C(26)-C(21)	120.2(9)	C(45)-C(44)-C(43)	121.2(8)
C(25)-C(26)-H(26)	119.9	C(45)-C(44)-H(44)	119.4
C(21)-C(26)-H(26)	119.9	C(43)-C(44)-H(44)	119.4
C(32)-C(27)-C(28)	118.2(8)	C(40)-C(45)-C(44)	121.0(8)
C(32)-C(27)-N(3)	119.4(7)	C(40)-C(45)-H(45)	119.5
C(28)-C(27)-N(3)	122.4(8)	C(44)-C(45)-H(45)	119.5
C(27)-C(28)-C(29)	120.5(9)	C(51)-C(46)-C(47)	119.7(8)
C(27)-C(28)-H(28)	119.8	C(51)-C(46)-N(5)	118.9(7)
C(29)-C(28)-H(28)	119.8	C(47)-C(46)-N(5)	121.2(8)
C(30)-C(29)-C(28)	121.8(8)	C(46)-C(47)-C(48)	119.6(9)
C(30)-C(29)-H(29)	119.1	C(46)-C(47)-H(47)	120.2
C(28)-C(29)-H(29)	119.1	C(48)-C(47)-H(47)	120.2
C(29)-C(30)-C(31)	118.7(9)	C(49)-C(48)-C(47)	120.1(9)
C(29)-C(30)-H(30)	120.6	C(49)-C(48)-H(48)	119.9
C(31)-C(30)-H(30)	120.6	C(47)-C(48)-H(48)	119.9
C(30)-C(31)-C(32)	120.5(9)	C(48)-C(49)-C(50)	119.2(10)
C(30)-C(31)-H(31)	119.7	C(48)-C(49)-H(49)	120.4
C(32)-C(31)-H(31)	119.8	C(50)-C(49)-H(49)	120.4
C(27)-C(32)-C(31)	120.2(8)	C(51)-C(50)-C(49)	121.3(10)
C(27)-C(32)-H(32)	119.9	C(51)-C(50)-H(50)	119.3
C(31)-C(32)-H(32)	119.9	C(49)-C(50)-H(50)	119.3
C(34)-C(33)-C(38)	117.1(10)	C(46)-C(51)-C(50)	120.0(9)
C(34)-C(33)-N(4)	120.3(9)	C(46)-C(51)-H(51)	120.0
C(38)-C(33)-N(4)	122.6(9)	C(50)-C(51)-H(51)	120.0
C(33)-C(34)-C(35)	120.4(12)	C(53)-C(52)-C(57)	118.6(8)
C(33)-C(34)-H(34)	119.8	C(53)-C(52)-N(6)	119.7(7)
C(35)-C(34)-H(34)	119.8	C(57)-C(52)-N(6)	121.0(8)
C(36)-C(35)-C(34)	121.3(16)	C(52)-C(53)-C(54)	121.8(9)
C(36)-C(35)-H(35)	119.4	C(52)-C(53)-H(53)	119.1
C(34)-C(35)-H(35)	119.4	C(54)-C(53)-H(53)	119.1
C(35)-C(36)-C(37)	120.5(14)	C(55)-C(54)-C(53)	119.2(10)
C(35)-C(36)-H(36)	119.7	C(55)-C(54)-H(54)	120.4
C(37)-C(36)-H(36)	119.8	C(53)-C(54)-H(54)	120.4
C(38)-C(37)-C(36)	117.8(16)	C(56)-C(55)-C(54)	119.4(10)
C(38)-C(37)-H(37)	121.1	C(56)-C(55)-H(55)	120.3
C(36)-C(37)-H(37)	121.1	C(54)-C(55)-H(55)	120.3
C(37)-C(38)-C(33)	122.9(13)	C(55)-C(56)-C(57)	121.5(10)
C(37)-C(38)-H(38)	118.5	C(55)-C(56)-H(56)	119.2
C(33)-C(38)-H(38)	118.5	C(57)-C(56)-H(56)	119.2
N(6)-C(39)-N(5)	118.5(6)	C(52)-C(57)-C(56)	119.4(10)
N(6)-C(39)-C(40)	121.6(7)	C(52)-C(57)-H(57)	120.3
N(5)-C(39)-C(40)	119.9(7)	C(56)-C(57)-H(57)	120.3
C(45)-C(40)-C(41)	118.9(7)	N(8)-C(58)-N(7)	118.3(6)
C(45)-C(40)-C(39)	121.6(7)	N(8)-C(58)-C(59)	120.6(7)
C(41)-C(40)-C(39)	119.5(7)	N(7)-C(58)-C(59)	121.2(7)
C(42)-C(41)-C(40)	119.7(8)	C(60)-C(59)-C(64)	119.4(7)

C(60)-C(59)-C(58)	120.8(7)	C(102)-C(101)-C(106)	120.0
C(64)-C(59)-C(58)	119.8(7)	C(102)-C(101)-C(100)	118.8(12)
C(61)-C(60)-C(59)	122.5(8)	C(106)-C(101)-C(100)	121.0(12)
C(61)-C(60)-H(60)	118.8	C(103)-C(102)-C(101)	120.0
C(59)-C(60)-H(60)	118.8	C(103)-C(102)-H(102)	120.0
C(60)-C(61)-C(62)	117.9(9)	C(101)-C(102)-H(102)	120.0
C(60)-C(61)-H(61)	121.1	C(104)-C(103)-C(102)	120.0
C(62)-C(61)-H(61)	121.1	C(104)-C(103)-H(103)	120.0
C(61)-C(62)-C(63)	121.2(8)	C(102)-C(103)-H(103)	120.0
C(61)-C(62)-Br(1)	119.4(7)	C(103)-C(104)-C(105)	120.0
C(63)-C(62)-Br(1)	119.4(6)	C(103)-C(104)-H(104)	120.0
C(62)-C(63)-C(64)	120.5(8)	C(105)-C(104)-H(104)	120.0
C(62)-C(63)-H(63)	119.8	C(106)-C(105)-C(104)	120.0
C(64)-C(63)-H(63)	119.8	C(106)-C(105)-H(105)	120.0
C(59)-C(64)-C(63)	118.4(8)	C(104)-C(105)-H(105)	120.0
C(59)-C(64)-H(64)	120.8	C(105)-C(106)-C(101)	120.0
C(63)-C(64)-H(64)	120.8	C(105)-C(106)-H(106)	120.0
C(70)-C(65)-C(66)	119.4(8)	C(101)-C(106)-H(106)	120.0
C(70)-C(65)-N(7)	120.4(7)	C(108)-C(107)-C(112)	120.0
C(66)-C(65)-N(7)	120.0(8)	C(108)-C(107)-C(100)	118.6(9)
C(65)-C(66)-C(67)	119.7(9)	C(112)-C(107)-C(100)	121.3(9)
C(65)-C(66)-H(66)	120.2	C(109)-C(108)-C(107)	120.0
C(67)-C(66)-H(66)	120.2	C(109)-C(108)-H(108)	120.0
C(68)-C(67)-C(66)	121.2(8)	C(107)-C(108)-H(108)	120.0
C(68)-C(67)-H(67)	119.4	C(110)-C(109)-C(108)	120.0
C(66)-C(67)-H(67)	119.4	C(110)-C(109)-H(109)	120.0
C(67)-C(68)-C(69)	120.1(9)	C(108)-C(109)-H(109)	120.0
C(67)-C(68)-H(68)	119.9	C(109)-C(110)-C(111)	120.0
C(69)-C(68)-H(68)	119.9	C(109)-C(110)-H(110)	120.0
C(70)-C(69)-C(68)	118.4(10)	C(111)-C(110)-H(110)	120.0
C(70)-C(69)-H(69)	120.8	C(110)-C(111)-C(112)	120.0
C(68)-C(69)-H(69)	120.8	C(110)-C(111)-H(111)	120.0
C(65)-C(70)-C(69)	121.2(8)	C(112)-C(111)-H(111)	120.0
C(65)-C(70)-H(70)	119.4	C(111)-C(112)-C(107)	120.0
C(69)-C(70)-H(70)	119.4	C(111)-C(112)-H(112)	120.0
C(72)-C(71)-C(76)	120.2(8)	C(107)-C(112)-H(112)	120.0
C(72)-C(71)-N(8)	120.3(7)	C(200)-N(200)-C(5)	105.8(14)
C(76)-C(71)-N(8)	119.3(8)	N(200)-C(200)-C(201)	133.3(15)
C(71)-C(72)-C(73)	119.9(9)	N(200)-C(200)-C(207)	109.3(13)
C(71)-C(72)-H(72)	120.1	C(201)-C(200)-C(207)	117.3(12)
C(73)-C(72)-H(72)	120.1	C(202)-C(201)-C(206)	120.0
C(74)-C(73)-C(72)	119.7(10)	C(202)-C(201)-C(200)	119.7(12)
C(74)-C(73)-H(73)	120.1	C(206)-C(201)-C(200)	120.2(12)
C(72)-C(73)-H(73)	120.1	C(203)-C(202)-C(201)	120.0
C(75)-C(74)-C(73)	120.9(10)	C(203)-C(202)-H(202)	120.0
C(75)-C(74)-H(74)	119.6	C(201)-C(202)-H(202)	120.0
C(73)-C(74)-H(74)	119.6	C(202)-C(203)-C(204)	120.0
C(74)-C(75)-C(76)	121.0(9)	C(202)-C(203)-H(203)	120.0
C(74)-C(75)-H(75)	119.5	C(204)-C(203)-H(203)	120.0
C(76)-C(75)-H(75)	119.5	C(203)-C(204)-C(205)	120.0
C(71)-C(76)-C(75)	118.3(9)	C(203)-C(204)-H(204)	120.0
C(71)-C(76)-H(76)	120.8	C(205)-C(204)-H(204)	120.0
C(75)-C(76)-H(76)	120.8	C(204)-C(205)-C(206)	120.0
C(100)-N(100)-C(5)	127.4(16)	C(204)-C(205)-H(205)	120.0
N(100)-C(100)-C(101)	121.6(14)	C(206)-C(205)-H(205)	120.0
N(100)-C(100)-C(107)	121.6(13)	C(205)-C(206)-C(201)	120.0
C(101)-C(100)-C(107)	116.6(12)	C(205)-C(206)-H(206)	120.0

C(201)-C(206)-H(206)	120.0	C(311)-C(312)-H(312)	120.0
C(208)-C(207)-C(212)	120.0	C(307)-C(312)-H(312)	120.0
C(208)-C(207)-C(200)	117.0(10)	C(400)-N(400)-C(43)	122.3(17)
C(212)-C(207)-C(200)	122.8(10)	N(400)-C(400)-C(401)	128.0(17)
C(209)-C(208)-C(207)	120.0	N(400)-C(400)-C(407)	113.7(15)
C(209)-C(208)-H(208)	120.0	C(401)-C(400)-C(407)	118.2(15)
C(207)-C(208)-H(208)	120.0	C(402)-C(401)-C(406)	120.0
C(208)-C(209)-C(210)	120.0	C(402)-C(401)-C(400)	119.7(15)
C(208)-C(209)-H(209)	120.0	C(406)-C(401)-C(400)	118.6(16)
C(210)-C(209)-H(209)	120.0	C(401)-C(402)-C(403)	120.0
C(211)-C(210)-C(209)	120.0	C(401)-C(402)-H(402)	120.0
C(211)-C(210)-H(210)	120.0	C(403)-C(402)-H(402)	120.0
C(209)-C(210)-H(210)	120.0	C(404)-C(403)-C(402)	120.0
C(210)-C(211)-C(212)	120.0	C(404)-C(403)-H(403)	120.0
C(210)-C(211)-H(211)	120.0	C(402)-C(403)-H(403)	120.0
C(212)-C(211)-H(211)	120.0	C(405)-C(404)-C(403)	120.0
C(211)-C(212)-C(207)	120.0	C(405)-C(404)-H(404)	120.0
C(211)-C(212)-H(212)	120.0	C(403)-C(404)-H(404)	120.0
C(207)-C(212)-H(212)	120.0	C(404)-C(405)-C(406)	120.0
C(300)-N(300)-C(43)	115.4(11)	C(404)-C(405)-H(405)	120.0
N(300)-C(300)-C(301)	131.3(11)	C(406)-C(405)-H(405)	120.0
N(300)-C(300)-C(307)	114.2(10)	C(405)-C(406)-C(401)	120.0
C(301)-C(300)-C(307)	114.3(9)	C(405)-C(406)-H(406)	120.0
C(302)-C(301)-C(306)	120.0	C(401)-C(406)-H(406)	120.0
C(302)-C(301)-C(300)	120.9(9)	C(408)-C(407)-C(412)	120.0
C(306)-C(301)-C(300)	119.1(9)	C(408)-C(407)-C(400)	119.7(12)
C(303)-C(302)-C(301)	120.0	C(412)-C(407)-C(400)	120.3(12)
C(303)-C(302)-H(302)	120.0	C(407)-C(408)-C(409)	120.0
C(301)-C(302)-H(302)	120.0	C(407)-C(408)-H(408)	120.0
C(302)-C(303)-C(304)	120.0	C(409)-C(408)-H(408)	120.0
C(302)-C(303)-H(303)	120.0	C(408)-C(409)-C(410)	120.0
C(304)-C(303)-H(303)	120.0	C(408)-C(409)-H(409)	120.0
C(305)-C(304)-C(303)	120.0	C(410)-C(409)-H(409)	120.0
C(305)-C(304)-H(304)	120.0	C(409)-C(410)-C(411)	120.0
C(303)-C(304)-H(304)	120.0	C(409)-C(410)-H(410)	120.0
C(304)-C(305)-C(306)	120.0	C(411)-C(410)-H(410)	120.0
C(304)-C(305)-H(305)	120.0	C(412)-C(411)-C(410)	120.0
C(306)-C(305)-H(305)	120.0	C(412)-C(411)-H(411)	120.0
C(305)-C(306)-C(301)	120.0	C(410)-C(411)-H(411)	120.0
C(305)-C(306)-H(306)	120.0	C(411)-C(412)-C(407)	120.0
C(301)-C(306)-H(306)	120.0	C(411)-C(412)-H(412)	120.0
C(308)-C(307)-C(312)	120.0	C(407)-C(412)-H(412)	120.0
C(308)-C(307)-C(300)	121.5(7)	C(500)-N(500)-C(24)	122.9(13)
C(312)-C(307)-C(300)	118.5(7)	N(500)-C(500)-C(501)	131.3(13)
C(307)-C(308)-C(309)	120.0	N(500)-C(500)-C(507)	114.7(12)
C(307)-C(308)-H(308)	120.0	C(501)-C(500)-C(507)	114.0(10)
C(309)-C(308)-H(308)	120.0	C(502)-C(501)-C(506)	120.0
C(310)-C(309)-C(308)	120.0	C(502)-C(501)-C(500)	120.1(13)
C(310)-C(309)-H(309)	120.0	C(506)-C(501)-C(500)	119.9(13)
C(308)-C(309)-H(309)	120.0	C(501)-C(502)-C(503)	120.0
C(309)-C(310)-C(311)	120.0	C(501)-C(502)-H(502)	120.0
C(309)-C(310)-H(310)	120.0	C(503)-C(502)-H(502)	120.0
C(311)-C(310)-H(310)	120.0	C(504)-C(503)-C(502)	120.0
C(310)-C(311)-C(312)	120.0	C(504)-C(503)-H(503)	120.0
C(310)-C(311)-H(311)	120.0	C(502)-C(503)-H(503)	120.0
C(312)-C(311)-H(311)	120.0	C(503)-C(504)-C(505)	120.0
C(311)-C(312)-C(307)	120.0	C(503)-C(504)-H(504)	120.0

C(505)-C(504)-H(504)	120.0	C(609)-C(610)-H(610)	120.0
C(504)-C(505)-C(506)	120.0	C(611)-C(610)-H(610)	120.0
C(504)-C(505)-H(505)	120.0	C(612)-C(611)-C(610)	120.0
C(506)-C(505)-H(505)	120.0	C(612)-C(611)-H(611)	120.0
C(505)-C(506)-C(501)	120.0	C(610)-C(611)-H(611)	120.0
C(505)-C(506)-H(506)	120.0	C(611)-C(612)-C(607)	120.0
C(501)-C(506)-H(506)	120.0	C(611)-C(612)-H(612)	120.0
C(508)-C(507)-C(512)	120.0	C(607)-C(612)-H(612)	120.0
C(508)-C(507)-C(500)	120.9(8)	C(736)-C(701)-C(704)	81(2)
C(512)-C(507)-C(500)	119.0(8)	C(736)-C(701)-C(719)	83(3)
C(507)-C(508)-C(509)	120.0	C(704)-C(701)-C(719)	91(2)
C(507)-C(508)-H(508)	120.0	C(704)-C(702)-C(707)	120(2)
C(509)-C(508)-H(508)	120.0	C(707)-C(703)-C(737)	63(2)
C(510)-C(509)-C(508)	120.0	C(702)-C(704)-C(701)	104(2)
C(510)-C(509)-H(509)	120.0	C(702)-C(704)-C(736)	68(2)
C(508)-C(509)-H(509)	120.0	C(701)-C(704)-C(736)	47.0(16)
C(511)-C(510)-C(509)	120.0	C(717)-C(706)-C(710)	136(3)
C(511)-C(510)-H(510)	120.0	C(717)-C(706)-C(709)	53(2)
C(509)-C(510)-H(510)	120.0	C(710)-C(706)-C(709)	102(2)
C(512)-C(511)-C(510)	120.0	C(703)-C(707)-C(737)	64(2)
C(512)-C(511)-H(511)	120.0	C(703)-C(707)-C(702)	104(2)
C(510)-C(511)-H(511)	120.0	C(737)-C(707)-C(702)	102(2)
C(511)-C(512)-C(507)	120.0	C(717)-C(709)-C(706)	46(2)
C(511)-C(512)-H(512)	120.0	C(717)-C(709)-C(725)	140(3)
C(507)-C(512)-H(512)	120.0	C(706)-C(709)-C(725)	139(2)
C(600)-N(600)-C(24)	108.8(15)	C(727)#1-C(711)-C(742)	80(3)
N(600)-C(600)-C(601)	130.4(15)	C(727)#1-C(711)-C(740)	81(4)
N(600)-C(600)-C(607)	113.7(14)	C(742)-C(711)-C(740)	45(3)
C(601)-C(600)-C(607)	115.9(12)	C(727)#1-C(711)-C(726)#1	97(3)
C(602)-C(601)-C(606)	120.0	C(742)-C(711)-C(726)#1	171(3)
C(602)-C(601)-C(600)	120.2(11)	C(740)-C(711)-C(726)#1	143(5)
C(606)-C(601)-C(600)	119.8(11)	C(727)#1-C(711)-C(712)#1	56(3)
C(603)-C(602)-C(601)	120.0	C(742)-C(711)-C(712)#1	125(3)
C(603)-C(602)-H(602)	120.0	C(740)-C(711)-C(712)#1	135(4)
C(601)-C(602)-H(602)	120.0	C(726)#1-C(711)-C(712)#1	48.8(19)
C(604)-C(603)-C(602)	120.0	C(735)-C(712)-C(727)	52(4)
C(604)-C(603)-H(603)	120.0	C(735)-C(712)-C(726)	96(5)
C(602)-C(603)-H(603)	120.0	C(727)-C(712)-C(726)	102(3)
C(603)-C(604)-C(605)	120.0	C(735)-C(712)-C(711)#2	83(5)
C(603)-C(604)-H(604)	120.0	C(727)-C(712)-C(711)#2	47(2)
C(605)-C(604)-H(604)	120.0	C(726)-C(712)-C(711)#2	63(2)
C(606)-C(605)-C(604)	120.0	C(735)-C(713)-C(727)	45(3)
C(606)-C(605)-H(605)	120.0	C(706)-C(717)-C(709)	80(3)
C(604)-C(605)-H(605)	120.0	C(706)-C(717)-C(708)	127(4)
C(605)-C(606)-C(601)	120.0	C(709)-C(717)-C(708)	93(3)
C(605)-C(606)-H(606)	120.0	C(701)-C(719)-C(736)	43.4(16)
C(601)-C(606)-H(606)	120.0	C(723)-C(721)-C(720)	103(4)
C(608)-C(607)-C(612)	120.0	C(733)-C(724)-C(731)	93(3)
C(608)-C(607)-C(600)	116.4(10)	C(718)-C(726)-C(712)	78(3)
C(612)-C(607)-C(600)	123.5(10)	C(718)-C(726)-C(711)#2	135(4)
C(607)-C(608)-C(609)	120.0	C(712)-C(726)-C(711)#2	68(2)
C(607)-C(608)-H(608)	120.0	C(735)-C(727)-C(711)#2	98(4)
C(609)-C(608)-H(608)	120.0	C(735)-C(727)-C(712)	37(3)
C(610)-C(609)-C(608)	120.0	C(711)#2-C(727)-C(712)	77(3)
C(610)-C(609)-H(609)	120.0	C(735)-C(727)-C(713)	59(3)
C(608)-C(609)-H(609)	120.0	C(711)#2-C(727)-C(713)	154(4)
C(609)-C(610)-C(611)	120.0	C(712)-C(727)-C(713)	76(3)

```
C(735)-C(727)-C(742)#2 149(4)
C(711)#2-C(727)-C(742)#251(2)
C(712)-C(727)-C(742)#2 119(3)
C(713)-C(727)-C(742)#2 149(3)
C(715)#1-C(732)-C(722) 105(3)
C(712)-C(735)-C(727)    91(6)
C(712)-C(735)-C(713)   109(6)
C(727)-C(735)-C(713)    75(4)
C(701)-C(736)-C(704)    51.5(18)
C(701)-C(736)-C(719)    54(2)
C(704)-C(736)-C(719)    70(2)
C(703)-C(737)-C(707)    53.3(19)
C(742)-C(740)-C(711)    61(5)
C(734)-C(742)-C(740)   106(6)
C(734)-C(742)-C(711)   148(4)
C(740)-C(742)-C(711)    74(5)
C(734)-C(742)-C(727)#1 164(4)
C(740)-C(742)-C(727)#1  77(5)
C(711)-C(742)-C(727)#1  49(2)
```

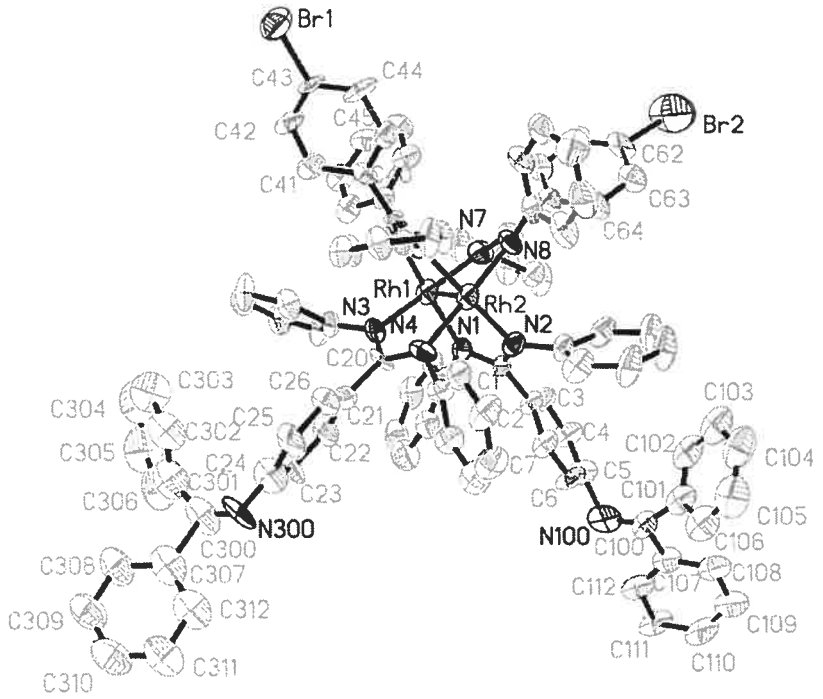

Table 1. Crystal data and structure refinement for ***cis*-V-8**.

Empirical formula	C102 H76 Br2 N10 Rh2	
Formula weight	1807.37	
Temperature	100(2)K	
Wavelength	1.54178 Å	
Crystal system	Monoclinic	
Space group	P21/c	
Unit cell dimensions	a = 17.580(4) Å	$\alpha = 90^\circ$
	b = 26.769(5) Å	$\beta = 95.080(12)^\circ$
	c = 24.033(4) Å	$\gamma = 90^\circ$
Volume	11266(4)Å^3	
Z	4	
Density (calculated)	1.066 g/cm^3	
Absorption coefficient	3.520 mm^{-1}	

F(000)	3672
Crystal size	0.28 x 0.12 x 0.10 mm
Theta range for data collection	2.48 to 66.99°
Index ranges	$-20 \leq h \leq 20$, $-31 \leq k \leq 31$, $-27 \leq \ell \leq 27$
Reflections collected	54125
Independent reflections	18314 [R_{int} = 0.072]
Absorption correction	Semi-empirical from equivalents
Max. and min. transmission	0.7800 and 0.5300
Refinement method	Full-matrix least-squares on F^2
Data / restraints / parameters	18314 / 1039 / 1196
Goodness-of-fit on F^2	0.774
Final R indices [I>2sigma(I)]	R1 = 0.0974, wR_2 = 0.2378
R indices (all data)	R1 = 0.2058, wR_2 = 0.2657
Largest diff. peak and hole	1.644 and -1.208 e/Å^3

Table 2. Atomic coordinates (x 10^4) and equivalent isotropic displacement parameters (Å^2 x 10^3) for ***cis*-V-8**.

U_{eq} is defined as one third of the trace of the orthogonalized Uij tensor.

	Occ.	x	y	z	U_{eq}
Rh(1)	1	2158(1)	6781(1)	5648(1)	71(1)
Rh(2)	1	3020(1)	7353(1)	5266(1)	71(1)
Br(1)	1	4466(1)	4532(1)	3667(1)	138(1)
Br(2)	1	6076(2)	6541(1)	8277(1)	280(2)
N(1)	1	1723(5)	7360(3)	6028(3)	63(2)
N(2)	1	2716(5)	7852(3)	5849(4)	71(3)
N(3)	1	1450(5)	6897(3)	4980(3)	68(2)
N(4)	1	2162(5)	7576(3)	4748(4)	75(3)
N(5)	1	2653(5)	6239(3)	5267(3)	67(2)
N(6)	1	3262(4)	6791(3)	4747(4)	73(3)
N(7)	1	2936(5)	6692(3)	6288(4)	85(3)
N(8)	1	3841(5)	7102(3)	5805(4)	77(3)
C(1)	1	2089(6)	7807(4)	6100(5)	68(3)

C(2)	1	1835(6)	8199(4)	6462(4)	70(3)
C(3)	1	1632(6)	8075(4)	7011(5)	79(3)
C(4)	1	1346(7)	8437(4)	7331(5)	101(4)
C(5)	1	1268(8)	8914(5)	7153(5)	113(5)
C(6)	1	1460(7)	9043(4)	6607(5)	106(4)
C(7)	1	1721(6)	8678(4)	6287(4)	87(4)
C(8)	1	977(8)	7355(4)	6137(5)	81(4)
C(9)	1	672(7)	7000(4)	6507(5)	84(4)
C(10)	1	-113(9)	6985(5)	6584(5)	107(5)
C(11)	1	-641(8)	7297(6)	6301(7)	122(5)
C(12)	1	-390(8)	7667(6)	5945(7)	129(5)
C(13)	1	410(7)	7667(5)	5874(5)	88(4)
C(14)	1	3255(6)	8227(4)	6047(5)	80(3)
C(15)	1	3620(7)	8235(4)	6584(5)	96(4)
C(16)	1	4168(7)	8568(5)	6785(5)	112(5)
C(17)	1	4423(9)	8914(5)	6419(6)	142(6)
C(18)	1	4116(9)	8944(5)	5882(7)	141(6)
C(19)	1	3538(7)	8606(5)	5677(5)	108(5)
C(20)	1	1513(6)	7321(5)	4650(4)	82(4)
C(21)	1	914(7)	7466(4)	4196(5)	77(3)
C(22)	1	143(7)	7487(4)	4289(5)	96(4)
C(23)	1	-419(6)	7633(5)	3876(5)	103(4)
C(24)	1	-278(9)	7753(6)	3330(6)	125(5)
C(25)	1	516(8)	7723(5)	3261(5)	113(5)
C(26)	1	1108(6)	7580(4)	3644(5)	82(4)
C(27)	1	967(7)	6520(4)	4790(5)	82(4)
C(28)	1	445(7)	6316(4)	5091(5)	88(4)
C(29)	1	39(7)	5913(5)	4950(5)	94(4)
C(30)	1	126(7)	5675(4)	4451(7)	108(5)
C(31)	1	615(7)	5843(5)	4077(6)	118(5)
C(32)	1	1027(6)	6255(5)	4252(5)	88(4)
C(33)	1	2170(7)	8091(4)	4540(5)	83(4)
C(34)	1	1639(7)	8442(5)	4690(5)	96(4)
C(35)	1	1722(9)	8960(6)	4574(6)	125(5)
C(36)	1	2371(10)	9088(5)	4289(6)	129(6)
C(37)	1	2901(9)	8750(5)	4171(5)	116(5)
C(38)	1	2812(7)	8243(5)	4300(5)	88(4)
C(39)	1	3098(6)	6311(4)	4865(4)	60(3)
C(40)	1	3417(6)	5906(4)	4540(4)	71(3)
C(41)	1	2929(7)	5495(4)	4265(5)	92(4)
C(42)	1	3285(8)	5107(4)	4032(4)	95(4)
C(43)	1	4039(7)	5065(4)	4020(4)	79(4)
C(44)	1	4524(8)	5456(4)	4226(5)	102(4)
C(45)	1	4200(7)	5856(4)	4491(4)	79(3)
C(46)	1	2674(7)	5753(4)	5505(5)	73(3)
C(47)	1	1991(7)	5483(4)	5511(4)	91(4)
C(48)	1	1984(8)	5005(4)	5801(5)	98(4)
C(49)	1	2662(9)	4853(5)	6049(6)	111(5)
C(50)	1	3340(7)	5090(5)	6051(5)	99(4)
C(51)	1	3308(7)	5543(4)	5754(5)	92(4)
C(52)	1	3522(6)	6918(4)	4185(5)	74(3)
C(53)	1	4150(6)	7229(4)	4155(5)	83(4)
C(54)	1	4376(7)	7377(4)	3629(5)	97(4)
C(55)	1	3996(6)	7219(4)	3164(5)	84(4)
C(56)	1	3353(7)	6932(4)	3192(4)	86(4)
C(57)	1	3093(6)	6759(4)	3688(4)	76(3)
C(58)	1	3609(7)	6826(4)	6288(5)	81(4)

C(59)	1	4247(6)	6738(5)	6737(5)	77(3)
C(60)	1	4309(8)	6284(5)	7002(5)	104(5)
C(61)	1	4852(9)	6204(5)	7411(7)	127(5)
C(62)	1	5338(7)	6595(7)	7627(5)	117(5)
C(63)	1	5274(7)	7051(6)	7371(6)	110(5)
C(64)	1	4738(7)	7116(5)	6942(5)	96(4)
C(65)	1	2674(6)	6574(4)	6846(5)	75(3)
C(66)	1	2246(6)	6159(4)	6892(5)	99(4)
C(67)	1	1929(7)	6039(5)	7400(5)	100(4)
C(68)	1	2043(7)	6393(5)	7821(5)	110(5)
C(69)	1	2442(7)	6800(5)	7804(4)	101(4)
C(70)	1	2771(6)	6912(4)	7277(5)	82(3)
C(71)	1	4590(8)	7104(5)	5691(5)	82(4)
C(72)	1	4886(8)	7574(6)	5576(5)	113(5)
C(73)	1	5606(9)	7611(6)	5365(7)	130(5)
C(74)	1	6055(10)	7207(7)	5290(7)	144(7)
C(75)	1	5769(8)	6751(6)	5402(6)	117(5)
C(76)	1	5036(7)	6702(5)	5615(4)	89(4)
N(100)	0.50	862(13)	9377(8)	7428(9)	111(8)
C(100)	0.50	1291(10)	9693(8)	7621(11)	94(7)
C(101)	0.50	2134(9)	9797(8)	7613(9)	117(7)
C(102)	0.50	2644(12)	9431(8)	7820(10)	131(8)
C(103)	0.50	3418(11)	9479(9)	7753(10)	150(9)
C(104)	0.50	3682(9)	9892(10)	7477(10)	172(10)
C(105)	0.50	3172(13)	10258(9)	7270(10)	164(9)
C(106)	0.50	2398(12)	10210(8)	7337(10)	140(8)
C(107)	0.50	890(11)	10038(7)	8044(8)	110(7)
C(108)	0.50	1298(10)	10398(8)	8362(9)	135(9)
C(109)	0.50	913(14)	10752(8)	8654(9)	133(9)
C(110)	0.50	120(14)	10746(9)	8627(10)	145(9)
C(111)	0.50	-288(10)	10386(10)	8309(10)	135(8)
C(112)	0.50	97(11)	10031(8)	8017(9)	126(8)
N(200)	0.50	942(13)	9225(6)	7558(9)	94(7)
C(200)	0.50	1287(11)	9606(8)	7676(13)	102(7)
C(201)	0.50	2016(10)	9808(8)	7471(9)	114(7)
C(202)	0.50	2664(12)	9532(8)	7646(10)	135(8)
C(203)	0.50	3372(10)	9675(10)	7486(11)	145(8)
C(204)	0.50	3433(11)	10094(10)	7150(10)	168(10)
C(205)	0.50	2786(15)	10370(8)	6976(10)	162(10)
C(206)	0.50	2077(12)	10226(8)	7136(9)	136(9)
C(207)	0.50	735(11)	10030(7)	7868(8)	99(7)
C(208)	0.50	1047(10)	10434(8)	8173(9)	107(7)
C(209)	0.50	587(13)	10725(8)	8485(10)	136(9)
C(210)	0.50	-184(13)	10613(9)	8493(10)	130(8)
C(211)	0.50	-495(10)	10210(9)	8189(10)	135(9)
C(212)	0.50	-36(11)	9918(7)	7876(9)	130(8)
N(300)	0.50	-742(11)	7933(9)	2894(10)	101(7)
C(300)	0.50	-1287(13)	7676(7)	2805(12)	122(7)
C(301)	0.50	-1468(13)	7120(6)	2832(11)	163(8)
C(302)	0.50	-865(14)	6811(8)	2718(13)	150(8)
C(303)	0.50	-873(15)	6309(8)	2865(14)	167(9)
C(304)	0.50	-1484(17)	6116(7)	3126(14)	183(10)
C(305)	0.50	-2087(14)	6424(9)	3239(13)	209(11)
C(306)	0.50	-2079(11)	6927(9)	3092(12)	201(10)
C(307)	0.50	-1900(11)	7928(8)	2352(9)	134(7)
C(308)	0.50	-2425(15)	7637(9)	2029(12)	145(8)
C(309)	0.50	-2995(15)	7864(12)	1680(13)	147(9)

C(310)	0.50	-3041(14)	8382(13)	1653(12)	153(10)
C(311)	0.50	-2516(14)	8673(9)	1975(12)	153(10)
C(312)	0.50	-1945(11)	8446(8)	2325(9)	137(8)
N(400)	0.50	-960(13)	8105(9)	3004(11)	128(9)
C(400)	0.50	-1170(13)	7730(8)	2761(13)	125(8)
C(401)	0.50	-1166(13)	7172(7)	2887(11)	142(8)
C(402)	0.50	-657(14)	6882(8)	2615(12)	160(9)
C(403)	0.50	-631(16)	6368(8)	2700(14)	184(10)
C(404)	0.50	-1113(16)	6145(7)	3055(14)	172(10)
C(405)	0.50	-1621(13)	6436(9)	3327(12)	191(10)
C(406)	0.50	-1647(12)	6949(9)	3242(11)	191(10)
C(407)	0.50	-2012(12)	7875(9)	2469(10)	145(8)
C(408)	0.50	-2413(16)	7551(9)	2098(13)	142(8)
C(409)	0.50	-2988(17)	7733(13)	1718(13)	147(9)
C(410)	0.50	-3162(15)	8239(13)	1708(13)	153(10)
C(411)	0.50	-2761(15)	8564(10)	2078(14)	154(9)
C(412)	0.50	-2187(13)	8382(9)	2459(11)	172(10)

Table 3. Hydrogen coordinates (x 10^4) and isotropic displacement parameters ($Å^2$ x 10^3) for ***cis*-V-8**.

	Occ.	x	y	z	U_{eq}
H(3)	1	1696	7744	7149	94
H(4)	1	1197	8352	7689	122
H(6)	1	1406	9376	6473	128
H(7)	1	1830	8760	5917	104
H(9)	1	1007	6769	6704	101
H(10)	1	-286	6752	6842	128
H(11)	1	-1170	7261	6347	146
H(12)	1	-730	7903	5763	155
H(13)	1	577	7905	5619	105
H(15)	1	3475	7986	6836	116
H(16)	1	4367	8560	7165	134
H(17)	1	4822	9137	6546	171
H(18)	1	4289	9194	5642	169
H(19)	1	3334	8625	5298	130
H(22)	1	-4	7399	4647	115
H(23)	1	-931	7652	3972	124
H(25)	1	658	7812	2902	136
H(26)	1	1618	7560	3546	98
H(28)	1	358	6472	5434	106
H(29)	1	-315	5788	5192	113
H(30)	1	-165	5382	4362	130
H(31)	1	663	5686	3728	141
H(32)	1	1380	6383	4010	106
H(34)	1	1213	8333	4874	115
H(35)	1	1369	9203	4680	150
H(36)	1	2433	9426	4178	154
H(37)	1	3339	8856	3998	139
H(38)	1	3191	8007	4221	106

H(41)	1	2388	5507	4256	110
H(42)	1	2974	4847	3865	114
H(44)	1	5056	5447	4184	123
H(45)	1	4530	6109	4649	95
H(47)	1	1533	5612	5327	109
H(48)	1	1531	4813	5814	118
H(49)	1	2663	4545	6245	133
H(50)	1	3799	4961	6236	119
H(51)	1	3776	5715	5728	110
H(53)	1	4428	7342	4488	100
H(54)	1	4804	7591	3611	116
H(55)	1	4166	7303	2812	100
H(56)	1	3068	6845	2851	103
H(57)	1	2658	6550	3693	91
H(60)	1	3959	6025	6892	125
H(61)	1	4917	5877	7563	153
H(63)	1	5602	7318	7495	132
H(64)	1	4693	7435	6770	115
H(66)	1	2155	5943	6580	119
H(67)	1	1658	5738	7447	120
H(68)	1	1805	6332	8154	132
H(69)	1	2519	7015	8119	121
H(70)	1	3046	7214	7235	98
H(72)	1	4603	7867	5641	136
H(73)	1	5785	7932	5270	156
H(74)	1	6549	7243	5164	172
H(75)	1	6059	6460	5338	140
H(76)	1	4859	6379	5705	107
H(102)	0.50	2464	9148	8009	158
H(103)	0.50	3766	9229	7895	180
H(104)	0.50	4211	9925	7431	206
H(105)	0.50	3352	10540	7082	197
H(106)	0.50	2050	10460	7195	169
H(108)	0.50	1840	10403	8381	161
H(109)	0.50	1191	10999	8871	159
H(110)	0.50	-144	10988	8826	174
H(111)	0.50	-830	10381	8290	162
H(112)	0.50	-181	9785	7800	152
H(202)	0.50	2622	9246	7875	162
H(203)	0.50	3815	9487	7605	174
H(204)	0.50	3918	10192	7041	202
H(205)	0.50	2827	10656	6747	194
H(206)	0.50	1635	10415	7017	163
H(208)	0.50	1573	10511	8167	128
H(209)	0.50	800	11001	8693	163
H(210)	0.50	-498	10813	8706	156
H(211)	0.50	-1022	10133	8194	162
H(212)	0.50	-249	9642	7668	156
H(302)	0.50	-447	6943	2540	180
H(303)	0.50	-461	6098	2788	201
H(304)	0.50	-1490	5773	3226	219
H(305)	0.50	-2505	6292	3417	250
H(306)	0.50	-2491	7138	3170	241
H(308)	0.50	-2394	7283	2048	174
H(309)	0.50	-3354	7666	1459	176
H(310)	0.50	-3430	8538	1414	183
H(311)	0.50	-2547	9027	1957	183

H(312)	0.50	-1587	8645	2546	164
H(402)	0.50	-328	7034	2372	192
H(403)	0.50	-284	6169	2514	220
H(404)	0.50	-1094	5794	3113	206
H(405)	0.50	-1950	6283	3570	229
H(406)	0.50	-1995	7148	3428	230
H(408)	0.50	-2294	7204	2105	170
H(409)	0.50	-3261	7511	1465	176
H(410)	0.50	-3555	8364	1447	183
H(411)	0.50	-2880	8910	2071	185
H(412)	0.50	-1913	8604	2712	206

Table 4. Anisotropic parameters ($Å^2$ x 10^3) for ***cis*-V-8**.

The anisotropic displacement factor exponent takes the form:

$$-2\,\pi^2\,[\,h^2\,a^{*2}\,U_{11} + \ldots + 2\,h\,k\,a^*\,b^*\,U_{12}\,]$$

	U11	U22	U33	U23	U13	U12
Rh(1)	103(1)	78(1)	31(1)	-2(1)	3(1)	3(1)
Rh(2)	105(1)	76(1)	32(1)	-3(1)	2(1)	0(1)
Br(1)	178(2)	124(1)	108(2)	-38(1)	-6(1)	39(1)
Br(2)	348(3)	345(3)	133(3)	-49(2)	-62(2)	134(3)
N(1)	79(6)	80(6)	29(5)	-15(4)	-6(4)	10(5)
N(2)	99(7)	60(6)	51(7)	-6(4)	1(6)	3(5)
N(3)	83(6)	92(7)	25(6)	3(4)	-18(5)	10(5)
N(4)	60(6)	99(7)	64(7)	12(5)	-1(5)	25(5)
N(5)	104(7)	61(5)	38(6)	6(4)	13(5)	3(5)
N(6)	85(6)	89(7)	44(6)	-1(5)	-1(5)	7(5)
N(7)	50(6)	87(7)	121(10)	-3(6)	24(6)	-3(5)
N(8)	44(5)	122(8)	63(8)	-16(6)	-2(5)	13(5)
C(1)	83(9)	72(8)	44(8)	-22(6)	-24(6)	15(7)
C(2)	118(9)	65(7)	29(7)	-7(5)	8(6)	12(7)
C(3)	112(9)	64(7)	61(9)	-4(6)	14(7)	8(6)
C(4)	179(12)	73(8)	55(9)	18(6)	28(9)	24(9)
C(5)	176(13)	122(11)	42(9)	-15(7)	18(9)	52(10)
C(6)	196(13)	64(8)	59(9)	-15(6)	14(9)	49(8)
C(7)	154(11)	81(8)	25(7)	-7(5)	10(7)	6(8)
C(8)	118(10)	71(8)	52(9)	-30(6)	-4(8)	26(8)
C(9)	120(10)	90(9)	41(8)	-16(6)	5(7)	-8(8)
C(10)	134(12)	150(13)	37(9)	-15(7)	14(9)	-20(10)
C(11)	103(11)	176(16)	86(14)	-38(11)	11(10)	-17(11)
C(12)	115(13)	157(14)	116(15)	-11(11)	5(10)	4(11)
C(13)	80(9)	120(10)	66(9)	-17(7)	21(7)	-4(8)
C(14)	103(9)	94(9)	41(8)	-15(7)	-1(7)	-3(7)
C(15)	150(12)	85(9)	57(10)	-16(7)	24(9)	-6(8)
C(16)	166(13)	130(12)	35(9)	3(8)	-14(9)	-47(10)
C(17)	214(16)	158(14)	49(12)	-19(9)	-19(12)	-72(12)
C(18)	209(16)	101(11)	112(15)	-4(10)	13(13)	-77(10)
C(19)	170(13)	111(10)	50(9)	5(7)	41(9)	-15(9)

C(20)	62(8)	169(12)	11(7)	-21(7)	-19(6)	61(8)
C(21)	83(9)	75(8)	73(10)	-4(6)	4(8)	11(6)
C(22)	90(9)	141(11)	56(10)	-10(7)	3(8)	14(8)
C(23)	59(8)	204(14)	43(10)	-3(9)	-17(7)	15(8)
C(24)	115(12)	183(15)	82(13)	9(10)	42(10)	-2(11)
C(25)	146(12)	157(12)	30(9)	19(8)	-23(9)	8(11)
C(26)	87(8)	118(9)	40(8)	16(6)	12(7)	13(7)
C(27)	92(9)	98(9)	54(9)	-23(7)	-14(7)	1(7)
C(28)	111(10)	87(9)	68(9)	-10(7)	21(8)	-42(8)
C(29)	108(10)	130(12)	46(9)	-4(7)	16(8)	-20(9)
C(30)	98(10)	94(10)	131(15)	0(9)	2(10)	-37(8)
C(31)	132(12)	137(12)	80(12)	-30(9)	-6(9)	-66(10)
C(32)	97(9)	132(11)	37(8)	14(7)	6(7)	-15(8)
C(33)	127(11)	82(9)	37(8)	8(6)	-11(7)	36(8)
C(34)	146(11)	92(9)	49(9)	14(7)	3(8)	14(9)
C(35)	181(15)	121(13)	69(12)	16(9)	-15(10)	0(11)
C(36)	219(17)	76(10)	87(13)	21(8)	-10(12)	1(11)
C(37)	213(16)	90(11)	46(9)	0(7)	21(10)	-5(11)
C(38)	127(10)	92(9)	40(8)	-9(7)	-14(7)	6(9)
C(39)	80(8)	58(7)	37(7)	-26(5)	-20(6)	44(6)
C(40)	59(7)	92(9)	60(9)	16(6)	-1(6)	9(7)
C(41)	124(10)	56(7)	96(11)	7(7)	16(8)	-1(7)
C(42)	176(12)	80(8)	30(7)	-9(5)	9(8)	54(9)
C(43)	124(10)	58(7)	57(8)	-23(5)	14(7)	44(7)
C(44)	177(12)	52(7)	83(10)	-9(6)	42(9)	37(8)
C(45)	115(10)	74(8)	46(8)	-3(6)	-9(7)	-1(7)
C(46)	98(9)	76(8)	44(8)	-18(6)	1(7)	15(8)
C(47)	137(11)	88(9)	49(9)	3(6)	15(8)	-11(8)
C(48)	117(11)	89(9)	90(12)	3(8)	22(9)	-7(8)
C(49)	124(12)	106(11)	105(13)	19(8)	22(11)	43(10)
C(50)	94(10)	117(11)	84(11)	18(8)	1(8)	4(9)
C(51)	125(11)	88(9)	64(10)	7(7)	20(8)	15(8)
C(52)	86(8)	79(8)	56(9)	-13(6)	-8(7)	8(6)
C(53)	102(9)	107(10)	37(8)	0(6)	-13(7)	-18(7)
C(54)	156(11)	116(9)	15(8)	-7(6)	-12(8)	-36(8)
C(55)	93(9)	114(10)	43(9)	6(6)	1(7)	-12(7)
C(56)	123(10)	114(10)	18(7)	-20(6)	-6(7)	13(8)
C(57)	92(8)	118(9)	16(7)	-3(6)	-12(6)	-6(7)
C(58)	100(10)	95(9)	42(9)	-2(6)	-29(8)	42(8)
C(59)	81(8)	100(9)	50(9)	5(7)	1(7)	5(8)
C(60)	140(12)	143(13)	24(9)	-12(7)	-24(8)	35(10)
C(61)	195(16)	105(11)	82(13)	-31(9)	20(11)	43(11)
C(62)	128(10)	183(12)	31(9)	-3(8)	-51(7)	58(9)
C(63)	114(11)	159(13)	55(11)	-8(9)	-7(9)	21(9)
C(64)	99(10)	153(12)	30(9)	-1(8)	-20(7)	15(9)
C(66)	140(11)	122(10)	35(8)	-3(6)	6(8)	-44(8)
C(67)	115(10)	124(11)	59(10)	14(8)	3(8)	-9(8)
C(68)	156(12)	147(13)	28(9)	-5(8)	17(8)	-28(10)
C(69)	156(12)	128(11)	19(7)	0(7)	12(7)	-36(9)
C(70)	123(9)	80(8)	41(8)	4(6)	-6(7)	3(7)
C(71)	85(10)	108(10)	48(9)	-9(7)	-14(7)	-10(9)
C(72)	96(10)	194(16)	51(10)	-10(9)	9(8)	-11(11)
C(73)	135(14)	149(14)	100(14)	18(11)	-25(11)	-29(12)
C(74)	136(15)	155(16)	145(17)	-30(13)	47(12)	-22(13)
C(75)	101(11)	163(15)	84(12)	-47(10)	-12(9)	11(11)
C(76)	81(9)	144(12)	41(8)	6(7)	-3(7)	13(9)
N(100)	180(16)	125(16)	26(13)	52(11)	2(12)	36(14)

C(100)	166(14)	85(12)	29(12)	3(10)	-4(12)	2(12)
C(101)	198(14)	105(13)	47(13)	-4(11)	5(13)	16(13)
C(102)	232(18)	125(16)	40(15)	-29(12)	26(14)	0(16)
C(103)	234(19)	147(18)	72(18)	-35(14)	32(17)	-8(17)
C(104)	260(19)	151(19)	107(19)	-17(17)	27(17)	-51(17)
C(105)	218(18)	194(17)	84(18)	1(16)	32(16)	-41(16)
C(106)	212(17)	136(15)	75(16)	7(14)	24(15)	-1(15)
C(107)	167(14)	116(14)	48(14)	-9(12)	4(13)	36(13)
C(108)	215(18)	117(15)	68(18)	-6(14)	-7(16)	62(15)
C(109)	207(19)	135(15)	55(16)	-7(13)	10(16)	66(16)
C(110)	270(20)	115(15)	49(15)	-41(12)	14(17)	59(17)
C(111)	264(17)	108(16)	32(14)	-30(12)	7(14)	78(14)
C(112)	246(17)	110(14)	21(13)	-11(11)	0(14)	70(15)
N(200)	165(15)	65(12)	57(14)	25(11)	30(12)	32(12)
C(200)	172(14)	103(13)	30(12)	-3(11)	2(12)	-1(12)
C(201)	188(15)	103(13)	49(14)	-23(12)	-12(13)	13(13)
C(202)	231(18)	124(15)	51(15)	-43(13)	8(15)	12(15)
C(203)	224(16)	135(16)	79(16)	-39(14)	24(15)	-38(15)
C(204)	254(19)	183(19)	69(19)	-33(16)	23(16)	-45(17)
C(205)	210(20)	200(18)	82(19)	-8(16)	23(17)	-15(18)
C(206)	202(18)	140(16)	65(17)	-2(14)	6(16)	-18(16)
C(207)	166(15)	113(13)	15(12)	10(10)	-19(12)	43(13)
C(208)	173(15)	99(14)	44(14)	-24(12)	-20(13)	62(13)
C(209)	217(19)	127(14)	62(16)	-23(13)	7(16)	51(15)
C(210)	254(19)	107(16)	27(14)	-50(12)	-4(15)	45(16)
C(211)	269(19)	98(17)	33(15)	-22(13)	-11(15)	55(15)
C(212)	254(18)	111(16)	26(14)	-11(12)	13(15)	56(15)
N(300)	66(13)	219(17)	17(11)	48(12)	-4(10)	36(12)
C(300)	111(13)	207(15)	51(12)	58(12)	12(12)	-11(13)
C(301)	163(16)	217(15)	109(14)	27(14)	15(14)	-10(14)
C(302)	126(16)	201(17)	127(16)	39(16)	30(14)	-10(16)
C(303)	166(17)	158(16)	183(18)	48(15)	52(16)	-38(16)
C(304)	170(20)	174(18)	210(20)	55(16)	42(19)	-85(17)
C(305)	220(20)	193(18)	210(20)	48(17)	43(19)	-112(18)
C(306)	210(20)	203(19)	190(20)	24(18)	-4(19)	-85(18)
C(307)	123(13)	222(15)	64(13)	29(13)	44(11)	-14(13)
C(308)	135(16)	220(17)	79(16)	24(15)	6(14)	1(15)
C(309)	126(15)	215(19)	100(16)	28(16)	10(14)	26(15)
C(310)	120(16)	210(20)	132(18)	55(17)	15(16)	18(16)
C(311)	133(18)	200(18)	126(18)	64(16)	17(16)	-22(16)
C(312)	131(15)	200(16)	85(15)	47(14)	43(13)	-16(15)
N(400)	77(14)	270(20)	38(15)	40(15)	-5(12)	7(15)
C(400)	102(14)	217(15)	54(13)	50(13)	2(12)	-16(14)
C(401)	129(15)	218(16)	82(14)	37(14)	27(13)	-28(15)
C(402)	135(16)	196(17)	148(17)	33(15)	13(15)	-23(15)
C(403)	172(19)	188(19)	190(20)	25(18)	25(18)	-16(18)
C(404)	140(20)	178(17)	210(20)	39(16)	66(18)	-65(16)
C(405)	182(19)	170(17)	219(18)	40(16)	4(17)	-133(16)
C(406)	197(19)	209(17)	165(18)	-12(17)	-1(17)	-67(17)
C(407)	141(14)	219(15)	78(14)	23(13)	21(13)	-17(14)
C(408)	136(15)	219(17)	70(15)	39(14)	7(14)	2(14)
C(409)	125(16)	217(19)	98(17)	11(17)	2(15)	29(16)
C(410)	124(16)	200(20)	128(18)	54(17)	2(15)	45(17)
C(411)	123(17)	203(17)	135(18)	61(16)	-1(16)	0(16)
C(412)	160(17)	229(18)	123(18)	37(16)	-8(16)	-17(16)

Table 5. Bond lengths [Å] and angles [°] for ***cis*-V-8**.

Rh(1)-N(5)	1.960(8)	C(24)-C(25)	1.421(15)
Rh(1)-N(3)	1.967(8)	C(24)-N(400)	1.66(3)
Rh(1)-N(7)	1.981(10)	C(24)-C(400)	1.99(3)
Rh(1)-N(1)	1.986(8)	C(25)-C(26)	1.381(14)
Rh(1)-Rh(2)	2.3929(12)	C(27)-C(28)	1.336(13)
Rh(2)-N(4)	1.961(8)	C(27)-C(32)	1.488(14)
Rh(2)-N(8)	1.971(9)	C(28)-C(29)	1.319(13)
Rh(2)-N(6)	2.023(8)	C(29)-C(30)	1.378(15)
Rh(2)-N(2)	2.042(8)	C(30)-C(31)	1.373(15)
Br(1)-C(43)	1.854(8)	C(31)-C(32)	1.365(14)
Br(2)-C(62)	1.945(11)	C(33)-C(38)	1.373(14)
N(1)-C(8)	1.360(13)	C(33)-C(34)	1.392(14)
N(1)-C(1)	1.364(11)	C(34)-C(35)	1.425(15)
N(2)-C(1)	1.307(11)	C(35)-C(36)	1.424(17)
N(2)-C(14)	1.431(12)	C(36)-C(37)	1.347(16)
N(3)-C(27)	1.370(12)	C(37)-C(38)	1.404(14)
N(3)-C(20)	1.394(13)	C(39)-C(40)	1.476(12)
N(4)-C(20)	1.333(13)	C(40)-C(45)	1.397(12)
N(4)-C(33)	1.468(12)	C(40)-C(41)	1.511(14)
N(5)-C(39)	1.311(11)	C(41)-C(42)	1.359(12)
N(5)-C(46)	1.419(12)	C(42)-C(43)	1.334(14)
N(6)-C(39)	1.353(11)	C(43)-C(44)	1.411(14)
N(6)-C(52)	1.501(13)	C(44)-C(45)	1.393(12)
N(7)-C(58)	1.236(13)	C(46)-C(51)	1.342(14)
N(7)-C(65)	1.490(13)	C(46)-C(47)	1.403(13)
N(8)-C(71)	1.367(13)	C(47)-C(48)	1.458(14)
N(8)-C(58)	1.465(13)	C(48)-C(49)	1.347(15)
C(1)-C(2)	1.459(12)	C(49)-C(50)	1.350(14)
C(2)-C(7)	1.357(12)	C(50)-C(51)	1.405(14)
C(2)-C(3)	1.436(13)	C(52)-C(53)	1.389(13)
C(3)-C(4)	1.361(13)	C(52)-C(57)	1.421(13)
C(4)-C(5)	1.349(14)	C(53)-C(54)	1.414(13)
C(5)-C(6)	1.427(15)	C(54)-C(55)	1.321(13)
C(5)-N(200)	1.44(2)	C(55)-C(56)	1.372(13)
C(5)-N(100)	1.60(3)	C(56)-C(57)	1.393(13)
C(6)-C(7)	1.349(12)	C(58)-C(59)	1.506(15)
C(8)-C(13)	1.406(14)	C(59)-C(60)	1.372(15)
C(8)-C(9)	1.438(14)	C(59)-C(64)	1.390(14)
C(9)-C(10)	1.408(14)	C(60)-C(61)	1.324(17)
C(10)-C(11)	1.382(16)	C(61)-C(62)	1.420(17)
C(11)-C(12)	1.406(18)	C(62)-C(63)	1.368(17)
C(12)-C(13)	1.431(14)	C(63)-C(64)	1.345(15)
C(14)-C(15)	1.391(15)	C(65)-C(66)	1.352(13)
C(14)-C(19)	1.465(14)	C(65)-C(70)	1.376(14)
C(15)-C(16)	1.368(14)	C(66)-C(67)	1.422(14)
C(16)-C(17)	1.380(16)	C(67)-C(68)	1.387(15)
C(17)-C(18)	1.358(18)	C(68)-C(69)	1.298(14)
C(18)-C(19)	1.416(16)	C(69)-C(70)	1.470(13)
C(20)-C(21)	1.499(14)	C(71)-C(76)	1.352(14)
C(21)-C(22)	1.395(13)	C(71)-C(72)	1.399(16)
C(21)-C(26)	1.430(14)	C(72)-C(73)	1.408(16)
C(22)-C(23)	1.393(14)	C(73)-C(74)	1.360(17)
C(23)-C(24)	1.396(16)	C(74)-C(75)	1.356(16)
C(24)-N(300)	1.36(3)	C(75)-C(76)	1.435(14)

N(100)-C(100)	1.199(16)	C(409)-C(410)	1.3900
C(100)-C(101)	1.510(15)	C(410)-C(411)	1.3900
C(100)-C(107)	1.585(15)	C(411)-C(412)	1.3900
C(101)-C(102)	1.3900		
C(101)-C(106)	1.3900	N(5)-Rh(1)-N(3)	90.6(3)
C(102)-C(103)	1.3900	N(5)-Rh(1)-N(7)	88.2(3)
C(103)-C(104)	1.3900	N(3)-Rh(1)-N(7)	175.4(4)
C(104)-C(105)	1.3900	N(5)-Rh(1)-N(1)	176.0(4)
C(105)-C(106)	1.3900	N(3)-Rh(1)-N(1)	90.6(3)
C(107)-C(108)	1.3900	N(7)-Rh(1)-N(1)	90.3(3)
C(107)-C(112)	1.3900	N(5)-Rh(1)-Rh(2)	88.5(2)
C(108)-C(109)	1.3900	N(3)-Rh(1)-Rh(2)	87.9(3)
C(109)-C(110)	1.3900	N(7)-Rh(1)-Rh(2)	87.6(3)
C(110)-C(111)	1.3900	N(1)-Rh(1)-Rh(2)	87.7(3)
C(111)-C(112)	1.3900	N(4)-Rh(2)-N(8)	176.7(4)
N(200)-C(200)	1.208(16)	N(4)-Rh(2)-N(6)	91.6(4)
C(200)-C(201)	1.512(15)	N(8)-Rh(2)-N(6)	88.2(3)
C(200)-C(207)	1.590(15)	N(4)-Rh(2)-N(2)	90.2(4)
C(201)-C(202)	1.3900	N(8)-Rh(2)-N(2)	89.6(3)
C(201)-C(206)	1.3900	N(6)-Rh(2)-N(2)	172.7(3)
C(202)-C(203)	1.3900	N(4)-Rh(2)-Rh(1)	87.7(3)
C(203)-C(204)	1.3900	N(8)-Rh(2)-Rh(1)	88.9(3)
C(204)-C(205)	1.3900	N(6)-Rh(2)-Rh(1)	86.3(2)
C(205)-C(206)	1.3900	N(2)-Rh(2)-Rh(1)	86.7(3)
C(207)-C(208)	1.3900	C(8)-N(1)-C(1)	115.9(9)
C(207)-C(212)	1.3900	C(8)-N(1)-Rh(1)	119.9(7)
C(208)-C(209)	1.3900	C(1)-N(1)-Rh(1)	123.1(7)
C(209)-C(210)	1.3900	C(1)-N(2)-C(14)	118.2(9)
C(210)-C(211)	1.3900	C(1)-N(2)-Rh(2)	122.6(7)
C(211)-C(212)	1.3900	C(14)-N(2)-Rh(2)	118.7(7)
N(300)-C(300)	1.183(17)	C(27)-N(3)-C(20)	119.2(10)
C(300)-C(301)	1.524(15)	C(27)-N(3)-Rh(1)	119.0(8)
C(300)-C(307)	1.611(15)	C(20)-N(3)-Rh(1)	121.0(8)
C(301)-C(302)	1.3900	C(20)-N(4)-C(33)	117.1(10)
C(301)-C(306)	1.3900	C(20)-N(4)-Rh(2)	123.7(8)
C(302)-C(303)	1.3900	C(33)-N(4)-Rh(2)	118.1(7)
C(303)-C(304)	1.3900	C(39)-N(5)-C(46)	115.8(8)
C(304)-C(305)	1.3900	C(39)-N(5)-Rh(1)	123.6(7)
C(305)-C(306)	1.3900	C(46)-N(5)-Rh(1)	119.2(6)
C(307)-C(308)	1.3900	C(39)-N(6)-C(52)	119.4(8)
C(307)-C(312)	1.3900	C(39)-N(6)-Rh(2)	121.2(7)
C(308)-C(309)	1.3900	C(52)-N(6)-Rh(2)	118.9(6)
C(309)-C(310)	1.3900	C(58)-N(7)-C(65)	115.7(11)
C(310)-C(311)	1.3900	C(58)-N(7)-Rh(1)	124.0(9)
C(311)-C(312)	1.3900	C(65)-N(7)-Rh(1)	118.5(7)
N(400)-C(400)	1.203(18)	C(71)-N(8)-C(58)	120.0(10)
C(400)-C(401)	1.522(15)	C(71)-N(8)-Rh(2)	122.0(8)
C(400)-C(407)	1.628(16)	C(58)-N(8)-Rh(2)	117.0(7)
C(401)-C(402)	1.3900	N(2)-C(1)-N(1)	115.5(9)
C(401)-C(406)	1.3900	N(2)-C(1)-C(2)	121.6(10)
C(402)-C(403)	1.3900	N(1)-C(1)-C(2)	122.8(10)
C(403)-C(404)	1.3900	C(7)-C(2)-C(3)	117.6(9)
C(404)-C(405)	1.3900	C(7)-C(2)-C(1)	122.5(10)
C(405)-C(406)	1.3900	C(3)-C(2)-C(1)	119.7(10)
C(407)-C(408)	1.3900	C(4)-C(3)-C(2)	119.2(10)
C(407)-C(412)	1.3900	C(5)-C(4)-C(3)	121.8(11)
C(408)-C(409)	1.3900	C(4)-C(5)-C(6)	119.7(11)

C(4)-C(5)-N(200)	111.6(13)	C(36)-C(37)-C(38)	120.7(14)
C(6)-C(5)-N(200)	128.5(13)	C(33)-C(38)-C(37)	119.3(12)
C(4)-C(5)-N(100)	129.6(13)	N(5)-C(39)-N(6)	116.5(8)
C(6)-C(5)-N(100)	110.0(13)	N(5)-C(39)-C(40)	124.2(10)
N(200)-C(5)-N(100)	18.9(12)	N(6)-C(39)-C(40)	119.3(10)
C(7)-C(6)-C(5)	117.9(11)	C(45)-C(40)-C(39)	122.6(10)
C(6)-C(7)-C(2)	123.7(11)	C(45)-C(40)-C(41)	114.8(10)
N(1)-C(8)-C(13)	124.5(11)	C(39)-C(40)-C(41)	122.5(9)
N(1)-C(8)-C(9)	123.0(12)	C(42)-C(41)-C(40)	118.1(11)
C(13)-C(8)-C(9)	112.4(12)	C(43)-C(42)-C(41)	124.6(12)
C(10)-C(9)-C(8)	121.5(12)	C(42)-C(43)-C(44)	120.1(9)
C(11)-C(10)-C(9)	122.9(13)	C(42)-C(43)-Br(1)	121.2(9)
C(10)-C(11)-C(12)	119.4(14)	C(44)-C(43)-Br(1)	118.4(9)
C(11)-C(12)-C(13)	115.9(14)	C(45)-C(44)-C(43)	118.1(11)
C(8)-C(13)-C(12)	127.8(13)	C(44)-C(45)-C(40)	123.9(11)
C(15)-C(14)-N(2)	123.8(11)	C(51)-C(46)-C(47)	117.1(12)
C(15)-C(14)-C(19)	113.5(11)	C(51)-C(46)-N(5)	123.8(12)
N(2)-C(14)-C(19)	122.4(11)	C(47)-C(46)-N(5)	119.0(11)
C(16)-C(15)-C(14)	126.2(12)	C(46)-C(47)-C(48)	120.2(12)
C(15)-C(16)-C(17)	118.1(14)	C(49)-C(48)-C(47)	115.5(12)
C(18)-C(17)-C(16)	121.5(14)	C(50)-C(49)-C(48)	127.4(14)
C(17)-C(18)-C(19)	120.3(14)	C(49)-C(50)-C(51)	114.0(13)
C(18)-C(19)-C(14)	120.3(13)	C(46)-C(51)-C(50)	125.8(13)
N(4)-C(20)-N(3)	115.2(10)	C(53)-C(52)-C(57)	120.0(11)
N(4)-C(20)-C(21)	122.1(12)	C(53)-C(52)-N(6)	119.3(10)
N(3)-C(20)-C(21)	122.6(11)	C(57)-C(52)-N(6)	120.5(10)
C(22)-C(21)-C(26)	117.0(11)	C(52)-C(53)-C(54)	120.2(11)
C(22)-C(21)-C(20)	121.6(11)	C(55)-C(54)-C(53)	120.3(12)
C(26)-C(21)-C(20)	121.4(11)	C(54)-C(55)-C(56)	119.7(11)
C(23)-C(22)-C(21)	122.3(11)	C(55)-C(56)-C(57)	124.1(11)
C(22)-C(23)-C(24)	124.2(12)	C(56)-C(57)-C(52)	115.6(11)
N(300)-C(24)-C(23)	131.5(15)	N(7)-C(58)-N(8)	118.7(11)
N(300)-C(24)-C(25)	117.4(14)	N(7)-C(58)-C(59)	127.4(12)
C(23)-C(24)-C(25)	110.7(14)	N(8)-C(58)-C(59)	113.9(11)
N(300)-C(24)-N(400)	22.8(15)	C(60)-C(59)-C(64)	117.3(13)
C(23)-C(24)-N(400)	113.0(14)	C(60)-C(59)-C(58)	119.7(12)
C(25)-C(24)-N(400)	130.7(14)	C(64)-C(59)-C(58)	122.7(12)
N(300)-C(24)-C(400)	25.4(13)	C(61)-C(60)-C(59)	120.7(15)
C(23)-C(24)-C(400)	116.4(14)	C(60)-C(61)-C(62)	121.5(14)
C(25)-C(24)-C(400)	129.9(14)	C(63)-C(62)-C(61)	118.1(13)
N(400)-C(24)-C(400)	37.1(7)	C(63)-C(62)-Br(2)	116.7(13)
C(26)-C(25)-C(24)	128.9(12)	C(61)-C(62)-Br(2)	125.2(13)
C(25)-C(26)-C(21)	116.8(11)	C(64)-C(63)-C(62)	119.0(14)
C(28)-C(27)-N(3)	123.9(11)	C(63)-C(64)-C(59)	123.2(14)
C(28)-C(27)-C(32)	112.4(11)	C(66)-C(65)-C(70)	120.8(11)
N(3)-C(27)-C(32)	123.4(11)	C(66)-C(65)-N(7)	117.8(10)
C(29)-C(28)-C(27)	125.3(12)	C(70)-C(65)-N(7)	120.7(10)
C(28)-C(29)-C(30)	120.2(12)	C(65)-C(66)-C(67)	121.3(12)
C(31)-C(30)-C(29)	122.7(12)	C(68)-C(67)-C(66)	115.5(12)
C(32)-C(31)-C(30)	114.2(13)	C(69)-C(68)-C(67)	126.4(12)
C(31)-C(32)-C(27)	125.2(11)	C(68)-C(69)-C(70)	117.0(11)
C(38)-C(33)-C(34)	120.3(12)	C(65)-C(70)-C(69)	118.8(11)
C(38)-C(33)-N(4)	117.0(11)	C(76)-C(71)-N(8)	127.2(12)
C(34)-C(33)-N(4)	121.1(11)	C(76)-C(71)-C(72)	117.2(13)
C(33)-C(34)-C(35)	121.4(13)	N(8)-C(71)-C(72)	115.1(13)
C(34)-C(35)-C(36)	115.5(14)	C(71)-C(72)-C(73)	119.9(14)
C(37)-C(36)-C(35)	122.4(14)	C(74)-C(73)-C(72)	122.8(16)

C(73)-C(74)-C(75)	117.4(16)
C(74)-C(75)-C(76)	120.8(15)
C(71)-C(76)-C(75)	121.8(13)
C(100)-N(100)-C(5)	115(2)
N(100)-C(100)-C(101)	135.3(18)
N(100)-C(100)-C(107)	111.0(17)
C(101)-C(100)-C(107)	113.2(14)
C(102)-C(101)-C(106)	120.0
C(102)-C(101)-C(100)	117.9(13)
C(106)-C(101)-C(100)	121.5(14)
C(101)-C(102)-C(103)	120.0
C(102)-C(103)-C(104)	120.0
C(105)-C(104)-C(103)	120.0
C(104)-C(105)-C(106)	120.0
C(105)-C(106)-C(101)	120.0
C(108)-C(107)-C(112)	120.0
C(108)-C(107)-C(100)	121.4(11)
C(112)-C(107)-C(100)	117.7(11)
C(109)-C(108)-C(107)	120.0
C(108)-C(109)-C(110)	120.0
C(109)-C(110)-C(111)	120.0
C(112)-C(111)-C(110)	120.0
C(111)-C(112)-C(107)	120.0
C(200)-N(200)-C(5)	115.2(19)
N(200)-C(200)-C(201)	130.4(19)
N(200)-C(200)-C(207)	111.3(16)
C(201)-C(200)-C(207)	113.3(14)
C(202)-C(201)-C(206)	120.0
C(202)-C(201)-C(200)	114.0(14)
C(206)-C(201)-C(200)	126.0(14)
C(203)-C(202)-C(201)	120.0
C(204)-C(203)-C(202)	120.0
C(203)-C(204)-C(205)	120.0
C(206)-C(205)-C(204)	120.0
C(205)-C(206)-C(201)	120.0
C(208)-C(207)-C(212)	120.0
C(208)-C(207)-C(200)	119.1(12)
C(212)-C(207)-C(200)	118.1(12)
C(207)-C(208)-C(209)	120.0
C(210)-C(209)-C(208)	120.0
C(209)-C(210)-C(211)	120.0
C(212)-C(211)-C(210)	120.0
C(211)-C(212)-C(207)	120.0
C(300)-N(300)-C(24)	111(2)
N(300)-C(300)-C(301)	137(2)
N(300)-C(300)-C(307)	111.1(18)
C(301)-C(300)-C(307)	108.0(14)
C(302)-C(301)-C(306)	120.0
C(302)-C(301)-C(300)	114.0(14)
C(306)-C(301)-C(300)	123.7(14)
C(303)-C(302)-C(301)	120.0
C(304)-C(303)-C(302)	120.0
C(303)-C(304)-C(305)	120.0
C(306)-C(305)-C(304)	120.0
C(305)-C(306)-C(301)	120.0
C(308)-C(307)-C(312)	120.0
C(308)-C(307)-C(300)	120.9(12)
C(312)-C(307)-C(300)	118.9(12)
C(309)-C(308)-C(307)	120.0
C(310)-C(309)-C(308)	120.0
C(309)-C(310)-C(311)	120.0
C(312)-C(311)-C(310)	120.0
C(311)-C(312)-C(307)	120.0
C(400)-N(400)-C(24)	86.2(18)
N(400)-C(400)-C(401)	136(2)
N(400)-C(400)-C(407)	103.8(17)
C(401)-C(400)-C(407)	108.0(14)
N(400)-C(400)-C(24)	56.6(15)
C(401)-C(400)-C(24)	84.5(13)
C(407)-C(400)-C(24)	157.0(19)
C(402)-C(401)-C(406)	120.0
C(402)-C(401)-C(400)	116.6(15)
C(406)-C(401)-C(400)	123.4(14)
C(401)-C(402)-C(403)	120.0
C(404)-C(403)-C(402)	120.0
C(403)-C(404)-C(405)	120.0
C(406)-C(405)-C(404)	120.0
C(405)-C(406)-C(401)	120.0
C(408)-C(407)-C(412)	120.0
C(408)-C(407)-C(400)	121.1(13)
C(412)-C(407)-C(400)	115.6(13)
C(407)-C(408)-C(409)	120.0
C(410)-C(409)-C(408)	120.0
C(409)-C(410)-C(411)	120.0
C(412)-C(411)-C(410)	120.0
C(411)-C(412)-C(407)	120.0

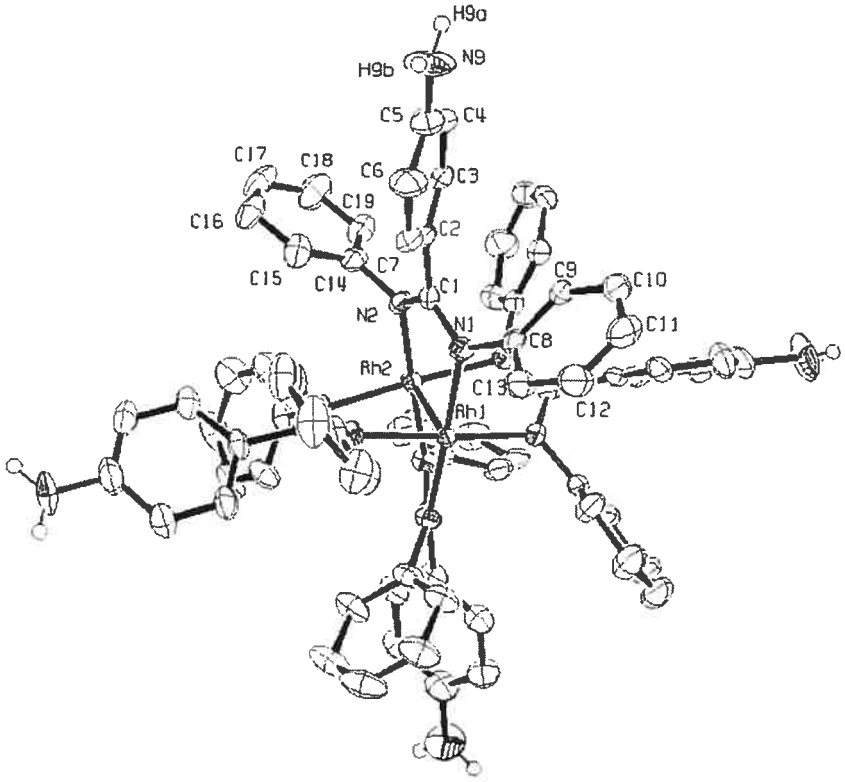

Table 1. Crystal data and structure refinement for **V-10**.

Empirical formula	C76 H64 N12 Rh2	
Formula weight	1351.21	
Temperature	100(2)K	
Wavelength	1.54178 Å	
Crystal system	Tetragonal	
Space group	P4/n	
Unit cell dimensions	a = 17.6228(9) Å	$\alpha = 90^\circ$
	b = 17.6228(9) Å	$\beta = 90^\circ$
	c = 11.8846(15) Å	$\gamma = 90^\circ$
Volume	3690.9(5)$Å^3$	
Z	2	
Density (calculated)	1.216 g/cm^3	
Absorption coefficient	3.985 mm^{-1}	

F(000)	1388
Crystal size	0.08 x 0.06 x 0.06 mm
Theta range for data collection	3.55 to 56.10°
Index ranges	$-18 \leq h \leq 18$, $-18 \leq k \leq 18$, $-10 \leq \ell \leq 12$
Reflections collected	33886
Independent reflections	2400 [R_{int} = 0.064]
Absorption correction	Semi-empirical from equivalents
Max. and min. transmission	0.8400 and 0.7800
Refinement method	Full-matrix least-squares on F^2
Data / restraints / parameters	2400 / 0 / 205
Goodness-of-fit on F^2	1.027
Final R indices [I>2sigma(I)]	R1 = 0.0363, wR_2 = 0.0884
R indices (all data)	R1 = 0.0459, wR_2 = 0.0905
Largest diff. peak and hole	1.455 and -0.545 e/Å^3

Table 2. Atomic coordinates (x 10^4) and equivalent isotropic displacement parameters (Å^2 x 10^3) for **V-10**.

U_{eq} is defined as one third of the trace of the orthogonalized Uij tensor.

	Occ.	x	y	z	U_{eq}
Rh(1)	1	2500	2500	3158(1)	24(1)
Rh(2)	1	2500	2500	5173(1)	26(1)
N(1)	1	2930(2)	1422(2)	3233(3)	27(1)
N(2)	1	2584(2)	1341(2)	5101(3)	28(1)
N(9)	1	3355(2)	-2165(2)	3649(4)	80(1)
C(1)	1	2814(2)	998(2)	4162(4)	30(1)
C(2)	1	2927(2)	162(2)	4101(3)	30(1)
C(3)	1	3378(2)	-229(2)	4864(4)	36(1)
C(4)	1	3520(2)	-999(2)	4719(4)	42(1)
C(5)	1	3206(2)	-1389(2)	3829(4)	53(1)
C(6)	1	2734(2)	-1002(2)	3066(4)	50(1)
C(7)	1	2611(2)	-237(2)	3202(4)	38(1)

C(8)	1	3432(2)	1170(2)	2365(4)	32(1)
C(9)	1	4148(2)	871(2)	2638(4)	40(1)
C(10)	1	4647(2)	669(2)	1759(4)	53(1)
C(11)	1	4436(3)	770(2)	655(4)	58(1)
C(12)	1	3735(3)	1070(2)	408(4)	52(1)
C(13)	1	3235(2)	1258(2)	1253(4)	40(1)
C(14)	1	2255(2)	924(2)	6006(4)	32(1)
C(15)	1	1599(2)	500(2)	5848(4)	41(1)
C(16)	1	1258(2)	135(2)	6748(4)	45(1)
C(17)	1	1563(3)	194(2)	7818(4)	54(1)
C(18)	1	2210(3)	617(2)	7977(4)	56(1)
C(19)	1	2551(2)	981(2)	7062(4)	43(1)

Table 3. Hydrogen coordinates (x 10^4) and isotropic displacement parameters ($Å^2$ x 10^3) for **V-10**.

	Occ.	x	y	z	U_{eq}
H(9A)	1	3655	-2413	4111	120
H(9B)	1	3147	-2402	3073	120
H(3)	1	3590	31	5489	43
H(4)	1	3836	-1258	5239	51
H(6)	1	2502	-1267	2461	60
H(7)	1	2304	26	2672	45
H(9)	1	4294	805	3402	48
H(10)	1	5131	463	1931	64
H(11)	1	4774	633	65	69
H(12)	1	3594	1147	-355	63
H(13)	1	2747	1452	1066	48
H(15)	1	1383	459	5118	49
H(16)	1	813	-158	6631	54
H(17)	1	1328	-54	8436	65
H(18)	1	2425	661	8706	67
H(19)	1	2997	1273	7178	51

Table 4. Anisotropic parameters ($Å^2$ x 10^3) for **V-10**.

The anisotropic displacement factor exponent takes the form:

$$-2\,\pi^2\,[\,h^2\,a^{*2}\,U_{11} + \ldots + 2\,h\,k\,a^*\,b^*\,U_{12}\,]$$

	U11	U22	U33	U23	U13	U12
Rh(1)	18(1)	18(1)	37(1)	0	0	0
Rh(2)	20(1)	20(1)	39(1)	0	0	0
N(1)	27(2)	21(2)	32(2)	-1(2)	6(2)	3(1)

N(2)	29(2)	22(2)	32(2)	5(2)	9(2)	0(1)
N(9)	95(3)	18(2)	127(4)	4(2)	-22(3)	11(2)
C(1)	22(2)	30(2)	39(3)	4(2)	9(2)	0(2)
C(2)	28(2)	21(2)	41(3)	8(2)	14(2)	-1(2)
C(3)	32(2)	29(2)	45(3)	11(2)	14(2)	1(2)
C(4)	35(2)	33(3)	59(3)	17(2)	8(2)	6(2)
C(5)	50(3)	25(2)	83(4)	8(3)	6(3)	1(2)
C(6)	54(3)	26(2)	70(4)	-1(2)	-6(2)	1(2)
C(7)	36(2)	25(2)	52(3)	10(2)	9(2)	-1(2)
C(8)	33(2)	17(2)	45(3)	5(2)	15(2)	2(2)
C(9)	36(2)	31(2)	52(3)	15(2)	19(2)	6(2)
C(10)	49(3)	41(2)	69(4)	18(2)	31(3)	18(2)
C(11)	74(4)	46(3)	53(4)	11(2)	36(3)	17(2)
C(12)	61(3)	53(3)	43(3)	8(2)	15(3)	18(2)
C(13)	44(2)	41(2)	34(3)	4(2)	12(2)	14(2)
C(14)	38(2)	21(2)	37(3)	-1(2)	10(2)	4(2)
C(15)	41(2)	35(2)	46(3)	-15(2)	11(2)	-6(2)
C(16)	55(3)	27(2)	54(4)	-11(2)	23(3)	-14(2)
C(17)	75(3)	39(3)	48(4)	2(2)	33(3)	-11(2)
C(18)	71(3)	60(3)	37(3)	3(2)	13(3)	-11(3)
C(19)	44(2)	42(2)	43(3)	5(2)	7(2)	-7(2)

Table 5. Bond lengths [Å] and angles [°] for **V-10**.

Rh(1)-N(1)	2.048(3)	C(9)-C(10)	1.410(5)
Rh(1)-N(1)#1	2.048(3)	C(9)-H(9)	0.95
Rh(1)-N(1)#2	2.048(3)	C(10)-C(11)	1.376(6)
Rh(1)-N(1)#3	2.048(3)	C(10)-H(10)	0.95
Rh(1)-Rh(2)	2.3950(9)	C(11)-C(12)	1.376(6)
Rh(2)-N(2)#1	2.051(3)	C(11)-H(11)	0.95
Rh(2)-N(2)#2	2.051(3)	C(12)-C(13)	1.377(6)
Rh(2)-N(2)#3	2.051(3)	C(12)-H(12)	0.95
Rh(2)-N(2)	2.051(3)	C(13)-H(13)	0.95
N(1)-C(1)	1.349(5)	C(14)-C(19)	1.363(5)
N(1)-C(8)	1.430(5)	C(14)-C(15)	1.390(5)
N(2)-C(1)	1.332(5)	C(15)-C(16)	1.385(5)
N(2)-C(14)	1.425(5)	C(15)-H(15)	0.95
N(9)-C(5)	1.410(5)	C(16)-C(17)	1.384(6)
N(9)-H(9a)	0.88	C(16)-H(16)	0.95
N(9)-H(9b)	0.88	C(17)-C(18)	1.375(6)
C(1)-C(2)	1.488(5)	C(17)-H(17)	0.95
C(2)-C(3)	1.389(5)	C(18)-C(19)	1.398(6)
C(2)-C(7)	1.394(5)	C(18)-H(18)	0.95
C(3)-C(4)	1.390(5)	C(19)-H(19)	0.95
C(3)-H(3)	0.95		
C(4)-C(5)	1.378(6)	N(1)-RH1-N(1)#1	174.97(18)
C(4)-H(4)	0.95	N(1)-RH1-N(1)#2	89.891(8)
C(5)-C(6)	1.406(6)	N(1)#1-RH1-N(1)#2	89.890(8)
C(6)-C(7)	1.375(5)	N(1)-RH1-N(1)#3	89.888(8)
C(6)-H(6)	0.95	N(1)#1-RH1-N(1)#3	89.890(8)
C(7)-H(7)	0.95	N(1)#2-RH1-N(1)#3	174.97(18)
C(8)-C(13)	1.376(6)	N(1)-RH1-RH2	87.48(9)
C(8)-C(9)	1.405(5)	N(1)#1-RH1-RH2	87.48(9)

N(1)#2-RH1-RH2	87.48(9)
N(1)#3-RH1-RH2	87.48(9)
N(2)#1-RH2-N(2)#2	89.902(8)
N(2)#1-RH2-N(2)#3	89.902(8)
N(2)#2-RH2-N(2)#3	175.26(18)
N(2)#1-RH2-N(2)	175.26(18)
N(2)#2-RH2-N(2)	89.902(8)
N(2)#3-RH2-N(2)	89.901(7)
N(2)#1-RH2-RH1	87.63(9)
N(2)#2-RH2-RH1	87.63(9)
N(2)#3-RH2-RH1	87.63(9)
N(2)-RH2-RH1	87.63(9)
C(1)-N(1)-C(8)	120.8(3)
C(1)-N(1)-RH1	119.6(2)
C(8)-N(1)-RH1	119.1(2)
C(1)-N(2)-C(14)	121.5(3)
C(1)-N(2)-RH2	120.6(2)
C(14)-N(2)-RH2	116.9(2)
C(5)-N(9)-H(9A)	120
C(5)-N(9)-H(9B)	120
H(9A)-N(9)-H(9B)	120
N(2)-C(1)-N(1)	118.7(3)
N(2)-C(1)-C(2)	122.0(3)
N(1)-C(1)-C(2)	119.2(4)
C(3)-C(2)-C(7)	118.6(3)
C(3)-C(2)-C(1)	122.4(4)
C(7)-C(2)-C(1)	118.9(3)
C(2)-C(3)-C(4)	120.4(4)
C(2)-C(3)-H(3)	119.8
C(4)-C(3)-H(3)	119.8
C(5)-C(4)-C(3)	120.6(4)
C(5)-C(4)-H(4)	119.7
C(3)-C(4)-H(4)	119.7
C(4)-C(5)-C(6)	119.4(4)
C(4)-C(5)-N(9)	121.7(4)
C(6)-C(5)-N(9)	118.9(4)
C(7)-C(6)-C(5)	119.5(4)
C(7)-C(6)-H(6)	120.2
C(5)-C(6)-H(6)	120.2
C(6)-C(7)-C(2)	121.4(4)
C(6)-C(7)-H(7)	119.3
C(2)-C(7)-H(7)	119.3
C(13)-C(8)-C(9)	119.4(4)
C(13)-C(8)-N(1)	120.1(3)
C(9)-C(8)-N(1)	120.4(4)
C(8)-C(9)-C(10)	118.9(4)
C(8)-C(9)-H(9)	120.6
C(10)-C(9)-H(9)	120.6
C(11)-C(10)-C(9)	120.4(4)
C(11)-C(10)-H(10)	119.8
C(9)-C(10)-H(10)	119.8
C(10)-C(11)-C(12)	119.7(4)
C(10)-C(11)-H(11)	120.2
C(12)-C(11)-H(11)	120.2
C(11)-C(12)-C(13)	120.8(5)
C(11)-C(12)-H(12)	119.6
C(13)-C(12)-H(12)	119.6
C(8)-C(13)-C(12)	120.7(4)
C(8)-C(13)-H(13)	119.6
C(12)-C(13)-H(13)	119.6
C(19)-C(14)-C(15)	118.8(4)
C(19)-C(14)-N(2)	120.1(3)
C(15)-C(14)-N(2)	121.0(4)
C(16)-C(15)-C(14)	120.4(4)
C(16)-C(15)-H(15)	119.8
C(14)-C(15)-H(15)	119.8
C(17)-C(16)-C(15)	120.4(4)
C(17)-C(16)-H(16)	119.8
C(15)-C(16)-H(16)	119.8
C(18)-C(17)-C(16)	119.3(4)
C(18)-C(17)-H(17)	120.4
C(16)-C(17)-H(17)	120.4
C(17)-C(18)-C(19)	119.9(5)
C(17)-C(18)-H(18)	120.1
C(19)-C(18)-H(18)	120.1
C(14)-C(19)-C(18)	121.2(4)
C(14)-C(19)-H(19)	119.4
C(18)-C(19)-H(19)	119.4